

# THE JOURNAL OF PHYSICAL CHEMISTRY

(Registered in U. S. Patent Office)

## CONTENTS

|  |     |
|--|-----|
| Keihei Ueno and Arthur E. Martell: Ultraviolet and Visible Absorption Spectra of Metal Chelates of Bisacetylacetonethylenediamine and Related Compounds.....   | 257 |
| Mary M. Williams, William S. McEwan and Ronald A. Henry: The Heats of Combustion of Substituted Triazoles, Tetrazoles and Related High Nitrogen Compounds.....   | 261 |
| S. Wagener: Adsorption Measurements at Very Low Pressures. II.....   | 267 |
| L. Mandelkern, L. C. Williams and S. G. Weissberg: Sedimentation Equilibrium of Flexible Chain Molecules.....  | 271 |
| Basil S. Strates, W. F. Neuman and George J. Levinskas: The Solubility of Bone Mineral. II. Precipitation of Near-Neutral Solutions of Calcium and Phosphate.....  | 279 |
| J. R. Zimmerman and M. R. Foster: Standardization of N.M.R. High Resolution Spectra.....   | 282 |
| J. P. McCullough, H. L. Finke, M. E. Gross, J. F. Messerly and Guy Waddington: Low Temperature Calorimetric Studies of Seven 1-Olefins: Effect of Orientation Disorder in the Solid State.....   | 289 |
| Andries Voet: Analysis of Structure in Channel Black Dispersions.....  | 301 |
| Frank E. Harris and Chester T. O'Konski: Dielectric Properties of Aqueous Ionic Solutions at Microwave Frequencies.....  | 310 |
| W. Forst, H. G. V. Evans and C. A. Winkler: The Kinetics of Nitrogen Atom Reactions Accompanied by Catalyzed Recombination of Atoms.....   | 320 |
| O. D. Bonner and Linda Lou Smith: A Selectivity Scale for Some Divalent Cations on Dowex 50.....   | 326 |
| Jay Vreeland and Robert Dunlap: The Ternary System Perfluorotri- <i>n</i> -butylamine-2,3,4-Trimethylpentane-Nitroethane.....  | 329 |
| R. Norman Diebel and D. F. Swinehart: The Ionization Constant of Orthoanthic Acid from 0 to 50° by Means of E.m.f. Measurements.....   | 333 |
| Karl A. Sense, C. A. Alexander, R. E. Bowman and R. B. Filbert, Jr.: Vapor Pressure and Derived Information of the Sodium Fluoride-Zirconium Fluoride System: Description of a Method for the Determination of Molecular Complexes Present in the Vapor Phase..... | 337 |
| John M. Googin and Hilton A. Smith: Vapor Pressure Studies Involving Solutions in Light and Heavy Waters. III. The Separation Factor for the Isotopes of Hydrogen during Distillation from Salt Solutions in the Mixed Waters at Room Temperature.....             | 345 |
| C. N. Spalaris, L. P. Bupp and E. C. Gilbert: Surface Properties of Irradiated Graphite.....   | 350 |
| Roger Sargent and William Rieman III: Salting-out Chromatography. I. Alcohols.....   | 354 |
| Chi-hsiang Wong and Verner Schomaker: An Electron Diffraction Investigation of the Structure of Cuprous Chloride Trimer.....   | 358 |
| V. Stannett, A. E. Woodward and R. B. Mesrobian: Autoxidation of 1,4-Dimethylcyclohexane.....  | 360 |
| K. H. Gayer and Leo Woontner: The Equilibria of Cadmium Hydroxide in Acidic and Basic Media at 25°.....  | 364 |
| NOTES: Max T. Rogers, John L. Speirs and Morton B. Panish: The Chlorine Trifluoride-Hydrogen Fluoride System. Some Vapor Pressure and Conductance Measurements.....  | 366 |
| Max T. Rogers and T. L. Brown: The Electric Moments of Lithium-alkyls.....   | 366 |
| E. Gerald Meyer and Mitchell A. Melnick: The Exchange Reaction between Tin(IV) Chloride and Tin(II) Chloride in Absolute Methanol.....   | 367 |
| N. W. Gregory: The Interaction of Iron(II) Bromide and Water.....  | 369 |
| L. M. Kushner, W. D. Hubbard and A. S. Doan: Light Scattering Measurements on a Fractionated Non-ionic Detergent.....  | 371 |
| Sidney A. Greenberg: The Chemical Reactions of Calcium Hydroxide, Silica and Water Mixtures at 82°.....  | 373 |
| S. Alexander Stern and Webster B. Kay: The Critical Pressure and Temperature of Dimethyl Oxalate.....  | 374 |
| Morton A. Golub: Shear Dependence of Viscosity of Natural Rubber Solutions.....  | 374 |
| George K. Estok: Some Considerations on the Guggenheim and Conventional Equations for Electric Moment Calculations.....  | 376 |
| Geoffrey Zubay: Chelate Formation between Cations and Polyelectrolytes.....  | 377 |
| R. W. Ramette and T. R. Blackburn: The Acid Dissociation Quotient of 3-Hydroxy-1,3-diphenyltriazine.....   | 378 |
| D. D. Williams, J. A. Grand and R. R. Miller: The Solubility of Sodium Hydroxide in Sodium.....  | 379 |
| F. B. Baker and T. W. Newton: The Effect of D <sub>2</sub> O on the Rate of the Reaction between Oxygen and Pu(III).....   | 381 |
| A. Greenville Whittaker and Charles M. Drew: Decomposition Study of Concentrated Hydrogen Peroxide.....  | 382 |
| S. F. Mason: The Structure of the Amide Ion.....   | 384 |
| Karl A. Sense, C. A. Alexander, R. E. Bowman, R. W. Stone and R. B. Filbert, Jr.: The Vapor Pressure of Sodium Fluoride.....   | 384 |

# THE JOURNAL OF PHYSICAL CHEMISTRY

(Registered in U. S. Patent Office)

W. ALBERT NOYES, JR., EDITOR

ALLEN D. BLISS

ASSISTANT EDITORS

ARTHUR C. BOND

## EDITORIAL BOARD

R. P. BELL

JOHN D. FERRY

S. C. LIND

R. E. CONNICK

G. D. HALSEY, JR.

H. W. MELVILLE

R. W. DODSON

J. W. KENNEDY

R. G. W. NORRISH

PAUL M. DOTY

A. R. UBBELOHDE

Published monthly by the American Chemical Society at 20th and Northampton Sts., Easton, Pa.

Entered as second-class matter at the Post Office at Easton, Pennsylvania.

The *Journal of Physical Chemistry* is devoted to the publication of selected symposia in the broad field of physical chemistry and to other contributed papers.

Manuscripts originating in the British Isles, Europe and Africa should be sent to F. C. Tompkins, The Faraday Society, 6 Gray's Inn Square, London W. C. 1, England.

Manuscripts originating elsewhere should be sent to W. Albert Noyes, Jr., Department of Chemistry, University of Rochester, Rochester 20, N. Y.

Correspondence regarding accepted copy, proofs and reprints should be directed to Assistant Editor, Allen D. Bliss, Department of Chemistry, Simmons College, 300 The Fenway, Boston 15, Mass.

Business Office: Alden H. Emery, Executive Secretary, American Chemical Society, 1155 Sixteenth St., N. W., Washington 6, D. C.

Advertising Office: Reinhold Publishing Corporation, 430 Park Avenue, New York 22, N. Y.

Articles must be submitted in duplicate, typed and double spaced. They should have at the beginning a brief Abstract, in no case exceeding 300 words. Original drawings should accompany the manuscript. Lettering at the sides of graphs (black on white or blue) may be pencilled in and will be typeset. Figures and tables should be held to a minimum consistent with adequate presentation of information. Photographs will not be printed on glossy paper except by special arrangement. All footnotes and references to the literature should be numbered consecutively and placed in the manuscript at the proper places. Initials of authors referred to in citations should be given. Nomenclature should conform to that used in *Chemical Abstracts*, mathematical characters marked for italic, Greek letters carefully made or annotated, and subscripts and superscripts clearly shown. Articles should be written as briefly as possible consistent with clarity and should avoid historical background unnecessary for specialists.

Notes describe fragmentary or less complete studies but do not otherwise differ fundamentally from articles. They are subjected to the same editorial appraisal as are Articles. In their preparation particular attention should be paid to brevity and conciseness.

Communications to the Editor are designed to afford prompt preliminary publication of observations or discoveries whose

value to science is so great that immediate publication is imperative. The appearance of related work from other laboratories is in itself not considered sufficient justification for the publication of a Communication, which must in addition meet special requirements of timeliness and significance. Their total length may in no case exceed 500 words or their equivalent. They differ from Articles and Notes in that their subject matter may be republished.

Symposium papers should be sent in all cases to Secretaries of Divisions sponsoring the symposium, who will be responsible for their transmittal to the Editor. The Secretary of the Division by agreement with the Editor will specify a time after which symposium papers cannot be accepted. The Editor reserves the right to refuse to publish symposium articles, for valid scientific reasons. Each symposium paper may not exceed four printed pages (about sixteen double spaced typewritten pages) in length except by prior arrangement with the Editor.

Remittances and orders for subscriptions and for single copies, notices of changes of address and new professional connections, and claims for missing numbers should be sent to the American Chemical Society, 1155 Sixteenth St., N. W., Washington 6, D. C. Changes of address for the *Journal of Physical Chemistry* must be received on or before the 30th of the preceding month.

Claims for missing numbers will not be allowed (1) if received more than sixty days from date of issue (because of delivery hazards, no claims can be honored from subscribers in Central Europe, Asia, or Pacific Islands other than Hawaii), (2) if loss was due to failure of notice of change of address to be received before the date specified in the preceding paragraph, or (3) if the reason for the claim is "missing from files."

Subscription Rates (1956): members of American Chemical Society, \$8.00 for 1 year; to non-members, \$16.00 for 1 year. Postage free to countries in the Pan American Union; Canada, \$0.40; all other countries, \$1.20. \$12.50 per volume, foreign postage \$1.20, Canadian postage \$0.40; special rates for A.C.S. members supplied on request. Single copies, current volume, \$1.35; foreign postage, \$0.15; Canadian postage \$0.05. Back issue rates (starting with Vol. 56): \$15.00 per volume, foreign postage \$1.20, Canadian, \$0.40; \$1.50 per issue, foreign postage \$0.15, Canadian postage \$0.05.

The American Chemical Society and the Editors of the *Journal of Physical Chemistry* assume no responsibility for the statements and opinions advanced by contributors to THIS JOURNAL.

The American Chemical Society also publishes *Journal of the American Chemical Society*, *Chemical Abstracts*, *Industrial and Engineering Chemistry*, *Chemical and Engineering News*, *Analytical Chemistry*, *Journal of Agricultural and Food Chemistry* and *Journal of Organic Chemistry*. Rates on request.



# THE JOURNAL OF PHYSICAL CHEMISTRY

(Registered in U. S. Patent Office) (© Copyright, 1957, by the American Chemical Society)

VOLUME 61

MARCH 25, 1957

NUMBER 3

## ULTRAVIOLET AND VISIBLE ABSORPTION SPECTRA OF METAL CHELATES OF BISACETYLACETONEETHYLENEDIIMINE AND RELATED COMPOUNDS<sup>1</sup>

By KEIHEI UENO<sup>2</sup> AND ARTHUR E. MARTELL

Contribution from the Chemical Laboratories of Clark University, Worcester, Mass.

Received December 9, 1956

Ultraviolet and visible absorption spectra are reported for bisacetylacetonethylenediimine, bisacetylacetonethylenediimine, bisbenzoylacetonethylenediimine, bisbenzoylacetonethylenediimine and bistrifluoroacetylacetonethylenediimine and many of the corresponding Cu(II), Ni(II) and Pd(II) chelate compounds. The strong absorption bands of the ligands in the ultraviolet region are attributed to the hydrogen-bonded conjugate chelate rings, and the double peaks of these bands are discussed in relation to the vibrational frequencies. An additional band at 244  $m\mu$  of the ligands derived from benzoylacetonethylenediimine is employed in a determination of the structure of these compounds. Absorption spectra of metal chelate compounds are classified into two groups, one of which is characteristic of the metal ions, while the other is characteristic of both the metal ions and the ligands.

In relation to investigations on infrared absorption<sup>3</sup> and dipole moment measurements<sup>4</sup> of the metal chelates of bisacetylacetonethylenediimine and related compounds, a study of the ultraviolet and visible absorption spectra was undertaken. The carbon skeleton and the conjugated system of these metal chelate compounds are similar to those of the synthetic chelate oxygen carrier,<sup>5</sup> bisacetylacetonethylenediimine-Co(II), with the exception that they do not contain the fused benzene ring. Bisacetylacetonethylenediimine was chosen for preliminary spectrophotometric study since it is the simplest possible tetradentate ligand having the same arrangement of donor groups as is found in the oxygen-carrying chelate compounds.

### Experimental

The composition and structures of the ligands and metal chelates employed in this investigation are summarized in Table I. The syntheses, physical properties and analyses of these substances are reported elsewhere.<sup>6</sup>

(1) This research was supported by the National Institutes of Health, U. S. Public Health Service, under Grant #G3819(C2).

(2) Dojindo & Co., Kumamoto-shi Japan. Postdoctoral Research Fellow, Clark University, 1953-1955.

(3) K. Ueno and A. E. Martell, *This Journal*, **59**, 998 (1955).

(4) P. J. McCarthy and A. E. Martell, *J. Am. Chem. Soc.*, **78**, 2106 (1956); P. J. McCarthy, Ph.D. Dissertation, Clark University, September, 1954.

(5) A. E. Martell and M. Calvin, "Chemistry of the Metal Chelate Compounds," Prentice-Hall, New York, N. Y., 1952, p. 337.

(6) P. J. McCarthy, R. J. Hovey, K. Ueno and A. E. Martell, *J. Am. Chem. Soc.*, **77**, 5820 (1955).

TABLE I

| Name of ligand  | R                             | R'              | R''             | Metal chelates         |
|---|-------------------------------|-----------------|-----------------|------------------------|
| 1. Bisacetylacetonethylenediimine                       | CH <sub>3</sub>               | CH <sub>3</sub> | H               | Cu(II), Ni(II), Pd(II) |
| 2. Bisacetylacetonethylenediimine-1,2-propylenediimine  | CH <sub>3</sub>               | CH <sub>3</sub> | CH <sub>3</sub> | Cu(II), Ni(II)         |
| 3. Bisbenzoylacetonethylenediimine                      | C <sub>6</sub> H <sub>5</sub> | CH <sub>3</sub> | H               | Cu(II)                 |
| 4. Bisbenzoylacetonethylenediimine-1,2-propylenediimine | C <sub>6</sub> H <sub>5</sub> | CH <sub>3</sub> | CH <sub>3</sub> | Cu(II)                 |
| 5. Bistrifluoroacetylacetonethylenediimine              | CH <sub>3</sub>               | CF <sub>3</sub> | H               | Cu(II)                 |

Absorption spectra were measured with a Beckman Model DU spectrophotometer equipped with a photomultiplier attachment. Weighed samples were dissolved in methanol (C.P. grade) or 0.1 N NaOH solution, and the solution was diluted to give a concentration of about  $10^{-5}$  M for the measurements in ultraviolet region and about  $10^{-4}$  M for measurements in the visible region. A set of matched silica cells of 10 mm. length were employed and optical densities were determined at 5  $m\mu$  intervals. All measure-

TABLE II

FREQUENCIES AND EXTINCTION COEFFICIENTS OF ABSORPTION BANDS IN METHANOL

| Lig-<br>and <sup>a</sup> | $\lambda_{\max}$<br>( $m\mu$ ) | $\epsilon^1$<br>$\times 10^{-3}$ | $\lambda_{\max}$<br>( $m\mu$ ) | $\epsilon^2$<br>$\times 10^{-3}$ | $\lambda_{\max}$<br>( $m\mu$ ) | $\epsilon^3$<br>$\times 10^{-3}$ | $\lambda_{\max}$<br>( $m\mu$ ) | $\epsilon^4$<br>$\times 10^{-3}$ | $\lambda_{\max}$<br>( $m\mu$ ) | $\epsilon^5$<br>$\times 10^{-3}$ | $\lambda_{\max}$<br>( $m\mu$ ) | $\epsilon^6$<br>$\times 10^{-3}$ | $\lambda_{\max}$<br>( $m\mu$ ) | $\epsilon^7$<br>$\times 10^{-3}$ |
|--------------------------|--------------------------------|----------------------------------|--------------------------------|----------------------------------|--------------------------------|----------------------------------|--------------------------------|----------------------------------|--------------------------------|----------------------------------|--------------------------------|----------------------------------|--------------------------------|----------------------------------|
| 1                        | 322                            | 29.5                             | 304                            | 31.7                             |                                |                                  |                                |                                  |                                |                                  |                                |                                  |                                |                                  |
| 2                        | 322-323                        | 31.3                             | 308                            | 29.5                             |                                |                                  |                                |                                  |                                |                                  |                                |                                  |                                |                                  |
| 3                        | 350                            | 37.5                             | (342 <sup>b</sup> )            | 37.0                             | 243                            | 17.4                             |                                |                                  |                                |                                  |                                |                                  |                                |                                  |
| 4                        | 350                            | 36.0                             | (342)                          | 35.5                             | 244                            | 15.8                             |                                |                                  |                                |                                  |                                |                                  |                                |                                  |
| 5                        | 322                            | 24.2                             | 311                            | 23.4                             |                                |                                  |                                |                                  |                                |                                  |                                |                                  |                                |                                  |
| Cu(II) Chelates          |                                |                                  |                                |                                  |                                |                                  |                                |                                  |                                |                                  |                                |                                  |                                |                                  |
| 1                        | 540                            | 0.18                             | (335                           | 5.9)                             | 306                            | 23.3                             | 275                            | 11.0                             |                                |                                  | 229                            | 17.5                             |                                |                                  |
| 2                        | 540                            | .19                              | (335                           | 8.0)                             | 306                            | 25.5                             | 276                            | 13.2                             |                                |                                  | 229                            | 19.7                             |                                |                                  |
| 4                        | 545                            | .22                              | (370                           | 11.5)                            | 334                            | 26.2                             | 278                            | 12.8                             | 242                            | 25.6                             | (230                           | 18.0)                            |                                |                                  |
| 5                        | 575                            | .13                              | (330                           | 4.0)                             | 305                            | 14.2                             | 268                            | 7.0                              |                                |                                  | 229                            | 7.6                              |                                |                                  |
| Ni(II) Chelates          |                                |                                  |                                |                                  |                                |                                  |                                |                                  |                                |                                  |                                |                                  |                                |                                  |
| 1                        | 562                            | 0.08                             | 357                            | 5.07                             | 352                            | 5.33                             | (305                           | 4.10)                            | 268                            | 13.3                             |                                |                                  | 234                            | 28.3                             |
| 2                        | 560                            | .08                              | 368                            | 5.10                             | 351                            | 5.21                             | (304                           | 4.00)                            | 269                            | 13.4                             |                                |                                  | 234                            | 28.2                             |
| 3                        | 555                            | .15                              | 395                            | 6.93                             |                                |                                  |                                |                                  | 292                            | 17.9                             | (248                           | 23.0)                            | 237                            | 27.7                             |

<sup>a</sup> Numbers refer to ligands listed in Table I. <sup>b</sup> The figures in parentheses indicate a shoulder.

ments were carried out at room temperature. The observed absorption curves in the ultraviolet region are shown in Figs. 1-5, and the principal absorption characteristics of the ligands and the metal chelate compounds are summarized in Table II.

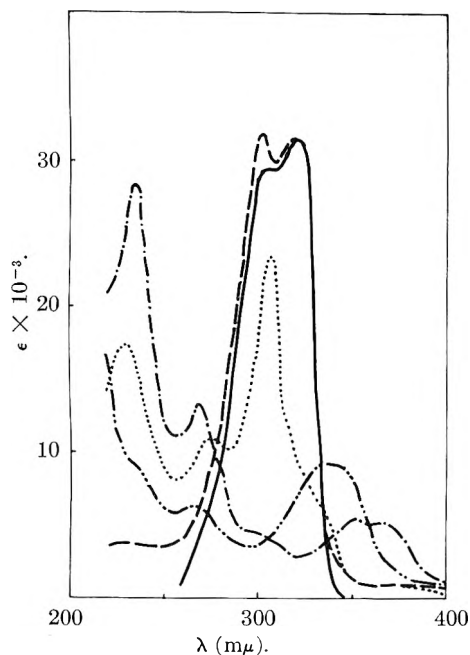


Fig. 1.—Ultraviolet absorption spectra of bisacetylacetonethylenediimine and metal chelate compounds: —, ligand in methanol; ---, ligand in 0.1 *N* NaOH; — — —, Cu(II) chelate in methanol; - - - - -, Ni(II) chelate in methanol; ·····, Pd(II) chelate in methanol.

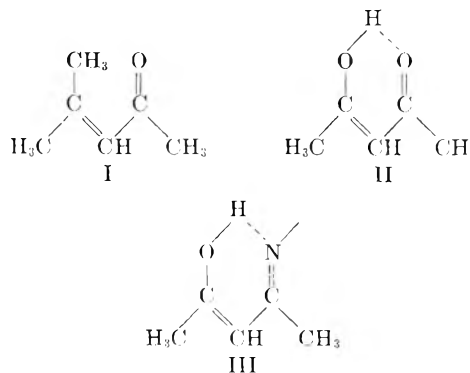
### Discussion

The absorption spectra of the metal chelates, illustrated in Figs. 1-5, are quite different from those of the ligands. The intense double bands of the Schiff bases disappear when they become coordinated with transition metal ions, and are replaced by a complicated system of bands of varying frequency and intensity. The lack of an obvious resemblance between the spectra of ligand and chelate may be taken as evidence for the highly-covalent character of the metal-donor bonds of the metal chelate compound. Similar conclusions have

been made concerning the structures of the analogous bisacetylacetonethylenediimine-Co(II) and -Ni(II),<sup>7</sup> both of which have been found to have magnetic moments corresponding to the formation of  $dsp^2$  covalent metal bonds.

The absorption spectra of bisacetylacetonethylenediimine, bisacetylacetonethylenediimine-1,2-propylenediimine and bistrifluoroacetylacetonethylenediimine were found to be very similar in the ultraviolet region. This similarity seems reasonable in view of the fact that they contain the same system of conjugated bonds, which is responsible for the ultraviolet absorption bands. The same may be said for the spectra, illustrated in Figs. 3 and 4, of bisbenzoylacetonethylenediimine and bisbenzoylacetonethylenediimine-1,2-propylenediimine, which also have similar resonating structures.

The absorption spectra of the Schiff bases (ligands 1, 2 and 5, Table II) are characterized by double peaks in the 300-325  $m\mu$  region, which arise from electronic transitions in the hydrogen-bonded chelate rings. A comparison of the absorption spectra of mesityl oxide (I) with that of acetylacetonethylenediimine (II) is of assistance in showing the full extent of the shift obtained by bridging an -O-H- group between the ends of the conjugated Schiff base studies in this investigation.



The absorption peaks of I and II, found by Grossmann<sup>8</sup> to occur at 238 and 270  $m\mu$ , indicate that the

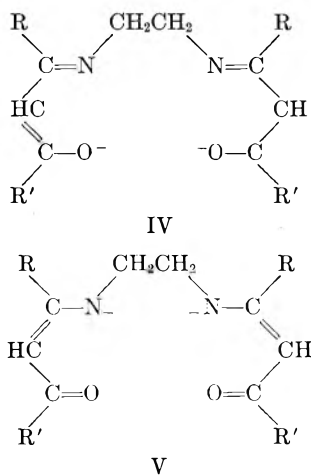
(7) Reference 5, p. 214.

(8) P. Grossmann, *Z. physik. Chem.*, **109**, 305 (1924).

replacement of  $\text{CH}_3$  by  $\text{OH}$  results in a bathochromic shift of  $32 \text{ m}\mu$ . It is also well known that the replacement of a carbonyl group by a  $\text{>C=N-}$  group in a conjugated system results in a considerable bathochromic shift.<sup>9</sup> On this basis the further bathochromic shifts ( $304\text{--}322 \text{ m}\mu$ ) of the compounds represented by III become understandable.

The spectra of the ligands derived from acetylacetone contain double peaks in the  $300\text{--}325 \text{ m}\mu$  region with a spacing which corresponds roughly to the infrared frequency range of  $1300\text{--}1800 \text{ cm.}^{-1}$ . The infrared absorption bands observed near  $1600 \text{ cm.}^{-1}$  were assigned in a previous publication<sup>3</sup> to stretching vibrations of the conjugated double bonds of the hydrogen-bonded chelate rings. The double peaks must correspond, therefore, to electronic transitions involving a change of vibrational energy states.

The hypsochromic shift observed in basic solution of the ligand containing trifluoro groups is interesting in view of the fact that the other Schiff bases show little if any frequency shift. It is interesting to note in this connection that this compound differs from the other ligands in that the trifluoromethyl group favors the ketonic form V rather than the normal Schiff base IV as the structure of the enolate ion. Hence the formation of the enolate in this case would result in a greater structural change in the resonating system than that which occurs in the other ligands.



Absorption spectra of the ligands derived from benzoylacetone (ligands 3 and 4), are characterized by similar double maxima at higher wavelength and by an additional band at  $243\text{--}244 \text{ m}\mu$ . This band in the  $243 \text{ m}\mu$  region is always observed in the ligands as well as in the metal chelate compounds of these ligands. Although the absorption spectra of the metal chelate compounds are much different from those of the ligands, a weak shoulder near  $240 \text{ m}\mu$  is still observed, whereas no corresponding band appears in the ligands of acetylacetone derivatives nor in their metal chelate compounds. It is quite certain, therefore, that the bands at  $243 \text{ m}\mu$  region are related to the conjuga-

(9) A. Gillam and E. S. Stern, "An Introduction to Electronic Absorption Spectroscopy in Organic Chemistry," Edward Arnold Ltd., London, 1954, p. 100.

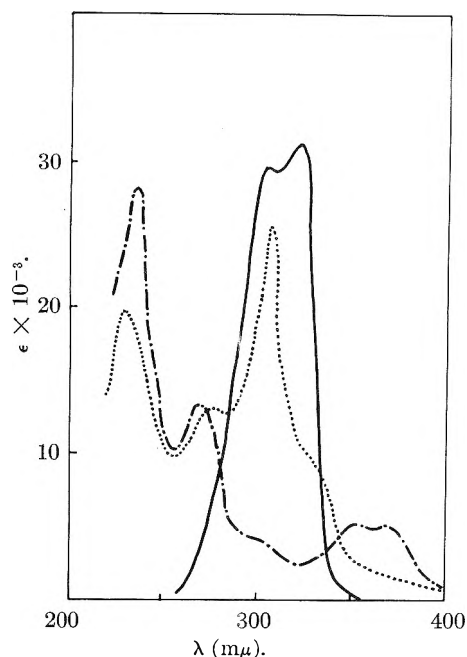


Fig. 2.—Ultraviolet absorption spectra of bisacetylacetone-1,2-propylenediimine and metal chelate compounds: —, ligand in methanol; ----, Cu(II) chelate in methanol; - · - ·, Ni(II) chelate in methanol.

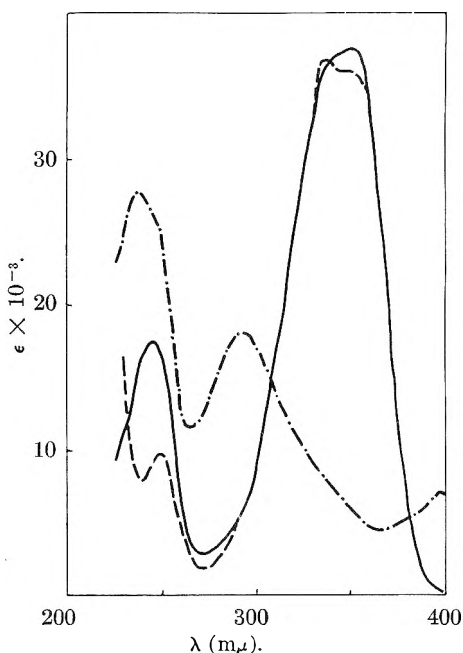
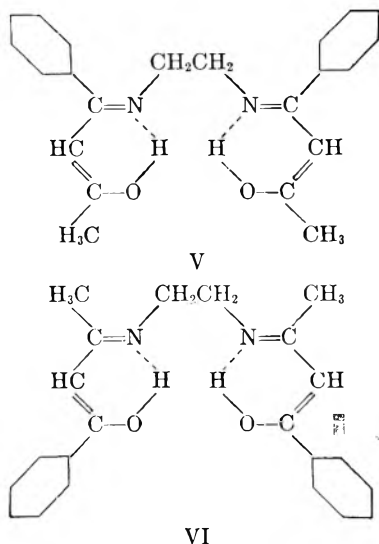


Fig. 3.—Ultraviolet absorption spectra of bisbenzoylacetoneethylenediimine and metal chelate compound: —, ligand in methanol; ----, ligand in  $0.1N \text{ NaOH}$ ; - · - ·, Ni(II) chelate in methanol.

tion of the aromatic ring with the unsaturated chelate ring system.

With regard to bisbenzoylacetoneethylenediimine, there are two possible structures corresponding to formulas V and VI, since this ligand was synthesized by the condensation of benzoylacetone and ethylenediamine.<sup>6</sup>

If the structure corresponds to formula V, conjugation with the phenyl ring is somewhat similar to that of bisbenzylideneethylenediimine, whereas the



conjugated system for the other possible structure, indicated by formula VI, would be similar to that of biscinnamylidenethylenediimine. The observed absorption maxima arising from these conjugated

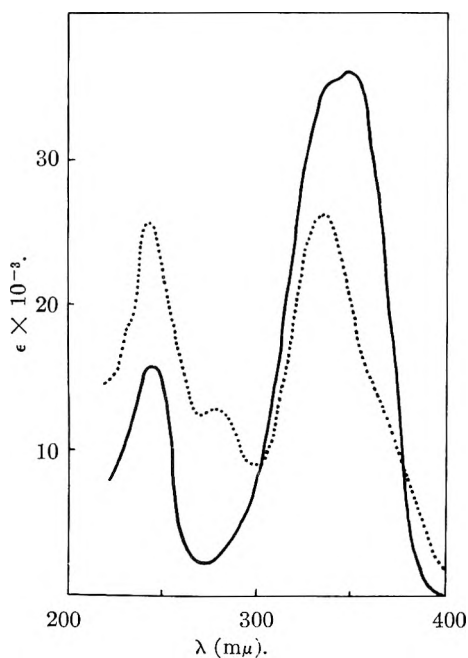


Fig. 4.—Ultraviolet absorption spectra of bisbenzoylacetone-1,2-propylenediimine and metal chelate compound: —, ligand in methanol; — — —, Cu(II) chelate in methanol.

systems were reported as 247 and 281  $m\mu$ , respectively.<sup>10</sup> The identity of the position of the absorption band of bisbenzylideneethylenediimine and of the 243–244  $m\mu$  band of the ligands indicates that the location of the phenyl rings is the one indicated by the formula V.

It also has been reported that, of the two absorption maxima of the enol form of benzoylacetone, the 310  $m\mu$  band was related to the conjugated chelate ring of the enol form, whereas a 247  $m\mu$  band was due to the aromatic ring which is con-

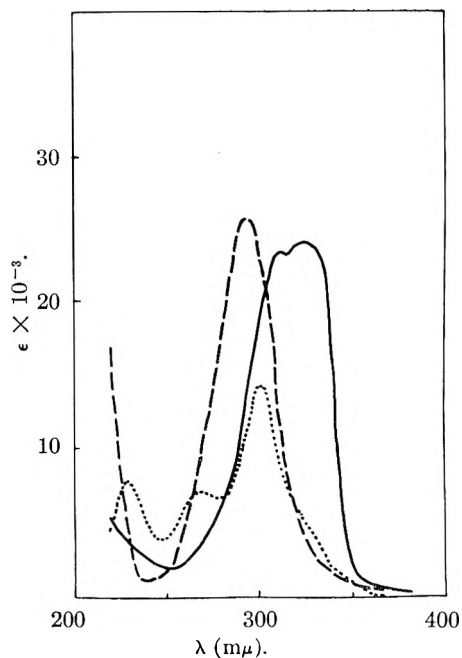


Fig. 5.—Ultraviolet absorption spectra of bistrifluoroacetylacetone ethylenediimine and metal chelate compound: —, ligand in methanol; — — —, ligand in 0.1N NaOH; — · — ·, Cu(II) chelate in methanol.

jugated with the unsaturated ketone.<sup>11</sup> This offers further evidence for the origin of the shorter wave length band of the ligand.

With regard to the main absorption band of bisbenzoylacetone ethylenediimine, a bathochromic shift of 40  $m\mu$  is observed when one goes from benzoylacetone to bisbenzoylacetone ethylenediimine. The size of shift is about the same as was observed in the case of bisacetylacetone ethylenediimine, and this bathochromic shift can be similarly explained by the different strengths of hydrogen bonded conjugate chelate rings between the simple diketone and the corresponding compound in which the hydrogen bond involves a basic nitrogen atom. The double maxima in the ligands derived from benzoylacetone are not so clear as in the case of acetylacetone derivatives. However, these double maxima may also be explained on the basis of vibrational fine structure, since a similar change of absorption intensities was observed in sodium hydroxide solution.

The absorption spectra of metal chelates of these ligands are quite different from those of the free ligands. For the metal chelates of bidentate ligands such as acetylacetone and salicylaldehyde, two kinds of absorption bands were observed: weak bands in the visible or near ultraviolet region which are characteristic of the central metal ions, and very strong bands in the ultraviolet region which are related with the ligands.<sup>12</sup> The absorption bands of the metal chelates under investigation can be classified in a similar manner. An absorption band in a region of 540–575  $m\mu$  for the Cu(II) chelates, and two bands near 350 and 570  $m\mu$  for Ni(II) chelates involve the central metal ions. However no corresponding band is observed

(10) L. N. Ferguson and G. E. K. Branch, *J. Am. Chem. Soc.*, **66**, 1467 (1944).

(11) E. S. Levin, *Bull. acad. sci. U.S.S.R., ser. phys.*, **11**, 413 (1947).

(12) K. Sone, *J. Am. Chem. Soc.*, **75**, 5207 (1953).

for the Pd(II) chelate, for which the first band appears at 340  $m\mu$ .

The crystal-field approach to the prediction of low-intensity "forbidden" absorption bands of the transition metal complexes, carried out with considerable success by Bjerrum, *et al.*,<sup>13</sup> was not attempted in this investigation, in view of the greater complexity and lower symmetry of the metal chelates of the tetradentate Schiff bases.

In a recent investigation on bisacetylaceton-

(13) J. Bjerrum, C. J. Ballhausen and C. K. Jorgensen, *Acta Chem. Scand.*, **8**, 1275 (1954), (and later papers).

Cu(II) by paramagnetic resonance absorption,<sup>14</sup> it was proved that the metal and ligand were involved in rather strong  $\pi$ -bonds. Bisacetylaceton-ethylenediimine-Cu(II), as well as the corresponding Ni(II) chelate, would have similar  $\pi$ -bond character, and the high degree of resonance in the chelate rings including the central metal ion would be responsible for the considerable change in the ultraviolet absorption spectra when one goes from the ligands to the metal chelates.

(14) B. R. McGarvey, *THIS JOURNAL*, **60**, 71 (1956).

## THE HEATS OF COMBUSTION OF SUBSTITUTED TRIAZOLES, TETRAZOLES AND RELATED HIGH NITROGEN COMPOUNDS

BY MARY M. WILLIAMS, WILLIAM S. McEWAN AND RONALD A. HENRY

*Contribution from the Chemistry Division of the U. S. Naval Ordnance Test Station, China Lake, Cal.*

*Received June 4, 1956*

The heats of combustion of some 36 substituted triazoles, tetrazoles and related high nitrogen compounds have been determined. The number of moles of nitric acid formed during the combustion process was found to be a function of the square root of the product of the heat of combustion and the number of nitrogen atoms present. Several new tetrazole compounds including the *cis* and *trans* isomers of 1,1'-dimethyl- and 1,1'-diethyl-5,5'-azotetrazole, are described.

The heats of combustion ( $H_c$ ) of a number of tetrazoles were reported by McEwan and Rigg<sup>1</sup> in 1951. Since that time the heats of combustion of a number of additional compounds have been determined. The samples were prepared as part of a study on preparation and properties of high nitrogen compounds and only in a few cases specifically for heat of combustion determinations. For this reason the amount of material available limited the number and size of samples to be run on a given compound.

Some of the triazoles did not burn cleanly or completely. Carbon deposits were found on the bomb wall after combustion; and increasing the oxygen pressure, decreasing the sample size or addition of benzoic acid did not always correct this tendency.

A number of azotetrazoles were prepared in order to have a series of compounds for combustion, which would contain more than one nitrogen-nitrogen double bond in the molecule per tetrazole ring. 5-Tetrazolylazo-(N)-piperidine met this requirement but like some of the triazole derivatives could not be burned cleanly. Compounds such as 3-(5-tetrazolylazo)-butanone-2, 3-(5-tetrazolylazo)-pentanedione-2,4, etc., also were made for this purpose; but some uncertainty exists, because of tautomerism, as to whether the compounds are present in the azo or hydrazo forms. Oxidation of 1- or 2-alkyl-5-aminotetrazole with sodium hypochlorite furnished the corresponding 5,5'-azotetrazoles; with the 1,1'-dimethyl- and the 1,1'-diethyl-5,5'-azotetrazole, both the *cis* and the *trans* isomers were ultimately isolated and characterized. With the 2,2'-dialkyl-5,5'-azotetrazoles only one isomer (probably the *cis*) was recovered.

Smooth combustion of some of these 5,5'-azo-

tetrazoles derivatives was also very difficult. The compounds would detonate (audible sound on ignition and shattered crucible) and deposit partially burned material on the bomb wall. Another apparent complication was noted: the heat of combustion of *trans*-1,1'-dimethyl-5,5'-azotetrazole seemed to increase with the age of the material (as much as 12 to 15 kcal. per mole in about four months time) although the melting point remained constant. The average heats of combustion for both the *cis* and the *trans* forms of 1,1'-dimethyl-5,5'-azotetrazole are given in Table I. Although an energy difference should exist between the *cis* and *trans* forms, the large deviations and lack of precision make any difference meaningless. Similar difficulties were encountered with the isomers of 1,1'-diethyl-5,5'-azotetrazole. A total of six samples were burned; of these only one burned cleanly enough to merit calculation. This single value of 1078 kcal. per mole was obtained on the more stable *cis* form.

An original intention in this work was to compute a set of standard bond energies applicable to high nitrogen compounds. Difficulties in obtaining compounds of unambiguous structure, in obtaining heat of sublimation values for all compounds, and the bulk of the data to be presented have caused this portion of the work to be deferred for later publication.

### Materials

**Tetrazole Derivatives.**—5-Dimethyl- and 5-diallyl-aminotetrazole were synthesized by the method of Garbrecht and Herbst.<sup>2</sup> The former compound melted at 237–239° dec. after four recrystallizations from water; the latter at 96–97° after five recrystallizations from benzene (calcd. eq. wt., 165.20; found, 165.24).

1-Allyl-5-aminotetrazole (four times recrystallized from ethyl acetate, m.p. 128.5–129.5°), 1-methyl-5-aminotetra-

(1) W. S. McEwan and M. W. Rigg, *J. Am. Chem. Soc.*, **73**, 4725 (1951).

(2) W. L. Garbrecht and R. M. Herbst, *J. Org. Chem.*, **18**, 1003 (1953).

TABLE I  
 COMBUSTION DATA

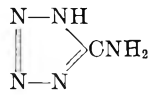
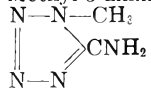
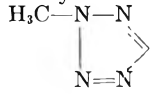
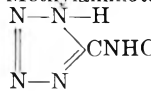
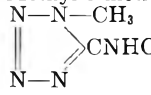
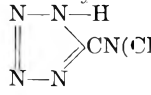
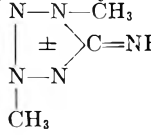
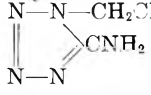
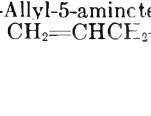
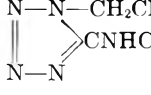
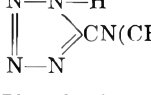
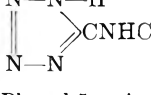
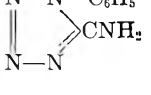
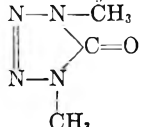
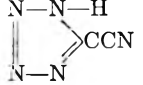
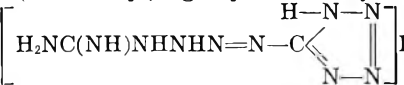
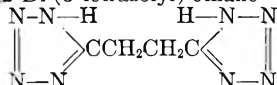
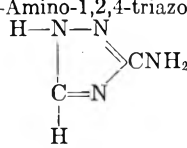
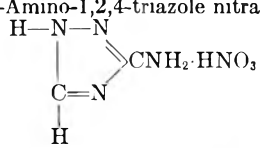
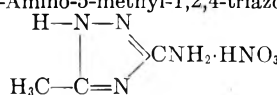
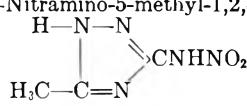
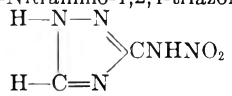
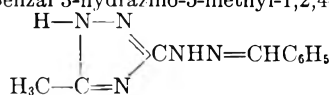
| Compound   | Formula                                    | Mol. wt. | Sampl. wt.   | $\frac{N_{HNO_3}}{N_{\text{sampl.}}}$        | $-\Delta H_c$  | $-\Delta H_c(\text{av.})$<br>kcal./mole | $-\Delta H_f$ |
|--|--|----------|--|--|--|---|---------------|
| 5-Aminotetrazole<br>                        | $\text{CH}_3\text{N}_5$                    |          |  |  |  | $246.20 \pm 0.56$                       | $-49.67$      |
| 1-Methyl-5-aminotetrazole<br>               | $\text{C}_2\text{H}_5\text{N}_5$           | 99.100   | 1.1215<br>0.9201<br>1.0258<br>1.0743                 | 0.213<br>.220<br>.221<br>.219                | 405.14<br>404.89<br>405.20<br>405.42                     | $405.16 \pm .11$                        | $-46.2$       |
| 2-Methyl-5-aminotetrazole<br>               | $\text{C}_2\text{H}_5\text{N}_5$           | 99.100   | 0.8520<br>.7134<br>.5686<br>.6132<br>1.0223          | .224<br>.229<br>.235<br>.229<br>.224         | 408.99<br>410.39<br>410.52<br>408.11<br>408.51           | $409.30 \pm .49$                        | $-50.40$      |
| 5-Methylaminotetrazole<br>                  | $\text{C}_2\text{H}_5\text{N}_5$           | 99.100   | 0.5926<br>.8878<br>.7785                             | .237<br>.225<br>.232                         | 406.61<br>407.12<br>408.20                               | $407.31 \pm .47$                        | $-48.41$      |
| 1-Methyl-5-methylaminotetrazole<br>         | $\text{C}_3\text{H}_7\text{N}_5$           | 113.126  | .9722<br>1.0489<br>1.0614                            | .267<br>.259<br>.262                         | 569.45<br>568.68<br>569.13                               | $569.09 \pm .70$                        | $-47.82$      |
| 5-Dimethylaminotetrazole<br>               | $\text{C}_3\text{H}_7\text{N}_5$           | 113.126  | 0.7821<br>.6945                                      | .275<br>.324                                 | 564.41<br>565.49   | $564.95 \pm .54$                        | $-43.68$      |
| 1,3-Dimethyl-5-iminotetrazole nitrate<br> | $\text{C}_3\text{H}_8\text{N}_6\text{O}_3$ | 176.142  | .5447<br>.5097                                       | .584<br>.693                                 | 554.45<br>553.84   | $554.15 \pm .30$                        | $+1.28$       |
| 1-Allyl-5-aminotetrazole<br>              | $\text{C}_4\text{H}_7\text{N}_5$           | 125.136  | .7131<br>.6327<br>.7356<br>.5859<br>1.1870<br>0.9929 | .282<br>.276<br>.271<br>.274<br>.249<br>.273 | 677.83<br>678.95<br>678.39<br>677.90<br>679.26<br>679.22 | $678.75 \pm .22$                        | $-63.43$      |
| 2-Allyl-5-aminotetrazole<br>              | $\text{C}_4\text{H}_7\text{N}_5$           | 125.136  | .4208<br>.5966                                       | .275<br>.273                                 | 683.12<br>682.74   | $682.93 \pm .19$                        | $-67.61$      |
| 1-Allyl-5-allylaminotetrazole<br>         | $\text{C}_7\text{H}_{11}\text{N}_5$        | 165.198  | .9346<br>.7959                                       | .342<br>.351                                 | 1117.33<br>1118.29                                       | $1117.81 \pm .52$                       | $-83.70$      |
| 5-Diallylaminotetrazole<br>               | $\text{C}_7\text{H}_{11}\text{N}_5$        | 165.198  | .8066<br>.7650<br>.5259<br>.4986                     | .305<br>.344<br>.356<br>.352                 | 1118.65<br>1118.32<br>1117.89<br>1117.26                 | $1118.03 \pm .54$                       | $-83.92$      |
| 5-Phenylaminotetrazole<br>                | $\text{C}_7\text{H}_7\text{N}_5$           | 161.166  | .3246<br>.3564                                       | .282<br>.315                                 | 970.40<br>970.35   | $970.37 \pm .02$                        | $-72.89$      |
| 1-Phenyl-5-aminotetrazole<br>             | $\text{C}_7\text{H}_7\text{N}_5$           | 161.166  | .5688<br>.4510<br>.4612                              | .297<br>.312<br>.318                         | 971.34<br>971.42<br>972.57                               | $971.78 \pm .40$                        | $-74.30$      |

TABLE I (Continued)

| Compound  | Formula           | Mol. wt. | Samp. wt.           | $\frac{N_{HNO_3}}{N_{\text{sample}}}$ | $-\Delta H_c$ | $-\Delta H_c(\text{av.})$<br>kcal./mole | $-\Delta H_f$ |
|---|-------------------|----------|---------------------|---------------------------------------|---------------|---|---------------|
| <i>trans</i> -1,1'-Dimethyl-5,5'-azotetrazole<br> | $C_4H_6N_{10}$    | 194.168  | 0.6502 <sup>a</sup> | 0.662                                 | 767.88        | $770.49 \pm 2.42$                       | -189.33       |
|   |                   |          | .5892               | .525                                  | 770.76        |   |               |
|   |                   |          | .4709               | .545                                  | 776.73        |   |               |
|   |                   |          | .3814               | .548                                  | 776.37        |   |               |
|   |                   |          | .8643 <sup>a</sup>  | .846                                  | 765.01        |   |               |
|   |                   |          | .6685               | .572                                  | 763.86        |   |               |
|   |                   |          | .6285               | .456                                  | 761.32        |   |               |
|   |                   |          | .5026 <sup>a</sup>  | .620                                  | 770.34        |   |               |
| <i>cis</i> -1,1'-Dimethyl-5,5'-azotetrazole<br>   | $C_4H_6N_{10}$    | 194.168  | .6184               | .445                                  | 769.69        | $769.78 \pm 0.09$                       | -188.62       |
|   |                   |          | .5884               | .397                                  | 769.87        |   |               |
| 2,2'-Dimethyl-5,5'-azotetrazole<br>               | $C_4H_6N_{10}$    | 194.168  | .4934               | .584                                  | 762.04        | $761.51 \pm .53$                        | -180.35       |
|   |                   |          | .4825               | .693                                  | 761.09        |   |               |
| 2,2'-Diethyl-5,5'-azotetrazole<br>                | $C_6H_{10}N_{10}$ | 222.22   | .3968               | .500                                  | 1061.39       | $1062.52 \pm .70$                       | -156.62       |
|   |                   |          | .3106               | .523                                  | 1062.65       |   |               |
|   |                   |          | .4673               | .529                                  | 1063.79       |   |               |
| 3-(5-Tetrazolylazo)-butanone-2<br>                | $C_5H_8N_6O$      | 168.162  | .4295               | .335                                  | 783.42        | $783.53 \pm .08$                        | -40.00        |
|   |                   |          | .4691               | .340                                  | 783.49        |   |               |
|   |                   |          | .3931               | .335                                  | 783.70        |   |               |
| 3-(5-Tetrazolylazo)-pentanedione-2,4<br>          | $C_6H_8N_6O_2$    | 196.172  | .6542               | .269                                  | 837.84        | $840.96 \pm 1.34$                       | -3.38         |
|   |                   |          | .6062 <sup>b</sup>  | .352                                  | 841.50        |   |               |
|   |                   |          | .8126               | .256                                  | 840.22        |   |               |
|   | $C_6H_8N_6O_2$    | 196.172  | .6153               | .303                                  | 844.29        | $840.96 \pm 1.34$                       | -3.38         |
|   |                   |          |                     |                                       |               |   |               |
| Benzal 5-hydrizinetetrazole<br>                   | $C_8H_8N_6$       | 188.192  | .9505               | .317                                  | 1130.99       | $1131.06 \pm 0.17$                      | -105.41       |
|   |                   |          | .7645               | .344                                  | 1130.86       |   |               |
|   |                   |          | .8970               | .312                                  | 1131.42       |   |               |
|   | $C_8H_8N_6$       | 188.192  |                     |                                       |               | $1131.06 \pm 0.17$                      | -105.41       |
|   |                   |          |                     |                                       |               |   |               |
| 1-Phenyl-5-methyltetrazole <sup>c</sup><br>       | $C_8H_8N_4$       | 160.176  | .7660               | .299                                  | 1095.07       | $1094.84 \pm .24$                       | -69.15        |
|   |                   |          | .7179               | .329                                  | 1094.60       |   |               |
| 1-Methyl-5-phenyltetrazole<br>                    | $C_8H_8N_4$       | 160.176  | .4593               | .323                                  | 1095.38       | $1095.53 \pm .15$                       | -69.84        |
|   |                   |          | .4462               | .324                                  | 1095.68       |   |               |
| 5-Methoxytetrazole<br>                            | $C_2H_4N_4O$      | 100.084  | .4471               | .190                                  | 341.50        | $341.25 \pm .17$                        | -16.51        |
|   |                   |          | .3843               | .198                                  | 341.33        |   |               |
|   |                   |          | .4611               | .190                                  | 340.93        |   |               |
| 5-Hydroxytetrazole<br>                            | $CH_2N_4O$        | 86.058   | .6396               | .113                                  | 163.49        | $163.88 \pm .23$                        | -1.50         |
|   |                   |          | .7436               | .108                                  | 163.54        |   |               |
|   |                   |          | .6181               | .109                                  | 164.32        |   |               |
|   |                   |          | .5520               | .102                                  | 163.47        |   |               |
|   |                   |          | 1.4491              | .106                                  | 164.56        |   |               |

TABLE I (Continued)

| Compound  | Formula           | Mol. wt. | Sampl. wt.  | $\frac{N_{HNO_3}}{N_{sampl.}}$ | $-\Delta H_c$                        | $-\Delta H_c(\text{av.})$<br>kcal./mole | $-\Delta H_f$ |
|---|-------------------|----------|---|--------------------------------|--------------------------------------|---|---------------|
| 1,4-Dimethyl-5-tetrazolone<br>                   | $C_3H_6N_4O$      | 114.100  | 0.6325<br>1.0038  | 0.213<br>.212                  | 479.92<br>480.93                     | $480.42 \pm .50$                        | -6.69         |
| 5-Cyanotetrazole<br>                             | $C_2HN_6$         | 95.068   | 0.4745<br>.5058 <sup>b</sup>  | .145<br>.147                   | 318.47<br>318.23                     | $318.35 \pm .12$                        | -96.09        |
| 1-(5-Tetrazolyl)-4-guanyltetrazene hydrate<br>   | $C_2H_5N_{10}O$   | 188.164  | .6282<br>.7957  | .455<br>.409                   | 506.66<br>507.50                     | $506.58 \pm .08$                        | -45.20        |
| 1,2-Di-(5-tetrazolyl)-ethane<br>                 | $C_4H_8N_8$       | 166.152  | .4227<br>.4157  | .393<br>.348                   | 687.21<br>687.50                     | $687.36 \pm .15$                        | -106.20       |
| Hydrazodicarbamide<br>$H_2NCONHNHCONH_2$  | $C_2H_6N_4O_2$    | 118.100  | .6852 <sup>b</sup><br>.3288 <sup>b</sup><br>.9890 <sup>b</sup><br>.7416 | .152<br>.178<br>.136<br>.153   | 273.97<br>273.53<br>274.19<br>273.79 | $273.87 \pm .14$                        | +119.19       |
| Azodicarbamide<br>$H_2NCON=NCONH_2$   | $C_2H_4N_4O_2$    | 116.084  | .9156<br>.5936  | .122<br>.106                   | 253.07<br>256.58                     | $254.83 \pm .25$                        | +69.91        |
| Acetamidoguanidine nitrate<br>$CH_3CONHNHC(NH)NH_2 \cdot HNO_3$   | $C_3H_9N_5O_4$    | 179.142  | .8407<br>.9197 <sup>b</sup>   | .215<br>.240                   | 471.09<br>472.00                     | $471.55 \pm .55$                        | +118.04       |
| 1-Acetamido-2-nitroguanidine<br>$CH_3CONHNHC(NH_2)NNO_2$  | $C_3H_7N_5O_3$    | 161.126  | 1.2724<br>1.2593  | .182<br>.162                   | 474.69<br>475.28                     | $474.99 \pm .70$                        | +46.28        |
| 1-Formamido-2-nitroguanidine<br>$HCONHNHC(NH_2)NNO_2$   | $C_2H_5N_5O_3$    | 147.100  | 0.8797<br>.7592   | .167<br>.173                   | 323.75<br>323.85                     | $323.80 \pm .05$                        | +35.10        |
| 3-Amino-1,2,4-triazole<br>                     | $C_2H_4N_4$       | 84.084   | 1.0300<br>1.0962<br>1.1441  | .165<br>.159<br>.159           | 343.72<br>342.11<br>343.48           | $343.10 \pm .47$                        | -18.36        |
| 3-Amino-1,2,4-triazole nitrate<br>             | $C_2H_5N_5O_3$    | 147.100  | 0.5470<br>1.0524<br>1.0988  | .172<br>.177<br>.173           | 320.01<br>315.95<br>318.06           | $318.01 \pm 1.17$                       | +140.89       |
| 3-Amino-5-methyl-1,2,4-triazole nitrate<br>    | $C_3H_7N_5O_3$    | 161.126  | 0.5621<br>.5351   | .228<br>.228                   | 467.09<br>466.27                     | $466.68 \pm 0.41$                       | +54.59        |
| 3-Nitramino-5-methyl-1,2,4-triazole<br>        | $C_3H_5N_5O_2$    | 143.100  | .6499<br>.8756 <sup>b</sup><br>1.1354<br>0.8032                         | .222<br>.256<br>.209<br>.218   | 465.06<br>465.50<br>465.80<br>465.51 | $465.67 \pm 0.19$                       | -12.72        |
| 3-Nitramino-1,2,4-triazole<br>                 | $C_2H_3N_5O_2$    | 129.084  | .7148<br>.4819<br>.4092<br>.8356  | .190<br>.190<br>.193<br>.196   | 314.91<br>318.47<br>319.48<br>316.94 | $317.45 \pm 1.00$                       | -26.87        |
| Benzal 3-hydrazino-5-methyl-1,2,4-triazole<br> | $C_{10}H_{11}N_5$ | 201.228  | .5849<br>.5644<br>.4540   | .356<br>.397<br>.360           | 1378.22<br>1377.38<br>1378.01        | $1377.87 \pm 0.25$                      | -61.60        |

<sup>a</sup> Sample detonated. <sup>b</sup> Benzoic acid added. <sup>c</sup> Rigg (ref. 1) reported  $1096.26 \pm 0.07$  kcal./mole for  $-\Delta H_c$ .

zole (three times recrystallized from water, m.p. 226.5–227.5°), 5-methylaminotetrazole, 1-phenyl-5-aminotetrazole, 5-anilinetetrazole (four times recrystallized from

33% aqueous ethanol, m.p. 209–210°) and 1-methyl-5-methylaminotetrazole (two times recrystallized from absolute ethanol, m.p. 173.5–174.5°) were prepared from

appropriate thioureas by previously reported procedures.<sup>3</sup> The samples of 2-allyl- and 2-methyl-5-aminotetrazole<sup>4</sup> melted at 67–68° and 105.5–106.5°, respectively, after several recrystallizations. 1,3-Dimethyl-5-iminotetrazole nitrate<sup>5</sup> was recrystallized three times from absolute ethanol, m.p. 152.5–153.5°. Benzal 5-hydrazinotetrazole<sup>6</sup> was recrystallized several times from acetic acid; m.p. 235–236° dec.

1-Allyl-5-allylamino-tetrazole was made in 82% yield from 1,3-diallylthiourea by the procedure outlined in ref. 3. After three recrystallizations from diethyl ether (1 ml. per g.) the compound melted at 48.5–49.5°.

*Anal.* Calcd. for C<sub>7</sub>H<sub>11</sub>N<sub>5</sub>: C, 50.39; H, 6.71; N, 42.40. Found: C, 51.09; H, 6.69; N, 41.89, 42.62.

1,2-Diallyl-3-aminoguanidine hydroiodide, an intermediate in the above preparation, melted at 126–127°, after recrystallization from absolute etharol.

*Anal.* Calcd. for C<sub>7</sub>H<sub>15</sub>N<sub>4</sub>I: C, 29.80; 5.36; I, 44.98. Found: C, 29.77; H, 5.35; I, 44.86.

1,2-Di-(5-tetrazolyl)-ethane.—A procedure described by Mihina and Herbst<sup>7</sup> was employed. A solution consisting of 8.81 g. (0.11 mole) of succinonitrile, 16.5 g. (0.23 mole) of sodium azide, 16.8 g. (0.28 mole) of acetic acid and 35 ml. of isopropyl alcohol was heated in a sealed ampule at 150° for 52 hours. The contents of the cooled ampule were dissolved in aqueous ethanol, filtered and evaporated to dryness under reduced pressure. The residue was redissolved in water, treated with 30 ml. of concentrated hydrochloric acid, and re-evaporated to dryness under reduced pressure. This residue was then extracted with two 100-ml. portions of 95% ethanol, and the extracts evaporated. This crude product was dissolved in 200 ml. of hot acetonitrile, filtered, cooled, and the compound removed by filtration; 8.6 g. (51.8%); m.p. 218–220°. One recrystallization from 400 ml. of acetonitrile plus 150 ml. of absolute ethanol raised the m.p. to 233–234° dec. Two recrystallizations from isopropyl alcohol finally yielded 2.0 g. of compound decomposing at 245–247°.

*Anal.* Calcd. for C<sub>4</sub>H<sub>6</sub>N<sub>8</sub>: C, 28.91; H, 3.64; eq. wt., 83.08. Found: C, 28.87; H, 3.74; eq. wt., 85.39.

Recrystallized samples of 5-cyano-, 5-hydroxy- and 5-methoxytetrazole, generously supplied by K. Hattori and E. Lieber, Illinois Institute of Technology, were used as received. The sample of 1,4-dimethyl-5-tetrazolone, also supplied by Hattori and Lieber, was purified by two low pressure sublimations. The purified 1-(5-tetrazolyl)-4-guanyltetrazene hydrate<sup>8</sup> was furnished by S. Patinkin.

1-Phenyl-5-methyltetrazole, made by the method of Dimroth and DeMontmollin,<sup>9</sup> was recrystallized twice from ethyl acetate, m.p. 97–98°. The isomeric 1-methyl-5-phenyltetrazole<sup>10</sup> was recrystallized three times from water, m.p. 104–105°.

The 2,2'-diethyl-5,5'-azotetrazole.—2-Ethyl-5-aminotetrazole (28.8 g., 0.255 mole) was dissolved in 200 ml. of water and treated all at once with 380 ml. of 5% sodium hypochlorite solution (0.255 mole). The solution was stirred for several hours at room temperature, then allowed to stand overnight at 5°. The product was removed by filtration, washed with a small volume of cold water, and recrystallized from 25% aqueous ethanol. The yield of once recrystallized compound was 17.8 g. (63%); orange needles, m.p. 110–111°;  $\lambda_{\max}$  293 m $\mu$  (25% C<sub>2</sub>H<sub>5</sub>OH),  $\epsilon$  14,370.

*Anal.* Calcd. for C<sub>8</sub>H<sub>10</sub>N<sub>10</sub>: C, 32.43; H, 4.54; N, 63.04. Found: C, 32.6; H, 4.56; N, 62.33.

1,1'-Diethyl-5,5'-azotetrazole was prepared in 29% yield from 1-ethyl-5-aminotetrazole<sup>3</sup> by the same procedure as above. After one recrystallization from 25% aqueous eth-

anol, the rosettes of very fine orange needles decomposed at 118–119°.

*Anal.* Calcd. for C<sub>6</sub>H<sub>10</sub>N<sub>10</sub>: C, 32.43; H, 4.54; Found: 32.46; H, 4.56.

This product was ultimately separated into two isomeric compounds by repeated fractional crystallizations from 25% ethanol: (1) a less soluble fraction; small bright yellow needles, m.p. 129–130° dec.;  $\lambda_{\max}$  375 m $\mu$  (25% C<sub>2</sub>H<sub>5</sub>OH),  $\epsilon$  9,230.

*Anal.* Calcd. for C<sub>6</sub>H<sub>10</sub>N<sub>10</sub>: C, 32.43; H, 4.54; N, 63.04. Found: C, 32.84; H, 4.59; N, 62.29.

(2) A more soluble fraction; large, flat orange needles, m.p. 168–169° dec.;  $\lambda_{\max}$  303–304 m $\mu$  (25% C<sub>2</sub>H<sub>5</sub>OH),  $\epsilon$  13,480.

*Anal.* Calcd. for C<sub>6</sub>H<sub>10</sub>N<sub>10</sub>: C, 32.43; H, 4.54; N, 63.04. Found: C, 32.22; H, 4.62; N, 63.16.

The low melting isomer is considered to be the *trans* compound since its ultraviolet absorption spectrum is almost identical with that for the *trans* 1,1'-dimethyl-5,5'-azotetrazole (see below).

2,2'-Dimethyl-5,5'-azotetrazole was made in a similar manner from 2-methyl-5-aminotetrazole; orange needles after recrystallization from water; m.p. 170–171° dec.

*Anal.* Calcd. for C<sub>8</sub>H<sub>6</sub>N<sub>10</sub>: C, 24.74; H, 3.12; N, 72.14. Found: C, 24.48, 24.88; H, 2.79, 3.27; N, 72.48.

1,1'-Dimethyl-5,5'-azotetrazole was obtained as bright yellow needles, decomposing at 149–150°, when the following procedure was employed. Recrystallized 1-methyl-5-aminotetrazole (10 g., 0.10 mole) was slurried with 100 ml. of water. Aqueous sodium hypochlorite solution (150 ml. of 5%, 0.1 mole) was added with good agitation during 2.5 hours; the stirring was continued for one hour. The solution, after dilution with 50 ml. of water, was heated to boiling to complete the reaction and to dissolve the precipitated azo compound. After the solution had been filtered and cooled to room temperature, the compound was removed and dried. The yield was 5.6 g. (58%). Recrystallization from water did not change the decomposition temperature. Single crystal X-ray patterns indicated that this compound had a center of symmetry<sup>11</sup>; primarily on this basis the *trans* configuration is assigned. An aqueous solution of this form showed a maximum absorption in the ultraviolet spectrum at 372 m $\mu$ ;  $\epsilon$  9,220.

*Anal.* Calcd. for C<sub>8</sub>H<sub>6</sub>N<sub>10</sub>: C, 24.74; H, 3.12; N, 72.14. Found: C, 24.72; H, 3.19; N, 72.78, 72.93.

The *trans* compound also exists in a polymorphic form; short, yellow prisms, m.p. 162–163° dec.;  $\lambda_{\max}$  372 m $\mu$  (H<sub>2</sub>O),  $\epsilon$  9190. Admixture with the low melting *trans* form did not depress the melting point.

*Anal.* Calcd. for C<sub>8</sub>H<sub>6</sub>N<sub>10</sub>: C, 24.74; H, 3.12; N, 72.14. Found: C, 24.73; H, 2.81; N, 72.50.

Attempts to convert this yellow form to an azoxy compound by heating with glacial acetic acid–30% hydrogen peroxide gave a product which melted at 183–184° dec., after recrystallization from water as orange, flat needles. Admixture with the starting compound lowered the melting point to 120–130°. However, the analyses did not indicate an azoxy compound but rather an azo compound. This orange form is more soluble in water than the yellow form and the maximum absorption in the ultraviolet spectrum of an aqueous solution occurs at 301–302 m $\mu$ ,  $\epsilon$  12,970. The *cis*-configuration is assigned tentatively. The *trans* form can also be converted quantitatively (based on the complete disappearance of the absorption peak at 372 m $\mu$  and the appearance of the peak at 302 m $\mu$ ) to the *cis* form by allowing an aqueous solution of the former to stand for several days in sunlight.

*Anal.* Calcd. for C<sub>8</sub>H<sub>6</sub>N<sub>10</sub>: C, 24.74; H, 3.12; N, 72.14. Found: C, 24.66, H, 3.17; N, 71.16.

Stollé, *et al.*,<sup>12</sup> reported 182° dec. for the melting point of 1,1'-dimethyl-5,5'-azotetrazole.

3-(5-Tetrazolylazo)-pentanedione-2,4<sup>13</sup> was recrystallized twice from 50% aqueous ethanol and once from ethyl acetate; m.p. 163–164° dec.

3-(5-Tetrazolylazo)-butanone-2<sup>13</sup> after two recrystalliza-

(11) Private communication from J. H. Bryden of this Laboratory.

(12) R. Stollé, K. Ehrmann, D. Rieder, H. Willie, H. Winter and F. Henke-Stark, *J. prakt. Chem.*, **134**, 282 (1932).

(13) Unpublished work of R. A. Henry and L. D. Dyer.

(3) W. G. Finnegan, R. A. Henry and E. Lieber, *J. Org. Chem.*, **18**, 779 (1953).

(4) R. A. Henry and W. G. Finnegan, *J. Am. Chem. Soc.*, **76**, 923 (1954).

(5) R. A. Henry, W. G. Finnegan and E. Lieber, *ibid.*, **76**, 2894 (1954).

(6) J. Thiele and J. T. Marais, *Ann.*, **273**, 144 (1893).

(7) J. S. Mihina and R. M. Herbst, *J. Org. Chem.*, **15**, 1082 (1950).

(8) S. H. Patinkin, J. P. Horwitz and E. Lieber, *J. Am. Chem. Soc.*, **77**, 562 (1955).

(9) O. Dimroth and G. DeMontmollin, *Ber.*, **43**, 2907 (1910).

(10) E. K. Harvill, R. M. Herbst, E. C. Schreiner and C. W. Roberts, *J. Org. Chem.*, **15**, 662 (1950).

tions from ethyl acetate-ethanol (2:1) melted at 175.5°.

**5-Tetrazolylazo-(N)-piperidine.**—5-Aminotetrazole monohydrate (4.85 g.) was diazotized according to the procedure of Bülow<sup>14</sup>; after 20 minutes 4 g. of piperidine in 15 ml. of water was added all at once. The resulting solution (*pH* ~ 4) was stirring for 25 minutes at 0–5°, then allowed to stand overnight at 0°. A white solid began to separate after five minutes and gradually increased in amount with the standing. The solid was removed by filtration and washed with two 15-ml. portions of cold water. The yield of air-dried product (m.p. 110–115°) was 6.6 g. (77.7%). Two recrystallizations in the following manner raised the melting point to 126–127° (vigorous decomposition): 150 ml. of water was heated to 65°, the compound was added with rapid stirring to assist the dissolution, and the solution was filtered into a flask cooled in an ice-bath. If the water is too hot or too much time is taken to effect the recrystallization, considerable decomposition with gassing occurs.

*Anal.* Calcd. for C<sub>6</sub>H<sub>11</sub>N<sub>7</sub>: C, 39.77; H, 6.12; N, 54.11; eq. wt., 181.22. Found: C, 40.09; H, 6.03; N, 53.82; eq. wt., 182.9, 181.8.

**Guanidine and Triazole Derivatives.**—Hydrazodicarbamide, made by the method of Leboucq,<sup>15</sup> was recrystallized twice from large volumes of water; m.p. 248°. Azodicarbamide<sup>16</sup> was made by oxidizing the hydrazo compound with potassium dichromate in sulfuric acid solution; recrystallization from water yielded small orange prismatic needles decomposing between 225–230° (depends on rate of heating).

1-Acetamido- and 1-formamido-2-nitroguanidine<sup>17</sup> after three recrystallizations from water decomposed at 195° and 190–191°, respectively. 3-Nitroamino-5-methyl-1,2,4-triazole<sup>17</sup> and 3-nitroamino-1,2,4-triazole<sup>17</sup> prepared from the preceding amides, were also recrystallized three times from water; m.p. 206–207° dec. and 221–222° dec., respectively. Formamidoguanidine nitrate was recrystallized three times from 95% ethanol; m.p. 144–145° (reported<sup>18</sup> 143°); whereas the homologous acetamido compound was recrystallized twice from absolute ethanol; m.p. 145.5–146.5° (reported<sup>19</sup> 142–143° (dec.)).

3-Amino-5-methyl-1,2,4-triazole was purified as follows. The crude compound was dissolved in absolute ethanol, decolorized with charcoal, filtered, cooled to 0° and treated with two volumes of diethyl ether. After several days at 0°, the crystalline material was removed and recrystallized twice from dioxane and finally from ethyl acetate. The resulting fine white needles melted at 151–152°; reported<sup>19</sup> 148°. The corresponding nitrate was recrystallized twice from absolute ethanol to give a product melting at 176–177° (reported<sup>19</sup> 171°).

3-Amino-1,2,4-triazole from Fairmount Chemical Co., after decolorization with charcoal in ethanol, was recrystallized three times from dioxane; m.p. 156–157°, reported<sup>18</sup> 159°. The nitrate was recrystallized three times from 95% ethanol; m.p. 180.5–181.5°, reported<sup>18</sup> 174° dec.

Benzal 3-hydrazino-5-methyl-1,2,4-triazole<sup>20</sup> was recrystallized from 30% ethanol; m.p. 266°; reported by Thiele and Manchot,<sup>18</sup> 263°.

### Experimental Details

An isothermal precision combustion calorimeter of local construction was used, calibrated with 1-g. samples of Bureau of Standards benzoic acid 39 g. Nineteen calibrations were made during the period in which these samples were run. The heat capacity of the calorimeter and the standard deviation was 2274.98 ± 0.35 cal./°. Other experimental details may be summarized as follows:

a. The calorimeter is completely surrounded by a constant temperature bath which is controlled to ±0.002°.

b. The same weighed quantity of water (±0.1 g.) is used in the calorimeter in each determination.

c. Temperature measurements were made with a platinum resistance thermometer and a Leeds and Northrup G-2 Mueller bridge to ±0.0003°.

d. A 360-ml. Parr double valve oxygen bomb was used. The electrodes of the bomb were modified to make more reliable and reproducible contacts with the fuse wire. The bomb was flushed twice with 25 atm. of oxygen and then filled to 30–31 atm. with oxygen.

e. The ignition system consisted of 90 v. d.c. through 4 to 6 cm. of 0.004 mil platinum wire which carried 0.0012 to 0.0024 g. of fuse paper.

f. One ml. of water was placed in the bomb before ignition.

g. Samples were in the form of 1/2 inch diameter pellets.

h. A very thin walled platinum crucible weighting 2 to 3 g. was used.

i. Provision was made for either heating or cooling the calorimeter so that adjustment of the calorimeter temperature at time of ignition with respect to bath temperature could be made easily.

### Corrections Applied

Heat transfer between the calorimeter and the constant-temperature bath is determined for each experiment by measuring the rate of temperature change before igniting the sample and after the reaction is complete. The time and resistance are recorded on a Gaertner four-channel chronograph. One channel records the time in seconds. The next channel records a code corresponding to a recorded thermometer resistance by means of a key switch. The third channel records the time at which the sample was fired. By following the temperature-time curve after firing and obtaining a second constant rate after the completion of the reaction the thermal-leakage coefficient and the heat of stirring are obtained by the solution of two equations of the form

$$dT/dt = (Q \times K) + W$$

where  $dT/dt$  is the change of temperature with respect to time in the calorimeter;  $Q$  the thermal head, is the difference between the bath temperature and the calorimeter temperature;  $K$  is the thermal-leakage coefficient and  $W$  is the rise in temperature produced through stirring.

The thermal-leakage coefficient for the calorimeter was approximately  $4.6 \times 10^{-5}$  degree/sec. and the correction to be applied was determined by graphical integration of the resistance *vs.* time curve. The temperature rise from stirring  $W$  was approximately  $1 \times 10^{-6}$  degree/sec. The average time from ignition to the final rate period was 500 seconds. A 10% deviation in the  $K$  value obtained was considered sufficient reason for disqualifying the result obtained on that particular determination.

Very small strips of ashless filter paper were threaded on the ignition wire as an igniter for the samples. The heat of combustion of the paper was found to be  $4032 \pm 2$  cal./g. on 6 determinations. The energy to the ignition wire was measured by a special watt meter and varied from 0.1 to 0.3 cal.

(14) C. Bülow, *Ber.*, **42**, 4429 (1909).

(15) J. Leboucq, *J. Pharm. Chem.*, **5**, 531 (1927).

(16) J. Thiele, *Ann.*, **271**, 127 (1892).

(17) R. A. Henry, *J. Am. Chem. Soc.*, **72**, 5343 (1950).

(18) J. Thiele and W. Manchot, *Ann.*, **303**, 33 (1898).

(19) J. Thiele and K. Heidenreich, *Ber.*, **26**, 2598 (1893).

(20) E. Lieber, S. Schiff, R. A. Henry and W. G. Finnegan, *J. Org. Chem.*, **18**, 218 (1952).

A correction for unburnt carbon was rarely used as there is always some uncertainty as to whether the unburnt residue is carbon, unburnt sample or some intermediate product. After the heat of combustion measurements were made, the crucible was removed from the bomb, dried and weighed. The crucible was then heated to red heat, cooled and weighed again. A loss in weight of 0.0002 g. or less was neglected. A loss in weight of 0.0003 to 0.0009 g., when visual inspection showed a thin black film, was treated as carbon and the heat of combustion correction of 7830 cal./g. was made. If a loss in weight of 0.0010 g. or more occurred the result was discarded.

The minimum and maximum amounts of water present in the bomb after completion of the reaction were calculated for the type of samples burnt in order to determine the dilution of the  $\text{HNO}_3$  formed. The molar ratio of  $\text{HNO}_3$  to  $\text{H}_2\text{O}$  varied from 1/24 to 1/40 from which the heat of formation of  $\text{HNO}_3(\text{aq})$  from  $\text{H}_2\text{O}$ ,  $\text{N}_2$  and  $\text{O}_2$  was computed as 15.07 kcal./mole. The number of moles of  $\text{HNO}_3$  formed was determined by thoroughly washing the interior walls of the bomb after each combustion and titrating the wash water to a phenolphthalein end-point with 0.1 *N* NaOH solution.

The heat of solution of  $\text{CO}_2$  was taken as 4050 cal./mole and the Washburn<sup>21</sup> figure of 0.004 was taken as the amount of  $\text{CO}_2$  going into solution. The heat of combustion was corrected to 25° and 1 atm. pressure by use of the standard Washburn corrections. The heats of formation ( $H_f$ ) of  $\text{CO}_2$  and  $\text{H}_2\text{O}(l)$  were 94.052 and 68.317 kcal./mole, respectively. The results are given in Table I. The standard deviation of the heat of combustion in kcal./mole also is listed.

**Nitric Acid Corrections.**—Inspection of the accumulated results of the nitric acid determination of these combustions leads one to the conclusion that for cases where a nitric acid determination has not been made a correction can be estimated. The number of moles of nitric acid formed ( $N_{\text{HNO}_3}$ ) by the combustion of  $N_s$  moles of  $\text{C}_a\text{H}_b\text{O}_c\text{N}_d$  may

(21) E. W. Washburn, *J. Research Natl. Bur. of Standards*, **10**, 525 (1933).

be calculated by use of the equation

$$N_{\text{HNO}_3} = 0.0045(H_c \times d)^{1/2} \times N_s$$

where the heat of combustion ( $H_c$ ) is measured in kcal./mole and  $d$  is the number of gram-atoms of nitrogen per formula weight. This equation represents the best straight line through 100 experimental points of a log-log plot. The average deviation of the experimental data from this equation, when converted to the per cent. error produced in the nitric acid correction, was 0.05%.

Three definite exceptions were noted in which the experimentally determined number of moles of nitric acid was significantly higher than the calculated value: (1) when the sample detonated, (2) when the sample was burned with an auxiliary material, and (3) when the sample was in the form of a hydrate (only one hydrate was burned so it is not definitely known whether this is a general exception or not). Only those samples which were definitely known to have detonated are marked. In material of the type burned it is possible that on numerous occasions a low order detonation occurred and there was no visible evidence when the bomb was opened after combustion.

It is felt that the nitric acid correction for combustion experiments of other laboratories will follow the general form of this equation; however, the constant may be a function of specific combustion apparatus employed. Sufficient data from other laboratories are not available to check this point.

The heats of combustion given in this paper have been corrected using the experimentally determined amount of nitric acid. The maximum deviation between the experimental correction and the calculated correction was 12 cal. This equation makes it possible to compute a nitric acid correction when none has been made and to adjust heat of combustion values for varying heats of formation of  $\text{HNO}_3$  when sufficient experimental data are not available.

**Acknowledgment.**—The assistance of William G. Finnegan in preparing and purifying some of the samples is appreciated.

## ADSORPTION MEASUREMENTS AT VERY LOW PRESSURES. II

BY S. WAGENER

*Kemet Company, A Division of Union Carbide and Carbon Corporation, Cleveland, Ohio*

Received July 12, 1956

Initial rates of adsorption are measured for  $\text{CO}$ ,  $\text{CO}_2$  and  $\text{N}_2$  on films prepared by evaporation from the metals Ba, Sr, La, Ti, Zr, Nb, Ta, Cr, Mo, W, Mn, Fe and Ni. While all metals absorb  $\text{CO}$  at a high rate of more than 2500  $\text{cm}^3/\text{sec. cm}^2$ , these metals behave in different ways when adsorbing  $\text{N}_2$ . Two groups can be distinguished, one of which, consisting of metals in the center of the periodic table, has a high rate for  $\text{N}_2$ , while the other one, consisting of metals located on the sides of the table, has a rate for  $\text{N}_2$  which is less than 1  $\text{cm}^3/\text{sec. cm}^2$ . The quantities adsorbed are about twice as large for carbon monoxide as for nitrogen. Both these quantities increase considerably if the temperature is raised above a critical value which ranges from 150 to 200° for Ba-CO and Ti-CO. This increase is believed to be due to the onset of surface migration. On titanium and tungsten, nitrogen may be adsorbed subsequent to carbon monoxide while the reverse procedure is not possible.

1. **Experimental Procedure.**—The method described in a recent publication<sup>1</sup> and illustrated in Fig. 1 has been improved further and measurements have been extended to

a number of transition metals. Experimental improvements

(1) S. Wagener, *THIS JOURNAL*, **60**, 567 (1956).

mainly consisted of the introduction of a bakable gas injection valve and of a copper foil trap as described by Alpert. These improvements made it possible to obtain a pressure of  $10^{-9}$  mm. after only one hour's bake at  $400^\circ$ .

Metals were investigated as films obtained by evaporation from helices. The glass on which the films were formed was cooled to about  $-20^\circ$  during evaporation. The pressure at the end of the evaporation period was  $10^{-8}$  mm. or less.

The gases used were carbon monoxide, carbon dioxide and nitrogen. If not indicated otherwise, measurements were done at room temperature.

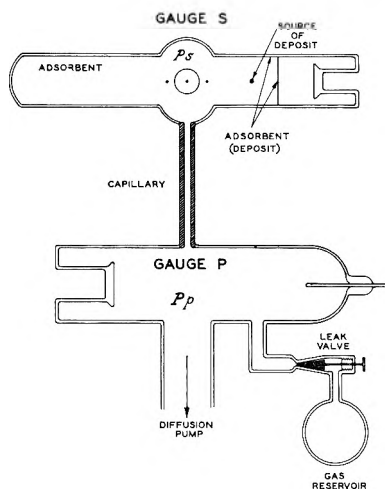


Fig. 1.—Experimental system.

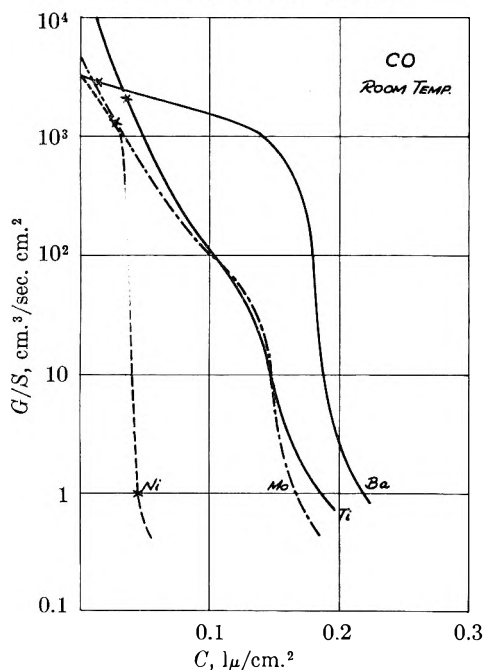


Fig. 2.—Rate of adsorption of carbon monoxide as a function of adsorbed quantity ( $1. \text{ at } 1\mu$ ) ( $p_p = 5 \times 10^{-5}$  mm.,  $F = 45 \text{ cm.}^3/\text{sec.}$ ): Ni,  $0.058 \text{ mg./cm.}^2$ ; Mo,  $0.046 \text{ mg./cm.}^2$ ; Ti,  $0.044 \text{ mg./cm.}^2$ ; Ba,  $0.045 \text{ mg./cm.}^2$

**2. Rates of Adsorption.**—Some of the results obtained with carbon monoxide are illustrated in Fig. 2. The metals investigated were Ba, Sr, La, Ti, Zr, Nb, Ta, Cr, Mo, W, Mn, Fe and Ni. All these give similar curves, beginning with an initial rate which is higher than  $2500 \text{ cm.}^3/\text{sec. cm.}^2$

Different results, such as illustrated in Fig. 3, were obtained for nitrogen. With one group of metals the initial rate for nitrogen was of the same

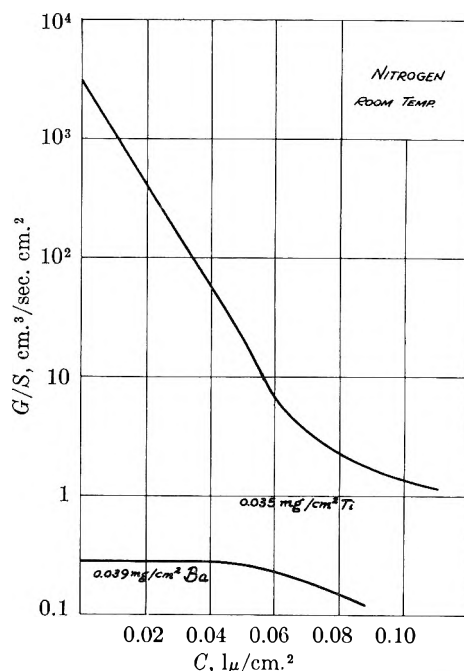


Fig. 3.—Rate of adsorption of nitrogen as a function of adsorbed quantity ( $p_p = 5.25 \times 10^{-5}$  mm.,  $F = 45 \text{ cm.}^3/\text{sec.}$ ).

order as that for carbon monoxide while with a second group this rate was less than  $1 \text{ cm.}^3/\text{sec. cm.}^2$ . Details of the classification into these two groups will be seen from Table I. Evidently the metals adsorbing nitrogen at a high rate are all located in the middle part of the periodic table while those adsorbing at a low rate are located on the two sides.

As discussed in the first paper (ref. 1, p. 571), the values measured for the initial adsorption rates may be used for deriving approximate values of the sticking probability. It follows, therefore, that the sticking probability for nitrogen on the metals in the outside columns (normal type in Table I) is  $1/10,000$  as large as that for carbon monoxide, while it is about the same as for carbon monoxide on the metals in the center columns (italic type in Table I). The low sticking probabilities which were measured for nitrogen cannot be due to contamination of the films. This is evident from the fact that films, adsorbing nitrogen at a low rate, were found to adsorb carbon monoxide at a high rate if exposed to this gas subsequently.

TABLE I

CLASSIFICATION OF METALS ACCORDING TO THEIR INITIAL RATE OF ADSORPTION FOR NITROGEN<sup>a</sup>

| I | II | III       | IV        | V         | VI        | VII | VIII    |
|---|----|-----------|-----------|-----------|-----------|-----|---------|
| . | .  | .         | <i>Ti</i> | .         | Cr        | Mn  | Fe . Ni |
| . | Sr | .         | Zr        | <i>Nb</i> | <i>Mo</i> | .   | .       |
| . | Ba | <i>La</i> | .         | <i>Ta</i> | <i>W</i>  | .   | .       |

<sup>a</sup> Italic type, high rates for CO and N<sub>2</sub> (>2500 cm.<sup>3</sup>/sec. cm.<sup>2</sup>); normal type, high rate for CO low rate for N<sub>2</sub> (<1 cm.<sup>3</sup>/sec. cm.<sup>2</sup>).

Although these rates, measured for nitrogen adsorbed on films, are low by our standards, they still are considerably higher than the rates determined for adsorption on powder catalysts. From

investigations by Emmett and Brunauer<sup>2</sup> and by Zwietering and Roukens,<sup>3</sup> rates of about 0.01 cm.<sup>3</sup>/sec. can be derived for nitrogen on iron powder (measured at temperatures between 200 and 400°). Since these rates refer to surface areas of probably many cm.<sup>2</sup>, division by this surface area will give values which are certain to be much smaller than those measured for nitrogen in the present investigation.

A slow adsorption of nitrogen on iron was also observed by Beeck and Wheeler.<sup>4</sup>

Results obtained with carbon dioxide adsorbed on barium and titanium are essentially the same as those with carbon monoxide.

**3. Interpretation of "Rate versus Quantity" Curves.**—In Fig. 2 and 3, the scale of the abscissa can be converted from  $l\mu/\text{cm}^2$  to monolayers of gas adsorbed, if an assumption is made on the number of sites available for adsorption. Let us assume that every surface atom of the film gives an adsorption site and that the surface atoms are equally spread over the main crystallographic planes 001, 011 and 111 (0001 and 0011 for the hexagonal lattice). Then the number of  $l\mu$  which may be adsorbed as a monolayer on 1 cm.<sup>2</sup> of the apparent surface area is given by the values in Table II.

TABLE II  
Quantity of gas adsorbed as a monolayer on 1 cm.<sup>2</sup> of apparent surface area,  $l\mu$

| Metal | Quantity of gas adsorbed as a monolayer on 1 cm. <sup>2</sup> of apparent surface area, $l\mu$ |
|-------|--|
| Ba    | 0.011  |
| Ni    | .046   |
| Mo    | .027   |
| Ti    | .035   |

In Fig. 2, the quantities of gas, corresponding to 1 monolayer, have been indicated as crosses on the respective curves. It will be seen that while the first monolayer is adsorbed on Ba, Mo and Ti, the rate remains high ( $>1000$  cm.<sup>3</sup>/sec. cm.<sup>2</sup>). This agrees with the results obtained by Becker<sup>5</sup> for adsorption of nitrogen on tungsten.

This result also shows that the greater part of the curves for Ba, Mo and Ti in Fig. 1 (that on the right hand side of the crosses) refers to adsorption on the internal surface area. The difference in shape between the curves for barium on one hand and those for molybdenum and titanium on the other, therefore, is due to differences in the configuration of the pores interconnecting the individual parts of the internal surface.

**4. Quantities of Gas Adsorbed.**—These quantities, as derived from the curves in Fig. 2 and 3, are given in Table III.

If comparing the two gases (making allowance for the difference in film weight), it will be observed that much less nitrogen than carbon monoxide is adsorbed in all cases. With titanium the adsorbed quantity of nitrogen is about one-half of that of carbon monoxide. This appears to confirm the view that nitrogen is adsorbed as atoms

(2) P. H. Emmett and S. Brunauer, *J. Am. Chem. Soc.*, **56**, 35 (1934).

(3) P. Zwietering and J. J. Roukens, *Trans. Faraday Soc.*, **51**, 178 (1954).

(4) O. Beeck and A. Wheeler, *J. Chem. Phys.*, **7**, 631 (1939).

(5) J. A. Becker, *Advances in Catalysis*, **VII**, 136 (1955).

TABLE III  
CAPACITY OF ADSORPTION FOR DIFFERENT METAL-GAS COMBINATIONS<sup>a</sup>

| Metal | Gas             | Wt. of deposit, mg./cm. <sup>2</sup> | Initial rate of adsorption, cm. <sup>3</sup> /sec. cm. <sup>2</sup> | Capacity in $l\mu/\text{cm}^2$ |       |           |
|-------|-----------------|--------------------------------------|---|--------------------------------|-------|-----------|
|       |                 |                                      |   | $C_{50}$                       | $C_5$ | $C_{0.1}$ |
| Ba    | CO              | 0.045                                | 3500  | 0.19                           | 0.20  | ..        |
|       | N <sub>2</sub>  | .039                                 | 0.3   | ..                             | ..    | 0.10      |
| Ti    | CO              | .044                                 | 1200  | .11                            | .15   | ..        |
|       | N <sub>2</sub>  | .034                                 | 300   | .040                           | .063  | ..        |
|       | CO <sub>2</sub> | .030                                 | 430   | .095                           | .13   | ..        |
| Mo    | CO              | .046                                 | 350   | .12                            | .14   | ..        |
|       | N <sub>2</sub>  | .052                                 | 270   | .044                           | .055  | ..        |
| Ni    | CO              | .058                                 | 4500  | .037                           | .040  | ..        |

<sup>a</sup> Here  $C_{50}$ ,  $C_5$  or  $C_{0.1}$  are the quantities of gas which are adsorbed until the rate falls to 50, 5 or 0.1 cm.<sup>3</sup>/sec. cm.<sup>2</sup>, resp.

while carbon monoxide is adsorbed as molecules.

The results given in the previous table do not agree with those by Trapnell<sup>6</sup> according to whom

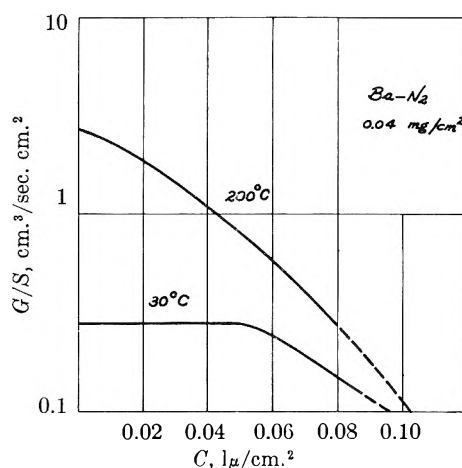


Fig. 4.—Influence of temperature of adsorbent on adsorption of nitrogen on barium ( $p_p = 5.25 \times 10^{-5}$  mm.,  $F = 45$  cm.<sup>3</sup>/sec.).

the quantity adsorbed should increase with the melting point of the material. On the contrary, barium with its comparatively low melting point was always found to adsorb larger quantities of carbon monoxide than all the other metals investigated. This different result may be due either to the different type of gas (Trapnell used hydrogen and oxygen) or, more likely, to the fact that Trapnell employed the conventional method in which adsorption is measured up to an ultimate rate which is very much lower than the ultimate rates of our measurements (50 or 5 cm.<sup>3</sup>/sec. cm.<sup>2</sup>).

**5. Adsorption of One Gas Subsequent to the Other.**—These results are shown in Table IV for titanium.

As indicated in the first line, nitrogen was adsorbed first until the rate had fallen to about 1 cm.<sup>3</sup>/sec. cm.<sup>2</sup> Subsequent to this, carbon monoxide still could be adsorbed with an initial rate of 750. The quantity of carbon monoxide adsorbed was comparable to that of nitrogen adsorbed previously. In the reverse experiment, however (second line of the table), no appreciable amount of

(6) R. M. W. Trapnell, *Trans. Faraday Soc.*, **51**, [III] 368 (1955).

TABLE IV

EXPOSURE OF TITANIUM DEPOSITS TO TWO GASES, ONE SUBSEQUENT TO THE OTHER, 0.040 MG./CM.<sup>2</sup> Ti

| Type           | First gas      |     |                         |  | Second gas     |                |                         |
|----------------|----------------|-----|-------------------------|--|----------------|----------------|-------------------------|
|                | Rate Initially | End | Capacity C <sub>s</sub> | Capacity C <sub>tot</sub> <sup>a</sup> | Type           | Rate Initially | Capacity C <sub>s</sub> |
| N <sub>2</sub> | 3500           | 1.3 | 0.070                   | 0.104                                  | CO             | 750            | 0.059                   |
| CO             | 10000          | 0.6 | .167                    | .19                                    | N <sub>2</sub> | 0.9            | 0                       |

<sup>a</sup> C<sub>tot</sub> is the total quantity of gas adsorbed at the end of the resp. measurement. Rates in cm.<sup>3</sup>/sec. cm.<sup>2</sup>; capacities in lμ/cm.<sup>2</sup>

nitrogen could be adsorbed subsequent to adsorption of carbon monoxide. Similar results were obtained with tungsten.

This result appears to show that a surface on which carbon monoxide molecules are adsorbed,

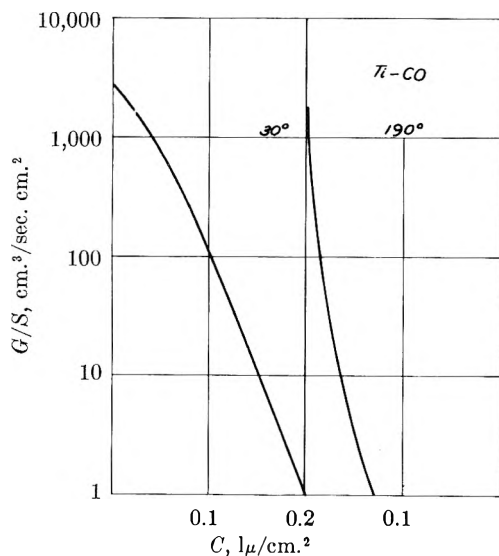


Fig. 5.—Influence of temperature of adsorbent on adsorption of carbon monoxide on titanium ( $p_p = 5 \times 10^{-3}$  mm.,  $F = 45$  cm.<sup>3</sup>/sec.)

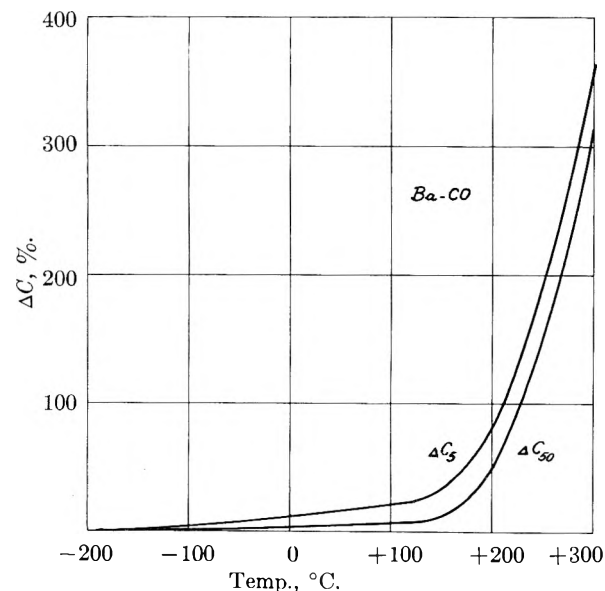


Fig. 6.—Increase of quantity of carbon monoxide adsorbed on barium with temperature of barium ( $\Delta C$  gives the increase in adsorbed quantity obtained when the temperature is raised from that of liquid nitrogen to the value indicated by the curves).

is saturated and that no bonds are left which are available for adsorption of another gas. On the other hand, adsorbed nitrogen atoms are too small to interfere sterically with the chemisorption of carbon monoxide.

**6. Influence of Temperature of Films.**—The influence of temperature on the low rate adsorption of nitrogen is illustrated in Fig. 4. There is an increase in rate with temperature indicating that a measurable activation energy is required for adsorption. The values measured for this activation energy show a rather wide spread, ranging from 2 to 4 kcal./mole for Ba-N<sub>2</sub>.

With high rate adsorption the activation energies are unmeasurably small, but another phenomenon then is observed, that of restoration of the rate, produced by an increase in temperature. This is illustrated in Fig. 5 for titanium-carbon monoxide. The rate, after having fallen to a low value, can be restored to a high value again, by increasing the temperature. Correspondingly, the adsorbed quantity increases with temperature. The percentage increase obtained when the temperature is raised from 30 to 200° is seen from Table V. The increase becomes less in the sequence Ba-Ti-Mo.

TABLE V

PERCENTAGE INCREASE IN CAPACITY, WHEN TEMPERATURE IS RAISED FROM 30 TO ABOUT 200°

| Metal | Carbon monoxide |                | Nitrogen        |                |                  |
|-------|-----------------|----------------|-----------------|----------------|------------------|
|       | C <sub>30</sub> | C <sub>5</sub> | C <sub>30</sub> | C <sub>5</sub> | C <sub>0.1</sub> |
| Ba    | 49              | 86             | ..              | ..             | 6                |
| Ti    | 14.5            | 26.5           | 0               | 28             | ..               |
| Mo    | 0.0             | 0.6            | Not measured    |                |                  |

If the increase in capacity is plotted as a function of temperature (see Fig. 6), one sees that there is a critical temperature below which the increase is slow and above which it is rapid.

As pointed out in the first article,<sup>1</sup> the rapid increase is believed to be due to the onset of surface migration. According to Fig. 6 and Table V, this onset occurs at about 150° for carbon monoxide on barium but above 200° for carbon monoxide on molybdenum. This temperature range agrees with that observed by Gomer<sup>7</sup> by means of the field emission microscope for adsorption of oxygen on tungsten.

**7. Conclusions.**—Frequently the hypothesis has been made that chemisorption is due to unfilled energy levels in the d-band.<sup>8</sup> The evidence put forward in this paper shows that the number of unfilled or filled levels in this band also fixes the rate at which this chemisorption occurs. Evidently, in the case of nitrogen, a high rate is obtained only if the number of filled levels has a medium value.

In conclusion the author wishes to express his renewed appreciation to Dr. J. P. Cels and Mr. E. Palsha for their assistance.

### Appendix

The units used for the adsorption rates in this paper are volume per sec. as opposed to the conventional units expressed in weight per sec. or molecules

(7) R. Gomer in, *Advances in Catalysis*, **VII**, 93 (1955).

(8) B. M. W. Trapnell, "Chemisorption," Academic Press, New York, N. Y., 1955, p. 153.

per sec. Reasons for the choice of these units were given in the first paper (p. 567). For converting these units into the conventional ones, equation 1 of the first paper may be used. According to this the rate expressed in conventional units is

$$R = Gp_s = F(p_p - p_s)$$

or for  $G \gg F$  and  $p_p \gg p_s$

$$R = Fp_p \text{ (in } \mu/\text{sec. or cm.}^3 \times (\text{mm. pressure})/\text{sec.)}$$

The values of  $F$  and  $p_p$  are indicated in each of the figures concerned or in the respective captions. The pressure  $p_s$  surrounding the adsorbent may in each instance be easily calculated from the values of  $G$ ,  $p_p$  and  $F$  given in the figures and their legends.

## SEDIMENTATION EQUILIBRIUM OF FLEXIBLE CHAIN MOLECULES<sup>1</sup>

BY L. MANDELKERN, L. C. WILLIAMS AND S. G. WEISSBERG

National Bureau of Standards, Washington 25, D. C.

Received July 26, 1956

The thermodynamic theory of sedimentation equilibrium is reviewed with special emphasis on solutions of flexible long chain molecules. The analyses indicate that the weight average molecular weight of this class of solutes, irrespective of the molecular weight heterogeneity, can be obtained in a straightforward manner only in ideal solutions. The molecular weight of a monodisperse polymeric solute in a non-ideal solution can in principle also be obtained from this type of experiment but with a great deal more difficulty. However, if the solute is polydisperse and the solution non-ideal, theory indicates that no reliable molecular weight average can be determined at present from experiments performed in the equilibrium ultracentrifuge. To investigate some of these conclusions it is first demonstrated that ideal solution of flexible chain molecules over a wide range of concentrations and of molecular weights can be achieved in the equilibrium centrifuge. For this initial study polyisobutylene was chosen as the polymer and ethyl *n*-heptanoate as solvent. Determination of the critical consolute temperature as a function of molecular weight indicated that ideal behavior could be attained at 34°, the temperature at which the sedimentation equilibrium experiments were carried out in a Svedberg ultracentrifuge. After the molecular weights were determined from these experiments, measurements were also made in a good solvent, isoöctane, and the methods and difficulties involved in interpreting such data are discussed.

### Introduction

The equilibrium ultracentrifuge was one of the earliest instruments developed to study the thermodynamic behavior of solutions of macromolecules. In principle, from an analysis of the mass distribution of solute along the length of the centrifuge cell, one can obtain information as to the molecular weight of the solute (or the average molecular weight if it is polydisperse) as well as information about deviations from ideal behavior. For thermodynamically ideal solutions a simple and exact analysis exists so that experimental results can be properly interpreted.<sup>2</sup> However, though all solutions must behave ideally as infinite dilution is approached it is usually experimentally impracticable to work at the extremely low concentrations required with solutions of macromolecules.

The introduction of the necessary corrections for non-ideality that are required to properly interpret experiments performed with solutions of flexible chain molecules is extremely difficult. The concentration of a single solute species in equilibrium in a centrifugal field will increase as the distance from the center of rotation increases. As the solute concentration increases, so must the magnitude of the correction for deviations from ideality. If the non-ideality correction is expressed as a power series expansion in concentration, it is *a priori* difficult to tell, except for initially very dilute solutions, how many terms will be adequate. For a heterogeneous solute the situation is further complicated by the fact that both the mass and the distribution of molecular weights will vary along the length of the cell. Recent theoretical and ex-

perimental studies<sup>3,4</sup> on the thermodynamic properties of solutions of chain molecules indicate that the non-ideality corrections will depend very markedly on molecular weight heterogeneity. Thus for this situation the necessary corrections will be further complicated.

A large majority of the experimental results reported<sup>5-7</sup> for long chain molecules have involved good solvents where the non-ideality corrections are severe. To interpret these results the various investigators have of necessity been forced to make certain arbitrary assumptions. It has been assumed that only the second virial coefficient need be considered, and further that the virial coefficient is independent, both of molecular weight and molecular weight distribution. The consequences of these assumptions in determining the molecular weights of long chain flexible molecules are considered in this paper. The deviations from ideality can, of course, be minimized by performing the experiments in poorer solvents. For the more compact macromolecules, such as the globular proteins, the deviations from ideality are not too severe in the accessible concentration range. Such systems will not be considered here.

On the other hand, it is now well known that ideal behavior can be attained for solutions of long chain flexible molecules over a wide range of solute concentrations by an appropriate choice of solvent and temperature. Under these conditions, com-

(3) P. J. Flory and W. R. Krigbaum, *J. Chem. Phys.*, **18**, 1086 (1950).

(4) W. R. Krigbaum and P. J. Flory, *J. Am. Chem. Soc.*, **75**, 1775 (1953).

(5) K. E. Van Holde and J. W. Williams, *J. Polymer Sci.*, **11**, 243 (1953).

(6) M. Wales, J. W. Williams, J. O. Thompson and R. H. Ewart, *THIS JOURNAL*, **52**, 983 (1948).

(7) M. Wales, F. T. Adler and K. E. Van Holde, *ibid.*, **55**, 145 (1951).

(1) Presented in part at the 128th American Chemical Society meeting, Minneapolis, Minn., Sept. 11-16, 1955.

(2) T. Svedberg and K. O. Pedersen, "The Ultracentrifuge," Oxford, 1940, p. 48.

monly call the " $\Theta$  temperature" or "Flory temperature," the second and all higher virial coefficients vanish for all molecular weights and molecular weight distributions. This situation arises because at the  $\Theta$  point the net interaction between segments of a pair of polymer molecules is zero so that molecules can freely overlap. These conditions are analogous to the Boyle point of a real gas, and therefore polymer solutions obey van't Hoff's law.<sup>8</sup> The rather important theoretical reason for performing sedimentation equilibrium experiments under these conditions has already been emphasized and the contributions that might result from experiments conducted in such a manner have been indicated.<sup>9</sup> The main purpose of this paper is to demonstrate experimentally that ideal solution behavior can be achieved in the equilibrium ultracentrifuge for solutions of long chain molecules over a wide range of molecular weights. Thus the theoretical difficulties in interpreting the experimental data are circumvented. It will be shown that under these conditions the analyses of the experimental data are extremely simple, both for homogeneous and heterogeneous solutes, and that many of the original objectives that led to the development of the instrument by Svedberg might be realizable for solutions of long chain molecules.

### Experimental Details

**Materials.**—The polyisobutylene fractions used in this study were obtained from two samples of commercially available whole polymer supplied by the Esso Standard Oil Company. Fractions A and F were obtained from the whole polymer designated as B-100 by fractional precipitation with acetone of an initial 0.5% solution in benzene, following the procedure described by Flory.<sup>10</sup> Fractions B, C, D and E were obtained from the whole polymer having the designation LMS. Fraction C was the first fraction obtained by the single precipitation of a 1% benzene solution; fractions B, D and E were obtained by further separation of the second fraction. The above letter designation of the fractions is merely for convenience in the subsequent discussion, and does not reflect the order in which they were obtained. For the present study no special effort was made to obtain sharp fractions. The viscosity average molecular weights of the fractions used are given in Table I and were determined from intrinsic viscosity measurements in benzene at 24° where the relation  $[\eta] = 10.7 \times 10^{-4} M^{1/2}$  has been shown to be valid.<sup>11</sup>

The solvents used, isoöctane and ethyl *n*-heptanoate, were of reagent grade and used as received.

**Precipitation Temperatures.**—The precipitation temperatures of solutions of the polymer fractions in ethyl *n*-heptanoate were obtained following the experimental procedure described by Shultz and Flory.<sup>12</sup> For this system it is important that drying columns be attached to the precipitation tubes in order to obtain reliable results. Precipitation temperatures reproducible to  $\pm 0.1^\circ$  were obtained, and when plotted against concentration for each fraction the curves pass through the expected maximum. The maximum temperature in this plot is the critical consolute temperature.

**Ultracentrifuge.**—A modified Svedberg equilibrium ultracentrifuge, manufactured by LKB Produkter (Sweden), was used in this investigation. The modifications of the standard instrument have been described previously.<sup>13</sup> Four different solutions can be studied at the same time without

the loss of any accuracy. The rotor of this instrument was immersed in a thermostat maintained constant to within  $\pm 0.007^\circ$ . For the systems studied here, equilibrium could be attained in four to fourteen days depending, of course, on the concentration, molecular weight and solvent used. The scale line displacement method was used, reference runs being made at each speed with each of the cells filled with pure solvent. The scale line displacements,  $Z$ , were measured from the reference lines using a Mann comparator having an accuracy of  $\pm 1 \mu$ . A synchropulsed Strobolux light source, appropriately filtered to isolate the 5460 Å. line, was used.

The scale line displacement is related to the index of refraction gradient  $dn/dx$  along the length of the cell by the relation

$$Z = Gab \, dn/dx$$

where  $G$  is the scale magnification factor obtained by direct measurement of the scale and scale photograph,  $a$  is the optical path length through the solution of a given cell, and  $b$  is the optical distance from the scale to the center of the cell. The index of refraction gradient is related to the concentration gradient of the solute in the cell by the relation

$$dc/dx = (dn/dx)/(dn/dc)$$

For dilute solutions of polyisobutylene in isoöctane the value of  $dn/dc$  has been reported<sup>6</sup> as  $1.42 \times 10^{-3} \text{ (g./dl.)}^{-1}$ . For polyisobutylene in ethyl *n*-heptanoate  $dn/dc$  was measured at 34°, using a Phoenix Differential Refractometer and is  $1.04 \times 10^{-3} \text{ (g./dl.)}^{-1}$ . To obtain the partial specific volume of this polymer in ethyl *n*-heptanoate at 34°, densities of dilute solutions were measured using a calibrated pycnometer and a semi-microbalance. The partial specific volume was calculated from these data by the method of intercepts as described by Lewis and Randall,<sup>14</sup> and was  $1.106 \text{ cm.}^3/\text{g.}$ ; the density of the solvent at this temperature is  $0.8563 \text{ g./cm.}^3$ . For polyisobutylene in isoöctane at 25°, the quantity of interest  $(1 - \bar{v}_p)$  is 0.272.<sup>5</sup>

The scale line displacements were plotted against  $x$ , for about 20 to 30 values of  $x$  for each experiment and a smooth curve drawn through the data from the meniscus to the bottom of the cell. The necessary integrations of the  $Z$  against  $x$  curves to obtain the molecular weights (see Discussion) were performed numerically using Simpson's rule.

### Discussion and Results

**General Theory.**—The analysis of the equilibrium state attained by a solution in the ultracentrifuge represents a special case of heterogeneous equilibrium in a force field. In this case the field can be described by the centrifugal potential  $\phi$  which assumes a definite value at each point  $x$ , the distance outward from the center of rotation. We shall consider a multicomponent solution composed of one solvent component designated by the subscript 1, and  $r - 1$  chemically identical polymeric solute components designated by the indices 2, 3, . . . ,  $r$ . The criterion for equilibrium is that for each of the components the total potential must be uniform throughout the force field. Thus at point  $x$

$$d\mu_i(x) + M_i d\phi(x) = 0 \quad (1)$$

there being  $r$  such equations, one for each component. In equation 1,  $\mu_i(x)$  is the chemical potential of species  $i$  at point  $x$ , and  $M_i$  is the molecular weight of this component. By applying standard thermodynamic methods as described by Pedersen<sup>2</sup> and Goldberg<sup>15</sup> one obtains the relation that

(14) G. N. Lewis and M. Randall, "Thermodynamics," McGraw-Hill Book Co., New York, N. Y., 1923, Chapter IV.

(15) R. J. Goldberg, *This Journal*, **57**, 194 (1953).

(8) P. J. Flory, "Principles of Polymer Chemistry," Cornell University Press, Ithaca, N. Y., 1953, p. 529 and 532.

(9) Ref. 8, p. 307.

(10) P. J. Flory, *J. Am. Chem. Soc.*, **65**, 372 (1943).

(11) T. G. Fox and P. J. Flory, *ibid.*, **73**, 1909 (1951).

(12) A. R. Shultz and P. J. Flory, *ibid.*, **74**, 4760 (1952).

(13) M. Wales, P. G. Sulzer and L. C. Williams, *J. Research Natl. Bur. Standards*, **50**, 69 (1953).

$$M_i (1 - \bar{v}_i^{(x)} \rho^{(x)}) \omega^2 x \, dx = \sum_{k=2}^r (\partial \mu_i / \partial N_k)^{(x)}_{T, P, N_1, \dots, N_i, \dots, N_r} dN_k^{(x)} \quad (2)$$

$N_i \neq N_k$

In equation 2,  $\bar{v}_i^{(x)}$  is the partial specific volume of component  $i$  at point  $x$ ,  $\rho^{(x)}$  the density of the solution at point  $x$ ,  $N_k$  the mole fraction of component  $k$  and the centrifugal potential  $d\phi^{(x)}$  has been replaced by its equivalent— $\omega^2 x \, dx$  where  $\omega$  is the angular speed of rotation.

In order to discuss the behavior of polymer solutions in the equilibrium ultracentrifuge it will be convenient to express the results obtained above in terms of the osmotic pressure at point  $x$ . This can be accomplished by multiplying both sides of equation 5 by  $n_i^{(x)}$  the number of moles of component  $i$  at point  $x$ , and summing over all polymer species. Then

$$\sum_{i=2}^r n_i^{(x)} M_i (1 - \bar{v}^{(x)} \rho^{(x)}) \omega^2 x \, dx = \sum_{i=2}^r \sum_{k=2}^r n_i^{(x)} (\partial \mu_i / \partial N_k)^{(x)}_{T, P, N_1, \dots, N_i, \dots, N_r} dN_k^{(x)} \quad (3)$$

$N_i \neq N_k$

the assumption being made that the partial specific volume is independent of molecular weight. By use of the relation

$$\mu_1^{(x)} - \mu_1^{(x,0)} = -\pi^{(x)} \bar{V}_1^{(x)} \quad (4)$$

and the Gibbs-Duhem relation in the form

$$\sum_{i=1}^r n_i^{(x)} (\partial \mu_i / \partial N_k)^{(x)}_{T, P} = 0 \quad (5)$$

there is obtained

$$\sum_{i=2}^r (n_i^{(x)} M_i / n_1^{(x)} \bar{V}_1^{(x)}) (1 - \bar{v}^{(x)} \rho^{(x)}) \omega^2 x \left( \frac{dc}{dx} \right)^{-1} = (\partial \pi / \partial c)^{(x)} \quad (6)$$

where  $\mu_1^{(x,0)}$  is the chemical potential of pure solvent at point  $x$ ,  $\pi^{(x)}$  is the osmotic pressure at point  $x$ , and  $c_x$  is the concentration at point  $x$  expressed as grams of solute per unit volume of solution. The expression

$$\sum_{i=2}^r n_i^{(x)} M_i / n_1^{(x)} \bar{V}_1^{(x)}$$

is equal to the number of grams of solute per unit volume of solvent at  $x$ . In dilute solution this quantity can be set equal to  $c_x$ . The error introduced is insignificant so that equation 6 can be written as

$$(1 - \bar{v}^{(x)} \rho^{(x)}) \omega^2 x c_x / (dc/dx)^x = (\partial \pi / \partial c)^x \quad (7)$$

Equation 7 is a general relation describing the equilibrium of a dilute solution in the ultracentrifuge. It is applicable to ideal as well as non-ideal solutions irrespective of the polydispersity of the solute. However, in interpreting the behavior of such solutions it is convenient to consider separately the problems involved in treating ideal and non-ideal solutions.

**Ideal Solutions.**—Over the concentration range in which a solution is ideal, van't Hoff's law is obeyed so that

$$\pi^{(x)} = (RT/M_n^{(x)}) c_x \quad (8)$$

where  $M_n^{(x)}$  is the number average molecular weight of the solute at  $x$ . For the special case of a single component solute equation 7 becomes

$$dc_x/dx = [(1 - \bar{v}^{(x)} \rho^{(x)}) \omega^2 x / RT] c_x M \quad (9)$$

which can be written in the alternative form as

$$H_u^{(x)} c_x / (dc/dx)^{(x)} = RT/M \quad (9-1)$$

As Goldberg<sup>15</sup> has pointed out a close analogy exists between equations 9 and 9-1 and the expression relating the excess turbidity of a polymer solution at zero angle and infinite dilution to the polymer molecular weight. The significant difference between the expressions is that in the light scattering case the equation is applicable to the solution as a whole; while for sedimentation equilibrium it is only applicable at point  $x$ .

For a multicomponent solute

$$(dc_x/dx)^x = \sum_{i=2}^r dc_{ix}/dx = [(1 - \bar{v}^{(x)} \rho^{(x)}) \omega^2 x / RT] \sum_{i=2}^r c_{ix} M_i \quad (10)$$

Since the weight average molecular weight at  $x$ ,  $M_{wx}$  is defined as

$$\sum_{i=2}^r c_{ix} M_i / c_x$$

we obtain the result that

$$M_{wx} = [RT / (1 - \bar{v}^{(x)} \rho^{(x)}) \omega^2 x] (dc_x/dx) c_x \quad (11)$$

Equation 11 gives the weight average molecular weight at point  $x$ , while the quantity of interest is the weight average molecular weight of the polymer. This quantity can be obtained by integrating equation 11 over the length of the centrifuge cell, taking cognizance of the fact that a sector shaped cell is used.<sup>16</sup> Thus for the weight average molecular weight of the polymer

$$M_w = \int_{x_a}^{x_b} M_{wx} c_x dx / \int_{x_a}^{x_b} x c_x dx \quad (12)$$

where the limits of integration represent the extremities of the cell,  $x_a$  being the meniscus position and  $x_b$  the bottom of the cell. If the necessary integrations are performed using equation 11 the result is

$$M_w = [2RT / (1 - \bar{v} \rho) \omega^2] [1/c_0 (x_b^2 - x_a^2)] \int_{x_a}^{x_b} (dc/dx) dx \quad (13)$$

where  $M_w$  is the weight average molecular weight of the solute and  $c_0$  is the initial solution concentration in the centrifuge cell. In performing the integration we have assumed that  $\bar{v}$  and  $\rho$  are independent of  $x$  and hence of polymer concentration and of pressure; these assumptions would appear to be adequate in dilute solutions.

Equation 13, valid only for ideal solutions, expresses the weight average molecular weight in terms of directly measurable quantities. The term  $(dc_x/dx)$  is directly related to the scale line displacements and the necessary integrations can be performed either numerically or graphically. The  $M_w$  calculated from equation 13 should be the

(16) T. Svedberg and K. O. Federsen, "The Ultracentrifuge," Oxford, 1940, p. 7.

same for different initial polymer concentrations, alleviating the necessity of making any arbitrary and hazardous extrapolations of the data to infinite dilution. Thus, if ideal solution behavior can be achieved in the ultracentrifuge,  $M_w$  can be very simply determined without reference to whether the solute is monodisperse or polydisperse, or to the nature of the polydispersity. The determination of  $M_w$  in the ultracentrifuge independent of total concentration and over a wide composition range can be taken as a sufficient criterion that ideal solution behavior has been achieved.

The attainment of ideal behavior for a given polymer involves the appropriate selection of solvent and temperature. This choice is not unlimited since the operation and design of the centrifuge itself impose certain restrictions. The temperature selected must, of course, lie within the operating range of the instrument. The solvent-polymer system must be such that the term  $(1 - \bar{v}\rho)$  is not so small as to make the rate of sedimentation too slow. Also the inherent lack of precision in measuring a small  $(1 - \bar{v}\rho)$  would be reflected in inaccurate molecular weights. Finally the indices of refraction of the polymer and solvent must differ appreciably so that the scale line displacement method can be used to measure the concentration gradient along the length of the cell. Though these conditions appear formidable they are not too difficult to fulfill. We have selected for our initial study the system polyisobutylene as polymer and ethyl *n*-heptanoate as solvent. We shall describe how the "θ temperature" or ideal solution conditions can be determined independent of the sedimentation equilibrium experiments and discuss the results of such experiments when performed under these conditions.

According to thermodynamic theory of polymer solutions the critical miscibility temperature,  $T_c$ , of a binary polymer-solvent system depends on molecular weight according to the following relation<sup>12</sup>

$$1/T_c = (1/\theta) [1 + (1/\psi_1) (1/X^{1/2} + 1/2X)] \quad (14)$$

when  $X$  is the ratio of the molar volume of the polymer to that of the solvent; *i.e.*, the number of segments per polymer chain.  $\psi_1$  is an entropy parameter, and  $\theta$  is the critical miscibility temperature for polymer species of infinite molecular weight, being defined as the maximum temperature for the coexistence of two liquid phases. At the temperature  $T = \theta$ , it has been shown theoretically<sup>8</sup> and verified experimentally<sup>17,18</sup> that polymer solutions of any molecular weight behave ideally. That is, van't Hoff's law is followed at all concentrations, for all molecular weights and molecular weight distributions. Thus the conditions for ideal solution behavior can be obtained from studies of the dependence of  $T_c$  on  $M$ . From such studies the  $\theta$  temperature can be deduced.<sup>11,12</sup> In Table I the values of  $T_c$  for fractions of polyisobutylene in ethyl *n*-heptanoate are given and the data are plotted in Fig. 1 according to the suggestion of equation 14. A linear plot results and  $\theta$  is

found to be  $33 = 1^\circ$  which is in very good agreement with the previous estimate of Fox and Flory.<sup>11</sup>

TABLE I  
CRITICAL MISCIBILITY TEMPERATURE OF POLYISOBUTYLENE  
FRACTIONS IN ETHYL *n*-HEPTANOATE

| Fraction | $M_v$     | $M_w$   | $T_c, ^\circ\text{C.}$ |
|----------|-----------|---------|------------------------|
| D        | 78,500    | 85,000  | 5.0                    |
| B        | 268,000   | 278,000 | 16.2                   |
| E        | 215,000   | ...     | 15.6                   |
| A        | 560,000   | 588,000 | 22.6                   |
| F        | 2,830,000 | ...     | 28.3                   |
| C        | ...       | 131,000 | ...                    |

Exploratory experiments utilizing the equilibrium ultracentrifuge were performed with this system in the temperature range of 32–34° and as a result of these measurements the  $\theta$  temperature was taken as 34°. The imposition of  $\theta$  conditions does not prevent the attainment of sedimentation equilibrium in a reasonable length of time; five to twelve days were usually required for the system studied here. Sedimentation equilibrium experiments were then made under these conditions with four of the polymer fractions over a wide initial concentration range for each. Weight average molecular weights were calculated from the data by means of equation 13 and the results are summarized in Table II. These calculations are, of course, performed without any regard to the polydispersity of the sample. For each of the fractions, the values of  $M_w$  that are obtained are independent of the initial concentration of polymer. The absolute value of the molecular weight of each fraction must of course reflect the uncertainty in the factor  $(1 - \bar{v}\rho)$ . Since for the system under consideration this quantity is equal to 0.053, a 1% error in the determination of  $\bar{v}$  can result in a 10% error in the molecular weight. However, any corrections from this cause would be uniformly applied to all molecular weights.

TABLE II  
 $M_w$  CALCULATED FROM EQUATION 13 FOR FRACTIONS OF  
PIB IN ETHYL *n*-HEPTANOATE AT 34.0°

| co, g./dl. | $M_w$           | co, g./dl. | $M_w$           |
|------------|-----------------|------------|-----------------|
|            | Fraction A      |            | Fraction C      |
| 0.122      | 604,000         | 0.5011     | 133,000         |
| .122       | 594,000         | .8150      | 130,000         |
| .229       | 583,000         | .9696      | 133,000         |
| .308       | 578,000         | 1.1695     | 128,000         |
| .381       | 582,000         |            |                 |
| av.        | 588,000 ± 4,000 | av.        | 131,000 ± 1,000 |
|            | Fraction B      |            | Fraction D      |
| 0.269      | 272,000         | 0.605      | 84,400          |
| .302       | 279,000         | 0.879      | 83,400          |
| .425       | 278,000         | 1.236      | 87,000          |
| .555       | 276,000         | 1.5116     | 83,000          |
| .636       | 282,000         | 1.8178     | 86,000          |
|            |                 | 2.0600     | 85,700          |
| av.        | 278,000 ± 2,000 | 2.3882     | 85,000          |
|            |                 | av.        | 85,000 ± 500    |

The deviation of molecular weights of each of the fractions at different concentration is small and

(17) W. R. Krigbaum and P. J. Flory, *J. Am. Chem. Soc.*, **75**, 5254 (1953).

(18) W. R. Krigbaum, *ibid.*, **76**, 3758 (1954).

well within the experimental error. These results, obtained under  $\Theta$  condition, are the theoretically expected ones and satisfy the condition for ideal solution behavior. For ideal solution the determination of the weight average molecular weight is, from a theoretical point of view, extremely simple. Extrapolation to infinite dilution is unnecessary since the molecular weight can be determined from an experiment involving only a single concentration. The thermodynamic analysis which allows the molecular weight to be calculated is almost exact; the only approximations are those pertaining to the solution concentration which introduce negligible error. Experiments performed in this manner yield absolute weight average molecular weights. Thus when sedimentation equilibrium experiments are performed under these conditions important and useful unambiguous information can be obtained. Though attainment of ideal behavior in the equilibrium centrifuge has only been demonstrated for a specific polymer-solvent system at an appropriate temperature there is no reason to expect that similar studies cannot be carried out with other polymer-solvent systems. If more heterogeneous polymeric solutes are studied under these conditions, then higher molecular weight averages could be obtained by methods of analysis previously described.<sup>15,19</sup> In practice, the determination of the higher molecular weight averages, such as  $M_z$  and  $M_{z+1}$ , require accurate values of the scale line displacement at the extremities of the cell. The optical system used with the centrifuge does not allow the direct determination of  $Z$  at  $x_a$  and  $x_b$ ; these quantities are usually determined by extrapolation.<sup>20,21</sup> For very polydisperse solutes this fact makes the reliable determination of the molecular weight averages greater than  $M_w$  difficult even under ideal conditions, but does not prevent the determination of  $M_w$ .

**Non-ideal Solutions.**—The results that have been obtained under " $\Theta$  conditions" can be immediately used to investigate the applicability of this experimental technique to the study of non-ideal solutions. In discussing the sedimentation equilibrium of non-ideal polymer solutions it is advisable to divide the discussion into two portions: One part deals with the problem of a monodisperse solute while the other portion considers the case where the solute is heterogeneous with respect to molecular weight.

For these purposes it is convenient to expand the osmotic pressure, at point  $x$  in the centrifugal field, in virial form. Thus

$$(\pi/c_x)^z = RT [A_1^{(z)} + A_2^{(z)}c_x + A_3^{(z)}c_x^2 + \dots] \quad (15)$$

If we consider first a monodisperse solute, then  $A_1$  can be set equal to  $1/M$  and the superscript  $z$  can be omitted from the higher virial coefficients since the molecular weight will be uniform throughout the entire centrifuge cell. Equation 15 can also be written in an alternative form<sup>3</sup>

(19) M. Wales, *THIS JOURNAL*, **52**, 235 (1948).

(20) T. Svedberg and K. O. Pedersen, "The Ultracentrifuge," Oxford, 1940, p. 319.

(21) J. B. Nichols and F. D. Bailey, Chapter XIII in "Physical Methods of Organic Chemistry," Vol. I, Part I, Edited by A. Weissberger, Interscience Publishers, New York, N. Y., 1949.

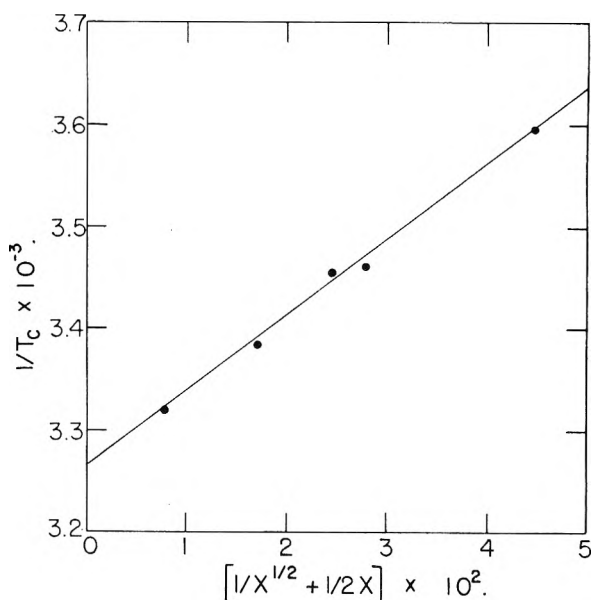


Fig. 1.—Plot of the reciprocal of the critical temperature against the molecular size function of equation 18 for polyisobutylene fractions in ethyl *n*-heptanoate.

$$(\pi/c_x)^z = (RT/M) [1 + \Gamma_2 c_x + \Gamma_3 c_x^2 + \dots] \quad (16)$$

where  $\Gamma_2 = MA_2$  and  $\Gamma_3 = MA_3$ . Relating the third virial coefficient to the second by the expression<sup>22</sup>  $\Gamma_3 = g\Gamma_2^2$  we obtain the following relation valid at any point  $x$  for a single solute component

$$((1 - \bar{v}\rho)\omega^2 x/RT) c_x / (dc_x/dx) = (1/M) [1 + 2\Gamma_2 c_x + 3g\Gamma_2^2 c_x^2 + \dots] \quad (17)$$

In good solvents  $g$  will have the value of about one third so that equation 17 becomes

$$((1 - \bar{v}\rho)\omega^2 x/RT) c_x / (dc_x/dx) \cong (1/M) [1 + \Gamma_2 c_x]^2 \quad (18)$$

Thus if  $dc_x/dx$  and  $c_x$  are known as a function of  $x$ , a point by point analysis can be made of a single experiment and the molecular weight and virial coefficients obtained.<sup>23</sup> By appropriately integrating the experimentally determined  $(dc_x/dx)$  against  $x$  curve, the values of  $c_x$  can be obtained. However, extremely accurate values of  $dc_x/dx$  are required for this purpose and the conditions of the experiments must be such that low values of  $dc_x/dx$  are avoided, otherwise the quantity of interest  $c_x/(dc_x/dx)$  will be unreliable. A further difficulty presents itself in that one does not know *a priori* how many terms in the virial expansion need be considered. In light scattering or osmotic pressure measurements, solutions sufficiently dilute can be studied so that the consideration of only the first three virial coefficients is usually adequate. However, in the equilibrium ultracentrifuge, for comparable initial concentrations, the mass of solute distributes itself along the length of the cell so that the concentration near the bottom of the cell may be two to three times the initial concentration. Thus at each point in the cell a different number of

(22) W. H. Stockmayer and E. F. Casassa, *J. Chem. Phys.*, **20**, 1560 (1952).

(23) Alternatively equation (17) can be integrated over the length of the centrifuge cell and the molecular weight and virial coefficients determined from the resulting equations.

virial terms will have to be considered. If these theoretical and experimental difficulties could be overcome, then the possibility exists that from a single observation one can obtain the same information utilizing the equilibrium ultracentrifuge that is obtained only after a series of measurements at different concentrations using other techniques, such as light scattering and osmotic pressure.

The appropriate expression for the sedimentation equilibrium of a heterogeneous solute can be obtained by using relations developed by Flory and Krigbaum<sup>3</sup> in treating the similar situation in light scattering. Thus, for a polydisperse non-ideal solution equation 17 can be written as

$$[(1 - \bar{v}\rho)\omega^2x/RT] [c_x/(dc_x/dx)] = 1/M_{wx} + 2A_2'^{(x)}c_x + \dots \quad (19)$$

For a heterogeneous solute the coefficient  $A_2'$  is not identical with  $A_2$ , the coefficient appropriate to osmotic pressure measurements. It has been theoretically predicted<sup>3</sup> and experimentally substantiated<sup>4</sup> that both these coefficients depend on molecular weight and molecular weight heterogeneity, though each in a different manner. Equation 19 is only valid at point  $x$ , and to determine the weight average molecular weight of the sample the integration indicated by equation 12 must be performed. However, since the distribution of molecular weights must vary with  $x$ , the term  $A_2'^{(x)}$  must in general also vary with  $x$ . Thus to perform the necessary integration, the dependence of  $A_2'^{(x)}$  on molecular weight and molecular weight distribution must be specified. However, the present theoretical and experimental understanding of the thermodynamic behavior of polymer solutions, does not allow the appropriate expression to be formulated in any tractable form. Hence, the necessary integration to obtain the weight average molecular weight of the polymer under these experimental conditions cannot be accomplished. From these considerations we conclude that unambiguous information cannot be obtained from a study of the sedimentation equilibrium of a non-ideal solution of polydisperse long chain molecules.

It has been suggested that the condition that  $A_2'$  must vary with molecular weight and molecular weight distribution can be relaxed. Thus procedures have been developed for treating the sedimentation equilibrium of non-ideal polydisperse polymer solutions by assuming  $A_2'$  is independent of  $x$  in these cases. Under these conditions equation 19 can then be written as<sup>19</sup>

$$1/M_{wx}^\circ = 1/M_{wx} + 2A_2'c_x \quad (20)$$

where  $M_{wx}^\circ$  represents a "molecular weight" at  $x$ , calculated as if the solution behaved ideally at this point, *i.e.*, the molecular weight calculated according to equation 13. Following the treatment of Williams and Van Holde<sup>5</sup> equation 20 is written as

$$M_{wx} = M_{wx}^\circ / (1 - 2A_2'c_x M_{wx}^\circ) \quad (21)$$

If the denominator is expanded in a power series

$$M_{wx} = M_{wx}^\circ [1 + 2A_2' M_{wx}^\circ c_x + 4A_2'^2 M_{wx}^\circ c_x^2 + \dots] \quad (22)$$

By multiplying each term in equation 22 by  $c_x x dx$  and integrating over the extremities of the centrifuge cell there is obtained

$$1/M_w^\circ \cong 1/M_w + \frac{2A_2}{c_0/2(x_b^2 - x_a^2)M_w^\circ} \left[ \int_{x_a}^{x_b} M_w^\circ c_x^2 x dx \right] \times \left\{ \frac{1 + 2A_2 \int_{x_a}^{x_b} M_w^\circ c_x^3 x dx}{\int_{x_a}^{x_b} M_w^\circ c_x^2 x dx} \right. \\ \left. \frac{1 + 2A_2 \int_{x_a}^{x_b} M_w^\circ c_x^2 x dx}{\int_{x_a}^{x_b} M_w^\circ c_x dx} \right\} \quad (23)$$

By assuming that the term in the brackets is approximately unity Van Holde and Williams<sup>5</sup> obtained

$$1/M_w^\circ = 1/M_w + \frac{2A_2}{c_0/2(x_b^2 - x_a^2)M_w^\circ} \int_{x_a}^{x_b} M_w^\circ c_x^2 x dx \quad (24)$$

or

$$1/M_w^\circ = 1/M_w + 2A_2 c'_0 \quad (25)$$

or where  $c'_0$  is a new concentration variable defined as

$$c'_0 = [2/(c_0(x_b^2 - x_a^2)M_w^\circ)] \int_{x_a}^{x_b} M_w^\circ c_x^2 x dx$$

For the concentration and molecular weights studied here  $c'_0$  exceeds  $c_0$  by about 15 to 30%. In this procedure only the second virial coefficient has been considered and its dependence on molecular weight and molecular weight distribution has been neglected. Furthermore, the series expansion of equation 21, which leads to equation 22, tacitly assumes a low value of the virial coefficient, since effectively only the second term is retained. On the other hand equation 25 offers the advantage that the weight average molecular weight of the solute is very simply expressed in terms of quantities readily obtainable from the experimental data. It is thus important to assess the validity or limitations of this analysis. To study this point, sedimentation equilibrium experiments were undertaken using a good solvent, isoöctane, with the same polymer fractions previously studied under "Θ conditions."

The data obtained from these studies are shown in Fig. 2 where according to equation 25 the reciprocal of  $M_w^\circ$  is plotted against  $c'_0$ . When the data are plotted in this manner straight lines result and if the analysis is correct the intercept at  $c'_0 = 0$  should represent the reciprocal of the weight average molecular weight. However, the horizontal dashed lines in this figure represent the results obtained for the same polymers under ideal solution conditions (the data of Table II), where the actual molecular weight is, of course, independent of concentration. The molecular weights obtained in the good solvent and the "Θ solvent" differ by about 25% in the higher molecular weight range. As the true molecular weight decreases this discrepancy becomes less and for a molecular weight of 85,000 the two results are virtually identical. Thus for low molecular weights, where the deviations from ideality will be less severe, the above analysis seems to be adequate. We therefore conclude that the suggested method of treating non-ideal solutions, equation 25, would be inaccurate except when ap-

plied to solutions of low molecular weight solutes. Other methods<sup>15,19</sup> suggested to treat this problem are similar in principle to the one just described and offer no substantial improvement in results.

The difficulties involved in treating the sedimentation equilibrium in good solvents can be realized if results with the same solute in good solvents and under ideal solution conditions are treated as though they behave as ideal two component system.<sup>5</sup> Lansing and Kraemer,<sup>24</sup> starting with equation 12, have derived an expression that is applicable to an *ideal two component system*. Their results are

$$\ln(Z/x) = \ln(Z/x)_a + (M(1 - \nu\rho)\omega^2/2RT)(x^2 - x_a^2) \quad (26)$$

Thus for an ideal two component solution a plot of  $\ln(Z/x)$  against  $x^2$  should be linear and the slope is directly related to the molecular weight. It has already been shown that weight average molecular weights can be determined unambiguously from equation 13 without having to assume that the solute consists of only one species. Thus a plot according to equation 26, of the data obtained under  $\Theta$  conditions will yield information as to the polydispersity of the solute since the slope at any point  $x$  is representative of the molecular weight, calculated as though the solute were monodisperse. For the experiments involving polyisobutylene in ethyl *n*-heptanoate at 34° straight lines should result if the fractions are monodisperse; deviations from linearity will be due solely to polydispersity. Once information regarding the polydispersity of the solute is obtained, treatment of experiments performed in isoöctane according to equation 26 should yield qualitative information as to the effect of deviations from ideality on the apparent molecular weight. It must be realized that non-ideal behavior will give an apparent molecular weight at any point which will be less than the true molecular weight of the solute.

Representative data obtained in both ethyl *n*-heptanoate and isoöctane for two different concentrations of each fraction are plotted in Fig. 3 according to equation 26. For illustrative purposes, apparent "ideal molecular weights" were calculated from the slopes at two points, the meniscus and at the bottom of the cell. These results are summarized in Table III. For fraction A straight lines result in these plots for the experiments performed under  $\Theta$  conditions (Fig. 3a). Since the slopes of these lines yield a molecular weight of 570,000, which is in excellent agreement with that previously deduced from equation 13, we can conclude that this sample is monodisperse as far as observations in the equilibrium ultracentrifuge are concerned. The results for the same solute in isoöctane are given in Fig. 3a, and curves with gradually decreasing slopes are obtained, indicating that the "apparent" ideal molecular weight is continuously decreasing. The initial apparent molecular weight is about 460,000 and gradually decreases to about 200,000. These observations can be explained by the fact that the concentration increases as the distance from the center of rotation

(24) W. D. Lansing and E. O. Kraemer, *J. Am. Chem. Soc.*, **57**, 1369 (1935).

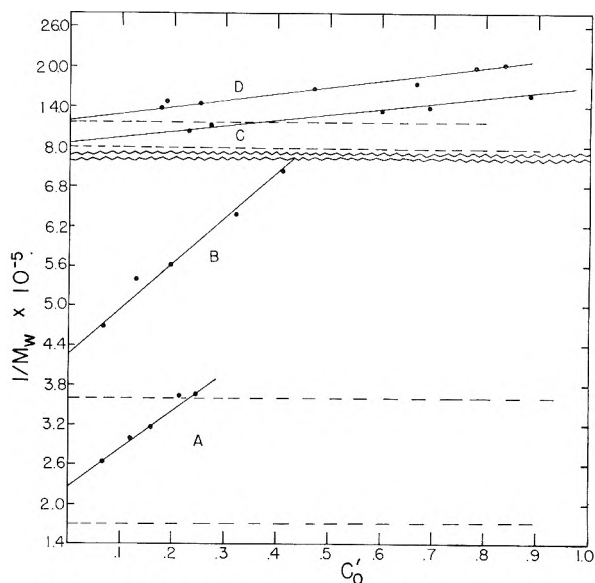


Fig. 2.—Plot of the reciprocal of the weight average molecular weight, calculated as though the solution were ideal, against the concentration variable  $c_0'$ . Solid lines for polyisobutylene fractions in isoöctane at 25°; dashed lines for same fractions in ethyl *n*-heptanoate at 34°.

increases. Since the non-ideality contribution to the total potential at any point is greater, the

TABLE III

APPARENT IDEAL MOLECULAR WEIGHTS AS DEDUCED FROM FIGURE 3 ACCORDING TO EQUATION 26<sup>a</sup>

| Fraction |              | In ethyl <i>n</i> -heptanoate 34° | Isoöctane, 25° |
|----------|--------------|-----------------------------------|----------------|
| A        | (a) Meniscus | 570,000                           | 460,000        |
|          | Base         |                                   | 193,000        |
|          | (b) Meniscus | 578,000                           | 470,000        |
|          | Base         |                                   | 206,000        |
| B        | (a) Meniscus | 296,000                           | 272,000        |
|          | Base         |                                   | 163,000        |
|          | (b) Meniscus | 306,000                           | 268,000        |
|          | Base         |                                   | 159,000        |
| D        | (a) Meniscus | 63,000                            | 60,500         |
|          | Base         | 173,000                           |                |
|          | (b) Meniscus | 60,000                            | 59,000         |
|          | Base         | 173,000                           |                |

<sup>a</sup> (a) Results at lower concentration. (b) Results at higher concentration.

greater the concentration, it will increase with increasing  $x$ . Therefore the apparent ideal molecular weight must be continually decreasing. The non-ideality contribution is appreciable in this case and these results illustrate the difficulties in trying to determine the true molecular weight from experiments in good solvents by calculating apparent ideal molecular weights at finite concentrations even when polydispersity complications are absent. Since fraction A behaves as a monodisperse solute, then the true molecular weight and higher virial coefficients should be obtainable from the experiments in isoöctane by use of equation 17 or 18. Unfortunately in these experiments, the scale line displacements at the low values of  $x$  were relatively small. Although this presents no difficulty in evaluating integrals of the type

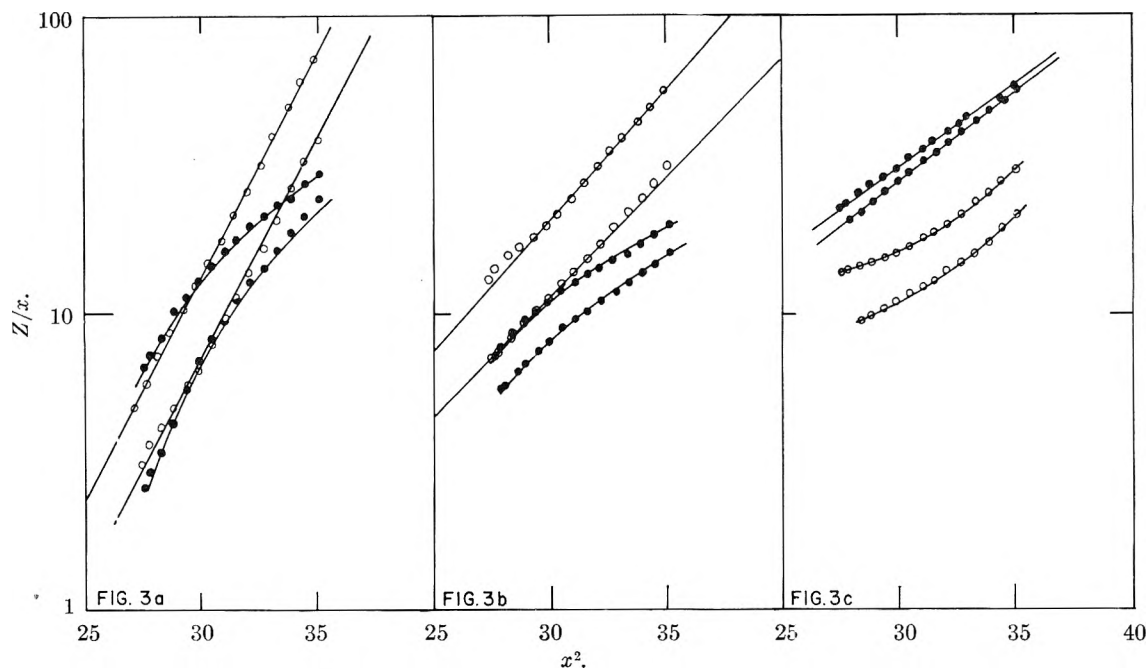


Fig. 3.—Plot of  $\log(Z/x)$  against  $x^2$ . *a* for fraction A, in ethyl *n*-heptanoate at 34° ○; upper curve  $c_0 = 0.229$  g./dl.; lower curve,  $c_0 = 0.122$  g./dl. in isoöctane at 25° ●; upper curve  $c_0 = 0.214$  g./dl.; lower curve  $c_0 = 0.118$  g./dl. *b* for fraction B, in ethyl *n*-heptanoate at 34° ○; upper curve  $c_0 = 0.555$  g./dl.; lower curve  $c_0 = 0.302$  g./dl. In isoöctane at 25° ●; upper curve  $c_0 = 0.285$  g./dl.; lower curve  $c_0 = 0.235$  g./dl. *c* for fraction D, in ethyl *n*-heptanoate at 34° ○; upper curve  $c_0 = 0.879$  g./dl.; lower curve  $c_0 = 0.605$  g./dl. In isoöctane at 25° ●; upper curve  $c_0 = 0.778$  g./dl.; lower curve  $c_0 = 0.614$  g./dl.

$$\int_{x_a}^{x_b} (dc/dx)_x dx$$

for use with equation 23, it is extremely difficult to obtain accurate values of the ratio  $c_x/(dc_x/dx)$  as a function of  $x$ , which is required for the correct evaluation of  $M$  and  $\Gamma_2$  according to equation 18.

Similar results are obtained when the data for fraction B,  $M_w$  278,000, are treated in this manner (Fig. 3b). Although under “ $\Theta$  conditions” the data can be fitted by a straight line, the molecular weight calculated from the slope of this line is slightly higher than the true molecular weight; the curve is probably slightly concave upward, indicative of a small amount of polydispersity. In the good solvent the data can be interpreted as for fraction A.

The results for fraction D, plotted in Fig. (3c), are quite different. For experiments in ethyl *n*-heptanoate at 34° straight lines do not result which can only mean that the solute is polydisperse. The “apparent ideal molecular weights” vary from 60,000 to 173,000, the higher molecular species occurring at the higher values of  $x$ , *i.e.*, in the direction of sedimentation. The weight average molecular weight of this sample is 85,000 which is consistent with the above observations. In the good solvent, surprisingly enough, straight lines do result and give an apparent molecular weight of 60,000. For this polydisperse solute at the higher  $x$  values, with its greater solute concentration and greater concentration of higher molecular weight species, the deviations from ideality are sufficient to give the same apparent ideal molecular weight that is obtained at lower values of  $x$  where for the lower molecular weight species and concentrations

involved the deviation from non-ideality should not be severe. However, even though straight lines are obtained when the data in a good solvent are treated in the manner described, the apparent molecular weight obtained is still appreciably lower than that obtained by the correct method.

### Conclusions

From the preceding discussion and consideration of experimental results it is clear that ideal solution behavior of flexible chain molecules can be attained in the equilibrium ultracentrifuge. An unambiguous and simple analysis can then be made of the experimental data. Thus the weight average molecular weight of a polymeric solute can be obtained without regard to its heterogeneity. The heterogeneity of a polydisperse polymeric solute is then describable by the relations previously developed.<sup>6</sup>

The difficulties of treating such experimental data obtained in non-ideal solution have been discussed and the inadequacies of the present empirical method of treatment have been indicated. On the other hand for a monodisperse polymeric solute, the possibility exists that the equilibrium centrifuge could be an important tool in studying the thermodynamic behavior of polymer solutions.<sup>25</sup> Verification of this latter point must await further experimental investigation.

NOTE ADDED IN PROOF.—Recent theoretical considerations of the thermodynamics of dilute polymer solutions by Orifino and Flory<sup>26</sup> indicate the possibility that the temperature at which the second virial coefficient vanishes might

(25) M. Wales, *J. Applied Phys.*, **22**, 735 (1951).

(26) T. A. Orifino and P. J. Flory, presented before 130th Meeting of the American Chemical Society, Atlantic City, N. J., September, 1956.

depend slightly upon the polymer molecular weight. Such an effect would not, however, significantly alter any of the major conclusions of this paper, which are concerned with much greater deviations from ideality.

**Acknowledgment.**—The authors wish to acknowledge very interesting discussions with H. Leaderman on this subject.

## THE SOLUBILITY OF BONE MINERAL. II.<sup>1,2</sup> PRECIPITATION OF NEAR-NEUTRAL SOLUTIONS OF CALCIUM AND PHOSPHATE

BY BASIL S. STRATES, W. F. NEUMAN AND GEORGE J. LEVINSKAS

From the Division of Pharmacology, Department of Radiation Biology, School of Medicine and Dentistry, University of Rochester, Rochester, New York

Received August 2, 1956

The precipitation of solutions of calcium and phosphate has been studied in the region of near neutrality. All results were expressed as the activity product,  $\alpha_{Ca^{++}} \times \alpha_{HPO_4^{--}}$ . It was necessary to exceed the  $K_{sp}$  of  $CaHPO_4 \cdot 2H_2O$  ( $2.7 \pm 0.3 \times 10^{-7}$  at 25°) to initiate precipitation in the absence of seeding materials, but the degree of required supersaturation varied with pH and temperature. At pH 6.9 or higher, the solid which first formed exhibited a molar Ca/P ratio of unity but rapidly hydrolyzed to hydroxy apatite. Both apatite crystals and collagen fibers were successful seeding materials, inducing solid formation between the point of spontaneous precipitation. It was concluded that serum is normally undersaturated,  $\alpha_{Ca^{++}} \times \alpha_{HPO_4^{--}}$ , in the absence of the solid phase but supersaturated with respect to bone mineral (hydroxy apatite). The physiological implications of this conclusion are indicated.

The solubility of calcium phosphate precipitates in the region of neutral pH has been the subject of intensive investigation for many years. This research interest is founded on the reasonable premise that an accurate knowledge of calcium phosphate solubility is prerequisite to an understanding of the biochemistry of bone formation and metabolism.

Despite the importance of the subject and despite frequent critical reviews of the literature<sup>3-12</sup> no general concept has been brought forth that has received wide-spread acceptance. A recent review<sup>11a</sup> supported the premise that the solubility product constant,  $K_{sp}$ , of  $CaHPO_4 \cdot 2H_2O$  governs the stability of solutions of calcium and inorganic orthophosphate—actually a restatement of an old suggestion by Shear and Kramer.<sup>13</sup> On this basis, normal serum is *undersaturated* (*vide infra*). On the other hand, the same review stated that, on theoretical grounds, basic calcium phosphate, (hydroxy apatite), the mineral phase stable at physiological pH, cannot exhibit a fixed  $K_{sp}$ . This lack of a fixed  $K_{sp}$  has since been established experimentally with dissolution data proven to have been derived from equilibrium conditions.<sup>14</sup> Unfor-

tunately, the solubilities observed, however variable with changing conditions, never approached the levels of calcium and phosphate observed in normal sera (*vide infra*). On this basis, normal serum is *supersaturated*.

To clarify this seemingly paradoxical conflict of data, a series of investigations was performed on the *formation* of precipitates of calcium and phosphate *in vitro* under approximately physiological conditions.

### Experimental

**Reagents and Preparations.**—All materials were dissolved in CO<sub>2</sub>-free, boiled, distilled water, the apparatus of Levinskas<sup>14</sup> being employed to maintain all transfers and aliquoting under an atmosphere of CO<sub>2</sub>-free nitrogen. KH<sub>2</sub>PO<sub>4</sub>, CaCl<sub>2</sub> and KCl were "Baker Analyzed" Reagent salts dried at 110° before use. Diethylbarbituric acid (Mallinckrodt Chemical Works) was shown by spectrographic analysis (courtesy Dr. L. Steadman) to be nearly free of contaminating cations. Maleic acid was obtained from Fisher Scientific Company. The hydroxy apatite preparation has been described previously.<sup>14-16</sup> Gelatin (Eastman Organic Chemicals) was repeatedly dialyzed against dilute disodium Versenate and distilled water to remove inorganic cations. Fibrin was prepared by agitating with a test-tube brush, fresh jugular blood from a dog. The fibrin threads adhering to the brush were washed repeatedly with Versenate solutions and distilled water. Collagen fibers were reconstituted from a 0.04% acetic acid solution of calf tail tendons.<sup>17</sup> One per cent. KCl precipitated the fibers which, upon electron microscopic examination (courtesy Dr. L. Peachey), appeared to have normal collagen structure with normal spacing (640 Å.).

**Methods and Procedures.**—Phosphorus was analyzed by the method of Fiske and SubbaRow<sup>18</sup>; calcium by the method of Sobel and Hanok.<sup>19</sup>

All solutions were buffered with a final concentration of 0.02 M barbital for pH's 7.8, 7.4 and 6.9 and 0.01 M maleic acid at pH 6.2. Ionic strength was maintained at 0.165 with KCl. The order of addition of solutions was always KH<sub>2</sub>PO<sub>4</sub>, buffer, KCl, CaCl<sub>2</sub> and CHCl<sub>3</sub> (5 ml./l. to inhibit

(1) Taken in part from the Masters Thesis of Basil S. Strates, June, 1956, The University of Rochester.

(2) This paper is based on work performed under contract with the United States Atomic Energy Commission at the University of Rochester Atomic Energy Project, Rochester, New York.

(3) W. D. Armstrong, *Ann. Rev. Biochem.*, **11**, 441 (1942).

(4) M. J. Dallemagne, *Ann. Rev. Physiol.*, **12**, 101 (1950).

(5) S. Eisenberger, A. Lehrman and W. D. Turner, *Chem. Revs.*, **26**, 257 (1940).

(6) D. M. Greenberg, *Ann. Rev. Biochem.*, **8**, 269 (1939).

(7) H. C. Hodge, Conference on Metabolic Interrelations, Transactions of the 3rd Conference, 1951, p. 194.

(8) C. Huggins, *Physiol. Rev.*, **17**, 119 (1937).

(9) M. A. Logan, *ibid.*, **20**, 522 (1940).

(10) (a) F. C. McLean, *Ann. Rev. Physiol.*, **5**, 79 (1943); (b) P. D. F. Murray, *ibid.*, **9**, 103 (1947).

(11) (a) W. F. Neuman and M. W. Neuman, *Chem. Revs.*, **53**, 1 (1953); (b) C. Ragan, *Ann. Rev. Physiol.*, **14**, 51 (1952).

(12) J. Sendroy, Jr., *Ann. Rev. Biochem.*, **14**, 407 (1945).

(13) M. J. Shear and B. Kramer, *J. Biol. Chem.*, **79**, 147 (1928).

(14) G. J. Levinskas and W. F. Neuman, *THIS JOURNAL*, **69**, 164 (1955).

(15) W. F. Neuman, Atomic Energy Report, UR-238 (1953).

(16) W. F. Neuman, T. Y. Toribara and B. J. Mulryan, *J. Am. Chem. Soc.*, **75**, 4239 (1953).

(17) F. O. Schmitt, C. E. Hall and M. A. Jakus, *J. Cell Comp. Physiol.*, **20**, 11 (1942).

(18) C. H. Fiske and Y. SubbaRow, *J. Biol. Chem.*, **66**, 375 (1925).

(19) A. E. Sobel and A. Hanok, *Proc. Soc. Exptl. Biol. Med.*, **77**, 737 (1951).

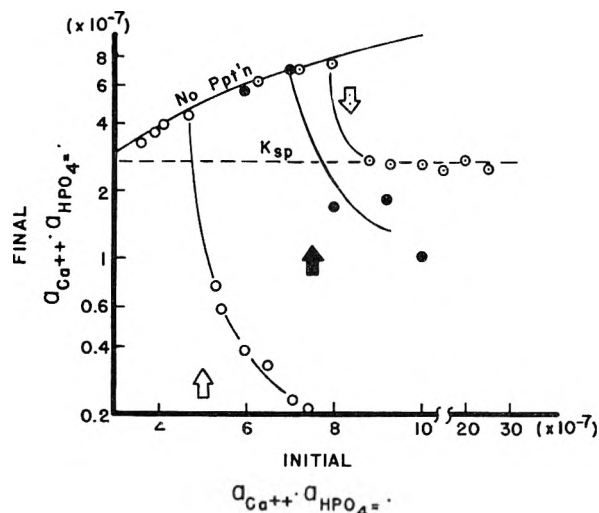


Fig. 1.—The determination of the precipitation point: open circles represent solutions initially at pH 7.4; solid circles at pH 6.9; dotted circles at pH 6.2; temperature 25°.

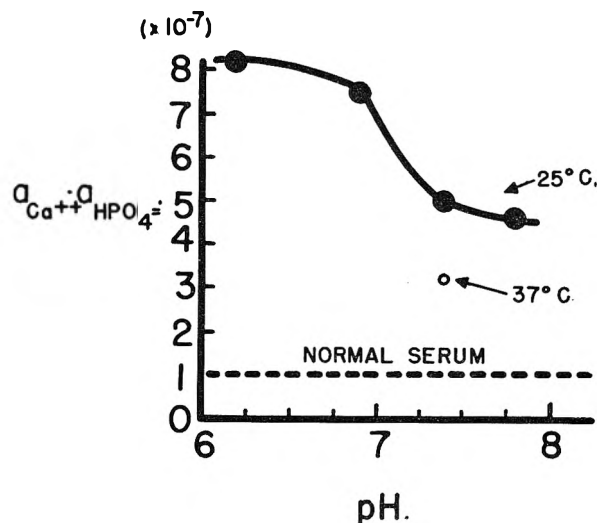


Fig. 2.—The effect of pH and temperature on the point of spontaneous precipitation.

bacterial growth.<sup>14</sup>) The mixed solutions were sealed in flasks, under nitrogen, with paraffin and parafilm.

In these studies, the flasks were shaken gently for 10 days at 25 ± 2°. While no claim is made that equilibrium was attained in every instance, it was shown that a steady state was achieved with  $\text{CaHPO}_4 \cdot 2\text{H}_2\text{O}$  as the solid phase by comparison with longer equilibration periods. Actually the question of attainment of equilibrium is somewhat irrelevant. Here, the aim was to establish conditions for solid formation. It is conceivable that, by some slow nucleation process, precipitates might ultimately appear in solutions that had stood more than 10 days, but such a process could hardly be of physiological significance because of its slow kinetics.

After equilibration, the precipitates were allowed to settle overnight and the supernatant fluid either centrifuged or filtered. Centrifugation was done on a Spinco Model L Ultracentrifuge, 80,000 × *g*.<sup>14</sup> Later, it was found more convenient to filter the supernatant solutions through molecular filter membranes (Millipore paper 450 *mμ* pore-size). Aliquots of the filtered or centrifuged supernatants were taken for duplicate analyses of calcium, phosphate and pH (Beckman pH meter). The composition of precipitates was deduced by the difference between initial and final concentrations.

Activity corrections were taken from Levinskas<sup>21</sup> ( $\gamma_{\text{Ca}^{++}}$

= 0.36,  $\gamma_{\text{H}_2\text{PO}_4^-}$  = 0.62,  $\gamma_{\text{HPO}_4^{2-}}$  = 0.23) and the  $pK_{11}$  of  $\text{H}_3\text{PO}_4$  was assumed to be 7.19.<sup>21</sup> No corrections were necessary for complexing of calcium by barbiturate ions but complexing by maleic was calculated from the formation constant,  $K_c$ , given by Schubert and Lindenbaum<sup>22</sup> using the dissociation constants of German, *et al.*<sup>23</sup>

## Results

**Determining of  $K_{sp}$   $\text{CaHPO}_4 \cdot 2\text{H}_2\text{O}$ .**—Expressed as an activity product, values given in the literature for  $K_{sp}$   $\text{CaHPO}_4 \cdot 2\text{H}_2\text{O}$  range from 2.19<sup>24</sup> to  $4 \times 10^{-7}$ .<sup>25,26</sup> Accordingly, an attempt was made to redetermine the solubility product under the conditions of our experiments. These data, assembled in Table I, give an average value of  $2.7 \times 10^{-7}$ , in reasonable agreement with published values.

**The Point of Spontaneous Precipitation.**—A series of experiments was performed to determine the product,  $\alpha_{\text{Ca}^{++}} \times \alpha_{\text{HPO}_4^{2-}}$ , at which spontaneous precipitation occurred. Typical results are given in Fig. 1. In Fig. 2 the effect of varying pH and temperature on the precipitation point is illustrated. Only at pH 6.2 did the final solution products stabilize to give a constant value. At the more alkaline pH's the final product was low and variable. Because, in these instances, the pH fell precipitously despite the presence of buffer, it appeared that the solid phase was undergoing rapid hydrolysis to a more alkaline substance.

This interpretation was confirmed by a study of the time course of the change in the solid phase.

TABLE I  
THE  $K_{sp}$  OF  $\text{CaHPO}_4 \cdot 2\text{H}_2\text{O}$  AT 25°  
Precipitation experiments

| Initial<br>[Ca],<br>$M \times 10^{-4}$ | [P] <sub>total</sub> ,<br>$M \times 10^{-4}$ | Final pH | Final<br>[Ca <sup>++</sup> ],<br>$M \times 10^{-4}$ | Final<br>[P] <sub>total</sub> ,<br>$M \times 10^{-4}$ | $\alpha_{\text{Ca}^{++}} \times$<br>$\alpha_{\text{HPO}_4^{2-}}$<br>( $\times 10^{-7}$ ) |
|--|--|----------|---|---|--|
| 123                                    | 42.9   | 6.02     | 123.  | 43.6  | ..   |
| 101                                    | 51.5   | 5.87     | 86.6  | 37.1  | 2.71   |
| 72.0                                   | 72.9   | 5.87     | 55.5  | 56.8  | 2.69   |
| 49.1                                   | 107.   | 5.90     | 32.6  | 91.3  | 2.73   |
| 40.9                                   | 129.   | 5.99     | 27.5  | 116.  | 3.54   |

## Dissolution experiments

| Initial<br>[Ca]<br>$M \times 10^{-4}$ | [P] <sub>total</sub> ,<br>$M \times 10^{-4}$ | $\text{CaHPO}_4 \cdot 2\text{H}_2\text{O}$ ,<br>g./100<br>ml. | Final<br>pH | Final<br>[Ca <sup>++</sup> ],<br>$M \times 10^{-4}$ | Final<br>[P] <sub>total</sub> ,<br>$M \times 10^{-4}$ | $\alpha_{\text{Ca}^{++}} \times$<br>$\alpha_{\text{HPO}_4^{2-}}$<br>( $\times 10^{-7}$ ) |
|---------------------------------------|--|---|-------------|---|---|--|
| 0.0                                   | 0.0  | 0.1   | 6.56        | 30.5  | 29  | 2.55   |
| 0.0                                   | 129  | .1  | 6.18        | 12.3  | 132   | 2.56   |
| 49.1                                  | .0   | .1  | 6.36        | 61.0  | 16.8  | 2.23   |
| 0.0                                   | .0   | .3  | 6.56        | 30.6  | 28.4  | 2.52   |
| 0.0                                   | 129  | .3  | 6.19        | 13.3  | 131   | 2.80   |
| 49.1                                  | .0   | .3  | 6.38        | 65.9  | 17.1  | 2.48   |

Av. ± S. Dev. =  $2.38 \pm 0.34 \times 10^{-7}$

**The Time Course of Solid Phase Conversion.**—A series of solutions having  $\alpha_{\text{Ca}^{++}} \times \alpha_{\text{HPO}_4^{2-}}$  above the precipitation point were mixed and, at varying time intervals, the solid which formed was isolated for analysis or X-ray examination. In all cases irrespective of pH the solid exhibited a Ca/P ratio

(21) L. F. Nims, *J. Am. Chem. Soc.*, **55**, 1946 (1933).

(22) J. Schubert and A. Lindenbaum, *ibid.*, **74**, 3529 (1952).

(23) W. L. German, A. I. Vogel and G. H. Jeffrey, *Phil. Mag.*, **22**, 790 (1953).

(24) Tennessee Valley Authority, Phosphorus, properties of the element and some of its compounds, Chem. Eng. Rept. No. 8, 1950.

(25) M. J. Shear and B. Kramer, *J. Biol. Chem.*, **79**, 125 (1928).

(26) L. E. Holt, Jr., V. K. LaMer and H. B. Chown, *ibid.*, **64**, 509 (1925).

TABLE II  
X-RAY ANALYSIS OF CALCIUM PHOSPHATE PRECIPITATES

Solutions buffered with barbital acid, filtered through molecular filters, and precipitates dried by lyophilization; samples No. 3 and 4 further lyophilized for two hours. Initial concentration of pH 6.18 and 6.90 samples  $1.1 \times 10^{-2} M P$  and  $6.4 \times 10^{-3} M Ca$ ; initial concentration of the pH 7.40 sample  $5.3 \times 10^{-3} M P$  and  $3.2 \times 10^{-3} M Ca$ . The X-ray analysis was performed by the Eastman Kodak Research Laboratories through the courtesy of Dr. R. L. Griffith.

| Sample no. | Initial pH | Time after mixing | Molar Ca/P in ppt. | CaHPO <sub>4</sub> ·2H <sub>2</sub> O | Estimated composition (X-ray analysis), % |           | KCl |
|------------|------------|-------------------|--------------------|---------------------------------------|---|-----------|-----|
|            |            |                   |                    |                                       | Hydroxy apatite                           | Amorphous |     |
| 1          | 6.18       | 24 hr.            | 1.02               | 60                                    | 0   | 0         | ?   |
| 2          | 7.40       | 48 hr.            | 1.60               | 0                                     | ~100                                      | 0         | 0   |
| 3          | 6.90       | 10 min.           | 1.19               | 0                                     | 20  | 60        | 20  |
| 4          | 6.90       | 25 min.           | 1.40               | 0                                     | 60  | 30        | 10  |
| 5          | 6.90       | 3 hr.             | 1.40               | 0                                     | 50  | 20        | 30  |
| 6          | 6.90       | 24 hr.            | 1.44               | 0                                     | 85  | 10        | 5   |

of about unity immediately after mixing. Only at pH 6.2 did the solid remain stable and form visible crystals. At the more alkaline pH's the Ca/P ratio rapidly rose. These data are given in Fig. 3.

TABLE III

PRECIPITATION SEEDING OF CALCIUM PHOSPHATE MIXTURES

Solutions buffered at pH 7.4. Mixtures equilibrated 10 days at 25°, filtered through molecular filters, and ashed. Initial calcium and phosphorus concentration just below point of spontaneous precipitation.

| Compd. added   | Amount, mg./cc. | Final concn.                       |                        | Solid phase molar Ca/P | Degree of pptn. |
|----------------|-----------------|------------------------------------|------------------------|------------------------|-----------------|
|                |                 | Liquid phase P, $M \times 10^{-4}$ | Ca, $M \times 10^{-4}$ |                        |                 |
| None (control) | ...             | 33.2                               | 20.0                   | ..                     | ...             |
| Apatite        | 3.0             | 20.6                               | 1.49                   | 1.47                   | 7+              |
| Apatite        | 3.0             | 21.0                               | 1.04                   | 1.75                   | 8+              |
| Gelatin        | 3.0             | 34.0                               | 19.5                   | ..                     | ...             |
| Fibrin         | 3.0             | 32.6                               | 20.2                   | ..                     | ...             |
| Collagen       | 3.0             | 29.6                               | 13.0                   | 1.43                   | 1+              |

Selected samples upon X-ray examination confirmed the analytical data suggesting a rapid conversion of the solid to hydroxy apatite at pH 6.9 or higher. These data are given in Table II.

**Seeding Experiments.**—It was of interest to determine what agents might induce crystallization by seeding solutions above the  $K_{sp}$  CaHPO<sub>4</sub>·2H<sub>2</sub>O but below the precipitation point. Accordingly, a preliminary experiment was performed, the results of which are given in Table III.

As expected,<sup>27</sup> the addition of hydroxy apatite crystals quickly catalyzed the separation of more solid phase. Fibrin and gelatin had no effect. Surprisingly, collagen, obtained from a tissue which does not normally calcify, did induce some crystallization.

Discussion

There is some question whether one may generalize from any single set of experiments. However, in these studies specific ion effects were minimized by expressing results in terms of ion activities. To this extent the data may be translated in physiological terms provided the normal thermodynamic ion product  $a_{Ca^{++}} \times a_{HPO_4^-}$  in serum is established. McLean and Hastings<sup>28</sup> provided the only direct measurement of the ionized calcium of serum using the frog heart method. Their value of 1.3

mM/l. is in agreement with recent unpublished calculations<sup>29</sup> based on studies of ultrafiltrates of normal human sera.<sup>30</sup> This concentration, converted to activity, multiplied by the  $a_{HPO_4^-}$  from Levinskas<sup>20</sup> (assuming a normal total inorganic HPO<sub>4</sub><sup>=</sup> of 3.5 mg. %) gives  $1 \times 10^{-7}$  as the thermodynamic product of normal serum.

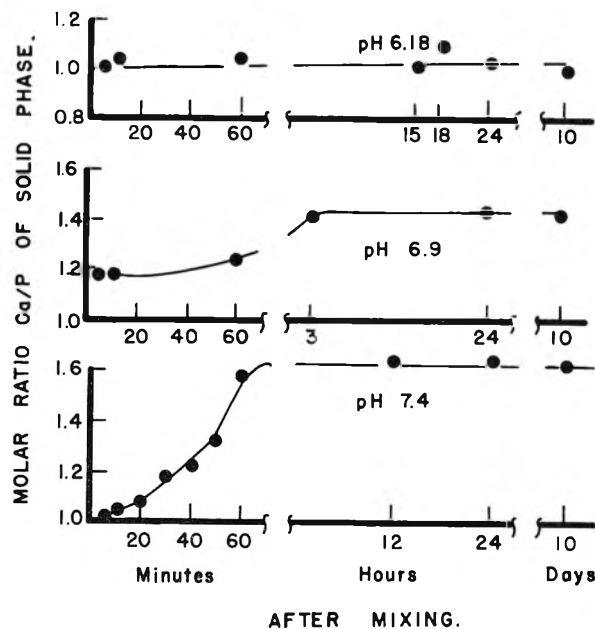


Fig. 3.—Variation of the Ca/P ratio of the solid phase with time after mixing.

The present data, therefore, indicate that serum is undersaturated but only in the absence of solid phase. The activity product of normal serum must be increased by a factor of three for spontaneous precipitation to occur. This is in agreement with the experience of a number of investigators.<sup>31-34</sup>

On the other hand, the data presented here also show that CaHPO<sub>4</sub>·2H<sub>2</sub>O is not stable above pH 6.9 and therefore hydroxy apatite governs the solubility equilibrium when solid phase is present. This, too, is in agreement with earlier studies.<sup>11a</sup>

(29) W. F. Neuman, "The Physical Chemistry of Bone," Chicago Univ. Press, to be published.

(30) A. R. Terepka and T. Y. Toribara, unpublished results.

(31) D. M. Greenberg and C. E. Larson, THIS JOURNAL, 43, 1139 (1939).

(32) T. Hopkins, J. E. Howard and H. Eisenberg, Bull. Johns Hopkins Hosp., 91, 1 (1952).

(33) M. Laskowski, Biochem. Z., 265, 401 (1933).

(34) F. C. McLean and M. A. Henrichs, Am. J. Physiol., 121, 580 (1938).

(27) W. F. Neuman, Metab. Interrelations, Josiah Macy, Jr., Foundation, 2nd Conf., 1950, p. 42.

(28) F. McLean and A. B. Hastings, J. Biol. Chem., 108, 285 (1935).

It would appear that the age-old question concerning whether serum is undersaturated, saturated or supersaturated can be resolved only by reference to the presence or absence of solid phase.

In the absence of solid phase, serum is undersaturated. It is below the point of spontaneous precipitation. In the presence of solid phase, it appears to be supersaturated since dissolution experiments at pH over 7 have never attained an activity product  $\alpha_{Ca^{++}} \times \alpha_{HPO_4^-}$  equalling that observed in normal serum.<sup>14</sup>

Space does not permit an adequate discussion of the many literature reports in relation to this interpretation but it is the authors' opinion that there exists virtually no disagreement.<sup>11a</sup>

The conclusion that serum is normally supersaturated (since solid phase is *always* present) with

respect to  $[Ca^{++}]$  and  $[HPO_4^-]$  has important physiological implications. In the first place, some cellular mechanism must be postulated by which such a supersaturated condition can be maintained *in vivo*. Secondly, the driving force of the mineralization process in calcification is easily seen to be present in serum itself. Given a "seed" crystal the supersaturated serum will spontaneously carry it to full mineralization. Thirdly, some active mechanism must be present in the gut wall to permit the absorption of calcium *against* an ion-gradient.

The first of these three corollaries already has been established.<sup>35</sup> The second and third corollaries are under study.

(35) W. F. Neuman, H. E. Firschein, P. S. Chen, B. J. Mulryan and V. DiStefano, *J. Am. Chem. Soc.*, **78**, 3863 (1956).

## STANDARDIZATION OF N.M.R. HIGH RESOLUTION SPECTRA

BY J. R. ZIMMERMAN AND M. R. FOSTER

*Magnolia Petroleum Company, Field Research Laboratories, Dallas, Texas*

*Received August 16, 1956*

An accurate method for referencing high resolution nuclear magnetic resonance spectra with respect to an external standard is described. Mathematical expressions are developed for determining chemical shift errors and effective line broadening arising from imperfections in a glass coaxial spinning system. With a properly designed precision system, errors in chemical shifts arising from tube imperfections can be reduced to less than 1 part in  $10^6$ . The magnetic field at the immediate vicinity of a nucleus is discussed in terms of the applied external field, susceptibility corrections, shape of sample and intermolecular association effects. Several experiments are discussed which illustrate molecular association in alcohol-water and in normal hexane-benzene mixtures and the corresponding necessity of exercising extreme caution in the use of internal reference standards.

### Introduction

High resolution spectroscopy involves the study of narrow line resonances—the fine structure phenomena of nuclear resonance arising from the electronic environment of nuclei. These narrow line resonances are usually described in terms of such measurable quantities as chemical shifts<sup>1-3</sup> and J-coupling splittings.<sup>4,5</sup> Because of the small separations of multiple narrow line resonances, high resolution spectroscopy is more often restricted to low viscosity liquids or gaseous samples, rather than solids.

Chemical shifts of resonance lines are field dependent and arise because the magnetic field at the nucleus is in general different from the applied external magnetic field. Any such difference can arise from either intermolecular or intramolecular effects or both. In the intramolecular sense, line separations or shifts are evident because of differences in the effective electron distribution about the nuclei being studied. Intermolecularly, these differences are derived from several causes, such as (a) intermolecular interactions, (b) exchange rate phenomena between different chemical environments and (c) bulk sample susceptibilities. J-Coupling splitting of resonance lines is an intra-

molecular, field independent, effect arising from an indirect interaction between the nuclear moments. The magnitude and multiplicity of this splitting depends on the number of nuclei involved and the types of chemical bonds separating the nuclei. The general reasons previously advanced in order for chemical shift and J-coupling phenomena to occur clearly suggest why high resolution spectroscopy has become an important tool for structural analysis and characterization of chemical systems.

As the number of chemical applications has increased, there has been an ever increasing refinement in observations which has pointed out the needs for better instrumentation, for higher resolution instruments, for proper corrections for small effects not necessarily related directly to the specific problem, and for more accurate measurements of resonance line positions. If an accurate quantitative analysis of electron distributions about nuclei in different molecular species is desired then appropriate procedures for standard line resonance comparisons must be adhered to. It is this problem of standardization of nuclear magnetic resonance high resolution spectra which forms the basis of this paper.

At the present time several laboratories, both academic and industrial, are already reporting intricate structural resonance lines separated by approximately one part in 100 million of the total applied magnetic field. One ultimate objective in n.m.r. chemical analysis is, of course, to be able to

(1) W. D. Knight, *Phys. Rev.*, **76**, 1259 (1949).

(2) W. D. Dickinson, *ibid.*, **77**, 736 (1950).

(3) W. G. Procter and F. C. Yu, *ibid.*, **77**, 717 (1950).

(4) H. Gutowsky, D. McCall, C. Slichter and E. McNeil, *ibid.*, **82**, 748 (1951).

(5) E. L. Hahn and D. E. Maxwell, *ibid.*, **84**, 1246 (1951); **88**, 1070 (1952).

standardize such small differences from one molecular species to another. Both internal and external standardization procedures have been widely used for several years. However, now with the increased resolution and stability of the spectrometer systems, differences in measurements from separate research laboratories are often common and sometimes even contradictory in qualitative deductions. In some instances differences of referenced chemical shift measurements exceed by more than ten times the reported deviations of the measurements. The importance of a proper referenced resonance line procedure for n.m.r. high resolution applications to chemical analysis has rapidly become apparent.

**Chemical Shifts.**—The precessional frequency of a nucleus when subjected to a magnetic field is given by the relation  $\omega = \gamma H_n$ , where  $\omega$  is the angular precessional frequency,  $\gamma$  is called the gyromagnetic ratio and is a property of the particular nuclear species, and where  $H_n$  is the magnetic field at the nucleus. The magnetic field applied externally to a sample compound is generally not the field  $H_n$  at the immediate vicinity of the nucleus. Likewise the local field at the vicinity of a particular molecule is generally not equal to the field  $H_n$ . It is the small differences in magnetic field, of course, that occur at the nuclei within the molecule that give rise to basic chemical shifts.

In a molecular system, the local field at the vicinity of a particular molecule is made up of the macroscopic field  $\vec{H}$  in the bulk sample plus contributions arising from the total magnetization  $\vec{M}$  of the system. If one assumes that the contribution of the molecules outside a physically infinitesimal sphere surrounding the molecule in question is the total contribution arising from any magnetization  $\vec{M}$  of the system, then by the method of Lorentz, the local field at the vicinity of the particular molecule is given by  $\vec{H} + 4\pi\vec{M}/3$ . This assumption, of course, neglects any contribution to the local field of the molecule from molecules inside the infinitesimal sphere. In instances where intermolecular interactions involve the electron distribution about the nuclei being investigated, this assumption no longer holds.

In principle one would like to study the chemical shifts of nuclei within an isolated molecule. With a macroscopic field  $\vec{H}$  existing in the molecular sample, the magnetic field  $\vec{H}_n$  at a particular nucleus might for convenience of discussion be written in the form

$$\vec{H}_n = (\vec{H}_0 + \vec{h}_1 + \vec{h}_2 + \vec{h}_3 + \vec{h}_4) \quad (1)$$

where  $\vec{H}_0$  is the applied external magnetic field, and where  $\vec{H}_0 + \vec{h}_1$  is the macroscopic field  $\vec{H}$  in the sample. The quantity  $\vec{h}_1$  is dependent on the shape of sample holder and the bulk susceptibility of the sample and the sample holder.  $\vec{h}_2$  is the contribution due to magnetization external to the Lorentz sphere; *i.e.*,  $\vec{h}_2 = 4\pi\vec{M}/3$ . In the case of

spherical samples, the contribution  $(\vec{h}_1 + \vec{h}_2)$  is zero; while for a cylindrical sample  $(\vec{h}_1 + \vec{h}_2) = (-2\pi/3)\kappa\vec{H}_0$ , where  $\kappa$  is the volume susceptibility of the sample.  $\vec{h}_3$  is an intermolecular interaction effect, and  $\vec{h}_4$  is the intramolecular chemical shift in an isolated molecule. In instances where a strong intermolecular association does occur between certain chemical groups of a chemical species but does not occur with other groups, the quantity  $\vec{h}_3$  can become an important factor. In a monomolecular species sample the question may arise regarding the relative importance of measuring shifts either when the molecule is isolated or when it is associated with its neighbors. But in a mixture of molecular species, erroneous conclusions can result regarding chemical shift measurements if proper allowance for variations of either the  $\vec{h}_3$  factor or combination of  $\vec{h}_3$  and  $\vec{h}_4$  factors is not made.

**Internal Standardization.**—An internal standardization procedure amounts to dissolving a small amount of the known reference standard into the sample. There are two specific advantages for using an internal reference standard: (a) simultaneous sweeping of the field or frequency spectrum for the unknown sample and reference standard and (b) the susceptibility corrections  $\vec{h}_1$  and  $\vec{h}_2$  in expression (1) are presumably common to both the reference and sample molecular systems. In the measurement of chemical shift differences between nuclei in a liquid system of a single molecular species, only the quantities  $\vec{h}_3$  and  $\vec{h}_4$  are factors for consideration. If a small amount of the reference standard can be dissolved into the system without affecting the  $\vec{h}_3$  and  $\vec{h}_4$  components of either the reference or unknown species, then one could conclude that an internal referencing procedure for comparing other molecular species would be satisfactory. However, this is not generally a valid assumption; and molecular association effects can, in many instances, contribute to effective chemical shift variations in magnetic field by as much as several parts in ten million.

A common example of this effect is observed when using water as an internal standard in ethyl alcohol. In Fig. 1 is shown a plot of the position of the internal water line with respect to the hydrogens of the methyl group as a function of the concentration of water. This chemical shift of the water line in comparison with pure water can vary as much as 11 sec.<sup>-1</sup> in  $40 \times 10^6$  sec.<sup>-1</sup> ( $\sim 2.6$  milligauss).<sup>6</sup>

It might be argued from Fig. 1 that so long as one uses small concentrations (<10% by volume) of water as an internal reference standard, then such a procedure would be satisfactory. In Fig. 2 one sees that this argument is not sound. Here the position of an internal water line with respect to the methyl group in *n*-propyl alcohol is plotted as a

(6) I. Weinberg, J. Fitch and J. Zimmerman, *Bull. Am. Phys. Soc.*, **1**, 92 (1956).

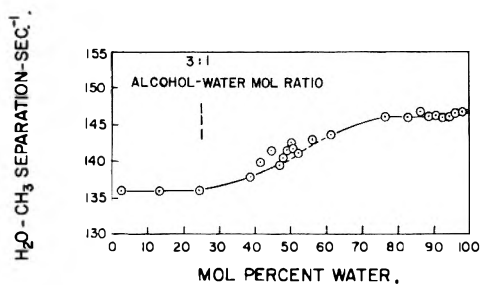


Fig. 1.—Chemical shift of water line in water-ethanol system.

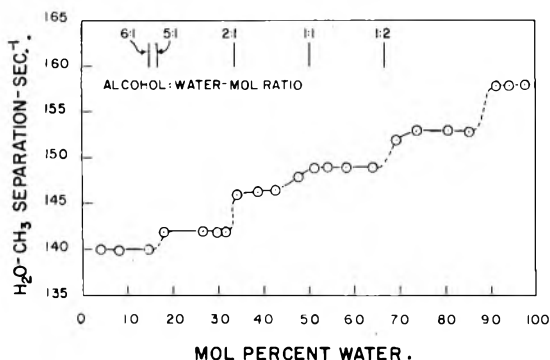


Fig. 2.—Chemical shift of water line in water-propanol system.

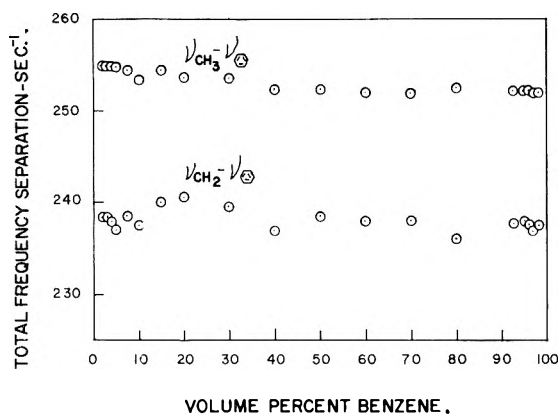


Fig. 3.—Resonance line separation of *n*-hexane and benzene mixtures.

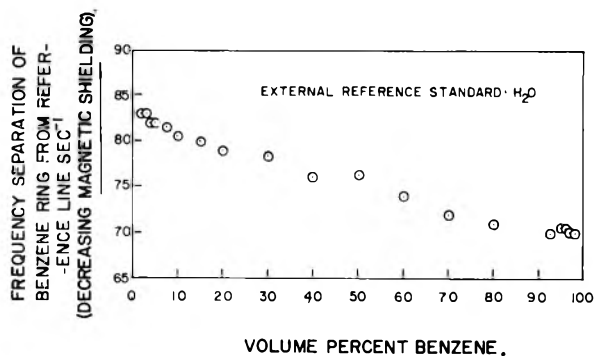


Fig. 4.—Chemical shift of benzene line in *n*-hexane-benzene system.

function of the concentration of water. Although this plot in Fig. 2 points out some excellent uses for nuclear magnetic resonance applications, the use of water as an internal standard without proper corrections for the effect of hydrogen bonding is an

improper standardization procedure which can lead to serious errors in chemical shift measurements.

In measurements made at very low concentrations of water (1% or less) in *n*-propyl alcohol, the resonance position of the isolated water is shifted approximately  $15 \text{ sec.}^{-1}$  with respect to a pure water resonance line. At these low concentrations of water, the difference in resonance line positions between the "isolated" water in *n*-propanol and the "isolated" water in ethanol is approximately  $4 \text{ sec.}^{-1}$  in  $40 \times 10^6 \text{ sec.}^{-1}$  ( $\sim 1$  milligauss).<sup>7</sup> It is apparent from these data that one must not only anticipate large chemical shifts because of hydrogen bonding or association of reference species but also must take into account that differences in association between the reference and unknown molecules can be appreciable—differences dependent on the unknown molecular species.

In liquid mixtures where large electric dipolar fields exist, strong molecular associations as those described above are usually predicted by the chemist by means other than n.m.r. Rather large shifts in electron density about certain chemical groups in such instances are not surprising. In the field of hydrocarbon chemistry, however, molecular species with strong electric dipole moments are not common. On this basis, there is a certain amount of logic in assuming that strong interaction effects (molecular association) between molecular species which might alter the effective electron density any appreciable amount in comparison with hydrogen bonding would be negligible. The question that arises, then, is whether internal standardization is appropriate in general for liquid hydrocarbon chemical shift measurements.

Benzene, because of its single sharp resonance line characteristic and its highly solvent behavior, has been used rather freely in the petroleum industry as an internal n.m.r. reference standard. In Fig. 3 the chemical shift between the benzene line and the major *n*-hexane line components are plotted as a function of the concentration of the reference standard (benzene). These results appear to verify the assumption that benzene would make a good internal standard in this instance; *i.e.*, the shift between the *n*-hexane groups and the benzene group remains approximately constant.

If the position of the benzene and *n*-hexane groups are measured with respect to an external reference standard, the result is shown in Fig. 4. It is true that both groups shift in unison with respect to the external standard as expected from Fig. 3. However, the total shift in going from 100% *n*-hexane to 100% benzene is approximately  $13.5 \text{ sec.}^{-1}$  (precessional frequency  $\sim 40 \times 10^6 \text{ sec.}^{-1}$ ); and the shift is toward higher magnetic field values. In expression 1, one notes that if the

variation of  $h_3$  and  $h_4$  effects are negligible then the only shift should be due to susceptibility differences between benzene and *n*-hexane. Such a correction amounts to a shift of only about  $4 \text{ sec.}^{-1}$  and is toward lower magnetic field strengths. Hence, one must conclude that not only is the

(7) I. Weinberg, J. Fitch and J. Zimmerman, to be published.

susceptibility shift much too small to account for the measured shift of  $13.5 \text{ sec.}^{-1}$ , but also is in the wrong direction.

A few conclusions summarizing the benzene-normal hexane mixtures as related to standardization are as follows: (a) The resonance line positions of pure benzene and benzene "isolated" in *n*-hexane differ by approximately  $18 \text{ sec.}^{-1}$  (b) The pure benzene hydrogens have a greater effective magnetic field shielding than do the hydrogens of the isolated benzene molecule. (c) The interaction effects which affect electron density about the hydrogen nuclei and which presumably are derived from the magnetic anisotropy of the  $\pi$ -electron structure of the benzene molecule arise not only between like molecular species (benzene-benzene) but also between unlike molecular species (benzene-*n*-hexane). (d) Such interaction phenomena can sometimes account for even greater electron density distortions of hydrogen groups than are observed in strong dipolar mixtures such as alcohol-water systems.

The use of benzene as an internal reference standard for n.m.r. chemical shift measurements, without proper corrections for interaction shifts, easily can lead to serious erroneous interpretations of data. Internal reference standards, especially in liquid hydrocarbon systems, must be considered with extreme caution.

**External Standardization.**—External standardization procedures for studying n.m.r. chemical shifts have two very distinct advantages over internal procedures in the case of pure chemical systems such as A.P.I. hydrocarbon standards. Measurements can be made without the pollution of the pure grade system and without introducing intermolecular effects arising from the presence of the reference standard compound. In terms of the magnetic field expression 1 for  $H_n$ , the  $h_3$  and  $h_4$  contributions to the field at the vicinity of the nuclei of the reference standard remain constant, and the corresponding contributions are fixed for the pure sample compound. Specifically, one can write for the *i*th sample and the *s*th reference standard that

$$\vec{H}_{ni} = (\vec{H}_{oi} + \vec{h}_{1i} + \vec{h}_{2i} + \vec{h}_{3i} + \vec{h}_{4i})$$

and

$$\vec{H}_{os} = (\vec{H}_{os} + \vec{h}_{1s} + \vec{h}_{2s} + \vec{h}_{3s} + \vec{h}_{4s})$$

The quantity  $(\vec{h}_{3i} + \vec{h}_{4i}) - (\vec{h}_{3s} + \vec{h}_{4s})$  is now a fixed quantity; and if the bulk effect differences  $(\vec{H}_{oi} + \vec{h}_{1i} + \vec{h}_{2i}) - (\vec{H}_{os} + \vec{h}_{1s} + \vec{h}_{2s})$  can be calculated or eliminated experimentally, then an accurate evaluation of chemical shifts is possible. It is true that association effects of a monomolecular species are not separable from "isolated" molecular chemical shifts, except by an independent experiment; but this is also true in the case of internal reference standard procedures. By external referencing, at least the quantities  $(\vec{h}_{3s} + \vec{h}_{4s})$  and  $(\vec{h}_{3i} + \vec{h}_{4i})$  are independent of one another.

The primary objection in the past to external referencing has been the problem of being certain

that both reference and unknown systems are subjected to a common external magnetic field, *i.e.*, that  $\vec{H}_{oi} = \vec{H}_{os}$ . Since independent measurements of the magnetic susceptibilities either are available or can be obtained readily, the difference quantity  $(\vec{h}_{1i} + \vec{h}_{2i}) - (\vec{h}_{1s} + \vec{h}_{2s})$  is an easily calculated correction.

Various methods of external standardization have been used by n.m.r. investigators. Most of the reported measuring techniques have involved obtaining independent sweeps of the spectra of the reference and unknown samples. With sufficient data for a proper statistical analysis, this procedure has been generally a good and widely used one for presentation of chemical shift measurements. The lack of a technique for simultaneous sweeping of reference and unknown samples does seriously limit the accuracy of line separation measurements; nevertheless, a few laboratories have reported accuracies to within one part in  $10^7$  by this method.

More recently procedures have been described which incorporate the principle of the simultaneous sweep. The basic problem is to be able to have both the reference and unknown samples in the same field  $H_0$ . The obvious advantage of simultaneous sweep is to be able to use side-band modulation techniques<sup>8</sup> of the spectra by superposing the side-band of one resonance upon the fundamental of another resonance. Chemical shifts can, in principle, be measured to an accuracy of a few parts in  $10^9$ .

One group of investigators<sup>9</sup> has approached this condition of placing both the reference and unknown samples in the same field  $H_0$  by separating the sample and the reference compounds by a thin glass membrane across a 5 mm. Pyrex glass tubing sample holder. The thickness of the membrane, of course, limits the accuracy of the  $H_0$  assumption. Also any symmetry in the glass membrane can distort the magnetic field so that  $H_{oi} \neq H_{os}$ . This asymmetric flux pattern was reportedly averaged out by rotating<sup>10</sup> the cell at a speed great enough to average out the inhomogeneity arising from the membrane. The reported reproducibility of measurements of this method is within plus or minus  $1 \text{ sec.}^{-1}$  at a Larmor frequency of  $30 \times 10^6 \text{ sec.}^{-1}$ . It should be emphasized that mere rotation of an asymmetric flux pattern does not assure that  $H_{oi}$  be equal to  $H_{os}$ ; *i.e.*, the two samples will not necessarily be subjected to the same effective average external magnetic field. A detailed clarification of this remark will be given later in this paper.

**An Accurate Method for External Standardization.**—We have been able to perfect a spinning external standardization procedure which encompasses simultaneous sweeping of reference and unknown samples and which does assure that  $H_{oi} = H_{os}$  to better than 1 part in  $10^8$ . Any sharp line reference standard may be used at the convenience of the observer. Side-band modulation techniques of the system are utilized, and the ultimate limitations

(8) J. Arnold and M. Packard, *J. Chem. Phys.*, **19**, 1608 (1951).

(9) J. Shoolery and B. Alder, *ibid.*, **23**, 805 (1955).

(10) F. Bloch, *Phys. Rev.*, **94**, 496 (1954).

of accuracy of this system are determined by the width of the resonance lines, the field sweep rate and the accuracy of the modulating audio oscillator.

The mechanics of this method is simply a spinning coaxial system of two precision glass tubes.<sup>11</sup> The sample to be studied is placed in the inner tube; the reference standard is placed in the annular region between the outer diameter of the inner tube and the inner diameter of the outer tube. Such a procedure can be dependable only if proper precautions are taken for averaging the asymmetric flux fields in the sample and reference regions. Both a theoretical and experimental evaluation of this external standardization procedure have been completed successfully.

To evaluate the proposed standardization procedure it is necessary to determine the field in the region occupied by the standard and the sample being studied. For mathematical purposes the problem is idealized if one regards the tubes as infinitely long and if one assumes that the field approaches the constant vector  $\vec{H}_0$  as the distance from the tubes becomes infinite. The problem is then to determine the magnetic field  $\vec{H} = \vec{H}_0 + \vec{h}_1$  which satisfies the following conditions: (a)  $\text{curl } \vec{H} = 0$ , (b)  $\text{div } \vec{H} = 0$ , (c) the normal component of  $\mu H$  is continuous at each interface, (d) the tangential component of  $\vec{H}$  is continuous at each interface, and (e)  $\vec{H} = \vec{H}_0$  as the distance from the tubes becomes infinite. Conditions (a) and (b) imply the existence of a potential satisfying  $\Delta\Phi = 0$  and  $H = \nabla\Phi$ .

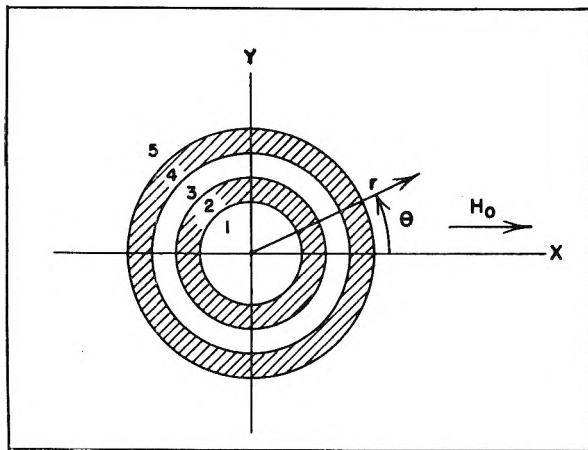


Fig. 5.—Coaxial system for standardization.

**The Ideal Case.**—If the tubes are circular and concentric and if  $H_0$  is perpendicular to the axis of the tubes, then the problem is a simple one in two dimensions. The coordinate system is chosen as shown in Fig. 5. The numbered regions from 1 to 5, respectively, are the sample, the glass wall of the inner tube, the standard, the glass wall of the outer tube and the unbounded region filled with air. The field in the  $i$ th region is given by

$$H_x(r, \theta) = [A_i - (B_i/r^2)\cos 2\theta] \quad (2)$$

(11) Wilmad Glass Company, Landisville, New Jersey.

and

$$H_y(r, \theta) = [-(B_i/r^2)\sin 2\theta] \quad (3)$$

where  $A_i$  and  $B_i$  are given to the first order in the susceptibilities by the expressions

$$A_i = [1 - 1/2(\mu_i - \mu_5)]H_0 \quad (4)$$

$$B_i = 1/2 \sum_{j=1}^{j=i-1} a_j^2 [\mu_{j+1} - \mu_j] H_0 \quad (5)$$

$$i > 1$$

$\mu_i$  is the permeability in the  $i$ th region and  $a_i$  is the radius of its outer boundary. It should be noted that  $B_i$  is of first order in the susceptibilities and so also is the  $y$ -component of the total field. The magnetic field strength is therefore  $H_x(r, \theta)$  to first order.

Particular interest centers on the first and third regions in Fig. 5. In the first region  $B_1 = 0$ ; hence the field strength is constant and equal to

$$H_1 = [1 - 1/2(\mu_1 - \mu_5)]H_0 \quad (6)$$

In the third region the field strength is given by

$$H_3 = \{1 - 1/2(\mu_3 - \mu_5) - [a_1^2(\mu_2 - \mu_1) + a_2^2(\mu_3 - \mu_2)] 1/2(1/r^2)\cos 2\theta\} H_0 \quad (7)$$

In the absence of rotation not all the molecules experience the same field. In fact, the field at the point  $(r, \theta)$  can be written

$$H_3 = \langle H_3 \rangle_{av} + \Delta H_3(a_2^2/r^2)\cos 2\theta$$

where

$$\Delta H_3 = -[a_1^2(\mu_2 - \mu_1) + a_2^2(\mu_3 - \mu_2)] (H_0/2a_2^2)$$

If a normalized field variable  $t$  is defined by  $t = (H_3 - \langle H_3 \rangle_{av})/(\Delta H_3)$ , there is some interest in calculating the number of molecules  $n(t)dt$  for which this field variable lies between  $t$  and  $t + dt$ . If the total number of molecules is  $N_0$ , then a plot of  $n(t)/N_0$  vs.  $t$  yields the curves shown in Fig. 6.

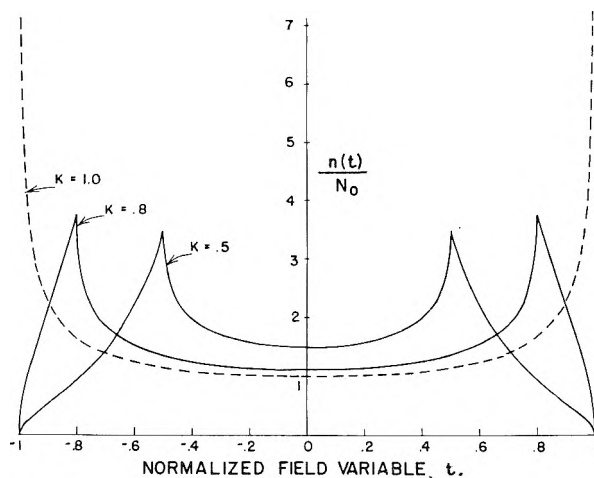


Fig. 6.—Particle density vs. field strength (static system).

In Fig. 6 the parameter  $k$  is  $(a_2/a_3)^2$ . A nuclear resonance spectrum obeying this field distribution is easily observed experimentally, and the distance between peaks can be determined.

If the coaxial system is rotated, the resultant effect is to average over  $\theta$ . Therefore, in the third region, Fig. 5

$$\langle H_3 \rangle_{av} = [1 - 1/2(\mu_3 - \mu_5)]H_0 \quad (8)$$

A comparison of this result with the average bulk field in the first region

$$\langle H_1 \rangle_{av} = H_1 = [1 - 1/2(\mu_1 - \mu_5)]H_0 \quad (9)$$

shows that the average bulk magnetic field experienced by a sample in region 3 is the same field that the sample would experience if it were placed in region 1 in the ideal case.

**Effects of Imperfect Tubing.**—In order to investigate the effect of imperfections in the glass tubing, standard perturbation techniques may be applied. The radius of the outer boundary of the *i*th region can be written as  $r_i(\theta) = a_i + \epsilon_i(\theta)$ , where  $\epsilon_i(\theta)$  is assumed to be so small that  $[\epsilon_i(\theta)]^2$  is negligible. The potential function is

$$\psi_i(r, \theta) = [A_i r + (B_i/r)] \cos \theta + V_i(r, \theta) \quad (10)$$

where the first term on the right is the potential function for the unperturbed problem, and where  $V_i(r, \theta)$  is the contribution due to the imperfections and is of the same order of magnitude as  $\epsilon_i(\theta)$ .

$\epsilon_i(\theta)$  can be represented by a trigonometric series

$$\epsilon_i(\theta) = 1/2 \rho_{0i} + \sum_{k=1}^{\infty} \rho_{ki} \cos(k\theta - \phi_{ki}) \quad (11)$$

and  $V_i(r, \theta)$  can be written as a series of solutions of Laplace's equation in the form

$$V_i(r, \theta) = \sum_{n=1}^{\infty} (b_{ni} r^n + d_{ni} r^{-n}) \cos n\theta + \sum_{n=1}^{\infty} (c_{ni} r^n + e_{ni} r^{-n}) \sin n\theta \quad (12)$$

The procedure is to determine the coefficients of the  $V_i(r, \theta)$  series in terms of the coefficients  $\rho_{ki}$  and  $\phi_{ki}$  subject to the requirement that  $\psi_i(r, \theta)$  satisfy the boundary conditions to first order.

The result of this calculation is that the additional contribution  $\eta_i(r, \theta)$  to the field strength is

$$\eta_i(r, \theta) = -1/2 H_0 \sum_{n=1}^{\infty} \left\{ \sum_{k=i}^4 a_k^{-n} (\mu_{k+1} - \mu_k) n r^{n-1} \rho_{n+1,k} \cos [(n-1)\theta - \phi_{n+1,k}] + \sum_{k=1}^{i-1} a_k^n (n r^{-n-1}) (\mu_{k+1} - \mu_k) \rho_{n-1,k} \cos [(n+1)\theta - \phi_{n-1,k}] \right\} \quad (13)$$

**Effect of Rotation.**—If the tube system is rotated at an angular frequency  $\Omega$  then expression 13 may be used to determine the additional field strength at a point rotating with the tubing. If the coordinates of this point at time  $t = 0$  are  $(r, \theta_0)$ , then the coordinates at time  $t$  will be  $(r, \theta_0 + \Omega t)$ . Moreover, since the tubing itself also rotates with the angular frequency  $\Omega$ ,  $\phi_{n,k}(t) = \phi_{n,k}(0) + \Omega t$ . If these values are inserted in expression 13 and averaged over time, the following result is obtained

$$\eta_i(r, \theta_0) = -H_0 \sum_{k=i}^4 a_k^{-2} (\mu_{k+1} - \mu_k) \rho_{3,k} r \cos [\theta_0 - \phi_{3,k}(0)] \quad (14)$$

Therefore, not even in a rotating system do all the particles experience the same average field. The reason is that the inhomogeneities in field strength arising from imperfections of the tubing are not static if the system rotates.

To further emphasize this point, suppose a normalized variable  $t_i$  is defined by

$$t_i = (\eta_i/H_0) \left\{ \left[ \sum_{k=i}^4 a_k^{-2} (\mu_{k+1} - \mu_k) \rho_{3k} \cos \phi_{3k} \right]^2 + \left[ \sum_{k=i}^4 a_k^{-2} (\mu_{k+1} - \mu_k) \rho_{3k} \sin \phi_{3k} \right]^2 \right\}^{-1/2} \quad (15)$$

The number of molecules experiencing a value of the normalized variable  $t_i$  between  $t$  and  $t + dt$  is  $n(t) dt$ . This field distribution function is shown in Fig. 7 for the interior (first) region. For the third region the distribution depends upon  $(a_2/a_3)$  and resembles the distributions graphed in Fig. 6.

The first-order effect of imperfections on the average magnetic fields experienced by the nuclei in regions 1 and 3 under rapid spinning conditions may be summarized as follows. In region 1 there is an effective broadening of the resonance line width with a single maximum (see Fig. 7). In region 3 there is a narrow spectral distribution of Larmor frequencies similar in shape to the distribution shown in Fig. 6.

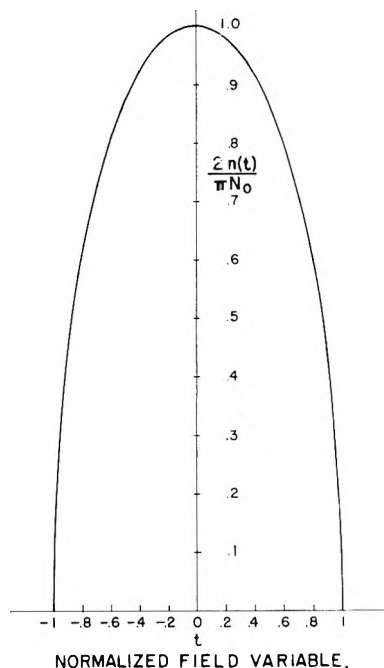


Fig. 7.—Particle density vs. average field strength (spinning system).

It should be observed that it is only imperfections exterior to a given region which affect that region. Moreover, the effect of imperfections in the *i*th boundary decreases as the inverse square of the radius of that boundary. It follows that the inner surfaces of both tubes in the coaxial system must be particularly precise.

**Effect of Tilting the Coaxial System.**—If a perfect tube system makes an angle  $\neq \pi/2$  with the magnetic field lines, then the average field strength in the *i*th region can be shown to be

$$H_i = [1 - 1/2(\mu_i - \mu_5)] H_0 + 1/2 \sin^2 \beta (\mu_i - \mu_5) H_0 \quad (16)$$

where  $\beta$  is the complement of the angle between the field lines and the axis of the tubing. Hence, there is a uniform shift of the average field by an amount

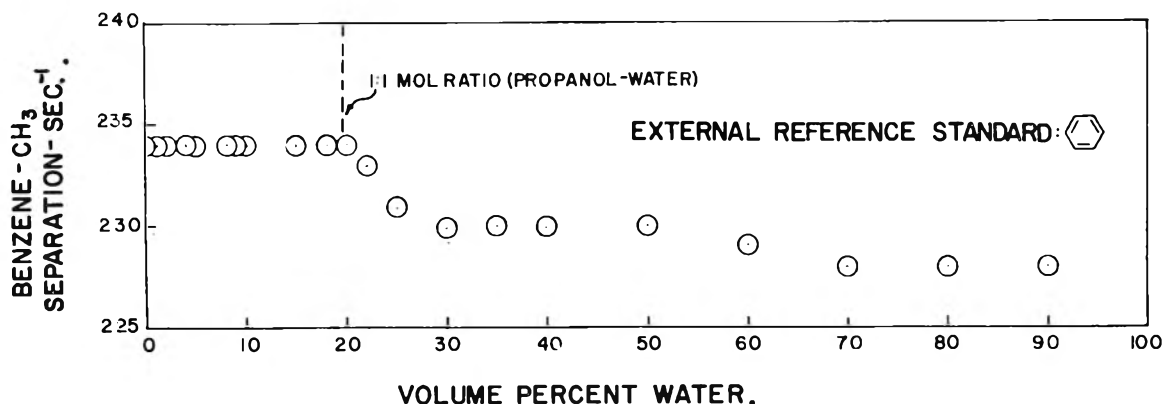


Fig. 8.—Susceptibility shift of water-propanol system.

$$\frac{1}{2} \sin^2 \beta (\mu_i - \mu_s) H_0 \approx \frac{1}{2} \beta^2 (\mu_i - \mu_s) H_0 \quad (17)$$

One might attempt to deduce this result from the perturbation theory by assuming that the effect of tilting is to distort the circular cross-sections into ellipses. If  $\beta$  is assumed small, this approach results in a field shift of

$$\frac{1}{4} [ \frac{1}{2} \beta^2 (\mu_i - \mu_s) H_0 ]$$

which depends in the same way on the parameters as does the correct result.

It, therefore, seems reasonable that the effect of tilting only one of the tubes can be roughly calculated in the same way. This results in the conclusion that the average fields in the first and third regions are shifted with respect to one another by roughly an amount

$$\frac{1}{2} \beta^2 (\mu_i - \mu_s) H_0 \quad (18)$$

The condition that this displacement be negligible together with the condition that the broadening effects previously considered be unimportant imposes rather stringent requirements on the precision of the glass tubing to be used in such a coaxial system of standardization. The required precision can be estimated from the preceding mathematical expressions.

### Conclusion

The use of internal reference standards does (a) permit simultaneous sweeping of the field or frequency spectrum for the reference standard and unknown sample and (b) make susceptibility corrections presumably common to both the reference and sample molecular systems. However, errors as large as several parts in  $10^7$  in chemical shift values for intramolecular hydrogen nuclei can arise from intermolecular effects. Hence, internal standardization methods should be used only with extreme caution. Chemical shift measurements, without quantitative corrections for molecular interaction effects, can lead to erroneous interpretations of data.

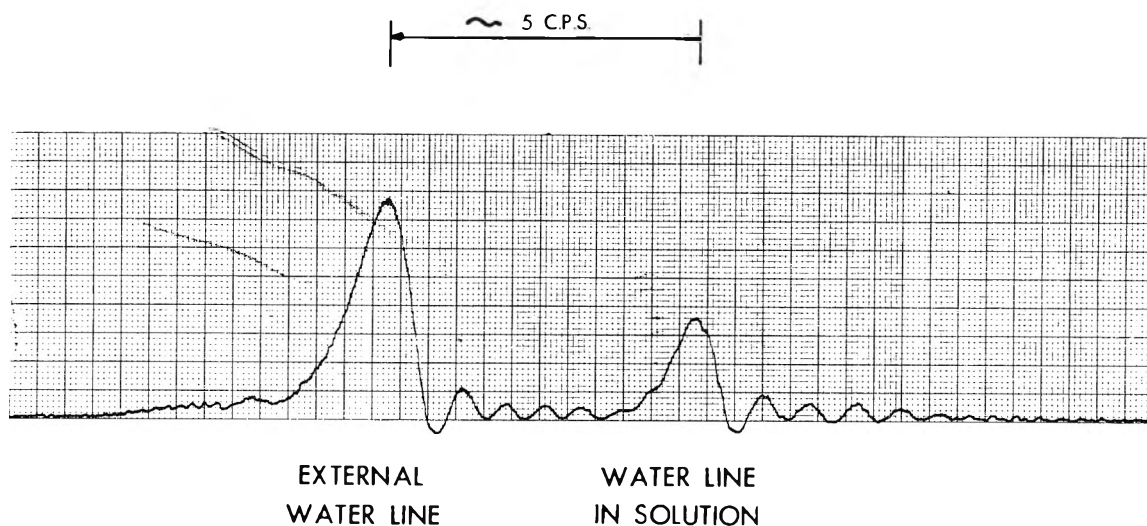
External reference standard measurements of pure monomolecular systems can be made (a) without polluting the pure system and (b) without introducing intermolecular effects arising from the presence of the reference standard compound. Association effects of a monomolecular species are not separable from "isolated" molecular chemical shifts except by an independent experiment but this is also true in internal reference standard

procedures. In external referencing for the case of cylindrically shaped samples, it is necessary to correct for magnetic susceptibilities of the reference and sample compounds. It should be emphasized that in the case of mixtures proper corrections for susceptibilities can become troublesome. The validity of simple extrapolation procedures often employed to correct for susceptibilities of mixtures is questionable. A plot of the position of the methyl group in *n*-propanol-water mixtures with respect to an external standard is shown in Fig. 8 to illustrate this point.

The primary problem in the use of an external referencing procedure is to be certain that both reference and unknown systems are subjected to a common effective external magnetic field. An accurate spinning coaxial system for external referencing has been developed at our laboratories which limits the errors arising from tube imperfections to less than 1 part in  $10^3$ . Any sharp line reference standard may be used in this system at the mere convenience of the observer. Side-band modulation techniques for frequency comparisons are utilized. Ultimate limitations of the accuracy of this system are determined by the width of the resonance lines, the field sweep rate, and the accuracy of the modulating audio source. A typical spectral display of this external referencing procedure is shown in Fig. 9. Here the external reference standard is water; the sample spectrum is the water line in a pyridine-water mixture.

Line broadening in the reference and sample compounds due to glass tubing imperfections has been considered under both static and spinning conditions. Certain line broadening phenomena are predicted in theory and observed experimentally which cannot be erased by rapid spinning of the coaxial system. This is due to the fact that the inhomogeneities in field strength due to imperfections of the tubing are not static if the system is spinning. The effects of tube tilting have been considered to show that the average fields in the reference and sample compound regions are shifted with respect to one another. Experimental measurements show that even in selected standard glass stock for the coaxial system, field shifts are often as large as 1 part in  $10^7$ .

The condition that the effects, line broadening and average field shifts, be negligible impose rather stringent requirements on the precision of the glass



### No Correction For Susceptibilities

Fig. 9.—Comparison of external reference water resonance with water resonance in pyridine solution.

tubing to be used in such a coaxial system of standardization. However, such a precise coaxial system is now readily available to n.m.r. spectroscopists.<sup>12</sup> This external standardization method for nuclear resonance spectra does give a practical means of

permitting reliable data exchange between research laboratories.

(12) The Wilmad Glass Company, Landisville, New Jersey, has recently marketed a precision coaxial glass system which fulfills the requirements necessary for accurate chemical shift measurements.

## LOW TEMPERATURE CALORIMETRIC STUDIES OF SEVEN 1-OLEFINS: EFFECT OF ORIENTATIONAL DISORDER IN THE SOLID STATE

BY J. P. McCULLOUGH, H. L. FINKE, M. E. GROSS, J. F. MESSERLY AND GUY WADDINGTON

Contribution No. 60 from the Thermodynamics Laboratory, Petroleum Experiment Station, Bureau of Mines, U. S. Department of the Interior, Bartlesville, Oklahoma

Received August 22, 1956

From low temperature calorimetric measurements, values of the heat capacities in the solid and liquid states and of the heats and temperatures of phase changes were obtained for the following compounds: 1-hexene, 1-heptene, 1-octene, 1-decene, 1-undecene, 1-dodecene and 1-hexadecene. Values of the entropy and other thermodynamic properties of each compound were calculated at selected temperatures in the range 10 to 360°K. The thermal behavior of this series of 1-olefin hydrocarbons is more complex than that of the corresponding series of *n*-paraffins. By comparing the entropy values of 1-olefins with those of the *n*-paraffins, it was found that 1-undecene, 1-dodecene and 1-hexadecene crystallize in a state of orientational disorder. In 1-hexadecene crystals, virtually complete end-for-end disorder occurs. Because 1-undecene and higher 1-olefins do not form perfect crystals, the Third Law cannot be used to calculate absolute entropy values from the experimental data for these three compounds. However, the results reported here and elsewhere for the C<sub>5</sub> to C<sub>16</sub> hydrocarbons, inclusive, show that the entropy of these 1-olefins in the liquid state at 298.16°K. is 0.19 ± 0.02 cal. deg.<sup>-1</sup> mole<sup>-1</sup> less than that of the corresponding *n*-paraffins. Thus, reliable values of the entropy of the higher 1-olefins may be calculated by subtracting 0.19 cal. deg.<sup>-1</sup> mole<sup>-1</sup> from the entropy value of the corresponding *n*-paraffin. The experimental and calculated entropy values of the 1-olefin hydrocarbons from 1-octene to 1-hexadecene are represented within 0.04% by the equation,  $S_{\text{intd.}}(\text{liq.}, 298.16^\circ\text{K.}) = 24.349 + 7.725 N \text{ cal. deg.}^{-1} \text{ mole}^{-1}$ , where *N* is the number of carbon atoms in the molecule.

Entropy data for selected members of homologous series of compounds found in petroleum are determined from low temperature calorimetric measurements as part of the program of this Laboratory. A recent study of the nine normal paraffin hydrocarbons from *n*-octane to *n*-hexadecane<sup>1</sup> showed, for the liquid state, that the increment of entropy per CH<sub>2</sub> group is constant above *n*-octane (7.725 ± 0.04 cal. deg.<sup>-1</sup> mole<sup>-1</sup> at 298.16°K.). The results of this investigation provided essential data

for calculation and compilation of the thermodynamic properties of the normal paraffins through *n*-tetracontane.<sup>2,3</sup> Low temperature calorimetric studies of selected 1-olefin hydrocarbons have been made to obtain data needed for similar calculations of the thermodynamic properties of the homologous series of 1-olefins. Results obtained for the following compounds are presented in this paper: 1-hex-

(2) W. B. Person and G. C. Pimentel, *ibid.*, **75**, 532 (1953).

(3) American Petroleum Institute Research Project 44, "Selected Values of Physical and Thermodynamic Properties of Hydrocarbons and Related Compounds," Carnegie Press, Carnegie Institute of Technology, Pittsburgh, Pennsylvania, 1953.

(1) H. L. Finke, M. E. Gross, Guy Waddington and H. M. Huffman, *J. Am. Chem. Soc.*, **76**, 333 (1954).

ene, 1-heptene, 1-octene, 1-decene, 1-undecene, 1-dodecene and 1-hexadecene.<sup>4</sup> Of the foregoing compounds, low temperature thermal data have been reported previously for 1-heptene<sup>5</sup> only.

The calorimetric investigations described in this paper gave, for each compound, values of the heat capacity in the solid and liquid states in the range 11 to 360°K. and values of the latent heats and temperatures of isothermal phase changes. From the observed data were calculated values of the free energy function, heat content function, heat content, entropy and heat capacity of the condensed phases at selected temperatures from 10 to 360°K. Details of the calorimetric studies and complete experimental results are given in the Experimental section at the end of this paper.

### Discussion of Results

In studies of an homologous series of compounds, it is to be expected that physical and thermodynamic properties will vary regularly with molecular size. Many regularities were found in the thermal properties of the *n*-paraffins from C<sub>5</sub> to C<sub>16</sub>.<sup>1</sup> For example, the entropy values in the liquid state were found to be linear functions of chain length. Also, it was found that each of the odd-numbered compounds (C<sub>9</sub>, C<sub>11</sub>, C<sub>13</sub> and C<sub>15</sub>) undergoes an enantiotropic transition in the solid state, while none of the even-numbered compounds studied exhibits such behavior. For the odd-numbered compounds the entropies of fusion and transition and the triple point and transition temperatures are smooth, nearly linear functions of chain length. The entropies of fusion and triple point temperatures of the even-numbered compounds also are smooth functions of chain length. Because the molecular structures of *n*-paraffins and 1-olefins are similar in many respects, analogous regularity might be expected for the latter; however, the thermal data for the 1-olefins show much less regularity than was found for the *n*-paraffins. The most important

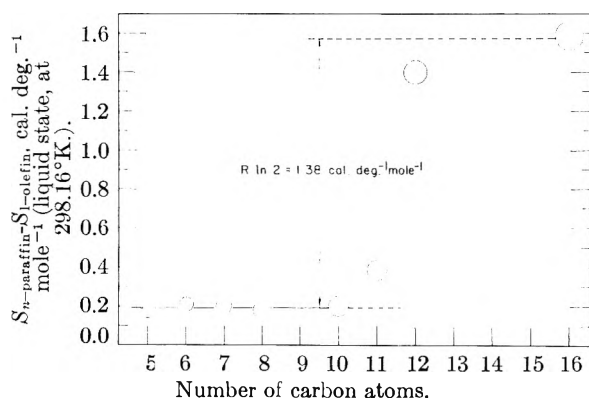


Fig. 1.—The entropy difference between liquid *n*-paraffins and 1-olefins at 298.16°K. as a function of number of carbon atoms. The diameters of the circles represent 0.1% of the observed entropy values for each pair of hydrocarbons.

(4) An attempt was made to determine the low temperature thermal properties of 1-nonene. Anomalous results were obtained in the melting region, and the study was discontinued. Anomalous results also were obtained in a study of the melting point of 1-pentene [S. S. Todd, G. D. Oliver and H. M. Huffman, *J. Am. Chem. Soc.*, **69**, 1519 (1947)]. Reinvestigations of these two compounds are planned.

(5) G. S. Parks, S. S. Todd and C. H. Shomate, *ibid.*, **58**, 2505 (1936).

dissimilarity in the results for the two groups of hydrocarbons is discussed in the following section.

**The Entropy of 1-Olefins and the Effect of Orientational Disorder in the Solid State.**—Values of the thermodynamic functions of seven 1-olefin hydrocarbons in the solid and liquid states are listed in Table VIII of the Experimental section. The entropies of the 1-olefins and *n*-paraffins in the liquid state at 298.16°K. are compared in Fig. 1. Because of the similarity in molecular structures, the entropy of each 1-olefin would be expected to differ from that of the corresponding *n*-paraffin by a constant amount for hydrocarbon chains as long as these. In other words, the increment of entropy per CH<sub>2</sub> group should be the same in the 1-olefin series as in the *n*-paraffin series. The results depicted in Fig. 1 show that from C<sub>5</sub> to C<sub>10</sub> the entropy value of a 1-olefin is  $0.19 \pm 0.02$  cal. deg.<sup>-1</sup> mole.<sup>-1</sup> less than that of the corresponding *n*-paraffin, a difference that is constant well within the accuracy uncertainty assigned to the experimental data. For the C<sub>11</sub> and higher hydrocarbons the difference is significantly greater.

In a paper on the thermodynamic properties of 1-butene, Guttman and Pitzer<sup>6</sup> stated: "It remains to be determined how long a 1-olefin molecule must be before random orientation will occur in the crystals." The end-for-end disorder that is possible in 1-olefin crystals could result in a residual entropy of  $R \ln 2$  at 0°K., and the measured entropy would be  $R \ln 2$  less than the true entropy. As shown in Fig. 1 the entropy of 1-hexadecene is almost exactly  $R \ln 2$  (1.38 cal. deg.<sup>-1</sup> mole.<sup>-1</sup>) less than the value that would be expected on the basis of the data for the C<sub>5</sub> to C<sub>10</sub> hydrocarbons. Thus, the results of this investigation show that random orientation does occur in the crystals of 1-undecene and higher 1-olefins. The results suggest that 1-undecene and 1-dodecene crystallize in a partially ordered state, but that 1-hexadecene crystallizes in a state of complete end-for-end disorder.

No evidence was obtained that the results were affected by the thermal treatment of the samples. It is possible that *extremely* slow crystallization of 1-undecene would have produced ordered crystals, but the procedures actually used always gave partially disordered crystals. In one experiment, 1-decene was crystallized as rapidly as possible, but the thermal properties of the crystals so obtained did not differ from those of ordered crystals obtained from a slower crystallization.

Because perfectly ordered crystals were not obtained in the studies of 1-undecene, 1-dodecene and 1-hexadecene, the Third Law cannot be used to compute absolute entropy values from the experimental data. Therefore, the thermodynamic properties given in Table VIII are *not absolute values*, but are *relative* to the disordered crystals at 0°K. The results obtained for the lower 1-olefins show that reliable entropy values of 1-undecene and higher 1-olefins can be computed by subtraction of 0.19 cal. deg.<sup>-1</sup> mole.<sup>-1</sup> from the entropy values of the corresponding *n*-paraffins.

Values of the entropy in the liquid state at 298.16°K. of 1-olefin and *n*-paraffin hydrocarbons

(6) L. Guttman and K. S. Pitzer, *ibid.*, **67**, 324 (1945).

from  $C_5$  to  $C_{16}$  are listed in Table I. The data for the *n*-paraffins and for 1-pentene, 1-hexene, 1-heptene, 1-octene and 1-decene are experimental values. The data for 1-nonene, 1-undecene and higher 1-olefins were computed by subtracting 0.19 cal. deg.<sup>-1</sup> mole<sup>-1</sup> from the entropy value of the corresponding *n*-paraffin. The entropy values given in Table I for the 1-olefins from  $C_8$  to  $C_{16}$ , inclusive, are represented within 0.04% by the equation

$$S_{\text{satd}}(\text{liq.}, 298.16^\circ\text{K.}) = 24.349 + 7.725N \text{ cal. deg.}^{-1} \text{ mole}^{-1}$$

where  $N$  is the number of carbon atoms in the 1-olefin chain.

#### Polymorphism in the 1-Olefin Hydrocarbons.

In contrast with the behavior of *n*-paraffins, both even and odd 1-olefins exhibit polymorphism, as may be seen by inspecting Fig. 2 and Table VIII of the Experimental part. Only two of the 1-olefins—1-hexene and 1-octene—do not show polymorphism. Two crystalline modifications of 1-heptene were obtained, and each was studied from 11°K. to its triple point. Three of the compounds—1-decene, 1-undecene and 1-dodecene—exhibit enantiotropic polymorphism, with first-order transitions 8, 6 and 25° below their respective triple points. The last compound of this series, 1-hexadecene, undergoes a second-order transition of the lambda type with maximum absorption of energy about 30° below the triple point.

TABLE I

THE MOLAL ENTROPIES IN THE LIQUID STATE AT 298.16°K. OF THE 1-OLEFIN AND *n*-PARAFFIN HYDROCARBONS FROM  $C_5$  TO  $C_{16}$ , IN CAL. DEG.<sup>-1</sup>

| No. carbon atoms | 1-Olefin <sup>a</sup>     | <i>n</i> -Paraffin <sup>a</sup> | $\Delta S^b$ |
|------------------|---------------------------|---------------------------------|--------------|
| 5                | 62.75 ± 0.20 <sup>c</sup> | 62.92 <sup>d</sup>              | 0.17         |
| 6                | 70.55 ± .14               | 70.76 ± 0.14 <sup>c</sup>       | .21          |
| 7                | 78.31 ± .15               | 78.51 ± .15 <sup>f</sup>        | .20          |
| 8                | 86.15 ± .17               | 86.33 ± .17 <sup>g</sup>        | .18          |
| 9                | 93.90 <sup>h</sup>        | 94.09 ± .19 <sup>g</sup>        |              |
| 10               | 101.58 ± .20              | 101.79 ± .20 <sup>g</sup>       | .21          |
| 11               | 109.31 <sup>h</sup>       | 109.50 ± .22 <sup>g</sup>       |              |
| 12               | 117.08 <sup>h</sup>       | 117.27 ± .23 <sup>g</sup>       |              |
| 13               | 124.78 <sup>h</sup>       | 124.97 ± .25 <sup>g</sup>       |              |
| 14               | 132.56 <sup>h</sup>       | 132.75 ± .26 <sup>g</sup>       |              |
| 15               | 140.23 <sup>h</sup>       | 140.42 ± .28 <sup>g</sup>       |              |
| 16               | 147.91 <sup>h</sup>       | 148.10 ± .29 <sup>g</sup>       |              |

<sup>a</sup> The uncertainty indicated is the estimated accuracy uncertainty. <sup>b</sup>  $\Delta S$  is the difference in observed entropy between a 1-olefin and the corresponding *n*-paraffin. <sup>c</sup> S. S. Todd, G. D. Oliver and H. M. Huffman, *J. Am. Chem. Soc.*, 69, 1519 (1947). <sup>d</sup> Ref. 3, Table 1p. <sup>e</sup> D. R. Douslin and H. M. Huffman, *J. Am. Chem. Soc.*, 68, 1704 (1946). <sup>f</sup> Unpublished datum, this Laboratory. <sup>g</sup> Ref. 1. <sup>h</sup> Values calculated by subtraction of 0.19 cal. deg.<sup>-1</sup> mole<sup>-1</sup> from the entropy values listed for the corresponding *n*-paraffin.

Results were obtained for two distinct polymorphs of 1-heptene (see Experimental part, Tables II, V and VI), and measurements were made on each from 11°K. to its triple-point temperature (153.89 and 154.30°K.). The lower melting polymorph, designated crystals II, was always obtained on initial crystallization, and the higher-melting form, crystals I, was obtained only by melting more than 50% of II and allowing the sample to warm to the melting point of I before recrystallization. The heat of fusion of crystals I is 57 cal.

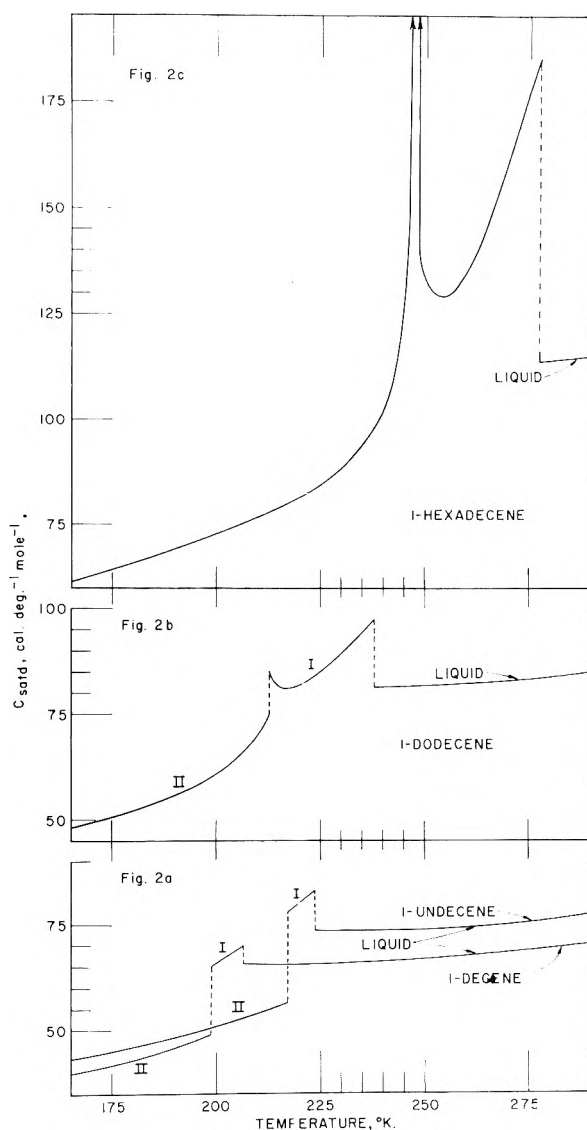


Fig. 2.—Portions of the heat capacity curves ( $C_{\text{satd.}}$  vs.  $T$ ) for 1-decene and 1-undecene (2a), 1-dodecene (2b) and 1-hexadecene (2c). The temperatures at which isothermal phase changes occur are indicated by vertical dashed lines.

mole<sup>-1</sup> less than that of crystals II, and the heat capacity of crystals I is several tenths of a per cent. greater than that of crystals II at all temperatures below the "premelting" region.

Calculation of the free energy difference between the two forms shows that the higher melting form, crystals I, is stable above 137°K., and that the lower melting form, crystals II, is stable below this temperature.<sup>7</sup> No experimental evidence of a transition near 137°K. was found. Evidently, the transformation between crystals II and crystals I occurs at a detectable rate only if a liquid phase is present.

The entropy of 1-heptene in the liquid state was calculated from data for both polymorphs, and the results differed by only 0.06 cal. deg.<sup>-1</sup> mole<sup>-1</sup>. Consequently, it is probable that both enantiotropic forms of 1-heptene are "perfect" crystals.

(7) To minimize the effect of experimental errors on the results of this calculation, the observed heat capacity and heat of fusion data given in the Experimental part were used to calculate the free energy of each polymorph relative to the liquid at 160°K.

The plots of heat capacity,  $C_{\text{satd}}$ , as a function of absolute temperature,  $T$ , given in Fig. 2 show the solid-state phenomena observed for the higher 1-olefins. In this figure and the following discussion, roman numeral I refers to crystals stable at high temperatures, and roman numeral II refers to crystals stable at low temperatures.<sup>8</sup> The transitions in 1-decene and 1-undecene (Fig. 2a) occur isothermally, and the heat capacity data for crystals II of these compounds show only slight upward curvature below the transition point. The transition in 1-dodecene (Fig. 2b) also occurred isothermally, in part, but the plot for crystals II shows appreciable upward curvature in this case. Also, the minimum in the heat capacity curve for 1-dodecene crystals I is similar in appearance to the high-temperature side of a lambda transition. A typical lambda transition is shown by the heat capacity curve of 1-hexadecene (Fig. 2c).

The isothermal entropies of transition for 1-decene and 1-undecene are about 10 cal. deg.<sup>-1</sup> mole<sup>-1</sup>, but the isothermal entropy of transition of 1-dodecene is only 5.11 cal. deg.<sup>-1</sup> mole<sup>-1</sup> (Table IV of the Experimental part). However, the non-isothermal entropy increases associated with the transitions in 1-dodecene and 1-hexadecene, estimated from the abnormal increase in heat capacity of these compounds, are 3.7 and 8.3 cal. deg.<sup>-1</sup> mole<sup>-1</sup>, respectively. These estimates show that the total entropies of transition are at least of the same order of magnitude for all four compounds. Consequently, it is probable that the same changes occur during the solid-state transitions in each of these 1-olefins, but the portion of the process that occurs isothermally decreases with increasing chain length. Crystallographic investigations that would permit an explanation of the thermal behavior of the 1-olefins have not yet been made. It is apparent from the results of this study that the regular alternation of structure found for the normal paraffins<sup>1,9</sup> is not duplicated in the 1-olefins.

A phenomenon termed "prerotation"<sup>10</sup> has been observed in the  $n$ -paraffins by means of thermal,<sup>1,11</sup> dielectric constant<sup>10,12</sup> and X-ray<sup>9</sup> studies. "Prerotation" is believed to cause the pronounced increase in heat capacity below the melting points of  $n$ -paraffins,<sup>1,11</sup> and such an effect might be expected in the 1-olefins. The proximity of the transitions and melting points of 1-decene and higher 1-olefins might obscure the effect of "prerotation" for these compounds. However, the heat capacity data for 1-hexene, 1-heptene and 1-octene, which do not undergo transitions, show no increase that cannot be attributed to premelting effects. It must be concluded, then, that the phenomenon of "prerotation" does not occur in these 1-olefins to the extent that it does in the corresponding  $n$ -paraffins. The melting points of 1-olefins are low compared to

those of  $n$ -paraffins, and it is probable that the crystal lattice of a 1-olefin does not expand sufficiently below the melting point to allow "prerotation" to take place.

**The Unusual Thermal Behavior of 1-Decene.**—The thermal behavior of 1-decene was more complex than is indicated by the results shown in Fig. 2a. It was possible to supercool the sample through the transition at 198.3°K., and below 190°K., supercooled crystals I transposed to another modification designated *metastable* crystals II. In attempts to determine the heat of transition between metastable crystals II and supercooled crystals I, the sample rapidly underwent further transformation to *stable* crystals II. The heat capacity of metastable crystals II was measured from 11 to 185°K. These results were uniformly 0.2% higher than those for stable crystals II, and they are not reported in this paper because the heat of the transition near 190°K. was not determined.

Unusual thermal behavior also was observed near the melting point of 1-decene and was believed at first to be evidence of polymorphism. As shown in Fig. 3a and Table II, two different and reproducible sets of heat capacity values were found between the transition at 198.3°K. and the triple point at 206.89°K. The two curves represent the heat capacity of crystals obtained directly from the liquid, curve IA, and from crystals II, curve IB. Two different and reproducible melting point curves were obtained, as shown in Fig. 3b, where the equilibrium melting temperatures,  $T$ , are plotted against the reciprocal of the fraction of sample melted,  $1/F$ . Melting point curves A and B were obtained on crystals that correspond to heat capacity curves IA and IB, respectively. The triple point temperatures obtained by extrapolation to  $1/F = 0$  agree within 0.003°.

It is believed that the results obtained near the melting point of 1-decene depended upon the extent to which the impurity formed a solid-solution. The A crystals were obtained by relatively fast crystallization. In a rapid crystallization it is possible that differences in the relative rates of deposition of impurity and 1-decene would result in crystals that contain *less* than equilibrium amounts of impurity *in solid-solution*. The impurity would then behave effectively as a *solid-insoluble* impurity, giving a more nearly linear melting curve (A) and raising the heat capacity curve (IA). On the other hand, if the crystals were held in the premelting region (10–20° below the melting point), it is possible that the impurity would slowly enter into solid-solution. These conditions were met in obtaining the B crystals; that is, to effect complete transposition to crystals II, the sample was held a few degrees below the transition temperature for several weeks. If the impurity did go into solid-solution in this period, the heat capacity values obtained after transposition to crystals I, curve (IB), would be lower because the effect of premelting would be smaller. Also, the melting point curve (B) would be higher and would show definite curvature.

Although the foregoing assumptions cannot be justified conclusively, a quantitative test was ob-

(8) This system of nomenclature of polymorphic forms is the reverse of that used in previous publications from this Laboratory. It is the system used in the International Critical Tables and in ref. 3.

(9) A. Müller, *Proc. Roy. Soc. (London)*, **A127**, 417 (1930); **A136**, 514 (1932).

(10) C. P. Smyth, *Trans. Faraday Soc.*, **42A**, 175 (1946).

(11) A. R. Ubbelohde, *ibid.*, **34**, 282 (1938).

(12) J. P. Hoffman and C. P. Smyth, *J. Am. Chem. Soc.*, **71**, 431 (1949); **71**, 3591 (1949); **72**, 171 (1950).

tained in the application of premelting corrections to the heat capacity data. *Upper limits* for the amount of *solid-insoluble* impurity calculated from a straight line through  $1/F$  values 4 and 10 are 0.09 and 0.05 mole % for curves A and B, respectively. When the heat capacity values for crystals IA and IB were corrected for premelting on the basis of 0.085 and 0.035 mole % solid-insoluble impurity, respectively, the results fell on a single straight line, curve IC of Fig. 3a. It is unlikely that data for true allotropic crystals could be reduced to the same "corrected" curve by using such reasonable values for the amount of solid-insoluble impurity. The fact that five experimental values of the heat of fusion agreed within the expected accuracy uncertainty (Table V) whether the initial crystals were A or B also indicates that A and B are *not* polymorphic.<sup>13</sup>

### Experimental

**Physical Constants.**—The 1951 International Atomic Weights<sup>14</sup> and the 1951 values of the fundamental physical constants<sup>15</sup> were used. Measurements of temperature were made with platinum-resistance thermometers calibrated in terms of the International Temperature Scale<sup>16</sup> from 90 to 400°K., and International Celsius Temperatures were converted to Kelvin Temperatures by addition of 273.16°. From 11 to 90°K., temperature measurements were made in terms of the provisional scale of the National Bureau of Standards.<sup>17</sup> Measurements of mass, potential and resistance were made in terms of standard devices calibrated at the National Bureau of Standards. Time measurements were made with an electric stopclock driven by 50 cycle alternating current obtained from the amplified output of a vacuum tube precision fork. The frequency of the current was constant within  $\pm 0.002\%$ , as determined by comparison with time signals from radio station WWV. Energy was measured in terms of international joules and converted to calories by the relation, 1 cal. = 4.1833 int. j.

**The Materials.**—The materials used in this investigation were A.P.I. Research samples.<sup>18</sup> With the exception of the sample of 1-hexadecene, the purities of these samples were above 99.7 mole %, as determined in calorimetric melting point studies described in another part of this paper. The samples were received in sealed ampoules with internal break-off tips and were transferred to the calorimeter by vacuum distillations. The samples of 1-hexene, 1-heptene and 1-octene were dried in the liquid phase with calcium hydride. Because the samples of 1-decene, 1-undecene, 1-dodecene and 1-hexadecene showed only traces of ice "floaters" on freezing and remelting, these materials were not dried.

**The Apparatus.**—All measurements were made in the apparatus described by Huffman and co-workers.<sup>19</sup> In each

(13) A presentation of somewhat similar results for 1-methylnaphthalene and *cis*-decahydronaphthalene will be given in a forthcoming publication from this Laboratory.

(14) E. Wichers, *J. Am. Chem. Soc.*, **74**, 2447 (1952).

(15) F. D. Rossini, F. T. Gucker, Jr., H. L. Johnston, L. Pauling and G. W. Vinal, *ibid.*, **74**, 2699 (1952).

(16) H. F. Stinson, *J. Research Natl. Bur. Standards*, **42**, 209 (1949).

(17) H. J. Hoge and F. G. Brickwedde, *ibid.*, **22**, 351 (1939).

(18) These samples of API-Research hydrocarbons were made available through the American Petroleum Institute Research Project 44 on the "Collection, Analysis and Calculation of Data on Properties of Hydrocarbons" and were purified by the American Petroleum Institute Research Project 6 on the "Analysis, Purification and Properties of Hydrocarbons" from materials supplied by the following laboratories: 1-hexene, 1-heptene and 1-undecene, by the American Petroleum Institute Research Project 45 at the Ohio State University, Columbus, Ohio; and 1-octene, 1-decene, 1-dodecene and 1-hexadecene, by the American Petroleum Institute Research Project 6 at the Carnegie Institute of Technology, Pittsburgh, Pa.

(19) (a) R. A. Ruehrwein and H. M. Huffman, *J. Am. Chem. Soc.*, **65**, 1620 (1943); (b) G. D. Oliver, M. Eaton and H. M. Huffman, *ibid.*, **70**, 1502 (1948).

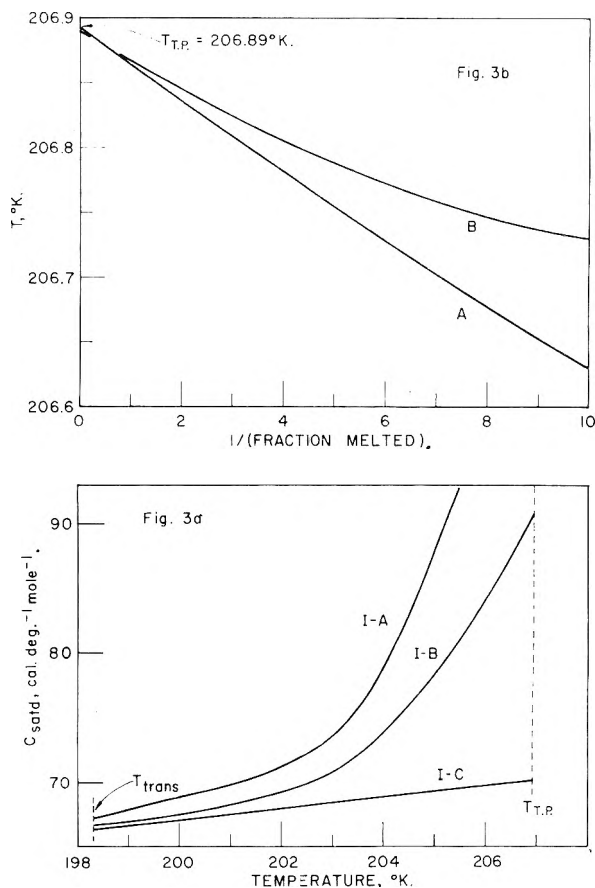


Fig. 3.—The heat capacity of 1-decene between the transition point and triple point temperatures (3a) and the observed melting point curves (3b).

study about 55 ml. of material was sealed in a copper calorimeter that contained horizontal, perforated copper disks to promote thermal equilibration and to prevent settling of the solid phase during fusion experiments. About 30 mm. helium pressure (at room temperature) was left in the calorimeter to promote thermal equilibration at low temperatures.

**The Heat Capacities in the Solid and Liquid States.**—Measurements were made of the heat capacity of each 1-olefin in the solid and liquid states in the range 11 to 360°K. The observed values of heat capacity at saturation pressure,  $C_{\text{satd}}$ , are recorded in Table II. The temperature increments employed in the measurements were small enough to obviate the need of corrections for non-linear variation of  $C_{\text{satd}}$  with  $T$ , except as noted in Table II. The precision of the heat capacity measurements was, in general,  $\pm 0.1\%$ , and above 30°K., the accuracy uncertainty should not exceed 0.2%. In some cases, the data for the heat capacity in the solid state may be less accurate near phase changes because of rapid changes of  $C_{\text{satd}}$  with  $T$ , slow equilibration, or uncertainties introduced by the presence of impurity. The data in Table II have not been corrected for premelting caused by impurity.

Two crystalline forms of 1-heptene were obtained, and data for both forms are listed in Table II. Crystals II were always obtained on first crystallizing 1-heptene. Crystals I were obtained only by melting more than 50% of II, after which treatment the sample warmed spontaneously to the melting point of I. Recrystallization then produced crystals I. Although these crystals are probably enantiotropic with a transition point near 137°K., it was possible to study each form from 11°K. to its triple point, and no direct evidence of transformation between the two forms was found except in the melting region.

Empirical cubic equations were obtained to represent the heat capacity of each compound in the liquid state. The constants for these equations are listed in Table III.

TABLE II  
THE MOLAL HEAT CAPACITIES OF SEVEN 1-OLEFIN HYDROCARBONS IN CAL. DEG. <sup>-1</sup>

| T, °K. <sup>a</sup> | ΔT <sup>b</sup> | C <sub>calc</sub> <sup>c</sup> | T, °K. <sup>a</sup> | ΔT <sup>b</sup> | C <sub>calc</sub> <sup>c</sup> |
|---------------------|-----------------|--------------------------------|---------------------|-----------------|--------------------------------|
| 1-Hexene            |                 |                                |                     |                 |                                |
| Crystals            |                 |                                |                     |                 |                                |
|                     |                 | 96.61                          | 8.085               | 18.430          |                                |
|                     |                 | 97.07                          | 5.570               | 18.536          |                                |
| 11.27               | 1.268           | 0.566                          | 102.53              | 5.349           | 19.230                         |
| 11.53               | 1.172           | .611                           | 104.46              | 7.619           | 19.458                         |
| 12.66               | 1.543           | .817                           | 104.58              | 5.694           | 19.474                         |
| 12.84               | 1.466           | .858                           | 110.16              | 5.482           | 20.173                         |
| 14.21               | 1.566           | 1.121                          | 112.33              | 8.128           | 20.455                         |
| 14.46               | 1.780           | 1.180                          | 120.26              | 7.735           | 21.454                         |
| 15.83               | 1.365           | 1.468                          | 127.41              | 6.549           | 22.578                         |
| 16.24               | 1.777           | 1.567                          |                     |                 |                                |
| 17.61               | 1.888           | 1.886                          |                     |                 |                                |
| 18.18               | 2.098           | 2.029                          |                     |                 |                                |
| 19.59               | 2.064           | 2.396                          | 135.19              | 3.932           | 36.88                          |
| 20.32               | 2.175           | 2.582                          | 140.60              | 4.898           | 36.85                          |
| 21.69               | 2.123           | 2.961                          | 142.88              | 5.895           | 36.85                          |
| 22.49               | 2.175           | 3.188                          | 146.95              | 7.794           | 36.86                          |
| 24.04               | 2.569           | 3.616                          | 148.76              | 5.862           | 36.89                          |
| 24.79               | 2.411           | 3.830                          | 154.71              | 7.739           | 36.93                          |
| 26.72               | 2.785           | 4.378                          | 159.41              | 9.621           | 36.95                          |
| 27.63               | 3.260           | 4.642                          | 163.38              | 9.594           | 37.00                          |
| 29.57               | 2.887           | 5.190                          | 168.98              | 9.532           | 37.09                          |
| 30.62               | 2.703           | 5.502                          | 178.94              | 10.381          | 37.28                          |
| 33.37               | 2.796           | 6.283                          | 189.27              | 10.269          | 37.54                          |
| 37.03               | 4.517           | 7.296                          | 199.48              | 10.150          | 37.88                          |
| 41.21               | 3.838           | 8.392                          | 209.56              | 10.027          | 38.27                          |
| 45.09               | 3.936           | 9.354                          | 219.53              | 9.899           | 38.71                          |
| 49.69               | 5.259           | 10.443                         | 229.36              | 9.768           | 39.21                          |
| 53.84               | 3.978           | 11.357                         | 239.50              | 10.508          | 39.76                          |
| 55.02               | 5.435           | 11.607                         | 245.76              | 10.434          | 40.13                          |
| 58.70               | 5.742           | 12.366                         | 256.11              | 10.258          | 40.78                          |
| 64.17               | 5.195           | 13.443                         | 266.29              | 10.095          | 41.46                          |
| 69.46               | 5.391           | 14.374                         | 276.71              | 10.755          | 42.20                          |
| 74.77               | 5.226           | 15.258                         | 287.38              | 10.571          | 42.99                          |
| 80.24               | 5.704           | 16.145                         | 297.86              | 10.394          | 43.78                          |
| 85.77               | 5.370           | 17.015                         | 308.16              | 10.217          | 44.63                          |
| 91.37               | 5.831           | 17.798                         |                     |                 |                                |
| Liquid              |                 |                                |                     |                 |                                |
| 1-Heptene           |                 |                                |                     |                 |                                |
| Crystals II         |                 |                                |                     |                 |                                |
|                     |                 | 22.13                          | 2.139               | 3.349           |                                |
|                     |                 | 23.33                          | 2.265               | 3.705           |                                |
| 11.40               | 1.164           | 0.629                          | 24.56               | 2.717           | 4.083                          |
| 11.61               | 1.107           | .661                           | 25.70               | 2.481           | 4.444                          |
| 12.61               | 1.284           | .857                           | 27.30               | 2.759           | 4.962                          |
| 12.93               | 1.613           | .906                           | 28.48               | 3.061           | 5.301                          |
| 14.17               | 1.854           | 1.174                          | 30.07               | 2.768           | 5.801                          |
| 14.57               | 1.723           | 1.259                          | 32.79               | 2.661           | 6.656                          |
| 15.91               | 1.624           | 1.556                          | 35.66               | 3.075           | 7.554                          |
| 16.30               | 1.750           | 1.645                          | 38.87               | 3.348           | 8.518                          |
| 17.81               | 2.170           | 2.002                          | 42.61               | 4.138           | 9.614                          |
| 18.49               | 2.640           | 2.187                          | 46.94               | 4.509           | 10.814                         |
| 19.88               | 1.966           | 2.555                          | 51.58               | 4.776           | 12.020                         |
| 20.82               | 2.026           | 2.819                          | 54.38               | 4.672           | 12.681                         |
| 21.89               | 2.049           | 3.119                          | 54.97               | 6.954           | 12.838                         |
| 23.39               | 3.107           | 3.563                          | 56.13               | 4.307           | 13.126                         |
| 24.02               | 2.209           | 3.746                          | 59.34               | 5.255           | 13.865                         |
| 26.36               | 2.446           | 4.444                          | 61.49               | 6.088           | 14.358                         |
| 26.46               | 3.027           | 4.481                          | 64.82               | 5.711           | 15.095                         |
| 28.63               | 2.086           | 5.128                          | 67.30               | 5.522           | 15.593                         |
| 29.23               | 2.506           | 5.311                          | 73.03               | 5.945           | 16.694                         |
| 32.35               | 3.731           | 6.282                          | 78.77               | 5.531           | 17.768                         |
| 35.79               | 3.133           | 7.332                          | 82.63               | 6.378           | 18.366                         |

|            |       |        |        |        |        |
|------------|-------|--------|--------|--------|--------|
| 39.05      | 3.396 | 8.305  | 84.73  | 6.393  | 18.871 |
| 42.54      | 3.572 | 9.318  | 87.08  | 6.200  | 19.278 |
| 46.64      | 4.630 | 10.441 | 88.69  | 6.948  | 19.524 |
| 51.39      | 4.863 | 11.710 | 90.93  | 6.019  | 19.871 |
| 54.49      | 5.866 | 12.459 | 93.12  | 5.880  | 20.201 |
| 56.00      | 4.364 | 12.842 | 95.90  | 7.475  | 20.604 |
| 60.03      | 5.218 | 13.780 | 96.81  | 5.739  | 20.738 |
| 65.48      | 5.681 | 14.990 | 102.88 | 6.400  | 21.614 |
| 70.94      | 5.233 | 16.079 | 109.14 | 6.135  | 22.471 |
| 76.39      | 5.680 | 17.121 | 111.36 | 5.216  | 22.720 |
| 82.26      | 6.048 | 18.239 | 115.16 | 5.903  | 23.310 |
| 88.35      | 6.139 | 19.320 | 116.90 | 5.866  | 23.537 |
| 94.81      | 6.771 | 20.303 | 121.43 | 6.637  | 24.169 |
| 101.41     | 6.442 | 21.287 | 123.13 | 6.591  | 24.382 |
| 102.05     | 5.471 | 21.326 | 128.65 | 7.802  | 25.167 |
| 107.42     | 5.261 | 22.124 | 131.15 | 10.421 | 25.470 |
| 107.71     | 6.158 | 22.180 | 141.26 | 9.789  | 27.249 |
| 112.59     | 5.083 | 22.851 |        |        |        |
| 114.17     | 6.747 | 23.083 |        |        |        |
| 116.89     | 6.771 | 23.464 |        |        |        |
| 117.59     | 4.928 | 23.547 | 157.13 | 4.337  | 43.38  |
| 120.78     | 6.481 | 24.011 | 161.19 | 5.304  | 43.35  |
| 122.45     | 4.789 | 24.218 | 162.76 | 6.912  | 43.37  |
| 123.53     | 6.507 | 24.394 | 167.36 | 7.040  | 43.41  |
| 127.14     | 6.247 | 24.919 | 169.65 | 6.875  | 43.42  |
| 130.43     | 7.295 | 25.363 | 177.35 | 8.537  | 43.54  |
| 138.07     | 7.986 | 26.549 | 185.86 | 8.469  | 43.73  |
|            |       |        | 194.29 | 8.399  | 43.96  |
|            |       |        | 202.65 | 8.324  | 44.27  |
|            |       |        | 210.94 | 8.243  | 44.62  |
| Crystals I |       |        |        |        |        |
| 11.35      | 1.135 | 0.651  | 219.14 | 8.163  | 44.99  |
| 12.09      | 0.950 | .775   | 227.26 | 8.078  | 45.44  |
| 12.65      | 1.456 | .888   | 235.29 | 7.991  | 45.89  |
| 13.26      | 1.453 | 1.015  | 239.81 | 7.827  | 46.17  |
| 14.13      | 1.511 | 1.212  | 243.63 | 8.688  | 46.42  |
| 14.77      | 1.617 | 1.353  | 248.36 | 9.270  | 46.73  |
| 15.70      | 1.627 | 1.566  | 257.56 | 9.144  | 47.37  |
| 16.41      | 1.661 | 1.746  | 266.64 | 9.019  | 48.02  |
| 17.42      | 1.830 | 1.999  | 275.60 | 8.830  | 48.74  |
| 18.08      | 1.678 | 2.173  | 284.43 | 8.772  | 49.44  |
| 19.35      | 2.011 | 2.528  | 293.14 | 8.653  | 50.17  |
| 19.99      | 2.136 | 2.709  | 299.61 | 4.279  | 50.76  |
| 21.27      | 1.836 | 3.087  |        |        |        |
| 1-Octene   |       |        |        |        |        |
| Crystals   |       |        |        |        |        |
|            |       | 99.41  | 8.406  | 23.153 |        |
|            |       | 107.40 | 7.581  | 24.336 |        |
| 11.27      | 1.195 | 0.783  | 115.69 | 9.003  | 25.566 |
| 11.48      | 1.123 | .831   | 118.69 | 6.188  | 26.000 |
| 12.52      | 1.307 | 1.073  | 119.18 | 6.169  | 26.070 |
| 12.75      | 1.453 | 1.124  | 124.47 | 8.559  | 26.814 |
| 13.97      | 1.598 | 1.422  | 124.52 | 6.840  | 26.814 |
| 14.25      | 1.553 | 1.495  | 125.20 | 6.822  | 26.914 |
| 15.63      | 1.704 | 1.853  | 125.79 | 6.829  | 26.990 |
| 15.96      | 1.852 | 1.942  | 131.64 | 7.412  | 27.825 |
| 17.46      | 1.950 | 2.367  | 132.28 | 7.335  | 27.901 |
| 17.98      | 2.180 | 2.532  | 132.81 | 7.408  | 27.992 |
| 19.64      | 2.394 | 3.049  | 140.32 | 7.604  | 29.032 |
| 20.20      | 2.251 | 3.231  | 140.86 | 11.033 | 29.096 |
| 21.80      | 1.921 | 3.755  | 141.97 | 10.798 | 29.246 |
| 22.46      | 2.257 | 3.975  | 148.31 | 8.380  | 30.148 |
| 23.93      | 2.312 | 4.470  | 150.99 | 7.247  | 30.493 |
| 25.01      | 2.824 | 4.833  | 161.47 | 13.711 | 32.459 |
| 26.37      | 2.554 | 5.302  |        |        |        |
| 27.86      | 2.876 | 5.817  |        |        |        |
| 28.99      | 2.675 | 6.210  |        |        |        |
| 31.37      | 4.129 | 7.042  | 175.43 | 4.522  | 50.86  |
| Liquid     |       |        |        |        |        |



TABLE II (Continued)

| $T, ^\circ\text{K.}^a$ | $\Delta T^b$ | $C_{\text{satd}}^c$ | $T, ^\circ\text{K.}^a$ | $\Delta T^b$ | $C_{\text{satd}}^c$ |
|------------------------|--------------|---------------------|------------------------|--------------|---------------------|
| 24.39                  | 3.072        | 5.964               | 200.80                 | 4.935        | 60.860              |
| 25.39                  | 2.133        | 6.402               | 203.59                 | 5.795        | 62.781              |
| 27.46                  | 3.055        | 7.329               | 204.90                 | 3.821        | 63.865              |
| 27.67                  | 2.414        | 7.415               | 207.93                 | 4.606        | 66.769              |
| 30.67                  | 3.354        | 8.777               |                        |              |                     |
| 34.19                  | 3.683        | 10.420              |                        |              |                     |
| 37.97                  | 3.865        | 12.138              |                        |              |                     |
| 42.22                  | 4.631        | 14.060              | 213.72                 | 1.475        | 84.42               |
| 47.00                  | 4.936        | 16.126              | 215.22                 | 1.519        | 81.22               |
| 52.04                  | 5.142        | 18.207              | 216.74                 | 1.519        | 81.08               |
| 55.38                  | 6.215        | 19.518              | 218.25                 | 1.515        | 81.25               |
| 56.90                  | 4.580        | 20.117              | 218.72                 | 3.938        | 81.40               |
| 61.74                  | 6.509        | 21.944              | 219.76                 | 1.504        | 81.89               |
| 67.92                  | 5.846        | 24.093              | 221.12                 | 3.920        | 82.43               |
| 73.96                  | 6.244        | 26.014              | 222.43                 | 4.751        | 83.07               |
| 79.97                  | 5.782        | 27.873              | 222.62                 | 3.860        | 83.29               |
| 85.95                  | 6.169        | 29.661              | 224.99                 | 3.820        | 84.98               |
| 91.95                  | 5.829        | 31.246              | 226.43                 | 3.746        | 86.20               |
| 93.23                  | 6.174        | 31.563              | 228.74                 | 3.685        | 88.65               |
| 97.85                  | 5.981        | 32.709              | 230.10                 | 3.605        | 90.21               |
| 99.25                  | 5.870        | 33.046              |                        |              |                     |
| 104.17                 | 6.648        | 34.224              |                        |              |                     |
| 110.67                 | 6.355        | 35.714              |                        |              |                     |
| 114.99                 | 5.316        | 36.736              | 240.33                 | 3.830        | 81.67               |
| 117.32                 | 6.953        | 37.241              | 244.54                 | 4.593        | 81.58               |
| 120.22                 | 5.149        | 37.886              | 247.36                 | 4.712        | 81.64               |
| 124.14                 | 6.683        | 38.755              | 249.13                 | 4.580        | 81.71               |
| 130.71                 | 6.446        | 40.171              | 252.07                 | 4.702        | 81.76               |
| 137.63                 | 7.406        | 41.666              | 256.01                 | 9.183        | 81.98               |
| 144.91                 | 7.146        | 43.271              | 265.12                 | 9.047        | 82.61               |
| 151.15                 | 5.951        | 44.679              | 274.86                 | 10.430       | 83.52               |
| 151.93                 | 6.907        | 44.859              | 285.23                 | 10.301       | 84.62               |
| 157.02                 | 5.791        | 46.029              | 295.46                 | 10.162       | 85.87               |
|                        |              |                     | 305.55                 | 10.026       | 87.12               |

Crystals I

Liquid

1-Hexadecene  
Crystals

|       |       |        |        |        |                     |
|-------|-------|--------|--------|--------|---------------------|
| 11.92 | 1.075 | 1.383  | 164.55 | 7.328  | 61.208              |
| 12.59 | 1.381 | 1.617  | 163.57 | 7.085  | 62.353              |
| 13.25 | 1.603 | 1.863  | 163.61 | 9.032  | 62.388              |
| 14.26 | 1.989 | 2.244  | 172.63 | 8.835  | 63.604              |
| 14.81 | 1.513 | 2.458  | 175.55 | 6.888  | 64.485              |
| 16.23 | 1.950 | 3.032  | 177.48 | 8.699  | 65.103              |
| 16.29 | 1.451 | 3.059  | 182.55 | 11.006 | 66.703              |
| 17.81 | 1.576 | 3.738  | 186.43 | 9.212  | 68.000              |
| 18.31 | 2.220 | 3.954  | 193.32 | 8.363  | 70.289              |
| 19.56 | 1.918 | 4.558  | 195.74 | 9.405  | 71.302              |
| 20.82 | 2.785 | 5.196  | 200.67 | 8.109  | 72.999              |
| 21.56 | 2.073 | 5.561  | 205.44 | 9.998  | 75.060              |
| 23.50 | 2.587 | 6.599  | 208.62 | 7.791  | 76.372              |
| 24.04 | 2.889 | 6.873  | 215.22 | 9.544  | 79.30 <sup>d</sup>  |
| 26.18 | 2.775 | 8.058  | 217.89 | 9.475  | 80.25 <sup>d</sup>  |
| 27.11 | 3.245 | 8.565  | 224.52 | 9.072  | 84.30 <sup>d</sup>  |
| 29.15 | 3.132 | 9.719  | 227.10 | 8.938  | 85.83 <sup>d</sup>  |
| 32.53 | 3.600 | 11.710 | 231.83 | 4.273  | 89.38 <sup>d</sup>  |
| 36.05 | 3.424 | 13.781 | 233.32 | 8.513  | 90.82 <sup>d</sup>  |
| 39.16 | 2.972 | 15.595 | 235.70 | 8.269  | 94.02 <sup>d</sup>  |
| 42.66 | 4.021 | 17.636 | 236.01 | 4.091  | 94.06 <sup>d</sup>  |
| 46.67 | 4.003 | 19.889 | 239.97 | 3.822  | 101.97 <sup>d</sup> |
| 50.88 | 4.414 | 22.199 | 241.28 | 7.414  | 106.4 <sup>d</sup>  |
| 55.45 | 4.714 | 24.590 | 243.57 | 3.372  | 118.5 <sup>d</sup>  |
| 55.90 | 6.081 | 24.812 | 250.52 | 1.741  | 133.12 <sup>d</sup> |
| 61.62 | 5.363 | 27.694 | 250.90 | 3.075  | 132.32 <sup>d</sup> |
| 67.21 | 5.819 | 30.277 | 252.28 | 1.775  | 129.96 <sup>d</sup> |

|        |       |        |        |       |                     |
|--------|-------|--------|--------|-------|---------------------|
| 72.79  | 5.346 | 32.617 | 254.00 | 3.130 | 129.20 <sup>d</sup> |
| 78.36  | 5.786 | 34.896 | 254.24 | 2.138 | 129.20 <sup>d</sup> |
| 84.12  | 6.168 | 37.166 | 256.54 | 2.469 | 130.84 <sup>d</sup> |
| 84.33  | 6.154 | 37.267 | 257.11 | 3.090 | 131.32 <sup>d</sup> |
| 90.19  | 5.122 | 39.318 | 260.22 | 3.002 | 135.82              |
| 90.45  | 6.507 | 39.424 | 263.10 | 2.887 | 142.10              |
| 91.04  | 7.265 | 39.602 | 265.93 | 2.753 | 150.13              |
| 96.25  | 7.000 | 41.253 | 273.47 | 2.140 | 186.24              |
| 97.12  | 6.825 | 41.531 |        |       |                     |
| 98.09  | 6.842 | 41.835 |        |       |                     |
| 103.52 | 7.552 | 43.537 |        |       |                     |
| 104.40 | 7.740 | 43.805 | 279.38 | 3.464 | 114.15              |
| 105.22 | 7.404 | 44.044 | 279.43 | 3.469 | 114.05              |
| 111.31 | 8.026 | 46.004 | 280.09 | 3.459 | 114.17              |
| 112.22 | 7.905 | 46.262 | 280.35 | 3.193 | 113.96              |
| 112.44 | 7.037 | 46.272 | 283.59 | 4.617 | 114.45              |
| 119.55 | 8.443 | 48.587 | 284.11 | 5.991 | 114.50              |
| 119.93 | 7.510 | 48.683 | 284.98 | 6.853 | 114.41              |
| 127.60 | 7.664 | 50.861 | 285.38 | 6.878 | 114.48              |
| 127.68 | 7.983 | 50.886 | 285.54 | 6.147 | 114.38              |
| 135.63 | 8.395 | 53.120 | 285.70 | 8.373 | 114.48              |
| 143.86 | 8.064 | 55.389 | 291.67 | 6.111 | 115.03              |
| 151.78 | 7.773 | 57.577 | 297.76 | 6.068 | 115.85              |
| 153.92 | 7.562 | 58.134 | 303.47 | 6.002 | 116.62              |
| 157.09 | 7.587 | 59.035 | 303.81 | 6.027 | 116.61              |

Liquid

<sup>a</sup>  $T$  is the mean temperature of each heat capacity measurement. <sup>b</sup>  $\Delta T$  is the temperature increment of each measurement. <sup>c</sup>  $C_{\text{satd}}$  is the heat capacity of the condensed phase at saturation pressure. <sup>d</sup> These values are corrected for the effect of curvature.

TABLE III

EQUATIONS FOR THE MOLAL HEAT CAPACITY IN THE LIQUID STATE

$$C_{\text{satd}}(\text{liq.}) = a + bT + cT^2 + dT^3, \text{ cal. deg.}^{-1} \text{ mole}^{-1}$$

| No. carbon atoms | $a$     | $b$      | $c \times 10^3$ | $d \times 10^6$ | Range, $^\circ\text{K.}^a$ |
|------------------|---------|----------|-----------------|-----------------|----------------------------|
| 6                | 47.387  | -0.15437 | 0.6502          | -0.579          | 150-310                    |
| 7                | 57.770  | -0.20286 | .8252           | -0.755          | 160-300                    |
| 8                | 80.470  | -0.38451 | 1.4907          | -1.535          | 200-310                    |
| 10               | 116.962 | -0.60967 | 2.1869          | -2.181          | 240-360                    |
| 11               | 129.669 | -0.63665 | 2.1538          | -1.979          | 245-310                    |
| 12               | 350.670 | -2.8766  | 9.9525          | -11.000         | 245-305                    |
| 16               | 328.58  | -2.0131  | 5.9000          | -5.167          | 280-310                    |

<sup>a</sup> The temperature range in which the heat capacity equation represents the observed data within about  $\pm 0.05\%$ .

The Heats of Transition and Transition Temperatures.—Isothermal phase transformations were found to occur in 1-decene, 1-undecene and 1-dodecene. For each compound two or more measurements were made of the total enthalpy increase over a finite temperature interval (5–20°) that included the transition temperature. To calculate the latent heats of transition, the energy absorbed non-isothermally was computed from the heat capacity data and subtracted from the total energy input. Corrections for premelting were applied as necessary. The results of these experiments are summarized in Table IV.

TABLE IV

THE MOLAL HEATS AND ENTROPIES OF TRANSITION AND TRANSITION TEMPERATURES

| Compound   | $T_{\text{trans.}}$ , $^\circ\text{K.}$ | $\Delta H_{\text{trans.}}$ , cal. | $\Delta S_{\text{trans.}}$ , cal. deg. <sup>-1</sup> |
|------------|---|-----------------------------------|--|
| 1-Decene   | 198.3                                   | 1900 <sup>a</sup>                 | 9.58   |
| 1-Undecene | 217.3                                   | 2202 $\pm$ 2 <sup>b</sup>         | 10.13  |
| 1-Dodecene | 212.9                                   | 1088 $\pm$ 4 <sup>b</sup>         | 5.11   |

<sup>a</sup> The value tabulated is the maximum value from four determinations; see text. <sup>b</sup> The uncertainty indicated is the maximum deviation of two results from the mean.

Relatively good precision was obtained in the measurements of the heats of transition of 1-undecene and 1-dodecene, but poor precision was obtained in the experiments on 1-decene. The results of four determinations of the heat of transition of 1-decene are: 1865, 1874, 1883 and 1903 cal. mole<sup>-1</sup>. For 1-decene, approximately three weeks was required to effect the transformation of crystals I to crystals II, and it is likely that complete transformation was not obtained before every determination. For this reason, it is believed that the highest value obtained for the heat of transition is the most reliable. A rounded value of 1900 cal. mole<sup>-1</sup> was chosen for the heat of transition of 1-decene.

The transition temperatures listed in Table IV were determined from observations of the temperature of a sample as a function of fraction transposed (fraction of sample present in the form of crystals I). In the studies of 1-decene and 1-dodecene true equilibrium was not observed and the results were extrapolated with the assumption that the equilibration rate was an exponential function of time. The results of the experiments are

|              |        |        |        |        |
|--------------|--------|--------|--------|--------|
| 1-Decene     |        |        |        |        |
| % Transposed | 13     | 27     | 80*    | 82*    |
| T, °K.       | 198.17 | 198.24 | 198.32 | 198.29 |
| 1-Undecene   |        |        |        |        |
| % Transposed | 19     | 47     | 76     |        |
| T, °K.       | 216.96 | 217.19 | 217.30 |        |
| 1-Dodecene   |        |        |        |        |
| % Transposed | 46*    | 53*    | 78*    |        |
| T, °K.       | 212.40 | 212.42 | 212.91 |        |

The results indicated by asterisks are single points observed in the course of separate heat of transition experiments.

**The Heats of Fusion, Triple Point Temperatures and Sample Purities.**—The heats of fusion of the seven 1-olefin hydrocarbons were determined in the manner described for the heats of transition. The results are presented in Table V. Four determinations of the heat of fusion of 1-octene gave the unusually large spread of values 3641 to 3660 cal. mole<sup>-1</sup>. This poor precision may have been due to incomplete crystallization or to formation of partially disordered crystals (see Discussion). In either case, the maximum value would be most reliable and, for this reason, was chosen as the heat of fusion. Poor precision also was obtained in three determinations of the heat of fusion of 1-heptene crystals II (3007 to 3021 cal. mole<sup>-1</sup>). The largest value obtained also was chosen for this compound because crystals II tended to transpose to crystals I (with smaller heat of fusion) in the region of the melting point.

TABLE V

THE MOLAL HEATS AND ENTROPIES OF FUSION AND THE CRYOSCOPIC CONSTANTS OF SEVEN 1-OLEFIN HYDROCARBONS

| No. carbon atoms | T <sub>T.P.</sub> <sup>a</sup> , °K. | ΔH <sub>fusion</sub> , cal. | ΔS <sub>fusion</sub> , cal. deg. <sup>-1</sup> | A, <sup>b</sup> deg. <sup>-1</sup> | B, <sup>c</sup> deg. <sup>-1</sup> |
|------------------|--------------------------------------|-----------------------------|--|------------------------------------|------------------------------------|
| 6                | 133.39                               | 2234 ± 0 <sup>d</sup>       | 16.75  | 0.06318                            | 0.00437                            |
| 7 (I)            | 154.30                               | 2964 ± 1 <sup>d</sup>       | 19.21  | .06265                             | .00396                             |
| 7 (II)           | 153.89                               | 3021 <sup>e</sup>           | 19.63  | .06419                             | .00403                             |
| 8                | 171.46                               | 3660 <sup>e</sup>           | 21.35  | .06265                             | .00343                             |
| 10               | 206.89                               | 3300 ± 2 <sup>d</sup>       | 15.95  | .03880                             | .00544                             |
| 11               | 223.99                               | 4061 ± 0 <sup>d</sup>       | 18.13  | .04073                             | .00563                             |
| 12               | 237.93                               | 4758 ± 0 <sup>d</sup>       | 20.00  | .04229                             | .00587                             |
| 16               | 277.51                               | 7216 ± 4 <sup>d</sup>       | 26.00  | .04715                             | .00856                             |

<sup>a</sup> The estimated accuracy uncertainty of the values listed is ±0.05°K. <sup>b</sup> A is the first cryoscopic constant, ΔH<sub>fusion</sub>/RT<sub>T.P.</sub><sup>2</sup>. <sup>c</sup> B is the second cryoscopic constant, 1/T<sub>T.P.</sub> - ΔC<sub>fusion</sub>/2ΔH<sub>fusion</sub>. <sup>d</sup> The uncertainty indicated is the maximum deviation from the mean of two to five determinations. <sup>e</sup> The value listed is the maximum value from several determinations; see text.

TABLE VI

MELTING POINT SUMMARIES FOR 1-OLEFIN HYDROCARBONS

| Liq. %                                   | 1/F   | T <sub>obsd.</sub> , °K. | T <sub>graph.</sub> , °K. <sup>b</sup> |
|--|-------|--------------------------|--|
| 1-Hexene (impurity = 0.04 ± 0.01 mole %) |       |                          |  |
| 11.86                                    | 8.432 | 133.3370                 | 133.3365                               |
| 26.01                                    | 3.845 | 133.3666                 | 133.3674                               |

|   |                    |                       |          |
|---|--------------------|-----------------------|----------|
| 50.36 <sup>a</sup>                            | 1.986 <sup>a</sup> | 133.3799 <sup>a</sup> | 133.3799 |
| 70.59   | 1.417              | 133.3847              | 133.3837 |
| 88.80 <sup>a</sup>                            | 1.126 <sup>a</sup> | 133.3857 <sup>a</sup> | 133.3857 |
| 100   | 1.00               |                       | 133.3865 |
| Pure  | 0                  |                       | 133.393  |
| 1-Heptene (I) (impurity = 0.24 ± 0.05 mole %) |                    |                       |          |
| 11.38   | 8.787              | 154.0303              | 153.96   |
| 27.06   | 3.695              | 154.1725              | 154.158  |
| 50.74 <sup>a</sup>                            | 1.971 <sup>a</sup> | 154.2233 <sup>a</sup> | 154.2232 |
| 71.26   | 1.403              | 154.2439              | 154.2447 |
| 82.32 <sup>a</sup>                            | 1.215 <sup>a</sup> | 154.2519 <sup>a</sup> | 154.2519 |
| 100   | 1.000              |                       | 154.2600 |
| Pure  | 0                  |                       | 154.298  |
| 1-Heptene (II) (impurity = 0.14 ± 0.1 mole %) |                    |                       |          |
| 21.03 <sup>a</sup>                            | 4.76 <sup>a</sup>  | 153.7859 <sup>a</sup> | 153.7859 |
| 50.16 <sup>a</sup>                            | 1.99 <sup>a</sup>  | 153.8470 <sup>a</sup> | 153.8470 |
| 100   | 1.00               |                       | 153.869  |
| Pure  | 0                  |                       | 153.89   |
| 1-Octene (impurity = 0.06 ± 0.02 mole %)      |                    |                       |          |
| 10.76   | 9.294              | 171.3808              | 171.369  |
| 25.57   | 3.911              | 171.4212              | 171.4209 |
| 50.58 <sup>a</sup>                            | 1.977 <sup>a</sup> | 171.4396 <sup>a</sup> | 171.4396 |
| 70.91   | 1.410              | 171.4475              | 171.4451 |
| 91.24 <sup>a</sup>                            | 1.096 <sup>a</sup> | 171.4481 <sup>a</sup> | 171.4481 |
| 100   | 1.000              |                       | 171.4490 |
| Pure  | 0                  |                       | 171.459  |
| 1-Decene (A) (impurity = 0.11 ± 0.02 mole %)  |                    |                       |          |
| 9.72  | 10.29              | 206.6281              | 206.60   |
| 21.86   | 4.575              | 206.7662              | 206.764  |
| 42.51 <sup>a</sup>                            | 2.352 <sup>a</sup> | 206.8259 <sup>a</sup> | 206.8259 |
| 59.10   | 1.692              | 206.8440              | 206.8444 |
| 75.71 <sup>a</sup>                            | 1.321 <sup>a</sup> | 206.8547 <sup>a</sup> | 206.8547 |
| 100   | 1.000              |                       | 206.8637 |
| Pure  | 0                  |                       | 206.892  |
| 1-Decene (B) (impurity = 0.09 ± 0.03 mole %)  |                    |                       |          |
| 11.04   | 9.057              | 206.7373              | 206.67   |
| 26.45   | 3.781              | 206.8094              | 206.797  |
| 47.85   | 2.090              | 206.8397              | 206.838  |
| 51.68   | 1.935              | 206.8461              | 206.842  |
| 52.31   | 1.912              | 206.8466              | 206.843  |
| 68.71   | 1.455              | 206.8497              | 206.854  |
| 71.13 <sup>a</sup>                            | 1.406 <sup>a</sup> | 206.8548 <sup>a</sup> | 206.8548 |
| 90.56 <sup>a</sup>                            | 1.104 <sup>a</sup> | 206.8621 <sup>a</sup> | 206.8621 |
| 100   | 1.000              |                       | 206.8646 |
| Pure  | 0                  |                       | 206.889  |
| 1-Undecene (impurity = 0.04 ± 0.01 mole %)    |                    |                       |          |
| 10.12   | 9.880              | 223.9144              | 223.89   |
| 24.37   | 4.103              | 223.9500              | 223.947  |
| 44.03 <sup>a</sup>                            | 2.271 <sup>a</sup> | 223.9648 <sup>a</sup> | 223.9648 |
| 63.66   | 1.571              | 223.9702              | 223.9715 |
| 86.88 <sup>a</sup>                            | 1.151 <sup>a</sup> | 223.9755 <sup>a</sup> | 223.9755 |
| 100.00  | 1.000              |                       | 223.9770 |
| Pure  | 0                  |                       | 223.987  |
| 1-Dodecene (impurity = 0.08 ± 0.04 mole %)    |                    |                       |          |
| 8.67  | 11.54              | 237.7961              | 237.71   |
| 23.36   | 4.281              | 237.8697              | 237.85   |
| 48.04   | 2.082              | 237.8944              | 237.891  |
| 67.82 <sup>a</sup>                            | 1.475 <sup>a</sup> | 237.9026 <sup>a</sup> | 237.9026 |
| 87.59 <sup>a</sup>                            | 1.142 <sup>a</sup> | 237.9090 <sup>a</sup> | 237.9090 |
| 100.00  | 1.000              |                       | 237.9117 |
| Pure  | 0                  |                       | 237.931  |

<sup>a</sup> A straight line through these points was extrapolated to 1/F = 0 to obtain the triple-point temperature, T<sub>T.P.</sub> <sup>b</sup> Temperatures read from the straight line of footnote a.

For each compound, a study of the equilibrium melting temperature as a function of the fraction of sample melted was made by the method outlined in an earlier publication from this Laboratory.<sup>20</sup> The results for each compound except 1-hexadecene are given in Table VI. The equilibrium temperatures,  $T_{\text{obsd}}$ , were plotted as a function of  $1/F$ , the reciprocal of the fraction of total sample in the liquid phase. Except for 1-hexadecene, the triple point temperatures,  $T_{\text{T.P.}}$ , listed in Table V were determined by linear extrapolations to zero value of  $1/F$ . If the impurities present in the samples form ideal solutions in the liquid phase and are insoluble in the solid phase the relation between mole fraction of total impurity,  $N_2^*$ , and melting point depression,  $\Delta T = T_{\text{T.P.}} - T_{\text{obsd}}$ , is<sup>21</sup>

$$-\ln(1 - N_2) = A\Delta T(1 + B\Delta T + \dots) \quad (1)$$

where  $N_2 = N_2^*/F$ . The cryoscopic constants,  $A = \Delta H_{\text{fusion}}/RT_{\text{T.P.}}^2$ , and  $B = 1/T_{\text{T.P.}} - \Delta C_{\text{fusion}}/2\Delta H_{\text{fusion}}$ , were calculated for each compound from the values of  $\Delta H_{\text{fusion}}$  and  $T_{\text{T.P.}}$  in Table V and values of  $\Delta C_{\text{fusion}}$  obtained from data in Table VIII (discussed in the following section). Values of  $A$  and  $B$  are included in Table V. The impurity values given in Table VI were calculated by application of eq. 1 in its simplified form (for  $N_2^* \ll 1$ ),  $N_2^* = \Delta F\Delta T$ .

A plot of  $T_{\text{obsd}}$  vs.  $1/F$  for 1-hexadecene departs markedly from linearity, perhaps because the impurity was partly soluble in solid 1-hexadecene. The results for 1-hexadecene were treated by the method described by Mastrangelo and Dornte,<sup>22</sup> which takes solid-solution formation into account. The calculations are summarized in Table VII. The effect of the relatively large amount of impurity on the entropy values reported for 1-hexadecene is probably insignificant because the impurity is most likely an isomeric substance with nearly the same thermodynamic properties.

TABLE VII

1-HEXADECENE: MELTING POINT SUMMARY<sup>a</sup>

$T_{\text{T.P.}} = 277.51 \pm 0.05^\circ\text{K.}$ ; impurity = 1.3 mole %; distribution coefficient,  $K = 0.252$ .

| Liq., % | $[F + K/(1 - K)]$ | $T_{\text{obsd.}}, ^\circ\text{K.}$ | $T_{\text{calcd.}}, ^\circ\text{K.}$ |
|---------|-------------------|-------------------------------------|--------------------------------------|
| 14.16   | 2.089             | 276.896                             | 276.938                              |
| 25.92   | 1.677             | 277.052                             | 277.051                              |
| 49.76   | 1.198             | 277.183                             | 277.183                              |
| 69.74   | 0.967             | 277.242                             | 277.246                              |
| 89.76   | 0.810             | 277.287                             | 277.289                              |

<sup>a</sup> Values of  $T_{\text{T.P.}}$ ,  $T_{\text{calcd.}}$ ,  $K$  and sample impurity were calculated with the aid of expressions given in ref. 22.

Although some of the other 1-olefins showed appreciable departure from linearity in plots of  $T_{\text{obsd}}$  vs.  $1/F$ , the data for these relatively pure samples were not treated by the solid-solution method.<sup>22</sup> Experience in this Laboratory has shown that the solid-solution treatment is best applied only to data for relatively impure samples or for compounds with low cryoscopic constants. Also, the presence of several impurities with different distribution coefficients is often a complicating factor.

**The Chemical Thermodynamic Properties in the Solid and Liquid States.**—The low temperature calorimetric data for each 1-olefin were used in calculating values of the free energy function, heat content function, heat content and entropy in the solid and liquid states at selected temperatures between 10 and 360°K. The values at 10°K. were calculated from Debye functions, the parameters for which were evaluated from the heat capacity data between 12 and 20°K.<sup>23</sup> The thermodynamic properties above 10°K. were

(20) S. S. Todd, G. D. Oliver and H. M. Huffman, *J. Am. Chem. Soc.*, **69**, 1519 (1947).

(21) A. R. Glasgow, Jr., A. J. Streiff and F. D. Rossini, *J. Research Natl. Bur. Standards*, **35**, 355 (1945).

(22) S. V. R. Mastrangelo and R. W. Dornte, *J. Am. Chem. Soc.*, **77**, 6200 (1955).

(23) The number of degrees of freedom and characteristic temperatures, respectively, of these Debye functions were: 1-hexene, 5 and 123.1°; 1-heptene(I), 5 and 119.1°; 1-heptene(II), 5 and 121.1°; 1-octene, 5, and 113.9°; 1-decene, 6 and 115.5°; 1-undecene, 7 and 123.4°; 1-dodecene, 6 and 106.0°; and 1-hexadecene, 8 and 113.3°.

calculated from the values for the heats and temperatures of phase changes and from increments computed by appropriate numerical integration of values  $C_{\text{satd}}$  read from large scale plots of the data of Table II. The results are recorded in Table VIII. Corrections for the effects of premelting were applied as necessary in computing the "smoothed" data in this table.

TABLE VIII

THE MOLAL THERMODYNAMIC PROPERTIES OF SEVEN 1-OLEFINS IN THE SOLID AND LIQUID STATES<sup>a</sup>

| $T, ^\circ\text{K.}$     | $-(F_{\text{satd}}/H_0^\circ)/T,$<br>cal.<br>deg. <sup>-1</sup> | $-(H_{\text{satd}}/H_0^\circ)/T,$<br>cal.<br>deg. <sup>-1</sup> | $H_{\text{satd}} - H_0^\circ,$<br>cal. | $S_{\text{satd.}}$<br>cal.<br>deg. <sup>-1</sup> | $C_{\text{satd.}}$<br>cal.<br>deg. <sup>-1</sup> |
|--------------------------|---|---|--|--|--|
| 1-Hexene<br>Crystals     |   |   |  |  |  |
| 10                       | 0.035   | 0.104   | 1.040                                  | 0.139  | 0.412  |
| 15                       | .116  | .339  | 5.080                                  | .455   | 1.292  |
| 20                       | .263  | .723  | 14.460                                 | .986   | 2.499  |
| 25                       | .475  | 1.217   | 30.42                                  | 1.692  | 3.892  |
| 30                       | .746  | 1.781   | 53.42                                  | 2.527  | 5.315  |
| 35                       | 1.066   | 2.388   | 83.57                                  | 3.454  | 6.733  |
| 40                       | 1.426   | 3.016   | 120.64                                 | 4.442  | 8.081  |
| 45                       | 1.818   | 3.649   | 164.20                                 | 5.467  | 9.330  |
| 50                       | 2.235   | 4.277   | 213.84                                 | 6.512  | 10.511   |
| 60                       | 3.123   | 5.498   | 329.8                                  | 8.621  | 12.647   |
| 70                       | 4.058   | 6.653   | 465.7                                  | 10.711   | 14.464   |
| 80                       | 5.018   | 7.733   | 618.6                                  | 12.751   | 16.108   |
| 90                       | 5.988   | 8.750   | 787.4                                  | 14.738   | 17.613   |
| 100                      | 6.960   | 9.701   | 970.1                                  | 16.661   | 18.899   |
| 110                      | 7.927   | 10.594  | 1165.3                                 | 18.521   | 20.141   |
| 120                      | 8.885   | 11.440  | 1372.7                                 | 20.325   | 21.339   |
| 130                      | 9.833   | 12.246  | 1591.9                                 | 22.079   | 22.503   |
| 133.39                   | 10.152  | 12.512  | 1668.9                                 | 22.664   | 22.891   |
| Liquid                   |   |   |  |  |  |
| 133.39                   | 10.152  | 29.259  | 3902                                   | 39.41  | 36.88  |
| 140                      | 11.57   | 29.618  | 4146                                   | 41.19  | 36.86  |
| 150                      | 13.63   | 30.10   | 4515                                   | 43.73  | 36.88  |
| 160                      | 15.59   | 30.52   | 4884                                   | 46.12  | 36.96  |
| 170                      | 17.45   | 30.91   | 5254                                   | 48.36  | 37.10  |
| 180                      | 19.23   | 31.25   | 5626                                   | 50.49  | 37.30  |
| 190                      | 20.93   | 31.58   | 6000                                   | 52.51  | 37.56  |
| 200                      | 22.55   | 31.89   | 6378                                   | 54.45  | 37.89  |
| 210                      | 24.12   | 32.18   | 6759                                   | 56.30  | 38.28  |
| 220                      | 25.62   | 32.47   | 7144                                   | 58.09  | 38.73  |
| 230                      | 27.07   | 32.75   | 7533                                   | 59.83  | 39.23  |
| 240                      | 28.47   | 33.03   | 7928                                   | 61.51  | 39.78  |
| 250                      | 29.83   | 33.31   | 8329                                   | 63.14  | 40.39  |
| 260                      | 31.14   | 33.60   | 8736                                   | 64.74  | 41.02  |
| 270                      | 32.41   | 33.89   | 9150                                   | 66.30  | 41.70  |
| 273.16                   | 32.81   | 33.98   | 9282                                   | 66.79  | 41.93  |
| 280                      | 33.65   | 34.18   | 9571                                   | 67.83  | 42.44  |
| 290                      | 34.85   | 34.48   | 9999                                   | 69.33  | 43.18  |
| 298.16                   | 35.81   | 34.72   | 10354                                  | 70.55  | 43.81  |
| 300                      | 36.03   | 34.78   | 10435                                  | 70.81  | 43.96  |
| 310                      | 37.17   | 35.09   | 10878                                  | 72.27  | 44.76  |
| 1-Heptene<br>Crystals II |   |   |  |  |  |
| 10                       | 0.036   | 0.109   | 1.091                                  | 0.145  | 0.433  |
| 15                       | .122  | .359  | 5.389                                  | .481   | 1.357  |
| 20                       | .277  | .755  | 15.102                                 | 1.032  | 2.582  |
| 25                       | .498  | 1.265   | 31.62                                  | 1.763  | 4.040  |
| 30                       | .779  | 1.852   | 55.56                                  | 2.631  | 5.552  |
| 35                       | 1.113   | 2.490   | 87.16                                  | 3.603  | 7.085  |
| 40                       | 1.488   | 3.159   | 126.36                                 | 4.647  | 8.600  |
| 45                       | 1.900   | 3.842   | 172.90                                 | 5.742  | 9.994  |





TABLE VIII (Continued)

|        |       |       |       |        |        |
|--------|-------|-------|-------|--------|--------|
| 273.16 | 49.13 | 60.31 | 16475 | 109.44 | 171.52 |
| 277.51 | 50.09 | 62.15 | 17243 | 112.24 | 185.32 |
| Liquid |       |       |       |        |        |
| 277.51 | 50.09 | 88.14 | 24459 | 138.24 | 113.85 |
| 280    | 50.89 | 88.39 | 24750 | 139.29 | 114.04 |
| 290    | 54.01 | 89.29 | 25895 | 143.30 | 114.95 |
| 298.16 | 56.50 | 90.01 | 26837 | 146.51 | 115.89 |
| 300    | 57.05 | 90.17 | 27050 | 147.22 | 116.14 |
| 310    | 60.02 | 91.03 | 28219 | 151.05 | 117.57 |

<sup>a</sup> The values tabulated are the free energy function, heat content function, heat content, entropy and heat capacity of the condensed phases at saturation pressure.

As stated in the Discussion, a thermodynamically feasible but unobserved transition should occur between crystals I and II of 1-heptene near 137°K. For convenience, this transition has been included in the table of thermodynamic properties of 1-heptene (Table VIII). The entropy of liquid 1-heptene was calculated independently from data for each of the two crystalline modifications, and the values obtained agreed within 0.06 cal. deg.<sup>-1</sup> mole<sup>-1</sup>. In Table VIII, the calculated heat of transition, 60.4 cal. mole<sup>-1</sup>, was selected to make the reported entropy values for liquid 1-heptene agree with the average of the values calculated independently from data for crystals I and crystals II.

It should be emphasized that 1-undecene, 1-dodecene and 1-hexadecene possess residual entropy at 0°K. and that the thermodynamic properties for these three compounds listed in Table VIII are not absolute values but are relative to orientationally disordered crystals at 0°K. (see Discussion).

## ANALYSIS OF STRUCTURE IN CHANNEL BLACK DISPERSIONS

BY ANDRIES VOET<sup>1</sup>

*J. M. Huber Corporation, Borger, Texas*

*Received August 27, 1956*

Recently developed electrical methods have clarified our insight into the processes of particle interaction in dispersions. In channel black dispersed in mineral oil not the elementary particle, but a much larger aggregate is the kinetic unit, even at high rates of shear. In stabilized systems at rest an interlinked particle network is not apparent, but the kinetic units join to form association complexes, partly coiled at rest, and uncoiled at low shear rates, which are destroyed at higher rates of shear. In quiescent unstabilized systems extensive reticulation is apparent, strongly promoted by an increased temperature, but destroyed at low shear rates. Pronounced hysteresis phenomena have been observed. Rheological data are misleading, since the measurement itself destroys the structures, while yield values are not indicative of the degree of structural involvement.

### 1. Introduction

The value of carbon blacks as reinforcing agents for rubber or as coloring and bodying agents in printing inks is controlled by both particle size and by the nature of the surface. While the particle size and the surface area are readily determined, the interaction between the carbon particles is more difficult to study. Such terms as "structure black" have gradually become common, with little more evidence of structure than accidental stringing in an electron micrograph or the stiffening effect when milled into unvulcanized rubber.

While the study of the action of carbon in rubber is difficult because of the semi-rigid nature of the hydrocarbon, it is possible to conduct such an investigation in liquid hydrocarbons. Electrical methods are now available for the study of the shape of the particle clusters or chains and to follow the rate and extent of the formation of such flocculates.<sup>2-7</sup> The application of shear during the electrical measurement may provide information regarding the forces involved in the chain formation.

2. Method.—Basically there are three electrical methods to evaluate particle flocculation. The d.c. conductivity method can follow the building of carbon chains in a system at rest and their destruction by shear. A second method makes use of the dielectric constant of the carbon dispersion, which does not vary with the size of the dispersed particles, but depends, at a given volume concentration, primarily

upon the particle shape. It is lowest for spherical particles and increases markedly with increasing particle asymmetry. Since flocculation generally leads to the formation of particle chains and other asymmetric structures, any increase in the dielectric constant of quiescent dispersions of carbon blacks may be related directly to particle flocculation or structure. The anisometry of the agglomerate has been quantitatively related to the particle shape for rotational ellipsoids.<sup>8</sup>

The third electrical method, by means of dielectric losses, appears to be unsatisfactory for carbon black dispersions, in view of the large contributions of eddy currents in systems of conductive particles.

### 3. Apparatus

A. The Cell.—The cell used for the measurement of the dielectric constant and the conductivity is a double cylindrical cell of the immersion type, with an outer stationary and an inner, rotating electrode, allowing a variable shear from 0-1200 reciprocal seconds and a rapid changeover in samples.

The cell assembly was kept at the selected temperature by submerging in an oil-bath, thermostated at the desired temperature with an accuracy of  $\pm 0.05^\circ$ .

B. D.c. Conductance.—The d.c. conductance was measured by applying a known voltage across the cell terminals and measuring the resulting current. The field strength applied was comparatively low in order to eliminate polarization effects and generally of the order of 100 mv. per cm. It was selected in such a way that Ohm's law was valid over the entire range of measurements. A Leeds & Northrup micro-micro ampere amplifier permitted accurate measurements at low field strengths. The cell constant of the rotating electrode was determined with the aid of liquids of known conductivity. The magnitude of the applied voltage was calibrated with a standard cadmium cell.

C. Dielectric Constant.—Dielectric constants were measured at a frequency of 4.8 megacycles by means of a Sargent Model V oscillometer. Complete calibration curves were established with the aid of known precision capacitors and resistors for the entire range of measurements. Conductance corrections had to be applied only at the highest concentration used.

(1) Presented before the Rubber Division, A.C.S., Cleveland, May 17-19, 1956.

(2) A. Voet, *THIS JOURNAL*, **51**, 1037 (1947).

(3) A. Voet and L. R. Suriani, *J. Coll. Sci.*, **6**, 1955 (1951).

(4) A. Voet and L. R. Suriani, *ibid.*, **7**, 1 (1952).

(5) A. Voet, *Am. Ink Maker*, **31**, (12), 34 (1953).

(6) M. J. Foster and D. J. Mead, *J. Appl. Phys.*, **22**, 705 (1951).

(7) A. A. Bondi and C. J. Penner, *THIS JOURNAL*, **57**, 72, 540 (1953).

(8) A. P. Altshuler, *ibid.*, **58**, 544 (1954).

#### 4. Preparation of Samples

A single grade of a dried commercial channel black of 6% volatile content was employed. The surface average diameter of 27  $m\mu$  compared favorably with the value 28.2  $m\mu$  derived from nitrogen adsorption area measurements, indicating essentially spherical and non-porous elementary particles.

The mineral oil used was a white mineral oil, "liquid petrolatum U.S.P.,"  $d_{40}^{20}$  0.8770;  $n_{D}^{25}$  1.4808; viscosity 160 c.p. at 30°C.

Maximum stability in the stabilized dispersions was achieved by combining an ionic stabilizer with a non-ionic stabilizer. Non-ionic stabilizers are generally of a resinous or asphaltic nature and provide steric protection by adsorption. Ionic stabilizers produce electrically charged particles. In the stabilized dispersions the vehicle consisted of 3% Gilsonite combined with 1% of a barium salt of a sulfonated petroleum product known as "mahogany acid," dissolved in the white mineral oil. In the unstabilized dispersions the white mineral oil was used as the vehicle.

Dispersions were prepared by incorporating 16 parts of black into 84 parts of vehicle with the aid of a three roller mill. All other concentrations were made by dilution with the vehicle.

#### 5. Experimental Results

##### A. Conductivity of Stabilized Dispersions.—

Table I gives the results for stabilized dispersions at rest as well as when subjected to varying rates of shear.

TABLE I

CONDUCTIVITY OF STABILIZED DISPERSIONS, EFFECT OF SHEAR

| Rate of shear, sec. <sup>-1</sup> | Temp., °C. | $K \times 10^{-12}$ at wt. % carbon |      |      |      |
|-----------------------------------|------------|-------------------------------------|------|------|------|
|                                   |            | 2                                   | 4    | 8    | 16   |
| 0                                 | 30         | 3.12                                | 8.81 | 23.0 | 76.8 |
| 320                               | 30         | 3.95                                | 10.7 | 26.6 | 84.0 |
| 426                               | 30         | 4.29                                | 11.3 | 27.8 | 85.8 |
| 632                               | 30         | 4.83                                | 12.5 | 29.8 | 90.3 |
| 800                               | 30         | 5.35                                | 13.5 | 32.1 | 94.0 |
| 957                               | 30         | 5.83                                | 14.5 | 33.9 | 98.0 |
| 0                                 | 60         | 11.6                                | 29.8 | 100  | 269  |
| 320                               | 60         | 14.4                                | 35.2 | 134  | 289  |
| 426                               | 60         | 15.2                                | 37.0 | 139  | 296  |
| 632                               | 60         | 16.8                                | 40.4 | 149  | 309  |
| 800                               | 60         | 18.4                                | 43.8 | 153  | 323  |
| 957                               | 60         | 19.7                                | 47.0 | 179  | 332  |
| 0                                 | 90         | 51.0                                | 141  | 402  | 958  |
| 320                               | 90         | 55.8                                | 149  | 415  | 990  |
| 426                               | 90         | 56.9                                | 152  | 422  | 998  |
| 632                               | 90         | 59.2                                | 158  | 429  | 1016 |
| 800                               | 90         | 62.6                                | 163  | 440  | 1035 |
| 957                               | 90         | 64.6                                | 167  | 449  | 1051 |

Table I indicates that the d.c. conductivity of stabilized dispersions shows a marked increase with the rate of shear.

Conductivities at rest  $K_0$ , when plotted against the concentration by volume  $C$  in a logarithmic plot, show linear relationships. In first approximation,  $K_0$  may be expressed as follows for the various temperatures.

$$K_0 = \frac{4.6 \times 10^{-9}}{\eta} C^{3/2} \quad (1)$$

where  $\eta$  is the viscosity of the vehicle at the indicated temperature, while  $C$  is the pigment concentration by volume, calculated from the weight concentration by using 1.85 as the density of the pigment and 0.8830, 0.8682 and 0.8501 as densities for the vehicle at 30, 60 and 90°, respectively.

In stabilized dispersions the rest conductivity  $K_0$  reaches a final value immediately after discontinuation of shear. The data of Table I also indicate that a linear relation exists between conductivities and rates of shear. Furthermore, the conductivity increment appears to be proportional to the volume concentration  $C$  of the black. Thus, for the increase in conductivity  $\Delta K$  per unit of shear rate the following empirical relation holds

$$\Delta K = PCD \quad (2)$$

whereby  $D$  is the rate of shear, expressed in reciprocal seconds, while  $P$  is a constant of the value 2.8, 8.6 and  $13.7 \times 10^{-13}$  at 30, 60 and 90°, respectively.

##### B. Conductivity of Unstabilized Dispersions.

I. Effect of Shear.—Conductivity coefficients for 16 and 8% by weight dispersions of channel black in white mineral oil, at different temperatures and at varying rates of shear, have been plotted in Figs. 1 and 2. At lower concentrations the pattern of the 8% dispersion is followed.

II. Effect of Time.—The changes in conductivity of unstabilized dispersions of channel black in mineral oil with time, after discontinuation of shear, are plotted in Figs. 3 and 4, for dispersions of 8 and 2% by weight at different temperatures.

##### C. Dielectric Constant of Stabilized Systems.

I. Effect of Shear.—The dielectric constants of the quiescent stabilized dispersions all showed a decrease upon being sheared. Table II indicates the magnitude of the decrease from the equilibrium value at rest at various rates of shear for dispersions of varying concentrations and temperatures.

TABLE II

DIELECTRIC PROPERTIES OF STABILIZED DISPERSIONS, EFFECT OF SHEAR

| Wt. % black | Temp., °C. | Decrease from rest in units $\times 10^3$ at following rates of shear in sec. <sup>-1</sup> |     |     |     |     |          |
|-------------|------------|---|-----|-----|-----|-----|----------|
|             |            | 245   | 373 | 584 | 783 | 981 | $\infty$ |
| 1           | 30         | 3   | 4   | 5   | 6   | 7   | 10       |
| 2           | 30         | 18  | 19  | 20  | 21  | 21  | 24       |
| 4           | 30         | 35  | 40  | 44  | 46  | 47  | 59       |
| 8           | 30         | 73  | 80  | 88  | 92  | 95  | 120      |
| 16          | 30         | 463   | 477 | 484 | 488 | 492 | 512      |
| 1           | 60         | 3   | 4   | 5   | 5   | 6   | 8        |
| 2           | 60         | 13  | 16  | 18  | 19  | 19  | 24       |
| 4           | 60         | 37  | 40  | 41  | 42  | 43  | 48       |
| 8           | 60         | 60  | 63  | 69  | 73  | 75  | 95       |
| 16          | 60         | 301   | 312 | 321 | 325 | 329 | 357      |
| 1           | 90         | 1   | 1   | 2   | 2   | 3   | 4        |
| 2           | 90         | 5   | 7   | 8   | 9   | 9   | 13       |
| 4           | 90         | 18  | 16  | 20  | 21  | 22  | 33       |
| 8           | 90         | 49  | 27  | 20  | 26  | 31  | 70       |
| 16          | 90         | 172   | 184 | 194 | 200 | 204 | 234      |

The value of the dielectric constant at an infinitely high rate of shear is significant, since it represents maximum separation of particles and the elimination of all structures in the dispersion. Such a value can be approximated by extrapolation. A straight line results from plotting the dielectric constants against the reciprocal value of the square root of the rate of shear for a 16% by weight stabilized dispersion of carbon black. This linear relationship allows extrapolation to "infinite shear rates" and  $\epsilon_\infty$ , the dielectric constant at an "infi-

TABLE III  
DIELECTRIC PROPERTIES OF STABILIZED DISPERSIONS

|                      | Temp., °C. | Wt. % carbon black |       |       |       |       |       |
|----------------------|------------|--------------------|-------|-------|-------|-------|-------|
|                      |            | 0                  | 1     | 2     | 4     | 8     | 16    |
| $\epsilon$           | 30         | 2.198              | 2.310 | 2.427 | 2.708 | 3.302 | 5.177 |
| $\epsilon_\infty$    | 30         | 2.198              | 2.300 | 2.403 | 2.649 | 3.182 | 4.665 |
| $\epsilon_{r\infty}$ | 30         | 1.000              | 1.047 | 1.094 | 1.205 | 1.448 | 2.122 |
| Vol. % Bl.           | 30         | ...                | 0.494 | 0.995 | 2.01  | 4.11  | 8.57  |
| $f$                  | 30         | ...                | 3.16  | 3.27  | 3.40  | 3.64  | 4.37  |
| $\epsilon$           | 60         | 2.165              | 2.278 | 2.401 | 2.666 | 3.251 | 5.064 |
| $\epsilon_\infty$    | 60         | 2.165              | 2.270 | 2.377 | 2.618 | 3.156 | 4.707 |
| $\epsilon_{r\infty}$ | 60         | 1.000              | 1.049 | 1.099 | 1.201 | 1.458 | 2.174 |
| Vol. % Bl.           | 60         | ...                | 0.484 | 0.975 | 1.970 | 4.025 | 8.41  |
| $f$                  | 60         | ...                | 3.30  | 3.38  | 3.54  | 3.74  | 4.66  |
| $\epsilon$           | 90         | 2.133              | 2.244 | 2.372 | 2.643 | 3.208 | 4.951 |
| $\epsilon_\infty$    | 90         | 2.133              | 2.240 | 2.359 | 2.610 | 3.138 | 4.717 |
| $\epsilon_{r\infty}$ | 90         | 1.000              | 2.050 | 1.105 | 1.223 | 1.470 | 2.210 |
| Vol. % Bl.           | 90         | ...                | 0.479 | 0.954 | 1.93  | 3.95  | 8.25  |
| $f$                  | 90         | ...                | 3.49  | 3.67  | 3.86  | 3.97  | 4.93  |

nite rate of shear" is found at the intersection of the line with the ordinate. The last column of Table II indicates the values for  $\epsilon_\infty$  obtained by graphic extrapolation.

The relative dielectric constant of a dispersed system of conductive particles at "infinite shear" may be expressed in terms of volume concentration  $C$  and a form factor  $f$  by the following equation, valid for the concentration range considered.<sup>2</sup>

$$\epsilon_{r\infty} = 1 + 3fc \tag{3}$$

The validity of this semi-empirical relationship has been established.<sup>2,7,8</sup> The value of  $f = 1.00$  for spherical particles and larger for non-spherical particles,<sup>3</sup> its value being indicative of the anisometry of the particle. The values for  $f$  have been calculated and are given in Table III, where the absolute values of the equilibrium dielectric constants at rest  $\epsilon$  have been indicated. In addition, values of  $\epsilon_{r\infty}$  are given.

From the data it appears that  $f$  is increasing with increasing concentration and is somewhat larger at higher temperatures. The magnitude of  $f$  indicates that the kinetic units are not spherical but have a decided anisometric character.

Data obtained at low shear rates indicate that the linear relations valid at higher rates of shear between  $\epsilon$  and  $D^{-1/2}$  break down at lower shear rates. They reveal the existence of a minimum of the  $\epsilon$ - $D$  relationship, the significance of which will be discussed later. The change of the dielectric constant for an 8% dispersion of black at lower rates of shear is indicated in Fig. 5.

**II. Effect of Time.**—Experimental evidence indicates that the dielectric constants of stabilized dispersions show an increase after discontinuation of shear, an effect not observed in conductivity measurements. Such an increase can only be caused by an increasing anisometry of the particles, as a result of the formation of more asymmetric flocculates. The dielectric effect of this process of flocculation is that the form factor increases, resulting in an increased dielectric constant. Defining as the agglomeration factor  $\alpha$  the change in form factor due to flocculation,<sup>2</sup> eq. 3 may be written in the form

$$\epsilon_r = 1 + 3\alpha fc \tag{4}$$

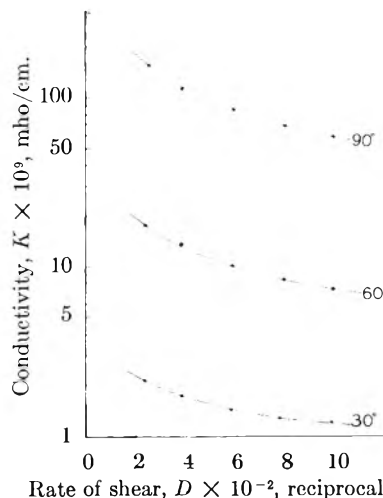


Fig. 1.—Conductivity of unstabilized dispersions of 16% carbon black, effect of shear.

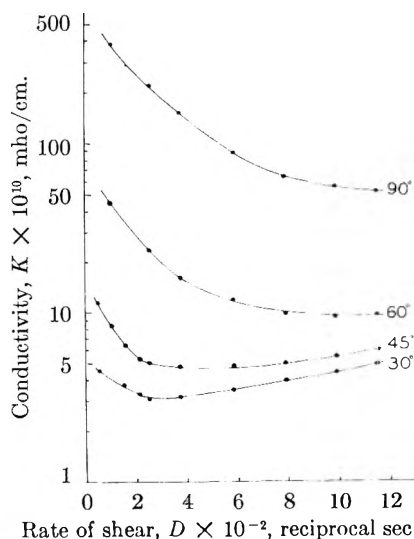


Fig. 2.—Conductivity of unstabilized dispersion of 8% carbon black, effect of shear.

and

$$\alpha = \frac{\epsilon - \epsilon_0}{\epsilon_\infty - \epsilon_0} \tag{5}$$

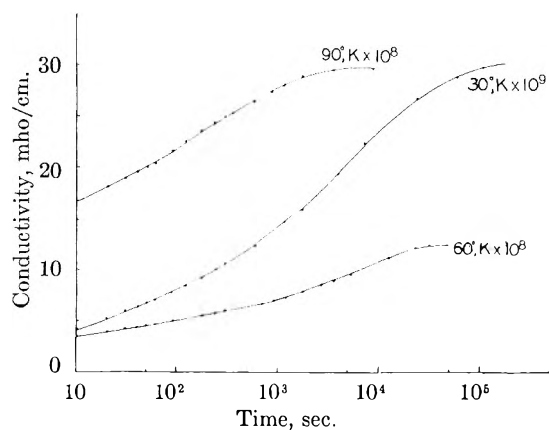


Fig. 3.—Conductivity of unstabilized quiescent dispersions of 8% carbon black, effect of time.

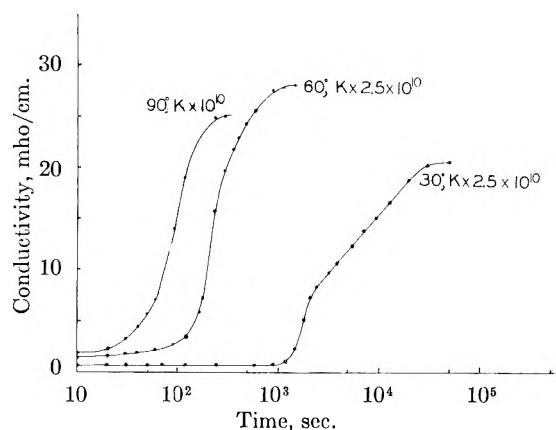


Fig. 4.—Conductivity of unstabilized quiescent dispersions of 2% carbon black, effect of time.

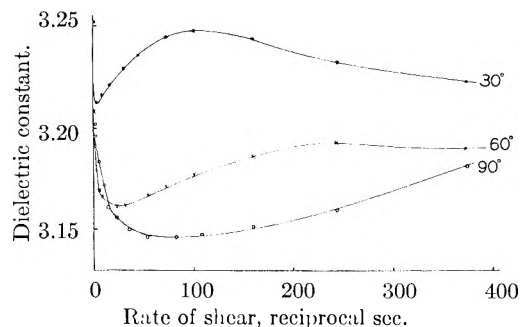


Fig. 5.—Dielectric constant of stabilized dispersions of 8% carbon black, effect of low shear.

where  $\epsilon_0$  represents the dielectric constant of the vehicle.

Figure 6 shows the change in dielectric constant with time for an 8% dispersion. More dilute systems show smaller changes. The increase in agglomeration factor  $\alpha$  is shown in Fig. 7 for a 16% by weight dispersion.

#### D. Dielectric Constant of Unstabilized Systems.

I. **Effect of Shear.**—Figure 8 indicates the decrease in dielectric constant with shear in an  $\epsilon-D^{-1/2}$  plot for a concentration of 16% by weight of carbon black in white mineral oil at varying shear rates. Other concentrations show a similar relationship.

II. **Effect of Time.**—The changes in dielectric constants with time after discontinuation of shear

are given in Fig. 9 for 16% dispersions and in Fig. 10 for 2% dispersions at varying temperatures. At 30° equilibrium is reached in 150 hours for a 16% dispersion; 28 hours for 8%, 2.5 hours for 4% and 0.5 hour for a 2% dispersion.

E. **Hysteresis Phenomena.**—It has been shown that in unstabilized dispersions the dielectric constant as well as the conductivity increases markedly with increasing temperatures. It appears that upon static cooling the process is not reversed and the higher values of the dielectric constant obtained at elevated temperature are only slightly reduced. Thus, of two samples of the same dispersion one may have a dielectric constant several units higher than the other at the same temperature. These differences appear to persist in quiescent dispersions. However, agitation will immediately reduce the dielectric constant and the original value reached at equilibrium will be restored.

Heating and cooling cycles have been indicated in Fig. 11 for a 16% unstabilized black dispersion, where a pronounced hysteresis effect is evident. The cycles can be repeated indefinitely, with identical results.

Hysteresis phenomena have also been observed in the conductivity of unstabilized dispersions, as is shown in Table IV for a 16% black dispersion. Equally, the equilibrium curve is followed upon heating, while upon static cooling the high conductivity values obtained at elevated temperatures are only slightly reduced. Thus, of two samples of the same dispersion one may have a conductivity twenty times as high as the other at the same temperature. Again, agitation restores the equilibrium values.

TABLE IV  
CONDUCTIVITY HYSTERESIS OF A 16% UNSTABILIZED DISPERSION

|                          | $K \times 10^8$ at |      |     |
|--------------------------|--------------------|------|-----|
|                          | 30°                | 60°  | 90° |
| Equilibrium conductivity | 8.8                | 60.0 | 152 |
| Static cooling from 90°  | 148                | 150  | ..  |
| Static cooling from 60°  | 55                 | ...  | ..  |

Hysteresis of the conductivity in unstabilized acetylene black dispersions in mineral oil has been reported by Bondi.<sup>9</sup>

F. **Rheological Properties.**—Plastic viscosities and yield values have been determined with the aid of a rotational viscometer and are indicated in Tables V and VI.

TABLE V  
RHEOLOGICAL PROPERTIES OF STABILIZED DISPERSIONS<sup>a</sup>

| % by wt. | Plastic viscosity in poises |      |      | Yield value, dynes/cm. <sup>2</sup> |     |     |
|----------|-----------------------------|------|------|-------------------------------------|-----|-----|
|          | 30°                         | 60°  | 90°  | 30°                                 | 60° | 90° |
| 0        | 1.60                        | 0.40 | 0.11 | 0                                   | 0   | 0   |
| 1        | 1.73                        | .43  | .12  | 0                                   | 0   | 0   |
| 2        | 1.83                        | .45  | .13  | 0                                   | 0   | 0   |
| 4        | 2.01                        | .51  | .15  | 0                                   | 0   | 0   |
| 8        | 2.60                        | .67  | .19  | 0                                   | 0   | 0   |
| 16       | 4.75                        | 1.20 | .39  | 80                                  | 40  | 0   |

<sup>a</sup> Most of the dispersions show Newtonian flow.

(9) A. A. Bondi, Proc. 2nd Int. Congress on Rheology, Oxford 1953, p. 274.

TABLE VI

RHEOLOGICAL PROPERTIES OF UNSTABILIZED DISPERSIONS<sup>a</sup>

| % black by wt. | Plastic viscosity in poises |      |      | Yield value in dynes/cm. <sup>2</sup> |      |     |
|----------------|-----------------------------|------|------|---------------------------------------|------|-----|
|                | 30°                         | 60°  | 90°  | 30°                                   | 60°  | 90° |
| 0              | 1.09                        | 0.24 | 0.10 | 0                                     | 0    | 0   |
| 1              | 1.17                        | .26  | .11  | 0                                     | 0    | 0   |
| 2              | 1.28                        | .29  | .13  | 0                                     | 0    | 0   |
| 4              | 1.44                        | .37  | .17  | 70                                    | 30   | 20  |
| 8              | 2.03                        | .54  | .30  | 160                                   | 90   | 60  |
| 16             | 4.14                        | 1.54 | 1.16 | 1400                                  | 1100 | 900 |

<sup>a</sup> These data indicate a decrease in yield value at the higher temperatures.

## 6. Discussion

### a. Conductivity Data. 1. Stabilized Systems.

—In stabilized dispersions the electrical current is conducted by ionic conductance. The particles act as insulators, in view of surface polarization.<sup>10,11</sup>

A theoretical explanation of the increase of the conductivity with shear has been offered by Bondi and Penther.<sup>7</sup> This phenomenon may be understood as a charge transfer from one electrode to the other through successive collisions of particles which carry an adsorbed charge in the interface. Thus, the conductivity increase with shear is proportional to the increase in number of collisions per unit of time and should therefore be proportional to the rate of shear, in complete accord with the experiments.

With respect to the relation between conductivity increment and concentration a difficulty seems to arise. While the number of collisions per particle is proportional to the number of particles per unit of volume, the total number of collisions, and therefore the total charge transfer in the dispersion is proportional to the square power of the number of particles per unit of volume, and thus proportional to  $C^2$ . However, only the collisions of particles with an electrode will contribute to the conductivity, resulting in the experimentally found relation.

**2. Unstabilized Systems.**—In unstabilized dispersions the concentration of the ions is several orders of magnitude lower than in stabilized systems. Actually the conductivity of the unstabilized systems is much higher, making it obvious that ionic conductance cannot be the cause of the conductivity of the systems. However, another mechanism of current conductance is now apparent.

In the absence of any significant ionic conductance in the vehicle, surface polarization of the particles cannot take place and the carbon black particles themselves remain conductors for the electric current. This is in agreement with the observation that in unstabilized dispersions no electrophoretic particle motion is observed.<sup>10</sup> As a result of the tendency of the particles to form chains in the absence of stabilizers, the distances between the electrodes are bridged by interlinked particles showing electronic conductance, of a much higher order of magnitude than the ionic conductance found in the

(10) J. Th. G. Overbeek, "Advances in Colloid Science," Vol. III, Interscience Publ., New York, N. Y., 1950, p. 107.

(11) J. C. Van der Minne and P. H. J. Hermanie, *J. Coll. Sci.*, **1**, 600 (1952).

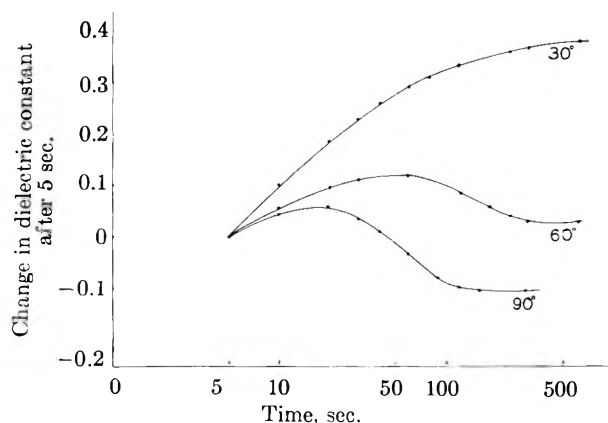


Fig. 6.—Change of dielectric constant with time in a stabilized quiescent dispersion of 8% carbon black.

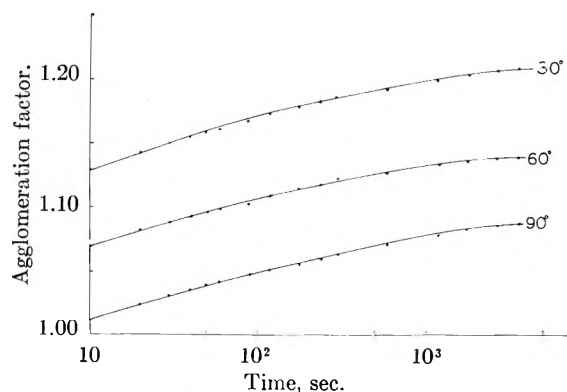


Fig. 7.—Agglomeration factor in stabilized quiescent dispersions of 16% carbon black, effect of time.

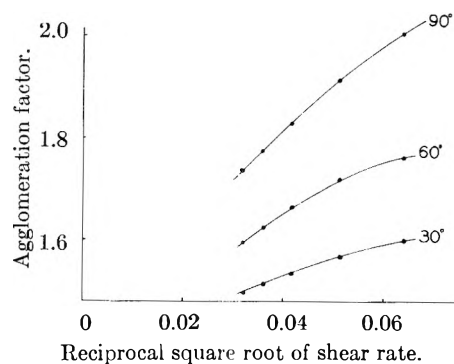


Fig. 8.—Agglomeration factor in unstabilized quiescent dispersions of 16% carbon black, effect of shear.

stabilized dispersions. Therefore, the only significant resistance encountered by the electrons in passing through the dispersion is in the small gaps between adjacent particle chains. By applying shear to the systems, the particle chains are broken up and the conductance drops to a much lower level. Thus, in a 16% by weight dispersion increasing rates of shear cause an increasing degree of destruction of the chains. At the highest rate of shear attainable the process has apparently not been completed, as is shown in Fig. 1, indicating a steady decline in conductivity with shear rate.

Figure 2 shows conductivity data for a concentration of 8% of channel black. While at 90° the general pattern of the 16% dispersion is repeated, at 60° a minimum is apparent at the higher shear

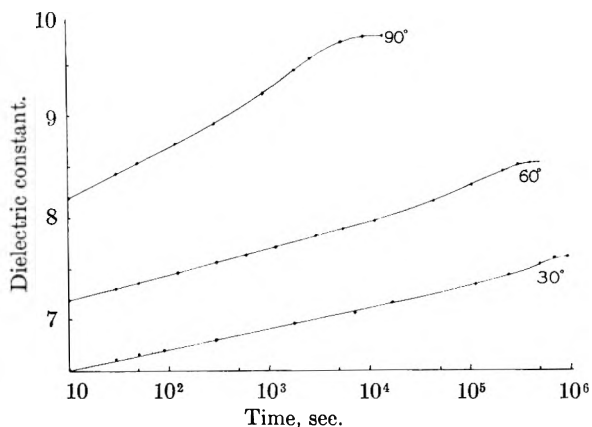


Fig. 9.—Dielectric constant in unstabilized quiescent dispersions of 16% carbon black, effect of time.

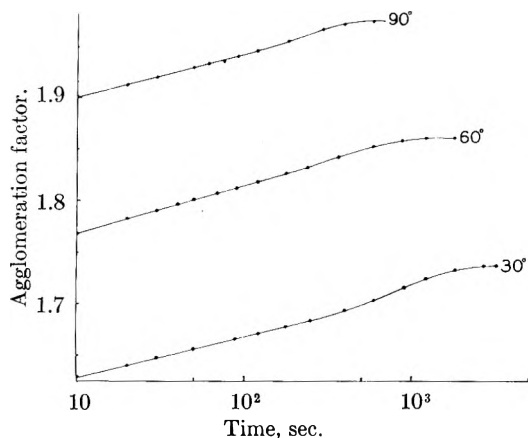


Fig. 10.—Agglomeration factor in unstabilized quiescent dispersions of 2% carbon black, effect of time.

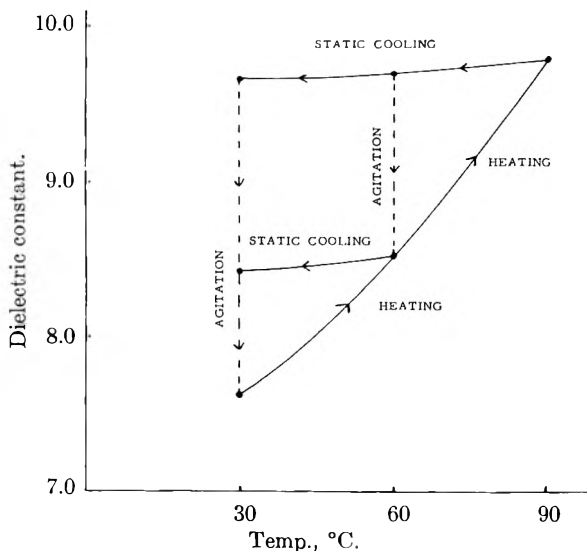


Fig. 11.—Dielectric hysteresis in unstabilized dispersions of 16% carbon black.

rates. At 45° and at 30° the minimum becomes more pronounced and is shifted toward the lower shear rates.

In the stabilized systems the increase in conductivity with increasing shear rates had been attributed to a charge transfer mechanism by colliding particles. The same mechanism must also be ac-

tive in unstabilized systems. While the particle charge in such systems is much smaller than in stabilized dispersions, collisions are likely to be much more frequent, in view of the predominating London-van der Waals particle attraction, as contrasted to the over-all repulsion in stabilized systems.

At low rates of shear there are not very many separate particle agglomerates in unstabilized dispersions, and the charge transfer mechanism contributes little to the conductivity. At increasing shear rates the destruction of particle chains, which causes a marked reduction in conductivity, will offset this action by providing more separate smaller particle agglomerates and chain fragments which in turn contribute to the conductivity by charge transfer. Finally, the charge transfer contributions to the conductivity balance the reductions caused by the elimination of structures. At this point the minimum in conductance is reached and any increase in shear will cause an increase in conductance. Obviously at higher concentrations, where particle chains are much more pronounced, the minimum is shifted toward higher rates of shear.

The influence of the temperature is more complex. The process of chain formation was found to be more pronounced at higher temperatures in unstabilized systems. This may be explained in the following manner. While stabilization by ionic and non-ionic stabilizers is not in effect in these systems, there is always adsorption of vehicle molecules on the surface of the carbon black, which will cause some stabilization, by reducing direct particle contacts, thus decreasing network formation. At more elevated temperatures this adsorption is markedly reduced, in view of the increased speed of the vehicle molecules, resulting in a more extended structural involvement. Thus, it is clear that the higher the temperature, the higher the rate of shear required to break up the particle structures. Consequently, the minimum of the conductance curves is shifted toward higher shear rates at higher temperatures.

The described phenomena make it possible to evaluate quantitatively the effect of stabilizers by establishing the minimum concentration required to change the sign of the conductivity-shear rate relationship.<sup>7</sup> The influence of time on the conductivity reveals an interesting side light on the mechanism of chain formation. A 2% dispersion, after discontinuation of shear, at 30° showed (Fig. 4) a constant conductivity for a period of about 1000 seconds. After this induction period there is a rapid rise in conductivity until the end point has been reached at nearly a tenfold increase. At 60° the same effect becomes apparent, though with a shorter induction period of 100 seconds. At 90° the induction period is still more reduced.

At higher concentrations the induction period is not quite as sharply defined, but a small rise in conductivity is observed in the beginning. Finally, at concentrations of 8% and higher, no induction period is apparent (Fig. 3), although the curves show an inflection point, indicating that the change in conductivity increases steadily, reaches a maximum and decreases thereafter.

The data of the more dilute dispersions indicate that effective interlinking of smaller agglomerates does not occur until at the end of the induction period. During the induction period the kinetic units of the dispersion will join to form smaller separate agglomerates, as may be derived from dielectric data. At the end of the induction period the agglomerates have grown enough to start the process of interlinking into a particle network. In this manner the electrodes are "bridged" by conductive particle chains, leading to the observed rapid increase in conductivity, until a saturation value has been reached.

At higher concentrations the newly formed smaller agglomerates are near enough to one another to start the process of interlinking at an earlier stage, resulting in a less pronounced induction period. Finally, at the highest concentrations, a mere inflection point in the curves indicates the existence of the two processes of growth.

In the stabilized dispersions the rest conductivity reaches its final value immediately after discontinuation of shear, indicating a complete absence of chain formation.

#### b. Dielectric Data. 1. Stabilized Systems.—

The form factor of the stabilized dispersions, as indicated in Table III, appears to vary within fairly narrow limits. Its value is somewhat higher in the more concentrated systems and at the higher temperatures. For spherical particles a value of 1.00 has been found repeatedly by experiments.<sup>2,7</sup> The conclusion must be that the kinetic units in the carbon black dispersions are not spherical. Yet, electron microscopy shows beyond any doubt that elementary particles of channel black are spherical.

This inconsistency can have only one reasonable explanation, namely, that in the systems considered the elementary particles are not the freely moving kinetic units. The actual kinetic unit must be an agglomerate of "fused" particles, although not greatly anisometric. The secondary variations in form factors at different concentrations and temperatures could point to small changes in the average shape of this kinetic unit.

Microscopic observations of the kinetic units were made in a 2% by weight dispersion by means of a homogeneous oil immersion system at 1500 $\times$ . The existence of independent non-spherical particles of a diameter of the order of somewhat below 1  $\mu$  was evident. These particles were observed to show a Brownian motion and collide regularly without breaking up and apparently are the independently moving kinetic units. Actual measurements reveal an average longest dimension of 0.8  $\mu$  and an average shortest dimension of 0.5  $\mu$ , while the shape is somewhat irregular.

The possibility existed that the optically visible particles are only a small fraction of the total and that much smaller and thus optically invisible particles form the bulk of the dispersion. However, a direct particle count showed that such is not the case.

Electron microscopic observation of the same dispersion appears to be possible. The mineral oil evaporates rapidly in the high vacuum upon being

subjected by the electron bombardment in an extremely thin film. The electron micrograph of the particles shows a similarity to a conventional powder electron micrograph, exhibiting clusters of fused elementary particles, irregularly shaped, and of the order of magnitude of somewhat below 1  $\mu$ , making an artifact rather improbable.

It is apparent that the relatively large stable kinetic units, visible as separate particles by optical microscopy, appear in the electron microscope as being built up from fused elementary carbon black particles.

Theoretical investigations<sup>8</sup> show that a form factor 3 corresponds to a particle of the shape of a rotational ellipsoid with an axial ratio of about 6 at random orientation. The fact that the actual axial ratio is slightly below 2 must be ascribed to the more or less irregular shape of the particle cluster.

The data of Table II reveal a small decrease in dielectric constant of the stabilized dispersion upon application of shear. The effect is more pronounced in the more concentrated dispersions.

A more complicated picture emerges at very low rates of shear. For example, in Fig. 5, at 30° initially a sharp drop in dielectric constant is observed at rates of shear below 3 reciprocal seconds, but a sharp rise occurs at a slightly higher shear rate, followed by a maximum. A steady decline is observed at higher rates of shear. Similar effects are observed at higher temperatures, although the location of the maximum is displaced toward higher shear rates.

Since the dielectric constant of dispersions is closely connected with particle anisometry, one must conclude that the effective shape of the secondary agglomerates undergoes important changes at lower rates of shear. The first minimum, at very low rates of shear, may be visualized as caused by a breaking-up of linkages between larger flocculates. However, the ensuing increase in dielectric constant is necessarily connected with an increasing anisometry of the flocculate. Generally it is assumed that increasing shear will cause the larger flocculates to break up into more isometric kinetic units. Apparently this process goes through an intermediate stage of higher dielectric constants, necessarily caused by more anisometric particle agglomerates.

A plausible explanation of this intermediate stage would be that the flocculates are originally formed from linear agglomerates, which at rest and at very low rates of shear will have a tendency to coil, in the same manner as occurs in linear polymers and as was actually optically observed in linear agglomerates of magnetized spherical iron particles dispersed in an organic liquid.<sup>3</sup> Preceding the process of the breaking up of the chains by shear must be the process of "uncoiling," leading to temporarily more anisometric particles. Such a sequence of processes explains the observed dielectric changes without difficulties. This "uncoiling" effect was not observed in 16% by weight dispersions. It seems likely that the more pronounced "crowding" of particles in the concentrated dispersions makes it much more difficult for particle chains to effectively uncoil before breaking up. In all dispersions of 8% and lower the "uncoiling" ef-

fect is apparent, although changes are smaller at lower concentrations and cannot be followed accurately at concentrations of 2% and below.

In concentrated dispersions at 16% by weight of black there is an increase in dielectric constant after discontinuation of shear, pointing to the formation of anisometric flocculates. The effect is more pronounced at lower temperatures, showing that the increased kinetic energy of the particle and the lower vehicle viscosity reduce the structural build-up in stabilized systems at higher temperatures (Fig. 7).

While a major structural build-up may occur within a few seconds after the discontinuation of shear, it is interesting to observe that the process of formation of structures is proceeding for several hours in the more concentrated systems at lower temperatures, until finally equilibrium has been attained.

In lower concentrations, again, the picture is somewhat more complicated. In stabilized dispersions of 8% of carbon black, at 30° an increase in dielectric constant is observed, reaching a saturation value in about 500 seconds (Fig. 6). However, at 60° and at 90° the initial increase is followed by a decrease. In accord with the previously discussed effect of shear, this phenomenon can be explained by assuming once formed linear aggregates to show coiling, thus reverting to a more isometric flocculate with a lower dielectric constant. The lower kinetic energy and the reduced mobility of the flocculate at lower temperatures make this effect more pronounced at higher temperatures. At lower concentrations the same effects are observed, but the magnitude of the changes is much smaller. In addition, it appears that at lower concentrations equilibria are reached much more rapidly, as a result of a freer particle motion. Again, these effects were not observed in 16% concentration, where particle crowding makes uncoiling impossible.

**2. Unstabilized Systems.**—Figure 8 indicates that the application of shear results in a very pronounced decrease in dielectric constant. Such changes are caused by the breaking-down of strongly anisometric particle agglomerates into less anisometric aggregates. However, at the limit of shear rate reached the agglomeration value still is much larger than unity, indicating that the highest value reached, 1200 reciprocal seconds, is utterly insufficient to break up the secondary aggregates, not even in dilute dispersions. It is interesting to note that the addition of chemical stabilizers immediately causes a breaking-up of structures. Thus, for instance, in an unstabilized dispersion of 16% black by weight at 90°, and at a rate of shear of 245 reciprocal seconds, the dielectric constant is 7.30, from which an agglomeration factor of 2.00 is calculated. Chemical stabilization causes a drop in dielectric constant to 5.00 with an agglomeration factor of 1.13, a drop not even remotely approached by the application of shear rate of 981 reciprocal seconds, which reduces the dielectric constant only to 6.59 with an agglomeration factor of 1.74.

As in conductivity, the dielectric data indicate a marked increase of structures at higher tempera-

tures in unstabilized dispersions, caused by the decrease in adsorption of vehicle molecules, which in the adsorbed state act to reduce particle union. In addition, the decreased vehicle viscosity results in an increase in the number of particle collisions per unit of time. Since collision is a prerequisite for the formation of particle agglomerates, the effect will promote the formation of structures.

In stabilized systems increased temperatures cause a decrease in agglomeration. In order to explain the different behavior in both types of dispersions, we must consider that in unstabilized systems the van der Waals attractive forces are counteracted only by the ineffective vehicle adsorption and any change in this adsorption greatly influences the agglomeration. In stabilized systems the attractive forces are counteracted not only by the much more effective steric protection by polar, non-ionic stabilizers, but in addition, by the repulsion of electric charges of equal sign, making the vehicle adsorption inconsequential. The electric repulsion, furthermore, is quite pronounced, since in the systems considered the ionic concentrations are so low that there is practically no screening of the particle charges by counter ions, and Debye's characteristic length of the double layer may be as large as several microns. While at higher temperatures the number of collisions will increase, the higher kinetic energy of the particles still further reduces the already low probability of the colliding particles to be captured in an agglomerate.

## 7. Association and Reticulation

Dielectric data showing the progress of the agglomeration with time after discontinuation of shear indicate that at all concentrations the process of formation of agglomerates is continuously progressing. Comparing this with the character of the changes in conductivity, especially in the lower concentrations, it is quite apparent that dielectric data and conductivity data indicate the existence of two processes active in the unstabilized dispersions. Dielectric data indicate the increasing anisometry of the growing secondary aggregates, while conductivity data show the progress made in the process of interlinking of the agglomerates, leading to a "bridging" of the gap between the electrodes. The latter process apparently occurs generally after the formation of the agglomerates has taken place.

We shall henceforth denote the interlinking of the agglomerates as "reticulation," while the formation of the agglomerates shall be termed "association." The data presented, therefore, indicate that flocculation in unstabilized systems is initiated by association of the existing units of the dispersion, followed by a process of reticulation.

A clear distinction between both processes can be made in dilute dispersions at lower temperatures. For instance, in a 2% unstabilized dispersion at 30°, association occurs continuously from the moment the shear has been discontinued until completed after about 2000 seconds (Fig. 10). Reticulation does not start until after 1000 seconds, apparently when enough association complexes have been formed, and is completed only after about 10,000 seconds (Fig. 4). At higher temperatures both association and reticulation are speeded up.

Thus, at 60° association is practically completed after 600 seconds, while reticulation starts already after 100 seconds and is practically ended after about 1000 seconds. At 90° the overlapping is even more pronounced and association is finished after about 300 seconds, while reticulation starts after 20 seconds and is ended after 300 seconds. At higher concentrations and at elevated temperatures both processes occur simultaneously, as indicated by conductivity and dielectric data. Thus, in a 16% concentration, both reticulation and association continue for long periods of time, of the order of a week or more at 30°, and only slightly shorter at elevated temperatures (Figs. 3 and 9).

#### 8. Electric Responses to Changes in Shear Rates

Upon discontinuation of shear in unstabilized dispersions equilibrium conditions are generally not re-established until after hours, or even days. The electrical responses to a change from one shear rate to another, however, are very rapid. The relaxation time is of the order of one second, both for conductivity and dielectric reactions.

In quiescent concentrated unstabilized dispersions in the equilibrium condition the kinetic units are arranged in a network. The structures can only be established by Brownian motion of the larger kinetic units and by vibrations around equilibrium positions of units partly bound in particle chains. Thus, the time element involved is necessarily long. In sheared dispersions, however, no network exists and equilibrium is rapidly reestablished, since it involves few contacts between large aggregates subject to shear and thus rotating and moving with respect to one another.

#### 9. Hysteresis Phenomena

The explanation of the hysteresis phenomena can be made on the basis of the previously developed picture. Structures formed at higher temperatures apparently are "frozen" at lower temperatures under quiescent conditions. Only upon agitation are the structures broken up and reform as equilibrium structures characteristic of the prevailing temperature. Conversely, structures formed at lower temperatures are able to change into the structures corresponding to higher temperatures upon static heating as a result of the motion of free aggregates and vibration of aggregates captured in chains.

Hysteresis phenomena are the more pronounced the higher the concentration and the larger the temperature differences. The fact that conditions reached upon static cooling seem to persist makes it essential to bring each sample in equilibrium at the measuring temperature before determining its properties.

It is interesting to note that hysteresis in stabilized systems is negligible.

#### 10. Rheological Characteristics

From Table V it appears that all stabilized dispersions show a Newtonian flow pattern, with the exception of the 16% concentration, which shows a very slight yield value. Since it is generally assumed that a Newtonian flow indicates the absence of particle interaction, it is obvious that the conclusions drawn from rheological data may be misleading. This might be caused by the phenomenon that the rheological measurement itself destroys the condition to be measured.

In unstabilized systems a yield value was found at concentrations of 4% by weight and higher. At increased temperatures the magnitude of the yield values decreased.

Electrical data show that structural involvements are much more pronounced at the higher temperatures, making it obvious, though contrary to current opinion, that the yield value is not a direct indication of particle structure. The ratio yield value to plastic viscosity shows at least qualitative agreement with electrical data.

The application of Reiner's criteria<sup>12</sup> in the systems considered leads to completely contradictory conclusions about the cause of the non-Newtonian flow character of the unstabilized dispersions.

In view of the serious discrepancy of the rheological approach to particle interaction in dispersions, much of the conclusions reported in the literature about structural involvements in dispersions based on rheological data alone must be considered questionable.

**Acknowledgment.**—I wish to express my appreciation to W. N. Whitten, Jr., for carrying out the rheological measurements with great precision, and to the J. M. Huber Corporation, for their permission to publish the data.

(12) M. Reiner, "Deformation and Flow," H. K. Lewis and Company, London, 1949.

# DIELECTRIC PROPERTIES OF AQUEOUS IONIC SOLUTIONS AT MICROWAVE FREQUENCIES<sup>1</sup>

By FRANK E. HARRIS<sup>2</sup> AND CHESTER T. O'KONSKI

*Contribution from the Department of Chemistry and Chemical Engineering, University of California, Berkeley, California*

*Received September 4, 1956*

The dielectric constants and loss factors of a number of aqueous ionic solutions were measured at 25° and at concentrations ranging from 0.5 *M* to saturation. Series of 1:1 electrolytes were studied, with constant cation and varying anion, and *vice versa*, to determine the effects of changing the ionic radius. Results were also obtained for some multivalent ions. Measurements were made at wave lengths of 1.17, 3.12 and 10.00 cm. Densities and audiofrequency conductivities of the same solutions were determined. From these primary data were determined relaxation times, parameters describing the extent of distribution of the relaxation times, and limiting values of the dielectric constant at low and high frequencies. At high concentrations, broad distributions of relaxation times are found, with the central relaxation often several times slower than that of pure water. The low frequency dielectric constant ( $\epsilon_0$ ) is not linear in the concentration. Large  $\epsilon_0$  (>30) are obtained even at the highest concentrations (10–12 *M*). Larger dielectric decrements are assigned to cations than to anions, although greater entropy decrements are generally ascribed to anions, a seemingly paradoxical situation. It is indicated how this can be explained in terms of models for cationic and anionic hydration which incorporate the important difference that nearest neighbor water molecules interact through both lone pairs with a given cation, but through a single hydrogen bond type linkage to a given anion. The low frequency dielectric increments are discussed with reference to an extension to ionic solutions of the statistical mechanical theory of dielectric polarization. It is shown how the dielectric constant data obtained at microwave frequencies can be employed to enable comparison of lower frequency measurements with the theory of Debye and Falkenhagen.

## I. Introduction

The dielectric properties of aqueous ionic solutions are of interest in studies of interactions between ions and polar solvent molecules as related to the thermodynamics and kinetics of ions in solution. Both the low frequency dielectric constant and the dielectric relaxation depend upon the molecular interactions, and can provide valuable information regarding the nature and effects of the forces between an ion and its hydration shell.

Dielectric constants of aqueous solutions at moderate concentrations are very difficult to determine at relatively low frequencies, since the high conductances and concomitant large loss angles seriously limit the accuracy of measurement. If the concentration is reduced to decrease the problem arising from conductivity, very high precision is required to determine the correspondingly smaller effects on the dielectric properties as compared with pure water.

A number of investigators have studied the dielectric constants and conductivities of dilute solutions at frequencies up to several hundred megacycles. The earliest such study was reported by Wien<sup>3</sup> in 1927. Data were also reported by Sack,<sup>4a</sup> Zahn,<sup>4b</sup> Deubner<sup>5</sup> and Malsch,<sup>6</sup> and are summarized by Harned and Owen<sup>7</sup> and by Falkenhagen.<sup>8</sup>

The theory of the effect of interionic electrostatic forces on the dielectric constant and conductivity, originally developed by Debye and Falkenhagen<sup>9</sup> and recently improved by Falkenhagen and oth-

ers,<sup>10</sup> indicates that these quantities will be affected by interionic forces at frequencies sufficiently low that the atmosphere about each ion, composed predominantly of ions of opposite charge, will have time to become appreciably asymmetric under the influence of the applied field. Some of the experimental results on very dilute solutions appear in accord with the predictions of these theories. The modified theory<sup>10</sup> is in better agreement with experimental values of conductance for relatively more concentrated solutions. However, it is not permissible to compare the changes in dielectric constants as calculated by the original or modified Debye–Falkenhagen theory with experimental results, since the important effects of the ions upon the orientational polarizability of the neighboring water molecules are completely omitted from consideration.

By going to microwave frequencies, dielectric properties can be measured over a greater concentration range, and with higher accuracy than the fragmentary results referred to above. This was recognized by Hasted, Ritson and Collie,<sup>11</sup> who applied two microwave methods for the measurement of the dielectric constant  $\epsilon'$  and the loss factor  $\epsilon''$  in aqueous ionic solutions. Their data are the most complete for NaCl, which was measured at 1.5 and 21° from 0.5 to 5 *M*, and from 0–40° at 0.66 *M*. Some other electrolytes were measured at 25° and concentrations from 0.33 to 1 or 2 *M*. Values of  $\epsilon'$  and  $\epsilon''$  determined at two or three frequencies were placed on a Cole–Cole diagram and relaxation times were obtained with the assumption that the points fell on semi-circular arcs with centers on the  $\epsilon'$  axis, *i.e.*, that the solutions could be characterized by single relaxation times. It was observed that the low frequency dielectric constants and the relaxation times decreased, essentially linearly, with increasing concentration. The dielectric decrements per unit concentration,  $-(d\epsilon'/dc)$ , were 10–16 for

(1) Based on the thesis submitted by Frank E. Harris in partial satisfaction of the requirements for the Ph.D. degree, University of California, 1954.

(2) Predoctoral Fellow, National Science Foundation, 1952–1953.

(3) M. Wien, *Ann. Physik*, [4] **83**, 840 (1927).

(4) (a) H. Sack, *Physik. Z.*, **29**, 627 (1928); (b) H. Zahn, *Z. Physik*, **51**, 350 (1928).

(5) A. Deubner, *ibid.*, **30**, 946 (1929).

(6) J. Malsch, *ibid.*, **33**, 19 (1932).

(7) H. S. Harned and B. B. Owen, "The Physical Chemistry of Electrolytic Solutions," Reinhold Publ. Corp., New York, N. Y., 1950, p. 211.

(8) H. Falkenhagen, "Electrolytes," Oxford University Press, London, 1934, p. 73.

(9) P. Debye and H. Falkenhagen, *Physik. Z.*, **29**, 121, 401 (1928).

(10) H. Falkenhagen, M. Leist and G. Kelbg, *Ann. Physik*, **11**, 51 (1952).

(11) J. B. Hasted, D. M. Ritson and C. H. Collie, *J. Chem. Phys.*, **16**, 1 (1948).

some alkali halides, and larger for mixed valence electrolytes. It was found that the cationic contribution to  $-d\epsilon'/dc$  depended upon the charge, and was greater for smaller cations. The relaxation time depressions were attributed to a "structure-breaking" effect postulated by Frank and Evans<sup>12</sup> to explain the entropies of aqueous ions.

Subsequently, additional measurements were made by Haggis, Hasted and Buchanan.<sup>13</sup> They reported data for some neutral molecules and generally confirmed the previous results for ionic solutions to 1.0 *M* in concentration. They assumed that the dielectric increment arising from ionic motions was negligible, since evidence for a change in conductivity with increasing frequency could not be found. The low frequency dielectric decrements were interpreted in terms of a simple model, which treats the electrolyte solution as a dielectric continuum of uniform dielectric constant with spherical inclusions of very low dielectric constant to represent non-polar ions and irrotationally bound water molecules. Then, by application of well known equations for the dielectric constant of such a mixture, the volume fractions of the inclusions were computed, and from these and the molar volumes of the salts, the volumes of irrotationally bound water molecules were calculated. It was suggested that for inorganic salts, the positive ions make the larger contributions to irrotational binding. The relaxation time changes were discussed with reference to the percentage of broken hydrogen bonds when solutes are dissolved. For ionic substances the relaxation times decreased, whereas for undissociated molecules likely to form hydrogen bonds, the relaxation times increased. This was interpreted as an increase in the percentage of broken hydrogen bonds when ions are added to water, and a decrease when hydrogen-bond forming molecules were added.

It became of particular interest to test the above interpretation of the dielectric properties of ionic solutions in the region of higher concentrations where any deviations from the simple models considered would be greater, particularly since many of the results were obtained near the upper limits of the previously employed experimental methods. For this study a new microwave technique applicable at very high concentrations was devised. It was found that the dielectric properties of ionic solutions above one molar show strong deviations from the behavior one would expect from an extrapolation of the data previously obtained at lower concentrations. With the aid of the statistical mechanical theory of electric polarization, the results are considered in relation to the various types of interactions in aqueous solutions of ions, with particular attention to the electrostatic forces between ions and water molecules.

## II. Experimental Techniques

The transmission line technique developed for this work has already been described.<sup>14</sup> The method was especially designed for liquids of high permittivity. Measurements were made at wave lengths of 1.17, 3.12 and 10.00 cm., and

(12) H. S. Frank and M. W. Evans, *J. Chem. Phys.*, **13**, 507 (1945).

(13) G. H. Haggis, J. B. Hasted and T. J. Buchanan, *ibid.*, **20**, 1452 (1952).

(14) F. E. Harris and C. T. O'Konski, *Rev. Sci. Inst.*, **26**, 482 (1955).

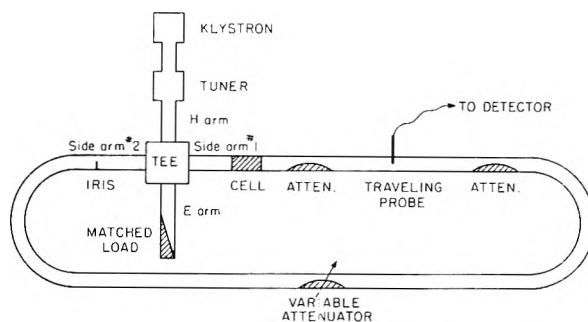


Fig. 1.—Apparatus used at 3 and 10 cm. wave lengths. All elements are constructed in rectangular wave guide,  $1'' \times 1/2''$  for 3 cm., and  $3'' \times 1.5''$  for 10 cm.

a temperature of 25°. Transmission coefficients of samples contained between mica windows in short sections of wave guide were measured by mixing the wave transmitted through the sample with a wave of known amplitude and phase traveling in the opposite direction. The resulting standing wave pattern was detected with a traveling probe. The primary data were related to the dielectric properties of the solutions by graphical methods.<sup>14</sup>

The apparatus used at 1.17 cm. is exactly as described previously.<sup>14</sup> A diagram of the 3 and 10 cm. apparatus, not given previously, is shown in Fig. 1.

The signal from a klystron is coupled through a tuner to transmit maximum power into the "H arm" of a magic tee. By means of an iris and matched load on the "E arm," the signal is divided among the side arms 1 and 2 of the tee. The arrangement is such that the net signal incident upon the cell is proportional to, and at constant phase relative to, the signal passing beyond the iris. The position and size of the iris are such as to maximize the power incident on the cell while permitting power equal to about 1% of the reference signal to pass the iris. By means of the traveling probe, the amplitude and phase of the radiation passing through the cell is compared with the signal from side arm 2 of the tee. This apparatus functions on the same principles as the 1.17 cm. apparatus which has already been described in detail.<sup>14</sup> The cell lengths employed in these studies were  $0.254 \pm 0.001$  cm.,  $0.381 \pm 0.001$  cm., and  $0.510 \pm 0.003$  cm., for 1.17, 3.12 and 10.00 cm., respectively.

Frequent measurements were made on water to ensure the best possible precision for the changes produced by addition of electrolytes. Readings for pure water were constant within 0.5 unit in both  $\epsilon'$  and  $\epsilon''$  for each series of measurements. The average deviation from the mean of 3 cm. measurements on two different samples of solution at different times, for a series of eight representative solutions, turned out to be 0.7 in  $\epsilon'$  (values from 23 to 50), and 0.5 in  $\epsilon''$  (values from 42 to 59). Comparable precision was obtained at other wave lengths.

Necessary auxiliary measurements included determinations of low frequency conductance, and of density. Conductance measurements were made using an audiofrequency shielded Wheatstone bridge. A conductance cell with a cell constant of  $724.6 \text{ cm.}^{-1}$  was employed. The cell, constructed according to the design recommended by Jones and Bollinger,<sup>15</sup> had bright platinum electrodes 1.5 cm. in diameter and 24 cm. apart, connected by a 3 mm. o.d. glass tube. The cell constant was found to be independent of frequency, for all solutions tested, from 100 to 1200 c.p.s. All measurements were made at 1 kc. The cell was calibrated with 1 *M* KCl ( $\sigma_{25} = 0.1118 \text{ ohm}^{-1} \text{ cm.}^{-1}$ ). The accuracy of the conductance measurements was better than 0.5%.

Density was determined by pipetting a 10-ml. portion of each solution into a stoppered flask and weighing to within 10 mg.

Reagent quality chemicals were used for the preparation of all solutions used in the present research. A stock solution of each solute was made up and its concentration determined by standard methods. Dilution was then made to the desired concentrations.

## III. Results

The dielectric constants and loss factors of a

(15) G. Jones and G. M. Bollinger, *J. Am. Chem. Soc.*, **53**, 411 (1931).

TABLE I

DIELECTRIC CONSTANTS AND LOSS FACTORS AT MICROWAVE FREQUENCIES, DENSITIES AND AUDIOFREQUENCY CONDUCTIVITIES OF AQUEOUS IONIC SOLUTIONS AT 25.0°

Units of concentration are moles/liter, of conductivity ohm<sup>-1</sup> cm.<sup>-1</sup>, of density g./cc.

| Solute                            | Concn. | Density | Audio cond. | $\epsilon'$ | 1.17 cm.<br>$\epsilon''_{\text{obsd}}$ | $\epsilon''_{\text{cor}}$ | $\epsilon'$ | 3.12 cm.<br>$\epsilon''_{\text{obsd}}$ | $\epsilon''_{\text{cor}}$ | $\epsilon'$ | 10.00 cm.<br>$\epsilon''_{\text{obsd}}$ | $\epsilon''_{\text{cor}}$ |
|-----------------------------------|--------|---------|-------------|-------------|--|---------------------------|-------------|--|---------------------------|-------------|---|---------------------------|
| LiCl                              | 2      | 1.044   | 0.1234      | 25.8        | 32.8                                   | 24.1                      | 42.8        | 40.7                                   | 17.6                      | 52.0        | 80.1                                    | 6.0                       |
|                                   | 4      | 1.087   | .1785       | 21.2        | 25.6                                   | 13.1                      | 35.0        | 46.4                                   | 12.9                      |             |   |                           |
|                                   | 8      | 1.164   | .1684       | 14.4        | 17.6                                   | 5.8                       | 22.0        | 40.2                                   | 8.6                       | 36.0        | 103.0                                   | 1.9                       |
| LiBr                              | 12     | 1.238   | .1020       | 11.8        | 12.6                                   | 5.4                       | 17.6        | 26.0                                   | 7.8                       | 34.0        | 60.0                                    | -1.3                      |
|                                   | 2      | 1.119   | .1346       | 26.3        | 32.9                                   | 23.4                      | 42.8        | 41.4                                   | 16.2                      |             |   |                           |
|                                   | 4      | 1.241   | .2022       | 22.3        | 25.7                                   | 12.5                      | 35.2        | 50.0                                   | 12.1                      |             |   |                           |
| NaCl                              | 10     | 1.591   | .1476       | 13.4        | 14.9                                   | 4.5                       | 20.8        | 33.7                                   | 6.0                       |             |   |                           |
|                                   | 2      | 1.077   | .1509       | 28.1        | 33.6                                   | 23.0                      | 49.2        | 45.5                                   | 17.2                      |             |   |                           |
|                                   | 4      | 1.150   | .2297       | 23.3        | 31.9                                   | 15.8                      | 38.2        | 55.7                                   | 12.7                      |             |   |                           |
| NaBr                              | 5      | 1.182   | .2481       | 21.2        | 31.0                                   | 13.6                      | 33.7        | 58.0                                   | 11.5                      |             |   |                           |
|                                   | 2      | 1.154   | .1602       | 27.8        | 33.4                                   | 22.1                      | 48.2        | 48.9                                   | 18.9                      | 60.0        | 103.4                                   | 7.2                       |
|                                   | 4      | 1.305   | .2441       | 23.6        | 32.0                                   | 14.8                      | 38.2        | 57.2                                   | 11.5                      |             |   |                           |
| NaI                               | 2      | 1.222   | .1628       | 29.0        | 33.9                                   | 22.5                      | 46.7        | 47.9                                   | 17.4                      |             |   |                           |
|                                   | 4      | 1.452   | .2534       | 23.8        | 32.0                                   | 14.2                      | 37.8        | 58.0                                   | 10.5                      |             |   |                           |
|                                   | 8      | 1.873   | .2221       | 16.0        | 22.6                                   | 7.0                       | 23.5        | 48.9                                   | 7.3                       | 35.0        | 135                                     | 2                         |
| KF                                | 1      | 1.043   | .0883       | 31.0        | 36.2                                   | 30.0                      | 56.0        | 41.5                                   | 25.0                      | 68.5        | 60.8                                    | 7.8                       |
|                                   | 4      | 1.177   | .2456       | 26.8        | 33.1                                   | 15.8                      | 42.4        | 62.1                                   | 16.1                      |             |   |                           |
|                                   | 8      | 1.332   | .3045       | 18.1        | 29.5                                   | 8.1                       | 29.2        | 69.2                                   | 12.1                      |             |   |                           |
| KCl                               | 12     | 1.469   | .2537       | 16.2        | 23.4                                   | 5.6                       | 22.3        | 57.0                                   | 9.5                       | 48.5        | 156                                     | 4                         |
|                                   | 1      | 1.039   | .1127       | 30.8        | 34.5                                   | 26.6                      | 54.4        | 42.8                                   | 21.7                      | 68.5        | 75.2                                    | 7.5                       |
|                                   | 2      | 1.100   | .2174       | 30.7        | 36.2                                   | 20.9                      | 50.7        | 58.9                                   | 18.2                      |             |   |                           |
| KBr                               | 4      | 1.174   | .3745       | 30.1        | 37.5                                   | 11.2                      | 44.0        | 80.4                                   | 10.2                      |             |   |                           |
|                                   | 1      | 1.081   | .1163       | 30.0        | 34.3                                   | 26.1                      | 55.4        | 44.2                                   | 22.4                      |             |   |                           |
|                                   | 2      | 1.164   | .2204       | 30.6        | 36.2                                   | 20.7                      | 51.9        | 59.1                                   | 17.8                      |             |   |                           |
| KI                                | 1      | 1.121   | .1177       | 30.1        | 34.4                                   | 26.1                      | 55.4        | 43.8                                   | 21.7                      |             |   |                           |
|                                   | 2      | 1.244   | .2260       | 35.9        | 36.7                                   | 20.8                      | 51.8        | 59.8                                   | 17.4                      |             |   |                           |
|                                   | 4      | 1.470   | .3968       | 29.8        | 34.2                                   | 6.3                       | 44.0        | 79.8                                   | 5.4                       |             |   |                           |
| Na <sub>2</sub> SO <sub>4</sub>   | 1      | 1.118   | .0961       | 27.1        | 33.2                                   | 26.4                      | 50.3        | 40.4                                   | 22.4                      |             |   |                           |
| NaNO <sub>3</sub>                 | 2      | 1.106   | .1257       | 28.4        | 33.8                                   | 25.0                      | 49.8        | 43.1                                   | 19.5                      |             |   |                           |
| NaClO <sub>4</sub>                | 4      | 1.210   | .1811       | 26.6        | 27.8                                   | 15.1                      | 38.7        | 45.9                                   | 12.0                      |             |   |                           |
|                                   | 2      | 1.152   | .1298       | 28.1        | 33.6                                   | 24.5                      | 48.4        | 42.5                                   | 18.2                      |             |   |                           |
|                                   | 4      | 1.305   | .1819       | 24.2        | 25.1                                   | 12.3                      | 34.5        | 44.6                                   | 10.5                      |             |   |                           |
| MgCl <sub>2</sub>                 | 1      | 1.073   | .1186       | 26.6        | 33.3                                   | 25.0                      | 46.2        | 42.9                                   | 20.7                      | 56.4        | 76.2                                    | 5.0                       |
|                                   | 2      | 1.145   | .1600       | 25.1        | 27.3                                   | 16.1                      | 35.0        | 45.0                                   | 15.0                      |             |   |                           |
|                                   | 3      | 1.202   | .1563       | 16.8        | 20.6                                   | 9.6                       | 28.0        | 39.9                                   | 10.6                      | 41.0        | 99.1                                    | 3.0                       |
| CaCl <sub>2</sub>                 | 4      | 1.269   | .1242       | 13.8        | 16.2                                   | 7.5                       | 24.1        | 33.2                                   | 9.9                       |             |   |                           |
|                                   | 0.5    | 1.043   | .0776       | 29.0        | 33.9                                   | 28.4                      | 52.6        | 37.7                                   | 23.2                      | 63.6        | 50.6                                    | 4.0                       |
|                                   | 1      | 1.086   | .1331       | 26.1        | 32.8                                   | 23.4                      | 46.1        | 43.9                                   | 19.0                      | 56.5        | 82.6                                    | 2.7                       |
| CaBr <sub>2</sub>                 | 2      | 1.167   | .1953       | 22.4        | 27.7                                   | 14.0                      | 35.8        | 50.7                                   | 14.1                      | 53.0        | 120                                     | 3                         |
|                                   | 4      | 1.316   | .1724       | 16.3        | 18.2                                   | 6.1                       | 24.5        | 40.3                                   | 8.0                       |             |   |                           |
|                                   | 0.5    | 1.078   | .0828       | 31.0        | 33.1                                   | 27.3                      | 52.2        | 38.2                                   | 22.7                      |             |   |                           |
| BaCl <sub>2</sub>                 | 1      | 1.156   | .1436       | 26.3        | 32.9                                   | 22.8                      | 45.9        | 47.0                                   | 20.1                      |             |   |                           |
|                                   | 0.5    | 1.085   | .0811       | 29.0        | 33.9                                   | 28.2                      | 53.9        | 39.1                                   | 23.9                      |             |   |                           |
|                                   | 1.0    | 1.171   | .1369       | 27.6        | 33.5                                   | 23.9                      | 49.2        | 46.0                                   | 20.3                      |             |   |                           |
| Al(NO <sub>3</sub> ) <sub>3</sub> | 1.5    | 1.258   | .1781       | 26.1        | 30.1                                   | 17.6                      | 44.2        | 48.3                                   | 14.9                      | 54.5        | 111.2                                   | 4.2                       |
|                                   | 1      | 1.154   | .1144       | 24.7        | 24.8                                   | 16.8                      | 38.3        | 38.2                                   | 16.8                      | 52.5        | 73.7                                    | 5.0                       |

number of inorganic electrolytes in aqueous solutions were measured at 25.0°, at concentrations ranging up to saturation. Data at the three wavelengths are listed in Table I, which also contains values of density and audiofrequency conductivity, determined on samples of the same solutions.

The correction of  $\epsilon''$  for ohmic conductance was calculated by the relation  $\epsilon''_{\text{cor}} = \epsilon''_{\text{obs}} - 2\sigma/\nu$ , where  $\nu$  is the frequency and  $\sigma$  the electrical conductivity in e.s.u. Following the suggestion in sections I and IV (5), we assume the ohmic conductance at microwave frequencies is the same as at audio frequencies, and therefore identify  $\sigma$  with the

audio frequency conductivity. Values of the corrected values,  $\epsilon''_{\text{cor}}$ , are also given in Table I.

The data were analyzed to characterize the relaxation, to determine a low frequency limiting value of the dielectric constant,  $\epsilon_0$ , and to obtain its high frequency limit,  $\epsilon_\infty$ . This was done by means of complex diagram plots of  $\epsilon'$  and  $\epsilon''$ . Cole and Cole<sup>16</sup> have discussed the use of such plots in studying relaxation phenomena, and have pointed out that many systems exhibit relaxation plots closely approximating circular arcs whose centers lie on or below the  $\epsilon'$  axis. The former case, which results

(16) K. S. Cole and R. H. Cole, *J. Chem. Phys.*, **9**, 341 (1941).

TABLE II

LIMITING LOW AND HIGH FREQUENCY DIELECTRIC CONSTANTS, RELAXATION TIMES, RELAXATION DISTRIBUTION PARAMETERS AND CORRELATION PARAMETERS OF AQUEOUS IONIC SOLUTIONS AT 25.0°

Units of concentration are moles/liter, of  $\lambda_D$ , cm. and of  $\mu$ , Debyes.

| Solute                            | Concn. solute | Concn. H <sub>2</sub> O | $\epsilon_0$ | $\epsilon_\infty$ | $\lambda_D$ | $\alpha$ | $\tau^2$ | $\mu^2\gamma$ | $a$  |
|-----------------------------------|---------------|-------------------------|--------------|-------------------|-------------|----------|----------|---------------|------|
| LiCl                              | 2             | 53.3                    | 52.5         | 5.5 ± 1           | 1.43        | 0.00     | 1.84     | 8.02          | 1.75 |
|                                   | 4             | 50.9                    | 50           | .....             | 1.75        | .28      | 1.91     | 7.98          | 1.74 |
|                                   | 8             | 45.8                    | 39           | 5.5 ± 2           | 4.3         | .50      | 2.02     | 6.66          | 1.45 |
|                                   | 12            | 40.5                    | 35           | 4.2 ± 1           | 8.0         | .57      | 2.13     | 6.52          | 1.42 |
| LiBr                              | 2             | 52.5                    | 51.8         | .....             | 1.34        | .00      | 1.84     | 8.18          | 1.78 |
|                                   | 4             | 49.6                    | 49.3         | .....             | 1.61        | .29      | 1.91     | 8.07          | 1.76 |
|                                   | 10            | 40.1                    | 39           | .....             | 7.2         | .53      | 2.12     | 7.40          | 1.61 |
| NaCl                              | 2             | 53.3                    | 59.5         | .....             | 1.33        | .10      | 1.83     | 9.32          | 2.03 |
|                                   | 4             | 50.8                    | 46.0         | .....             | 1.22        | .14      | 1.88     | 7.40          | 1.62 |
|                                   | 5             | 49.3                    | 42.0         | .....             | 1.32        | .18      | 1.90     | 6.90          | 1.51 |
| NaBr                              | 2             | 52.6                    | 62.4         | 5.5 ± 1           | 1.47        | .13      | 1.84     | 9.88          | 2.16 |
|                                   | 4             | 49.6                    | 47.2         | .....             | 1.24        | .19      | 1.92     | 7.69          | 1.68 |
| NaI                               | 2             | 51.2                    | 55.5         | .....             | 1.28        | .06      | 1.89     | 8.88          | 1.94 |
|                                   | 4             | 47.3                    | 45.7         | .....             | 1.16        | .20      | 2.01     | 7.61          | 1.66 |
|                                   | 8             | 37.4                    | 37.0         | 4.8 ± 1           | 2.8         | .40      | 2.20     | 7.35          | 1.60 |
| KF                                | 1             | 54.7                    | 70.0         | 5.0 ± 1           | 1.60        | 0.00     | 1.79     | 10.83         | 2.36 |
|                                   | 4             | 52.4                    | 64.0         | .....             | 1.96        | .32      | 1.86     | 10.12         | 2.21 |
|                                   | 8             | 48.1                    | 60           | .....             | 6.7         | .47      | 1.93     | 10.13         | 2.21 |
|                                   | 12            | 42.8                    | 57           | 4.0 ± 1           | 19          | .58      | 2.00     | 10.60         | 2.31 |
| KCl                               | 1             | 53.4                    | 70.5         | 5.5 ± 1           | 1.52        | .11      | 1.80     | 11.15         | 2.43 |
|                                   | 2             | 52.8                    | 66.3         | .....             | 1.36        | .22      | 1.83     | 10.50         | 2.29 |
|                                   | 4             | 48.6                    | 62           | .....             | 1.10        | .56      | 1.89     | 10.48         | 2.29 |
| KBr                               | 1             | 53.3                    | 69.3         | .....             | 1.46        | .09      | 1.81     | 10.94         | 2.39 |
|                                   | 2             | 51.4                    | 67.5         | .....             | 1.36        | .23      | 1.85     | 10.92         | 2.38 |
| KI                                | 1             | 53.0                    | 69.5         | .....             | 1.45        | .11      | 1.84     | 10.94         | 2.39 |
|                                   | 2             | 50.6                    | 67.6         | .....             | 1.35        | .25      | 1.89     | 11.00         | 2.40 |
|                                   | 4             | 44.7                    | 57.5         | .....             | 1.07        | .68      | 2.01     | 10.21         | 2.23 |
| Na <sub>2</sub> SO <sub>4</sub>   | 1             | 54.2                    | 62.5         | .....             | 1.46        | .04      | 1.83     | 9.63          | 2.10 |
| NaNO <sub>3</sub>                 | 2             | 51.9                    | 60.3         | .....             | 1.37        | .05      | 1.83     | 9.70          | 2.12 |
|                                   | 4             | 48.3                    | 48.4         | .....             | 1.15        | .21      | 1.87     | 8.22          | 1.79 |
| NaClO <sub>4</sub>                | 2             | 50.3                    | 57.8         | .....             | 1.31        | .05      | 1.83     | 9.58          | 2.09 |
|                                   | 4             | 45.2                    | 45.2         | .....             | 1.30        | .30      | 1.87     | 8.19          | 1.79 |
| MgCl <sub>2</sub>                 | 1             | 54.3                    | 57.1         | 5.5 ± 1           | 1.51        | .00      | 1.84     | 8.74          | 1.91 |
|                                   | 2             | 53.0                    | 49.0         | .....             | 1.20        | .19      | 1.90     | 7.53          | 1.64 |
|                                   | 3             | 50.8                    | 44.3         | 3.3 ± 1           | 1.70        | .37      | 1.96     | 6.96          | 1.52 |
|                                   | 4             | 49.3                    | 42.0         | .....             | .....       | .39      | 2.02     | 6.68          | 1.46 |
| CaCl <sub>2</sub>                 | 0.5           | 54.8                    | 64.3         | 5.5 ± 1           | 1.41        | .01      | 1.81     | 9.86          | 2.15 |
|                                   | 1             | 54.1                    | 57.5         | 5.2 ± 1           | 1.43        | .07      | 1.85     | 8.81          | 1.92 |
|                                   | 2             | 52.4                    | 54.0         | 5.0 ± 1           | 1.55        | .29      | 1.92     | 8.37          | 1.83 |
|                                   | 4             | 48.4                    | 49           | 5.0 ± 2           | 5.6         | .53      | 2.04     | 7.93          | 1.73 |
| CaBr <sub>2</sub>                 | 0.5           | 54.3                    | 65.0         | .....             | 1.45        | .03      | 1.82     | 10.03         | 2.19 |
|                                   | 1             | 53.1                    | 60.2         | .....             | 1.55        | .09      | 1.87     | 9.36          | 2.04 |
| BaCl <sub>2</sub>                 | 0.5           | 54.4                    | 68.9         | .....             | 1.60        | .04      | 1.84     | 10.57         | 2.31 |
|                                   | 1.0           | 53.4                    | 63.4         | .....             | 1.52        | .09      | 1.89     | 9.76          | 2.13 |
|                                   | 1.5           | 52.5                    | 58.2         | 5.5 ± 1           | 1.3         | .22      | 1.94     | 8.97          | 1.96 |
| Al(NO <sub>3</sub> ) <sub>3</sub> | 1             | 52.2                    | 55.7         | 5.5 ± 1           | 1.51        | .22      | 1.87     | 8.79          | 1.92 |

in a semi-circular relaxation diagram, corresponds to a system whose relaxation obeys the Debye equations with a single relaxation time. When the center of the circle lies below the  $\epsilon'$  axis, Cole and Cole show that the angle  $\alpha\pi/2$  between the  $\epsilon'$  axis and a radius of the circular arc drawn to its inner intercept upon the  $\epsilon'$  axis may be used to characterize the width of the distribution of relaxation times necessary to describe the system. The limit  $\alpha = 0$ , then, refers to a system with a single relaxation time, and larger values of  $\alpha$  correspond to broader distributions.

Circular arcs were drawn through the experimental points of the present research. Since the

maximum number of points available for any one solution was three, it was not possible to determine whether or not the relaxation curves were actually circular. However, the limiting values,  $\epsilon_0$  and  $\epsilon_\infty$ , behaved in such a way as to suggest that circular arcs were a reasonable approximation to the data within the experimental accuracy. Moreover, experimental results for water are available at more than five frequencies, and all these data lie on the same semi-circle,<sup>17</sup> thus establishing that a circular arc is the limiting form of the relaxation plots at low concentrations.

(17) C. H. Collie, J. B. Hasted and D. M. Ritson, *Proc. Phys. Soc. (London)*, **60**, 145 (1948).

Values of  $\epsilon_\infty$  could be determined from the inner intercept of the arcs with the  $\epsilon'$  axis. These values, in the more dilute solutions, were close to 5.5, the value for water; however, in the more concentrated solutions, significant decrements were observed.

Data at 10 cm. were not taken for some solutions. To define relaxation curves for these solutions, a value for  $\epsilon_\infty$  was assumed, either by interpolation or extrapolation from other concentrations of the same solute, or by comparison with other solutions of the same cationic composition. This procedure did not seriously influence the interpretation of the results, since the range of values of  $\epsilon_\infty$  was insufficient to produce much uncertainty in either  $\epsilon_0$ , or  $\lambda_s$ , the wave length at the maximum value of  $\epsilon''$ .

For each solution, values of  $\epsilon_0$ ,  $\epsilon_\infty$ ,  $\lambda_s$  and  $\alpha$  were determined and these are given in Table II.

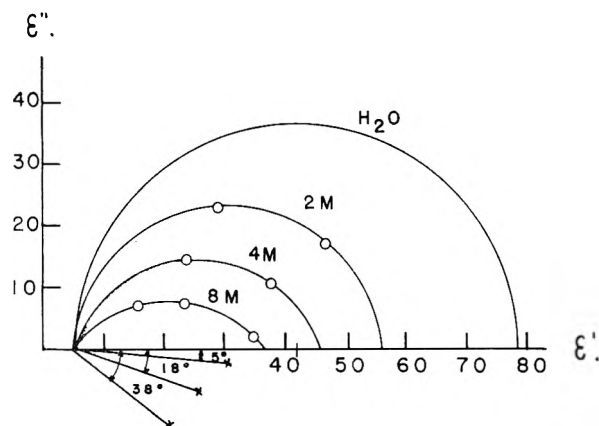


Fig. 2.—Dielectric relaxation in NaI solutions.

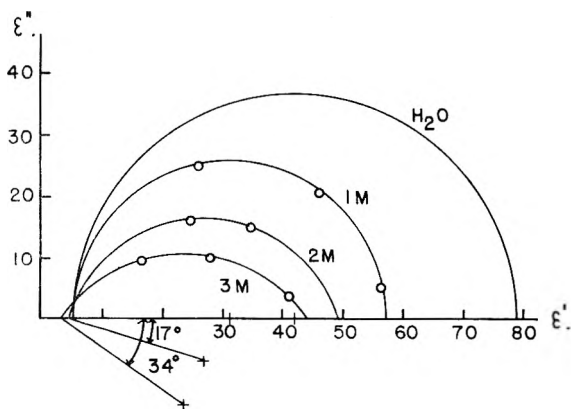


Fig. 3.—Dielectric relaxation in  $MgCl_2$  solutions.

The methods used for treatment of the results differ from the procedures used by previous investigators of ionic solutions. Hasted, Ritson and Collie<sup>11</sup> assumed that their data could be interpreted on the basis of a single relaxation time, and drew semi-circles through their experimental points. For many of the solutions studied, they had but one experimental point, so it was necessary for them to make the additional assumption that  $\epsilon_\infty = 5.5$  to completely define the curves. Their justification of the procedure was that the resulting values of the extrapolated low frequency dielectric constant and of the relaxation time showed a consistent, regular

behavior which suggested that the assumptions made were not unreasonable. More recently, Haggis, Hasted and Buchanan<sup>12</sup> presented results which they too analyzed in terms of a single relaxation time. In that research there were at least two points available for most of the solutions and it was not necessary to assume a value for  $\epsilon_\infty$ . Both of the above-mentioned studies were primarily concerned with relatively dilute solutions, below 1 M, and the present study indicates that the assumption of a single relaxation time was not in serious error at those concentrations.

Typical sets of relaxation plots are shown in Figs. 2 and 3. It can be seen that the distribution of relaxation times becomes quite broad at high concentrations, so that the assumption of a single relaxation time is clearly inadequate.

The values of  $\epsilon_0$  were plotted against the concentration of solute, and limiting slopes at low concentration were obtained. These plots showed considerable curvature, with the slopes decreasing in absolute value at higher concentrations. Examples of such curves appear in Figs. 4 and 5. In Table III the limiting slopes are listed for each electrolyte.

Plots of  $\lambda_s$  vs. concentration typically show the behavior illustrated by the examples of sodium and lithium salts in Fig. 6. Evidently the effect which tends to decrease  $\lambda_s$  at low concentrations is opposed by another effect which becomes more important at the higher concentrations.

#### IV. Discussion

**1. Low Frequency Dielectric Constants at Low Concentration.**—Let us first consider the dependence of the low frequency dielectric constants upon concentration, in the limit of low concentration. From the limiting slopes presented in Table III, it can be seen that the charge on the cation is an important factor influencing the dielectric constant depression. The results are, within experimental error, the same for a bromide or iodide as they are for the corresponding chloride. This suggests that a zero contribution can be assigned to the ions  $Cl^-$ ,  $Br^-$ ,  $I^-$ . Accordingly, to facilitate comparison of the various cations, the slopes for different compounds containing the same cations have been averaged, and the result listed in the columns for ions in the table. The slope for KF is considerably larger than that for any of the other potassium salts. Therefore, KCl, KBr and KI were used to compute the average slope listed for  $K^+$ , and the excess slope present in KF has been attributed to the fluoride ion.

The cation slopes of Table III indicate that the dielectric constant depression decreases with increasing size among cations of the same charge, but that this effect is not as large as that caused by changes in charge. Graphs showing the effect of cationic charge and size upon  $\epsilon_0$  are shown in Figs. 4 and 5. The depression associated with the fluoride ion is considerably smaller than that associated with any of the cations studied.

All the discussion of the data has, up to this point, been with regard to the solution as a whole. If we are interested in finding out about the effect of the ions on the water molecules, we must take

TABLE III

(a) SLOPES OF DIELECTRIC CONSTANT AND WATER DIPOLE CORRELATION PARAMETER AGAINST CONCENTRATION. EXTRAPOLATED TO ZERO CONCENTRATION

(b) MONATOMIC ION ASSIGNMENTS

| Solute                                | $\frac{-d\epsilon}{dc}$<br>(moles/l.) <sup>-1</sup> | Ion              | $\left(\frac{-d\epsilon}{dc}\right)_{av.}$<br>(moles/l.) <sup>-1</sup><br>(±2) | $\left(\frac{-d\theta}{dc}\right)_{av.}$ | $\bar{S}$ (e.u.) <sup>a</sup> |
|---------------------------------------|---|------------------|--|--|-------------------------------|
| LiCl                                  | 14 ± 2  | Li <sup>+</sup>  | 14   | 0.40                                     | 3.4                           |
| LiBr                                  | 15  | Na <sup>+</sup>  | 10   | .26                                      | 14.4                          |
| NaCl                                  | 10  | K <sup>+</sup>   | 7  | .13                                      | 24.5                          |
| NaBr                                  | 8   | Mg <sup>++</sup> | 28   | .65                                      | -28                           |
| NaI                                   | 12  | Ca <sup>++</sup> | 27   | .57                                      | -13.2                         |
| KF                                    | 10  | Ba <sup>++</sup> | 21   | .42                                      | 3.0                           |
| KCl                                   | 7   | Al <sup>±s</sup> | 30 (?)   | .7 (?)                                   | -74.9                         |
| KBr                                   | 8   | F <sup>-</sup>   | 3  | .08                                      | -2.3                          |
| KI                                    | 6   | Cl <sup>-</sup>  | (0)  | (0)                                      | 13.2                          |
| 1/2(Na <sub>2</sub> SO <sub>4</sub> ) | 9   | Br <sup>-</sup>  | (0)  | (0)                                      | 19.2                          |
| NaNO <sub>3</sub>                     | 10  | I <sup>-</sup>   | (0)  | (0)                                      | 26.1                          |
| NaClO <sub>4</sub>                    | 11  |                  |  |  |                               |
| MgCl <sub>2</sub>                     | 28  |                  |  |  |                               |
| CaCl <sub>2</sub>                     | 27  |                  |  |  |                               |
| CaBr <sub>2</sub>                     | 27  |                  |  |  |                               |
| BaCl <sub>2</sub>                     | 21  |                  |  |  |                               |
| Al(NO <sub>3</sub> ) <sub>3</sub>     | 30 ± 5  |                  |  |  |                               |

<sup>a</sup> The zero of  $\bar{S}$  is defined by setting  $\bar{S}_{H^+} = 0$ .

into account the reduced concentration of water in the solution. It would be desirable to allow for the dilution of the water in a manner which does not require the assumption of any particular model for the solution. We shall accomplish this by applying the theory of dielectric polarization in polar substances<sup>18</sup> to the low frequency dielectric constants. The theory may be applied in the form derived for solutions,<sup>18b</sup> with the assumption that the motion of the ions contributes negligibly to the polarization. The result is

$$\frac{\epsilon - 1}{\epsilon + 2} = \frac{n^2 - 1}{n^2 + 2} + \frac{4\pi N_1 \mu^2 g}{3V 3kT} \frac{9\epsilon}{(2\epsilon + 1)(\epsilon + 2)} \quad (1)$$

where  $n^2$  is an effective refractive index of the solution which includes the effects of both electronic and atomic polarization,<sup>19</sup>  $N_1/V$  is the number of water molecules per unit volume,  $k$  is Boltzmann's constant,  $T$  is the absolute temperature and  $\mu$  is the average dipole moment of a water molecule in the solution. The correlation parameter,  $g$ , is defined so that  $g\mu$  is the average total moment, excluding distortion polarization produced by an external field, of a macroscopic specimen of the solution when one water molecule is fixed in position. The dipole moment fluctuations<sup>18b</sup> which affect  $g$  are considered negligible.

Values of  $\mu^2 g$  for each solution were calculated by means of eq. 1 and listed in Table II. The necessary values of  $n^2$  for the solutions were obtained from visible frequency data available in the literature,<sup>20</sup> and are also given in Table II. The con-

(18) (a) F. E. Harris and B. J. Alder, *J. Chem. Phys.*, **21**, 1031 (1953); (b) F. E. Harris and S. G. Brush, *J. Am. Chem. Soc.*, **68**, 1280 (1956).

(19) This includes polarization due to motions of nuclei, but not that due to torsional oscillations of water molecules against their neighbors, which is included in  $g$ . Thus, the proper values of  $n^2$  to use in application of eq. 1 to aqueous solutions will be close to the values observed at optical frequencies.

(20) "International Critical Tables," Vol. 7, McGraw-Hill Book Co., New York, N. Y., p. 63 ff.

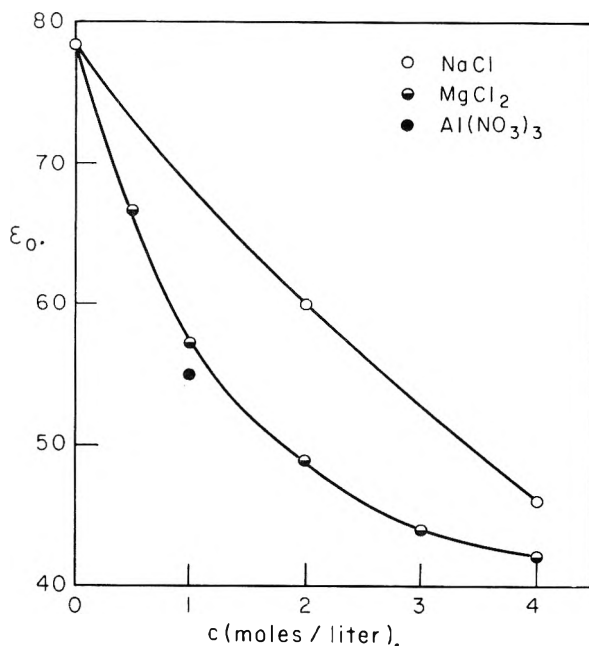


Fig. 4.—Effect of cationic charge upon low frequency dielectric constants.

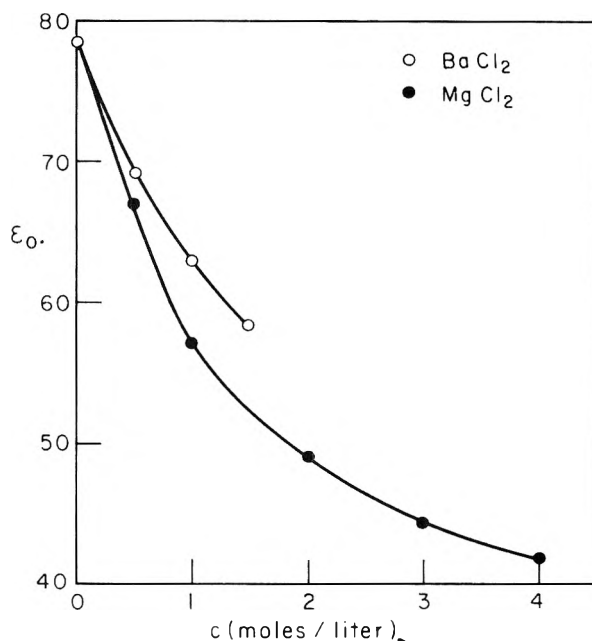


Fig. 5.—Effect of cationic size upon low frequency dielectric constants.

centrations of water were calculated from the densities measured in this research.

In order to calculate the correlation parameter,  $g$ , it is necessary to know the dipole moment of a water molecule in the solution. Although the strong electric field of the ions will polarize the water molecules sufficiently to change their dipole moment considerably, the induced moments give rise to a polarization which vanishes in the first approximation when the ions are non-polar. The effective dipole moment of the water molecules will therefore be determined primarily by the interaction between the water molecules, and can be approximated by the moment of molecules in pure

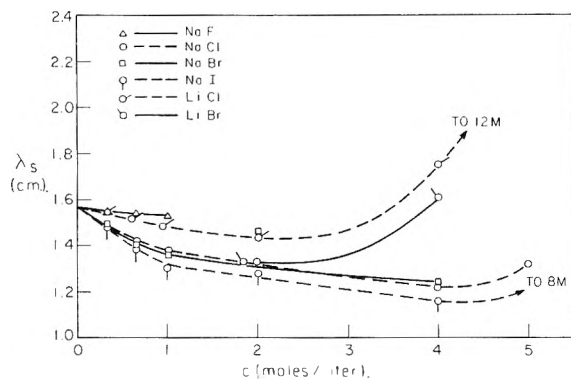


Fig. 6.—Wave length of central relaxation *vs.* concentration for various electrolytes at 25°. Values to 1 *M* from reference 13.

water. Pople has calculated this moment from a four-coördinated bendable hydrogen bond model for liquid water,<sup>21</sup> and shows that the main contribution to the increase over the vacuum moment is that of the first shell of neighbors. Therefore, the approximation considered should be adequate when most of the water molecules have four other water molecules as first neighbors. In the more concentrated solutions this condition is far from satisfied. However, we shall use the moment calculated in this way for lack of a better approximation. Values of *g* obtained using the pure water moment,  $\mu = 2.14 D$ , are listed in the last column of Table II.

The values of *g* obtained for the ionic solutions showed a behavior similar to that of the values of  $\epsilon_0$  from which they were derived. There are significant decrements from  $g = 2.55$ , the value for pure water, and they increase with cationic charge and decrease with increasing cationic size. Clearly, there is a substantial effect beyond that caused by the dilution of the water. The behavior noted above will be discussed in subsequent sections in relation to probable configurations of water molecules around ions.

Upon comparing the present results with those of the previous investigators,<sup>11,12</sup> we observe rough qualitative agreement. However, the present work provides a more definite indication that the contributions of the anions are small, that there is a noticeable and regular trend of the low frequency decrements with ionic size, and that the general conclusions remain unaltered when the effect of the dilution of the water is more rigorously taken into account.

**2. High Frequency Dielectric Constants.**—It has been pointed out that the high frequency limiting values of the dielectric constant fall near to or less than 5.5, the limiting value for pure water. The decrease in  $\epsilon_\infty$ , most marked in the more concentrated solutions, is, in part, caused by the dilution of water by ions of lower refractive index. However, since a substantial portion of the polarization effecting a dielectric constant of 5.5 in water probably is due to bending at the hydrogen bonds,<sup>13a,21</sup> this contribution will undoubtedly change as the environment of the water molecules is altered. If the ions are assumed to have a dielectric constant of approximately 2, the high frequency

dielectric constant of the surrounding water may be estimated from the experimental value of  $\epsilon_\infty$  and the volume occupied by the ions. The volume occupied by the ions can be estimated from crystal radii, and the volume fraction of solute,  $\delta$ , calculated. Böttcher has derived a simple formula relating the dielectric constant of a suspension of spheres to their volume fraction<sup>22</sup> in which  $\epsilon_1$  and  $\epsilon_2$  are the high frequency dielectric constants of the water and solute, respectively. The formula

$$\frac{\epsilon_\infty - \epsilon_1}{3\epsilon_\infty} = \delta \frac{\epsilon_2 - \epsilon_1}{2\epsilon_\infty + \epsilon_2} \quad (2)$$

is derived assuming a random distribution of spherical particles of arbitrary size in a continuous medium. While a detailed treatment should consider the discrete nature of the water molecules around the ions, the formula will give an idea of the magnitude of the difference between  $\epsilon_1$  and  $\epsilon_\infty$ .

The calculation indicated above reveals that the decrease in volume fraction of the water is much too small to explain the decrease of  $\epsilon_\infty$ . We therefore conclude that the polarization due to bending of the hydrogen bonds is substantially decreased at high concentrations. This is attributed to high deformation force constants associated with the relatively strong interaction<sup>23</sup> between ions and water molecules.

**3. Relaxation Times.**—In agreement with previously reported work,<sup>11,13</sup> the relaxation phenomena at low concentrations may be approximately characterized by a single Debye relaxation time, the relaxation time initially becoming shorter with increasing concentration. Haggis, Hasted and Buchanan<sup>13</sup> attributed the decrease of the relaxation time, which is proportional to the critical wave length,  $\lambda_s$ , to an increase in the number of broken hydrogen bonds produced by the addition of ions to the water. This concept clearly fails when applied to the more concentrated solutions, where the relaxation times are often much greater than the relaxation time of pure water. Thus the new results suggest that a more detailed consideration of the ion-solvent interactions is in order.

The electric field intensity *E* at a point outside of an isolated ion at a distance *r* from the center is given by  $Ze/r^2$ , and the coupling energy of a dipole in such a field is given by  $\mu \cdot E$ . It seems reasonable to suppose that when this energy is large compared to the binding energy of a water molecule in liquid water, the electric field will disrupt the normal short-range structure in water,<sup>24,25</sup> which is essentially that of ice, and produce structurally well defined configurations. It is important to recognize that to establish a criterion for saturation of the orientation in water, the dipole coupling energy should be compared to the energy of breaking hydrogen bonds in water rather than to *RT*, unlike the case of dielectric saturation in a gas.

The energy of a hydrogen bond in water was estimated by Pauling<sup>26</sup> to be roughly 4.5 kcal./mole of

(22) J. C. F. Böttcher, "Theory of Electric Polarization," Elsevier Pub. Co., Amsterdam, 1952.

(23) E. J. W. Verwey, *Rec. trav. chim.*, **61**, 127 (1942).

(24) J. D. Bernal and R. H. Fowler, *J. Chem. Phys.*, **1**, 515 (1933).

(25) J. Morgan and B. E. Warren, *ibid.*, **6**, 666 (1938).

(26) L. Pauling, "The Nature of the Chemical Bond," Cornell University Press, Ithaca, N. Y., 1948.

(21) J. A. Pople, *Proc. Roy. Soc. (London)*, **A205**, 163 (1951).

bonds. Later, Searcy<sup>27</sup> suggested a value somewhat higher,  $\sim 6.4$  kcal. Pauling attributed  $1/4$  of the heat of sublimation of ice at  $0^\circ$  (12.2 kcal./mole) to van der Waals forces, and the remainder to hydrogen bonds. Searcy refined the estimate by considering the packing situation in relation to similar substances, and obtained a repulsive energy of 4.5 kcal./mole and a London energy of  $-2.6$  kcal./mole, which led to a hydrogen bond energy of  $6.4 \pm 0.5$  kcal. at  $0^\circ\text{K}$ . Verwey,<sup>28</sup> in a relatively direct calculation of the repulsive and London energies, obtained  $8.5 \pm 2$  kcal./mole and  $-5.3$  kcal./mole for the repulsive and London energies, respectively. From this it appears that the London attractive potential is not enough to outweigh the repulsive forces, which seems reasonable in view of the relatively strong electrostatic attractions between water molecules, and the extremely open lattice of the ice structure. We now may estimate the hydrogen bond energy as  $1/2(12.2 - 5.3 + 8.5 \pm 2)$  or  $7.7 \pm 1$  kcal./mole of hydrogen bonds at  $0^\circ$ . This is of the order of magnitude of the values ( $6.8 \pm 0.5$ ) obtained by Verwey<sup>28</sup> from his model calculation, but is independent of the particular choice of model.

From computations, as indicated above, of the coupling energies for representative monatomic ions, it appears clear that nearest neighbor water molecules will have configurations determined primarily by the ionic field and by geometrical packing considerations, rather than the tetrahedral symmetry characteristic of the short-range order in ice and water. This is more in accord with the view of Verwey,<sup>23</sup> as opposed to that of Bernal and Fowler,<sup>24</sup> who consider that the ions replace water molecules in the tetrahedral structure. The calculations of Verwey, who employed a quadrupolar model to represent the spatial distribution of charge in the water molecule, provide numerical results which support this view.

Let us now consider roughly the coupling situation with regard to second shell water molecules, which is very complex, as recognized by Verwey. The electric field acting upon these molecules is greatly reduced because of the increase in  $r^2$ , and because of the polarization of the first shell molecules, and may be represented by  $Zc/\epsilon_e r^2$ , where  $\epsilon_e$  is an effective dielectric constant for the strongly polarized first shell. For univalent ions and any physically reasonable values of  $\epsilon_e$  and  $r$ , calculations show that the dipole coupling energy will be somewhat less than the energy of a hydrogen bond. Accordingly it is reasonable to suppose that the normal water structure will begin in the second shell and be regained almost completely in the third shell.

It remains to select and reject probable water molecule configurations from the considerable number suggested by other workers. First of all, the suggestion<sup>11</sup> that second shell molecules may be regarded as oriented in a well defined manner by the field of univalent ions is clearly contrary to the above point of view. Even for small trivalent and quadrivalent ions, the approximate calculations in-

dicating that it is not permissible to assert that the ionic field will strongly predominate over the hydrogen bond forming tendency in second shell molecules. However, the normal tetrahedral structure cannot as readily form about these molecules, because of the directing effect of the field and the consequent limitation of the configurations available to the first shell molecules, which are involved as nearest neighbors to the molecules in the second shell, and because of the appreciable directing field at the second shell. Thus the second shell may be regarded as possessing less structure than either normal water or the first hydration shell, and it is suggested that this shell contributes strongly to the "breaking down" of the water structure proposed by Frank and Evans on the basis of entropy considerations. Experimental studies of the fluidities<sup>29</sup> of aqueous ionic solutions and of the self-diffusion<sup>30</sup> of water in ionic solutions support the concept of Frank and Evans. Similarly, the decrease of the relaxation time for water in the more dilute solutions can be attributed to the competition between the above-described effects of the field and the tendency to form hydrogen bonds with tetrahedrally situated and properly oriented neighbors. In terms of the dielectric relaxation as a chemical rate process,<sup>31</sup> the increased relaxation rate can be explained by a raising of the minima in the potential energy curve for rotation of a second shell molecule with respect to its neighbors, with a consequent reduction of the potential barrier, and hence of the activation energy, for rotation of the dipole. The relaxation time depression was associated in a less definite manner with structure breaking by previous investigators.<sup>11</sup>

As the ionic concentrations are increased, it is seen from the results that the dielectric relaxation typically becomes characterized by a rapidly broadening distribution of relaxation times, with the longer times becoming relatively more important. This can be explained on the basis of several effects. First of all, the system is rapidly depleted of water molecules which would be expected to have relaxation times essentially equal to the one for pure water at the same temperature, let us say, molecules separated from ions by two or more intervening shells. Therefore the contribution from the "normal" relaxation processes is less. Secondly, at higher concentrations, the second shell molecules, in addition to experiencing a directing field from the central ion under consideration, are becoming polarized in the same direction by the fields from oppositely charged ions which on the average predominate in the vicinity of any given ion, so their configurations become relatively more stable. The longer relaxation times of the nearest neighbors become relatively more important. In terms of the shell model, at least four or six relaxation times can be expected for the nearest, second nearest and third nearest neighbors about cation and anion. Because the entire system is characterized by strong interactions and a mixing of the roles of a given water molecule between different ions, with a time depend-

(27) A. W. Searcy, *J. Chem. Phys.*, **17**, 210 (1949).

(28) E. J. W. Verwey, *Rec. trav. chim.*, **60**, 887 (1941).

(29) E. C. Bingham, *This Journal*, **45**, 885 (1941).

(30) J. H. Wang, *J. Am. Chem. Soc.*, **76**, 4755 (1954).

(31) W. Kauzmann, *Rev. Mod. Phys.*, **14**, 12 (1942).

ence associated with the random translational motions of the ions, the various relaxation times probably become smeared into a broad distribution, with the central relaxation time increasing at high concentrations because of depletion of the system with respect to relatively mobile water molecules.

**4. The Hydration of Ions.**—Verwey<sup>23</sup> concluded that monatomic anions probably interact with a nearest neighbor water molecule through what may be regarded as a hydrogen bond type linkage involving only one hydrogen. Water molecules so coordinated experience less repulsion for a given H . . . anion distance, and can form one more hydrogen bond with neighbors than can molecules which bend an anion in a symmetrical coplanar arrangement involving both hydrogens. Since the uncoordinated hydrogen can rotate about the anion . . . H-O direction, the molecular dipole can rotate, and there will be a contribution to the orientation polarization or to  $g$ . This is in accord with the low values for  $-dg/dc$  assigned above.

The large values for  $-dg/dc$  assigned to cations are not as easily explained. They are associated with the relatively large dielectric decrements produced by cations and attributed by Haggis, Hasted and Buchanan<sup>13</sup> to "irrotational binding." Their adopted configuration—a coplanar arrangement of the cation, oxygen and the two hydrogens—presumably does not permit rotation of the water molecule except possibly around the axis of the dipole. Since such motion does not contribute to the orientation polarization, this arrangement would produce a relatively large positive contribution to  $-dg/dc$ , which is qualitatively consistent with our results. However, the proposed arrangement is contrary to the conclusion of Verwey, and this was not adequately discussed.

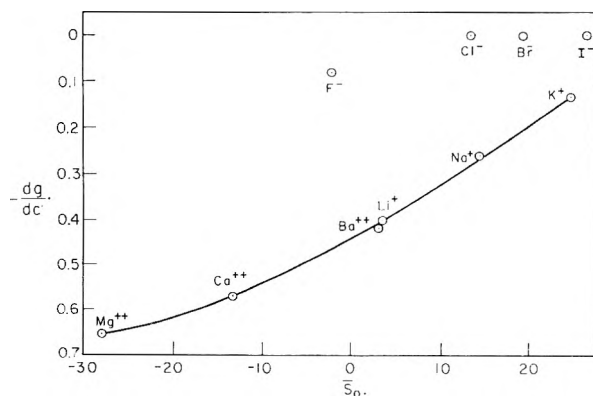


Fig. 7.—Limiting slope of the water dipole correlation parameter-concentration curve vs. standard ion entropy for monatomic ions.

Verwey<sup>23</sup> calculated that the binding energy between a singly charged cation 1.36 Å. in radius and a water molecule coordinated in the coplanar arrangement (a) is 2.5 to 3.5 kcal. greater (depending upon the value chosen for the screening parameter of the proton in his model) than the corresponding energy for a water molecule coordinated in a tetrahedral (c) manner. Nevertheless, he concluded that arrangement (c) would be energetically more favored on the basis of the fact that a water mole-

cule so bound can hydrogen bond to three surrounding water molecules, rather than two, as in (a). The corresponding energy difference was less (2.0 to 2.3 kcal.) for a 2.00 Å. cation, and undoubtedly would be greater for univalent cations less than 1.36 Å. in radius, and for multiply charged cations. The calculations did not include the effect of polarization of the surrounding molecules in the field of the cation, which would probably decrease the energy of the hydrogen bonds to the molecule in question in arrangement (c). Accordingly, for  $K^+$  ( $r = 1.33$  Å.) it appears that there would be no strong preference for either (a) or (c), but that the coplanar linkage (a) is progressively more favored as the cationic radius decreases, or the charge increases. Since  $K^+$  appears at one end of the cation curve in Fig. 7 (to be discussed), and there is an indication of a saturation of the  $-dg/dc$  values vs.  $S_0^0$  as  $S_0^0$  becomes more negative, it appears that the range represented by that curve may correspond to a transition toward the coplanar hydration linkage for cations as charge increases or cationic radius decreases. The suggested tendency might be greater than one might infer from Verwey's calculations, because of the neglect in his models of the concentration of negative charge in the lone pair orbitals of the water molecule.<sup>32</sup>

Further indications of the interactions between ions and water molecules are available in the thermodynamic functions for aqueous ions. Powell and Latimer<sup>33</sup> have examined the entropies of a large number of aqueous ions differing in charge and size, and found a correlation of solvation entropies with  $Z/r_e^2$  where  $Z$  is the absolute value of the ionic charge and  $r_e$  is an effective ionic radius. A further study by Powell<sup>34</sup> showed that a relation which correlates the entropies of monatomic cations and anions is

$$\bar{S}^0 = 47 - 154 Z/r_e^2 \quad (3)$$

where  $\bar{S}^0$  is the conventional ( $\bar{S}_{H^+}^0 = 0$ ) standard (1  $M$ ) partial molal ionic entropy,  $Z$  is the absolute value of the charge in electronic units, and  $r_e$  is an effective radius, in ångströms, taken to be 1.3 Å. greater than the Pauling crystal radius for cations, and 0.4 Å. greater than the Pauling crystal radius for anions. The physical basis for a choice of smaller interaction distance for an anion is that the anion may approach more closely the effective center of the water dipole than may a cation.<sup>35</sup> Comparing  $K^+$  and  $F^-$  which have equal crystal radii, it is seen that the effect of the  $K^+$  upon  $d\epsilon/dc$  as assigned in Table III is greater than that of  $F^-$ , although  $F^-$  has the smaller interaction distance, and therefore a stronger interaction with a water molecule. This is attributed to the special manner, discussed above, in which the cation immobilizes the dipoles of the nearest neighbor water molecules.

When a plot of  $d\epsilon/dc$  vs. ionic entropy is constructed from the data in Table III, the anions, the

(32) J. Lennard-Jones and J. A. Pople, *Proc. Roy. Soc. (London)*, **A205**, 155 (1951).

(33) R. E. Powell and W. M. Latimer, *J. Chem. Phys.*, **19**, 1139 (1951).

(34) R. E. Powell, *This Journal*, **58**, 528 (1954).

(35) W. M. Latimer, K. S. Pitzer and C. M. Slansky, *J. Chem. Phys.*, **7**, 108 (1939).

singly charged cations and the doubly charged cations fall into separate groups. However, when the quantity  $dg/dc$  is computed from eq. 1, which takes into account the dilution of water by the ions, and is plotted *vs.* ionic entropy, all of the cations characterized in this study are correlated by the smooth curve of Fig. 7. The anions still fall within a separate group and would not appear on the curve regardless of the manner in which the dielectric increment is arbitrarily divided between anion and cation for a given reference salt. This is considered a separate indication of the different modes of interaction between a water molecule and a cation and an anion, already inferred above.

**5. Ion Atmosphere Asymmetry.**—It has been shown by Debye and Falkenhagen<sup>9</sup> that there is a positive contribution to the dielectric constant as a result of the asymmetry produced in an ion atmosphere by the application of an external field. The theory of this effect for dilute solutions leads to an equation of the form

$$\Delta\epsilon_0' = \alpha c^{1/2} \quad (4)$$

where  $\Delta\epsilon_0'$  is the low frequency dielectric constant increment, and the coefficient  $\alpha$  is determined by the ionic charges and mobilities, the dielectric constant of the solvent and the temperature. Some values of  $\alpha$  in water at 18° are 3.8, 10.9, 13.8 and 30.3 for KCl, MgCl<sub>2</sub>, LaCl<sub>3</sub> and MgSO<sub>4</sub>, respectively.<sup>36</sup> At concentrations around 1 *M* the effect is probably smaller than might be expected from eq. 4 because of the overlap of ion atmospheres which would tend to reduce the asymmetry polarization. Now the depression of the dielectric constant by ion-solvent coupling interaction would be expected to be linear in the concentration on the basis of any model which treats the ions as acting independently. One therefore expects that in dilute solutions the total low frequency dielectric increment will be given by the sum of two terms

$$\Delta\epsilon_0 = \alpha c^{1/2} - \beta c \quad (5)$$

where the first term is the asymmetry contribution of Debye and Falkenhagen, and the second is the resultant of the ion-solvent coupling effects for the ions in question. It is of interest to examine the slope of the  $\Delta\epsilon_0$  *versus*  $c$  curve

$$\frac{d(\Delta\epsilon_0)}{dc} = \alpha/2c^{1/2} - \beta \quad (6)$$

from which it is seen that the Debye-Falkenhagen effect will dominate at low concentrations, but may be small compared to the ion-solvent coupling effects at high concentrations. In the transition region, the curve of  $\Delta\epsilon_0$  *vs.*  $c$  should be concave downward. The fact that it is typically concave upward in the 1 *M* region (Figs. 4 and 5) suggests that the first term may be negligible at such concentrations, and that  $\beta$  may be identified with  $-d\epsilon/dc$  of Table III. It appears evident that the term  $\beta c$  should be added to experimentally observed values of dielectric increments of dilute solutions of electrolytes before comparison is made with the Debye-Falkenhagen theory. When dealing with polyelectrolytes, a similar situation may be expected. The suggestion has been made<sup>37</sup> that the dielectric increments and the dispersion observed, for example, in the 1-10 megacycle region for protein solutions, may have their primary origin in an ion atmosphere polarization effect. Accordingly, the electrolyte composition of the solution should be specified when reporting experimental results for polyelectrolytes, to make comparisons with theory possible.

**6. Very Concentrated Solutions.**—It is of interest to note the high dielectric constants ( $\epsilon_0$ , Table II) of the most concentrated solutions, *e.g.*, 12 *M* LiCl(35), 10 *M* LiBr(39), 12 *M* KF(57). Although the relaxation times found in the more concentrated systems were helpful in understanding certain qualitative aspects of the dielectric properties of aqueous ionic solutions, a quantitative interpretation of the Kirkwood correlation parameters ( $g$ -values) was not attempted for those systems. The nature of the assumptions involved in obtaining eq. 1 preclude the consideration of polarization mechanisms involving ion clusters, or possible alternative ionic mechanisms. To the extent that this may be valid, the occurrence of correlation values greater than unity may be interpreted as indicating strong hydrogen-bond couplings between water molecules even in solutions where there are scarcely enough water molecules to hydrate the ions. This may be of importance in understanding the thermodynamic and dielectric properties of solid hydrates.

(36) Reference 8, p. 220.

(37) C. T. O'Konski, *J. Chem. Phys.*, **23**, 1559 (1955).

# THE KINETICS OF NITROGEN ATOM REACTIONS ACCOMPANIED BY CATALYZED RECOMBINATION OF ATOMS<sup>1</sup>

BY W. FORST, H. G. V. EVANS AND C. A. WINKLER

*Contribution from the Physical Chemistry Laboratory, McGill University, Montreal, Canada*

*Received September 6, 1956*

Theoretical considerations indicate that temperature dependence of the limiting hydrogen cyanide yield in reactions of active nitrogen with organic molecules may be explained by assuming that hydrogen cyanide formation is accompanied by recombination of nitrogen atoms catalyzed by reactant.

## Introduction

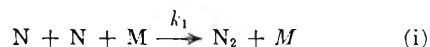
When the flow and activation of nitrogen is kept constant, it has generally been observed<sup>2-6</sup> that the yield of hydrogen cyanide becomes constant above a certain minimum input of organic reactant, and that this limiting yield of hydrogen cyanide is apparently independent of temperature. Such behavior has been attributed to complete consumption of active nitrogen.

This paper discusses two recent studies<sup>6,7</sup> in which the limiting yield of hydrogen cyanide was found to depend on temperature. To explain this behavior, it seems reasonable to assume that some process destroys the activity of the nitrogen (without forming hydrogen cyanide) to a different extent at different temperatures. If, for reasons indicated elsewhere,<sup>8</sup> it is assumed that the main reactive species in active nitrogen is atomic nitrogen, the most obvious mechanism of specific deactivation is by nitrogen atom recombination catalyzed by the reactants, methyl chloride<sup>6</sup> and methyl cyanide.<sup>7</sup> It is well known that the rate of recombination of nitrogen atoms due to wall reaction and to the presence of excess molecular nitrogen is slow in a suitably poisoned reaction vessel.<sup>9,10</sup> The main products of both reactions are much simpler molecules than the reactants, with fewer degrees of freedom. Hence, it seems unlikely that the products would be as efficient recombination catalysts as the reactants.<sup>11</sup> Direct evidence in favor of this conclusion is to be found in a comparison of the behavior of methyl cyanide with that of the hydrocarbons. The only main products of the methyl cyanide reaction, H<sub>2</sub> and HCN, are also main prod-

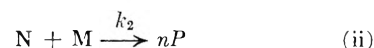
ucts of the reactions of the hydrocarbons with active nitrogen, none of which have shown a marked change of the limiting yield of HCN with change of temperature.

The observed kinetic behavior can be explained satisfactorily by a competition between direct reaction and catalyzed recombination. The simplest possible reaction scheme will be considered first, after which will be discussed the modifications necessary to take into account a relatively long life for an intermediate reactant-nitrogen atom complex that apparently is formed in most active nitrogen reactions.<sup>13</sup>

**I. Simple Reaction Scheme.**—The recombination reaction is taken to be third order.



and the direct reaction second order



where M represents methyl chloride or methyl cyanide, and P represents hydrogen cyanide.

The kinetics will depend on the nature of the flow in the reaction vessel. The assumption that the flow pattern corresponds to instantaneous mixing at the inlet, followed by essentially uniform flow out of the reaction vessel with only localized mixing, provides the best explanation of the observed kinetic behavior and also explains the observed shape of the reaction flame.<sup>14</sup> The error involved in the assumption of instantaneous mixing at the inlet to the reaction vessel is probably more important than the error that results from neglect of mixing along the path of flow. It is very difficult to make a quantitative treatment of the amount of reaction during the initial mixing period, but it seems likely that the assumption of instantaneous mixing should give the essential features of the kinetics.

For this flow pattern

$$\frac{-dN}{dt} = k_1 N^2 M + k_2 N M \quad (1)$$

(13) H. G. V. Evans, G. R. Freeman and C. A. Winkler, *Can. J. Chem.*, **34**, 1271 (1956).

(14) Equations 1 and 2 hold rigorously only for stream line flow in a cylindrical reactor in the absence of diffusion for isothermal gas phase reactions that occur without a change in volume. For small  $n$  in reaction (ii) the volume change will be small and can be neglected. Equations 1 and 2 will also give a good approximation if a certain amount of localized turbulence and diffusion occur, since localized mixing would lead only to second-order effects. It seems quite safe to neglect the rate of diffusion from one part of the reaction vessel to another compared with the rate of reaction, since both the linear gas velocity (30 cm./sec.) and the reaction rate (about  $10^5$  l. mole<sup>-1</sup> sec.<sup>-1</sup>) are large. For the same reason, the existence of predominantly turbulent flow conditions would seem unlikely.

(1) Contribution from the physical chemistry laboratory, McGill University, with financial assistance from the National Research Council, Ottawa, Ontario.

(2) J. H. Greenblatt and C. A. Winkler, *Can. J. Res.*, **B27**, 731 (1949).

(3) (a) G. S. Trick and C. A. Winkler, *Can. J. Chem.*, **30**, 915 (1952); (b) J. Versteeg and C. A. Winkler, *ibid.*, **31**, 1 (1953).

(4) H. Gesser, C. Luner and C. A. Winkler, *ibid.*, **31**, 346 (1953).

(5) M. Onyszchuk, L. Breitman and C. A. Winkler, *ibid.*, **32**, 351 (1954).

(6) H. B. Dunford, H. G. V. Evans and C. A. Winkler, *ibid.*, **34**, 1074 (1956).

(7) W. Forst and C. A. Winkler, *This Journal*, **60**, 1424 (1956).

(8) H. G. V. Evans and C. A. Winkler, *Can. J. Chem.*, **34**, 1217 (1956).

(9) Rayleigh (Lord), *Proc. Roy. Soc.*, **A151**, 567 (1935).

(10) L. H. Reinecke, *Z. Physik*, **135**, 361 (1953).

(11) The effects of a significant contribution from recombination catalyzed by one of the products, by the excess molecular nitrogen present, or by the wall of the reaction vessel, in a very fast reaction can be investigated by an extension of the treatment given in this paper.<sup>12</sup> The results indicate that the contribution from these reactions would have to be of major importance before the effects could be distinguished in the experimental results.

(12) H. G. V. Evans, Ph.D. Thesis, McGill University, 1955.

$$-\frac{dM}{dt} = k_2NM \quad (2)$$

where  $k_1$  and  $k_2$  are the rate constants for reactions (i) and (ii), and  $N$  and  $M$  represent the concentrations of the reactants (nitrogen atom and organic molecule) in the part of the reaction vessel that is reached by the flow  $t$  sec. after it leaves the point of entry.<sup>14</sup>

Dividing (1) by (2)

$$\frac{dN}{dM} = \frac{k_1N}{k_2} + 1 \quad (3)$$

Changing to dimensionless variables  $x$  and  $y$  defined by

$$x = \frac{M}{M_0} \text{ and } y = \frac{N}{N_0} \quad (4)$$

where  $M_0$  and  $N_0$  are the initial concentrations of reactant and nitrogen atoms ( $t = 0$  at point of entry), eq. 2 and 3 become

$$\frac{dx}{dt} = -k_2N_0xy \quad (5)$$

and

$$\frac{dy}{dx} = \frac{k_1}{k_2} M_0y + \frac{M_0}{N_0} \quad (6)$$

Integration of (6), using the initial condition  $y = 1$  for  $x = 1$ , gives

$$y = f(x) = \left(1 + \frac{k_2}{k_1N_0}\right) \exp\left\{\frac{-k_1M_0}{k_2}(1-x)\right\} \frac{-k_2}{k_1N_0} \quad (7)$$

where  $f(x)$  is an abbreviation for the function of  $x$ ,  $M_0/N_0$  and  $k_1N_0/k_2$  on the right side of eq. 7.

Substituting for  $y$  in eq. 5 and integrating

$$k_2N_0t = \int_x^1 \frac{dx}{x.f(x)} \quad (8)$$

If  $\tau$  is the mean time spent in the reaction vessel,<sup>15</sup> and  $x_1$  and  $y_1$  are the final values of  $x$  and  $y$  (corresponding to the mean concentrations of M and N leaving the reaction vessel), then

$$y_1 = f(x_1) \quad (7a)$$

$$k_2N_0\tau = \int_{x_1}^1 \frac{dx}{x.f(x)} \quad (8a)$$

Inspection of reaction (ii) shows that

$$P_1 = nM_0(1 - x_1) \quad (9)$$

where  $P_1$  is the mean concentration of hydrogen cyanide leaving the reaction vessel.

Two cases may now be considered, depending on the value of  $k_2N_0\tau$ .

#### Case A. Fast Reactions, e.g., Methyl Chloride.

—According to eq. 8a, a very small value for either  $x_1$  or  $y_1 = f(x_1)$  corresponds to a very large value for  $k_2N_0\tau$ , and it is obvious that for very fast reactions one or other of  $N$  and  $M$  will be completely consumed. Thus, for very fast reactions, there are two regions defined by: (a) Complete consumption of M, giving

(15) For stream line flow in a spherical reactor such as used in this study, the time spent in the reaction vessel will be different for different stream lines. Thus, the value of  $\tau$  that should be used in eq. 8a would depend on the geometry of the system as well as the reaction kinetics, but should not be very different from the mean time calculated from the volume of the reaction vessel and the total flow through it. Localized mixing would tend to remove differences in the reaction time for different paths, and it seems likely that putting  $\tau$  equal to the mean time is a reasonably good approximation.

$$x_1 = 0 \quad (10)$$

$$y_1 = f(0) = \left(1 + \frac{k_2}{k_1N_0}\right) \exp\left\{\frac{k_1M_0}{k_2}\right\} \frac{-k_2}{k_1N_0} \quad (11)$$

$$P_1 = nM_0 \quad (12)$$

(b) Complete consumption of N, giving

$$y_1 = f(x_1) = 0 \quad (13)$$

$$x_1 = 1 - \frac{k_2}{k_1M_0} \ln\left(1 + \frac{k_1N_0}{k_2}\right) \quad (14)$$

$$P_1 = \frac{nk_2}{k_1} \ln\left(1 + \frac{k_1N_0}{k_2}\right) \quad (15)$$

Since, by definition,  $y_1$  cannot be negative, it can be seen from eq. 11 that the first region corresponds to  $0 < M_0 \leq M_0'$ , and the second region to  $M_0 \geq M_0'$ , where  $M_0'$ , the critical reactant concentration that divides the two regions, is given by the simultaneous solution of eq. 12 and 15

$$M_0' = \frac{k_2}{k_1} \ln\left(1 + \frac{k_1N_0}{k_2}\right) \quad (16)$$

Thus, at constant  $N_0$ ,  $P_1$  increases linearly with  $M_0$  until  $M_0$  reaches  $M_0'$  and then remains constant at the value given by eq. 15 as  $M_0$  increases further. The limiting value of  $P_1$  given by eq. 15 increases with  $k_2/k_1$ , and hence the limiting yield of HCN<sup>16</sup> will increase with temperature if  $k_2/k_1$  increases with temperature, i.e., if  $k_2$  has the larger temperature coefficient.

The reaction of methyl chloride with nitrogen atoms appears to be an example of a system in which both the reaction itself and the catalyzed recombination are very fast. As can be seen in Fig. 1A, the yield of HCN increases linearly with the methyl chloride flow rate for low flow rates and is independent of temperature in this region. At higher flow rates, the yield of HCN increases with increase of temperature. Because the reaction is so fast, accurate temperature measurements could not be made,<sup>6</sup> and the results in the high flow rate region are only of qualitative significance. They do indicate, however, that  $k_2/k_1$  increases with temperature, and it seems likely, therefore, that a significant activation energy is required for the reaction.

**Case B. Slow Reactions, e.g., the Reactions of Methyl Cyanide with H Atoms<sup>17</sup> or N Atoms.**—Even if  $k_2N_0\tau$  is not very large, it is obvious physically, and can be demonstrated easily from the equations that, as  $M_0$  increases,  $y_1$  tends to zero, i.e., for high enough  $M_0$  nearly all the nitrogen atoms will be consumed. It will be shown later that for not too small values of  $k_2N_0\tau$  the convergence is quite rapid and that  $P_1$  will approach the limiting value  $P_1'$ , given by eq. 15

$$P_1' = \frac{nk_2}{k_1} \ln\left(1 + \frac{k_1N_0}{k_2}\right) \quad (15a)$$

for reasonable values of  $M_0$  (see Fig. 2). Thus, from known values of  $N_0$  and  $P_1'$ , the value of  $k_1/k_2$  can

(16) Multiplication of  $N_0$ ,  $M_0$  and  $P_1$  by the total flow rate gives the flow rate of N and M entering, and of P leaving the reaction vessel. A large excess of molecular nitrogen was always present so that the total flow rate did not change very much with change in the reactant flow rate. For the same reason, the value of  $N_0$  was essentially constant when the flow and activation of the nitrogen were kept constant.

(17) W. Forst and C. A. Winkler, *Can. J. Chem.*, **33**, 1814 (1955).

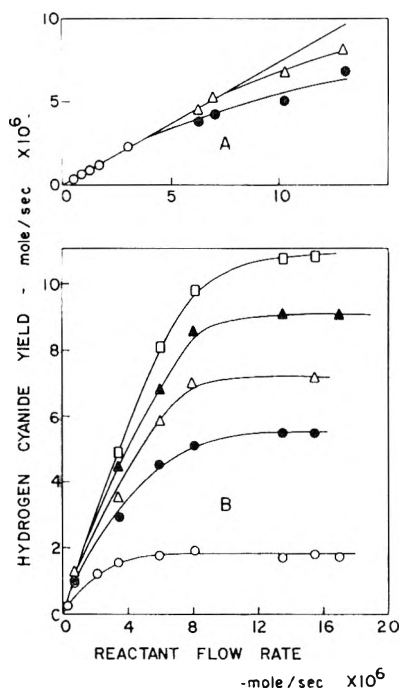


Fig. 1.—Dependence of hydrogen cyanide yield on temperature in reactions of active nitrogen with methyl chloride (A) and methyl cyanide (B): A, O, average temp.,  $\Delta$ , high temp.;  $\bullet$ , low temp.; B, O,  $90 \pm 30^\circ$ ;  $\bullet$ ,  $150 \pm 15^\circ$ ;  $\Delta$ ,  $245 \pm 10^\circ$ ;  $\blacktriangle$ ,  $345 \pm 5^\circ$ ;  $\square$ ,  $460 \pm 5^\circ$ .

be determined. The rate constant  $k_2$  can be determined from the initial slope of the  $P_1$  vs.  $M_0$  curve. For very small values of  $M_0$ , eq. 7 and 8a give

$$x_1 = e^{-k_2 N_0 \tau} \quad (17)$$

and, from eq. 9

$$P_1 = nM_0(1 - e^{-k_2 N_0 \tau}) \quad (18)$$

Thus, the initial slope,  $S_0$ , is given by

$$S_0 = n(1 - e^{-k_2 N_0 \tau}) \quad (19)$$

and

$$k_2 = -\left(\frac{1}{N_0 \tau}\right) \ln\left(1 - \frac{S_0}{n}\right) \quad (20)$$

The reaction of methyl cyanide with active nitrogen is slower than the methyl chloride reaction and it is possible to make a quantitative test of the validity of the treatment. As shown in Fig. 1B, both the limiting yield of HCN, and the initial slope of the plot of yield against methyl cyanide flow rate, depend on temperature. Thus, both  $k_1$  and  $k_2$  can be calculated as functions of temperature, using eq. 15a and 20. The main reaction is



so that  $n = 2$ . The total flow rate, the reaction pressure (1.03 mm.), and the volume of the reaction vessel were measured, and have been used to calculate  $\tau$  and to convert flow rates into concentrations. From values of  $P'$  and  $S_0$  estimated from plots of  $P$  against  $M_0$ , values of  $k_2$  and  $k_1/k_2$  have been calculated from eq. 20 and 15a (which were solved graphically). The results are summarized in Table I.

To estimate the value of  $N_0$ , it has been assumed that the constant production of HCN ( $6.72 \times 10^{-6}$  mole/sec.) observed at high flow rates in ex-

periments with ethylene at  $460^\circ$  was a direct measure of the atomic nitrogen flow rate at all temperatures. The justification for this assumption is that constant production of HCN from ethylene is attained at higher temperatures, and is not affected by further temperature increase.<sup>18</sup> Moreover, no reactant has yet been studied that gives, in the same system, higher conversions of atomic nitrogen to HCN, and a few others, like propylene,<sup>18</sup> have been found to give maximal HCN values nearly identical with that determined with ethylene.

Both  $N_0$  and  $\tau$  at a given temperature depend on the total flow rate, hence change with reactant flow rate. Average values of  $N_0$  and  $\tau$  are given in Table I. The maximum deviation at the highest and lowest flow rates studied was about  $\pm 10\%$  of the average values.

At this point, it is of interest to see whether the substitution of appropriate constants from Table I into the theoretical expressions will give a plot of  $P$  against  $M_0$  that is reasonably similar to the experimental curve. The integration in eq. 8a cannot be performed in terms of known functions, but numerical integration is possible after the integral is transformed to

$$k_2 N_0 \tau = \int_0^{1-x_1} \frac{dx}{(1-x) \frac{(1+k_2)}{k_1 N_0} \exp\left(\frac{-k_1}{k_2} M_0 x\right) \frac{-k_2}{k_1 N_0}} \quad (8b)$$

Figure 2 shows the experimental plot of  $P$  against  $M_0$  at  $460^\circ$  and the theoretical plot for the same temperature calculated from eq. 8b and 9, using the constants given in Table I. The agreement is quite satisfactory. It can be made nearly perfect by a slight modification in the reaction scheme (see later), but it is doubtful that it is worthwhile attempting to do this since errors resulting from secondary reactions that accompany the main reaction, and from the idealized treatment of the flow pattern could easily account for the difference between the curves.

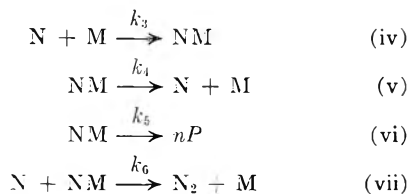
A further test of the theory was possible by varying  $N_0$ . For this purpose, several experiments at  $460^\circ$  were made, with the capacitance in the discharge circuit reduced to one-half to reduce the nitrogen atom concentration. From experiments with ethylene the new value of  $N_0$  was found to be  $1.025 \times 10^{-5}$  mole/liter, and the limiting yield of HCN from methyl cyanide corresponded to a value of  $P_1'$  of  $1.84 \times 10^{-5}$  mole/liter. Substituting this value for  $N_0$  into eq. 15a, using for  $k_1$  and  $k_2$  the values given in Table I, gives a calculated value for  $P_1'$  of  $1.89 \times 10^{-5}$  mole/liter. Again, the agreement is quite satisfactory.

**II. Reaction Scheme Involving Intermediate Complex.**—In the methyl chloride reaction<sup>6</sup> and several other reactions with active nitrogen<sup>12</sup> there is good evidence that complexes of relatively long life-times are formed between nitrogen atoms and organic molecules. It would be expected that the existence of this type of complex would be most favorable for catalyzed recombination. Thus, the reaction scheme to be considered should probably be

TABLE I<sup>a</sup>

| <i>T</i> | <i>N</i> <sub>0</sub> × 10 <sup>5</sup> | <i>τ</i> | <i>P</i> ' × 10 <sup>5</sup> | <i>S</i> <sub>0</sub> | <i>k</i> <sub>1</sub> × 10 <sup>-10</sup> | <i>k</i> <sub>2</sub> × 10 <sup>-5</sup> | <i>k</i> <sub>3</sub> × 10 <sup>-6</sup> |
|----------|---|----------|------------------------------|-----------------------|---|--|--|
| 160      | 1.25                                    | 0.27     | 1.02                         | 1.04                  | 6.75                                      | 2.17                                     | 0.738                                    |
| 245      | 1.48                                    | 0.228    | 1.80                         | 1.2                   | 2.76                                      | 2.71                                     | 3.60                                     |
| 345      | 1.83                                    | 0.185    | 2.75                         | 1.4                   | 1.61                                      | 3.56                                     | 8.58                                     |
| 460      | 2.14                                    | 0.16     | 3.75                         | 1.6                   | 0.67                                      | 4.7                                      | 30.95                                    |

<sup>a</sup> *T*, reaction temperature in degrees centigrade; *N*<sub>0</sub>, initial concentration of nitrogen atoms in mole/liter; *τ*, reaction time in seconds; *P*', hydrogen cyanide plateau value in mole/liter; *k*<sub>1</sub>, rate constant of reaction (i) in liter<sup>2</sup> mole<sup>-2</sup> sec.<sup>-1</sup>; *k*<sub>2</sub>, rate constant of reaction (ii) in liter mole<sup>-1</sup> sec.<sup>-1</sup>; *S*<sub>0</sub>, initial slope of the *P* vs. *M*<sub>0</sub> curves.



With the same assumption about the flow pattern as in section I, the rate equations are

$$\frac{dN}{dt} = -k_3NM + k_4C - k_6NC \quad (21)$$

$$\frac{dM}{dt} = -k_3NM + k_4C + k_6NC \quad (22)$$

$$\frac{dC}{dt} = k_3NM - (k_4 + k_5)C - k_6NC \quad (23)$$

where *C* represents the concentration of the complex NM, and the other symbols have the same significance as before.

It is now assumed that  $|dC/dt| \ll k_3NM$ . This corresponds to the assumption usually made in the stationary state treatment of fleeting intermediates, and leads to expressions that are similar in form to those obtained for the simple kinetic scheme treated in section I. (The validity of the assumption is discussed in Appendix A where it is shown that it can be expected to be reasonably good for the methyl cyanide reaction).

With this approximation, eq. 23 gives

$$C = \frac{k_3NM}{k_4 + k_5 + k_6N} \quad (24)$$

and eq. 21 and 22 become

$$\frac{dN}{dt} = \frac{-k_3NM(2k_6N + k_5)}{k_4 + k_5 + k_6N} \quad (25)$$

$$\frac{dM}{dt} = -\frac{k_3k_5NM}{k_4 + k_5 + k_6N} \quad (26)$$

Dividing (25) by (26)

$$\frac{dN}{dM} = \frac{2k_6N}{k_5} + 1 \quad (27)$$

It can be seen that eq. 27 is of the same form as eq. 3, with *k*<sub>1</sub>/*k*<sub>2</sub> replaced by 2*k*<sub>6</sub>/*k*<sub>5</sub>. Changing to dimensionless variables defined by eq. 4 and integrating gives, as before

$$y = f(x) = \left(1 + \frac{k_5}{2k_6N_0}\right) \exp\left\{-\frac{2k_6}{k_5} M_0(1-x)\right\} - \frac{k_5}{2k_6N_0} \quad (28)$$

and the value of the limiting yield, for *y* → 0, will now be

$$P_1' = \frac{nk_5}{2k_6} \ln\left(\frac{1 + 2k_6N_0}{k_5}\right) \quad (29)$$

From eq. 26

$$\frac{d\tau}{dt} = -\frac{k_3k_5N_0x^2y}{k_4 + k_5 + k_6N_0y} \quad (30)$$

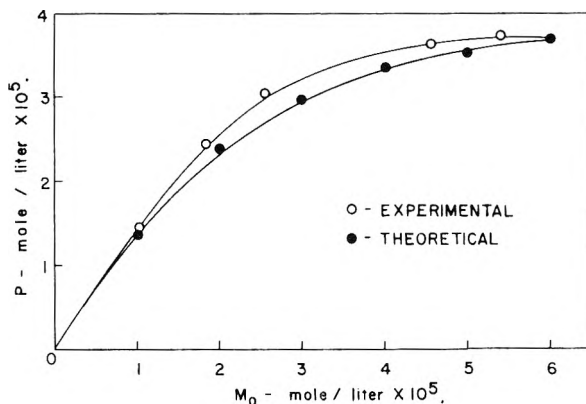


Fig. 2.—Experimental and calculated relations between hydrogen cyanide yield (*P*) and reactant flow rate (*M*) in the active nitrogen-methyl cyanide reaction.

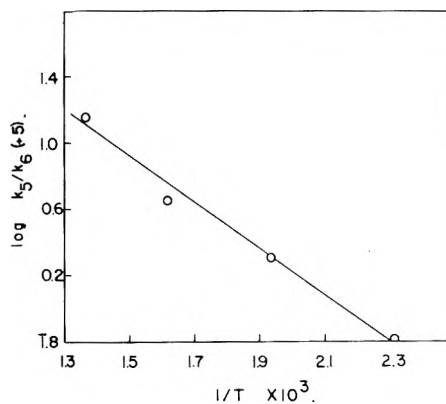


Fig. 3.—Plot of *k*<sub>5</sub>/*k*<sub>6</sub> against 1/*T* for the active nitrogen-methyl cyanide reaction.

which can be integrated to give

$$k_3k_5N_0\tau = -(k_4 + k_5) \int_{x_1}^1 \frac{dx}{x f(x)} + k_6N_0 \int_{x_1}^1 \frac{dx}{x} \quad (31)$$

where *f*(*x*) is the expression on the right side of eq. 28. From eq. 28, *y* = 1 for very small *M*<sub>0</sub>, and eq. 31 gives

$$x_1 = \exp\left\{-\frac{k_3k_5N_0\tau}{k_4 + k_5 + k_6N_0}\right\} \quad (32)$$

Thus, the initial slope of the curve relating *P*<sub>1</sub> to *M*<sub>0</sub> is now given by

$$S_0 = n \left[1 - \exp\left\{-\frac{k_3k_5N_0\tau}{k_4 + k_5 + k_6N_0}\right\}\right] \quad (33)$$

Comparing eq. 29 and 33 with the corresponding eq. 15a and 19 that were used in section I to calculate *k*<sub>1</sub> and *k*<sub>2</sub>, it can be seen that

$$\frac{k_1}{k_2} = \frac{2k_6}{k_5} \quad (34)$$

$$k_2 = \frac{k_3k_5}{k_4 + k_5 + k_6N_0} \quad (35)$$

$$k_1 = \frac{2k_3k_6}{k_4 + k_5 + k_6N_0} \quad (36)$$

Using eq. 35, eq. 31 can be written in the form

$$k_2N_0\tau = \int_{x_1}^1 \frac{dx}{x f(x)} - \left( \frac{k_6N_0}{k_4 + k_5 + k_6N_0} \right) \int_{x_1}^1 \frac{1}{x} \left( \frac{1}{f(x)} - 1 \right) dx \quad (37)$$

Comparing eq. 37 with 8a

$$k_2N_0\tau = \int_{x_1}^1 \frac{dx}{x f(x)} \quad (8a)$$

it can be seen that, for a given initial slope  $S_0$ , and asymptotic value,  $P_1'$ , the plot of  $P_1$  against  $M_0$  calculated from eq. 37 will start from zero with the same slope, and will approach the same limiting value for large  $M_0$ , as the curve calculated from eq. 8a, but will lie above it for intermediate values of  $M_0$ .<sup>19</sup>

Inspection of Fig. 2 shows that better agreement between theory and experiment would be obtained by using eq. 37, rather than 8a, with a fairly small value of  $k_6N_0/(k_4 + k_5 + k_6N_0)$ . Because of the other possible sources of error mentioned previously, it is probably not legitimate to deduce an absolute value for this ratio from the shape of the experimental curve, but the methyl cyanide results are at least not inconsistent with a value of  $k_4$  of the same order of magnitude as  $k_5$ .<sup>20</sup>

Relatively long-lived complexes seem to be involved in many of the atomic nitrogen reactions<sup>12</sup> and it is of some interest to consider the implications of a value for  $k_4$  of the same order as  $k_5$  ( $1/k_4$  will be approximately equal to the mean "collisional life-time" of the complex with respect to formation of  $N + M$ , see reaction v). An upper limit of approximately  $10^6$  sec.<sup>-1</sup> for the value of  $k_6N_0$  can be obtained from the frequency of collision between a given complex and nitrogen atoms (at a concentration  $N_0$ ) calculated by the usual methods. This value, together with the value of  $k_6N_0/k_5$  (Table I), gives an upper limit of  $k_5$  of about  $10^7$  sec.<sup>-1</sup>. The time between collisions for a given complex (with all the other molecules in the reaction vessel) was of the order  $10^{-7}$  sec. Thus, a value of  $k_4$  of the same order as  $k_5$  implies that the collisional life-time is of the order  $10^{-7}$  sec., *i.e.*, very long compared with the periods of molecular vibration ( $\sim 10^{-13}$  sec.) and of the same order as the time between collisions. Under these conditions, it would be quite possible for collision complexes to be stabilized by having the initial translational energy of the collision partners removed in a subsequent collision. There is some indication that stabilization of the

(19) This follows from the sign of the second term on the right side of (37). By definition  $1/f(x) = 1/y \gg 1$ , so that the second integral is always positive and the second term negative. Thus, for a given  $M_0$ , the values of  $x_1$  required to satisfy eq. 37 are smaller, and the corresponding values of  $P_1$  (*cf.* eq. 9) higher than for eq. 8a.

(20) Using the value of  $k_6N_0/k_5 = k_1N_0/k_2$  from Table I, the values of this ratio can be calculated for various values of  $k_4/k_5$ , thus

| $\frac{k_4}{k_5}$                     | 0    | 0.1  | 1    | 10   | 100   |
|---------------------------------------|------|------|------|------|-------|
| $\frac{k_6N_0}{(k_4 + k_5 + k_6N_0)}$ | 0.13 | 0.12 | 0.07 | 0.01 | 0.001 |

Rough calculations show that a reasonably good fit of the theoretical to the experimental curve will be obtained for  $k_4/k_5$  values less than 100, and probably less than 10.

complexes in this way does occur in the methyl chloride reaction, leading to recovery of methyl chloride when the complexes decompose on the cold surface of the trap.<sup>6</sup>

An interesting result of the treatment is that the limiting yield of product depends only on the ratio  $k_6N_0/k_5$  (equation 29) and is independent of  $1/k_4$ , the collisional lifetime. Thus, for a reaction to show a shift in the limiting yield with temperature, the life-time of the complex with respect to decomposition into products must be relatively long, and this process must require an activation energy so that  $k_6N_0/k_5$  will change with temperature. A reaction might therefore not show a marked shift in limiting yield with temperature, even though it involves the formation of a complex with relatively long collisional life-time.

For the methyl cyanide reaction, the values of  $k_5/k_6$  given in Table I can be calculated from eq. 34. Figure 3 shows a plot of  $\log k_5/k_6$  against  $1/T$ . From this plot, the difference in activation energies of reactions vi and vii is found to be approximately 6.6 kcal., and the ratio of the frequency factor of reaction vi to the steric factor of reaction vii to be of the order  $10^{10}$ . (The collision frequency for reaction vii was calculated in the usual way, taking a collision diameter of  $3 \times 10^{-8}$  cm. for the nitrogen atom<sup>2</sup> and  $5 \times 10^{-8}$  cm. for the complex.) It seems reasonable that the steric factor for reaction vii will be fairly close to unity; hence the frequency factor for reaction vi should be of the order  $10^{10}$  sec.<sup>-1</sup>. This is much smaller than the frequency factors generally found for unimolecular decompositions ( $10^{13}$ – $10^{14}$  sec.<sup>-1</sup>). A possible explanation is that the decomposition reaction has a transmission coefficient of the order  $10^{-3}$  to  $10^{-4}$  because it is accompanied by a change in electron spin. (It seems quite certain that the over-all reaction does involve a change in spin.<sup>8,12</sup>) The activation energy for reaction vii would be expected to be quite small, and a consideration of the kind of rearrangement required for decomposition makes it appear quite reasonable that the activation energy for reaction vi should be about 7 kcal.

To discuss the other rate constants, it is convenient to consider two limiting cases.

**Case A.**  $k_4 \gg (k_5 + k_6N_0)$ .—For this condition, the kinetic behavior is the same as for the simple scheme treated in Section I (see eq. 37) and both

$$k_2 = \frac{k_3k_6}{k_4} \quad (35a)$$

and

$$k_1 = \frac{k_3k_6}{k_4} \quad (36a)$$

are true rate constants.<sup>21</sup>

**Case B.**  $k_4 \ll (k_5 + k_6N_0)$ .—For this condition

$$k_2 = \frac{k_3k_5}{(k_5 + k_6N_0)} \quad (35b)$$

$$k_1 = \frac{k_3k_6}{(k_5 + k_6N_0)} \quad (36b)$$

The quantities  $k_1$  and  $k_2$  are no longer true rate

(21) The ratio  $k_2/k_1$  may be considered as the equilibrium constant for the formation of a critical complex from the reactants, so that the expressions are a partial development of the Theory of Absolute Reaction Rates applied to the reactants.

constants, but a value for  $k_3$  can be found. From (35b) and (34)

$$k_3 = k_2 + k_1 N_0 \quad (38)$$

It is easy to see that the slow stage of the reaction is decomposition of a fleeting intermediate complex for Case A (with a rate constant  $k_2$ ) while for Case B it is complex formation (with a rate constant  $k_3$ ).

An Arrhenius plot of the values of  $k_2$  given in Table I is shown in Fig. 4. This would give a value for the activation energy of reaction ii of about 1.6 kcal., and a steric factor<sup>22</sup> of the order  $10^{-6}$ . The values of  $k_2$  are comparable with those determined for other nitrogen atom reactions,<sup>12</sup> but the activation energy and steric factor are smaller.

The values of the third order rate constant  $k_1$  (Table I) are of the same order of magnitude as those for the recombination of bromine<sup>23-26</sup> iodine<sup>27-29</sup> and hydrogen<sup>30-34</sup> atoms in the presence of various third bodies, and are somewhat larger than the estimated value for the recombination of nitrogen atoms with  $N_2$  as the third body.<sup>35</sup> They show a negative temperature coefficient that is larger than that predicted by the theory of absolute reaction rates for reaction i occurring as a termolecular reaction.

Values of  $k_3$  calculated from eq. 38 and collision yields corresponding to these values, are given in Table I. The collision yields would indicate that no activation energy is required for the complex formation reaction, and that it has a steric factor of about  $10^{-6}$ . It seems rather more reasonable that complex formation should require a small activation energy than that the third order rate constant should have a large negative temperature coefficient, and this might be interpreted as further evidence in favor of a fairly small value of  $k_4/k_5$ . However, there can be large experimental errors in the values of the activation energies, which have been determined in a very indirect manner, and it is probably safe to conclude only that the suggested mechanism leads to reasonable values of the rate constants.

(22) The collision diameter of methyl cyanide was assumed to be  $5 \times 10^{-8}$  cm.

(23) W. Jost, *Z. physik. Chem.*, **B3**, 95 (1929).

(24) E. Rabinowitch and H. L. Lehman, *Trans. Faraday Soc.*, **31**, 689 (1935).

(25) E. Rabinowitch and W. C. Wood, *ibid.*, **32**, 907 (1936).

(26) K. Hilferding and W. Steiner, *Z. physik. Chem.*, **B30**, 399 (1935).

(27) E. Rabinowitch and W. C. Wood, *J. Chem. Phys.*, **4**, 497 (1936).

(28) N. Davidson, R. Marshall and L. T. Carrington, *ibid.*, **19**, 1311 (1951).

(29) M. I. Christie, R. G. W. Norrish and G. Porter, *Proc. Roy. Soc. (London)*, **A216**, 152 (1953).

(30) H. M. Smallwood, *J. Am. Chem. Soc.*, **51**, 1985 (1929).

(31) W. Steiner and E. W. Wicke, *Z. physik. Chem., Bodenst. Festband*, 817 (1931).

(32) W. Steiner, *Trans. Faraday Soc.*, **31**, 623 (1935).

(33) I. Amdur and A. L. Robinson, *J. Am. Chem. Soc.*, **55**, 1395 (1933).

(34) L. Farkas and H. Sachsse, *Z. physik. Chem.*, **B27**, 111 (1934).

(35) E. Rabinowitch, *Trans. Faraday Soc.*, **33**, 283 (1937).

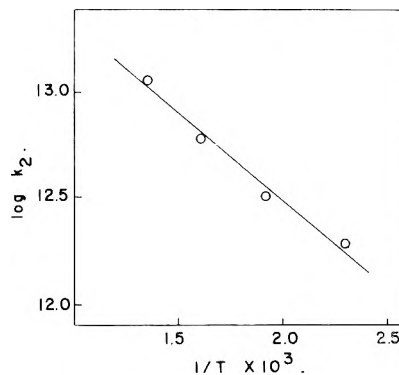


Fig. 4.—Plot of  $k_2$  against  $1/T$ .

### Appendix A

It is easy to show that the approximation

$$\left| \frac{dc}{dt} \right| \ll k_3 N M \quad (39)$$

is self-consistent for the methyl cyanide results. Differentiating eq. 24 with respect to time, and using eq. 24, 25 and 26 to simplify the result, 39 becomes

$$\frac{(k_3 k_6 N)/(k_4 + k_5 + k_6 N)^2 + k_3 M(k_4 + k_5)(k_5 + 2k_6 N)/(k_4 + k_5 + k_6 N)^3 \ll 1 \quad (40)$$

Now

$$\frac{k_4 + k_5}{k_4 + k_5 + k_6 N} \approx 1 \quad (41)$$

and

$$\frac{k_5 + 2k_6 N}{k_4 + k_5 + k_6 N} \approx \frac{k_5 + 2k_6 N_0}{k_4 + k_5 + k_6 N_0} \approx \frac{k_5 + 2k_6 N_0}{k_5 + k_6 N_0} \sim 1 \quad (42)$$

(The experimental values of  $(k_5 + 2k_6 N_0)/(k_5 + k_6 N_0)$  range from 1.5 at  $160^\circ$ , to 1.1 at  $460^\circ$ .) Thus, considering the second term of (40), it will be  $\ll 1$  if

$$k_3 M/(k_4 + k_5 + k_6 N) \ll 1 \quad (43)$$

The most stringent test of (43) will be for the largest values of  $M$ . Thus it will certainly be satisfied if

$$k_3 M_0/(k_4 + k_5 + k_6 N_0) \ll 1 \quad (43a)$$

for the largest value of  $M_0$  used in the study. From eq. 35 this can be written in the form

$$k_2 M_0/k_5 \ll 1 \quad (44)$$

The largest value of  $k_2 M_0$  was about  $20 \text{ sec.}^{-1}$ , and the value of  $k_5$  was probably between  $10^4$  and  $10^7$ , (corresponding to a collision yield for the recombination reactions between  $10^{-3}$  and 1, see Section II) so that condition (44) is satisfied. In a similar way, it can be shown that the first term of (40) is  $\ll 1$ , if

$$\frac{k_3 N}{k_4 + k_5 + k_6 N} \ll 1 \quad (45)$$

and comparing (45) with (43) it can be seen that this condition is also satisfied since the greatest value of  $N$  is less than the greatest value of  $M$ .

## A SELECTIVITY SCALE FOR SOME DIVALENT CATIONS ON DOWEX 50

BY O. D. BONNER AND LINDA LOU SMITH<sup>1,2</sup>*Dept. of Chemistry, University of South Carolina, Columbia, South Carolina**Received September 10, 1956*

Equilibrium studies involving cupric, zinc, cobaltous, nickel, magnesium, cadmium, uranyl and lead ions on Dowex 50 resins of approximately 4, 8 and 16% divinylbenzene content have been made at a constant ionic strength of approximately 0.1 *M*. These ions in addition to barium, strontium and calcium ions have been included in the same selectivity scale as the common univalent cations. Activity coefficient corrections have been made for the ions in the aqueous solution phase, and these corrections have been substantiated in some instances by the results of exchange reactions carried out at lower ionic strengths. It is observed that the order of decreasing activity coefficients for the nitrates of both the univalent and the divalent ions is the same as that of the selectivity scale. The characteristic maximum water uptake of the resin in these ionic forms is reported.

A summary of the results of ion-exchange equilibria and maximum water uptake of Dowex 50 resins of 4, 8 and 16% DVB content involving the common univalent cations has been reported previously.<sup>3</sup> The results of ion-exchange equilibria involving the four divalent cations cupric, barium, strontium and calcium also have been reported.<sup>4</sup> All of these exchange reactions were carried out at an aqueous solution ionic strength of approximately 0.1 *M*. The activity coefficient ratio term for the ions in the aqueous solution which appears in the expression for the equilibrium constant was ignored, although it was realized that it might differ from unity by as much as 20% in some exchanges.<sup>4</sup>

Experimental data on exchanges involving seven additional divalent ions are reported herewith. An activity coefficient correction is made for these as well as for all previously calculated equilibrium constants. This permits the establishment of a single selectivity scale which includes the nine univalent ions and the 11 divalent ions studied up to this time.

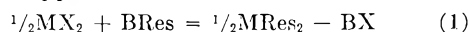
### Experimental

The methods of equilibration and separation of aqueous and resin phases have been described previously.<sup>4</sup> In preparation for analysis the resin phase was first washed free of adhering electrolyte and then exhaustively eluted with an electrolyte which would not interfere with the analysis for the ions in question. Aliquots of this effluent and also of the solution phase were then analyzed for both ions being exchanged. Cobalt and zinc ion concentrations were determined radiometrically, Co<sup>60</sup> and Zn<sup>65</sup> being used as tracers. Nickel ion concentration was determined by titration with standard potassium cyanide solution. Lead and cadmium ion concentrations were determined by complexometric titration with the disodium salt of ethylenediaminetetraacetic acid in acidic media, PAN serving as indicator. Calcium and magnesium ion concentrations were determined by a similar titration in ammoniacal solution. Copper ion concentrations were determined either by complexometric titration with standard disodium EDTA in acidic media, by titration of the iodine liberated by cupric ion from an excess of acidified potassium iodide solution with standard thiosulfate solution, or by electrolytic deposition of copper on weighed platinum electrodes. Uranyl ion concentrations were determined by reduction of the uranium from the +6 to the +4 state in a Jones reductor and subsequent titration with standard dichromate solution. The uranyl-hydrogen exchange is the only one studied in which both ions in both

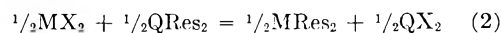
the resin and solution phases cannot be determined directly. Aqueous solutions of known compositions were passed over columns of resin until equilibrium was reached. Since the uranyl ion interferes with acid-base titrations, the hydrogen ion in the resin phase was then calculated as the difference between the capacity of the resin and the uranyl ion found.

### Discussion and Results

It has been indicated<sup>4</sup> previously that if exchanges between univalent and divalent ions or between two divalent ions are represented by equations of the type



and



they are directly comparable with exchanges between univalent ions which are represented by the equation



The equilibrium constants for the above reactions are

$$K_{1,2} = \frac{N^{1/2}MRes_2m_{BX}f^{1/2}MRes_2\gamma_{BX}^2}{N_{BRes}m^{1/2}MX_2f_{BRes}\gamma^{3/2}MX_2} = k \frac{f^{1/2}MRes_2\gamma_{BX}^2}{f_{BRes}\gamma^{3/2}MX_2} \quad (4)$$

$$K_{2,2} = \frac{N^{1/2}MRes_2m^{1/2}QX_2f^{1/2}MRes_2\gamma^{3/2}QX_2}{N^{1/2}QRes_2m^{1/2}MX_2f^{1/2}QRes_2\gamma^{3/2}MX_2} = k \frac{f^{1/2}MRes_2\gamma^{3/2}QX_2}{f^{1/2}QRes_2\gamma^{3/2}MX_2} \quad (5)$$

and

$$K_{1,1} = \frac{N_{ARes}m_{BX}f_{ARes}\gamma_{BX}^2}{N_{BRes}m_{AX}f_{BRes}\gamma_{AX}^2} = k \frac{f_{ARes}\gamma_{BX}^2}{f_{BRes}\gamma_{AX}^2} \quad (6)$$

respectively, where *m* is the aqueous phase molality, *N* is the molar fraction of the ion in the resin phase, *f* is the activity coefficient of the resin,  $\gamma$  is the mean activity coefficient of the electrolyte in the aqueous phase and *k* is the quantity later referred to as the equilibrium quotient.

When the exchange reactions are represented in this manner, triangular comparisons may be obtained by addition or subtraction of two equations to yield a third, and the resultant equilibrium constant for the third reaction will be the product or quotient of the first two constants. This logarithmic additivity of equilibrium constants has also permitted the establishment of a quantitative selectivity scale<sup>3</sup> for the common univalent ions by the arbitrary assignment of a value of unity for the affinity of each resin sample for lithium ion. The equilibrium constant for each exchange reaction has

(1) These results were developed under a project sponsored by the United States Atomic Energy Commission.

(2) Part of the work described herein was included in a thesis submitted by Linda Lou Smith to the University of South Carolina in

$$\log K = \int_0^1 \log k \, dX \quad (7)$$

where  $X$  is the equivalent fraction of the preferred ion in the resin phase.

**Activity Coefficient Corrections.**—It has been realized that the  $K$  values calculated in this manner are in error<sup>6</sup> because the activity coefficient ratios of the ions in the aqueous solution were assumed to be unity. This assumption was made because few activity coefficient values are available for mixed electrolytes at an ionic strength of 0.1. The error in  $K$  caused by neglect of solution phase activity coefficients becomes appreciably larger, however, in exchanges involving divalent ions than was the case for univalent ion exchanges, and a correction becomes necessary. This correction may be made by application of the ionic strength principle and use of the activity coefficients for the electrolytes in pure solutions at an ionic strength of 0.1. Although this procedure probably does not completely eliminate the error, it reduces it considerably. As an example the activity coefficient ratio  $\gamma_{\text{HNO}_3}/\gamma_{\text{AgNO}_3}$  may be cited. The value of this ratio<sup>7</sup> for pure solutions of nitric acid and silver nitrate may be calculated to be 1.078 for 0.1  $M$  solutions. The value in mixed solutions<sup>8</sup> is nearly constant for all ratios of nitric acid to silver nitrate, and has an average value of 1.060. Since one of the ions involved is silver ion, the difference in the activity coefficient ratio for pure and mixed solutions observed here is probably as great as will be encountered in most systems. A slightly greater refinement in this correction might be made by use of the interaction coefficients of Guggenheim.<sup>9,10</sup> This was not done, however, because these coefficients are not known for all of the univalent electrolytes which were studied, and only for barium ion of the divalent ions studied.

The calculated values of the activity coefficient correction term for these exchanges range from 1.016 for the hydrogen-lithium system to 1.280 for the cupric-hydrogen system in chloride media. These activity coefficient corrections have been verified in several instances by the study of exchanges at several lower ionic strengths, extrapolation of the  $k$  values to infinite dilution, and comparison with the value of  $k$  calculated from exchanges at the ionic strength of 0.1  $M$  to which the activity coefficient correction had been made. Examples of these comparisons are given in Table I. The calculated activity coefficient correction factor for almost all of the systems was greater than unity, the calcium-cupric exchange constituting one of the few exceptions. There is a very large correction in the case of the magnesium-hydrogen exchange even at an ionic strength of 0.01. This is to be expected because of the differences in the rate

(6) Oscar D. Bonner and Vickers Rhett, *THIS JOURNAL*, **57**, 254 (1953).

(7) R. A. Robinson and R. H. Stokes, *Trans. Faraday Soc.*, **45**, 612 (1949).

(8) O. D. Bonner, A. W. Davidson and W. J. Argersinger, *J. Am. Chem. Soc.*, **74**, 1047 (1952).

(9) E. A. Guggenheim, "Thermodynamics," Interscience Publishers, Inc., New York, N. Y., 1949, p. 315.

(10) E. A. Guggenheim and J. C. Turgeon, *Trans. Faraday Soc.*, **51**, 747 (1955).

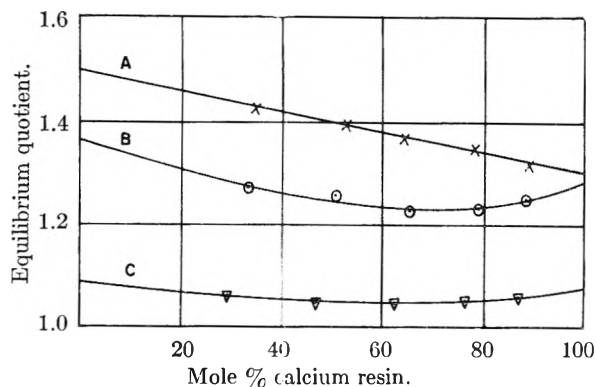


Fig. 1.—Calcium-cadmium exchange: A, 16% DVB; B, 8% DVB; C, 4% DVB.

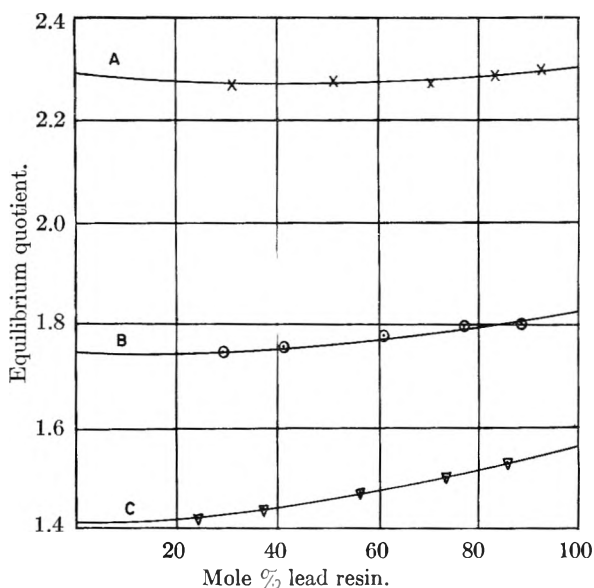


Fig. 2.—Lead-calcium exchange: A, 16% DVB; B, 8% DVB; C, 4% DVB.

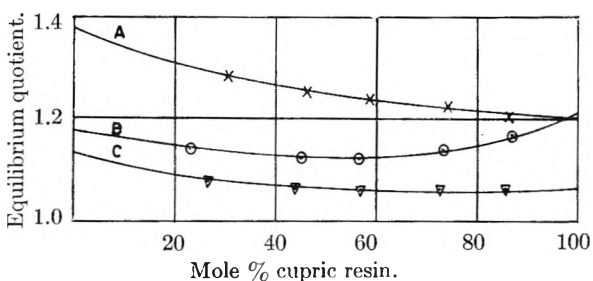


Fig. 3.—Cupric-magnesium exchange: A, 16% DVB; B, 8% DVB; C, 4% DVB.

of change of the activity coefficients with concentration between 1,1 and 2,1 electrolytes in very dilute solutions.

**Selectivity Data.**—The experimental data for the new exchange systems studied are presented graphically in Figs. 1–8 as plots of the equilibrium quotient,  $k$ , as a function of resin loading. The value of  $k$  does not change markedly with resin loading for many of the divalent ion exchanges studied. The lead-calcium exchange is interesting in that  $k$  increases with increased lead (the preferred ion) loading. It is more common for  $k$  to decrease with an increase in the resin content of

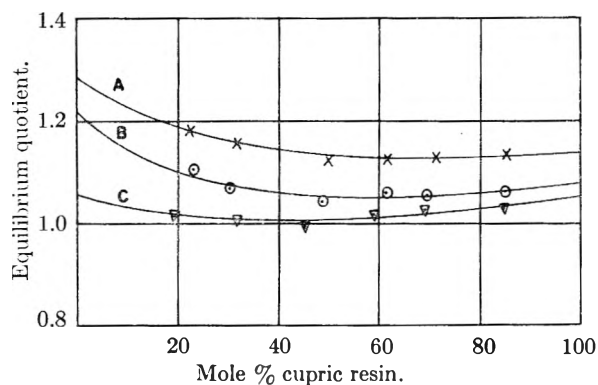


Fig. 4.—Cupric-zinc exchange: A, 16% DVB; B, 8% DVB; C, 4% DVB.

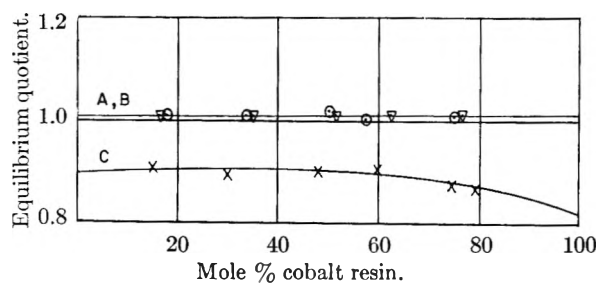


Fig. 5.—Cobalt-cupric exchange: A, 4% DVB; B, 8% DVB; C, 16% DVB.

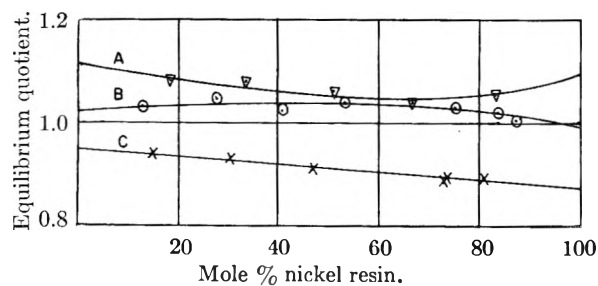


Fig. 6.—Nickel-cupric exchange: A, 4% DVB; B, 8% DVB; C, 16% DVB.

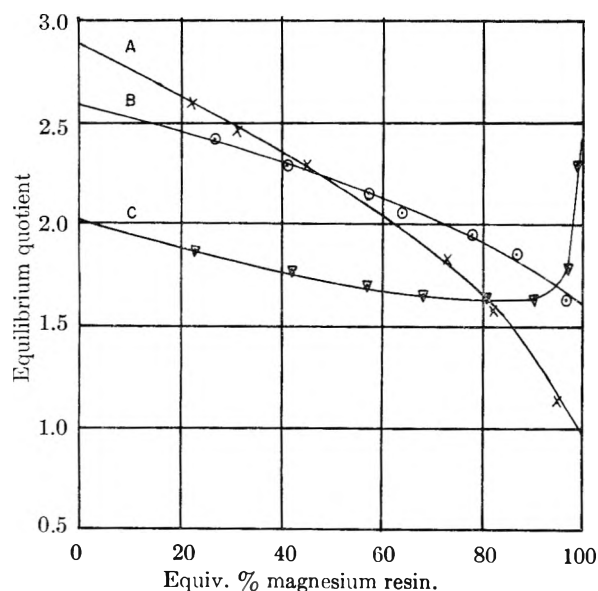


Fig. 7.—Magnesium-hydrogen exchange: A, 16% DVB; B, 8% DVB; C, 4% DVB.

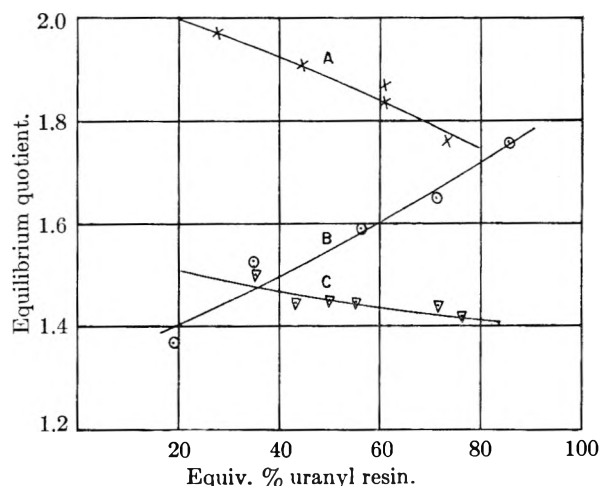


Fig. 8.—Uranyl-hydrogen exchange: A, 16% DVB; B, 8% DVB; C, 4% DVB.

TABLE I

EQUILIBRIUM QUOTIENT VARIATION WITH IONIC STRENGTH (8% DVB resin)

| Ex-change | Resin loading % preferred ion | $\mu =$ |      |      |       |                  |                  |
|-----------|-------------------------------|---------|------|------|-------|------------------|------------------|
|           |                               | 0.1     | 0.07 | 0.01 | 0.001 | 0.0 <sup>a</sup> | 0.0 <sup>b</sup> |
| Ca-Cd     | 54.2                          | 1.25    |      | 1.28 |       | 1.33             | 1.31             |
| Ca-Cu     | 56.5                          | 1.40    |      | 1.36 |       | 1.34             | 1.32             |
| Mg-H      | 87.5                          | 1.67    | 1.70 | 1.74 |       | 2.00             | <sup>d</sup>     |
| Pb-Ca     | 76.1                          | 1.79    |      | 1.86 | 1.93  | <sup>c</sup>     | 1.94             |

<sup>a</sup> Calculated by the application of solution phase activity coefficient corrections to exchanges performed at  $\mu = 0.1$ .  
<sup>b</sup> Extrapolated values. <sup>c</sup> Activity coefficient of  $\text{Pb}(\text{NO}_3)_2$  not known. <sup>d</sup> Extrapolation uncertain.

TABLE II

REVISED SELECTIVITY SCALE FOR UNIVALENT IONS ON DOWEX 50

|               | 4% DVB | 8% DVB | 16% DVB |
|---------------|--------|--------|---------|
| Li            | 1.00   | 1.00   | 1.00    |
| H             | 1.32   | 1.27   | 1.47    |
| Na            | 1.58   | 1.98   | 2.37    |
| $\text{NH}_4$ | 1.90   | 2.55   | 3.34    |
| K             | 2.27   | 2.90   | 4.50    |
| Rb            | 2.46   | 3.16   | 4.62    |
| Cs            | 2.67   | 3.25   | 4.66    |
| Ag            | 4.73   | 8.51   | 22.9    |
| Tl            | 6.71   | 12.4   | 28.5    |

the preferred ion, although there are several instances where  $k$  passes through a maximum or a minimum value. The nickel-cupric system is unusual in that nickel ion is preferred to cupric ion on the 4 and 8% DVB resins, while cupric ion is preferred on the 16% DVB resin.

A selectivity scale for nine of the univalent ions, which has been revised by the correction for solution phase activity coefficients, is given in Table II. A similar selectivity scale for eleven divalent ions is given in Table III. Both scales are based upon the arbitrary assignment of the value of unity to affinity of lithium ion for each resin. Four univalent-divalent ion exchange systems provide the data for comparison of univalent and divalent ion affinities in these tables, namely, the cupric-hydrogen and silver-cupric systems, which have been reported

previously,<sup>4</sup> and the cupric-magnesium and magnesium-hydrogen systems.

TABLE III

| SELECTIVITY SCALE FOR DIVALENT IONS ON DOWEX 50 | IONIC FORMS (g./equiv.) |        |         |
|---|-------------------------|--------|---------|
|   | 4% DVB                  | 8% DVB | 16% DVB |
| UO <sub>2</sub>                                 | 2.36                    | 2.45   | 3.34    |
| Mg  | 2.95                    | 3.29   | 3.51    |
| Zn  | 3.13                    | 3.47   | 3.78    |
| Co  | 3.23                    | 3.74   | 3.81    |
| Cu  | 3.29                    | 3.85   | 4.46    |
| Cd  | 3.37                    | 3.88   | 4.95    |
| Ni  | 3.45                    | 3.93   | 4.06    |
| Ca  | 4.15                    | 5.16   | 7.27    |
| Sr  | 4.70                    | 6.51   | 10.1    |
| Pb  | 6.56                    | 9.91   | 18.0    |
| Ba  | 7.47                    | 11.5   | 20.8    |

TABLE IV

| MAXIMUM WATER UPTAKE OF DOWEX 50 RESINS IN VARIOUS | IONIC FORMS (g./equiv.) |        |         |
|--|-------------------------|--------|---------|
|  | 4% DVB                  | 8% DVB | 16% DVB |
| UO <sub>2</sub>                                    | 339                     | 167    | 121     |
| Mg   | 315                     | 175    | 129     |
| Zn   | 313                     | 178    | 127     |
| Co   | 306                     | 177    | 129     |
| Cu   | 303                     | 173    | 124     |
| Cd   | 313                     | 166    | 117     |
| Ni   | 298                     | 157    | 118     |
| Ca   | 282                     | 159    | 115     |
| Sr   | 250                     | 153    | 113     |
| Pb   | 203                     | 130    | 106     |
| Ba   | 167                     | 122    | 97      |

It is interesting to compare the above selectivity scales with values of the activity coefficients of salts of these ions. If one chooses the nitrates, which are similar to the sulfonates in that they are large oxygenated anions with a somewhat diffuse negative charge, the order of the selectivity scale is exactly the same as the order of decreasing activ-

ity coefficients<sup>7,11</sup> for all of the univalent and divalent ions for which such activity coefficient data are available.

**Swelling Data.**—The data representing the maximum water uptake of the 4, 8 and 16% DVB resins in the various divalent ionic forms are presented in Table IV. Similar moisture data for the univalent cations<sup>3</sup> closely follow the order of the selectivity scale in that the ions which cause the resin to swell the most are the least preferred. This is not so generally true for divalent cations, except for the 4% DVB resin. There are two possible reasons for this. The error in these moisture uptake data is probably of the order of  $\pm 2\%$ , and this uncertainty in several instances could reverse the positions of the ions in the moisture uptake table. Also, it is not a thermodynamic necessity that the resin imbibe more solvent in the less preferred form. If the osmotic pressure effect and the solution phase activity coefficients are ignored, the equation for the equilibrium quotient is<sup>12</sup>

$$\ln K = \int_0^{m_\phi} \left( \frac{1}{m_{A_{Res}}} - \frac{1}{m_{B_{Res}}} \right)_{m_\phi} dm(\phi) \quad (8)$$

where BRes refers to the resin containing B<sup>+</sup>, the preferred ion. The water uptake of the resin equals 1000/*m*. The data for the solution of this equation are, of course, not obtainable experimentally, since the swelling of the resin is limited by its cross-linking and the state of infinite dilution can never be reached. The equation does illustrate, however, that it is the value of the integral and not the value of (1/*m*<sub>ARes</sub> - 1/*m*<sub>BRes</sub>) for the wet swollen cross-linked resins which must be positive.

(11) H. S. Harned and B. B. Owen, "The Physical Chemistry of Electrolytic Solutions," Reinhold Publ. Corp., New York, N. Y., 1950, pp. 567, 602.

(12) O. D. Bonner, V. F. Holland and Linda Lou Smith, *THIS JOURNAL*, **60**, 1102 (1956).

## THE TERNARY SYSTEM: PERFLUOROTRI-*n*-BUTYLAMINE-2,2,4-TRIMETHYLPENTANE-NITROETHANE<sup>1</sup>

By JAY VREELAND<sup>2</sup> AND ROBERT DUNLAP

*Department of Chemistry, University of Maine, Orono, Maine*

*Received September 13, 1956*

The mutual solubilities of 2,2,4-trimethylpentane with perfluorotri-*n*-butylamine and with nitroethane were determined. The ternary system composed of these substances, studied at six temperatures between 25 and 51.3°, is the first ternary system to be reported with a fluorocarbon as one of the components. The existence of three liquid phases above the temperature at which two of the components become completely miscible is a novel phenomenon. The study demonstrates exactly what happens to the phase boundaries of the internal triangle in the phase diagrams as the temperature is increased to 34.8°, the highest temperature at which three liquid phases are stable. The properties of the ternary system are in accord with the theory of regular solutions when compared with the properties of the binary systems, but not when compared with thermodynamic properties of the pure components.

Hildebrand has used the solubility parameter,<sup>3</sup>  $\delta$ , the square root of the internal pressure, as a meas-

ure of solvent power. In general, the larger the difference in  $\delta$  values for two particular substances the lower their mutual solubility. The magnitude of these parameters ranges from  $\delta = 7$  (cal.<sup>1/2</sup> cm.<sup>-3/2</sup>) for hydrocarbons to  $\delta = 24$  for water. In contrast to all other organic liquids which have higher parameters than the hydrocarbons, the fluorocarbons have  $\delta$  values near 6. The mutual

(1) Presented before the 126th Meeting of the American Chemical Society, New York City, September, 1954.

(2) Submitted as a thesis in partial fulfillment of the requirements of the Bachelor of Science degree in Chemistry at the University of Maine.

(3) J. H. Hildebrand and R. L. Scott, "Solubility of Nonelectrolytes," Reinhold Publ. Corp., New York, N. Y., 1950, pp. 129, 423.

solubility of fluorocarbons and hydrocarbons is even lower than one would predict on the basis of these parameters.<sup>4-10</sup> Fluorocarbons are relatively insoluble in such liquids as carbon disulfide,  $\delta = 10$ , and the nitroparaffins,  $\delta = 11-12$ , thus making it possible for the first time to select for study a ternary system having two components, each partially miscible with a hydrocarbon, yet relatively insoluble in each other.

The system perfluorotri-*n*-butylamine-2,2,4-trimethylpentane (isoöctane)-nitroethane satisfies these requirements at temperatures convenient for study. The perfluorotri-*n*-butylamine and nitroethane were found to have mutual solubilities of less than one part per thousand at 25° and the critical solution temperatures of the hydrocarbon-fluorocarbon pair and the hydrocarbon-nitroethane pair were found to be 48.65 and 29.8°, respectively, indicating limited solubility at room temperature.

### Experimental

Perfluorotri-*n*-butylamine, obtained from the Minnesota Mining and Manufacturing Company, was distilled through a Todd column and a middle cut, b.p. 178.0-178.1° at 761 mm., was used.

Nitroethane, research grade, obtained from the Matheson Chemical Company, was distilled through a Todd column and a middle cut with a boiling range 114.7-114.8° at 760 mm. was used.

Isoöctane (Pure Grade, 99 mole % minimum) was obtained from the Phillips Petroleum Company. Its density was 0.68774 at 25.0° as compared with 0.68777 given by Timmermans.<sup>11</sup> This material was used without further purification.

The phase boundaries for the ternary system were determined at 25.0, 31.5, 33.7, 35.0, 45.0 and 51.3° and are shown in Figs. 2-6.<sup>12</sup> The method for obtaining the experimental data depended on the temperature and composition range but, in general, binary solutions were made up volumetrically with calibrated graduated pipets and the third component was added until a phase just disappeared or reappeared. These titrations were carried out in stoppered 150 mm. test-tubes which were supported in temperature baths held at the desired temperature to  $\pm 0.01^\circ$ . In cases where a shift from two phases to one was approached, the size of one layer usually decreased faster than the other upon addition of the third component. When such behavior was observed, addition of the third component was made dropwise until the system became homogeneous. Near the end-point, ten minutes was allowed between drops in order to establish temperature equilibrium. In cases requiring a shift from two to three phases, it was found difficult to observe the appearance of the third phase when it appeared at the interface or the meniscus. In such cases, greater reproducibility was obtained by making up a three-phase solution and titrating with a third component until the shift from three to two phases was observed.

Calibrations of the pipets were made by weighing the volumes of liquid delivered allowing five seconds drainage time when held in a vertical position. Volumes could be reproduced to  $\pm 0.002$  ml. The maximum error in the

compositions at the phase boundaries was estimated to be not greater than one per cent.

The points on the borders of the phase diagrams were obtained from solubility data on the binary systems. Refractive index determinations of perfluorotri-*n*-butylamine saturated with nitroethane and of nitroethane saturated with perfluorotri-*n*-butylamine showed that the solubility of these substances in each other was less than one part per thousand. In the cases of the systems nitroethane-isoöctane and perfluorotri-*n*-butylamine-isoöctane, solutions of determined composition were heated above the critical solution temperature and placed in a bath which was cooled at the rate of 0.01° per minute. The solutions were agitated and the temperature at which phase separation occurred was observed. The experimental data<sup>12</sup> for the two binary systems studied are shown in Fig. 1.

### Results

The critical solution temperature and composition for the binary system perfluorotri-*n*-butylamine-isoöctane are 48.65° and 0.768 mole fraction of the hydrocarbon. The mutual solubility of these substances is significantly different from that reported by Rotariu, Hanrahan and Fruin<sup>7</sup> who give 53.7° as the critical solution temperature for this system.

There is a possible explanation for this discrepancy. The above investigators have reported the temperature at which opalescence was first noticed as the consolute solution temperature. In our laboratory, however, we have found when investigating solutions of fluorocarbons and hydrocarbons that opalescence sometimes appears 4-5° above the temperature at which phase separation occurs. Solutions of these substances which are virtually opaque can be kept in this state for days without phase separation at temperatures slightly above the consolute solution temperature.

The critical solution temperature and composition for the binary system nitroethane-isoöctane are 29.8° and 0.509 mole fraction of hydrocarbon.

Figure 2 shows the incomplete miscibility of the three components at 25°. The corners of the internal triangle give the equilibrium compositions of the three phases when the over-all composition is represented by a point within the triangle. A typical example of this phenomenon is given by F. A. H. Schreinemakers.<sup>13</sup> Figure 3 shows a three-phase region above the temperature at which two of the components, nitroethane and isoöctane, become completely miscible. No examples showing such behavior for three components have been published, although the system phenol-water-mixed pentenes<sup>14</sup> is somewhat similar. The crescent shaped area at the side of the internal triangle is a two-phase area, but does not reach the border of the diagram because nitroethane and isoöctane are completely miscible at this temperature. This novel phenomenon is of interest because it is an example of behavior discussed by Ricci<sup>15</sup> and Francis.<sup>14</sup> It is similar to the diagram for the system phenol-water-mixed pentenes and different from that postulated by Ricci inasmuch as two of the components are practically immiscible. This is usually an essential requirement for a three-liquid system, especially when a hydrocarbon is chosen

(4) J. H. Simons and R. D. Dunlap, *J. Chem. Phys.*, **18**, 335 (1950).

(5) J. H. Simons and J. W. Mausteller, *ibid.*, **20**, 1516 (1952).

(6) J. H. Hildebrand, B. B. Fisher and H. A. Benesi, *J. Am. Chem. Soc.*, **72**, 4348 (1950).

(7) G. J. Rotariu, R. J. Hanrahan and R. E. Fruin, *ibid.*, **76**, 3752 (1954).

(8) F. P. McLaughlin and R. L. Scott, *ibid.*, **76**, 5276 (1954).

(9) N. Thorp and R. L. Scott, *THIS JOURNAL*, **60**, 670 (1956).

(10) James B. Hickman, *J. Am. Chem. Soc.*, **77**, 6154 (1955).

(11) J. Timmermans, "Physico-Chemical Constants of Pure Hydrocarbons," Elsevier Publishing Co., Houston, Texas, 1950, p. 94.

(12) The experimental data have been deposited as Document number 5047 with the ADI Auxiliary Publication Project, Photoduplication Service, Library of Congress, Washington 25, D. C. A copy may be secured by citing the Document number and by remitting in advance \$1.25 for photoprints, or \$1.25 for 35 mm. microfilm, payable to Chief, Photoduplication Service, Library of Congress.

(13) F. A. H. Schreinemakers, *Z. physik. Chem.*, **25**, 543 (1898).

(14) A. W. Francis, "Physical Properties of Hydrocarbons," by A. Farkas, Academic Press, Inc., New York, N. Y., 1950, p. 253.

(15) J. E. Ricci, "The Phase Rule and Heterogeneous Equilibrium," D. Van Nostrand Co., Inc., New York, N. Y., 1951, p. 215.

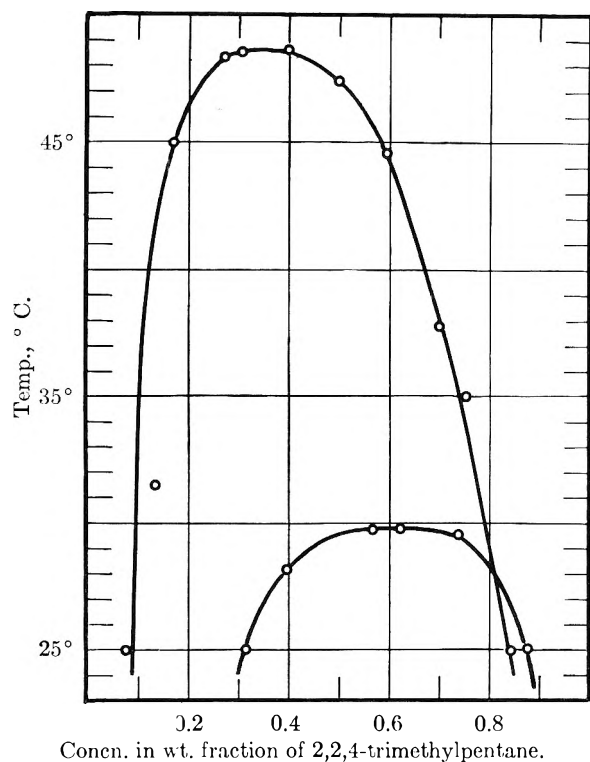


Fig. 1.—The mutual solubilities of 2,2,4-trimethylpentane with perfluorotri-*n*-butylamine (upper curve) and with nitroethane (lower curve).

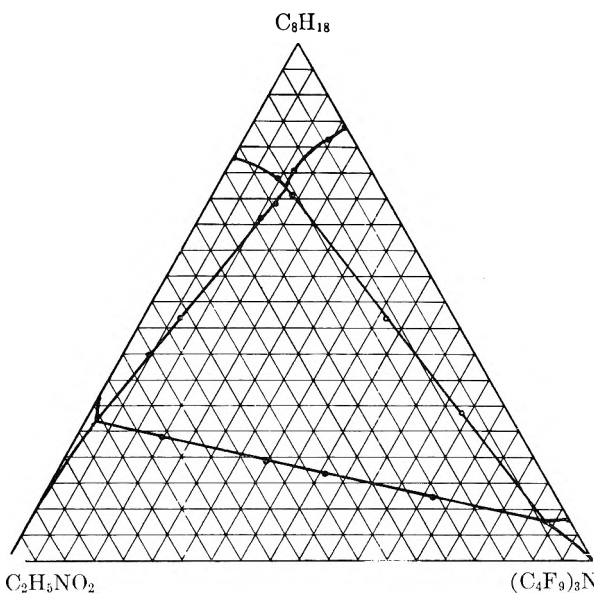


Fig. 2.—Isothermal solubility diagram: perfluorotri-*n*-butylamine-2,2,4-trimethylpentane-nitroethane at 25°; concentration in % by weight.

as the component with limited miscibility in each of the others.

At 25° and 31.5° (Figs. 2, 3) only one of the three two-phase areas has a base which is wider on the internal triangle than on the border. In this respect, these phase diagrams differ from those mentioned above. At higher temperatures, however, the miscibility gap for the hydrocarbon-fluorocarbon pair also has its wider base along the border of the three-phase region. This is shown in Fig. 4 at 33.7°.

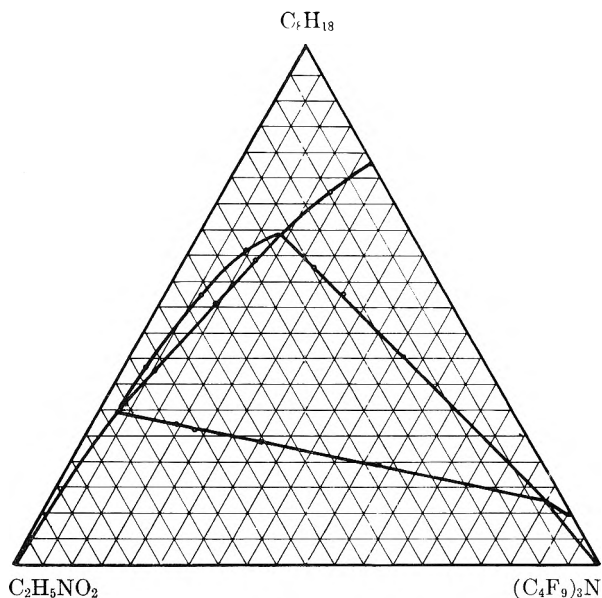


Fig. 3.—Isothermal solubility diagram: perfluorotri-*n*-butylamine-2,2,4-trimethylpentane-nitroethane at 31.5°; concentration in % by weight

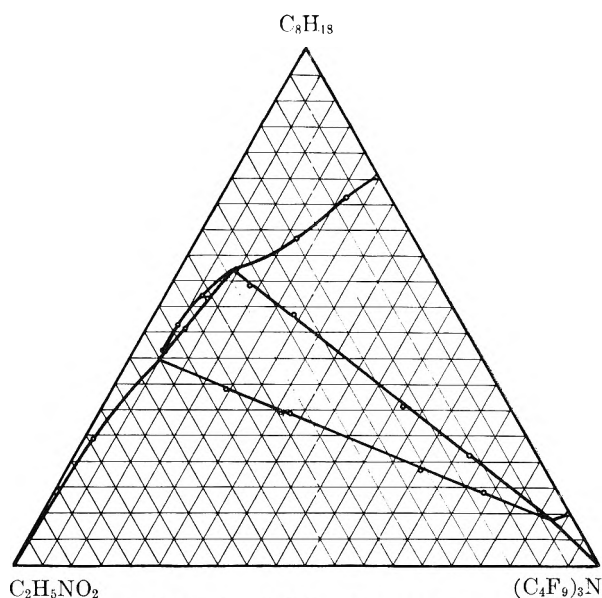


Fig. 4.—Isothermal solubility diagram: perfluorotri-*n*-butylamine-2,2,4-trimethylpentane-nitroethane at 33.7°; concentration in % by weight.

As the temperature is raised, the crescent shaped area becomes smaller and the sides of the triangle separating two- and three-phase regions approach each other until the three-phase region degenerates to the two-phase region shown in Fig. 5. The highest temperature at which three phases can exist was found to be 34.8°.

In order to determine whether the binodal curve for the fluorocarbon-hydrocarbon pair would separate from the binodal curve for the fluorocarbon-nitroethane pair, the isothermal solubility curve<sup>12</sup> was determined at 45°, *i.e.*, slightly below the critical solution temperature of the fluorocarbon-hydrocarbon pair. The solubility diagram is similar to that shown in Fig. 5, the only difference being a smaller two-phase region. A few experiments

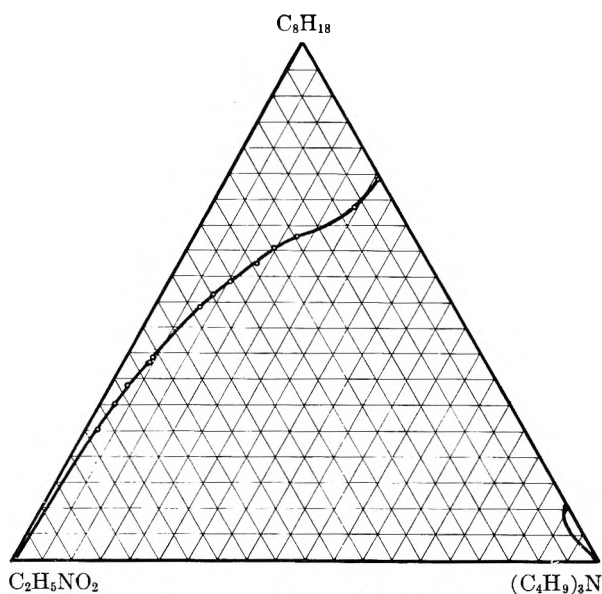


Fig. 5.—Isothermal solubility diagram: perfluorotri-*n*-butylamine-2,2,4-trimethylpentane-nitroethane at 35.0°; concentration in % by weight.

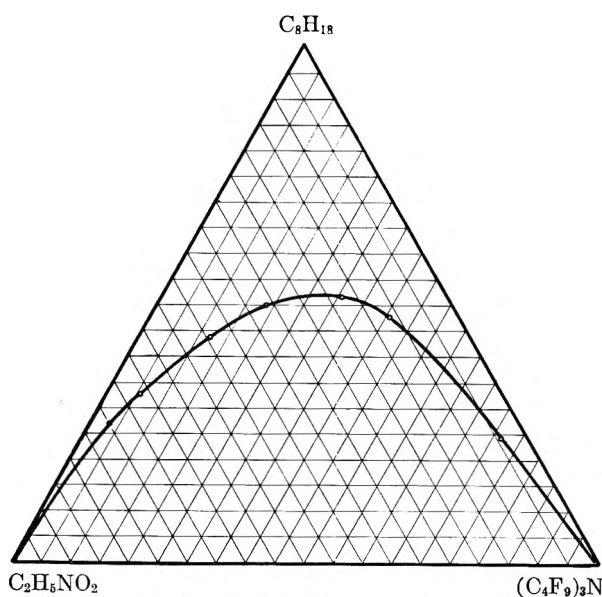


Fig. 6.—Isothermal solubility diagram: perfluorotri-*n*-butylamine-2,2,4-trimethylpentane-nitroethane at 51.3°; concentration in % by weight.

carried out at less than 0.1° below the critical solution temperature of this pair showed that the two-phase region converges to a point on the fluorocarbon-hydrocarbon border of the three phase diagram. There was no indication of a "col" or saddle point<sup>16</sup> in this region.

Figure 6 at 51.3°, where both the nitroethane-isoöctane and perfluorotri-*n*-butylamine-isoöctane binary systems are completely miscible, is typical of a three-component system showing enhancement of the solubility of two relatively insoluble liquids due to the presence of a third component which is compatible with each.

#### Discussion

From the theory for regular solutions, as de-

(16) A. W. Francis, *J. Am. Chem. Soc.*, **76**, 393 (1954).

veloped by Hildebrand and Wood<sup>17</sup> and Scatchard,<sup>18</sup> equations relating the activity to the equilibrium compositions and the solubility parameters are

$$RT \ln \frac{a_1}{x_1} = \phi_2^2 V_1 (\delta_2 - \delta_1)^2 \quad (1)$$

for a binary system, and

$$RT \ln \frac{a_H^H}{x_H^H} = V_H [(\delta_H - \delta_N)\phi_N^H + (\delta_H - \delta_F)\phi_F^H]^2 \quad (2)$$

$$RT \ln \frac{a_N^N}{x_N^N} = V_H [(\delta_H - \delta_N)\phi_N^N + (\delta_H - \delta_F)\phi_F^N]^2 \quad (3)$$

$$RT \ln \frac{a_F^F}{x_F^F} = V_H [(\delta_H - \delta_N)\phi_N^F + (\delta_H - \delta_F)\phi_F^F]^2 \quad (4)$$

for a ternary system,<sup>19</sup> where the *a*'s, *x*'s, *φ*'s and *δ*'s represent the activities, mole fractions, volume fractions and solubility parameters, respectively. The subscripts designate the component referred to and the superscripts designate the component which has the largest mole fraction in the phase considered. For example  $a_H^H$  and  $\phi_N^H$  represent the activity of hydrocarbon and the volume fraction of the nitroethane in the isoöctane phase and  $a_F^F$  and  $\phi_N^F$  represent the activity of the hydrocarbon and the volume fraction of the nitroethane in the fluorocarbon phase. Six equations similar to 2, 3 and 4 can be obtained for the activities of the other two components. From the condition that the activity of each component be the same in each of these phases, it is possible to calculate the equilibrium composition of the conjugate phases and thus the phase boundary in the ternary diagram. The calculations are complicated because the compositions appear as squared terms in the nine equations.

A test of the theory which lends itself more readily to calculation is to compare the differences in the *δ* values calculated from the energies of vaporization and molal volumes of the pure components with the differences in *δ* values calculated by simultaneous solution of equations 2, 3 and 4 using the experimentally determined compositions of the conjugate phases. These are shown in Table I. For each set of three equations, two differences in *δ* values are obtained, *e.g.*, when the activity of the hydrocarbon in the hydrocarbon phase is equated to the activities of the hydrocarbon in the nitroethane and fluorocarbon phases, two quadratic equations are obtained. Their simultaneous solution gives the values: 2.34 cal.<sup>1/2</sup> cm.<sup>-3/2</sup> for  $\delta_H - \delta_F$  and 3.5 for  $\delta_N - \delta_H$  as shown in column five of Table II. The other values shown are obtained in the same manner by equating the activities of the fluorocarbon and nitroethane in their conjugate phases at 25, 31.5 and 33.7°, respectively.

The solubility parameters calculated from the energies of vaporization and molal volumes at 25° for perfluorotri-*n*-butylamine,<sup>7</sup> 2,2,4-trimethylpentane<sup>20</sup> and nitroethane<sup>21</sup> are 5.9, 6.85 and 11.38,

(17) J. H. Hildebrand and S. E. Wood, *J. Chem. Phys.*, **1**, 817 (1933).

(18) G. Scatchard, *Chem. Revs.*, **8**, 321 (1931).

(19) See ref. 3, p. 200.

(20) See ref. 3, p. 436.

(21) D. E. Holcomb and C. L. Dorsey, Jr., *Ind. Eng. Chem.*, **41**, 2788 (1949).

TABLE I  
 CONCENTRATIONS OF THE THREE SATURATED PHASES WT. %

| Temp. °C. | Isooctane phase |               |              | Perfluorotri- <i>n</i> -butylamine phase |               |              | Nitroethane phase |               |              |
|-----------|-----------------|---------------|--------------|--|---------------|--------------|-------------------|---------------|--------------|
|           | Iso-octane      | Fluoro-carbon | Nitro-ethane | Iso-octane                               | Fluoro-carbon | Nitro-ethane | Iso-octane        | Fluoro-carbon | Nitro-ethane |
| 25.0      | 72.2            | 11.9          | 15.9         | 7.5                                      | 88.3          | 4.2          | 26.9              | 1.9           | 71.2         |
| 31.5      | 64.2            | 13.7          | 22.1         | 12.4                                     | 84.8          | 2.8          | 29.5              | 2.9           | 67.6         |
| 33.7      | 57.5            | 8.9           | 33.6         | 8.7                                      | 87.8          | 3.5          | 39.6              | 4.9           | 55.5         |

respectively. The differences in  $\delta$  values are shown in column 2 of Table II for comparison with those calculated from the data for the binary and ternary systems. The values shown in column 3 were calculated from the critical solution temperatures of the hydrocarbon-fluorocarbon and hydrocarbon-nitroethane binary systems using equation 5

$$RT_c = \frac{2x_1x_2V_1^2V_2^2}{(x_1V_1 + x_2V_2)^3} (\delta_2 - \delta_1)^2 \quad (5)$$

which has been derived from equation 1.<sup>22</sup>

 TABLE II  
 SOLUBILITY PARAMETER DIFFERENCES  
 $(\frac{\Delta E}{V})^{1/2}$ 

| $\delta_H - \delta_F$ | $T_c$ | Phase boundaries |       |
|-----------------------|-------|------------------|-------|
|                       |       | $a_F$            | $a_N$ |
|                       | 2.20  |                  |       |
| 25.0°                 | 0.95  | 2.39             | 2.34  |
| 31.5°                 |       | 2.31             | 2.24  |
| 33.7°                 |       | 2.40             | 2.45  |
|                       | 3.80  |                  |       |
| $\delta_N - \delta_H$ |       |                  |       |
| 25.0°                 | 4.53  |                  | 3.50  |
| 31.5°                 |       |                  | 3.44  |
| 33.7°                 |       |                  | 3.48  |
|                       |       |                  | 3.50  |
| $\delta_N - \delta_F$ |       |                  |       |
| 25.0°                 | 5.48  | 3.48             | 3.78  |
| 31.5°                 |       | 3.44             | 5.65  |
| 33.7°                 |       | 3.33             | 4.20  |

The differences in  $\delta$  values calculated from the data for the ternary and binary systems are not in

(22) See ref. 1, p. 253.

agreement with those calculated from the physical properties of the pure components. Similar discrepancies were found in the case of solutions of hydrocarbons and fluorocarbon amines by Simons and Linevsky,<sup>23</sup> Rotariu, Hanrahan and Fruin<sup>7</sup> and McLaughlin and Scott.<sup>8</sup> Reed<sup>24</sup> has been able to explain at least part of the discrepancy by considering the deviation from the geometric mean approximation due to the differences of the ionization potentials of the molecules.

Discrepancies for solutions of hydrocarbons in solvents with a higher internal pressure have been observed and discussed by Hildebrand.<sup>25</sup>

The parameter differences calculated from the phase boundaries in the three-component system agree with those calculated from the critical solution temperatures and compositions of the perfluorotri-*n*-butylamine-iso-octane and nitroethane-iso-octane systems. The low values for  $\delta_F - \delta_N$  obtained from the ternary data were unexpected.

**Acknowledgment.**—We wish to thank the Minnesota Mining and Manufacturing Company for the perfluorotri-*n*-butylamine used in this investigation and The National Science Foundation for supporting the program of which this work was a part.

(23) J. H. Simons and M. J. Linevsky, *J. Am. Chem. Soc.*, **74**, 4750 (1952).

(24) T. M. Reed, III, *This Journal*, **59**, 425 (1955).

(25) J. H. Hildebrand, *J. Chem. Phys.*, **18**, 1337 (1950).

## THE IONIZATION CONSTANT OF ORTHANILIC ACID FROM 0 TO 50° BY MEANS OF E.M.F. MEASUREMENTS<sup>1</sup>

BY R. NORMAN DIEBEL AND D. F. SWINEHART

*Department of Chemistry, University of Oregon, Eugene, Oregon*

*Received September 21, 1956*

The ionization constant of orthanilic acid has been determined from 0 to 50° by the use of cells without liquid junction. The equation  $-\log K = 1160.68/T + 0.0066339T - 3.2314$  expresses the experimental data as a function of temperature in the above temperature range with a standard deviation of 0.0008 in  $-\log K$  for 11 experimental points. The standard entropy of ionization,  $\Delta S^\circ$ , was found to be  $-3.3$  e.u., a value much larger than that for sulfanilic and metanilic acids.

### Introduction

The ionization constants and related thermodynamic quantities for sulfanilic acid<sup>2</sup> and metanilic acid<sup>3</sup> (*p*- and *m*-aminobenzenesulfonic acids, respectively) have been reported previously from this Laboratory. Both acids are zwitterions with large charge separations and both show a remarkably

small entropy of ionization. It has been suggested<sup>3,4</sup> that the small entropy of ionization of these two acids can be understood on the basis of a qualitative picture of the interaction of water dipoles and these zwitterions. On this basis a prediction was made regarding the entropy of ionization for orthanilic acid.

The present paper reports experimental data for the determination of the ionization constant of orthanilic acid (*o*-aminobenzenesulfonic acid) as a function of temperature and confirms the prediction regarding entropy of ionization.

(1) Taken in part from the master's thesis of R. Norman Diebel.

(2) R. O. MacLaren and D. F. Swinehart, *J. Am. Chem. Soc.*, **73**, 1822 (1951).

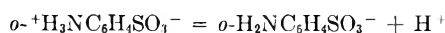
(3) R. D. McCoy and D. F. Swinehart, *ibid.*, **76**, 4708 (1954).

(4) D. F. Swinehart, paper presented at the Northwest Regional Meeting of the A.C.S., Pullman, Wash., June 12-13, 1953.

Previously reported values for the ionization constant of orthanilic acid were obtained from conductivity measurements and calculations were made without the benefit of the Debye-Hückel interionic attraction theory. These values are

| Investigator        | $K$                   | $t$ (°C.) |
|---------------------|-----------------------|-----------|
| Oswald <sup>5</sup> | $3.3 \times 10^{-3}$  | 25        |
| Boyle <sup>6</sup>  | $4.29 \times 10^{-3}$ | 25        |

It has been shown by Carr and Shutt<sup>7</sup> from measurements of the change in dielectric constant with pH for sulfanilic acid solutions that sulfanilic acid behaves as a zwitterion. Even though orthanilic acid is somewhat stronger than sulfanilic acid, it is not nearly as strong as the unsubstituted aromatic sulfonic acids<sup>8</sup> and it is reasonable to assume that orthanilic acid also exists in solution largely as the zwitterion. Hence the ionization constant is written for the reaction



The general method of investigation is that developed by Harned and co-workers.<sup>9</sup> The cells were of the type Pt,  $\text{H}_2/\text{HOr}(m_1)$ ,  $\text{NaOr}(m_2)$ ,  $\text{NaCl}(m_3)/\text{AgCl}-\text{Ag}$  where HOr and NaOr are orthanilic acid and its sodium salt, respectively, and  $m_1$ ,  $m_2$  and  $m_3$  are molalities. By elimination of  $m_{\text{H}^+} + \gamma_{\text{H}^+}$  from the cell potential equation

$$E = E^\circ - \frac{2.30259RT}{F} \log m_{\text{H}^+} m_{\text{Cl}^-} \gamma_{\text{H}^+} \gamma_{\text{Cl}^-} \quad (1)$$

and the thermodynamic ionization constant expression

$$K = \frac{m_{\text{H}^+} m_{\text{Or}^-} \gamma_{\text{H}^+} \gamma_{\text{Or}^-}}{m_{\text{HOr}} \gamma_{\text{HOr}}} \quad (2)$$

there results the relation

$$\frac{(E - E^\circ)F}{2.30259RT} + \log \frac{m_{\text{HOr}} m_{\text{Cl}^-}}{m_{\text{Or}^-}} = -\log K - \log \frac{\gamma_{\text{HOr}} \gamma_{\text{Cl}^-}}{\gamma_{\text{Or}^-}} \quad (3)$$

The ionization constant was determined from eq. 3 by extrapolation of the left-hand side to zero ionic strength using a method of calculation similar to that developed by Hamer<sup>10</sup> and essentially identical with that used in the previous papers.<sup>2,3</sup> However, due to the fact that orthanilic acid is the strongest acid of the three isomers, the calculations were long and tedious. The full calculation required four complete successive approximations at each temperature in order to be sure that the extrapolations of the left-hand side of eq. 3 had converged to give constant values of  $-\log K$  at zero ionic strength. This full calculation was carried out at 0, 25 and 50° only. The final hydrogen ion molalities obtained at these temperatures were used to interpolate initial hydrogen ion molalities at the remaining temperatures and successive approximation started with the resulting values. This procedure saved two complete successive approxi-

mations at the remaining eight temperatures. However, the effect was to have made four complete approximations at each temperature.

The values of the molal electrode potentials,  $E^0$ , of the silver-silver chloride electrode have been determined by Harned and Ehlers<sup>11</sup> and recalculated, along with  $2.30259RT/F$ , in absolute volts by Swinehart<sup>12</sup> using the constants of Bearden and Watts.<sup>13</sup>

## Experimental

The materials and reagents other than orthanilic acid were purified in a manner similar to that described by MacLaren and Swinehart.<sup>2</sup>

Eastman Kodak white label orthanilic acid, when first dissolved in hot water, gave a noticeable odor of sulfur dioxide which was eliminated by addition of strong acid. Therefore the first crystallization was made from a solution containing approximately 20 ml. of concd. HCl per liter of solution. This was followed by two or three recrystallizations from pure water. The white crystals were dried in a vacuum desiccator over 90–95%  $\text{H}_2\text{SO}_4$ . A solution of this product gave no visible test for chloride ion with silver nitrate.

Solutions of the impure acid developed a pink color fairly rapidly when exposed to light. This sensitivity decreased markedly on further purification. Samples of purified acid in solution in contact with air were left in the dark for 8 months and did not become colored but turned pink when left standing in daylight for several days. Solutions used in the measurements took at least one week to become visibly tinted unless exposed to bright sunlight. The various purification operations were carried out in a semi-darkened room.

Analysis for purity was made by titration with NaOH which had been standardized vs. National Bureau of Standards potassium acid phthalate. Weight buret techniques were applied and a pH meter was used to detect the endpoint which occurred at pH 7.5. The resulting values of purity varied from 99.72 to 99.94%, the value increasing with the drying time. A sample, oven dried at 110°, analyzed 100.01% pure. Each desiccator-dried batch of recrystallized acid was analyzed separately; the difference between the analysis and 100% was assumed to be water.

The most likely impurity neglecting moisture is sulfanilic acid. The problem of detecting this impurity in our product and estimating its amount has not been solved satisfactorily. In the ultraviolet absorption spectra of these acids, the molar extinction coefficient of sulfanilic acid is approximately ten times that of orthanilic acid at 2550 Å. We estimate that such measurements would permit us to detect 1 or 2% of sulfanilic acid as an impurity but not lesser amounts. We can only express confidence in the absence of sulfanilic acid to this degree.

The cells, electrodes, measuring instruments and procedure of the measurements were the same as those described by MacLaren and Swinehart.<sup>2</sup>

## Results

The results are shown in Table I. Each potential difference is the average of 16 potential measurements obtained from two cells, run in duplicate, except where noted in the table by the footnote, "one cell only." These latter values are the averages of eight measurements from one cell only. The average deviations of the potentials from any one cell from the mean potential were about  $\pm 0.02$  mv. The mean potentials of duplicate cells showed an average difference of 0.062 mv. and no difference was greater than 0.16 mv.

The data were treated as indicated in the introduction. Representative extrapolations of the last approximation of the left-hand side of eq. 3

(5) W. Oswald, *Z. physik. Chem.*, **3**, 406 (1889).  
 (6) M. Boyle, *J. Chem. Soc.*, **115**, 1505 (1919).  
 (7) W. Carr and W. J. Shutt, *Trans. Faraday Soc.*, **35**, 579 (1939).  
 (8) W. J. Hamer, G. D. Pinching and S. F. Acree, *J. Research Natl. Bur. Standards*, **31**, 291 (1943).  
 (9) H. S. Harned and B. B. Owen, "The Physical Chemistry of Electrolytic Solutions," 2nd Ed., Reinhold Publ. Corp., New York, N. Y., 1950.  
 (10) W. J. Hamer, *J. Am. Chem. Soc.*, **56**, 860 (1934).

(11) H. S. Harned and J. W. Ehlers, *ibid.*, **55**, 2179 (1933).  
 (12) D. F. Swinehart, *ibid.*, **74**, 1100 (1952).  
 (13) J. A. Bearden and H. M. Watts, *Phys. Rev.*, **81**, 73 (1951).

TABLE I  
ELECTROMOTIVE FORCE OF THE CELL  
Pt, H<sub>2</sub>/HOr(m<sub>1</sub>), NaOr(m<sub>2</sub>), NaCl(m<sub>3</sub>)/AgCl-Ag

| μ<br>(approx.) | Absolute volts       |                      |                      |                      |                      |                      |                      |                      |                      |                      |                      |
|----------------|----------------------|----------------------|----------------------|----------------------|----------------------|----------------------|----------------------|----------------------|----------------------|----------------------|----------------------|
|                | 0.01 <sup>a</sup>    | 0.01 <sup>a</sup>    | 0.02                 | 0.02                 | 0.03                 | 0.04                 | 0.04 <sup>a</sup>    | 0.06                 | 0.06                 | 0.08                 | 0.1                  |
| m <sub>1</sub> | 0.00593 <sub>6</sub> | 0.00506 <sub>4</sub> | 0.01323 <sub>7</sub> | 0.01020 <sub>2</sub> | 0.01520 <sub>3</sub> | 0.01976 <sub>5</sub> | 0.02011 <sub>4</sub> | 0.03057 <sub>7</sub> | 0.02995 <sub>2</sub> | 0.03983 <sub>8</sub> | 0.05019 <sub>1</sub> |
| m <sub>2</sub> | .00424 <sub>5</sub>  | .00508 <sub>6</sub>  | .00693 <sub>0</sub>  | .01014 <sub>1</sub>  | .01503 <sub>3</sub>  | .01993 <sub>1</sub>  | .02049 <sub>1</sub>  | .03014 <sub>4</sub>  | .03018 <sub>6</sub>  | .03966 <sub>7</sub>  | .05028 <sub>1</sub>  |
| m <sub>3</sub> | .00511 <sub>4</sub>  | .00499 <sub>0</sub>  | .01014 <sub>1</sub>  | .01015 <sub>0</sub>  | .01559 <sub>2</sub>  | .01984 <sub>2</sub>  | .02039 <sub>1</sub>  | .03190 <sub>7</sub>  | .03023 <sub>3</sub>  | .03969 <sub>0</sub>  | .05010 <sub>5</sub>  |
| t (°C.)        |                      |                      |                      |                      |                      |                      |                      |                      |                      |                      |                      |
| 0              | 0.51336              | 0.51911              | 0.48762              | 0.49741              | 0.48504              | 0.47877              | 0.47811              | 0.46582              | 0.46734              | 0.46020              | ...                  |
| 5              | .51484               | .52060               | .48850               | .49830               | .48555               | .47914               | .47844               | .46584               | .46739               | .46004               | 0.45430              |
| 10             | .51617               | .52200               | .48929               | .49906               | .48596               | .47936               | .47859               | .46574               | .46730               | .45974               | .45385               |
| 15             | .51741               | .52324               | .48990               | .49970               | .48626               | .47948               | .47866               | .46551               | .46709               | .45934               | .45330               |
| 20             | .51848               | .52436               | .49042               | .50022               | .48647               | .47949               | .47860               | .46517               | .46674               | .45886               | .45264               |
| 25             | .51952               | .52541               | .49084               | .50068               | .48660               | .47942               | .47858               | .46476               | .46636               | .45826               | .45190               |
| 30             | .52041               | .52632               | .49116               | .50106               | .48664               | .47920               | .47834               | .46425               | .46592               | .45758               | .45107               |
| 35             | .52121               | .52708               | .49137               | .50130               | .48650               | .47894               | .47810               | .46365               | .46533               | .45681               | .45012               |
| 40             | .52190               | .52776               | .49148               | .50144               | .48635               | .47857               | .47770               | .46294               | .46466               | .45596               | .44910               |
| 45             | .52249               | .52839               | .49152               | .50152               | .48607               | .47814               | .47722               | .46217               | .46392               | .45502               | .44798               |
| 50             | .52302               | .52896               | .49145               | .50154               | .48578               | .47762               | .47661               | .46136               | .46304               | .45396               | .44676               |

<sup>a</sup> One cell only.

to zero ionic strength yielding thermodynamic values of  $-\log K$  are shown in Fig. 1.

The resulting values of  $-\log K$  were fitted by the equation

$$-\log K = A/T + CT - D \quad (4)$$

using the method of least squares, yielding the values 1106.68, 0.0066339 and 3.2314 for  $A$ ,  $C$  and  $D$ , respectively. The calculated values of  $-\log K$  using these constants together with the experimental values of  $-\log K$  and the values of  $K$  itself are shown in Table II. The standard deviation of the calculated values of  $-\log K$  from the experimental values is 0.0008 in  $-\log K$ . This quantity is calculated from the equation

$$\text{Standard deviation} = \left( \frac{\sum \Delta^2}{n - c} \right)^{1/2}$$

where  $\Delta$  is the deviation of the experimental point from the fitted curve in the direction of the  $-\log K$  axis,  $n$  is the number of experimental points and  $c$  is the number of constants in the equation.<sup>14</sup>

**Discussion**

By means of the usual relations, standard thermodynamic quantities for the ionization reaction

TABLE II

THE IONIZATION CONSTANT OF ORTHANILIC ACID IN WATER FROM 0 TO 50°

| t (°C.) | K × 10 <sup>3</sup> | -log K |        | Δ × 10 <sup>3</sup> |
|---------|---------------------|--------|--------|---------------------|
|         |                     | Obsd.  | Calcd. |                     |
| 0       | 2.328               | 2.6330 | 2.6321 | -9                  |
| 5       | 2.563               | 2.5912 | 2.5925 | 13                  |
| 10      | 2.782               | 2.5557 | 2.5554 | -3                  |
| 15      | 3.016               | 2.5206 | 2.5208 | 2                   |
| 20      | 3.254               | 2.4876 | 2.4884 | 8                   |
| 25      | 3.475               | 2.4592 | 2.4583 | -9                  |
| 30      | 3.707               | 2.4310 | 2.4302 | -8                  |
| 35      | 3.943               | 2.4042 | 2.4042 | 0                   |
| 40      | 4.169               | 2.3798 | 2.3800 | 2                   |
| 45      | 4.399               | 2.3567 | 2.3576 | 9                   |
| 50      | 4.597               | 2.3375 | 2.3370 | -5                  |

Stand. dev. in  $-\log K = 0.0008$

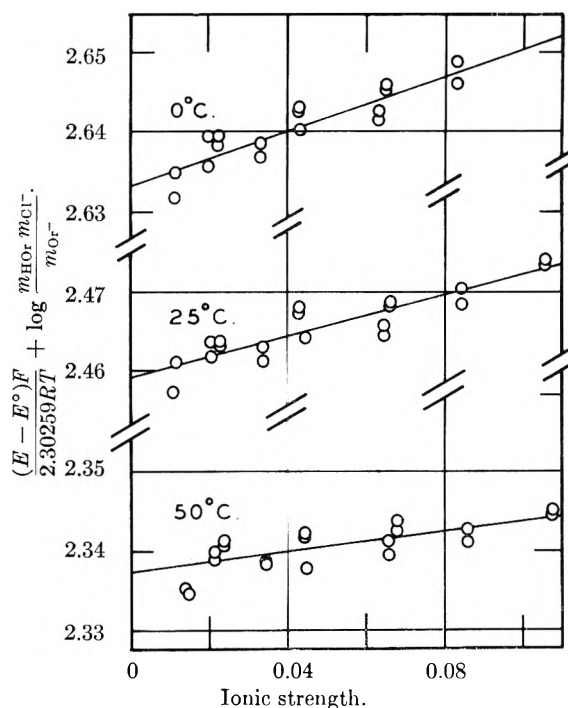


Fig. 1.—Representative extrapolations for the evaluation of  $-\log K$ .

may be calculated<sup>15</sup> from the constants in eq. 4.

It is worthwhile to note the remarkably small values of the entropies and heat capacity changes for the ionization of sulfanilic<sup>2</sup> and metanilic<sup>3</sup> acids and to compare these quantities with the corresponding values for orthanilic acid and certain other acids. In Table III these two thermodynamic quantities are listed for a number of selected uncharged acids. All these data were taken from Harned and Owen<sup>16</sup> except the values for sulfamic acid<sup>17</sup> and taurine,<sup>18</sup> and for the three isomeric aminobenzenesulfonic acids which were taken from references previously given<sup>2,3</sup> and this paper.

(16) Reference 9, p. 514.

(17) E. J. King and G. W. King, *J. Am. Chem. Soc.*, **74**, 1212 (1952).

(18) E. J. King, *ibid.*, **75**, 2204 (1953).

(14) T. B. Crumpler and J. H. Yoe, "Chemical Computations and Errors," John Wiley and Sons, Inc., New York, N. Y., 1940, p. 222.

(15) Reference 9, p. 583.

TABLE III  
ENTROPIES AND HEAT CAPACITY CHANGES FOR THE IONIZATION OF SOME WEAK ACIDS AT 25°

| Acid                                | $\Delta S^\circ$<br>(cal./deg.) | $\Delta C_p^\circ$<br>(cal./deg.) |
|-------------------------------------|---------------------------------|-----------------------------------|
| Water                               | -18.7                           | -46.5                             |
| Formic                              | -17.6                           | -41.7                             |
| Acetic                              | -22.1                           | -36.5                             |
| Propionic                           | -22.8                           | -38.3                             |
| Butyric                             | -24.4                           | -36.4                             |
| Chloroacetic                        | -17.0                           | -40.0                             |
| Lactic                              | -18.0                           | -40.7                             |
| Glycolic                            | -16.9                           | -38.8                             |
| Phosphoric (1st H <sup>+</sup> )    | -15.7                           | -50.7                             |
| Glycine                             | -6.9                            | -32.2                             |
| <i>dl</i> -Alanine                  | -8.3                            | -34.2                             |
| <i>dl</i> -Amino- <i>n</i> -butyric | -9.5                            | -34.1                             |
| <i>dl</i> -Leucine                  | -9.4                            | -36.8                             |
| <i>dl</i> -Valine                   | -9.9                            | -32.7                             |
| Sulfamic                            | -3.0                            | -110                              |
| Taurine                             | -7.9                            | -8.4                              |
| Sulfanilic                          | -0.37                           | -7.1                              |
| Metanilic                           | -0.57                           | -7.7                              |
| Orthanilic                          | -3.32                           | -18.6                             |

It is remarkable that the standard entropies of ionization of many uncharged acids are approximately constant at about -20 e.u. and that the heat capacity changes for ionization hover about -40 cal./degree/mole. However, when the corresponding values for the classical zwitterions, *i.e.*, the aliphatic amino acids, are considered, the entropies of ionization decrease to about half the values for the neutral acids. The heat capacity changes seem to be lowered only slightly in magnitude. The entropies of ionization of sulfanilic and metanilic acids are *very* small indeed as are the changes in heat capacity.

These observations are interpreted following the ideas of Frank and Evans<sup>19</sup> and of Powell and Latimer.<sup>20</sup> An entropy decrease occurs when neutral molecules are dissolved in water. Part of this entropy loss is due to restriction of the molecule to a small volume or "cage" of solvent molecules and part is due to the immobilization of water molecules adjacent to the solute molecule. Now, if the molecule separates into two charged ions, many *more* water molecules are "frozen" and a large entropy loss occurs. This effect is so large that, to a first approximation, the entropy is the same for all neutral, *i.e.*, uncharged, acids.

A zwitterion, on the other hand, such as an amino acid, binds many more water molecules due to interaction of the water dipoles with the widely separated

charges of the zwitterions. Thus, when such a zwitterion separates into two independent ions, the *change* in amount of water bound is much smaller than for neutral acids, resulting in a markedly smaller entropy of ionization for the zwitterion.

Sulfanilic and metanilic acids are zwitterions with such large charge separations that essentially as much water is bound by the zwitterions as for the separated ions, yielding a very small entropy effect on ionization.

For the case of orthanilic acid, the charge separation must be markedly less than for its isomers. Space considerations then limit the amount of water bound by the zwitterions and results in a much larger entropy effect than for the isomeric acids,  $\Delta S^\circ$  being, for this case, approximately ten times larger than for the isomers, although not quite as large as predicted.<sup>3</sup> This indicates that the charge separation, *i.e.*, the dipole moment, of orthanilic, although smaller than that of its isomers, is still considerably larger than that of the aliphatic amino acids. Direct measurements of the dipole moments of metanilic and orthanilic acids have not been reported.

It has been claimed that sulfamic acid exists in solution as the neutral molecule, *i.e.*, not as the zwitterion,<sup>17,21</sup> even though other evidence indicates that it does exist in the crystalline state as the zwitterion.<sup>22</sup> The entropy of ionization of sulfamic acid<sup>17</sup> shown in Table III supports strongly the idea that it also exists in solution as the zwitterion. The entropy and heat capacity change for taurine agree with other evidence<sup>23,24</sup> that this acid exists in solution as a zwitterion. In this picture, only the heat capacity change for sulfamic acid appears to be anomalously high.

King has reported difficulty in the interpretation of e.m.f. data for the estimation of the ionization constant for sulfamic acid<sup>17</sup> due to its being a fairly strong acid and suggests that if an acid with an accurately known ionization constant of about  $1 \times 10^{-3}$  were available, a method involving a mixture of a salt of sulfamic acid and the second weak acid, as suggested by Bates,<sup>25</sup> might be used to check his e.m.f. data. It is suggested that sulfanilic or orthanilic acid might serve this purpose.

**Acknowledgment.**—This research was supported by a fellowship and grant from the Graduate Council of the University of Oregon.

(21) P. Baumgarten, *Ber.*, **62B**, 820 (1929).

(22) F. A. Kanda and A. J. King, *J. Am. Chem. Soc.*, **73**, 2315 (1951).

(23) G. LeVoto, *Gazz. chim. ital.*, **61**, 897 (1931)

(24) M. Freymann and P. Rumpf, *Compt. rend.*, **201**, 606 (1935).

(25) R. G. Bates, *J. Am. Chem. Soc.*, **73**, 2259 (1951).

(19) H. S. Frank and M. W. Evans, *J. Chem. Phys.*, **13**, 507 (1945).

(20) R. E. Powell and W. M. Latimer, *ibid.*, **19**, 1139 (1951).

# VAPOR PRESSURE AND DERIVED INFORMATION OF THE SODIUM FLUORIDE-ZIRCONIUM FLUORIDE SYSTEM. DESCRIPTION OF A METHOD FOR THE DETERMINATION OF MOLECULAR COMPLEXES PRESENT IN THE VAPOR PHASE<sup>1</sup>

BY KARL A. SENSE, C. A. ALEXANDER, R. E. BOWMAN AND R. B. FILBERT, JR.

*Battelle Memorial Institute, Columbus, Ohio*

*Received September 27, 1956*

By use of the transpiration method, the vapor pressures of the NaF-ZrF<sub>4</sub> system were measured over the range 599–1075°. On the basis of the Duhem-Margules equation and the thermodynamic stability of a system, it was deduced that, in addition to NaF and ZrF<sub>4</sub>, a compound composed of NaF and ZrF<sub>4</sub> must exist in the vapor phase. The molar composition ratio of this compound must be NaF/ZrF<sub>4</sub> < 1.38. The assumption is made that the complex has the simple structure NaZrF<sub>5</sub>. On the basis of this assumption, partial pressures of NaF, ZrF<sub>4</sub>, and NaZrF<sub>5</sub> are calculated. As a first approximation, the dissociation constant for the reaction, NaZrF<sub>5</sub> = NaF + ZrF<sub>4</sub>, was determined as a function of the temperature. A partial phase diagram of the NaF-ZrF<sub>4</sub> system derived from the vapor pressure data shows a constant boiling point to exist at 25 mole % ZrF<sub>4</sub>. The composition at this constant boiling point does not seem to change with pressure. This behavior, considered together with an activity plot of the system NaF-NaZrF<sub>5</sub>, suggests the existence of Na<sub>3</sub>ZrF<sub>7</sub> in the liquid state. The extent of dissociation of Na<sub>3</sub>ZrF<sub>7</sub> in the vapor phase could not be determined. Plots showing vapor-liquid-solid equilibria are presented. A plot is given showing the change of the total vapor pressure of the NaF-ZrF<sub>4</sub> system with composition for various temperatures.

This work was undertaken as part of a program to investigate the physical properties of fused-salt systems.

## Experimental

The method and apparatus have been described in sufficient detail in previous papers.<sup>2,3</sup> A slight change from previous procedure consisted in the use of argon rather than nitrogen as a carrier gas. The results obtained when argon was used were fully comparable with those when nitrogen was used. The use of another vapor pressure apparatus similar to the one built originally permitted the detection of systematic errors peculiar to either set. A revised schematic diagram is given in Fig. 1.

The low melting mixtures of NaF and ZrF<sub>4</sub>, as well as pure ZrF<sub>4</sub>, were provided by the Oak Ridge National Laboratory. The NaF was J. T. Baker highest grade.

Except for a few prefused salt mixtures, the desired compositions were obtained by adding the proper amounts of NaF or ZrF<sub>4</sub> to a prefused NaF-ZrF<sub>4</sub> mixture. The components necessary to make up a desired composition were first ground to a fine powder. The necessary quantities of the powdered components were then intimately mixed to ensure homogeneity. The results obtained using charges prepared in this manner were checked against results obtained with a prefused salt having the same composition. Although the manually prepared charges produced more scatter about the vapor pressure curve obtained, the results were comparable with those from prefused salts.

All results were corrected for composition changes which occurred while the runs were being made.

## Results and Discussion

**Molecular Species in the Vapor Phase.**—Initially, in the absence of any information regarding complex molecules in the vapor phase, the partial pressures of NaF and ZrF<sub>4</sub> were calculated on the assumption that only NaF and ZrF<sub>4</sub> exist in the vapor phase. The results are presented graphically in Figs. 2, 3 and 4, and in terms of the constants *A* and *B* defined by the vapor pressure equation in Table I

$$\log p = A - \frac{B \times 10^3}{T(^{\circ}\text{K.})}$$

Figure 3 shows plots of *p*NaF as a function of the reciprocal temperature for the NaF-rich region of

(1) Work performed under AEC Contract W-7405-eng-92.

(2) K. A. Sense, M. J. Snyder and J. W. Clegg, *THIS JOURNAL*, **58**, 223 (1954).

(3) K. A. Sense, M. J. Snyder and R. B. Filbert, Jr., *ibid.*, **58**, 995 (1954).

the NaF-ZrF<sub>4</sub> system. The curves behave as expected, since for a given temperature *p*NaF decreases as the NaF-ZrF<sub>4</sub> system becomes poorer in NaF. Figure 4 also shows plots of *p*NaF as a function of the reciprocal temperature for NaF-ZrF<sub>4</sub> compositions poorer in NaF than those shown in Fig. 3. In spite of the rather considerable scatter, it is quite evident, and interesting, that *p*NaF increases as the composition of the liquid becomes poorer in NaF. This behavior is brought out more clearly by Fig. 5 which shows how the partial pressures of NaF and ZrF<sub>4</sub> vary with composition for a given temperature. It is noted that for compositions greater than about 34 mole % ZrF<sub>4</sub>, the partial pressure of NaF is greater than the vapor pressure of pure NaF. In terms of activities, this means that the apparent activity of NaF is greater than 1.

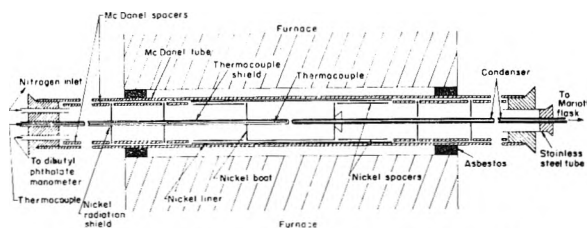


Fig. 1.—Cross-section of vapor pressure apparatus.

Such a condition is not admissible for a thermodynamically stable system.<sup>4</sup> Furthermore, beginning with about 25 mole % ZrF<sub>4</sub>, both *p*NaF and *p*ZrF<sub>4</sub> increase as the salt composition becomes richer in ZrF<sub>4</sub>. This behavior is contrary to the Duhem-Margules equation

$$x_1 \frac{d \ln p_1}{d x_1} = x_2 \frac{d \ln p_2}{d x_2} \quad (1)$$

where *x* is the mole fraction of either component 1 or 2, and *p* is the partial pressure of the corresponding component.

According to this equation, for a two-component system, the partial pressure of one component must decrease as the other one increases, when the

(4) J. H. Hildebrand and R. L. Scott, "Solubility of Non-Electrolytes," 3rd Ed., Reinhold Publ. Corp., New York, N. Y., 1950, p. 41.

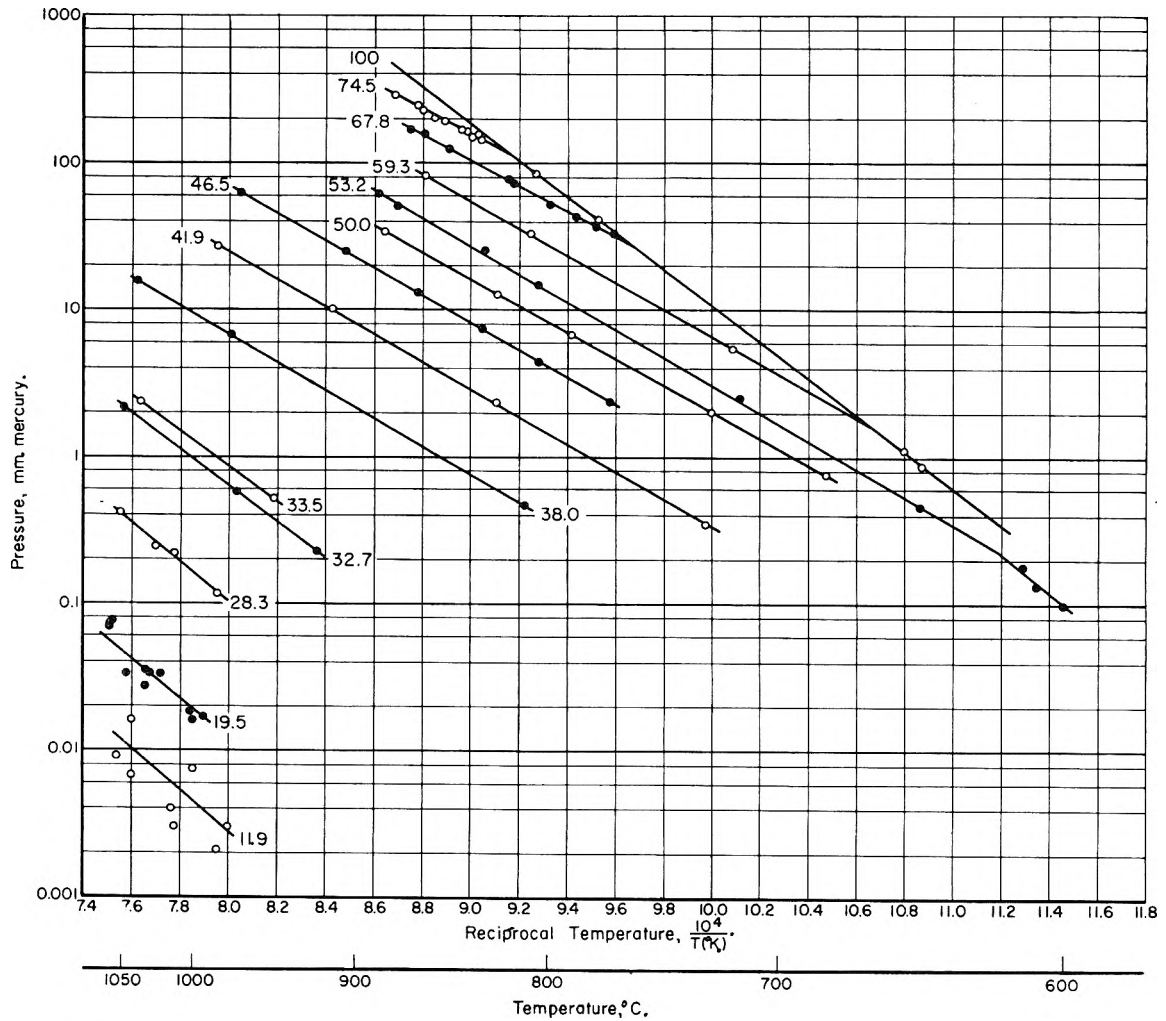


Fig. 2.—Partial pressure of  $ZrF_4$  based on assumption that only  $NaF$  and  $ZrF_4$  exist in vapor phase. Figures on plot denote mole per cent.  $ZrF_4$ .

TABLE I

VAPOR PRESSURE CONSTANTS FOR THE  $NaF-ZrF_4$  SYSTEM BASED ON THE ASSUMPTION THAT ONLY  $NaF$  AND  $ZrF_4$  EXIST IN THE VAPOR PHASE

$$\log p = A - \frac{B \times 10^3}{T(^{\circ}K.)}$$

| Composition, mole % $ZrF_4$ |          | $p_{ZrF_4}$ |         |                            | $p_{NaF}$ |         |                          | Temp. range, $^{\circ}C$ |
|-----------------------------|----------|-------------|---------|----------------------------|-----------|---------|--------------------------|--------------------------|
|                             |          | A           | B       | Temp. range, $^{\circ}C$ . | A         | B       | Temp. range, $^{\circ}C$ |                          |
| 100                         | (solid)  | 13.3995     | 12.3760 | 616-881                    | ...       | ...     | ...                      |                          |
| 74.50 <sup>a</sup>          | (liquid) | 9.869       | 8.528   | 817-878                    | ...       | ...     | ...                      |                          |
| 67.79 <sup>a</sup>          | (liquid) | 9.887       | 8.745   | 760-870                    | ...       | ...     | ...                      |                          |
| 59.33 <sup>a</sup>          | (liquid) | 10.040      | 9.227   | 664-862                    | ...       | ...     | ...                      |                          |
| 53.16                       | (liquid) | 9.939       | 9.448   | 621-887                    | ...       | ...     | ...                      |                          |
| 53.16                       | (solid)  | 13.86       | 12.95   | 599-621                    | ...       | ...     | ...                      |                          |
| 50.00                       | (liquid) | 9.3510      | 9.0432  | 682-884                    | ...       | ...     | ...                      |                          |
| 46.50                       | (liquid) | 9.263       | 9.267   | 771-969                    | ...       | ...     | ...                      |                          |
| 41.88                       | (liquid) | 8.862       | 9.338   | 729-985                    | 9.10      | 11.45   | 825-985                  |                          |
| 38.00                       | (liquid) | 8.441       | 9.511   | 811-1039                   | 9.10      | 11.67   | 811-1039                 |                          |
| 33.50                       | (liquid) | 9.498       | 11.950  | 948-1037                   | 9.42      | 12.5    | 948-1037                 |                          |
| 32.72                       | (liquid) | 9.643       | 12.303  | 922-1049                   | 9.33      | 12.6    | 873-1049                 |                          |
| 28.27                       | (liquid) | 9.675       | 13.33   | 984-1051                   | 8.990     | 12.569  | 978-1067                 |                          |
| 19.54                       | (liquid) | 8.8         | 13.3    | 994-1059                   | 9.087     | 12.396  | 994-1059                 |                          |
| 11.89                       | (liquid) | 8.7         | 14.0    | 976-1053                   | 9.190     | 12.276  | 976-1058                 |                          |
| Pure $NaF$                  | (liquid) | ...         | ...     | ...                        | 9.4188    | 12.4283 | 996-1075                 |                          |
| Pure $NaF$                  | (solid)  | ...         | ...     | ...                        | 11.3315   | 14.8557 | 934-996                  |                          |

<sup>a</sup> The constants for the solidus region are the same as those for  $ZrF_4$ .

composition is changed. To resolve the problem presented in Fig. 5 where the partial pressures of both NaF and  $ZrF_4$  increase as the composition is shifted toward pure  $ZrF_4$ , the assumption was made that a complex molecule composed of NaF and  $ZrF_4$  exists in the vapor phase. In accordance with the Duhem-Margules equation, the exact molecular composition of this complex is given by the peak of the partial pressure curve of NaF.

From Fig. 5, it is noted that the peak of the partial pressure curve has obviously not yet been reached over the 0-42 mole %  $ZrF_4$  composition range. Hence, the peak of the apparent activity curve of NaF must occur in the 42-100 mole %  $ZrF_4$  composition region which means that in the complex, the mole ratio of NaF to  $ZrF_4$  must be smaller than 1.38. Unfortunately, the limitations of the chemical analysis for NaF in the condensates in that region were such that  $p_{NaF}$  was known only as having less than a certain maximum value. This maximum was too high to be of any use in locating the maximum in the partial pressure curve.

A plot of the activity of  $ZrF_4$  of the NaF- $ZrF_4$  system at  $918^\circ$  (Fig. 6) suggests the possibility that the complex has a NaF to  $ZrF_4$  ratio of 1:1, *i.e.*, that the simple complex  $NaZrF_5$  exists in the vapor phase. Such a complex would satisfy the requirement that it occur in the 42-100 mole %  $ZrF_4$  region.

On the basis that  $NaZrF_5$  exists in the vapor phase, a plot of the activity of  $ZrF_4$  at  $918^\circ$  was constructed for the  $NaZrF_5$  system (Fig. 7).<sup>6</sup> The fact that the deviations from Raoult's law in Fig. 7 are not nearly as great as those in Fig. 6 makes the assumption that the complex is  $NaZrF_5$  seem reasonable. The fact that the activity of  $ZrF_4$  does not go to zero at zero mole fraction  $ZrF_4$  implies partial dissociation of  $NaZrF_5$ .

**Derived Partial Pressures of NaF,  $ZrF_4$ , and  $NaZrF_5$ .**—As a first approximation, the vapor phase of the NaF- $ZrF_4$  system was treated as consisting only of NaF,  $ZrF_4$ , and  $NaZrF_5$ . Furthermore,  $NaZrF_5$  was considered to dissociate partially into NaF and  $ZrF_4$ , the extent of dissociation being a function of the temperature. The partial pressures of the various vapor phase components were calculated by the following procedure. (Refer to Fig. 5.) For compositions containing more than about 30 mole %  $ZrF_4$ , the vapor phase was assumed to consist almost entirely of  $p_{ZrF_4}$  and  $p_{NaZrF_5}$  with  $p_{NaF}$  being considered negligible. Hence, the apparent  $p_{NaF}$  in this re-

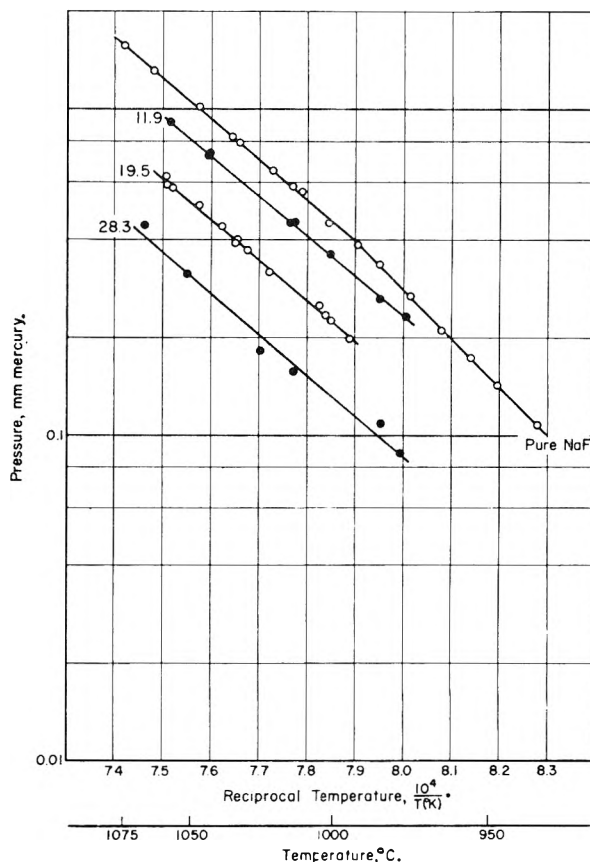


Fig. 3.—Partial pressures of NaF for the 0 to 28.3 mole %  $ZrF_4$  region. Values based on assumption that only NaF and  $ZrF_4$  exist in vapor phase. Figures denote mole %  $ZrF_4$ .

gion became  $p_{NaZrF_5}$ .<sup>8</sup> The  $ZrF_4$  tied up as  $NaZrF_5$  was then subtracted from that given by the  $ZrF_4$  curve to yield the true  $p_{ZrF_4}$ . In the composition region of 0 to about 20 mole %  $ZrF_4$ , the vapor phase was assumed to consist almost entirely of NaF and  $NaZrF_5$ , with  $ZrF_4$  making only a negligible contribution to the total vapor pressure. Hence, the apparent  $p_{ZrF_4}$  in this region became the  $p_{NaZrF_5}$ . The NaF tied up as  $NaZrF_5$  was then subtracted from that given by the NaF curve to give the true  $p_{NaF}$ . The  $p_{NaZrF_5}$  for the 28.3 mole %  $ZrF_4$  composition could not be determined in this manner since all the components exert comparable vapor pressures. However, from a plot of  $p_{NaZrF_5}$  values already calculated for the other compositions, an interpolated value for the 28.3 mole per cent. composition could be obtained. This  $p_{NaZrF_5}$  was then subtracted, respectively, from the apparent  $p_{NaF}$  and  $p_{ZrF_4}$  to give the true  $p_{NaF}$  and  $p_{ZrF_4}$ . Figure 8 shows the resulting curves of  $p_{NaF}$ ,  $p_{ZrF_4}$  and  $p_{NaZrF_5}$  at  $1026^\circ$ . The vertical lines through the  $p_{NaZrF_5}$  curve qualitatively reflect the degree of uncertainty of the partial pressures of NaF and  $ZrF_4$  (see Figs. 2 and

(8) This is so since for the transpiration method

$$\text{partial pressure of component} = \frac{(\text{moles of component}) (\text{total pressure of system})}{\text{moles carrier gas} + \Sigma(\text{moles of components})}$$

From the standpoint of  $ZrF_4$ , the number of moles is the same whether  $ZrF_4$  is present as such or whether it is part of the  $NaZrF_5$  complex.

(5) Defined as  $p_{ZrF_4}/p^0_{ZrF_4}$ . The standard state,  $p^0_{ZrF_4}$ , is the vapor pressure of liquid  $ZrF_4$ . Since  $ZrF_4$  sublimates at a pressure of 1 atm., the vapor pressure at the melting point ( $918^\circ$ ) had to be calculated from the  $P$ - $T$  equation for  $ZrF_4$ , namely,  $p_{ZrF_4} = 13.3995 - 12376.0/T(^\circ K)$ . From this equation,  $p^0_{ZrF_4} = 1020$  mm. mercury at  $918^\circ$ .

(6) The mole fraction,  $N'_0$ , of  $ZrF_4$  in the  $NaZrF_5$   $ZrF_4$  system is given by  $N'_0 = (N_0 - N)/N_0$ , where  $N_0$  and  $N$  are the mole fractions of  $ZrF_4$  and NaF, respectively, in the NaF- $ZrF_4$  system.

(7) Throughout the following discussion the "apparent" partial pressures are those which were calculated for a vapor phase assumed to consist simply of NaF and  $ZrF_4$ . Since the vapor phase is more accurately described as consisting of  $NaZrF_5$ , NaF and  $ZrF_4$ , the partial pressures of NaF and  $ZrF_4$  where  $NaZrF_5$  is taken into account will be referred to as the "true" partial pressures.

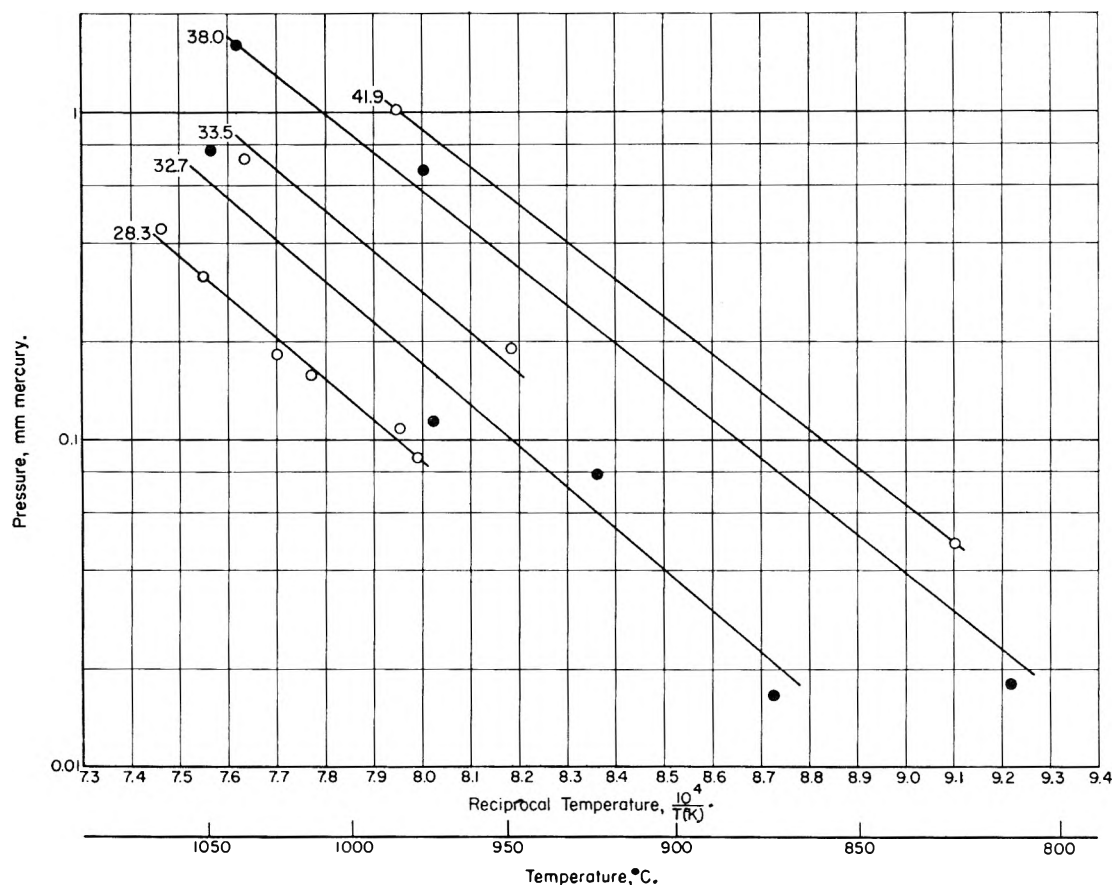


Fig. 4.—Partial pressures of NaF for the 28.3 to 41.9 mole %  $ZrF_4$  region. Values based on assumption that only NaF and  $ZrF_4$  exist in vapor phase. Figures give mole %  $ZrF_4$ .

TABLE II  
PARTIAL PRESSURES AS A FUNCTION OF RECIPROCAL TEMPERATURE AND COMPOSITION

| Composition, mole % $ZrF_4$ | $pZrF_4$ , mm., at given reciprocal temp., |       |       | $\frac{10^4}{T(^{\circ}K.)}$<br>8.395 | $pNaZrF_5$ , mm., at given reciprocal temp. |       |        | $\frac{10^4}{T(^{\circ}K.)}$<br>8.395 | $pNaF$ , mm., at given reciprocal temp. |       |        | $\frac{10^4}{T(^{\circ}K.)}$<br>8.395 |
|-----------------------------|--|-------|-------|---------------------------------------|---|-------|--------|---------------------------------------|---|-------|--------|---------------------------------------|
|                             | 7.50                                       | 7.70  | 8.00  |                                       | 7.50  | 7.70  | 8.00   |                                       | 7.50                                    | 7.70  | 8.00   |                                       |
| 41.9                        | 69.0                                       | 45.1  | 23.8  | 10.3                                  | 3.3   | 1.94  | 0.88   | 0.31                                  |   |       |        | negligible                            |
| 38.0                        | 18.2                                       | 11.8  | 6.21  | 2.66                                  | 2.24  | 1.29  | 0.58   | 0.20                                  |   |       |        | negligible                            |
| 33.5                        | 2.32                                       | 1.30  | 0.61  | 0.20                                  | 1.07  | 0.60  | 0.26   | .085                                  |   |       |        | negligible                            |
| 32.7                        | 1.85                                       | 1.06  | 0.45  | 0.15                                  | 0.88  | .51   | 0.21   | .070                                  |   |       |        | negligible                            |
| 28.3                        | 0.150                                      | 0.074 | 0.025 | 0.0067                                | .33   | .185  | 0.078  | .024                                  | 0.036                                   | 0.020 | 0.0081 | 0.0011                                |
| 19.5                        | negligible                                 |       |       |                                       | .054  | .028  | 0.012  | .0036                                 | .560                                    | .317  | .136   | .0443                                 |
| 11.9                        | negligible                                 |       |       |                                       | .0138                                       | .0062 | 0.0026 | .00075                                | .948                                    | .540  | .231   | .0725 <sup>a</sup>                    |
| 0                           | 0  | 0     | 0     | 0                                     | 0   | 0     | 0      | 0                                     | 1.25                                    | .706  | .280   | .0725 <sup>a</sup>                    |

<sup>a</sup> These values are the same since the solid NaF phase is present in both cases.

4) from which  $pNaZrF_5$  is derived. This calculation procedure was carried out also for other temperatures. Table II gives the partial pressures as a function of composition and reciprocal temperatures obtained from smoothed-out plots of the information obtained. Table III gives the derived values for the constants of the partial pressure equations for NaF,  $ZrF_4$  and  $NaZrF_5$ .

With the aid of this information, an activity plot (Fig. 9) was constructed for the pseudo-binary system NaF- $NaZrF_5$ .<sup>9</sup> The marked negative deviations from Raoult's law indicate strong attraction of the components in the liquid phase, suggesting the presence of a complex such as  $Na_3ZrF_7$  in the

(9) The activity of  $NaZrF_5$  is defined as  $pNaZrF_5/p^0NaZrF_5$ , where  $p^0NaZrF_5$  is approximated by the extrapolated  $pNaZrF_5$  value at 50 mole %  $ZrF_4$  (Fig. 8).

liquid phase. To what extent such a complex is present in the vapor phase is not readily apparent. It is evident that because of possible further complexities in the vapor phase, the treatment of the NaF- $ZrF_4$  system as consisting of NaF,  $ZrF_4$  and  $NaZrF_5$  in the vapor phase must be regarded only as approximate.

**Dissociation of  $NaZrF_5$ .**—From Fig. 8 and others constructed for different temperatures, approximate values were obtained for the dissociation constant  $K_p = [(pNaF)(pZrF_4)]/(pNaZrF_5)$  as a function of temperature. For least uncertainty, data were obtained for the 25, 27 and 28.3 mole %  $ZrF_4$  region. The results are given in Table IV. An average value was obtained for each of these reciprocal temperatures, and the best curve was drawn. The following results were obtained over

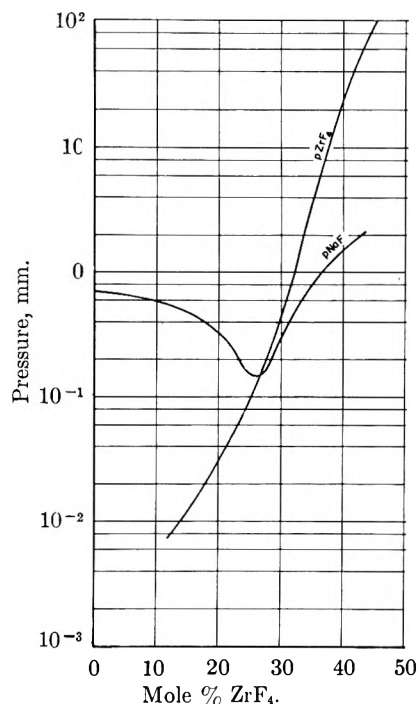


Fig. 5.—Apparent partial pressures at 1026° C.

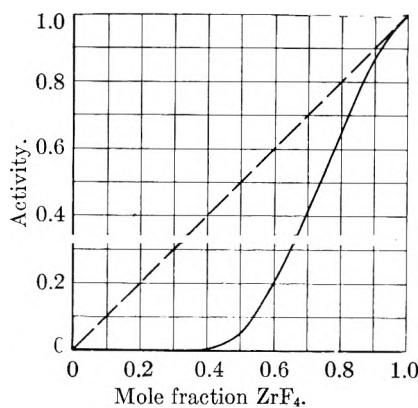


Fig. 6.—Activity of ZrF<sub>4</sub> for the NaF-ZrF<sub>4</sub> system at 918°.

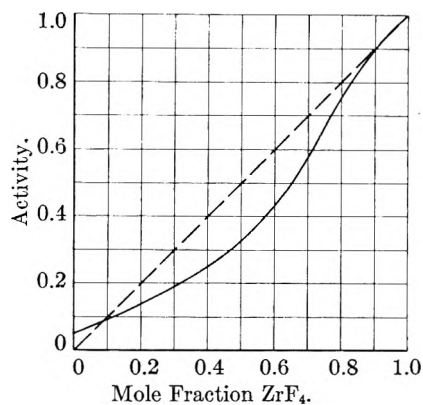


Fig. 7.—Activity of ZrF<sub>4</sub> for the pseudo binary system Na<sub>3</sub>ZrF<sub>5</sub>-ZrF<sub>4</sub> at 918°.

the 918-1060° temperature interval

$$\log K_p = 6.4 - \frac{1.47 \times 10^4}{T(^{\circ}\text{K.})} \quad (2)$$

$$\Delta S = 29 \text{ e.u.} \quad (3)$$

and

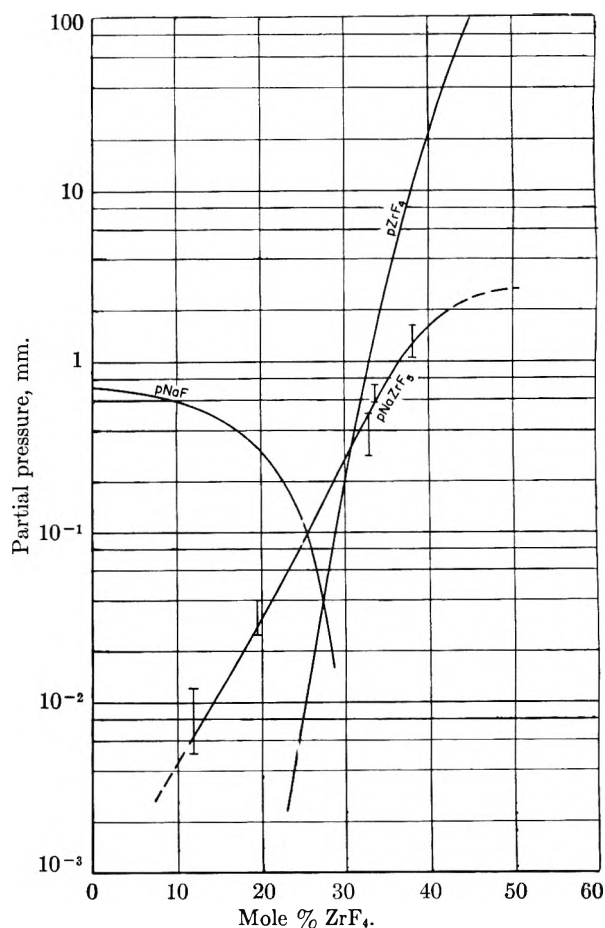


Fig. 8.—Partial pressures at 1026°.

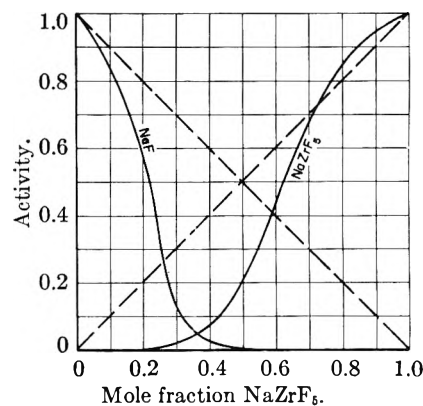
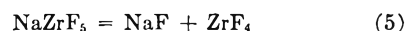


Fig. 9.—Activities of NaF and Na<sub>3</sub>ZrF<sub>5</sub> for the system NaF-Na<sub>3</sub>ZrF<sub>5</sub> at 1026°.

$$\Delta H = 67 \text{ kcal./g. mole} \quad (4)$$

for the reaction



**Partial Phase Diagrams Derived from Vapor Pressure Data.**—With the aid of Table III, partial phase diagrams were constructed. Figure 10 shows such a phase diagram for a total pressure of 1 mm. mercury. A constant-boiling mixture corresponding to the compound Na<sub>3</sub>ZrF<sub>7</sub> is shown to exist. To determine whether or not the composition of the constant-boiling mixture changed with pressure, phase diagrams for various pressures were constructed. Figure 11 shows the results in the vicinity

TABLE III

DERIVED VAPOR PRESSURE CONSTANTS FOR THE NaF-ZrF<sub>4</sub> SYSTEM BASED ON THE ASSUMPTION THAT THE VAPOR PHASE IS COMPOSED OF NaF, ZrF<sub>4</sub> AND NaZrF<sub>5</sub>

$$\log p = A - \frac{B \times 10^3}{T(^{\circ}\text{K.})}$$

| Composition, mole % ZrF <sub>4</sub> | <i>p</i> ZrF <sub>4</sub> |         | <i>p</i> NaF |         | <i>p</i> NaZrF <sub>5</sub> |       | $\Delta H_v$ , kcal./mole | M.p., <sup>d</sup> °C. | S.p., <sup>d</sup> °C. |
|--------------------------------------|---------------------------|---------|--------------|---------|-----------------------------|-------|---------------------------|------------------------|------------------------|
|                                      | A                         | B       | A            | B       | A                           | B     |                           |                        |                        |
| 100 (solid)                          | 13.3995                   | 12.3760 | ...          | ...     | ...                         | ...   | 56.63 <sup>b</sup>        | 918 <sup>c</sup>       | 903 <sup>c</sup>       |
| 74.50 <sup>a</sup> (liquid)          | 9.869                     | 8.528   | ...          | ...     | ...                         | ...   | 39.0                      | 817                    | 947                    |
| 67.79 <sup>a</sup> (liquid)          | 9.887                     | 8.745   | ...          | ...     | ...                         | ...   | 39.9                      | 760                    | 976                    |
| 59.33 <sup>a</sup> (liquid)          | 10.040                    | 9.227   | ...          | ...     | ...                         | ...   | 42.2                      | 664                    | 1016                   |
| 53.16 (liquid)                       | 9.939                     | 9.448   | ...          | ...     | ...                         | ...   | 43.2                      | ...                    | 1072                   |
| 53.16 (solid)                        | 13.86                     | 12.95   | ...          | ...     | ...                         | ...   | 59                        | 621                    | ...                    |
| 50.00 (liquid)                       | 9.3431                    | 9.0372  | ...          | ...     | 9.1                         | 11.2  | 41.4                      | ...                    | 1125                   |
| 46.50 (liquid)                       | 9.243                     | 9.252   | ...          | ...     | 9.1                         | 11.3  | ...                       | ...                    | 1177                   |
| 41.88 (liquid)                       | 8.762                     | 9.229   | ...          | ...     | 9.13                        | 11.48 | ...                       | ...                    | ...                    |
| 38.00 (liquid)                       | 8.259                     | 9.332   | ...          | ...     | 9.14                        | 11.72 | ...                       | ...                    | ...                    |
| 33.50 (liquid)                       | 9.249                     | 11.845  | ...          | ...     | 9.25                        | 12.30 | ...                       | ...                    | ...                    |
| 32.72 (liquid)                       | 9.338                     | 12.095  | ...          | ...     | 9.16                        | 12.28 | ...                       | ...                    | ...                    |
| 28.27 (liquid)                       | 10.49                     | 15.08   | 8.3          | 12.9    | 8.90                        | 12.51 | ...                       | ...                    | ...                    |
| 19.54 (liquid)                       | 8.7                       | 15.3    | 8.92         | 12.23   | 8.59                        | 13.14 | ...                       | ...                    | ...                    |
| 11.89 (liquid)                       | ...                       | ...     | 9.323        | 12.467  | 8.76                        | 14.16 | ...                       | ...                    | ...                    |
| Pure NaF (liquid)                    | ...                       | ...     | 9.4188       | 12.4283 | ...                         | ...   | 56.9                      | ...                    | 1628                   |
| Pure NaF (solid)                     | ...                       | ...     | 11.3315      | 14.8557 | ...                         | ...   | 68.0 <sup>b</sup>         | 996                    | ...                    |

<sup>a</sup> The constants for the solidus region are the same as those for ZrF<sub>4</sub>. <sup>b</sup> This denotes the heat of sublimation. <sup>c</sup> This is the sublimation point. <sup>d</sup> Derived from vapor pressure curves. <sup>e</sup> From thermal analysis.

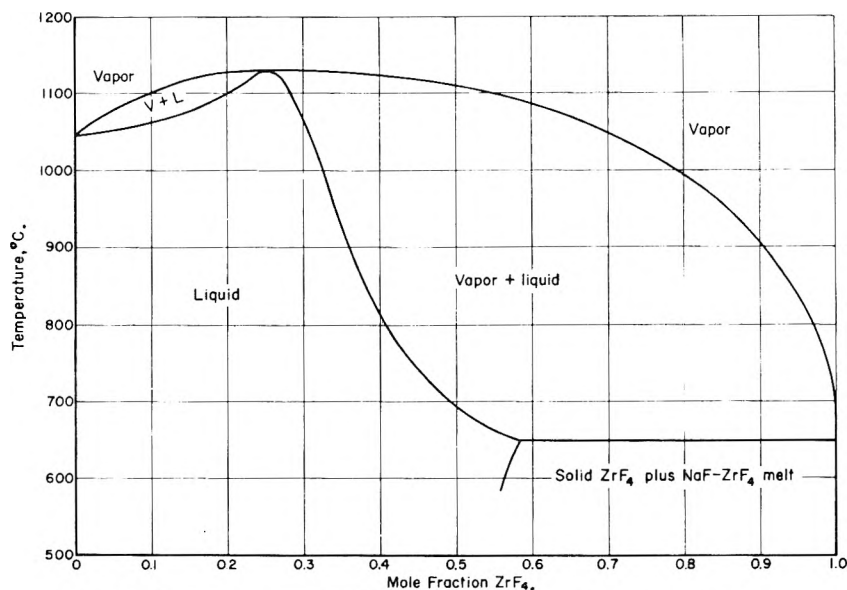


Fig. 10.—Phase diagram for the NaF-ZrF<sub>4</sub> system at a pressure of 1 mm.

of the azeotrope. The fact that the composition of the azeotrope does not appear to change with a change in pressure seems to indicate that Na<sub>3</sub>ZrF<sub>7</sub> exists in the liquid state. Previous indications that such a complex might exist in the liquid state were already apparent from the activity plot given in Fig. 9.

From the vapor pressure data obtained, a melting point curve also could be constructed. Figure 12 shows this liquidus curve as part of a phase diagram for  $P = 760$  mm. The experimental point at the lower end of the curve was obtained by filtration and subsequent analysis of the filtrates of two NaF-ZrF<sub>4</sub> salt mixtures at  $586 \pm 2^{\circ}$ . The compositions of the initial salt mixtures were 41 mole % NaF-59 mole % ZrF<sub>4</sub>, and 30 mole % NaF-70 mole %

ZrF<sub>4</sub>. The two filtrates were found to contain ZrF<sub>4</sub> mole fractions of 0.554 and 0.567, respectively. The difference between these two figures was not considered to be significant. The melting point ( $918^{\circ}$ ) of pure ZrF<sub>4</sub> was obtained by thermal analysis.

From Fig. 2, it is noted that the *p*ZrF<sub>4</sub>'s in the solid region for the 74.5 and 59.3 mole % ZrF<sub>4</sub> compositions coincide with the vapor pressure of pure ZrF<sub>4</sub>. This implies that the solid phase for compositions from 100 down to at least 59.3 mole % ZrF<sub>4</sub> consists of ZrF<sub>4</sub>. However, the *p*ZrF<sub>4</sub> curve for the solidus region of the 53.2 mole % ZrF<sub>4</sub> system (*i.e.*, where  $1/^{\circ}\text{K.} > 11.2 \times 10^{-4}$ ) is displaced from the pure ZrF<sub>4</sub> vapor pressure curve (if extended). This implies that the solid phase for this particular

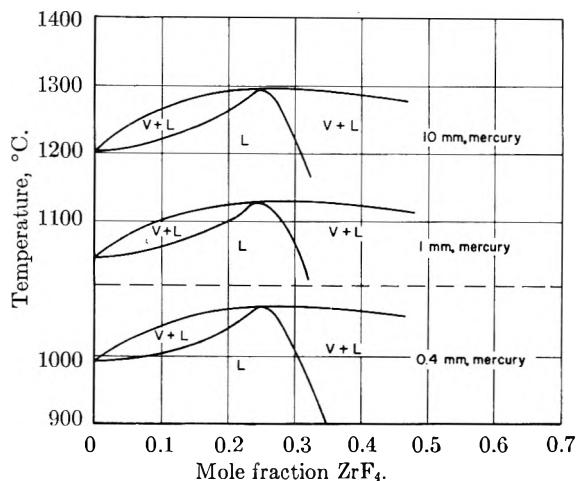


Fig. 11.—Phase diagrams in vicinity of azeotropes for various pressures.

exists in the vapor phase, the results would be affected in the following manner. As an extreme case, if  $\text{Na}_3\text{ZrF}_7$  existed virtually undissociated in the vapor phase at a  $\text{ZrF}_4$  mole fraction of 0.25, the total vapor pressure would have a value about one-third<sup>10</sup> of that indicated in Fig. 13. As the salt composition becomes either richer or poorer in  $\text{ZrF}_4$  than 0.25, the change in the indicated total pressure decreases. For compositions in which the  $\text{ZrF}_4$  mole fraction is greater than 0.38, the change in the total vapor pressure would not be discernible on this plot. It is likely that  $\text{Na}_3\text{ZrF}_7$  is largely dissociated in the vapor phase. Depending on the extent of dissociation of  $\text{Na}_3\text{ZrF}_7$ , the total vapor pressure at 0.25 mole fraction  $\text{ZrF}_4$  would then be somewhere between the value given in Fig. 13 and one-third of that value.

**Acknowledgments.**—The authors wish to thank Dr. J. W. Droege for the many stimulating and in-

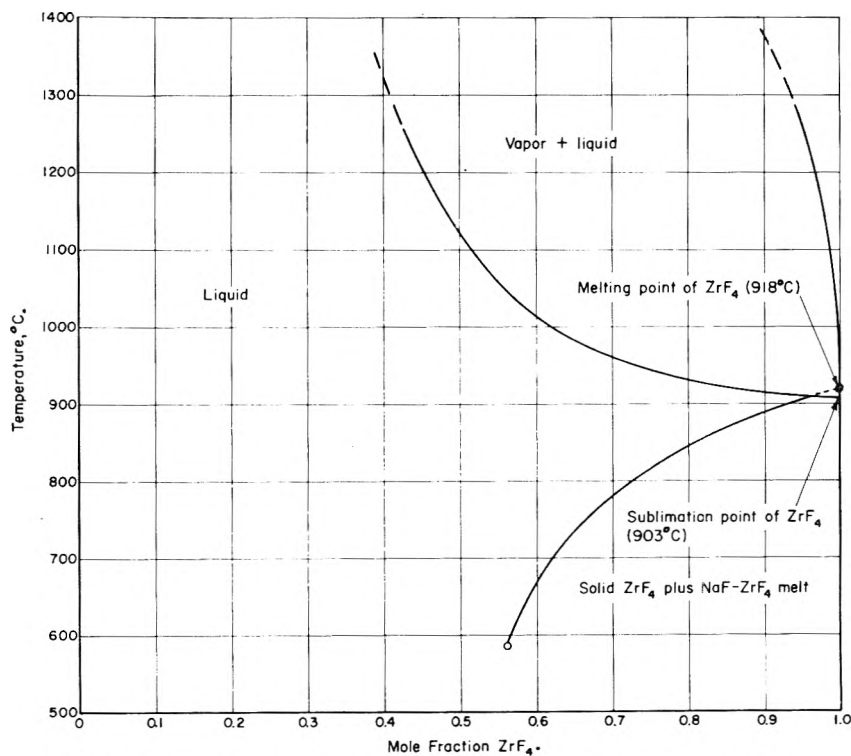


Fig. 12.—Partial phase diagram of NaF-ZrF<sub>4</sub> system at a pressure of 760 mm.

system is different from  $\text{ZrF}_4$ . The exact composition of this solid phase is not immediately evident. No liquidus curve could be constructed for this solid phase, since only one melting point was available. The melting point,  $621^\circ$ , was obtained from the intersection of the liquidus and solidus vapor pressure curves of the 53.2 mole %  $\text{ZrF}_4$  composition.

**Total Vapor Pressures of the NaF-ZrF<sub>4</sub> System.**—The total vapor pressure as a function of composition for various temperatures is given in Fig. 13. This plot was constructed from information given in Table III. A vapor pressure minimum is present at a  $\text{ZrF}_4$  mole fraction of 0.25. Because of insufficient information about the degree of dissociation of  $\text{Na}_3\text{ZrF}_7$  in the vapor phase, the total pressures were calculated on the basis that only NaF,  $\text{ZrF}_4$  and  $\text{NaZrF}_5$  exist in the vapor phase. If  $\text{Na}_3\text{ZrF}_7$

TABLE IV  
EQUILIBRIUM CONSTANTS CALCULATED FOR VARIOUS RECIPROCAL TEMPERATURES FOR THE REACTION



$$K_p = \frac{(p_{\text{NaF}})(p_{\text{ZrF}_4})}{(p_{\text{NaZrF}_6})}$$

| Composition, mole % $\text{ZrF}_4$ | Equilibrium constant, $K_p$ , at given reciprocal temp., |                      |                      | $\frac{10^4}{T(^{\circ}\text{K.})}$<br>8.395 |
|------------------------------------|--|----------------------|----------------------|--|
|                                    | 7.50   | 7.70                 | 8.00                 |  |
| 25                                 | $2.5 \times 10^{-5}$                                     | $1.7 \times 10^{-5}$ | $3.8 \times 10^{-6}$ | $1.1 \times 10^{-6}$                         |
| 27.5                               | $2.8 \times 10^{-5}$                                     | $1.4 \times 10^{-5}$ | $5.4 \times 10^{-6}$ | $1.6 \times 10^{-6}$                         |
| 28.3                               | $2.1 \times 10^{-5}$                                     | $1.1 \times 10^{-5}$ | $3.4 \times 10^{-6}$ | $1.4 \times 10^{-6}$                         |

formative discussions, and Messrs. Richard W. Stone and Val Hemm for their assistance in carry-

(10) See Appendix for discussion.

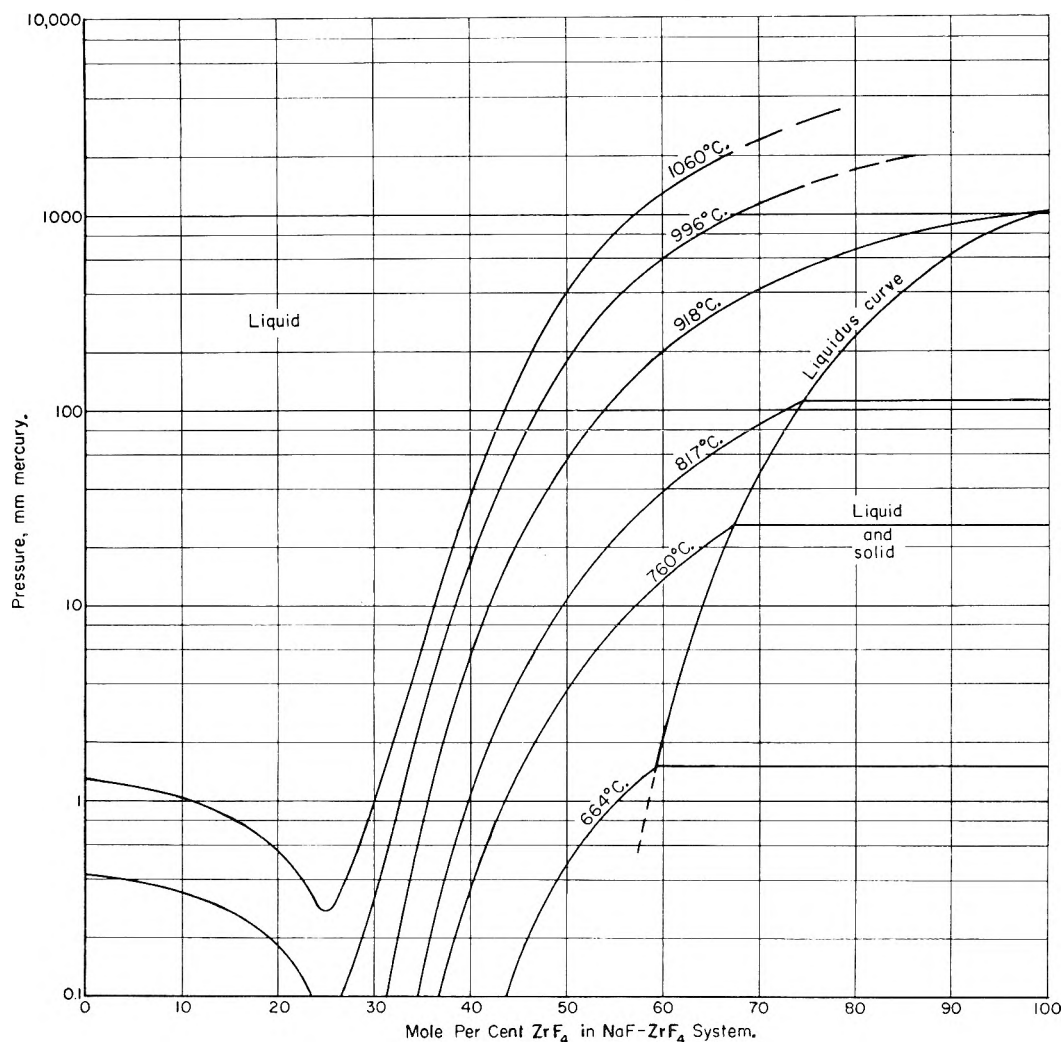


Fig. 13.—Total vapor pressure of the NaF-ZrF<sub>4</sub> system for various temperatures.

ing out the experimental work. They further wish to thank Messrs. L. K. Jones and Aaron Eldridge for performing the chemical analyses.

#### Appendix

**Calculations of Partial Pressures.**—The partial pressures of the components of a system are calculated according to the relation

$$p_i = \frac{m_i}{M + \sum_i m_i} P \quad (a)$$

where

$p_i$  = partial pressure of the  $i$ th component  
 $P$  = total pressure of system  
 $m_i$  = moles of  $i$ th component in condenser (corrected for quantity which diffused into condenser)  
 $M$  = moles of carrier gas collected

$P$  remains essentially constant, since the total pressure was always only slightly greater than atmospheric. Hence

$$p_i \propto \frac{m_i}{M + \sum_i m_i} \quad (b)$$

Since for vapor pressures of about 10 mm. or less, the number of moles of inert gas collected is much greater than the number of moles of salt collected, there results for low vapor pressures

$$M \gg \sum_i m_i \quad (c)$$

and therefore

$$p_i \propto m_i \quad (d)$$

For the extreme case discussed previously,<sup>10</sup> the sum of the partial pressures of the components was less than 1 mm. for the 25 mole % region (Fig. 13). Therefore, inequality (c) is satisfied and equation (d) is applicable.

Hence, two moles of NaF and one mole of NaZrF<sub>5</sub> in the vapor phase exert a vapor pressure of three arbitrary units. If the two moles of NaF combined with one mole of NaZrF<sub>5</sub> to form one mole of Na<sub>3</sub>ZrF<sub>7</sub> in the vapor phase, a vapor pressure of one arbitrary unit would result. The summation value in the denominator of (b) would change but the total value of the denominator would remain essentially the same because of (c).

# VAPOR PRESSURE STUDIES INVOLVING SOLUTIONS IN LIGHT AND HEAVY WATERS. III. THE SEPARATION FACTOR FOR THE ISOTOPES OF HYDROGEN DURING DISTILLATION FROM SALT SOLUTIONS IN THE MIXED WATERS AT ROOM TEMPERATURE

BY JOHN M. GOOGIN AND HILTON A. SMITH

*Department of Chemistry, University of Tennessee, Knoxville, Tennessee*

*Received October 1, 1956*

An investigation has been made into the possibility of changing the separation factor for the fractionation of the isotopes of hydrogen during the distillation of water by the addition of various solutes to the system. The experimental procedure involved the direct determination of the separation factor for the system under study by analysis of the two phases at equilibrium, rather than carrying out experiments on solutions in the pure waters and attempting subsequent predictions which could be in serious error. The results indicate that there is little possibility of improving the separation by additions to the water phase at room temperature. Apparently anything which is added to water disrupts its structure to some extent and thus reduces the separation factor. This reduction in the separation factor amounts to more than 60% of its excess over one when zinc iodide is used as solute.

Distillation of water at low temperatures has been proposed<sup>1</sup> as a method for the separation of the isotopes of hydrogen because of the increase of the separation factor. There are cases<sup>2,3</sup> reported in which distillation at moderately low pressures has proved successful, but the lowest temperature reached was approximately 40° at the top of the column and 65° at the bottom ( $\Delta p = 128$  mm.). Here the separation factor for a single stage is 1.05 compared to 1.03 at 100°. If a material could be found which would, when added to the liquid phase, increase the separation of the isotopes from that found for pure water, the ordinary distillation operation could be modified to extractive distillation.<sup>4,5</sup> This research has consisted primarily of the measurements of the effects of a series of salts on the separation factor of the isotopes of hydrogen during distillation. The separation factor ( $\alpha$ ) may be defined by

$$\alpha = \frac{(H/D)_{\text{gas}}}{(H/D)_{\text{liquid}}}$$

where (H/D) is the molar ratio of hydrogen to deuterium in the gas or the liquid phase as is indicated by the subscript.

In order to obtain the desired results, either the bonding of the hydrogen in the water structure is going to have to be increased to some small extent or it is going to have to be decreased greatly. In this connection, a survey of the literature gives some interesting theories of the structure of water<sup>6-8</sup> and of its solutions.<sup>6,9-11</sup> The small

cations produce no change, or changes which are similar to those produced by decreases in the temperature of the solvent, while the large cations and the anions produce changes similar to increases in temperature when the X-ray spectra, Raman spectra, temperature of maximum density and viscosity of the solutions are considered. The concept of a structural temperature has received further support in the effect of salts on the infrared spectrum of water<sup>12</sup> although one investigator<sup>13</sup> regards the observed changes as more characteristic of the salt added than of a change in the temperature of the solvent. The water relaxation time as indicated by the dielectric properties of water is shortened by the addition of positive ions and is lengthened by hydrogen bond-forming molecules.<sup>14</sup>

Considering next some possible differences in the properties of light and heavy water, some investigators<sup>15,16</sup> found the ratio of the vapor pressures of the solvents (light to heavy water) is not affected by the addition of potassium chloride within the experimental error of the determination which is about 0.01 mm. When data<sup>17</sup> for saturated solutions of sodium sulfate are calculated on the same basis, using solubility data from another source,<sup>18</sup> there is no difference in the ratios. From a series of determinations on saturated solutions of cupric sulfate<sup>19</sup> it was found that the lowering of the vapor pressure of the light water was that expected from Raoult's law multiplied by 1.022 while the results for the heavy water required a factor of 1.030. Only one determination<sup>20</sup> with the mixed waters, where H<sub>2</sub>O, D<sub>2</sub>O and HDO species are present, was found. Here, the separation was

(1) G. N. Lewis and R. E. Cornish, *J. Am. Chem. Soc.*, **55**, 2616 (1933).

(2) M. Randall and W. A. Webb, *Ind. Eng. Chem.*, **31**, 227 (1939); I. Dostrovsky, E. D. Hughes and D. R. Llewellyn, *Nature*, **161**, 858 (1948).

(3) J. O. Maloney, G. F. Quinn and H. S. Ray in "Production of Heavy Water," McGraw-Hill Book Co., New York, N. Y., 1955, p. 73; P. J. Selak and J. Finke, *Chem. Eng. Prog.*, **50**, 221 (1954).

(4) J. H. Perry, "Chemical Engineers Handbook," 3rd ed., McGraw-Hill Book Co., Inc., New York, N. Y., 1950, p. 629.

(5) A. Weissberger, "Technique of Organic Chemistry," Vol. 4, Interscience Publishers, Inc., New York, N. Y., 1951, pp. 317-356.

(6) J. D. Bernal and R. H. Fowler, *J. Chem. Phys.*, **1**, 515 (1933).

(7) J. Morgan and B. E. Warren, *ibid.*, **6**, 666 (1938).

(8) J. Lennard-Jones and J. A. Pople, *Proc. Roy. Soc. (London)*, **A205**, 155 (1951).

(9) E. J. W. Verwey, *Rec. trav. chim.*, **61**, 127 (1942).

(10) G. W. Stewart, *J. Chem. Phys.*, **11**, 72 (1943).

(11) E. C. Bingham, *This Journal*, **45**, 885 (1941).

(12) E. Ganz, *Ann. Physik*, [5] **28**, 445 (1937).

(13) T. H. Kujumzelis, *Z. Physik*, **110**, 742 (1938).

(14) G. H. Haggis, J. B. Hasted and T. J. Buchanan, *J. Chem. Phys.*, **20**, 1452 (1952).

(15) K. Niwa and E. Shimazaki, *J. Faculty Sci. Hokkaido Imp. Univ., Ser. III*, **3**, 35 (1940).

(16) Z. Shibata and K. Niwa, *Z. physik. Chem.*, **A173**, 415 (1935).

(17) L. Higuchi, *J. Chem. Soc. Japan*, **58**, 193 (1937); *C. A.*, **31**, 3363 (1937).

(18) R. D. Eddy and A. W. C. Menzies, *This Journal*, **44**, 207 (1940).

(19) F. T. Miles and A. W. C. Menzies, *J. Am. Chem. Soc.*, **60**, 87 (1938).

(20) E. Lange, W. Martin and H. Sattler, *Z. ges. Naturw.*, **1**, 441 (1936).

better when r.o salt was added to the pot than when either sodium chloride or magnesium sulfate was present. The vapor pressures of the two waters over solid solvates have been investigated to some extent,<sup>17,19,21</sup> and, in the majority of cases, the differences between the vapor pressures of the waters over the solvates are less than that for the pure liquids at the same temperature. Some exceptions are potassium fluoride dihydrate and nickelous chloride hexahydrate in which the ratios of the vapor pressures are 1.4 and 1.25, respectively, at 25°. The ratio for the pure solvents at the same temperature is 1.158.<sup>22</sup> There are some data available on the isotopic variation of water removed from cupric sulfate pentahydrate crystals<sup>23</sup> which indicate that the sulfate ion, which is supposed to hold the last molecule of water by means of hydrogen bonds, favors the light isotope of hydrogen as compared to the four molecules of water about the cation. The distribution of the isotopes between the water of hydration and the mother liquor has been measured for a few hydrates,<sup>24</sup> and this distribution indicates that no separation takes place within the experimental error which should have allowed detection of a factor of about 1.001. The heat of solution of salts in heavy water is smaller than in the light water except for some fluorides of small cations.<sup>25,26</sup> In the halogen series, the difference in the heats of solution increases with the increasing size of the anions reported, being the greatest for the iodide. The cations produce less difference as the size of the ion is decreased. Light water is generally a better solvent than is heavy water, but one instance, lithium fluoride,<sup>26</sup> has been found where the unhydrated salt is more soluble in heavy water. For hydrates, it has been reported<sup>18</sup> that sodium iodide dihydrate, lithium chloride monohydrate, lithium bromide dihydrate and strontium chloride hexahydrate are less soluble in the light water system, but the differences observed may be due to the change in the structure of the solid phase as much as to the properties of the solution. For potassium salts, the salts of large anions, like the iodide and the dichromate, show greater solubility differences than those of the smaller anions like the nitrate and sulfate.<sup>27</sup> This survey indicates possible solutes to be used in an extractive distillation process for the separation of hydrogen and deuterium as well as possible properties for correlation of the results obtained in this investigation.

### Experimental

The experimental procedure has been the direct determination of the separation factor for the system under study by analysis of the two phases at equilibrium. This was done to avoid predictions attempted on the basis of data for

the pure waters, making correction for the presence of protium deuterium oxide. The Rayleigh method of distillation<sup>28,29</sup> was used to determine the actual separation factor for the distillation process, and the calculations will be described later. To allow measurement of the separation factor with the greatest ease for a given accuracy, the solvent was mixed to contain approximately 50 mole % of heavy water, as the greatest actual change in the concentration was produced by a single stage separation at this concentration. The method of analysis involved the determination of the density of the water by means of the time of fall of a drop of known size through a column of an immiscible liquid of smaller density and has been previously described.<sup>22</sup> To ensure the purity of the water required by this method, the apparatus, which is shown in Fig. 1, and in which the Rayleigh distillation was carried out, was constructed so that the water could be redistilled. With the pot held at  $27 \pm 2^\circ$  and the condensing trap at  $0^\circ$  the condition of zero reflux which was necessary for the success of this distillation was maintained easily. To ensure equilibrium within the body of the liquid in the pot, agitation was supplied with a magnetic stirrer which also turned another agitator in the beaker of liquid used to control the temperature of the pot. Investigation of alpha as a function of agitation indicated that some agitation (80 and 400 r.p.m. were satisfactory) was necessary to prevent too low an apparent alpha, due probably to a concentration of the heavy isotope on the surface. The rate of stirring of 80 r.p.m. was used in the subsequent experiments. The several joints and stopcocks in the apparatus were lubricated with "Apicizon M"<sup>30</sup> which had neither exchangeable hydrogen nor high enough vapor pressure to contaminate the condensate. A typical experiment was performed in the following manner. The salt to be used was added to a tared pot with caps and dried by heating under vacuum to  $290^\circ$  using a glycerol-bath. This system was pumped through a trap cooled in Dry Ice-acetone mixture until no further accumulation of ice was observed, when the cooling bath was raised to an ice-free part of the trap. With this procedure, it was found that a sample of 20 g. of calcium sulfate could be freed from light water, wet with a half-gram sample of 48.26 mole % heavy water, and then dried, with the water recovered analyzing 48.22 mole % heavy water. After drying the salt and removing the grease with carbon tetrachloride, the weight of the salt was obtained. Next, water of known isotopic composition was added, and its weight (varying from one to three grams) was obtained. The water which was added was expected to give a solution which was between one-half and two-thirds of saturation at the operating temperature. Then, the pot containing the solution was returned to the distillation train, was frozen with the Dry Ice-acetone mixture, and was evacuated through a trap in a similar cooling mixture. The latter trap served to catch any water which might have been above the cold zone in the pot. When the pressure had been reduced to less than one mm., the system was isolated from the pump and the water in the trap was allowed to distil back to the pot. The pot was then warmed to the desired temperature and the agitator was started. When there was no further rise in the temperature of the pot, as indicated by a constant pressure in the apparatus, the trap was cooled in ice-water for the Rayleigh distillation. The area of the trap cooled, or the stopcock between the pot and the trap was adjusted so that 5 to 15 minutes were required for the collection of the sample, usually consisting of about 25% of the original solvent. With the pot shut off from the rest of the apparatus, the condensate was redistilled to the removable sample holder which was kept at ice-water temperature while the trap was warmed. It was found that the amount of water vapor remaining using this method was enough to affect significantly the analysis of the recovered water and, thus, the vapor was condensed with the Dry Ice-acetone mixture after the distillation was completed. This cooling mixture was not used initially because the liquid which was distilling froze, and this slowed the distillation considerably. After the last distillation and before the removal or warming up of the sample, air was admitted to the system through a

(21) J. Bell, *J. Chem. Soc.*, 459 (1937); 72 (1940).

(22) R. L. Combs, J. M. Googin and H. A. Smith, *THIS JOURNAL*, **58**, 1000 (1954).

(23) J. C. Anderson, R. H. Purcell, T. G. Pearson, A. King, F. W. James, H. J. Emeleus and H. V. A. Briscoe, *J. Chem. Soc.*, 1392 (1937).

(24) J. N. E. Dzy, E. D. Hughes, C. K. Ingold and C. L. Wilson, *ibid.*, 1593 (1934).

(25) E. Lange and W. Martin, *Z. physik. Chem.*, **A180**, 233 (1937).

(26) W. Birnthal and E. Lange, *Z. Elektrochem.*, **44**, 679 (1938).

(27) T. Chang and Y. Hsieh, *Sci. Repts. Natl. Tsing Hua Univ.*, **A5**, 252 (1948), (*C.A.*, **43**, 6492c (1949)); *J. Chinese Chem. Soc.*, **16**, 10, 65 (1949), (*C.A.*, **43**, 8321g (1949); **44**, 28f (1950)).

(28) J. W. S. Rayleigh, *Phil. Mag.*, [5] **42**, 493 (1896); [6] **4**, 521 (1902).

(29) J. H. Perry, ref. 4, p. 580.

(30) Obtained from the James G. Biddle Co., Philadelphia, Pennsylvania.

drying tube containing magnesium perchlorate. The errors of the distillation process were few, and it was found that samples of water could be carried through all the operations with the exception of the Rayleigh distillation with errors no larger than 0.01%. This included those errors which might result from the short time when the water was exposed to moist air during the transfer from the storage container to the pot and from the sample receiver to the analysis pipet. After the distillation and analysis, the weight of solvent lost was determined by reweighing the pot. This, with the analysis of the condensate, and the weight and the composition of the original solvent, were all the data needed for the calculation of alpha.

The above methods could not apply for solutions of sodium hydrogen sulfate and potassium hydroxide where the solute contained exchangeable hydrogen. After a Rayleigh distillation of a sodium hydrogen sulfate solution, the residue was analyzed for heavy water by neutralizing with anhydrous potassium carbonate and recovering the water for isotopic analysis by the usual vacuum drying technique. With the potassium hydroxide solution, the water was recovered after neutralizing with anhydrous carbon dioxide added through the drying tube used for the admission of air to the apparatus. Aluminum sulfate and zinc sulfate gave trouble because of their tendency to hydrolyze to sulfuric acid on dehydration and this difficulty was eliminated, as above, by neutralization, recovery and analysis of the water remaining in the pot. For the zinc sulfate solution, a material balance for the water recovered indicated an original composition of 47.74 mole % heavy water in satisfactory agreement with the analysis of 47.80 mole % of the original water added.

The values for alpha were relatively insensitive to small errors in the weight of the condensate of the fraction removed and were less sensitive as the weight of the condensate decreased. As an example, for the removal of 20% of the solvent, a 10% error in weight removed would only change an alpha of 1.060 to 1.059. The value obtained for alpha was more sensitive to errors in one of the water analyses. An error of 0.03% in one of the values at the 50% level would make an error of 0.001 in alpha. A constant error in both of the compositions, however, had little effect on the value of alpha. An error of this kind amounting to 0.1% produced a change of less than 0.0001. Thus, the internal consistency of the results was much more important than absolute accuracy.

In the distillation step, there would be fractionation of the isotopes of oxygen as well as the isotopes of hydrogen. Since the separation factor for the oxygen isotopes is low (1.007), and the oxygen in the water which was used had been normalized to give only a small concentration of the heavy isotope ( $O^{16}/O^{18} = 511$  and the abundance ratio for  $O^{16}/O^{17}$  is five times that for  $O^{16}/O^{18}$ ),<sup>31</sup> no correction of the derived results was made.

If the effect is assumed to be entirely due to  $O^{18}$  and this isotope causes the same change in the density of water as the presence of two deuterium atoms, the fractionation of the oxygen isotopes produced less than 0.01% error in the deuterium analysis. This would be true even with the increased separation factors reported for the oxygen when salts are present.<sup>32</sup>

The substances examined were generally limited to those which could be separated from water by the application of heat and which were free of hydrogen atoms which could undergo exchange with water under the experimental condition. These limitations were imposed so that an effective agent, if found, could be used in extractive distillation. Most of the salts were used as they are commercially supplied in the reagent grade. Those which were unavailable in this form were prepared, where possible, from the reagent grade oxide or carbonate of the metal and the reagent grade of the desired acid. In preparation for an experiment, the salts were pulverized before they were completely dehydrated in the vacuum apparatus. Sodium dichromate, available in only the technical form, was purified by recrystallization to give about 20% yield. For lithium ferrocyanide, the required acid was prepared by the addition of hydrochloric acid and ether to a concentrated solution of potassium

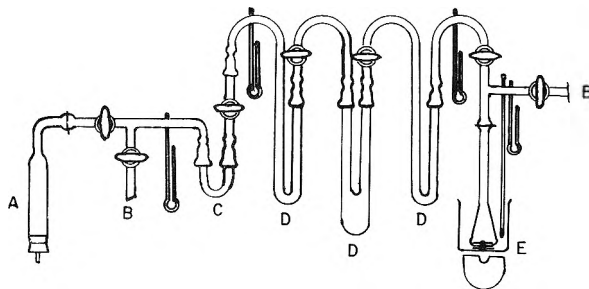


Fig. 1.—The distillation apparatus: A, drying tube; B, to pump; C, sample holder; D, traps; E, pot.

ferrocyanide.<sup>33</sup> The precipitated, solvated acid was washed with cold water and then was used to neutralize a solution of reagent grade lithium hydroxide. The tetramethylammonium bromide was the white label grade supplied by Eastman Kodak Company. No additional purification was attempted with this salt.

### Calculations

A Rayleigh distillation<sup>28,29</sup> requires that a portion of the solvent be vaporized from the solution under equilibrium conditions at zero reflux. From the analysis of the condensate and the original solvent, and a knowledge of the amount of each, the separation factor (alpha) can be calculated from an equation due to Rayleigh

$$\alpha = \frac{\ln(D_{1,i}/D_{1,f})}{\ln(H_{1,i}/H_{1,f})}$$

where  $D_1$  and  $H_1$  are the moles of deuterium and hydrogen, respectively, in the liquid phase initially or finally as is indicated by the subscript. In the experiments performed, it was inconvenient to determine the composition of the solvent in the pot after the distillation because of the salt present, so the material balance equation

$$D_{1,f} = D_{1,i} - D_{1,c}$$

where the c references to the condensate, was incorporated into the above equation to give

$$\alpha = \frac{\ln\left(\frac{1}{1 - D_{1,c}/D_{1,i}}\right)}{\ln\left(\frac{1}{1 - H_{1,c}/H_{1,i}}\right)}$$

As the use of this equation involved considerable computation time, an apparent alpha, defined by

$$\alpha^1 = \frac{(H/D)_c}{(H/D)_i}$$

was calculated and a graphical approximation outlined by Cohen<sup>34</sup> was set up to allow a more rapid solution. Plots were made of the quantity  $(\alpha^1 - \alpha)/(\alpha - 1)$  vs. fraction of solvent removed for values of alpha in the desired range, and alphas determined from the apparent alphas with the aid of these plots. The apparent alpha is equal to alpha when the amount of condensate is vanishingly small, and the difference between the two alphas increases as the fraction of condensate increases.

As there was a considerable change in the concentration of the salt during the Rayleigh distilla-

(33) N. V. Sidgwick, "The Chemical Elements and Their Compounds," Oxford University Press, London, 1950, p. 1336.

(34) K. Cohen, "The Theory of Isotope Separation as Applied to the Large-Scale Production of  $U^{235}$ ," McGraw-Hill Book Co., Inc., New York, N. Y., 1951, pp. 150-153.

(31) I. Kirshenbaum, "Physical Properties and Analysis of Heavy Water," McGraw-Hill Book Co., Inc., New York, N. Y., 1951, p. 29, p. 416.

(32) H. M. Feder and H. Taube, *J. Chem. Phys.*, **20**, 1335 (1952).

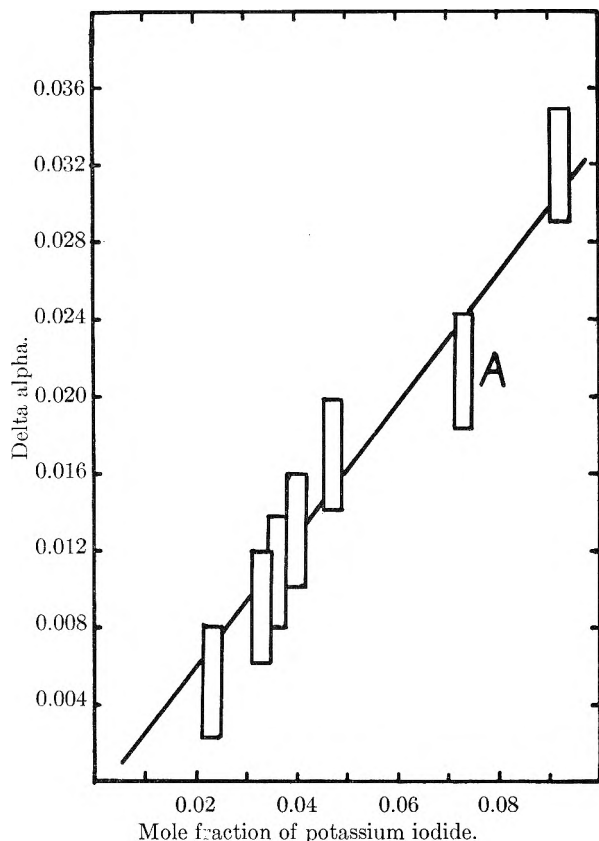


Fig. 2.—The relationship of delta alpha to concentration for solutions of potassium iodide: A, from data of R. L. Combs obtained by method of Smith, Combs and Googin.<sup>35</sup>

tion, the average value was used for the calculation of the effective concentration. The concentration of the salt was expressed as the mole fraction of the anion in the solvent as most of the literature<sup>6,10,11,25-27</sup> indicated that this ion is more influential in the structure of the solution containing the hydrogen atoms. This fact should be kept in mind for the comparisons of salts with ions of different valences. In order to test a postulated linear relationship between the change in the separation factor and concentration of the solution, a series of determinations was made with potassium iodide which was found to have one of the larger effects on the separation factor. The results are given in Fig. 2 with the point "from data by R. L. Combs" coming from his dissertation<sup>35</sup> and made by an independent method on apparatus which is described elsewhere.<sup>36</sup> With the confidence interval found for the distillation of water (see Results), and an estimated uncertainty in the concentration of 0.002, the experimental relationship was found to be in agreement with the postulated linearity. Some of the experiments with other salts have been made using two concentrations to give a further check of the linearity of the relationship, and these are given in the first four lines in Table I. The agreement of the determinations of  $k$  was as good as could be expected from the standard deviation on the value of alpha. Thus, for the expression

(35) R. L. Combs, Ph.D. Dissertation, The University of Tennessee, Knoxville, Tennessee, 1955.

(36) H. A. Smith, E. L. Combs and J. M. Googin, *THIS JOURNAL*, **58**, 997 (1954).

of the results, it has been assumed that the change in the value of alpha is proportional to the concentration of substance added. On the basis of this linear relationship, a constant,  $k$ , characteristic of the solute was calculated for each anion according to the equation

$$\Delta\alpha = kN$$

where delta alpha is the separation factor for the pure solvent at the experimental temperature minus the separation factor for the solution, and  $N$  is the average mole fraction of the anion. The results of this investigation are summarized and compared with others on the basis of the values of  $k$ .

### Results and Discussion

The first determination was the separation factor for the distillation of the pure solvent in the apparatus. An average of four results, with the stirring equal to or greater than 80 r.p.m., was 1.078 with a standard deviation of 0.0015. The 90% confidence interval would thus be  $\pm 0.003$  on the value of a single determination. Determination of the value of alpha by a more precise method gave a value of 1.078 at 27°, while interpolation of Kirshenbaum's data gives the figure of 1.074.<sup>37</sup> The value of 1.078 was used as alpha for the pure solvent in all subsequent calculations. In the calculations of the values of the error(s) placed on the determinations of  $k$ , it was assumed that the determination of the value  $k$  was only in error by the amount introduced by the uncertainty in the value of alpha, and that the standard deviation for this was the same as that found for the experiments above on the pure solvent in which there could be but one correct result. The results obtained from the salts examined are presented in Table I. The relatively small effect of variation in the cation size can be seen from the similarity of the  $k$ 's for the chlorides of lithium, potassium and cesium. A much greater change has been found for the variations in the size of the anions, with the lowering for the iodide being definitely outside of experimental error. No salt examined increased alpha and there is no possibility indicated of improving the isotopic separation by addition of a salt to the water phase. Apparently anything which is added to water disrupts its structure to some extent, and, since it is the structure of the liquid which makes the separation by distillation possible, the alpha is reduced.

Those salts which disrupt the structure most on a per mole of anion basis are potassium ferrocyanide, potassium orthophosphate, lithium ferrocyanide, sodium hydrogen sulfate and potassium iodide. Due to its greater solubility, zinc iodide gave the lowest alpha of 1.029 which is a reduction of the separation to less than 40% of its excess over one. There are indications<sup>38,39</sup> that the separation for the distillation process reverses at higher temperatures and that the above salts could increase the separation at these high temperatures.

(37) I. Kirshenbaum, ref. 31, p. 25.

(38) F. T. Miles and A. W. C. Menzies, *J. Am. Chem. Soc.*, **58**, 1067 (1936).

(39) E. H. Riesenfeld and T. L. Chang, *Z. physik. Chem.*, **B33**, 120 (1936).

TABLE I  
THE EFFECTS OF SALTS ON ALPHA AT 27°

| Salt  | Alpha                  | N     | k           |
|---|------------------------|-------|-------------|
| K <sub>2</sub> CO <sub>3</sub>                  | 1.051                  | 0.136 | 0.20 ± 0.01 |
| K <sub>2</sub> CO <sub>3</sub>                  | 1.060                  | .086  | .21 ± .02   |
| NaClO <sub>4</sub>                              | 1.059                  | .232  | .08 ± .01   |
| NaClO <sub>4</sub>                              | 1.067                  | .171  | .06 ± .01   |
| LiCl  | 1.056                  | .210  | .10 ± .01   |
| KF  | 1.063                  | .128  | .12 ± .01   |
| KCl   | 1.068                  | .091  | .11 ± .02   |
| KBr   | 1.065                  | .081  | .16 ± .02   |
| KI  | (From slope of Fig. 2) |       | .34 ± .02   |
| CsCl  | 1.061                  | .100  | .17 ± .02   |
| N(CH <sub>3</sub> ) <sub>4</sub> Br             | 1.061                  | .084  | .21 ± .02   |
| LiNO <sub>3</sub>                               | 1.072                  | .151  | .04 ± .01   |
| NaNO <sub>3</sub>                               | 1.073                  | .159  | .03 ± .01   |
| KNO <sub>3</sub>                                | 1.073                  | .044  | .11 ± .04   |
| Ca(NO <sub>3</sub> ) <sub>2</sub>               | 1.065                  | .126  | .10 ± .01   |
| Al <sub>2</sub> (SO <sub>4</sub> ) <sub>3</sub> | 1.061                  | .051  | .33 ± .04   |
| MnSO <sub>4</sub>                               | 1.062                  | .069  | .27 ± .03   |
| Na <sub>2</sub> SO <sub>4</sub>                 | 1.076                  | .022  | .09 ± .08   |
| ZnSO <sub>4</sub>                               | 1.064                  | .047  | .30 ± .04   |
| NaHSO <sub>4</sub>                              | 1.067                  | .026  | .42 ± .07   |
| K <sub>4</sub> Fe(CN) <sub>6</sub>              | 1.064                  | .014  | 1.0 ± .13   |
| Li <sub>4</sub> Fe(CN) <sub>6</sub>             | 1.055                  | .053  | 0.43 ± .03  |
| LiIO <sub>3</sub>                               | 1.059                  | .085  | .22 ± .02   |
| Na <sub>2</sub> Cr <sub>2</sub> O <sub>7</sub>  | 1.063                  | .066  | .23 ± .03   |
| K <sub>2</sub> C <sub>2</sub> O <sub>4</sub>    | 1.068                  | .045  | .22 ± .04   |
| KOH   | 1.015                  | .217  | .29 ± .01   |
| K <sub>3</sub> PO <sub>4</sub>                  | 1.060                  | .038  | .47 ± .05   |
| NiCl <sub>2</sub>                               | 1.070                  | .083  | .10 ± .02   |
| ZnI <sub>2</sub>                                | 1.029                  | .260  | .19 ± .01   |

A determination of the value for potassium chloride also has been made by independent means<sup>35</sup> involving no change in the concentration of the solute and using better temperature control, giving a  $k$  value of 0.14 which is in substantial agreement with the 0.11 found by the Rayleigh distillation method. However, computing a  $k'$ , equivalent to that used here, from the determination of the vapor pressures of solutions of potassium chloride in heavy<sup>15</sup> and light<sup>16</sup> water for the highest concentration of the salt used, a mole fraction of 0.0601 and 0.0535, gives a value of less than 0.01 for approximately 10° if the assumption of Lewis and Cornish<sup>1</sup> is used. This difference, 0.11 versus 0.01, illustrates very well the difficulty of deriving accurate separation factors for the water systems from the properties of the pure waters.

Because of the rather small effect of sodium nitrate on the separation factor, an experiment was performed at -10° which is near the eutectic of the system. The temperature of the pot was maintained during the distillation by the manual addition of Dry Ice to a bath of acetone. The very low vapor pressure of the water over the solution at this temperature made the time necessary for the accumulation of a sample a matter of hours rather than the few minutes involved in the 27° experiments. The condenser had to be kept in the Dry Ice-acetone bath to get the needed temperature differential. The separation factor found at this temperature was 1.122, uncorrected for the salt present. A linear extrapolation of other

data<sup>22</sup> at higher temperatures gave an expected value of 1.126 for the solvent at this temperature, indicating that the sodium nitrate still has little effect at low temperatures.

The  $k$  values indicate that the salts all produce a higher structural temperature, and that, as with the temperature of maximum density, the smaller effects are produced by the salts of the smaller ions.<sup>6</sup> Comparison of the apparent volumes of the ions in solutions<sup>6</sup> with the  $k$  values indicates that there is essentially no correspondence between the two. A comparison of the  $k$  values with heat<sup>40</sup> and entropy<sup>41</sup> for the hypothetical process of vaporization of the ions from the solution and with the molar fluidity elevations<sup>11</sup> indicates that the alkali halides fit into a qualitative trend with all of the properties listed. As soon as one applies the same information to salts of the other metals, there is essentially a complete breakdown in the agreement even on a qualitative basis. Evidently the process of solution of the gaseous ions involves reactions other than those in which the bonding of the hydrogen is an important factor. The larger the value of the fluidity, the more the water structure in the solution is supposed to be broken down, but some of the salts which would be expected to have the least effect, such as aluminum sulfate, have some of the largest values of  $k$ .

There is again a qualitative agreement between the  $k$  values and the differences in the heats of solution of salts in heavy and light water<sup>25</sup> as long as one restricts the comparison to a common ion. There is also qualitative agreement between the ratio of the solubility of the salts in heavy water to that in light water<sup>18,27</sup> to the  $k$  values for several salts, but others such as aluminum sulfate are completely out of line. This salt is also out of line with respect to the other properties discussed.

Most of the salts which fell in the category of salts of weak acids and bases showed relatively large effects on the separation factor. This might be due either to the formation of the hydronium and hydroxide ions in the solution or to the formation of the undissociated acid or base. It has been shown by analogy with other compounds for which spectra are available, hydronium ion compared to ammonia, etc., that one can expect a concentration of light isotope of hydrogen in the hydronium and hydroxide ions when these ions are in equilibrium with liquid water.<sup>42</sup> There is a qualitative correlation between the solubility of the hydroxides of the metal in terms of the hydroxide ion concentration<sup>43,44</sup> and the value of  $k$ . Thus, the reduction in the separation produced by the alkali metal salts of the weaker acids may be the result of a similar combination of circumstances since both species, hydroxide ion and the hydrogen form of the anion, produced by hydrolysis of the anion are expected to show a preference for the light hydro-

(40) W. M. Latimer, K. S. Pitzer and C. M. Slansky, *J. Chem. Phys.*, **7**, 108 (1939).

(41) H. S. Frank and M. W. Evans, *ibid.*, **13**, 507 (1945).

(42) H. Sness and H. Jensen, *Naturwissenschaften*, **32**, 372 (1944).

(43) W. M. Latimer and J. H. Hildebrand, "Reference Book of Inorganic Chemistry," Revised Ed., The Macmillan Co., New York, N. Y., 1940, p. 506.

(44) N. A. Lange, "Handbook of Chemistry," Fourth Ed., Handbook Publishers, Sandusky, Ohio, 1941, p. 1143.

gen as compared to the water. The difference between potassium hydroxide with a ( $k$ ) of 0.29 and potassium phosphate with 0.47 could be interpreted as an indication of a stronger preference of the phosphate ion for the light hydrogen. In most of the comparisons with the other properties of the solutions, the difficulties encountered with potassium fluoride may arise from the weakness of the acid. The hydrogen involved in the un-ionized

hydrofluoric acid and the hydrogen difluoride ion which are found in such a solution would be expected to favor the light isotope as do the other weak acids.

**Acknowledgment.**—The authors are indebted to the United States Atomic Energy Commission for support of this work. They are also indebted to Mr. Robert L. Combs for his interest and aid in various phases of this research.

## SURFACE PROPERTIES OF IRRADIATED GRAPHITE<sup>1</sup>

BY C. N. SPALARIS,<sup>2</sup> L. P. BUPP AND E. C. GILBERT

*Engineering Department, General Electric Company, Richland, Washington*  
*Chemistry Department, Oregon State College, Corvallis, Oregon*

Received October 1, 1956

The surface characteristics of neutron irradiated graphite have been investigated. Studies include measurements of surface area, density, heat of adsorption and pore size distribution. The results obtained indicate that the magnitude of these properties decreases with increasing irradiation exposures. It has been proposed that the graphite crystallites in expanding upon neutron irradiation, occupy the voids in their immediate vicinity, thus causing the changes in surface properties.

### Introduction

The use of graphite as moderator material in atomic reactors resulted in the accumulation of a large quantity of information concerning the effects of radiation flux on its physical and chemical properties. Research undertaken at various laboratories dealt primarily with the effects of radiation flux on physical properties of graphite such as dimensional characteristics, electrical resistivity, thermal conductivity, Hall coefficient, crystalline structure and stored energy. All of these properties undergo significant changes when graphite is subjected to radiation flux, and in particular, energetic neutron flux.

One of the most important effects induced by neutron irradiation on graphite, in a low temperature (20–100°) environment, is the change of its physical dimensions.<sup>3</sup> This radiation effect can be detrimental to the over-all structure of an atomic reactor. Although X-ray diffraction studies on graphite have indicated a crystalline growth or expansion along the C axis caused by neutron irradiation, this crystalline expansion has been found to be many times greater than the increase in physical length experienced for irradiated artificial graphite.<sup>4</sup> This phenomenon has been attributed to the fact that the individual crystallites, in expanding during neutron irradiation, have occupied neighboring empty pore space.<sup>5</sup>

The existence of this empty pore space has been found by comparing apparent graphite density to crystallite density.<sup>6</sup>

The purpose of this study was to investigate the changes that take place on the surface of the graphite after its exposure to radiation. These investigations include measurements of the surface area magnitude, pore-size distribution, density and heat of adsorption.

### Methods and Materials

**Samples.**—The graphite samples used throughout the experiments were all manufactured artificially. Almost any organic material that yields a high carbon content on pyrolysis can be used as a raw material. Typical examples are anthracite coke and petroleum coke. Unless otherwise specified, all types of graphite used in this work were manufactured from petroleum coke. The various letter titles used in this report to designate the samples in the experiments, denote the kind of commercial coke and pitch binder used in their manufacture.<sup>3,4</sup> Artificially manufactured graphite has crystalline characteristics similar to natural graphite. The crystallites in the formed artificial graphite are held together with a "binder" which is graphitized at high temperatures. The manufactured graphite is extruded in bars of desired size with the long dimension parallel to the extrusion axis. The crystallites are preferentially oriented parallel to the extrusion axis, as evidenced by the anisotropy of physical properties such as thermal conductivity. Samples exposed in various atmospheres, and *in vacuo*, were enclosed in quartz containers equipped with a break-off seal.

**Irradiation Flux.**—Irradiation exposures for the graphite samples were obtained in the production reactors at Hanford. Thermal neutron flux is calculated from specific power generation in the Hanford reactors. It is assumed that all heat generation originates from fission of uranium and is transferred to the water since heat loss by other means in a pile is negligible.

The radiation flux in the Hanford reactors is usually expressed in megawatts per central ton of active metal (MW/CT). This value is obtained from the average heat generation of the uranium loaded tubes surrounding the exposure facility and an assumed cosine flux distribution along the tube. The nvt values in neutrons per square centimeter used in this report express the total integrated flux to which the adjacent uranium columns were exposed during the time the samples were in the pile.

The exposure of a sample in a given position is expressed in megawatt day per central ton of active metal (MWD/CT). The conversion factor of flux from MWD/CT to nvt is:  $1 \text{ MWD/CT} = 3 \times 10^{17} \text{ nvt}$ . The neutron flux (neutron/cm.<sup>2</sup>/sec.) gives the rate of bombardment with

(1) Excerpted from the thesis of C. N. Spalaris submitted to Oregon State College in partial fulfillment of the requirements for the Ph.D. degree.

(2) General Electric Company, APED, San Jose, California.

(3) W. K. Woods, L. P. Bupp and J. F. Fletcher, Paper #746 presented at the Geneva Conference on Peaceful Uses of Atomic Energy.

(4) W. C. Riley, "Technical Activities Report, Graphite Development," Hanford Report HW-25678, 1953.

(5) C. N. Spalaris, "Surface Studies of Irradiated Graphite," Hanford Report HW-29082, 1953.

(6) L. E. J. Roberts and E. M. Dresel, *Nature*, **171**, 170 (1953).

neutrons; the integrated neutron flux or integrated flux is the product of neutron flux and the length (time) of irradiation. The integrated flux thus represents the amount of bombardment by neutrons in neutrons/cm.<sup>2</sup> denoted by the conventional symbol nvt. The MWD/CT and nvt values reported are accurate to within a nominal 10 to 20%. The description of test hole and process tube experimental facilities at the Hanford piles is given in detail elsewhere.<sup>7</sup> The radioactivity level of graphite samples after exposure never exceeded 1/50 of a roentgen at a distance of 2 cm. from the surface. When the samples were enclosed in glass containers the radioactivity level was reduced to 1/250 of a roentgen. There was no particular difficulty, therefore, in handling the irradiated samples.

**Experimental Procedures.**—An experimental system was designed to investigate the surface characteristics of graphite. This apparatus was similar to that suggested and used by Brunauer, Emmett and Teller.<sup>8</sup> Graphite-nitrogen gas adsorption isotherms were obtained at liquid nitrogen and liquid oxygen temperatures. Desorption isotherms were determined at liquid nitrogen temperatures only. The BET method was used to compute the surface area. The pore size distribution curves were obtained from the analysis of the nitrogen desorption isotherms using the BJH method.<sup>9</sup> The heat of adsorption of nitrogen on graphite was calculated from the isotherms obtained at the two temperatures (*e.g.*, liquid nitrogen—195° and liquid oxygen—183°) using the Clausius-Clapeyron equation. Prior to the determination of the surface characteristics, each sample was evacuated for three hours at high temperature to remove most of the adsorbed bases. The surface area of graphite increased with increasing outgassing temperature, but such increase was very small beyond 500°. For this reason all of the outgassing in these experiments was done between 500 and 1000° unless otherwise mentioned. Density studies were made at 25.0 ± 0.1° using the helium immersion method described elsewhere.<sup>10</sup>

### Experimental Results

For this experiment a large number of graphite samples was exposed to radiation under different flux and atmosphere conditions. The surface area of all graphites decreased during irradiation regardless of the surrounding atmosphere in which they were exposed. The area of the irradiated specimens increases with increasing annealing temperature, but never reaches the pre-irradiation value recorded for the sample. Furthermore, the samples initially having large surface area show the greatest decrease as compared to their corresponding pre-irradiation values. Data for some samples are shown in Table I. The surface area decrease, due to irradiation in high flux environment, depends on the total amount of integrated radiation flux received by the sample. If the total exposure is plotted *versus* the change in surface area a linear curve is obtained as in Fig. 1. A relatively large change in surface area occurs during the initial stages of neutron irradiation. Unfortunately, data for short pile exposures are not available to justify the extension of the curve in Fig. 1 to the origin.

Experimental runs with non-irradiated and irradiated graphites reveal some important changes of their pore size distribution caused by radiation. In general, samples initially having large surface area were effected more by irradiation than those having small surface area. Typical nitrogen gas desorption isotherms of graphite before and after irradiation

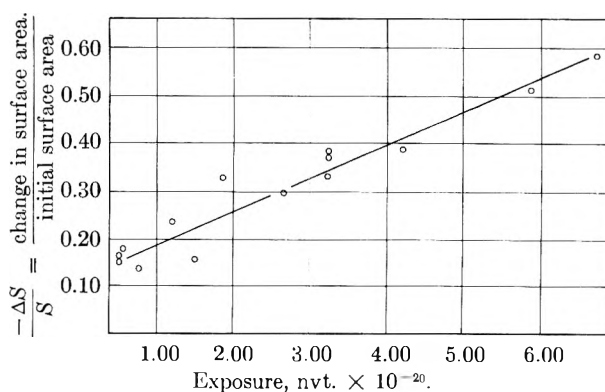


Fig. 1.—Decrease of surface area of graphite due to radiation exposure in a Hanford reactor at low temperatures (20–50°).

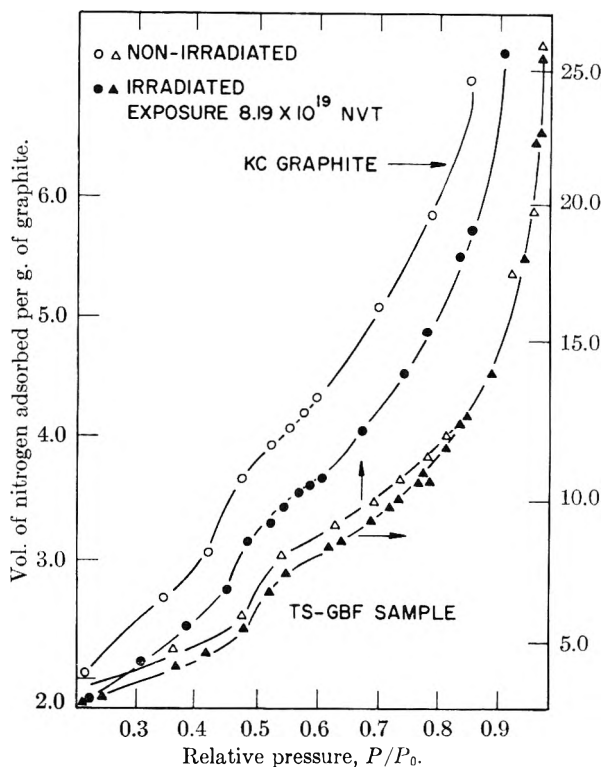


Fig. 2.—Typical desorption isotherms for two types of graphite (powdered form) before and after irradiation.

are presented in Fig. 2 for convenient comparison. In all cases the adsorption and desorption isotherms coincided below relative pressure of 0.4 with only one hysteresis loop occurring between 0.4 and 0.5  $P/P_0$ . The adsorption isotherms were omitted from Fig. 2 because of space limitations. The pore size distribution curves computed from these isotherms and illustrated in Fig. 3, indicate clearly the effect of radiation on the pore sizes of artificial graphite.

A general "shrinkage" or porosity decrease is observed for all sizes of pore radii, which is typical of all graphites studied. The irradiation exposure took place in a water-cooled process tube (annulus tube) in a Hanford reactor with an average temperature of about 20°. The samples, both in formed as well as in powdered state were enclosed in quartz tubes, outgassed at 660° and evacuated

(7) J. C. Fox, "Special Irradiations Manual," Hanford Report HW-29548, 1954.

(8) S. Brunauer, P. H. Emmett and E. Teller, *J. Am. Chem. Soc.*, **60**, 309 (1938).

(9) E. P. Barrett, L. G. Joyner and P. P. Halenda, *ibid.*, **73**, 363 (1951).

(10) C. N. Spalaris, *This Journal*, **60**, 1480 (1956).

TABLE I  
EFFECT OF RADIATION ON THE SURFACE AREA OF GRAPHITE<sup>a</sup>

| Sample and type   | Exposure<br>(nvt × 10 <sup>19</sup> ) | Before irradiation<br>Outgassing<br>temp.<br>(°C.) | Surface<br>area<br>(m. <sup>2</sup> /g.) | After irradiation<br>Annealing<br>temp.<br>(°C.) | Surface<br>area<br>(m. <sup>2</sup> /g.) |
|---|---------------------------------------|--|--|--|--|
| KC (cylindrical form, exposed <i>in vacuo</i> )         | 14.47 <sup>b</sup>                    | 1000   | 0.52                                     | 350  | 0.47                                     |
|   |                                       |  |  | 450  | .49                                      |
|   |                                       |  |  | 550  | .49                                      |
| WSF (powder, exposed <i>in vacuo</i> )                  | 14.47 <sup>b</sup>                    | 1000   | 4.04                                     | 300  | 3.50                                     |
|   |                                       |  |  | 420  | 3.87                                     |
|   |                                       |  |  | 650  | 3.96                                     |
| CSF (powder, exposed <i>in vacuo</i> )                  | 8.21 <sup>c</sup>                     | 1000   | 6.20                                     | 75   | 5.05                                     |
|   |                                       |  |  | 145  | 5.10                                     |
|   |                                       |  |  | 165  | 5.18                                     |
|   |                                       |  |  | 300  | 5.51                                     |
|   |                                       |  |  | 500  | 6.02                                     |
|   |                                       |  |  | 550  | 6.06                                     |
| Lamp Black (powder, exposed <i>in vacuo</i> )           | 8.21 <sup>c</sup>                     | 1000   | 14.44                                    | 70   | 11.97                                    |
|   |                                       |  |  | 160  | 12.67                                    |
|   |                                       |  |  | 300  | 13.08                                    |
|   |                                       |  |  | 520  | 13.62                                    |
|   |                                       |  |  | 660  | 13.62                                    |
|   |                                       |  |  | 75   | 13.62                                    |
|   |                                       |  |  | 75   | 13.62                                    |
| KC (powder, exposed in oxygen)                          | 8.21 <sup>c</sup>                     | 900  | 6.01                                     | 65   | 3.56                                     |
|   |                                       |  |  | 125  | 3.66                                     |
|   |                                       |  |  | 350  | 4.44                                     |
|   |                                       |  |  | 550  | 4.58                                     |
|   |                                       |  |  | 630  | 4.69                                     |
|   |                                       |  |  | 650  | 4.84                                     |
|   |                                       |  |  | 720  | 4.84                                     |
| KC (cylindrical form, exposed in carbon monoxide)       | 8.21 <sup>c</sup>                     | 950  | 0.60                                     | 85   | 0.42                                     |
|   |                                       |  |  | 150  | .43                                      |
|   |                                       |  |  | 300  | .43                                      |
|   |                                       |  |  | 450  | .44                                      |
|   |                                       |  |  | 450  | .44                                      |
| WSF (two cylindrical pieces, exposed in carbon dioxide) | 8.24 <sup>c</sup>                     | 600  | 0.95                                     | 280  | .82                                      |
|   |                                       |  |  | 450  | .85                                      |
|   |                                       |  |  | 500  | .85                                      |

<sup>a</sup> This table includes only samples irradiated and then annealed in an oven. The number of samples examined in this manner is limited because of the lengthy experimental procedures involved. The change in surface area with increasing neutron exposure is best illustrated in Fig. 1. <sup>b</sup> Reactor exposures were carried out at temperatures not exceeding 50°. <sup>c</sup> Reactor exposures were carried out at temperatures not exceeding 20°.

to 10<sup>-6</sup> mm. for three hours before sealing. Several of the quartz containers in addition to graphite samples were filled with gases after evacuation. Samples exposed *in vacuo*, oxygen, carbon dioxide and carbon monoxide have been studied, and it was observed that there is no difference of irradiation effects among samples exposed in these atmospheres.<sup>5</sup> The quartz containers for most of the samples were found in good condition after exposure to radiation, although a good number of them developed microscopic leaks during reactor exposure. All containers were leak-tested with a mercury manometer before and after the break-off seal was opened.

The density of the artificial graphites studied decreases upon irradiation. The density decrease depends upon the length of exposure as well as the temperature maintained during irradiation. If the reactor exposure is carried out at low temperatures, below 50°, the surrounding atmosphere has no effect on density. If, however, the temperature is high and the surrounding atmosphere is capable of oxidizing the graphite sample, then the density increases as a result of oxidation. In other words,

the effect of oxidation on the density at high temperatures is greater than that induced by irradiation alone. Densities of a few samples irradiated at low temperatures are presented in Table II.

TABLE II  
EFFECT OF LOW TEMPERATURE IRRADIATION ON THE DENSITY OF ARTIFICIAL GRAPHITE

| Sample  | Type of graphite <sup>a</sup> | Total exposure, nvt × 10 <sup>20</sup> | Density                                   |  |
|---------|-------------------------------|--|---|--|
|         |                               |  | Before irradiation (g./cm. <sup>3</sup> ) | After irradiation (g./cm. <sup>3</sup> ) |
| 106-28  | CSF                           | 6.62                                   | 2.07                                      | 1.81                                     |
| 111-95  | CSF                           | 4.52                                   | 2.11                                      | 2.07                                     |
| 107-251 | CSF                           | 4.82                                   | 2.15                                      | 2.09                                     |

<sup>a</sup> Density decrease due to reactor exposure was also observed for TS-GBF, WSF and KC graphite.

All samples in Table II were exposed to temperatures not exceeding 50°. They were 10 cm. in length and 1 cm. in diameter. It can be concluded from the data on Table II that the density decrease of artificial graphite depends on the total irradiation exposure. The decrease of graphite surface area and density are concurrent with the shrinkage in the pore-size distribution. After being reduced

by irradiation, the surface area of a given graphite sample increases on thermal annealing and approaches asymptotically the value found before irradiation. It was first thought that this variation in an area was just a normal increase with increasing outgassing temperature, as is the case of non-irradiated samples. This was proved not to be the

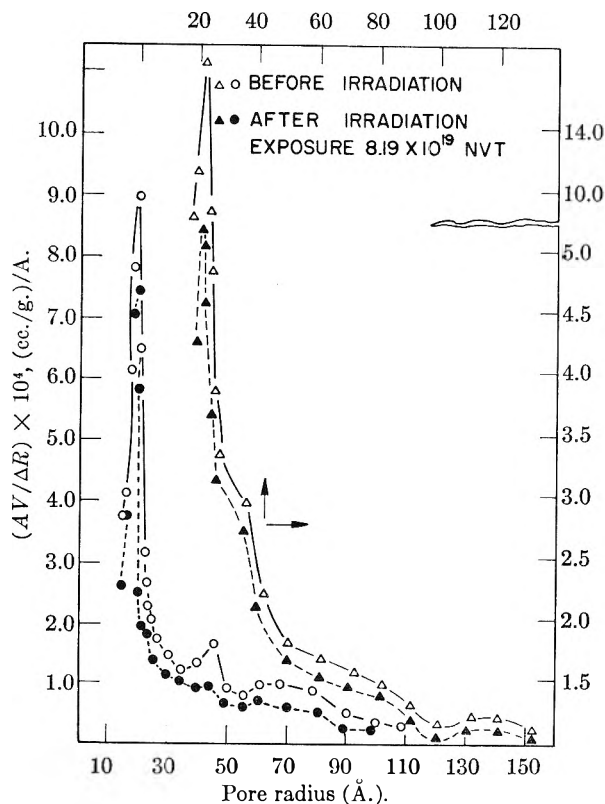


Fig. 3.—Typical pore distribution curves for ○● KC and ▲▲ TS-GBF graphite before and after irradiation.

case. The samples in Table I were all outgassed at high temperatures. Some of them were enclosed in vacuum before pile exposure, then opened *in vacuo*. The pre-irradiation outgassing temperatures were high, beyond which further surface area increase is quite small. The vacuum was maintained during the reactor exposure. Because of the reasons stated above, it was concluded that the surface area increase of irradiated graphites upon heat treatment was due to temperature annealing. This effect is illustrated in Fig. 4. Furthermore, the density decrease and pore shrinkage which occur during reactor exposure anneal upon heat treatment. The heat of adsorption of nitrogen on graphite was determined isothermally by the method of Clausius-Clapeyron. In order to use this equation, two adsorption isotherms obtained at different temperatures were needed. The adsorption isotherms at  $-183$  and  $-195^\circ$  were obtained using liquid oxygen and liquid nitrogen cooling baths, respectively. Volume-pressure plots of graphite-nitrogen isotherms determined at the two temperatures were used to calculate the heat of adsorption at constant volume, by the Clausius-Clapeyron equation in the form

$$\Delta H = 2.303R \left( \frac{T_1 T_2}{T_2 - T_1} \right) (\log P_2 - \log P_1)$$

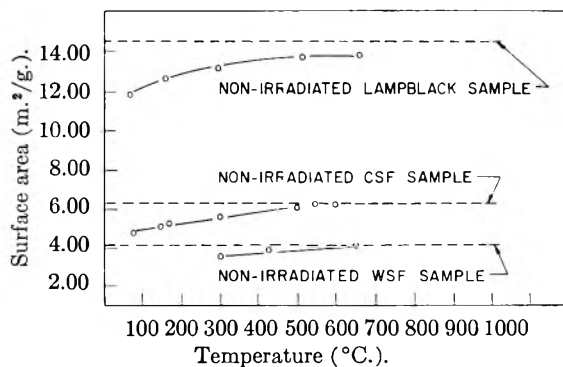


Fig. 4.—Temperature effect (annealing) on the surface area of graphite irradiated *in vacuo*.

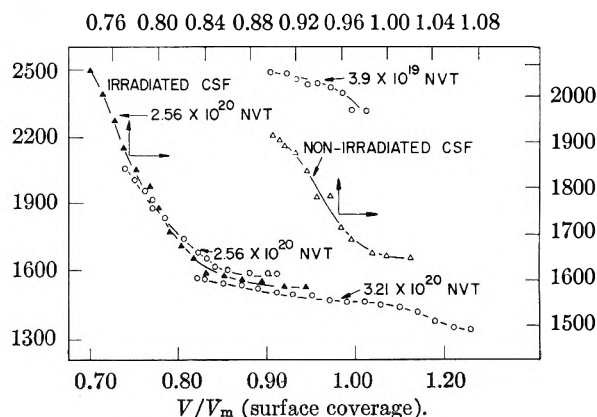


Fig. 5.—Effect of low temperature reactor exposure on the heat of adsorption (nitrogen on graphite). Circles on graph represent TS-GBF graphite data.

In Fig. 5,  $\Delta H$  (differential heat of adsorption) is plotted against  $V/V_m$  or  $\theta$ , which represents the fraction of surface covered by the gas molecules. These curves show that the heat of adsorption of artificial graphite decreases with increasing radiation exposure. A small quantity of nitrogen gas is adsorbed at first evolving high heat, then  $\Delta H$  falls, approaching rapidly a nearly constant value at high surface coverages. The heat of adsorption for the TS-GBF sample (lowest neutron exposure) is abnormally high even at complete coverage of the surface with a monolayer. No explanation can be offered at this time for this behavior, although the experimental points near  $V/V_m = 1$  show a decline toward lower  $\Delta H$  values. High heats of adsorption are usually attributed to adsorption of gas molecules in cracks and crevices whereas the low values are due to adsorption on plane surfaces. Because a large number of small pores in irradiated graphite have been blocked by crystallite expansion, their heats of adsorption at a given  $V/V_m$  region are lower than their corresponding non-irradiated samples.

### Discussion and Summary of Results

For all types of artificial graphite investigated the surface area decreased upon low temperature irradiation. This was true for samples irradiated *in vacuo* as well as for those irradiated in various atmospheres. Density and porosity of graphite also decrease upon irradiation. If samples which were irradiated at low temperatures were afterwards heated at relatively high temperatures in the lab-

oratory, their surface area increases and gradually approaches the area value before irradiation. The decrease in surface area, density and pore shrinkage of the irradiated graphite can be attributed to the expansion of the individual crystallites. The crystallites expand upon neutron radiation and in so doing occupy the microscopic void spaces available in their immediate vicinity, thus causing a decrease in porosity. Although many pores are known to be very small in size, others are large, but have small bottle-neck-like openings. The small pores are partially or completely blocked by graphite crystalline expansion. The subject of graphite crystalline expansion has been treated in detail at Hanford, and elsewhere.<sup>3,4,11,12</sup>

It has been proposed that crystalline expansion is caused by interstitial atoms, or groups of atoms, tending to position themselves between graphite layers. Atoms, acquiring a certain amount of energy from an incoming neutron, vibrate vigorously until their bonds break from the regular network of hexagons. Once free, they may either move to an interstitial position, leaving a vacancy, or replace another atom at a regular position, or fill an existing

vacancy. At the end of an irradiation period, the once regular structure possesses a large number of lattice imperfections which are chiefly responsible for crystallite expansion.

Measurements of the physical expansion of formed irradiated graphite show a 0.20 to 0.60% increase at the most, depending on the length of the exposure.<sup>3</sup> The range of the irradiation exposures studied was up to about  $7.53 \times 10^{20}$  nvt. total. The same samples, however, show a 15% increase in C axis as determined by X-ray measurements. The difference in crystallite expansion was absorbed into the voids, or micropore structure. This fact was substantiated by the observed pore shrinkage found for low temperature irradiated graphites.

The time lapse for the establishment of gas-solid equilibrium during the adsorption isotherms for irradiated graphite was approximately three to four times longer than the time ordinarily necessary for the non-irradiated solid sample-gas equilibria. This also supports the hypothesis of crystallite expansion into the voids. Because the entrances of a large number of pores are partially blocked, the molecules of nitrogen gas have difficulty in entering these pores. The gas molecules diffuse slowly through the restricted entrances. This slow equilibrium phenomenon was not observed after the irradiated samples were subjected to high temperature treatment.

(11) E. P. Warekois, "Pile graphite sampling production tests. Pile graphite expansion," Hanford Report HW-21930, 1951.

(12) B. E. Warren and D. R. Chipman, "X-Ray measurement of radiation damage in graphite," Knolls Atomic Power Laboratory Report, KAPL-938, 1953.

## SALTING-OUT CHROMATOGRAPHY. I. ALCOHOLS

BY ROGER SARGENT AND WILLIAM RIEMANN III

*Ralph G. Wright Chemical Laboratory, Rutgers University, New Brunswick, New Jersey*

*Received October 18, 1956*

The separation of water-soluble non-electrolytes by elution through a column of ion-exchange resin with an aqueous salt solution as eluent is designated as "salting-out chromatography." Variables such as the functional group, mesh size and cross-linkage of the resin, the sample size and flow rate were studied with several alcohols as solutes. The usefulness of the method is demonstrated by a separation of nine alcohols in a 12-hr. elution.

A process for the chromatographic separation of water-soluble non-electrolytes with ion-exchange resins and aqueous salt solutions as the stationary and mobile phases, respectively, was reported recently.<sup>1</sup> The designation, "salting-out chromatography" is proposed for this method.

In the interpretation of the results, use is made of the equation<sup>2</sup>

$$U^* = CV + V \quad (1)$$

where  $U^*$  is the volume of effluent collected from the addition of the sample to the peak, and  $C$  is the distribution ratio of the alcohol (quantity of the alcohol in the resin of any plate divided by the quantity in the interstitial solution of the same plate). The interstitial volume of the column is represented by  $V$ .

### Experimental

**Alcohols.**—All alcohols were of the best grade obtainable. No further purification was necessary for this study.

(1) R. Sargent and W. Rieman, *J. Org. Chem.*, **21**, 594 (1956).

(2) J. Beukenkanp, W. Rieman and S. Lindenbaum, *Anal. Chem.*, **26**, 505 (1954).

**Resins.**—Three types of anion-exchange resins were used. Dowex 1, Dowex 2 and Dowex 3 were converted to the sulfate form (in columns) by the passage of 3.0 *M* ammonium sulfate until the effluent gave a negative test for chloride. The resins were removed from the columns, slurried with the desired eluent and poured into columns, 30 cm.  $\times$  3.90 cm.<sup>2</sup> (Ace Glass Co., drawing T-3422). After 5 min. the excess eluent was drained. An additional 1 l. of eluent was passed through the bed at a maximum flow rate with occasional tapping of the side of the column. This procedure ensures air-free and reasonably uniform packing of the resin. Considerable shrinking or swelling of the resin occurs when the concentration of the eluent is changed markedly. In order to avoid the formation of channels in the column from this cause, the column was repoured before determining distribution ratios with a different concentration of eluent. Two cation exchangers, Dowex 50 and Amberlite IRC-50(H) were similarly converted to the ammonium form and packed.

The interstitial volume,  $V$ , was found to be 44.0% of the bed volume for Dowex 1-X8, 200-400 mesh. The values of  $V$  for Dowex 50-X8, 100-200 mesh and 200-400 mesh were, respectively, 36.6 and 39.1% of the bed volume. Values of 44.0% for Dowex 1 and 38.0% for Dowex 50 were used to evaluate the elution data.

**Elution and Analysis.**—The eluent was drained to the top of the bed of resin and the sample of approximately 0.1 mmole of the alcohol in 1 ml. of water was pipetted onto the bed without disturbing the resin. The sample was drained

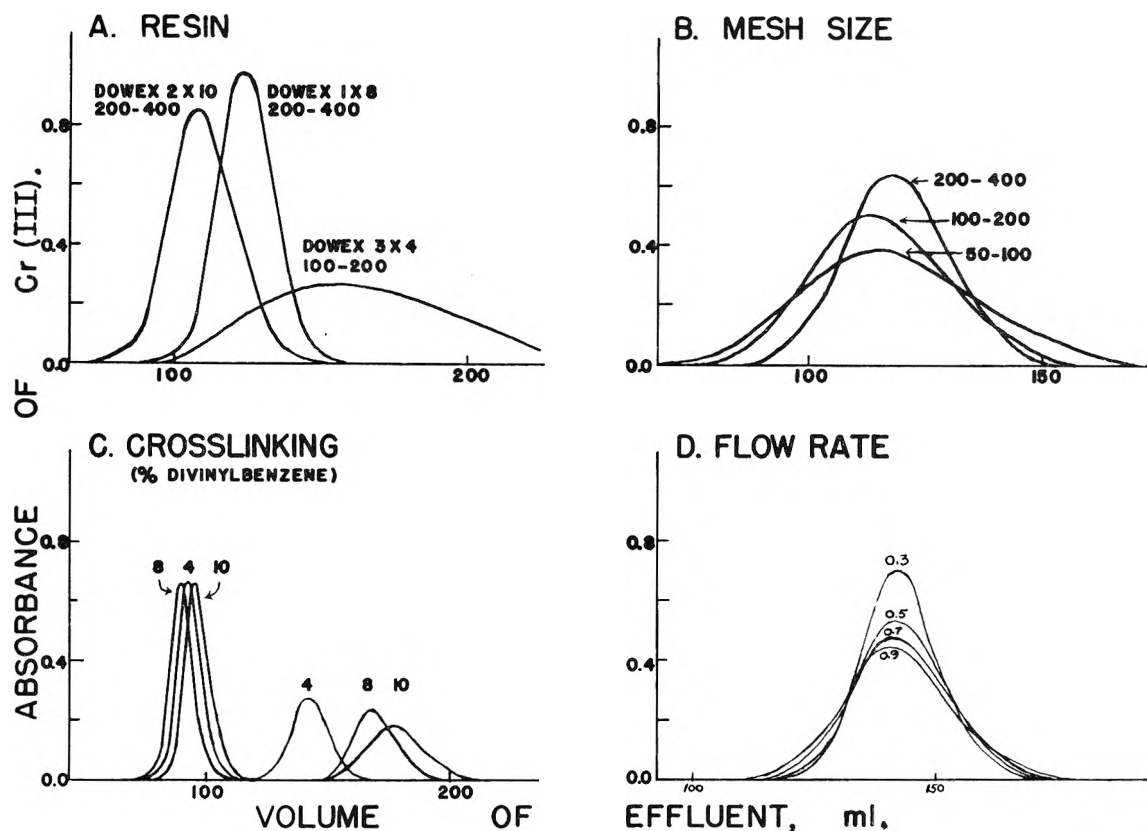


Fig. 1.—Variables in salting-out chromatography.

to the top of the bed, and the sides of the column were washed with two 1-ml. portions of eluent. The alcohol was then eluted with a flow rate of 0.5 cm. per min. unless otherwise specified. Fractions of 6 ml. were collected with the aid of a fraction collector.<sup>2</sup> The fractions were analyzed by mixing them with 0.1 *N* sodium dichromate dissolved in concentrated sulfuric acid and subsequent measurement of the absorbance of the resulting Cr(III).<sup>3,4</sup>

**Solubility Studies.**—Salting-out constants for *n*-propyl and *sec*-butyl alcohol were obtained by the determination of relative solubility by shaking an excess quantity of alcohol with 2 to 4 *M* ammonium sulfate solutions. The relative quantity of alcohol in the aqueous phase was determined by oxidation of an aliquot with dichromate.<sup>3</sup>

### Results and Discussion

**Resins.**—Propylene glycol was eluted with 3.0 *M* ammonium sulfate from 20-cm. columns of each resin. The elution graphs for Dowex 50 and Amberlite IRC-50 were very similar to the graphs obtained for Dowex 1 and Dowex 3 (Fig. 1a), respectively. Dowex 1 and Dowex 50 were chosen as the best resins for the separation of alcohols.

**Mesh Size.**—Similar elutions of propylene glycol were run on 20-cm. columns of Dowex 1-X10 of various particle sizes. Figure 1b shows that the smallest mesh, 200-400, produced the sharpest elution graph. No significant shift of  $U^*$  was observed for a change in mesh size of resin.

**Cross-linking.**—The effect of cross-linking was investigated by eluting a mixture of methyl and ethyl alcohols with 3.0 *M* ammonium sulfate from columns containing 20 cm. of Dowex 1-X10, Dowex 1-X8 and Dowex 1-X4. All resins were 200-400 mesh. Although the selectivity of the 10% divinylbenzene resin (Fig. 1c) was the greatest, Dowex

1-X8 was chosen as the resin that gave good selectivity and the best elution graph. Slight differences in the peaks of methyl alcohol (first peak) with the various resins probably are due to the physical inability to prepare columns whose interstitial volumes are identical, and not to the nature of the resin itself.

**Flow Rate.**—Figure 1d shows the gradation from narrow to broad elution graphs when ethyl alcohol was eluted from 16.8 cm. of Dowex 1-X8, 200-400 mesh, at flow rates ranging from 0.3 to 0.9 cm. per min. A mixture which is very difficult to separate may require the slower flow rate; conversely, the flow rate for less-difficult separations may be increased. No change in the position of  $U^*$  was discernible for a change of flow rate.

**Sample Size.**—An almost linear decrease in the value of the distribution ratio  $C$  was found with increasing the amounts of alcohol eluted. This effect shows up as a shift of the leading edge and the peak of the elution graph toward the left while the trailing edge remains constant. The shift is much greater when the alcohol has a large distribution ratio. The quantity of alcohol that may be taken for an elution so that the value of  $C$  remains within 2% of its limiting value, was found to be 0.23, 0.11 and 0.088 mmole for alcohols with  $C$  values of 1.02, 5.55 and 12.4, respectively. As a first approximation the sample size in millimoles,  $S$ , is governed by the empirical equation  $S = 0.022 A / \log(C + 1)$ , where  $A$  is the cross-sectional area of the column.

**Choice of Salt.**—The only convenient method known to the authors for the determination of the

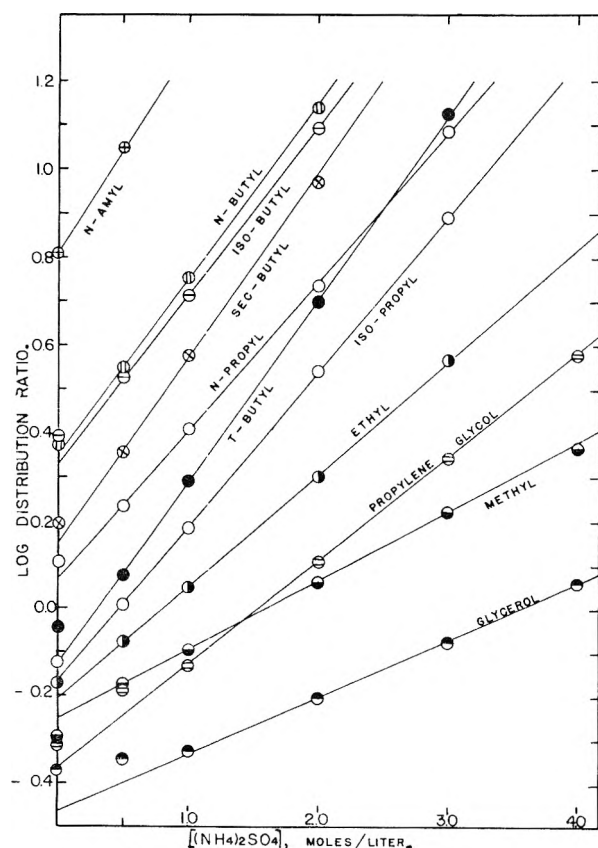
(3) R. Sargent and W. Rieman, *Anal. Chim. Acta*, **14**, 381 (1956).

(4) R. Sargent and W. Rieman, *J. Phys. Chem.*, **60**, 1370 (1956).

TABLE I  
 VALUES OF  $C$  FOR VARIOUS ALCOHOLS AND RESINS

| Resin<br>[(NH <sub>4</sub> ) <sub>2</sub> SO <sub>4</sub> ] | Dowex 1-X8 |       |       |       |       | Dowex 50-X8 |       |       |       |       |      |
|---|------------|-------|-------|-------|-------|-------------|-------|-------|-------|-------|------|
|   | 0.0        | 0.5   | 1.0   | 2.0   | 3.0   | 4.0         | 0.0   | 0.5   | 1.0   | 2.0   | 3.0  |
| Glycerol  | 0.427      | 0.453 | 0.473 | 0.622 | 0.843 | 1.16        | 0.586 | 0.635 | 0.688 | 0.901 | 1.20 |
| Propylene glycol  | .477       | .647  | .740  | 1.29  | 2.21  | 3.83        | .644  | .856  | 1.08  | 1.77  | 3.07 |
| Methyl alcohol  | .507       | .670  | .804  | 1.15  | 1.68  | 2.33        | .839  | .950  | 1.13  | 1.59  | 2.29 |
| Ethyl alcohol   | .673       | .843  | 1.12  | 2.00  | 3.72  | ...         | .839  | 1.08  | 1.46  | 2.46  | 4.57 |
| Isopropyl alcohol   | .753       | 1.02  | 1.53  | 3.48  | 7.76  | ...         | .744  | 1.21  | 1.61  | 3.58  | 8.34 |
| <i>t</i> -Butyl alcohol                                     | .883       | 1.19  | 1.96  | 5.12  | 13.4  | ...         | .662  | 1.20  | 1.90  | 4.78  | 12.9 |
| <i>n</i> -Propyl alcohol                                    | 1.28       | 1.71  | 2.57  | 5.45  | 12.3  | ...         | 1.03  | 1.62  | 2.35  | 5.01  | ...  |
| <i>sec</i> -Butyl alcohol                                   | 1.56       | 2.26  | 3.79  | 9.30  | 26.5  | ...         | 1.07  | 1.73  | 2.88  | 7.48  | ...  |
| Isobutyl alcohol  | 2.47       | 3.34  | 5.17  | 12.3  | ...   | ...         | 1.33  | 2.20  | 3.38  | 8.74  | ...  |
| <i>n</i> -Butyl alcohol                                     | 2.37       | 3.52  | 5.67  | 13.8  | ...   | ...         | 1.28  | 2.17  | 3.53  | 8.44  | ...  |
| <i>n</i> -Amyl alcohol                                      | 6.63       | 11.0  | ...   | ...   | ...   | ...         | 2.69  | 5.03  | 8.33  | ...   | ...  |

very small concentrations of alcohol in the effluent fractions is the spectrophotometric determination of chromic ion produced by the reduction of dichromate.<sup>4</sup> Oxidizing anions such as nitrate and reducing ions such as the halides would interfere in this determination. These facts imposed a severe restriction on the salts suitable for use as eluents. Actually, only ammonium, sodium and magnesium sulfates were tried. Ammonium sulfate was best because of its large solubility and great salting-out power.


 Fig. 2.—Plot of  $\log C$  for Dowex 1.

**Salting-out Constants.**—Values of  $C$  (Table I) were calculated from the data of the various elutions by eq. 1. The logarithms of these values are plotted against the concentrations of ammonium sulfate for Dowex 1 in Fig. 2. These plots follow fairly closely the equation

$$\log C = \log C_0 + kM \quad (2)$$

where  $C_0$  is the distribution ratio in pure water,  $k$  is the salting-out constant and  $M$  is the molarity of ammonium sulfate. The constants of eq. 2 are given in Table III.

Salting-out constants in the absence of resin have been determined<sup>5</sup> by use of eq. 3

$$\log S = \log S_0 - kM \quad (3)$$

where  $S$  is the solubility in ammonium sulfate of molarity  $M$  and  $S_0$  is the solubility in water. The agreement of the  $k$  values in eq. 2 and 3 is shown by solubility measurements for *n*-propyl and *sec*-butyl alcohol. Table II lists the logarithms of the quantities of alcohol (in arbitrary units of absorbance) that were plotted against the concentration of ammonium sulfate to obtain the slope of the line.

 TABLE II  
 SOLUBILITIES IN SOLUTIONS OF AMMONIUM SULFATE  
 Arbitrary units

| [(NH <sub>4</sub> ) <sub>2</sub> SO <sub>4</sub> ] | 2.0   | 2.5   | 3.0   | 3.5   | 4.0      |
|--|-------|-------|-------|-------|----------|
| <i>n</i> -Propyl alcohol                           | 1.240 | 1.063 | 0.897 | 0.781 | <i>a</i> |
| <i>sec</i> -Butyl alcohol                          | 1.069 | 0.867 | 0.601 | 0.438 | 0.233    |

<sup>a</sup> Ammonium sulfate precipitated.

 TABLE III  
 COMPARISON OF VALUES FOR  $C_0$  AND  $k$ 

| Alcohol           | Dowex 1-X8 |       | Dowex 50-X8 |       | Eq. 3<br>$k$ |
|-------------------|------------|-------|-------------|-------|--------------|
|                   | $\log C_0$ | $k$   | $\log C_0$  | $k$   |              |
| Glycerol          | -0.465     | 0.129 | -0.282      | 0.120 |              |
| Propylene glycol  | -.362      | .210  | -.188       | .224  |              |
| Methyl            | -.252      | .158  | -.095       | .151  |              |
| Ethyl             | -.208      | .256  | -.083       | .243  |              |
| Isopropyl         | -.170      | .353  | -.135       | .350  |              |
| <i>t</i> -Butyl   | -.125      | .414  | -.130       | .408  |              |
| <i>n</i> -Propyl  | .070       | .336  | .043        | .330  | 0.341        |
| <i>sec</i> -Butyl | .150       | .422  | .039        | .419  | .420         |
| Isobutyl          | .33        | .38   | .130        | .407  |              |
| <i>n</i> -Butyl   | .35        | .40   | .125        | .405  |              |
| <i>n</i> -Amyl    | .82        | .45   | .44         | .50   |              |

Table III reveals the following facts. (1) The  $C_0$  values of the alcohols increase as their hydrophilic nature decreases. (2) Salting-out constants  $k$  show a rough tendency to increase as the hydrophilic nature of the alcohol decreases. (3) For any one alcohol, the  $k$  values for Dowex 1, Dowex 50 and eq. 3 agree within experimental error.

(5) Setschenow, *Z. physik. Chem.*, **4**, 117 (1889).

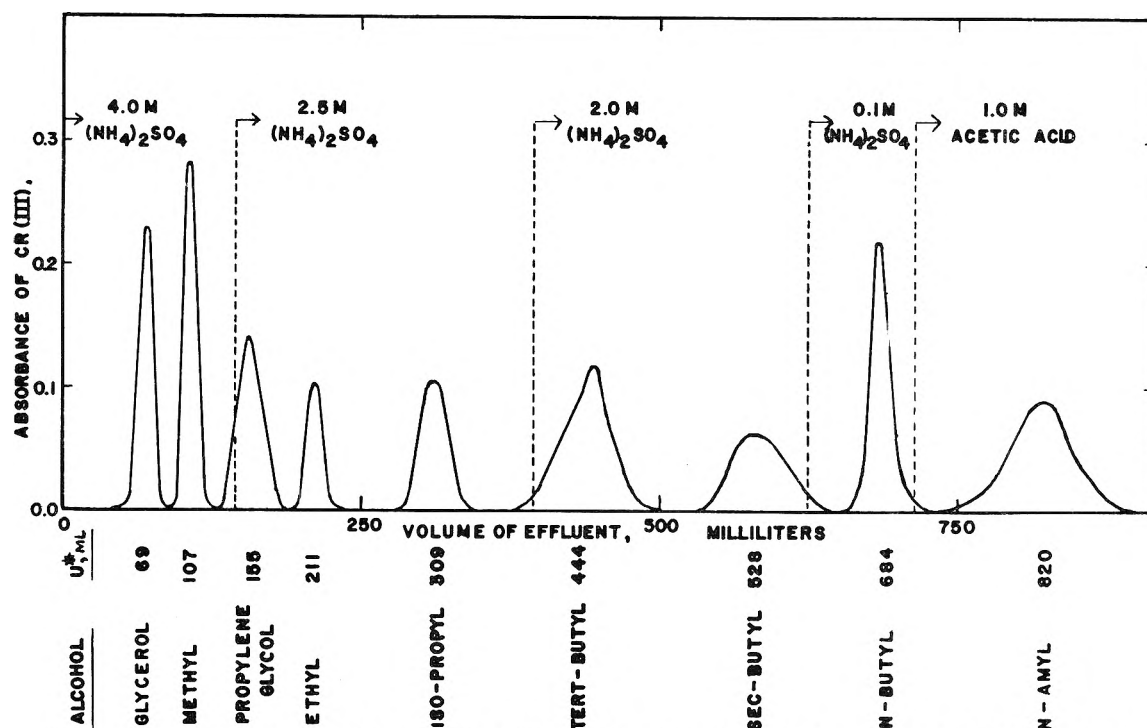


Fig. 3.—Elution of alcohols on Dowex 1X8, 200–400 mesh, sulfate form, 32.0 cm.  $\times$  2.28 cm.<sup>2</sup>, 0.6 cm./min.

In salting-out chromatography, a linear increase in the electrolyte concentration of the eluent produces an exponential increase in the distribution ratio for a given alcohol, *i.e.*, the affinity of the resin for the alcohol is greater for high eluent concentrations. This is a major difference from ion-exchange chromatography where an increase in eluent concentration decreases the distribution ratio of the sample constituent.

**Separation of Alcohol Mixtures.**—Figure 3 shows the separation obtained for a mixture of nine alcohols and the changes of eluent that are required for the separation. Acetic acid was used to “salt-in” the amyl alcohol to the aqueous phase so that it is eluted more rapidly than with water. Acetic acid was chosen since it is one of the few organic compounds which will not reduce dichromate in the analytical procedure. The elution with the specified flow rate required 12 hr. for completion. Normal propyl and isobutyl alcohols, not included in the separation, would be eluted under these conditions with  $U^*$  values very close to *t*-butyl and *n*-butyl alcohols, respectively. Straight-chain, primary alcohols above amyl are absorbed by the resins so tenaciously that excessively long elutions would ensue.

The conditions for the separation represented by Fig. 3 were found almost entirely by calculations based on the plate theory. The concentration of ammonium sulfate was determined that would give a ratio of the values of  $C \geq 1.5$  which is necessary to separate the alcohols by elution from a 30-cm. column. For example, 4 *M* ammonium sulfate is needed to separate the first three alcohols. The eluent concentration is then lowered as much as possible for the rapid elution of the higher alcohols. The positions of peak concentration of the alcohols in the effluent,  $U^*$ , were calculated and

later compared with the experimental values. Sample calculations for  $U^*$  of isopropyl alcohol are given below.

$$\begin{aligned} \log C &= \log C_0 + kM \\ \log C &= -0.170 + (0.353)(4.0) \\ C &= 17.5 \\ U^* &= CV + V \\ U^* &= (17.5)(32.1) + 32.1 \end{aligned}$$

$$U^* (4.0 M \text{ ammonium sulfate}) = 594$$

When the eluent was changed to 2.5 *M* ammonium sulfate at 150 ml., the isopropyl alcohol had moved down the column

$$\frac{150}{594} \times 32.0 = 8.08 \text{ cm.}$$

At the change of eluent, the interstitial volume above the isopropyl alcohol was 8.1 ml. of 4.0 *M* ammonium sulfate. Before the 2.5 *M* ammonium sulfate reaches the isopropyl alcohol, it will have moved an additional 0.4 cm. or 8.5 cm. down the column. The remaining interstitial volume is now 23.6 ml.

$$\begin{aligned} C (2.5 M \text{ ammonium sulfate}) &= 5.14 \\ U^* &= 150 + 8.1 + (5.14)(23.6) + 23.6 \\ U^* &= 303 \end{aligned}$$

The calculated values of  $U^*$  for the 9 alcohols were, respectively, 70, 109, 154, 206, 303, 444, 549, 694 and 880. The observed values are listed in Fig. 3. Agreement was excellent for most of the alcohols.

The height of the column necessary for the separation was calculated from the results of a preliminary elution on a 24.8-cm. column of the same resin. This elution indicated that the separation of propylene glycol from methyl alcohol would be the most difficult. Application of the equation<sup>2</sup> for the calculation of column height necessary to separate these alcohols gave a value of 32.0 cm., which was

used for the separation in Fig. 3.

**Mechanism of Salting-out Chromatography.**—It is suggested that the mechanism for the chromatographic process is governed by solvation. Consider a ternary mixture of resin, water and a small amount of alcohol. The ionic groups on the resin are solvated chiefly by water because its solvation power and concentration are larger than those of the alcohol. When a salt is added, such as ammonium sulfate, which is not soluble in (not solvated by) alcohol, the resin shrinks because part of the water is withdrawn to solvate the ions of the salt. The salt, by virtue of its removal of water from the resin, has therefore increased the number of solvation positions around the ionic groups of the resin which can now be occupied by the hydroxyl groups of the alcohols. The hydrocarbon tail of the

alcohol would be attracted toward the resin matrix. The process is definitely not simple sorption on the resin matrix since the value of  $C$  for the elution of the alcohols from a column of polystyrene-divinylbenzene copolymer with 3.0  $M$  ammonium sulfate is zero.

A study of the salting-out chromatography of the ketones is now being pursued in this Laboratory. Additional studies of other organic compounds and more detailed studies of the nature of the process are planned.

**Acknowledgment.**—The authors express their gratitude to the Dow Chemical Company for generous financial support of this investigation and for the resins used in the work, also to R. M. Wheaton for reading the manuscript and suggesting several changes.

## AN ELECTRON DIFFRACTION INVESTIGATION OF THE STRUCTURE OF CUPROUS CHLORIDE TRIMER<sup>1,2</sup>

BY CHI-HSIANG WONG AND VERNER SCHOMAKER

Contribution No. 2142 from the Gates and Crellin Laboratories of Chemistry, California Institute of Technology, Pasadena, Cal.

Received October 22, 1956

Electron diffraction photographs have been made of cuprous chloride vapor. The Cu-Cl distance is  $2.160 \pm 0.015$  Å. A six-membered alternating ring model of the trimer molecule with  $\angle\text{Cu-Cl-Cu} \sim 90^\circ$  and very large amplitude of symmetric bending vibration seems plausible and is shown to be in agreement with the diffraction pattern.

Cuprous chloride vapor was long regarded as dimeric, on the basis of early vapor density measurements, but in 1948 Brewer and Lofgren<sup>3</sup> reported it to consist of monomer and trimer with no dimer, and said that at 1000°K. the saturated vapor should be 100.0 mole % trimeric. The present diffraction data are apparently similar to those obtained earlier by Maxwell and Mosley and not found to be entirely compatible with any dimer model<sup>4</sup>; our interpretation in terms of the trimer differs, however, from Maxwell's. He reports<sup>5</sup> disagreement with "a six-membered ring structure" and agreement with "a configuration consisting of two sphenoids sharing an edge for the trimer in equilibrium with a relatively high concentration of the monomer." We find agreement with an alternating six-ring structure, of the sort proposed by Brewer and Lofgren (ref. 3, p. 3044) to account for the stability and low entropy of the trimer as well as the relative instability of the dimer, but with a remarkably great amplitude of vibration toward and away from the configuration proposed<sup>6</sup> by Professor Pauling, in which "the copper atoms form a small triangle and the chlorine atoms a large triangle, each chlorine atom being bonded to two copper atoms and each copper atom being bonded to two

chlorine atoms and also the two other copper atoms."

**Experimental.**—Greenish cuprous chloride of C.P. grade was washed in dilute sulfuric acid to obtain a purified white powder which was heated to about 450° in a simple monometal boiler inside our new electron diffraction camera. The photographs (Kodak-50 plates;  $L \sim 10$  cm.;  $\lambda \sim 0.06$  Å.) were interpreted visually in the usual way.<sup>7</sup>

The boiler had a total volume of 0.8 ml. and was usually somewhat less than half full, so that the liquid sample surface was about 0.6 cm.<sup>2</sup>. The orifice was a tube about 1 mm. long and 0.3 mm. or 1 mm. in diameter.

**Results.**—Our photographs show about eight main rings (Fig. 1), graced with a few weak, close-in outer shoulders (1, 3, *a* and *b*); the radial distribution curve correspondingly has a sharp main peak at 2.16 Å. and a very broad secondary peak at about twice the distance (4.23 Å.). There is thus substantial agreement with Maxwell and Mosley's<sup>4</sup> report of "two prominent distances  $l$  and  $2l$ " with  $l$  equal to 2.13 Å.

The necessary information for a detailed demonstration of the trimer structure is clearly not at hand. First of all, there is the possibility that the vapor photographed was a non-equilibrium mixture of evaporated molecular fragments. We have assumed otherwise, however, partly because (1) Professor Brewer has given us his opinion that, under the conditions of the experiment, the vapor from our boiler would probably be predominantly trimeric (the estimated fraction of monomer in the saturated vapor at 450° being only about  $4 \times 10^{-5}$ ),<sup>8</sup> and (2) the change in orifice noted in "Ex-

(1) Presented at the Pasadena Meeting of the American Crystallographic Association, June, 1955.

(2) This work was supported by the Office of Naval Research under Contract N6onr-24423. Reproduction in whole or in part is permitted for any purpose of the United States Government.

(3) L. Brewer and N. L. Lofgren, *J. Am. Chem. Soc.*, **72**, 3038 (1950).

(4) L. R. Maxwell and V. M. Mosley, *Phys. Rev.*, **55**, 238 (A) (1939).

(5) L. R. Maxwell, Abstract, American Crystallographic Association Meeting at Pennsylvania State College, April, 1950.

(6) L. Pauling, private communication to V.S., January 31, 1950.

(7) K. Hedberg and A. J. Stosick, *J. Am. Chem. Soc.*, **74**, 954 (1952).

(8) Leo Brewer, private communication to C. W.

perimental" has no perceptible effect on the diffraction pattern. There is also the possibility that the vapor contains a significant fraction of higher polymers—the tetramer has been found in the vapor at  $150^\circ$  (Rosenstock, *et al.*; see below), and its presence at higher temperatures is suggested by the negative value for  $K_2$  obtained by Brewer and Lofgren (ref. 3, p. 3040) when they interpreted their data on the reaction of Cu with HCl on the assumption that monomer, dimer and trimer might be present. Nevertheless, we have assumed that our diffraction pattern is due entirely to trimer, and this is probably substantially correct. Even so, more than one model can be made to fit. One that has to be rejected as structurally impossible consists of an equilateral triangle of copper atoms, each bonded to a chlorine atom at about 2.16 Å. and to two copper atoms, also at about 2.16 Å.; Cu-Cu = 2.16 Å. cannot be accepted.

The planar alternating six-ring with large  $\angle$ Cl-Cu-Cl ( $\sim 150^\circ$ ) and small  $\angle$ Cu-Cl-Cu ( $\sim 90^\circ$ ) seems the most likely; it has general advantages as cited by Brewer and Lofgren; the bond angles are reasonable<sup>9</sup>; and the great amplitude of symmetric in-plane bending vibration that is required to wash out the unobserved Cu . . . Cu term suggests that Cu . . . Cu is a bonding interaction, as suggested by Professor Pauling, but only weakly and only when all three copper atoms are brought together in quasi-metallic fashion.<sup>10</sup> As may be seen from the plots of distance *vs.*  $\angle$ Cu-Cl-Cu in Fig. 1, almost any equilibrium angle value will lead to a fit with the radial distribution if the temperature factors are properly adjusted,  $90^\circ$  (or even the complementary  $150^\circ$ ) then leading to the greatest conspicuous area above background for the outer peak, whereas larger or smaller angles, with temperature factors adjusted to emphasize the longer of the distances Cu . . . Cl and Cl . . . Cl, center the peak more accurately on the distance 4.23 Å. Angles of much less than  $80^\circ$ , however, would imply too short Cu . . . Cu distances,<sup>11</sup> or else too narrow a Cu . . . Cu distribution, and angles greater than about  $100^\circ$  would hardly represent a reasonable approximation to the structural ideals that we have taken as giving support to the ring model. *A priori* estimates of the vibrational amplitudes would be most helpful but can hardly be made, since we know neither the frequencies nor the actual forms of the several normal modes. We therefore must be content to note that the bending amplitudes quite clearly predominate over the stretching, as expected, and that the symmetrical in-plane bending apparently dominates the asymmetrical, as is made plausible by the argument of quasi-metallic bonding. The relative smallness of the vibrational amplitude for the longest distance

(9) In  $\text{Cu}_2\text{O}$  as well as, presumably, other bicoordinate complexes of  $\text{Cu}^+$ ,  $\angle$ X-Cu-X is  $180^\circ$ ;  $\angle$ M-Cl-M is about  $90^\circ$ , the nominal for  $\text{p}^2$  bonds, in  $\text{PdCl}_2$  and many other bicoordinate complexes of  $\text{Cl}^-$ .

(10) It could even be suggested that this last aspect of the trimer structure has something to do with its stability relative to the corresponding tetramer, which could have just the ideal bond angles of  $90^\circ$  and  $180^\circ$  but would contain the germ of a different, possibly less stable fragment of metal structure.

(11) The shortest Cu . . . Cu distance in cuprite is 3.01 Å., both for inter- and intra-network contacts. In copper itself, Cu-Cu is 2.55 Å.

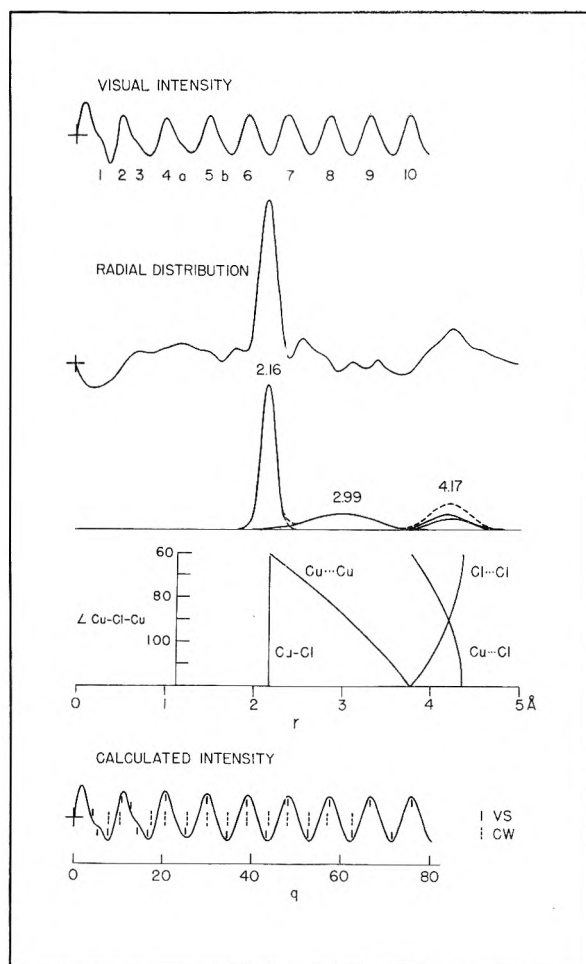


Fig. 1.—Visual intensity and radial distribution curves for cuprous chloride. A synthetic radial distribution, plots of interatomic distance *vs.*  $\angle$ Cu-Cl-Cu, and a theoretical intensity curve for the alternating, planar, trimeric ring model described in the text.

in the molecule then invariably follows from the *r vs.*  $\angle$ Cu-Cl-Cu plots, which of course describe the relative effects of the symmetrical bending mode. The illustrated theoretical intensity curve<sup>12</sup> and synthetic distance distribution (drawn with approximate allowance for the artificial temperature factor) and the  $q_{\text{calc}}$  values for the best rings (Table I) are for a model with Cu-Cl = 2.16 Å.,  $\angle$ Cu-Cl-Cu =  $87.5^\circ$ ,  $a_{\text{Cu} \dots \text{Cu}} = \frac{1}{2}(\delta r^2_{\text{Cu} \dots \text{Cu}} - \delta r^2_{\text{Cu-Cl}}) = 0.06 \text{ \AA.}^2$ ,  $a_{\text{Cu} \dots \text{Cl}} = a_{\text{Cl} \dots \text{Cl}} = 0.02 \text{ \AA.}^2$ , and  $\{(Z-f)_{\text{Cu}}/(Z-f)_{\text{Cl}}\}_{\text{effective}} = 1.3$ , as is a fair approximation<sup>13</sup> for the range  $0 < q < 20$  of greatest relevance. The theoretical curve is in good agreement with our observations, both of the qualitative aspects ( $a_{\text{Cl} \dots \text{Cl}}$  should probably be reduced somewhat) and, as shown by the arrows, of the ring diameters. The determination of Cu-Cl in Table I is substantially independent of the exact choice of angle and *a* values, the temperature factor for all terms except Cu-Cl being so severe. We conclude that Cu-Cl is 2.160 Å. with limit of error  $\pm 0.015 \text{ \AA.}$  and that the trimer structure is probably the alternating planar six-ring, with  $\angle$ Cu-Cl-Cu  $\sim 90^\circ$

(12) Various theoretical curves were calculated to test our conclusions from the radial distribution curve.

(13) J. A. Ibers and Jean A. Hoerni, *Acta Cryst.*, **7**, 405 (1954).

and with a very large amplitude of symmetrical bending vibration.

**Discussion.**—A Cu-Cl distance of 2.16 Å. corresponds to a Cu radius of 1.17 Å., in good agreement with the value of 1.18 Å. from Cu<sub>2</sub>O,<sup>14</sup> and considerably shorter than the tetrahedral value, 1.35 Å. The difference between the tetrahedral radius and the Ag<sub>2</sub>O radius for Ag<sup>+</sup> is similar,<sup>14</sup> but we know no other examples for Cu<sup>+</sup>.<sup>16</sup>

Some recent mass-spectrometric observations<sup>16</sup> on the cuprous halides seem to tie in with the notion that the copper atoms in (CuCl)<sub>3</sub> have a tendency to form a bonded group of some stability. With 75-volt electrons, the vapor from cuprous chloride held at about 150° produced a main sequence of ions derivable from a parent trimer ion by removal of successive chlorine atoms (Cu<sub>3</sub>Cl<sub>3</sub><sup>+</sup>,

(14) See L. Pauling, "The Nature of the Chemical Bond," Cornell University Press, Ithaca, N. Y., 2nd Ed., 1940, p. 186.

(15) N. V. Sidgwick ("The Chemical Elements and Their Compounds," Oxford University Press, Oxford, England, 1950, p. 116) in discussing AgCN did not allow for the Ag<sup>+</sup> difference and so was misled into ascribing the correspondingly very large decrement in the observed distance entirely to resonance; Ag(CN)<sub>2</sub><sup>-</sup> (p. 134) similarly shows a large decrement.

(16) H. M. Rosenstock, J. R. Sites, J. R. Walton and Russell Baldoek, *J. Chem. Phys.*, **23**, 2442 (1955).

TABLE I  
DETERMINATION OF  $\tau_{\text{Cu-Cl}}$  IN (CuCl)<sub>3</sub>

| Min. | Max. | $q_{\text{calcd}}^a$ | $\frac{(q_{\text{calcd}}/q_{\text{obsd}})_{\text{V.S.}}}{(q_{\text{calcd}}/q_{\text{obsd}})_{\text{C.W.}}}$ |
|------|------|----------------------|---|
|      | 4    | 20.6                 | (0.982)   |
| 5    |      | 25.6                 | (1.008)   |
|      | 5    | 29.9                 | 0.995   |
| 6    |      | 34.5                 | .993  |
|      | 6    | 39.1                 | .999  |
| 7    |      | 43.7                 | .999  |
|      | 7    | 48.3                 | .995  |
| 8    |      | 52.9                 | .996  |
|      | 8    | 57.5                 | .991  |
| 9    |      | 62.1                 | .983  |
|      |      | av. <sub>3</sub>     | 0.9939  |
|      |      | a.d.                 | .0036   |

$$\tau_{\text{Cu-Cl}} = 2.175 \times 0.9933 = 2.160 \text{ \AA.}$$

<sup>a</sup> For model described in text.

Cu<sub>3</sub>Cl<sub>2</sub><sup>+</sup>, Cu<sub>3</sub>Cl<sup>+</sup> and Cu<sub>3</sub><sup>+</sup>) and weaker sequences of ions containing one, two or four copper atoms but almost no ions containing more chlorine atoms than copper atoms.

We wish to express our thanks to Professor Pauling for suggesting the problem and to Professor Brewer for advice about the properties of cuprous chloride vapor.

## AUTOXIDATION OF 1,4-DIMETHYLCYCLOHEXANE<sup>1</sup>

BY V. STANNETT, A. E. WOODWARD AND R. B. MESROBIAN

Contribution from Institute of Polymer Research, Polytechnic Institute of Brooklyn, Brooklyn 1, N. Y.

Received October 24, 1956

The kinetics of the liquid phase autoxidation of 1,4-dimethylcyclohexane have been studied. Following the initial auto-catalytic increase in both the amount of oxygen absorbed and the formation of 1,4-dimethylcyclohexane hydroperoxide, maximum rates of oxidation and steady hydroperoxide concentrations are attained. The results indicate that a chain mechanism is followed. A value of 31 was found for the initial chain length of the reaction at 95°. In later stages of the reaction, the products of oxidation reduce the rate of oxygen absorption while accelerating the decomposition of the hydroperoxide. The decomposition of 1,4-dimethylcyclohexane hydroperoxide in its parent hydrocarbon also was studied. A second-order dependence of the hydroperoxide concentration was operative at the concentrations and temperatures employed in the autoxidations. At higher temperatures and low hydroperoxide concentrations a first-order dependence was obtained.

The first comprehensive interpretation of the kinetics of the autoxidation of various hydrocarbons was reported by Bolland and Gee.<sup>2,3,4</sup> Since that time a number of olefinic hydrocarbons in the initial stages of autoxidation have been found to follow the kinetic scheme proposed by those authors.<sup>4</sup> This scheme involves a free radical chain process with the initial formation of a hydroperoxide which acts as the initiator of further autoxidation.

The Bolland and Gee mechanism can be extended mathematically, as shown previously by Tobolsky and co-workers<sup>5</sup> to predict the kinetic behavior occurring upon extensive autoxidation. A recent study of the kinetics of tetralin oxidation activated by cobaltous acetate<sup>6</sup> gave support to this theory.

To explore the occurrence of maximum rates of oxidation accompanied by steady hydroperoxide concentrations as predicted,<sup>5</sup> the kinetics of 1,4-dimethylcyclohexane (DMCH) autoxidation initiated thermally has been studied and the results presented herein. This specific hydrocarbon was selected for reasons of ready availability, ease of purification, oxidizability at measurable rates below the boiling point, and previous knowledge of the oxidation products.<sup>7</sup>

### Experimental

**Reagents.**—1,4-Dimethylcyclohexane (Dougherty Chemical, technical grade) was freed from olefins by shaking with sulfuric acid and fractionally distilled, the fraction boiling at 120° being taken for use. Only minute traces of peroxide could be detected iodometrically in the hydrocarbon after purification.

1,4-Dimethylcyclohexane hydroperoxide was prepared by the thermal oxidation of 1,4-dimethylcyclohexane at 95° up to a point where all the oxygen gas absorbed could still be accounted for as the hydroperoxide. The solution obtained was then concentrated at room temperature under

(1) This work was supported by the Office of Naval Research, Project Number NR 033-292.

(2) J. L. Bolland and G. Gee, *Trans. Faraday Soc.*, **42**, 236 (1946).

(3) J. L. Bolland, *Proc. Roy. Soc. (London)*, **186A**, 218 (1946).

(4) L. Bateman, *Quart. Revs.*, **8**, 147 (1954).

(5) A. V. Tobolsky, D. J. Metz and R. B. Mesrobian, *J. Am. Chem. Soc.*, **72**, 1942 (1950).

(6) A. E. Woodward and R. B. Mesrobian, *ibid.*, **75**, 6189 (1953).

(7) G. Chavanne and E. Bode, *ibid.*, **52**, 1609 (1930); P. George and A. D. Walsh, *Trans. Faraday Soc.*, **42**, 94 (1946).

vacuum to give a solution containing 45% of the hydroperoxide. Portions of this solution were diluted with a given amount of pure 1,4-dimethylcyclohexane and used for the kinetic studies of the hydroperoxide decomposition.

A commercial grade of benzoyl peroxide was purified by dissolving in chloroform and precipitating by the addition of methanol, the precipitated peroxide then being filtered and dried under vacuum.

Reagent grade chlorobenzene was taken from freshly opened bottles and distilled before use.

Reagent grade materials were employed in the analytical procedure for estimation of hydroperoxides.

**Procedures.**—The simultaneous measurement of oxygen absorption and hydroperoxide content were carried out using a constant pressure type apparatus. A U-tube manometer containing tricresyl phosphate was used to detect small changes in internal pressure. The reaction flask was of the erlenmeyer type fitted with an extra ground glass socket on the side of the flask by which a thermometer was placed in the oxidizing liquid. Stirring was carried out magnetically. The reaction flask, stirrer and a compensation vessel were enclosed in a constant temperature box.

Measured amounts of each reagent used in a particular run were added to the reaction vessel, the flask connected to a manifold line with a mercury sealed ground glass joint and the whole apparatus flushed with oxygen. The box was raised to the desired temperature, the excess gas released, and stirring started. As oxygen was absorbed the pressure was adjusted back to atmospheric. The volume of gas absorbed was read off on a graduated buret and the readings corrected to 0°. The data were further corrected in order to express the amount of oxygen absorbed in terms of the unreacted hydrocarbon content of the reaction mixture.

Stirring rates of 75 r.p.m. or greater gave rates of oxidation independent of the stirring speed. The same oxidation rates were found when different sized reaction vessels were used and when glass beads were added to increase the surface area.

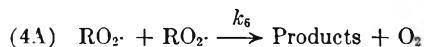
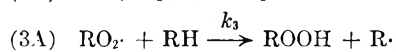
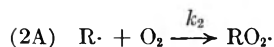
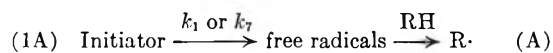
To measure the hydroperoxide content of the hydrocarbon, the thermometer was removed from the reaction vessel and a slow stream of oxygen passed through the apparatus. A one-ml. sample of hydrocarbon was then removed using a pipet fitted with a rubber bulb. The oxygen flow was stopped, the thermometer replaced and the gas buret set back to zero at atmospheric pressure. As the whole operation only took about three minutes, whereas the absorption experiments lasted several days, no appreciable error was involved by the temporary opening of the apparatus.

The hydrocarbon samples were analyzed for hydroperoxide using a procedure which was essentially that of Wagner, Smith and Peters.<sup>8</sup>

The kinetics of the decomposition of 1,4-dimethylcyclohexane hydroperoxide under non-oxidizing conditions were studied, using an experimental method described previously.<sup>9</sup>

## Results and Discussion

The Bolland and Gee mechanism<sup>2,3</sup> may be represented as follows when the oxygen pressure is sufficiently high to produce termination by equation 4A



The free radicals formed by decomposition of the initiator extract a hydrogen atom from the hydrocarbon (RH) to give the hydrocarbon radical (R·) which enters into a chain reaction to form the hy-

droperoxide (ROOH). In the case of the oxidation of 1,4-dimethylcyclohexane, product analysis indicates<sup>7</sup> that the tertiary hydrogen atom is extracted and the hydroperoxide group is found at that position on the ring.

Termination steps other than the one represented in this mechanism (step 4) are not appreciable when [RO<sub>2</sub>·] is large with respect to [R·]. Under these conditions the rate of oxygen absorption is independent of the oxygen pressure.<sup>2,3</sup> To check this independence the rate of oxygen uptake of a given amount of DMCH at 95° using pure oxygen was studied and then a similar run with dry air substituted for the oxygen was made. The oxygen absorption rates were found to be the same.

Kinetic analysis of mechanism A, when benzoyl peroxide (BzO<sub>2</sub>) is acting as the sole initiator, leads to the following equation for the initial rate of oxygen absorption

$$-\frac{d[\text{O}_2]}{dt} = k_3(e_i k_7 / 2k_6)^{1/2} [\text{RH}] [\text{Initiator}]^{1/2} \quad (1)$$

where  $e_i$  is the efficiency of the initiator and  $k_7$  the rate constant for the decomposition of the initiator. Since the decomposition of benzoyl peroxide in the presence of radical acceptors is essentially first order,<sup>10</sup> the initiator concentration appears in the rate expression to the  $1/2$  power.

The half power dependence of the rate of oxidation on the benzoyl peroxide concentration has been found for 1,4-dimethylcyclohexane oxidation as is shown in Table I.

TABLE I  
OXIDATION OF 1,4-DIMETHYLCYCLOHEXANE AT 71°  
Initial rate vs. [BzO<sub>2</sub>]      Initial rate vs. [ROOH]

| Rate <sup>a</sup> | [BzO <sub>2</sub> ],<br>moles/l. | Cor.<br>rate <sup>b</sup><br>[BzO <sub>2</sub> ] <sup>-1/2</sup> | Rate <sup>a</sup> | [ROOH],<br>moles/l. | Cor.<br>rate <sup>b</sup><br>[ROOH] |
|-------------------|----------------------------------|--|-------------------|---------------------|-------------------------------------|
| 0.37              | 0                                | ..   | 0.37              | 0                   | ..                                  |
| 3.20              | 0.104                            | 8.5  | 2.04              | 0.315               | 5.3                                 |
| 6.03              | 0.489                            | 8.1  | 2.76              | .442                | 5.4                                 |
| 8.05              | 1.00                             | 7.7  | 3.74              | .662                | 5.2                                 |
| 10.4              | 1.52                             | 8.1  | 4.75              | .843                | 5.2                                 |

<sup>a</sup> Moles of oxygen absorbed/25 ml. of soln./hour. <sup>b</sup> The corrected rates were obtained by subtraction of the rate in the absence of initiator from the observed rates.

When DMCH hydroperoxide is used as the initiator, a *first* power dependence of the initial rate of oxygen absorption on the initiator concentration, [ROOH], is found, as can be seen in Table I. This proportionality between the oxidation rate and the hydroperoxide concentration has been obtained previously for certain olefins<sup>2-4</sup> and indicates the participation of two hydroperoxide molecules in the decomposition step. This behavior was explained as being due to the formation of hydroperoxide dimers,<sup>11</sup> strong association in concentrated solutions being indicated from infrared data.

For a further confirmation of the oxidation rate dependence on the initiator concentration, the decomposition of DMCH hydroperoxide in DMCH was studied, as briefly reported elsewhere.<sup>12</sup> At a

(8) C. D. Wagner, E. H. Smith and E. D. Peters, *Anal. Chem.*, **19**, 976 (1947).

(9) V. Stannett and R. B. Mesrobian, *J. Am. Chem. Soc.*, **72**, 4125 (1950).

(10) C. E. H. Bawn and S. F. Mellish, *Trans. Faraday Soc.*, **47**, 1216 (1951).

(11) L. Bateman and H. Hughes, *J. Chem. Soc.*, 4594 (1952).

(12) V. Stannett and R. B. Mesrobian, *Faraday Soc. Disc.*, **14**, 242 (1953).

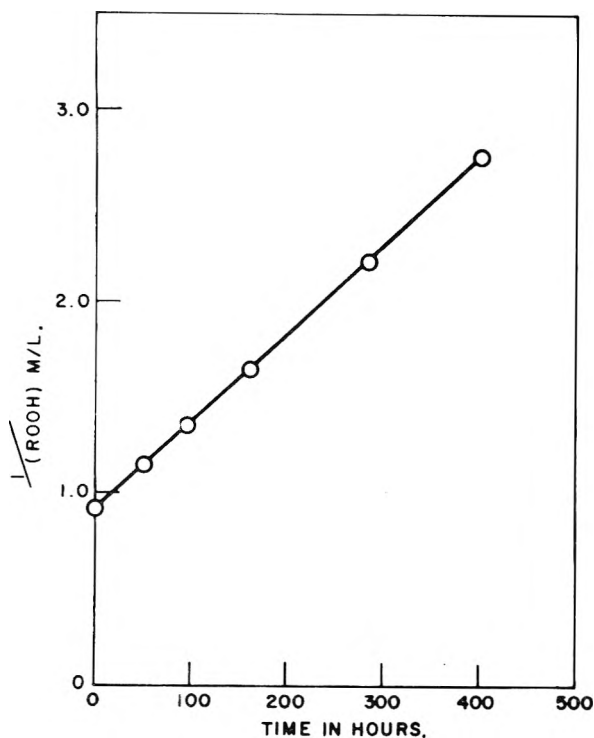


Fig. 1.—The decomposition of 1,4-dimethylcyclohexane hydroperoxide in 1,4-dimethylcyclohexane at 85°.

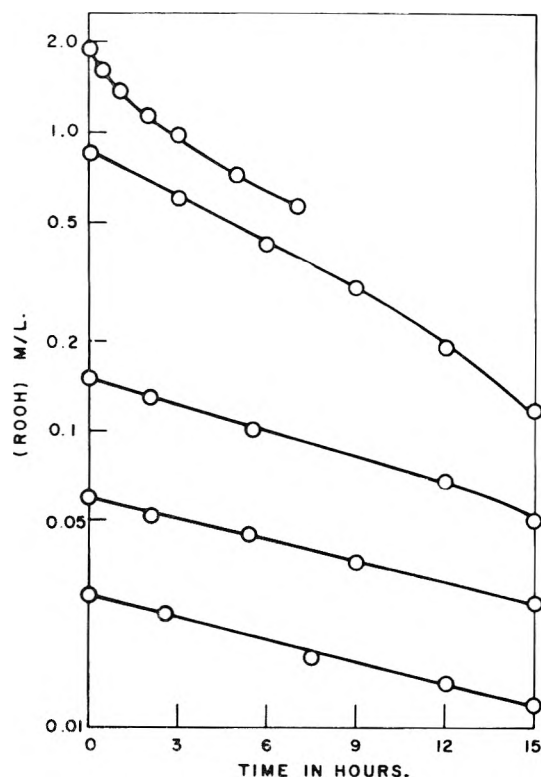


Fig. 2.—The decomposition of 1,4-dimethylcyclohexane hydroperoxide in 1,4-dimethylcyclohexane at 120°.

temperature of 85° and an initial hydroperoxide concentration of 1.09 molar, a reaction second order with respect to the hydroperoxide concentration occurred; a plot of these data is given in Fig. 1. However, other studies at high temperatures and more dilute initial hydroperoxide concentrations

gave a first-order dependence as is seen from the log concentration *versus* time plot in Fig. 2. This same behavior has been reported for cyclohexenyl hydroperoxide<sup>11</sup> and is consistent with the postulate of hydroperoxide association mentioned above. The first- and second-order rate constants for the decomposition of DMCH hydroperoxide were determined at a number of temperatures and are given in Table II. From these data activation energies of 32.8 kcal. for the first-order reaction and 28.6 kcal.

TABLE II  
DECOMPOSITION OF 1,4-DIMETHYLCYCLOHEXANE HYDROPEROXIDE AT VARIOUS TEMPERATURES

| Temp., °C. | 1st order-hr. <sup>-1</sup> | Rate constants<br>2nd order-moles ROOH/mole RH/<br>hr. |        |
|------------|-----------------------------|--|--------|
|            |                             | Obsd.  | Calcd. |
| 85         | ...                         | 0.026  | 0.018  |
| 95         | ...                         | 0.091  | 0.098  |
| 100        | ...                         | 0.141  | ...    |
| 106        | ...                         | 0.300  | 0.45   |
| 110        | 0.017                       | ...  | ...    |
| 120        | 0.059                       | 1.00   | ...    |
| 137        | 0.114                       | ...  | ...    |

for the second-order reaction were calculated. The calculated values listed in the fourth column are discussed in the last paragraph of this article.

In accord with the results given above, the breakdown of the hydroperoxide during oxidation of DMCH would be concurrently first and second order with respect to the hydroperoxide concentration. However, due to the temperatures employed for the oxidations and the hydroperoxide levels reached in the early stages, the second-order decomposition would predominate, as is indicated by the first-order dependence of the initial oxidation rate on the hydroperoxide concentration.

The rate of autooxidation, as given by mechanism A, would be<sup>2,3</sup>

$$-\frac{d[\text{O}_2]}{dt} = k_3 \left(\frac{k_1}{k_6}\right)^{1/2} [\text{ROOH}] [\text{RH}] \quad (2)$$

assuming the initiation step<sup>2,3</sup>



occurs. During the early stages of autooxidation the amount of hydroperoxide present is equal to the amount of oxygen absorbed. Under these conditions the hydroperoxide which decomposes to initiate further oxidation is very small. However, as the hydroperoxide concentration increases, with a proportional increase in the rate of oxidation, the rate of decomposition increases to a point where it equals the rate of formation. The steady concentration of hydroperoxide,  $[\text{ROOH}]_\infty$ , which results is given by<sup>5</sup>

$$[\text{ROOH}]_\infty = \frac{k_3 [\text{RH}]}{(k_1 k_6)^{1/2}} \quad (3)$$

The resulting maximum rate of oxidation,  $(d[\text{O}_2]/dt)_\infty$ , is found to be<sup>5</sup>

$$[-d[\text{O}_2]/dt]_\infty = \frac{k_3^2 [\text{RH}]^2}{k_6} \quad (4)$$

As can be seen in Fig. 3, where plots of oxygen absorption and hydroperoxide content of DMCH with time at 95° are given, the general qualitative fea-

tures outlined above are apparent. There is, however, a decrease of the hydroperoxide content after attainment of the steady concentration, accompanied by a falling off of the rate of oxygen absorption. These effects occur at a point where appreciable amounts of hydroperoxide decomposition products,<sup>7</sup> principally 1,4-dimethylcyclohexane-1-ol, are present. Since water and acids<sup>7</sup> are also products, this decomposition may proceed partly by an ionic mechanism<sup>13</sup> giving products which do not initiate oxidation.

The dependence of the maximum rate of oxidation on the square of the hydrocarbon concentration, predicted in equation 4, was confirmed for DMCH oxidation at 100° in chlorobenzene solutions. A plot of the maximum rate values *versus* the square of the appropriate hydrocarbon concentration of the oxidizing solution gives a straight line passing through the origin, as shown in Fig. 4.

As demonstrated previously,<sup>5</sup> integrated expressions, assuming the hydrocarbon concentration is constant, can be obtained which express the amount of oxygen absorbed,  $-[O_2]_t$ , and the concentration of hydroperoxide present,  $[ROOH]_t$ , at time  $t$  during hydrocarbon autoxidation in terms of  $[ROOH]_\infty$ , a constant,  $a$ , equal to  $k_3(k_1/k_6)^{1/2}/[RH]$ , the initial hydroperoxide content,  $[ROOH]_0$ , and the time,  $t$ . These expressions can be written as<sup>5</sup>

$$\ln \left\{ \frac{[ROOH]_\infty}{[ROOH]_t} - 1 \right\} = \ln \left\{ \frac{[ROOH]_\infty}{[ROOH]_0} - 1 \right\} - at \quad (5)$$

$$-[O_2]_t = [ROOH]_\infty at + [ROOH]_\infty \ln \left( \frac{[ROOH]_0}{[ROOH]_\infty} \right) \left( 1 - \left( 1 - \frac{[ROOH]_\infty}{[ROOH]_0} \right) e^{-at} \right) \quad (6)$$

The quantity  $[ROOH]_\infty/[ROOH]_0$  appearing in these equations has been shown<sup>5</sup> to be equal to the initial chain length of the reaction.

As is evident in Fig. 3 at 95° the hydroperoxide concentrations reach a maximum value of 0.267 mole/mole RH. Taking this value as  $[ROOH]_\infty$ , a plot of  $[ROOH]_t$  as a function of time using equation 5 gives a straight line from which values of 0.060 for  $a$  and 31 for  $[ROOH]_\infty/[ROOH]_0$  were obtained. Since the latter value, as pointed out above, is equal to the initial chain length, 31 molecules of hydroperoxide are formed per free radical initiating the reaction before termination occurs in the initial stages of the autoxidation of DMCH at 95°. By substitution of these values for  $a$  and  $[ROOH]_\infty/[ROOH]_0$  in equation 6, a curve expressing the amount of oxygen absorbed as a function of time was calculated and is shown in Fig. 3. It is seen that the theoretical curve, although in agreement with the experimental points in the autocatalytic region, exhibits a higher maximum rate. The reason for this discrepancy is not completely clear but may be connected with the decrease of the hydroperoxide content at relatively high extents of oxidation. Among the major products of the oxidation other than the hydroperoxide is the tertiary alcohol, 1,4-dimethylcyclohexane-1-ol.<sup>7</sup> For this reason the effects of adding small amounts of a tertiary alcohol, *t*-amyl alcohol, were studied. Defi-

(13) A. V. Tobolsky and R. B. Mesrobian, "Organic Peroxides," Interscience Publishers, New York, N. Y., 1954, pp. 117-120.

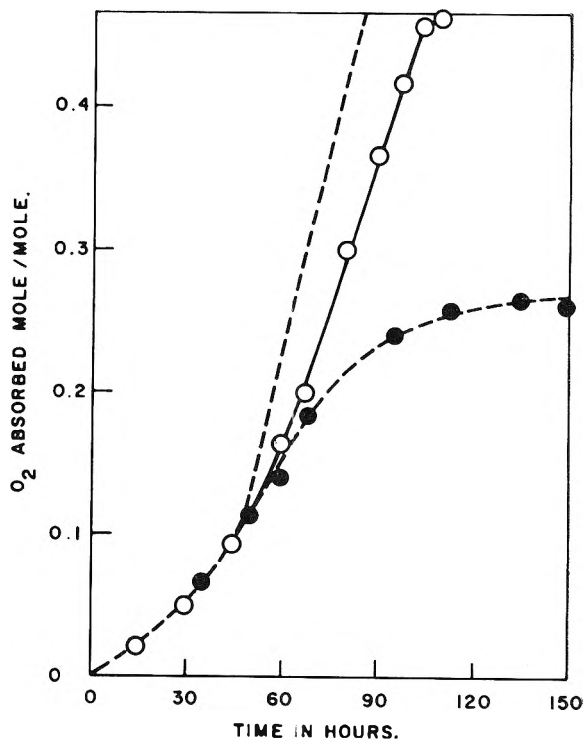


Fig. 3.—Thermal autoxidation of 1,4-dimethylcyclohexane at 95°: O, oxygen absorbed; ●, oxygen absorbed as ROOH; - - - - , theoretical curve.

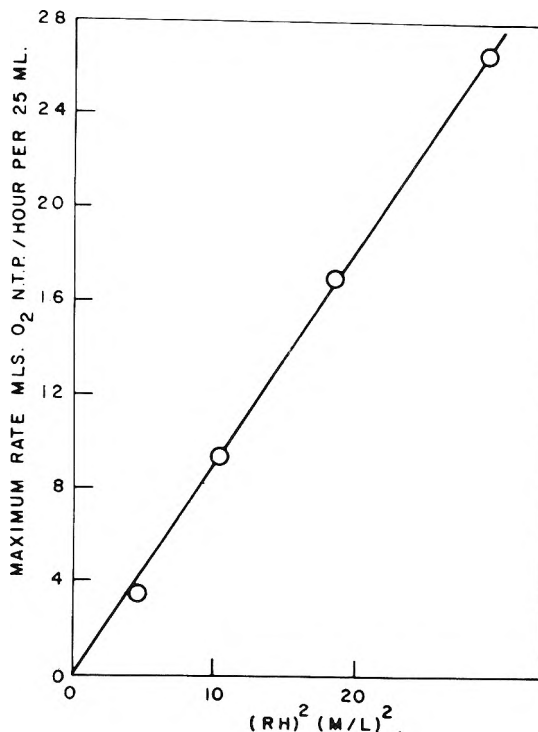


Fig. 4.—Dependence of the maximum rate of oxidation on the square of the 1,4-dimethylcyclohexane concentration in chlorobenzene at 100°.

nite decreases in the oxidation rates occurred. This effect of alcohols on the rate of oxidation of hydrocarbons also has been noted by other workers.<sup>14</sup>

(14) A. Robertson and W. A. Waters, *Trans. Faraday Soc.*, **42**, 201 (1946); P. George, E. K. Rideal and A. Robertson, *Proc. Roy. Soc. (London)*, **185A**, 288 (1946).

Rates of oxidation and hydroperoxide concentrations also were measured at two other temperatures, the experimental curves showing similar behavior to that seen in Fig. 3. The observed maximum rates and steady hydroperoxide values at the three temperatures are given in Table III. Using these data, activation energies of 16.8 kcal. for the experimental maximum rate and  $-10.7$  kcal. for the steady hydroperoxide concentration  $[\text{ROOH}]_{\infty}$  were calculated. From the theoretical plots of the oxygen absorbed as a function of time, obtained as outlined above, maximum oxidation rates at 85, 95 and  $106^{\circ}$  were calculated and are compared with the observed values in Table III.

By inspection of equations 3 and 4, it is seen that  $k_2$ , the rate constant for the decomposition of

TABLE III  
MAXIMUM RATES OF OXIDATION AND STEADY HYDROPEROXIDE CONCENTRATIONS FOR 1,4-DIMETHYLCYCLOHEXANE

| Temp., $^{\circ}\text{C}$ . | Max. rate, moles obsd. | $\text{O}_2/\text{mole RH/hr.}$ calcd. | $[\text{ROOH}]_{\infty}$ , moles/mole RH/hr. |
|-----------------------------|------------------------|--|--|
| 85                          | 0.0037                 | 0.0069                                 | 0.45   |
| 95                          | .0070                  | .0099                                  | .267   |
| 106                         | .0136                  | .028                                   | .173   |

the hydroperoxide, is equal to  $[-d[\text{O}_2]/dt]_{\infty}/[\text{ROOH}]_{\infty}^2$ . Rate constants calculated in this manner from the data given in Table III, using the observed maximum rate values, are compared in Table II with those found by measurements of hydroperoxide decomposition under non-oxidizing conditions.

## THE EQUILIBRIA OF CADMIUM HYDROXIDE IN ACIDIC AND BASIC MEDIA AT $25^{\circ}$

BY K. H. GAYER AND LEO WOONTNER<sup>1</sup>

Contribution from the Department of Chemistry, Wayne State University, Detroit, Michigan

Received October 26, 1956

The solubility of cadmium hydroxide has been studied in perchloric acid and in sodium hydroxide solution at  $25^{\circ}$ . Cadmium hydroxide was found to have fairly strong basic properties but it was also found to exhibit some acidic properties.

The purpose of this investigation was to obtain solubility and reaction data for cadmium hydroxide in dilute perchloric acid and sodium hydroxide solutions. At present the published work is incomplete (1) in regard to reaction of cadmium hydroxide in acidic and basic media, (2) the ionic species involved in these reactions, and (3) the thermodynamic quantities involved.

A summary of published work on cadmium hydroxide equilibria is collected in Table I.

TABLE I

| Source                               | Equilibria reported | Value reported                         |
|--------------------------------------|---------------------|--|
| Bodlander <sup>2</sup>               | Water solubility    | $8.1 \times 10^{-6}$ mole/l.           |
| Piater <sup>3</sup>                  | Water solubility    | $1.8 \times 10^{-6}$ mole/l.           |
| Ishikawa and Shibata <sup>4</sup>    | Water solubility    | $1.4 \times 10^{-5}$ mole/l.           |
| Oka <sup>5</sup>                     | Water solubility    | $8.5 \times 10^{-6}$ mole/l.           |
| DeWys <sup>6</sup>                   | Solubility product  | $K_{\text{SP}} = 2.8 \times 10^{-14}$  |
| Ishikawa and Shibata <sup>4</sup>    | Solubility product  | $K_{\text{SP}} = 1.18 \times 10^{-14}$ |
| Moeller and Rhymer <sup>7</sup>      | Solubility product  | $K_{\text{SP}} = 3.2 \times 10^{-14}$  |
| Feitknecht and Reinmann <sup>8</sup> | Solubility product  | $K_{\text{SP}} = 6.1 \times 10^{-16}$  |

Piater<sup>3</sup> reported a solubility minimum of  $1.3 \times 10^{-6}$  mole/l. between 0.01 and 0.10 *N* NaOH and

a primary acid dissociation constant of  $1 \times 10^{-19}$ . Scholder and Staufebiehl<sup>9</sup> obtained a solid,  $\text{Na}_2\text{Cd}(\text{OH})_4$ , from 15 *N* NaOH solutions of  $\text{Cd}(\text{OH})_2$  while Latimer<sup>10</sup> states that no appreciable amounts of cadmate ion are formed in dilute hydroxide solutions.

### Experimental

The preparation of general reagents (conductivity water, NaOH solutions,  $\text{HClO}_4$  solutions), equilibration samples and the procedures and equipment used in equilibration, filtration and the determination of hydrogen ion concentration have been previously described by Gayer and Leider.<sup>11</sup>

**Cadmium Hydroxide.**—Relatively large crystals of  $\text{Cd}(\text{OH})_2$  were obtained by means of the slow hydrolysis of a dilute solution of cadmium acetate. The cadmium acetate was prepared by dissolving 10 g. of Merck cadmium metal in 100 ml. of B. & A. acetic acid and 5 ml. of Mallinckrodt 30% hydrogen peroxide. The crystals obtained by evaporation were dissolved in conductivity water and boiled for several weeks while maintaining a constant solution volume by the addition of water. An intermediate fraction of the hydrolysis-deposited solid was thoroughly washed and transferred to the sample preparation apparatus together with a few drops of carbonate free NaOH solution. Washing was then continued to the absence of a sodium flame test. The product was found to be both carbonate and acetate free.

**Analysis for Cadmium.**—The concentration of the cadmium-bearing species in solution was determined by means of a model B Beckman spectrophotometer as the cadmium dithione complex. The analytical procedure was adapted from that described by Saltzman.<sup>12</sup>

### The Data and Calculated Results

**The Equilibria in Dilute Acid.**—The solubility data and the numerical values of the equilibrium

(1) From a dissertation submitted by Mr. Woontner in partial fulfillment of the requirements for the Doctor of Philosophy degree at Wayne State University.

(2) G. Bodlander, *Z. physik. Chem.*, **27**, 66 (1898).

(3) J. Piater, *Z. anorg. allgem. Chem.*, **174**, 321 (1938).

(4) F. Ishikawa and E. Shibata, *Sci. Reports Tohoku Imp. Univ.*

(5) Y. Oka, *J. Chem. Soc. Japan*, **61**, 311 (1940).

(6) H. J. deWys, *Rec. trav. chim.*, **44**, 663 (1925).

(7) T. Moeller and P. W. Rhymer, *This Journal*, **46**, 477 (1942).

(8) W. Feitknecht and R. Reinmann, *Helv. Chim. Acta*, **34**, 2255 (1951).

(9) E. P. Scholder and E. Staufebiehl, *Z. anorg. Chem.*, **247**, 259 (1941).

(10) W. M. Latimer, "Oxidation Potentials," Prentice-Hall, Inc., New York, N. Y., 2nd Edition, 1952, p. 172.

(11) K. H. Gayer and H. Leider, *J. Am. Chem. Soc.*, **77**, 1448 (1955).

(12) B. E. Saltzman, *Anal. Chem.*, **25**, 493 (1953).

constant for the reaction in acid solution are collected in Table II.

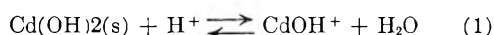
TABLE II

SOLUBILITY OF CADMIUM HYDROXIDE IN PERCHLORIC ACID AT 25°

| Obsd. pH<br>(equilibrium) | Activity of<br>HClO <sub>4</sub><br>× 10 <sup>8</sup> | Molal concn.<br>of cadmium<br>× 10 <sup>4</sup> | K <sub>1</sub> × 10 <sup>-4</sup> |
|---------------------------|---|---|-----------------------------------|
| 8.98                      | (Water solubility)                                    | 0.15  | 1.4                               |
| 7.62                      | 2.4   | 15.1  | 6.3                               |
| 7.35                      | 4.5   | 19.5  | 4.3                               |
| 7.05                      | 8.5   | 44  | 5.2                               |

The range of data obtainable in the presence of acid was quite limited due to the basic nature of cadmium hydroxide. Several additional samples which were prepared so as to yield information in more acidic solution are not included in Table II since they had no solid phase remaining at equilibrium. This roughly supports the observation of Britton,<sup>13</sup> who reported that the formation of a precipitate during the titration of a cadmium salt with base first appears between pH 7 and pH 8.

Within the limited range of concentration over which data are available, the absence of drift in the equilibrium constant for reaction 1



indicates this to be the principal reaction governing the dissolution of cadmium hydroxide in dilute acid. The average value of K<sub>1</sub> in this region is 4.3 × 10<sup>4</sup> for which ΔF°<sub>298</sub> = -4600 cal./mole.

The data cannot be interpreted as indicating any significant contribution of either divalent or undissociated cadmium-bearing species in this pH range.

**The Equilibria in Basic Solution.**—The solubility data and the numerical value of the equilibrium constants for the reactions in sodium hydroxide solutions are collected in Table III.

TABLE III

THE SOLUBILITY OF CADMIUM HYDROXIDE IN SODIUM HYDROXIDE AT 25°

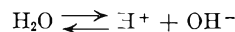
| M <sub>OH<sup>-</sup></sub><br>× 10 <sup>5</sup> | M <sub>Cd<sup>++</sup></sub><br>× 10 <sup>6</sup> | K <sub>2</sub><br>× 10 <sup>10</sup> | K <sub>3</sub><br>× 10 <sup>6</sup> | K <sub>4</sub><br>× 10 <sup>6</sup> |
|--|---|--------------------------------------|-------------------------------------|-------------------------------------|
| 1.00   | 15.0  | 1.5                                  | 15                                  | 1.5 × 10 <sup>5</sup>               |
| 1.60   | 7.9   | 1.3                                  | 7.9                                 | 4.9 × 10 <sup>4</sup>               |
| 2.30   | 7.0   | 1.6                                  | 7.0                                 | 3.0 × 10 <sup>4</sup>               |
| 66   | 3.5   | 23                                   | 3.5                                 | 530                                 |
| 560  | 3.6   | 183                                  | 3.6                                 | 64                                  |
| 5500   | 5.9   | 2200                                 | 5.9                                 | 10.7                                |
| 10100  | 6.2   | 3700                                 | 6.2                                 | 6.1                                 |
| 2.8 × 10 <sup>6</sup>                            | 7.5   | 10500                                | 7.5                                 | 2.7                                 |
| 5.4 × 10 <sup>4</sup>                            | 8.8   | 2.2 × 10 <sup>4</sup>                | 8.8                                 | 1.6                                 |
| 9.0 × 10 <sup>4</sup>                            | 13.0  | 5.4 × 10 <sup>4</sup>                | 13.0                                | 2.0                                 |
| 1.4 × 10 <sup>5</sup>                            | 22  | 1.4 × 10 <sup>5</sup>                | 22                                  | 1.6                                 |
| 1.8 × 10 <sup>5</sup>                            | 38  | 3.3 × 10 <sup>5</sup>                | 38                                  | 2.1                                 |
| 2.1 × 10 <sup>5</sup>                            | 63  | 6.3 × 10 <sup>5</sup>                | 63                                  | 3.1                                 |

(13) H. T. S. Britton, *J. Chem. Soc.*, **127**, 2148 (1925).

The constancy of K<sub>2</sub> in the region of low basicity—before the solubility minimum—indicates that reaction 2



can account satisfactorily for the solubility. This reaction, however, is related to reaction 1 by the water ionization reaction



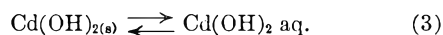
and it seems reasonable that K<sub>1</sub> should continue to be valid in this region. A value for K<sub>1</sub> can be determined from the average K<sub>2</sub> as

$$K_2 = 1.5 \times 10^{-10}$$

$$K'_1 = \frac{K_2}{K_w} = \frac{1.5 \times 10^{-10}}{1.0 \times 10^{-14}} = 1.5 \times 10^4$$

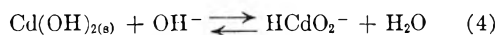
This shows fair agreement with K<sub>2</sub>, 4.3 × 10<sup>4</sup>, while the relative magnitudes of K<sub>1</sub> and K<sub>2</sub> indicate that the reaction represented by the former accounts for the dissolution of cadmium hydroxide in slightly basic and neutral solution. The average over-all constant throughout this extended concentration range is 3.2 × 10<sup>4</sup> ± 2.0 × 10<sup>4</sup> and ΔF°<sub>298</sub> = -4800 cal./mole.

A solubility minimum exists between 10<sup>-4</sup> and 10<sup>-2</sup> molar sodium hydroxide, in which region it may be assumed that the undissociated species predominates. The average value of K<sub>3</sub> for the reaction



is 4.3 × 10<sup>-6</sup> ± 1 × 10<sup>-6</sup> for which ΔF°<sub>298</sub> = 5900 cal./mole.

As the basicity increases, the concentration of cadmium in solution also increases. Such behavior can only be attributed at low ionic strength to amphoteric properties of the oxide. This is best supported by the constancy of K<sub>4</sub>, representing the reaction



The average value of K<sub>4</sub>, selected from those in which the hydroxyl ion concentration is greater than 10<sup>-2</sup> molar, is 2.1 × 10<sup>-5</sup> ± 0.5 × 10<sup>-5</sup> and ΔF°<sub>298</sub> = 6400 cal./mole.

In the region of highest basicity studied, K<sub>5</sub> also exhibits constancy, which appears to indicate the occurrence of the cadmate ion as a product of reaction 5



This reaction is apparently simultaneous with reaction 4 above 1 N sodium hydroxide and the data are insufficient to indicate over what concentration range reaction 5 extends. A tentative value of 7.3 × 10<sup>-6</sup> ± 2.5 × 10<sup>-6</sup> can be selected as a lower limit for K<sub>5</sub>. The corresponding value of ΔF°<sub>298</sub> for this reaction is 7000 cal./mole.

## NOTES

THE CHLORINE TRIFLUORIDE-HYDROGEN FLUORIDE SYSTEM. SOME VAPOR PRESSURE AND CONDUCTANCE MEASUREMENTS<sup>1</sup>

BY MAX T. ROGERS, JOHN L. SPEIRS AND MORTON B. PANISH

*Kedzie Chemical Laboratory, Michigan State University, East Lansing Michigan*

Received September 20, 1956

The possible existence of a stable complex between chlorine trifluoride and hydrogen fluoride<sup>2</sup> made further study of this system desirable. We have therefore investigated the vapor pressures and specific conductances of liquid solutions of hydrogen fluoride in chlorine trifluoride.

The vapor pressure-composition data at 0° are shown in Table I.

TABLE I

THE VAPOR PRESSURES OF CHLORINE TRIFLUORIDE-HYDROGEN FLUORIDE SOLUTIONS AT 0°

| Mole % HF | Pressure, mm. | Mole % HF | Pressure, mm. |
|-----------|---------------|-----------|---------------|
| 0.0       | 448           | 69.0      | 645           |
| 10.5      | 562           | 86.0      | 527           |
| 33.2      | 592           | 100.0     | 398           |

The system shows large positive deviations from Raoult's law at this temperature. There is an azeotropic mixture with maximum vapor pressure the composition of which is about  $65 \pm 10$  mole % hydrogen fluoride.<sup>3</sup> Although the probable error in our pressure measurements was not over  $\pm 5.0$  mm. we would not claim an accuracy in the vapor pressures better than about  $\pm 3\%$  since there was some evidence of reaction of the materials with the apparatus and consequent drift of pressure with time.

The specific conductance of chlorine trifluoride and of various solutions of hydrogen fluoride in chlorine trifluoride at 25 and  $-78^\circ$  are shown in Table II. The specific conductance of chlorine trifluoride may be compared with an unpublished value<sup>4</sup> of  $3 \times 10^{-9}$  ohm<sup>-1</sup> cm.<sup>-1</sup> at 0°. The addition of hydrogen fluoride increases the conductance markedly but molar conductances are low indicating a low degree of ionization.

A measurement of the density of a single solution (53.0 mole % hydrogen fluoride,  $d_4^{25}$  1.60 g./cc.) gave an observed average molar volume of 33.8

(1) Physical Properties of the Halogen Fluorides. X. For the preceding article of this series see M. T. Rogers and J. L. Speirs, *THIS JOURNAL*, **60**, 1462 (1956).

(2) D. F. Smith and J. P. Pemsler, "Symposium on Spectroscopy," Ohio State University, June 18, 1954; M. T. Rogers and J. J. Katz, *J. Am. Chem. Soc.*, **74**, 1375 (1952).

(3) An azeotrope containing 67 mole % hydrogen fluoride has been reported recently by another method; R. M. McGill, W. S. Wendolkowski and E. J. Barber, Abstracts of the 126th National Meeting of the American Chemical Society, New York, N. Y., September, 1954.

(4) A. A. Banks quoted by N. N. Greenwood, *Revs. Pure and Applied Chem. (Australia)*, **1**, 84 (1951).

TABLE II

CONDUCTANCES OF CHLORINE TRIFLUORIDE-HYDROGEN FLUORIDE SOLUTIONS AND OF CHLORINE TRIFLUORIDE AT 25 and  $-78^\circ$ 

| (moles HF/l. at 25°) | $L$ , ohms <sup>-1</sup> cm. <sup>-1</sup> × 10 <sup>8</sup> at $-78^\circ$ | $\Lambda \times 10^4$ (at 25°) |
|----------------------|---|--------------------------------|
| 0                    | 0.65  | 0                              |
| 1.00                 | 4.5   | 2.96                           |
| 1.35                 | 9.5   | 5.49                           |
| 2.57                 | 82.5  | 43.7                           |
| 4.67                 | 460   | 350                            |
|                      |   | 7.5                            |

cc./mole which is 3.3% smaller than the ideal average molar volume (35.0 cc./mole). This is close to the observed decrease in volume found in other hydrogen fluoride-halogen fluoride systems<sup>5</sup>; molar conductances  $\Lambda$  were calculated with the aid of this result.

## Experimental

**Materials.**—Chlorine trifluoride and hydrogen fluoride (Harshaw Chemical Co.) were purified by a simple distillation in Monel apparatus. For conductance work the hydrogen fluoride was dried over cobaltic fluoride ( $L = 2.9 \times 10^{-4}$  ohm<sup>-1</sup> cm.<sup>-1</sup> at 25°).

Our data provide no evidence for the existence of a stable complex between chlorine trifluoride and hydrogen fluoride. While it is possible that such a complex exists as a transient intermediate in exchange reactions it evidently does not exist in important concentrations at room temperature.

**Apparatus and Method.**—These were essentially the same as described elsewhere.<sup>6,6</sup> All measurements were made as soon as possible after the mixtures were prepared.

**Acknowledgment.**—This work was supported by the Atomic Energy Commission through contract AT (11-1)-151.

(5) M. T. Rogers, J. L. Speirs and M. B. Panish, *J. Am. Chem. Soc.*, **78**, 3283 (1956); M. T. Rogers, J. L. Speirs, M. B. Panish and H. B. Thompson, *ibid.*, **78**, 936 (1956).

(6) H. B. Thompson and M. T. Rogers, *Rev. Sci. Instr.*, **27**, in press.

## THE ELECTRIC MOMENTS OF LITHIUM-ALKYLS

BY MAX T. ROGERS AND T. L. BROWN<sup>1</sup>*Kedzie Chemical Laboratory, Michigan State University, East Lansing, Michigan*

Received September 7, 1956

The only electric moment measurement reported for an organolithium compound is the value 0.97 *D.* computed for *n*-butyllithium by Rogers and Young<sup>2</sup> from the measured dielectric constants of a series of solutions of *n*-butyllithium in benzene. They assumed that the compound was a monomer but it is now known that these compounds are polymerized in benzene solution.<sup>3</sup> In view of the interest in the carbon-lithium bond moment, and

(1) DuPont Teaching Fellow, Michigan State University 1955-1956; Noyes Chemical Laboratory, University of Illinois, Urbana, Illinois.

(2) M. T. Rogers and A. Young, *J. Am. Chem. Soc.*, **68**, 2748 (1946).

(3) E. Warhurst, *Disc. Faraday Soc.*, **2**, 239 (1947).

in the nature of the polymer in solution, it seemed desirable to make measurements on another alkyl-lithium compound. We report here some measurements on ethyllithium, a substance which can be isolated as a pure crystalline material. The degree of polymerization in benzene is available.

#### Experimental

**Materials.**—Crystalline ethyllithium of at least 99% purity was used. The preparation and methods of analysis have been described elsewhere.<sup>4</sup> A series of solutions of this material in benzene were prepared in an atmosphere of dry, oxygen-free nitrogen. The concentrations were measured by direct titration of an aliquot with standard acid after the material had been decomposed with water.

Benzene was purified by a single fractional-freezing step followed by distillation over calcium hydride,  $d_{25}^{25}$ , 0.87356; it was stored over sodium wire.

**Apparatus and Method.**—The densities and dielectric constants of the solutions were measured by use of apparatus described elsewhere.<sup>5</sup> The dielectric constant cell was made of nickel with Teflon insulation and had a replaceable capacitance of 84.4  $\mu\text{farads}$ . From the dielectric constants of three solutions of molalities 0.0779, 0.249 and 0.347, a value of the molar polarization of ethyllithium of 26.9  $\text{cm}^3$  was calculated for the monomer by the method of Halverstadt and Kumler. The constants of their equation were found to be  $a = 0.78$ ,  $b = 0.1225$ ,  $\epsilon_0 = 2.2725$  and  $\nu_{10} = 1.14530$ . The molar refraction of lithium ethyl was found to be 14.3 from measurements of the refractive indices and densities of the solutions. However, because the probable error in the measurements of refractive index was rather large we prefer to use a value of 11.5  $\text{cm}^3$  for the electronic polarization of lithium ethyl which is just the molar refraction calculated from atomic constants with the atomic refraction of lithium estimated at 1.5  $\text{cm}^3$ . The electric moment, computed assuming a monomer, and making no correction for atomic polarization, is then 0.87  $D$ ; for reasons discussed below this number has only formal significance.

#### Discussion

The average degree of association reported for ethyllithium in benzene, on the basis of freezing point depression measurements, is nearly six and appears to be independent of concentration in the range of concentrations employed here.<sup>4</sup> If the monomer were highly polar and the polymer non-polar and there were an equilibrium between these species then the dielectric constants of the solutions would not be expected to be the linear function of concentration which we observe; also, the infrared data indicate that the relative amount of monomer must be quite small even in the most dilute solution run.<sup>4</sup> If it is assumed that all the ethyllithium is present as hexamer the molar polarization of the hexamer would be 161.4  $\text{cm}^3$  and the sum of the atomic and orientation polarizations would be 90.6  $\text{cm}^3$ . The atomic polarization,  $P_a$ , is unknown and may be rather large in a compound of this type with many low frequency stretching and bending modes. An approximate upper limit of 44  $\text{cm}^3$  may be placed on the atomic polarization of the hexamer by consideration of the values found by measurements on analogous compounds. The contribution of the C-Li bending modes should be less than half the value of  $P_a = 3.19$  found for dimethylmercury<sup>6</sup> since there is only one carbon-metal bond in the former and the frequencies are lower. For the

hexamer then the contribution of the C-Li bending modes to  $P_a$  should be less than 19  $\text{cm}^3$  (assuming, at most, two lithium-carbon bonds per lithium atom). The skeletal modes of vibration in the polymer would surely contribute less to  $P_a$  than the value  $P_a = 25 \text{ cm}^3$  observed for beryllium acetoacetate in which there are two non-planar six-membered rings.

The minimum orientation polarization for the hexamer would then be estimated at 46.6  $\text{cm}^3$  and the minimum dipole moment would be 1.50  $D$ .

Our present knowledge of these systems suggests that *n*-butyllithium is probably also best represented as a hexamer in benzene solution. Recalculating the data of Rogers and Young on this assumption and assigning a maximum value of 50  $\text{cm}^3$  to the atomic polarization, the electric moment of the hexamer of *n*-butyllithium would be 1.43  $D$ .

It is interesting that the electric moment of the associated species is about 1.4–1.5  $D$  for both *n*-butyl- and ethyllithium. Since nothing is known of the configuration of this species the calculation of C-Li bond moment made by Rogers and Young is scarcely justified.

## THE EXCHANGE REACTION BETWEEN TIN(IV) CHLORIDE AND TIN(II) CHLORIDE IN ABSOLUTE METHANOL

BY E. GERALD MEYER AND MITCHELL A. MELNICK<sup>1</sup>

Department of Chemistry, New Mexico Highlands University, Las Vegas, New Mexico

Received October 8, 1956

Previous investigations of the exchange between Sn(IV) and Sn(II) in absolute ethanol<sup>2</sup> and in 10  $F$  hydrochloric acid<sup>3</sup> solutions have produced rate of exchange equations,  $R = 1.4 \times 10^{13} e^{-23,700/RT}$  (SnCl<sub>2</sub>) (SnCl<sub>4</sub>), and  $R = 7.5 \times 10^5 e^{-10,800/RT}$  (Sn II) (Sn IV) where  $R$  is in units of moles liter<sup>-1</sup> sec.<sup>-1</sup>. From these equations molar activation entropy values of -0.4 and -50 e.u. are obtained. Due to the considerable divergence of these rate equations it seemed appropriate to run the exchange in absolute methanol.

#### Experimental

The radioactivity employed was 1.1 day Sn<sup>121</sup> prepared and used as described in the earlier work.<sup>2</sup> The chemicals used were also the same with the addition of absolute methanol which was Baker C.P. Analyzed. The methanol was stored over Drierite, and deoxygenated with oxygen-free, dried nitrogen gas.

The irradiated sample of SnCl<sub>4</sub> was distilled into dried, oxygen-free methanol discarding the first third and last third of distillate and keeping the entire system closed and moisture free. The SnCl<sub>2</sub> was then dissolved in treated methanol using a nitrogen-filled dry-box. Aliquots of each solution were analyzed, the Sn(IV) gravimetrically by precipitation with phenylarsonic acid<sup>4</sup> and the Sn(II) iodimet-

(1) (a) A portion of this work is abstracted from the thesis of Mitchell A. Melnick submitted in partial fulfillment of the requirements for the M.S. degree, New Mexico Highlands University, September, 1955. (b) Los Alamos Scientific Laboratory, Los Alamos, New Mexico. (c) Presented in part before the Division of Physical and Inorganic Chemistry, 129th Meeting of the American Chemical Society, Dallas, Texas, April, 1956.

(2) E. G. Meyer and M. Kahn, *J. Am. Chem. Soc.*, **73**, 4950 (1951).

(3) C. I. Browne, R. P. Craig and N. Davidson, *ibid.*, **73**, 1946 (1951).

(4) S. Knapper, K. A. Craig and G. C. Chandler, *ibid.*, **55**, 3945 (1933).

(4) T. L. Brown and M. T. Rogers, unpublished results.

(5) M. T. Rogers, *J. Am. Chem. Soc.*, **77**, 3681 (1955).

(6) E. Bergmann and W. Schutz, *Z. physik. Chem.*, **B19**, 401 (1932).

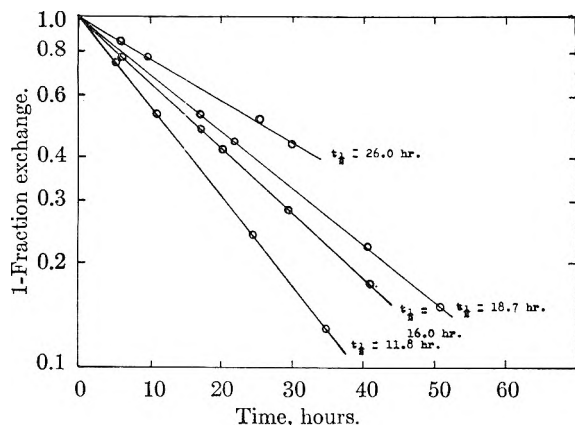


Fig. 1.—Semi-logarithmic plot of (1-fraction exchange) against time for runs 33.1°.

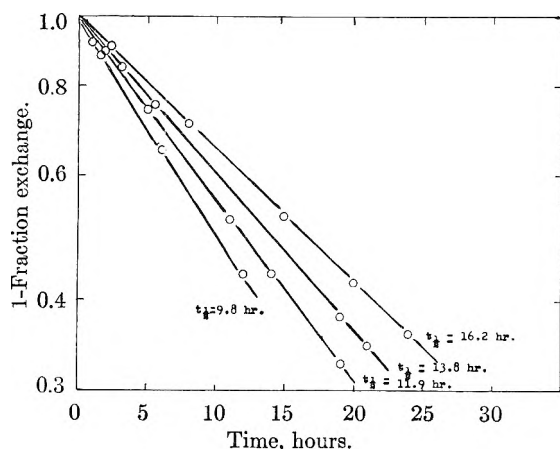


Fig. 2.—Semi-logarithmic plot of (1-fraction exchange) against time for runs 40.5°.

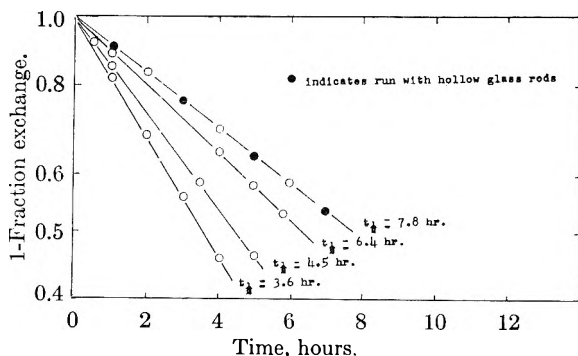


Fig. 3.—Semi-logarithmic plot of (1-fraction exchange) against time for runs 47.2°.

rically. The solutions were then placed in a thermostated bath ( $\pm 0.1^\circ$ ) to bring them to the reaction temperature. At all times an atmosphere of nitrogen was kept over the solution surfaces.

At a predetermined time the active  $\text{SnCl}_4$  solution was mixed with the  $\text{SnCl}_2$  solution and an aliquot taken for Sn(II) analysis. Additional aliquots were taken at specific time intervals: one such aliquot being analyzed for Sn(II) and a second being subjected to the Sn(IV)–Sn(II) separation procedure. The separation was accomplished by pipetting the exchange mixture aliquot into a nitrogen-filled test-tube containing an excess of powdered oxalic acid. A precipitate of stannous oxalate was thus formed which was separated by centrifugation along with the unreacted oxalic acid. The precipitate was washed twice with methanol to remove  $\text{SnCl}_4$  and then dissolved in hydrochloric acid. The Sn(II) was oxidized with an excess of iodine solution which was then back-titrated with sodium thiosulfate, and pre-

cipitated with phenylarsonic acid.<sup>4</sup> The precipitate was then ignited to  $\text{SnO}_2$ , weighed and transferred to a 1 in. diameter filter circle which was placed in the center of a 2.5 in.  $\times$  3.5 in. aluminum plate. The oxide was spread evenly over the filter circle and covered with a gummed label having a 1 in. diameter cellophane window. The sample was counted with a methane proportional counter so that the counting error was less than 1%. The sample size and specific activity were regulated so that no self absorption or coincidence corrections were necessary. An appropriate aliquot was taken from each run and oxidized without separation of the species. This sample was precipitated and mounted as described above, and counted to determine the equilibrium activity.

## Results

As shown in Table I, a series of runs were made at 33.1, 40.5 and 47.2°. In each of these the Sn(IV) and Sn(II) concentrations were varied, and the values of  $\ln(1 - F)$  were plotted against time in accordance with the well-known first-order exchange law

$$-\ln(1 - F) = \frac{R((\text{SnCl}_4) + (\text{SnCl}_2))}{(\text{SnCl}_4)(\text{SnCl}_2)} t$$

where  $(\text{SnCl}_2)$  = total concentration (active + inactive) of  $\text{SnCl}_2$  in moles per liter;  $(\text{SnCl}_4)$  = total concentration (active + inactive) of  $\text{SnCl}_4$  in moles per liter;  $F$  = fraction exchanged at time,  $t$ , = specific activity of stannous chloride at time,  $t$ , divided by the equilibrium specific activity of stannous chloride (specific activity of stannous chloride at time,  $t = \infty$ ) where the specific activity of stannous chloride = 0 at time,  $t = 0$ .  $R$  is the actual rate at which the exchange of tin atoms between  $\text{SnCl}_2$  and  $\text{SnCl}_4$  takes place. For any one experiment,  $R$  will be constant because  $(\text{SnCl}_2)$  and  $(\text{SnCl}_4)$  are constant.

TABLE I

| BASIC DATA OF ALL EXCHANGES |                     |                     |                       |                 |   |         |
|-----------------------------|---------------------|---------------------|-----------------------|-----------------|---|---------|
| Temp., °C.                  | Sn(IV) molar concn. | Sn(II) molar concn. | Total Sn molar concn. | Half-times, hr. | $K$ , mole <sup>-1</sup> l. hr. <sup>-1</sup> | Av. $K$ |
| 33.1—1                      | 0.0523              | 0.0523              | 0.1046                | 26.0            | 0.255   |         |
|                             | 0.0865              | 0.0822              | .1687                 | 16.0            | .257  |         |
|                             | 0.0979              | 0.0464              | .1443                 | 18.7            | .257  |         |
|                             | 0.1345              | 0.0958              | .2303                 | 11.8            | .255  | 0.256   |
| 40.5—1                      | 0.0453              | 0.0307              | 0.0760                | 16.2            | .563  |         |
|                             | 0.0638              | 0.0242              | .0880                 | 13.8            | .568  |         |
|                             | 0.0510              | 0.0527              | .1037                 | 11.9            | .566  |         |
|                             | 0.0838              | 0.0416              | .1254                 | 9.8             | .564  | 0.565   |
| 47.2—1 <sup>a</sup>         | 0.0315              | 0.0444              | 0.0759                | 7.8             | 1.171   |         |
|                             | 0.0491              | 0.0451              | .0942                 | 6.4             | 1.149   |         |
|                             | 0.0845              | 0.0493              | .1338                 | 4.5             | 1.151   |         |
|                             | 0.1056              | 0.0634              | .1690                 | 3.6             | 1.139   | 1.156   |

<sup>a</sup> Run with small hollow glass rods to demonstrate the absence of heterogeneous catalysis.

The graphs thus produced are shown in Figs. 1, 2 and 3. The half-times of exchange obtained from these graphs were then plotted against the reciprocal of the total tin concentration as shown in Fig. 4. The straight lines thus obtained indicate that the rate of exchange is first order with respect to the concentrations of Sn(II) and Sn(IV) at each of the three temperatures investigated. From the slopes of the three lines of Fig. 4 the velocity constant was determined at each temperature. A semi-logarithmic plot of these velocity constants *vs.*  $1/T$  as shown in Fig. 5 yielded a straight line from whose slope an activation energy of 20.9 kcal. was

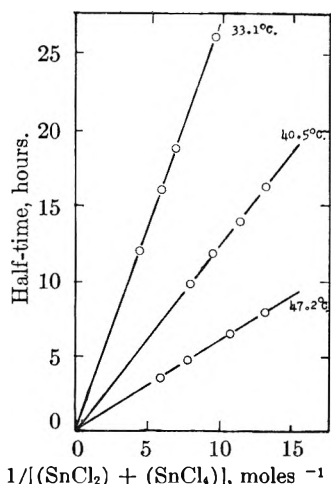


Fig. 4.—Effect of total tin concentration on the half-time of the exchange.

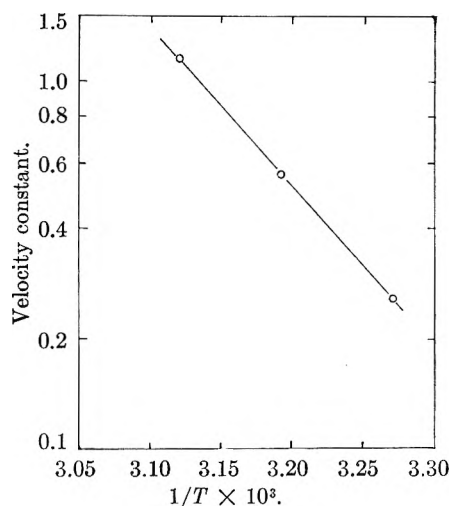


Fig. 5.—The temperature dependence of the exchange reaction.

calculated. An over-all rate of exchange equation  $R = 5.5 \times 10^{10} e^{-20,900/RT} (\text{SnCl}_4)(\text{SnCl}_2)$  mole liter<sup>-1</sup> sec.<sup>-1</sup> was obtained which is valid within the indicated concentration and temperature ranges. The molar activation entropy calculated from this equation is  $-11.5$  e.u. It is estimated that the data are accurate to  $\pm 2\%$ . The principal sources of error are the uncertainty in the solution concentrations (*ca.*  $\pm 1\%$ ), the uncertainty in the counting sample weights (*ca.*  $\pm 0.5\%$ ), and the statistical fluctuation in the counting rate (*ca.*  $\pm 0.5\%$ ).

**Acknowledgment.**—The authors wish to thank the Research Corporation for financial support, and the water-boiler reactor group of the Los Alamos Scientific Laboratory for irradiating the  $\text{SnCl}_4$  samples.

## THE INTERACTION OF IRON(II) BROMIDE AND WATER

BY N. W. GREGORY

Department of Chemistry, University of Washington, Seattle, Washington

Received September 10, 1956

During studies on the iron-bromine system, it

became necessary to investigate the interaction of water with  $\text{FeBr}_2$  in the temperature range 25–400°. Equilibrium water vapor pressures characterizing the decomposition of  $\text{FeBr}_2 \cdot \text{H}_2\text{O}$ ,  $\text{FeBr}_2 \cdot 2\text{H}_2\text{O}$  and  $\text{FeBr}_2 \cdot 4\text{H}_2\text{O}$ , respectively, have been measured and X-ray powder patterns obtained from the solid phases participating in the equilibria. In the absence of oxygen, appreciable amounts of  $\text{HBr}$  were not observed in the vapor phase over the entire temperature range.

Equilibrium pressures are shown in Fig. 1. At least four independent samples were used to establish each curve. From 0.2 to 0.8 g. of anhydrous

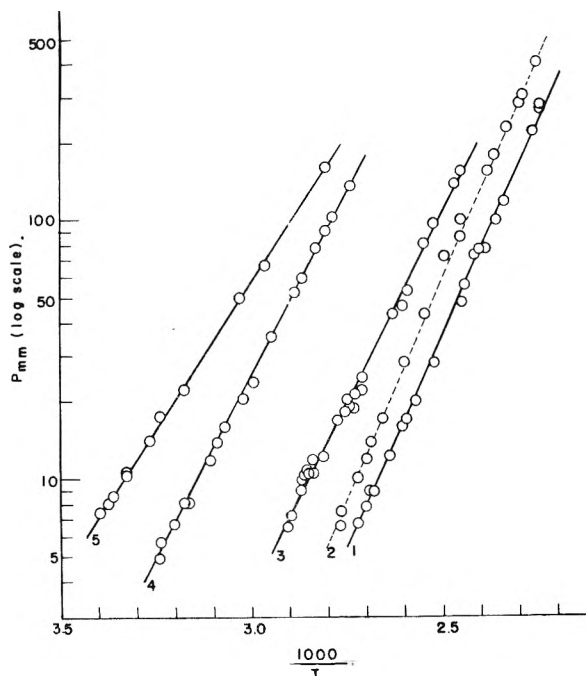


Fig. 1.—Equilibrium water vapor pressure over  $\text{FeBr}_2$  and its hydrates.

$\text{FeBr}_2$ , prepared by reaction of bromine with A.R. iron wire, was initially sublimed under high vacuum, either directly into the Pyrex equilibrium vessel, volume *ca.* 20 ml., or subsequently transferred into the vessel in a dry-box. Water vapor was then admitted and equilibrium pressures, usually established within 30 minutes or less, measured in one of three ways: below 20 mm., the vapor phase was allowed to come into direct contact with a mercury manometer at room temperature; at higher pressures, a glass diaphragm gage<sup>1</sup> (lines 1 and 2) or alternately (lines 3, 4, 5) a mercury U-tube extending to the opening of the electric furnace was placed between the sample and manometer to prevent condensation of water vapor. Pressures were read with an uncertainty of  $\pm 0.5$  mm.; temperatures were controlled to  $\pm 0.7^\circ$ . No change in total moles of vapor with temperature could be detected in diaphragm gage measurements above the region of hydrate formation (200–400°); neither were appreciable amounts of  $\text{HBr}$  released on decomposition of the hydrates at lower temperatures. Water collected from complete dehydration of a

(1) For design see R. O. MacLaren and N. W. Gregory, *THIS JOURNAL*, 59, 184 (1955).

solution of  $\text{FeBr}_2 \cdot 4\text{H}_2\text{O}$  (volume *ca.* 1 ml.) was found to have *pH ca.* 3. Sublimation of the remaining anhydrous  $\text{FeBr}_2$  left only a trace of oxide residue. If air is not rigorously excluded during the hydration, however, significant amounts of  $\text{FeO}$  are formed in this treatment.

Formulas of the hydrates were ascertained from data shown in Fig. 2. In two series of measurements known amounts of water, determined by measuring the volume of liquid removed from a calibrated 2-mm. capillary tube, were added to known amounts of  $\text{FeBr}_2$ . The results are shown by plotting the temperature at which the pressure of water vapor is 10 mm. as a function of the ratio of moles of water to  $\text{FeBr}_2$ . Aliquots of water were added until the sample had dissolved completely; the equilibrium points were measured again during dehydration. The mono- and dihydrates are white; the tetrahydrate is a light green.

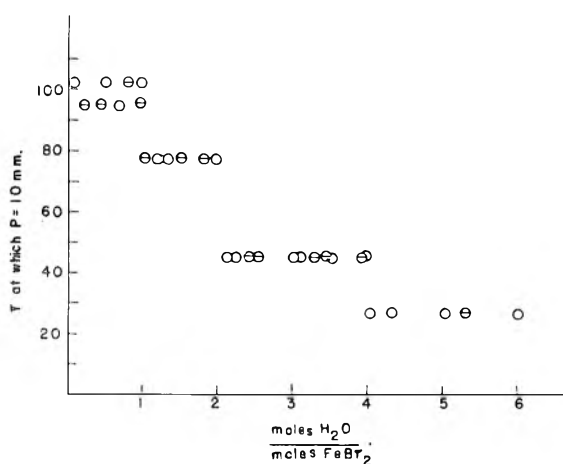


Fig. 2.—Temperatures at which hydrate decomposition pressures are 10 mm. Points indicated by  $\ominus$  correspond to measurements made after successive additions of aliquots of water; those by  $\circ$  at various stages of dehydration.

An interesting problem arose in the study of the first stage of the hydration. With the addition of small amounts of water to anhydrous  $\text{FeBr}_2$  prepared by vacuum sublimation at  $475^\circ$  (crystals formed in the sublimation have a  $\text{Cd}(\text{OH})_2$  type structure<sup>2</sup> with the halogen atoms in a hexagonal close-packed array (HCP) and with dimensions of the order of one mm.) apparent equilibrium pressures lying on line 2 (Fig. 1) were observed in both direct and diaphragm gage measurements. In the latter, a sequence of measurements up to  $180^\circ$  made during a two-day period gave pressures mutually consistent for ascending and descending temperatures. However, when a limited amount of water vapor was left in contact with the  $\text{FeBr}_2$  at  $100^\circ$  for several weeks, a slow change of pressure from line 2 to line 1 was observed. If the  $\text{FeBr}_2$  is converted completely to mono-hydrate (or higher hydrates) by addition of sufficient water (the reaction occurs quite rapidly at lower temperatures) subsequent study of the dehydration and rehydration equilibrium always gave pressures falling on line 1.

(2) R. O. MacLaren and N. W. Gregory, *J. Am. Chem. Soc.*, **76**, 5874 (1954).

Hence only line 1 has been assumed to give an equilibrium relationship between the monohydrate and anhydrous forms. However, the anhydrous phase participating in this equilibrium is found to have a crystal structure somewhat different from that of the starting material. X-Ray powder patterns (Fig. 3) of  $\text{FeBr}_2$ , formed by dehydration of the monohydrate at *ca.*  $110^\circ$ , show layers of bromine atoms packed in a random fashion instead of the HCP arrangement characteristic of the original crystals. (This modification of structure has also been observed on similar treatment of  $\text{FeCl}_2$ .<sup>2</sup>) In addition the random packed material appears to be finely divided and consequently to have a greater surface area than the starting material.

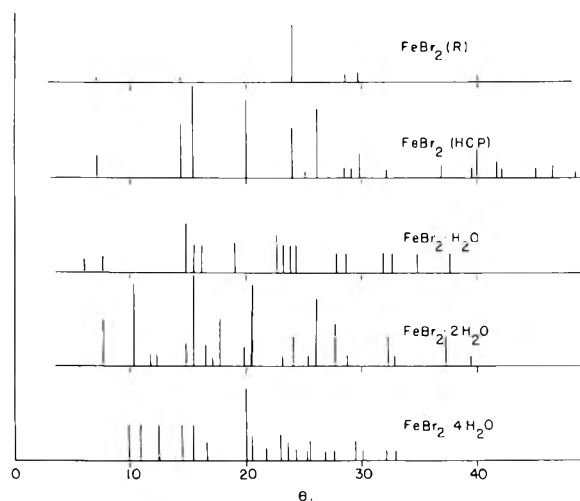


Fig. 3.—Powder patterns of  $\text{FeBr}_2$  and its hydrates.

If these changes are responsible for the shift in equilibrium pressures from line 2 to line 1, the anhydrous phase must be thermodynamically less stable than the starting material (since the  $\text{H}_2\text{O}$  pressures are lower) and its formation attributed to kinetic factors. The vapor pressure of  $\text{FeBr}_2$  in the vicinity of  $100^\circ$  is not sufficient to facilitate crystal growth (v.p. *ca.*  $2 \times 10^{-5}$  mm. at  $350^\circ$ ); hence the random structure, if formed by the dehydration, could not easily change to the ordered form by a vaporization mechanism. On this basis lines 1 and 2 might serve to relate thermodynamic properties of the ordered- and random-packed phases; however, the structural and concomitant crystal size effects cannot be separated from the present information alone.

Alternately, changes in the monohydrate phase may be largely responsible for the observed shift although no other evidence was observed to support this. Water pressures above the mono- and dihydrates did not show irregularities; also once the random form of  $\text{FeBr}_2$  had been prepared, equilibrium pressures throughout its hydration were found to fall on line 1.

The data summarized in Fig. 1 lead to the relationships

(3) R. O. MacLaren and N. W. Gregory, *THIS JOURNAL*, **59**, 184 (1955).

| Line | Equilibrium<br>(temp. range studied)  | $\Delta F^\circ = \Delta H^\circ - T\Delta S^\circ = -RT \ln P_{\text{atm}}$<br>(cal./mole) |
|------|---|---|
| (1)  | $\text{FeBr}_2 \cdot \text{H}_2\text{O}(\text{s}) = \text{FeBr}_2(\text{R.P., s}) + \text{H}_2\text{O}(\text{g})$ (90–160°)   | $\Delta F^\circ = 15250 - 32.1T$  |
| (3)  | $\text{FeBr}_2 \cdot 2\text{H}_2\text{O}(\text{s}) = \text{FeBr}_2 \cdot \text{H}_2\text{O}(\text{s}) + \text{H}_2\text{O}(\text{g})$ (70–150°)                       | $\Delta F^\circ = 13460 - 29.7T$  |
| (4)  | $\frac{1}{2}\text{FeBr}_2 \cdot 4\text{H}_2\text{O}(\text{s}) = \frac{1}{2}\text{FeBr}_2 \cdot 2\text{H}_2\text{O}(\text{s}) + \text{H}_2\text{O}(\text{g})$ (35–92°) | $\Delta F^\circ = 13070 - 32.4T$  |
| (5)  | Vapor pressure of water above a satd. soln. of $\text{FeBr}_2 \cdot t\text{H}_2\text{O}$ (20–84°)   | $\Delta F^\circ = 10400 - 26.1T$  |

An uncertainty of  $\pm 400$  cal. in  $\Delta H^\circ$  and of  $\pm 1$  e.u. in  $\Delta S^\circ$  is estimated. Calculation of absolute thermodynamic properties of the hydrates must await determination of the relationship of the random and HCP packed forms of  $\text{FeBr}_2$ ; standard values are available only for the latter.

The two levels seen in Fig. 2 (at 102 and 95°) in the region of mono-hydrate formation correspond to lines 1 and 2, respectively, in Fig. 1. No evidence to indicate existence of hydrates with less than one mole of water for each mole of  $\text{FeBr}_2$  was observed. With the mole ratio of  $\text{H}_2\text{O}/\text{FeBr}_2$  between five and six, liquid became visible in the system at 25°. The actual solubility limit was not determined. The existence of higher hydrates at lower temperatures has been reported.<sup>4</sup> The heat of vaporization of water from the saturated solution corresponds to that of pure water within limits of the rather large experimental error.

Nearly pure samples of each hydrate phase were prepared and placed in Pyrex capillary tubes. X-Ray powder patterns were obtained using  $\text{Cu K}\alpha$  ( $\lambda = 1.542$ ) radiation. Values of the Bragg angle theta are shown for the principal reflections in Fig. 3, along with those observed for the two anhydrous phases, HCP and RP. Relative intensities, estimated visually, are indicated by the heights of the lines. Cell dimensions for the random packed structure were not materially different from those previously reported for the HCP structure.<sup>2</sup>

This work was supported in part by the Office of Ordnance Research, U. S. Army.

(4) F. Schimmel, *Ber.*, **62**, 963 (1929).

## LIGHT SCATTERING MEASUREMENTS ON A FRACTIONATED NON-IONIC DETERGENT

BY L. M. KUSHNER, W. D. HUBBARD AND A. S. DOAN  
*Surface Chemistry Section, National Bureau of Standards, Washington 25, D. C.*

Received September 18, 1956

In an earlier publication<sup>1</sup> the results of viscometric and turbidimetric measurements on dilute aqueous solutions of the non-ionic detergent, Triton X-100, were presented. At that time it was pointed out that, in contrast to the ionic types of detergents, there was no well defined critical micelle concentration apparent from the turbidity data. Instead, in the concentration range from 0 to 0.3 g./dl. of Triton X-100, there is a gradual increase in the fraction of added detergent forming micelles. At concentrations higher than about 0.3 g./dl., virtually all of each increment of detergent added to the solution becomes micellar.

An explanation for this behavior was presented in terms of the distribution of polyether chain

lengths that must necessarily occur in a material such as Triton X-100, which is prepared by a polycondensation reaction. Those molecules in the sample having short polyether chains would be expected to undergo micelle formation at lower concentrations than those having the longer chain lengths. Even if each molecular species had a sharp critical micelle concentration, the net result would be the gradual appearance of micelles, as observed, rather than a single, well-defined critical micelle concentration. This does not mean that above a concentration of about 0.3 g./dl. of Triton X-100, each micelle is composed of molecules all having the same length of polyether chain, since it must be remembered that a dynamic equilibrium exists among all of the molecular and micellar species in the solution.

In order to provide additional data pertinent to the question of micelle formation in non-ionic detergent solutions, a sample of Triton X-100 was fractionated by molecular distillation and turbidity measurements were made on aqueous solutions of two water-soluble fractions.

### Experimental

**Materials.**—The sample of Triton X-100 which was fractionated was from a different batch than that used in our earlier work.<sup>1</sup> However, since measurements of turbidity as a function of concentration for the two samples were identical within the limits of experimental error, it was assumed that they are virtually identical in composition and the two sets of data were combined. According to the manufacturer (Rohm and Haas Company, Philadelphia, Pa.), Triton X-100 is the product of the condensation of a highly branched octyl phenol and ethylene oxide. Its formula can be represented by



where the average value of  $n$  is close to 10

**Distillation.**—The separation of the sample into fractions was performed with a molecular still similar to that described by Matalon and Smith.<sup>2</sup> The still was operated at a pressure of about  $10^{-4}$  mm. The first step was to split the sample into two fractions, one distilling below 200° and the other between 200 and 220°. The low boiling fraction was insoluble in water. The high boiling fraction dissolved to give clear solutions. Each of these fractions was then re-introduced into the still and split into a high- and a low-boiling sub-fraction. In each case, the low-boiling sub-fraction was insoluble in water at room temperature but the high boiling sub-fraction dissolved to give a clear solution. The two soluble sub-fractions were used for the subsequent measurements. Measurements of freezing point depression in benzene indicated that  $n \approx 12$  for the higher boiling of the two soluble sub-fractions and  $n \approx 8$  for the lower boiling soluble sub-fraction.

Recombination of the fractions obtained in any one of the distillations always gave a substance whose solubility characteristics were the same as those of the starting material for that distillation. This leads one to conclude that the distillation procedure did not involve significant amounts of degradation or other changes in the samples.

**Measurements.**—Turbidity and differential refractive index measurements were made at 23° and at 436  $\mu$  as previously described.<sup>1</sup>

(1) L. M. Kushner and W. D. Hubbard, *This Journal*, **58**, 1163 (1954).

(2) R. Matalon and C. C. Smith, *Nature*, **165**, 613 (1950).

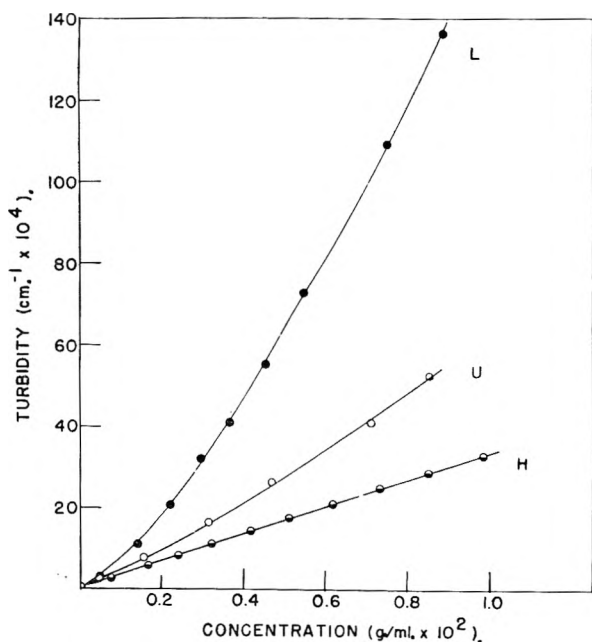


Fig. 1.—The dependence of turbidity on concentration for unfractionated Triton X-100 (U), for a high- (H), and for a low-boiling (L) fraction derived from it.

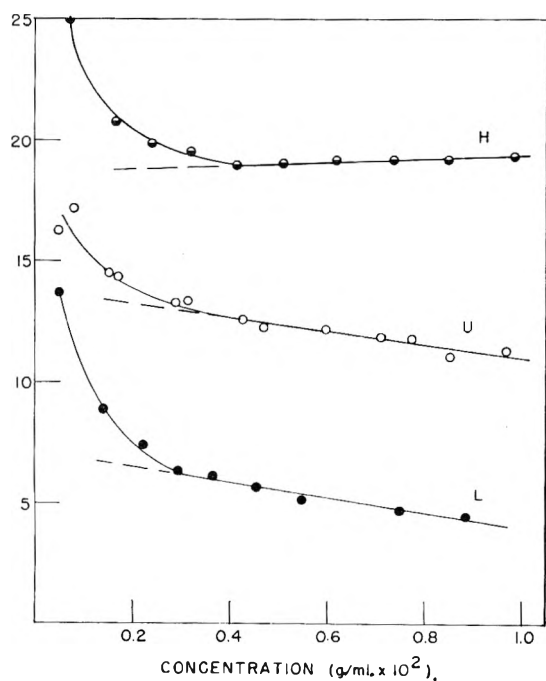


Fig. 2.—The dependence of  $H(c/\tau)$  on  $c$  for Triton X-100 and for two fractions derived from it. U, H and L designate the unfractionated detergent, and high- and the low-boiling fractions, respectively.

### Results and Discussion

In Fig. 1 is shown the dependence of turbidity on concentration for the unfractionated detergent U, the high-boiling soluble sub-fraction H, and the low-boiling soluble sub-fraction L. At any given concentration L has the highest turbidity and H the lowest.

In Fig. 2, the data have been plotted according to the method of Debye.<sup>3</sup>  $H$  is the usual light

scattering constant. The quantity  $c$  is concentration of detergent in g./ml. and  $\tau$  is the turbidity of the solution minus that of the solvent. For a solution of colloidal particles whose size distribution is independent of concentration, a straight line should result. The intercept at  $c = 0$  is the reciprocal of the weight average molecular weight of the particles.

For each sample, it is clear that below a concentration of about 0.3 to 0.4 g./dl. (Fig. 2), the mean degree of association of the detergent is a rapidly changing function of the concentration. Under the circumstances it is not possible to determine unequivocally the molecular weight of the detergent micelles. However, by a procedure previously discussed,<sup>1</sup> it is possible to reduce the data so that straight lines are obtained and the following micellar weights calculated:

| Sample | Micellar wt. |
|--------|--------------|
| L      | 208,000      |
| U      | 90,000       |
| H      | 53,500       |

Because the extrapolation by which they were obtained was not to infinite dilution of micelles, the percentage error in each micellar weight is about 5–10%. This is larger than is ordinarily the case with light scattering measurements; however, the substantial differences between the micellar weights of the samples are greater than can be accounted for by experimental and other errors.

It is of interest to compare these experimental results with a theory for non-ionic detergent micelles recently presented by Reich.<sup>4</sup> From considerations of the change of interfacial energy involved in the aggregation of  $N$  detergent molecules into a micelle and the entropy change accompanying the association process, Reich is able to calculate the size distribution of the micelles as a function of the concentration of monomeric detergent. His conclusions are (1) the formation of micelles of non-ionic detergents occurs at a sharp critical micelle concentration, (2) for a given hydrophobic group, the critical micelle concentration should increase with increasing length of the hydrophilic chain, and (3) the most probable number of detergent molecules/micelle depends on the ratio  $S/A$ , where  $A$  is the total area of the hydrocarbon portion of the molecule and  $S$  is that portion of  $A$  that is covered by the polar group.

The data shown in Fig. 1 do not indicate a sharper critical micelle concentration for either of the fractions than for the unfractionated sample. This may be due to insufficient resolution of the fractions in the two distillations, although the difference between sub-fractions L and H is substantial as shown in Figs. 1 and 2. In Reich's theory, however, the sharpness with which micelles appear is markedly dependent on the values assigned to the entropy and energy change associated with micelle formation. His assignment of a high negative value (–20k) for the entropy change is probably unwarranted since it is based primarily on considerations of the heat of vaporization of dodecane and neglects the positive contribution to the total

(3) P. Debye, *Ann. N. Y. Acad. Sci.*, **51**, Art. 4, 575 (1949).

(4) I. Reich, *This Journal*, **60**, 257 (1956).

entropy change which results from the uncurling of the hydrocarbon portion of the detergent molecule when it enters a micelle. Choice of a smaller value for the entropy change would reduce the predicted sharpness of micelle formation.

Although no critical micelle concentrations were observed in this work, the data in Fig. 2 suggest that a mean micelle size which is concentration independent is achieved at a lower concentration with sample L than with the unfractionated detergent or fraction H. This is expected on the basis of solubility considerations and is predicted by Reich.

The very large difference between the micelle weights for fractions L and H is surprising, and shows that the ratio  $S/A$ , which should be identical for the two fractions and the unfractionated sample, is not the primary factor determining the most probable size of a stable micelle. The higher micelle weight for the lower molecular weight fraction shows that the mean degree of association increases as the hydrophilic group is shortened. The micelles formed by L contain at least four times as many detergent molecules as those formed by sub-fraction H. Such a large difference, if the hydrocarbon portions of the molecule are identical in the two fractions, probably reflects a different type of packing and micelle shape.

## THE CHEMICAL REACTIONS OF CALCIUM HYDROXIDE, SILICA AND WATER MIXTURES AT 82°

BY SIDNEY A. GREENBERG<sup>1</sup>

*Johns-Manville Research Center, Manville, New Jersey*

*Received September 17, 1956*

The chemical reaction of calcium hydroxide with colloidal silicas in the presence of excess water was investigated by examining periodically the liquid and solid phases during the course of the reaction. Electrical conductivity and pH measurements were used to follow the changes in composition of the liquid phases. The formation of the solid products was studied by differential thermal analysis (DTA), surface area, weight loss and X-ray techniques.

### Experimental

**Materials.**—The Mallinckrodt Sp.B., S.L. and aerogel silicas have been described.<sup>2</sup> The diatomaceous silica D.S. (Celite 403, Johns-Manville Corp.) was mined at Lompoc, Calif. Both Baker A.R. calcium hydroxide and some prepared from Mallinckrodt S.L. calcium carbonate were used.

**Equipment.**—Most of the apparatus<sup>3</sup> has been described. The differential thermal analysis equipment is essentially like one in the laboratory of Professor P. Kerr at Columbia University.<sup>3</sup>

**Procedure.**—In each experiment 25 g. of calcium hydroxide was allowed to react with an equimolar quantity of SiO<sub>2</sub> in 800 ml. of water at 82°. Samples were removed periodically and the phases were separated by filtration.

### Results and Conclusions

**Liquid Phases.**—After 20 minutes of reaction the pH values of the solutions were between 12.1

and 12.3 and remained at this level for the greater part of the reaction period. The conductivity of the solution containing Sp.B. silica decreased from 3.0 to  $1.3 \times 10^{-3}$  ohms<sup>-1</sup> in four hours. In contrast the solution with S.L. silica showed a small increase from 3.8 to  $4.3 \times 10^{-3}$  ohms<sup>-1</sup> in agreement with the pH measurements. The electrical conductance of the solution with D.S. fluctuated between 4.0 and  $5.8 \times 10^{-3}$  ohms<sup>-1</sup> during the course of the reaction. Essentially, therefore, most of the reaction proceeds in a saturated solution of calcium hydroxide.<sup>2</sup>

**Solid Phases.**—The DTA curves showed endothermic peaks at 490° for the decomposition of calcium hydroxide and at 825° exothermic peaks were found which correspond to the conversion to β-wollastonite of tobermorite.<sup>2,4</sup> The peak heights at 490° decrease with reaction time for samples containing S.L. and D.S. silicas; however, only a very small peak was found for the sample with Sp.B. silica after 20 minutes of reaction. The peak heights at 825° increased rapidly with reaction time for the S.L. and Sp.B. samples, and somewhat less rapidly for the mixture with D.S. silica, but after 3 hours of reaction all the peaks reached the same height. There is a rapid rise in surface area for the mixture with D.S. silica from 15 to 78 sq.m./g. in 210 minutes. In Table I the surface area of products after 3 to 4 hours of reaction are listed.

TABLE I

| Silica type | Surface areas, sq. m./g. SiO <sub>2</sub> | Reaction time, hr. | Surface areas, sq. m./g. sample |
|-------------|---|--------------------|---------------------------------|
| S.L.        | 750                                       | 4                  | 61                              |
| Sp. B.      | 383                                       | 3                  | 54                              |
| D.S.        | 22  | 3                  | 61                              |
| Aerogel     | 247                                       | 3                  | 45                              |

The 1000° weight losses of the solid phases initially dried at 115° decrease with reaction time and level off at 12.5 to 13.8% (g. loss/100 g. ignited sample) after two hours of reaction. After 45 minutes of reaction the X-ray patterns of the mixtures with S.L. and Sp.B. silicas showed evidence for the presence of tobermorite in lines at 3.05 and 1.82 Å.<sup>4</sup> No such lines were found in the pattern of the sample containing D.S. silica.

**Conclusions.**—The reactions rates are different but are not necessarily proportional to the surface areas of the silicas. (It should be noted that the absolute rate of reaction is slower for these large crystallite size, chemically-pure, calcium hydroxides than for fine-particle size, commercial grade limes.<sup>5</sup>) Although the products show essentially the same surface areas (Table I), those with D.S. or Sp. B. silicas are thixotropic gels,<sup>5</sup> but high surface area, S.L. silica does not form such a gel. It is clear that tobermorite forms immediately on reaction. Both the thixotropic behavior and electron microscopy<sup>6</sup> indicate that the products are plate-like crystals. Although it is difficult to propose a complete mechanism, nevertheless because of the insolubility of calcium silicate in the presence of excess calcium

(1) Chemistry Department, Seton Hall University, South Orange, New Jersey.

(2) S. A. Greenberg, *THIS JOURNAL*, **58**, 362 (1954); **60**, 325 (1956).

(3) P. Kerr, *et al.*, Preliminary Reports, Reference Clay Minerals, American Petroleum Institute, Research Project 49, Columbia University, New York, N. Y., 1951.

(4) H. F. M. Taylor, *J. Chem. Soc.*, 3682 (1950); 163 (1953).

(5) S. A. Greenberg, unpublished results.

(6) A. Grudemo, in article by J. D. Bernal, "The Structures of Cement Hydration Compound," Proceedings of the Third International Symposium on the Chemistry of Cement, London, 1952.

hydroxide,<sup>2</sup> it seems reasonable to assume that reaction of colloidal silica with calcium hydroxide solutions must occur *in situ* and not in solution. (The same kind of reaction would be expected for the hydrolysis of tricalcium silicate.) According to this hypothesis calcium hydroxide would first be chemisorbed by silica, then in the presence of the  $\text{Ca}^{++}$  and  $\text{OH}^-$  ions and water, which would diffuse into the silica structure, hydrolysis of  $\text{SiOSi}$  bonds results ( $\text{pH } 12.3 \pm 0.2$ ) and simultaneously the  $\text{SiO}_4$  tetrahedra reorient into the tobermorite structure.

**Acknowledgments.**—The assistance of Mr. J. Pellicane in the performance of most of the experimental work is gratefully acknowledged. Thanks are also due to Mr. J. McGourty of this Laboratory for the Debye-Scherrer patterns and to Mr. G. Reimschuessel for the surface area measurements.

## THE CRITICAL PRESSURE AND TEMPERATURE OF DIMETHYL OXALATE

BY S. ALEXANDER STERN AND WEBSTER B. KAY

Department of Chemical Engineering, The Ohio State University, Columbus, Ohio

Received October 19, 1956

The critical pressure and temperature of dimethyl oxalate,  $(\text{COOCH}_3)_2$ , are reported in the International Critical Tables<sup>1</sup> as 9.48 atmospheres and  $260^\circ$ , respectively, based on older experimental data.<sup>2,3</sup> A critical pressure of 9.48 atmospheres appears abnormally low for this compound when compared with that of other esters of organic acids. Consequently, it was decided to measure the critical constants of dimethyl oxalate in order to determine whether the low value reported for the critical pressure is in error or whether it represents a possible anomalous behavior.

### Experimental

Eastman Kodak Co. research grade dimethyl oxalate was fractionally crystallized from ethyl alcohol five times. The purified fraction was then degassed under high vacuum (less than  $1 \times 10^{-5}$  mm.) and a portion was distilled into the experimental tube, and was frozen, and the remainder of the tube filled with mercury preparatory to the determination of the critical constants.

The experimental method for the determination of the critical constants consisted essentially in the determination of the temperature at which the liquid-vapor interface disappeared when the sample was heated. The apparatus has been described elsewhere.<sup>4</sup>

Dimethyl oxalate was found to be thermally unstable above  $200^\circ$ , decomposing to form a dark colored liquid and a relatively insoluble gas. It was necessary therefore to raise the temperature of the sample rapidly to the critical temperature in order to minimize the effect of the decomposition products on the value of the critical constants. While this procedure results in a fair approximation of the critical temperature, the pressure observed is considerably higher than the true critical pressure because of the presence of the gaseous decomposition product.

To obtain a value of the pressure consistent with the experimental critical temperature the critical pressure was calculated from a Clausius-Clapeyron vapor pressure equation of the form  $\log P = A - B/T$  established at lower tem-

peratures. Such a procedure is justified, as the above equation is known to fit the vapor pressure data of a large number of substances reasonably well up to the critical point, even though the basic assumptions usually made in its derivation are not valid over so extensive a range.<sup>5</sup> While of a lower order of accuracy, the above method is capable of bracketing the values of the critical constants within reasonable limits.

### Results

In order to evaluate the constants, "A" and "B," of the equation  $\log P = A - B/T$ , the following vapor pressure data were obtained for dimethyl oxalate.

|                |       |      |      |      |
|----------------|-------|------|------|------|
| Temp., °C.     | 163.3 | 180  | 220  | 260  |
| Pressure, atm. | 1.03  | 1.56 | 3.99 | 8.87 |

The values of "A" and "B" were calculated by the least-squares method and found to be 5.2240 and 2280, respectively, when the pressure is given in atmospheres and the temperature in °K. The average deviation of the vapor pressures computed by means of the equation from the experimental data is less than  $\pm 3\%$ .

The critical temperature of dimethyl oxalate was observed to be  $355 \pm 7^\circ$ , while the critical pressure, calculated by means of the vapor pressure equation as the pressure at the critical temperature, was estimated to be  $39.3 \pm 4$  atm. The pressure observed at the critical temperature was 55.4 atm, indicating the presence of gaseous decomposition products.

Using the empirical methods for estimating critical constants developed by Lyderson,<sup>6</sup> the critical temperature and critical pressure of dimethyl oxalate were calculated to be  $366^\circ$  and 39.4 atmospheres, respectively, in fair agreement with the values reported here.

It is concluded, therefore, that the critical temperature and pressure previously reported for dimethyl oxalate are grossly in error.

(5) B. F. Dodge, "Chemical Engineering Thermodynamics," 1st Ed., McGraw-Hill Book Co., Inc., New York, N. Y., 1934, p. 248.

(6) O. A. Hougen, K. M. Watson and R. A. Ragatz, "Chemical Process Principles," Vol. I, John Wiley and Sons, Inc., New York, N. Y., 1954, p. 87.

## SHEAR DEPENDENCE OF VISCOSITY OF NATURAL RUBBER SOLUTIONS

BY MORTON A. GOLUB

Contribution from the B. F. Goodrich Company Research Center, Brecksville, Ohio

Received October 19, 1956

In an earlier paper<sup>1</sup> viscosity measurements on dilute Alfin polyisoprene solutions at quite low shear rates were reported. It was shown that the limiting slope of the intrinsic viscosity *vs.* rate of shear plot at low shear rates,  $(\Delta[\eta]/\Delta D)_{D \rightarrow 0}$ , is proportional to the square of the zero shear intrinsic viscosity  $[\eta]_0^2$ . This relationship suggested the possibility of using the slope of the  $(\Delta[\eta]/\Delta D)_{D \rightarrow 0}$  *vs.*  $[\eta]_0^2$  plot as a molecular weight-independent parameter expressing the magnitude of the shear dependence of intrinsic viscosity, and thus as a possible means for studying polymer microstructure. It

(1) "International Critical Tables," Vol. III, McGraw-Hill Book Co., New York, N. Y., 1928, p. 248.

(2) H. V. Regnault, *Mem. Acad. Roy. Sci.*, **26**, 335 (1862).

(3) F. Weger, *Ann.*, **221**, 61 (1883).

(4) W. B. Kay and G. M. Rambow, *Ind. Eng. Chem.*, **45**, 221 (1953).

(1) M. A. Golub, *This Journal*, **60**, 421 (1956).

was thought that polymers having different structures would give rise to linear plots of the latter type, but with different slopes. To test this view, it was deemed desirable to extend viscosity measurements to another polyisoprene system, namely, natural rubber. This note describes the results obtained from viscosity measurements on Hevea fractions, and shows the comparative shear effects for both the natural *cis* and the predominantly *trans* Alfin polyisoprenes.

#### Experimental

The Hevea was a sample of pale crepe. The polymer was dissolved in benzene and the gel fraction extracted by filtration through a fine wire screen. The soluble portion was then fractionated by the usual precipitation of polymer from benzene solution with methanol. The six highest fractions, varying in molecular weight from about one to four million (Table I), were employed. The natural rubber solutions were stabilized by incorporation of tetramethylthiuram disulfide to the extent of 1% on polymer. Viscosity measurements were carried out on benzene solutions of polymer fractions at  $25 \pm 0.01^\circ$  over the approximate shear range of 100 to 600  $\text{sec}^{-1}$  in the horizontal capillary viscometer previously described,<sup>1</sup> following the same procedure as before.

TABLE I

| MOLECULAR WEIGHTS OF HEVEA FRACTIONS |            |                           |
|--------------------------------------|------------|---------------------------|
| Fraction                             | $[\eta]_0$ | Mol. wt. $\times 10^{-4}$ |
| A                                    | 14.0       | 3.87                      |
| B                                    | 12.1       | 3.12                      |
| C                                    | 10.8       | 2.70                      |
| D                                    | 9.2        | 2.25                      |
| E                                    | 8.4        | 1.95                      |
| F                                    | 5.8        | 1.07                      |
| U (Unfractd.)                        | 8.8        | 2.10                      |

#### Results and Discussion

Experimental curves of reduced viscosity *vs.* rate of shear were obtained for three concentrations of each of the various fractions, as well as for the un-fractionated polymer. Typical plots are shown in Fig. 1. From such graphs, isoshear plots of  $\eta_{sp}/c$  *vs.*  $c$  at various gradients were constructed, and these in turn were extrapolated to zero concentration to give intrinsic viscosity at various rates of shear over the range considered. Figure 2 shows the shear dependence of intrinsic viscosity for the various Hevea fractions. The slopes of these lines were then plotted against the squares of the zero shear intrinsic viscosities, as shown in Fig. 3, where they are seen to fall along the straight line obtained previously for Alfin polyisoprene.<sup>1</sup> Now, the all-*cis*-1,4-polyisoprene structure of Hevea contrasts with the very high *trans*-1,4-structure of the Alfin polymer which also contains substantial pendant vinyl and isopropenyl groups.<sup>2</sup> Thus, in spite of the known structural differences between the two polyisoprenes, the non-Newtonian behavior of their dilute solutions as represented by the suggested molecular weight-independent parameter is virtually the same.

There is, however, one interesting qualitative difference between the shear effects for the two polymers. The slopes of the lines in Fig. 1 are all greater than corresponding ones for the Alfin polymers of roughly the same molecular weight and solution concentration. (Compare Fig. 1 of the

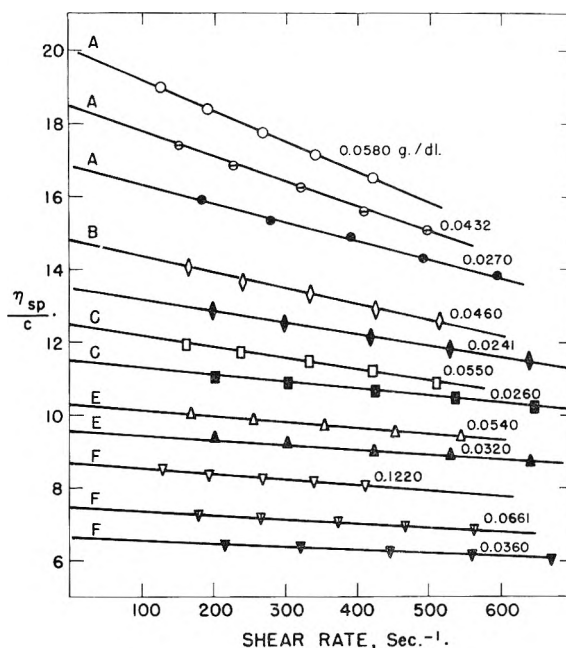


Fig. 1.—Reduced viscosity *vs.* rate of shear for Hevea fractions of different molecular weight in benzene at  $25^\circ$ .

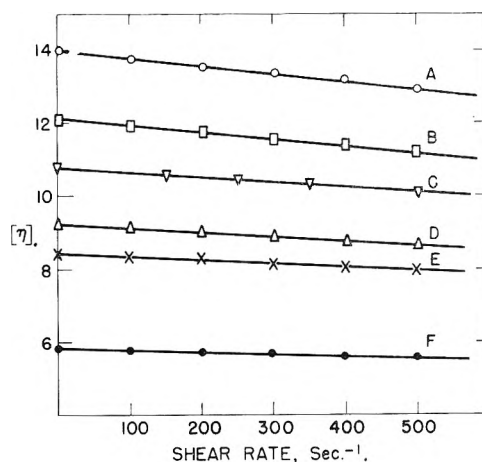


Fig. 2.—Shear dependence of intrinsic viscosity for various Hevea fractions in benzene.

present paper with Fig. 2 of ref. 1). This may be seen from Table II, although, fortuitously, no

TABLE II

SLOPES OF TYPICAL VISCOSITY-SHEAR PLOTS FOR VARIOUS POLYMERS

| Fraction | $[\eta]_0$ | Concn. g./dl. | $(\eta_{sp}/c)_0$ | $-\left(\frac{\Delta\eta_{sp}/c}{\Delta D}\right) \times 10^3$ |
|----------|------------|---------------|-------------------|--|
| Hevea—B  | 12.1       | 0.0460        | 14.80             | 4.20   |
| B        | ...        | .0241         | 13.50             | 3.00   |
| C        | 10.8       | .0550         | 12.55             | 3.24   |
| C        | ...        | .0260         | 11.47             | 1.84   |
| Alfin—1c | 12.8       | .0500         | 16.24             | 2.86   |
| 1c       | ...        | .0250         | 14.62             | 2.24   |
| 3c       | 10.3       | .0595         | 14.00             | 2.68   |
| 3a       | ...        | .0298         | 12.10             | 1.64   |

strictly comparable results are available. Nevertheless, it is evident that Hevea fraction B, with a somewhat smaller estimated molecular weight than Alfin 1c, has a much larger viscosity-shear slope

(2) W. S. Richardson and A. Sacher, *J. Polymer Sci.*, **10**, 353 (1953).

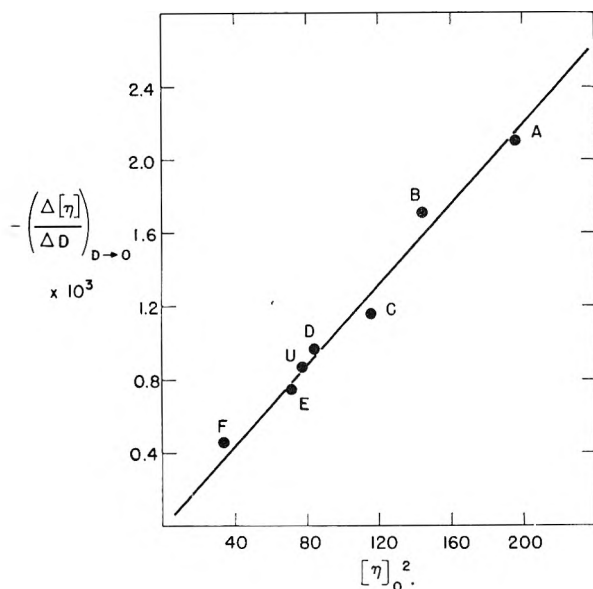


Fig. 3.—The limiting slope of the intrinsic viscosity-rate of shear curve plotted against the square of the zero shear intrinsic viscosity. The circles correspond to present data for Hevea fractions and the line represents the relation obtained previously for Alfin polyisoprene.

than does the latter, at more or less the same concentrations; similarly for Hevea fraction C and Alfin 3a. Unfortunately, these results cannot be conveniently reduced to any common denominator for comparison short of the molecular weight-independent parameter already mentioned. This, of course, has been shown to be insensitive to the structural differences between the two samples of polyisoprene under consideration.

As pointed out by Goldberg and Fuoss,<sup>3</sup> the non-Newtonian behavior of polymer solutions can arise from either the shear dependence of interaction between polymer molecules or the shear dependence of the intrinsic viscosity, or both. Since the latter factor is apparently the same for the two polymers in question, it follows that the remaining difference between them must be ascribed to the difference in the shear dependence of polymer interaction. Now, examination of the isoshear plots of Alfin polyisoprene<sup>1</sup> reveals that the Huggins  $k'$  is more or less constant over the shear range 0–600 sec.<sup>-1</sup> (e.g., 0.36 for fraction 1a), whereas with the natural rubber molecule  $k'$  decreases with shear rate (e.g., from  $k' = 0.41$  at  $D = 0$  to  $k' = 0.25$  at 600 sec.<sup>-1</sup> for Hevea fraction B). The explanation for this disparity in the shear dependence of interaction is presently unknown.

It appears from the above that the shear effect in dilute solutions may not be used readily for studying microstructural differences in polymers, although concentrated solutions may actually show definite differences between such polymers. Moreover, for most polymers of interest, the dilute solution viscosities are smaller than those considered here and as a result their shear effects are much less pronounced, in which case the suggested parameter would be even less likely to be useful for microstructural studies.

(3) P. Goldberg and R. M. Fuoss, *THIS JOURNAL*, **53**, 648 (1954).

**Acknowledgment.**—The assistance of Mrs. Corinne Bonar with the experimental work is gratefully acknowledged.

## SOME CONSIDERATIONS ON THE GUGGENHEIM AND CONVENTIONAL EQUATIONS FOR ELECTRIC MOMENT CALCULATIONS<sup>1</sup>

BY GEORGE K. ESTOK

*Department of Chemistry and Chemical Engineering, Texas Technological College, Lubbock, Texas*

Received October 27, 1956

The Guggenheim method for determining electric moments, using dielectric constant and refraction measurements on solutions, has been developed in recent years.<sup>2–4</sup>

Some confusion, however, appears to have arisen<sup>5,6</sup> as an outgrowth of the original manner of deriving the equation,<sup>2</sup> in which an arbitrary symbol representing a fictitious atomic polarizability,  $\gamma_a'$ , was introduced. Another contributing factor was the elimination of two small terms from the original exact equation, yielding an approximate equation.

The purpose here is to derive, in a concurrent and completely analogous manner, both the conventional and Guggenheim equations, starting with the same initial equations used by Guggenheim. This aids in making a simple comparison of the two equations. It will further be demonstrated that the derivation made by Palit,<sup>5</sup> who used a different set of starting equations, leads to exactly the same equation as that of Guggenheim.

Symbols used in the following treatment are:  $M$ ,  $v$ ,  $V$ ,  $\epsilon$ ,  $n$ ,  $P$ ,  $\gamma$  and  $\mu$ , which refer, respectively, to: molecular weight, specific volume, molar volume, dielectric constant, index of refraction, molar polarization, polarizability and electric moment. Subscripts are: 1 (pure solvent); 2 (pure solute); a, atomic; and e, electronic. For convenience, symbols without subscripts refer to solution values, except that  $x$  and  $w$  refer to mole fraction solute and weight fraction solute, respectively, in the solution.

The original derivation by Guggenheim<sup>2</sup> used the Debye equations as a basis

$$\left(\frac{\epsilon - 1}{\epsilon + 2}\right) V = \left(\frac{\epsilon_1 - 1}{\epsilon_1 + 2}\right) V_1(1 - x) + \frac{4\pi N}{3} \left(\gamma_e + \gamma_a + \frac{\mu^2}{3kT}\right) x \quad (1)$$

$$\left(\frac{n^2 - 1}{n^2 + 2}\right) V = \left(\frac{n_1^2 - 1}{n_1^2 + 2}\right) V_1(1 - x) + \frac{4\pi N}{3} \gamma_e x \quad (1a)$$

where  $V_1$  and  $V_2$  are partial molar volumes of solvent and solute and  $V = V_1 + x(V_2 - V_1)$

By subtracting equation 1a from equation 1 Guggenheim obtained

(1) Presented at the 130th meeting of the American Chemical Society, Atlantic City, Sept., 1956.

(2) E. A. Guggenheim, *Trans. Faraday Soc.*, **45**, 714 (1949).

(3) J. W. Smith, *ibid.*, **46**, 394 (1950).

(4) E. A. Guggenheim, *ibid.*, **47**, 573 (1951).

(5) S. R. Palit, *J. Am. Chem. Soc.*, **74**, 3952 (1952).

(6) E. A. Guggenheim, *Proc. Phys. Soc.*, **68B**, 186 (1955).

$$\left(\frac{\epsilon - 1}{\epsilon + 2} - \frac{n^2 - 1}{n^2 + 2}\right) [V_1 + x(V_2 - V_1)] = \left(\frac{\epsilon_1 - 1}{\epsilon_1 + 2} - \frac{n_1^2 - 1}{n_1^2 + 2}\right) V_1(1 - x) + \frac{4\pi N}{3} \left(\gamma_a + \frac{\mu^2}{3kT}\right) x \quad (2)$$

To simplify the following treatment, let  $4\pi N/3 = K$ ,  $\mu^2/3kt = F$ ,  $\epsilon - 1/\epsilon + 2 = H$ , and  $(\epsilon - 1/\epsilon + 2) - (n^2 - 1/n^2 + 2) = G$ . Then equations 1 and 2 may be written, respectively

$$H[V_1 + x(V_2 - V_1)] = H_1V_1(1 - x) + K(\gamma_e + \gamma_a + F)x \quad (3)$$

$$G[V_1 + x(V_2 - V_1)] = G_1V_1(1 - x) + K(\gamma_a + F)x \quad (4)$$

Expanding and rearranging equation 3 gives

$$HV_1 + Hx(V_2 - V_1) - H_1V_1(1 - x) = K(\gamma_e + \gamma_a + F)x$$

Differentiation with respect to  $x$  yields

$$V_1 \frac{dH}{dx} + HV_2 - HV_1 + x(V_2 - V_1) \frac{dH}{dx} + H_1V_1 = K(\gamma_e + \gamma_a + F)$$

At infinite dilution  $HV_2 = H_1V_2$ ,  $HV_1 = H_1V_1$ , and  $x(V_2 - V_1) (dH/dx) = 0$ , so that the following conventional equation results

$$V_1 \left(\frac{dH}{dx}\right)_\infty = K(\gamma_e + \gamma_a + F) - H_1V_2 \quad (5)$$

Analogous treatment of equation 4 leads directly to the Guggenheim equation

$$V_1 \left(\frac{dG}{dx}\right)_\infty = K(\gamma_a + F) - G_1V_2 \quad (6)$$

Equation 6 is analogous to equation 5, except that the electronic polarizability has been eliminated.

Conversion of the concentration unit from mole fraction solute  $x$  to weight fraction  $w$  may be accomplished by using the following general relation, valid at infinite dilution:  $(dA/dx)_\infty = M_2/M_1 \cdot (dA/dw)_\infty$ , where  $A$  may be  $H$  or  $G$ .

The conventional and Guggenheim equations may now be written, respectively

$$M_2v_1(dH/dw)_\infty = K(\gamma_e + \gamma_a + F) - H_1V_2 \quad (5a)$$

$$M_2v_1(dG/dw)_\infty = K(\gamma_a + F) - G_1V_2 \quad (6a)$$

where  $v_1$  is the partial specific volume of the solvent.

By further differentiating, with respect to  $w$ , the quantities represented by  $H$  and  $G$ , letting  $\epsilon = \epsilon_1$  and  $n = n_1$  at infinite dilution, and resubstituting for  $K$  and  $F$ , the following working forms are obtained

$$\mu^2 = \frac{9kT}{4\pi N} \left[ \left(\frac{3M_2v_1}{(\epsilon_1 + 2)^2} \left(\frac{d\epsilon}{dw}\right)_\infty + \left(\frac{\epsilon_1 - 1}{\epsilon_1 + 2}\right) M_2v_2 - P_{2e} - P_{2a} \right) \right] \quad (7)$$

$$\mu^2 = \frac{9kT}{4\pi N} \left\{ 3M_2v_1 \left[ \frac{d\epsilon/dw_\infty}{(\epsilon_1 + 2)^2} - \frac{dn^2/dw_\infty}{(n_1^2 + 2)^2} \right] + \left(\frac{\epsilon_1 - 1}{\epsilon_1 + 2} - \frac{n_1^2 - 1}{n_1^2 + 2}\right) M_2v_2 - P_{2a} \right\} \quad (8)$$

where  $P_{2e} = (4\pi N/3)\gamma_e =$  electronic polarization, usually taken equal to the molar refraction,  $MR_D$ ;  $P_{2a} = (4\pi N/3)\gamma_a =$  atomic polarization, often taken as  $0.05 MR_D$ .

In either equation, if the specific volume of the pure solute (as a liquid) is available, it may be substituted for the partial specific volume  $v_2$  without

significant error, thus obviating the need for density measurements on the solutions.<sup>7</sup>

If the  $MR_D$  for a solid solute is obtainable without making refraction measurements, then equation 7 is much simpler to use, since only dielectric constant data need be gathered. In the event refraction measurements must be made, there is little to choose between equations 7 or 8, except that the latter is less sensitive to an approximate value of  $v_2$  inasmuch as  $(\epsilon_1 - 1/\epsilon_1 + 2) - (n_1^2 - 1/n_1^2 + 2)$  is normally much smaller than  $\epsilon_1 - 1/\epsilon_1 + 2$  for non-polar solvents.

S. R. Palit<sup>6</sup> criticized and discussed the Guggenheim *approximate* equation (which neglected the last two terms of equation 8; *i.e.*,  $G_1M_2v_2$  and  $P_{2a}$ ) but did not appear to recognize that the Guggenheim *exact* equation was identical with his own derived *exact* equation. It may not be readily apparent that Palit's term  $B$  is identical with Guggenheim's  $G_1M_2v_2$  (also called  $[4\pi N/3]\gamma_a'$  by Guggenheim). This identity may be demonstrated as

$$\text{Palit's } B = \frac{3M_2(\epsilon_1 - n_1^2)}{d_1(\epsilon_1 + 2)(n_1^2 + 2)} \left(1 - \frac{\beta_0}{d_1}\right)$$

where  $d =$  density, and  $\beta_0 = (\partial d/\partial w)_\infty$ , also

$$G_1 = \frac{\epsilon_1 - 1}{\epsilon_1 + 2} - \frac{n_1^2 - 1}{n_1^2 + 2} = \frac{3(\epsilon_1 - n_1^2)}{(\epsilon_1 + 2)(n_1^2 + 2)}$$

It has been shown previously<sup>7</sup> that  $\beta_0$ , at infinite dilution, is equal to  $d_1^2(v_1 - v_2)$ , and thus Palit's  $(1 - \beta_0/d_1)$  is equal to  $d_1v_2$ . Therefore Palit's term  $B$  is identical with Guggenheim's  $G_1M_2v_2$  (or  $[4\pi N/3]\gamma_a'$ ).

In conclusion, it is felt that the derivations of the conventional and Guggenheim equations as here outlined permit an easy comparison and better understanding of the equations. In general the conventional approach is simpler, although occasionally the Guggenheim method could be preferred.

(7) G. K. Estok, *THIS JOURNAL*, **60**, 1336 (1956).

## CHELATE FORMATION BETWEEN CATIONS AND POLYELECTROLYTES

BY GEOFFREY ZUBAY<sup>1</sup>

Received November 1, 1956

Wolcott Gibbs Memorial Laboratory, Harvard University, Cambridge, Mass.

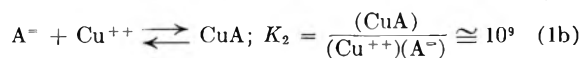
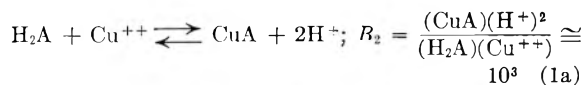
Chelate formation between cations and simple dicarboxylic acids may be treated adequately as a binding problem in terms of the mass action law. The situation is more complicated with polyelectrolytes because of the very large electrostatic energy term which in general makes the binding much stronger than in the corresponding monomeric case. Considerable progress has been made in treating the case of univalent counterions. The purpose of this note is to point out the additional difficulties that arise in the case of multivalent counterions and the inadequacy of a recent attempt to overcome these difficulties.

The binding of copper to oxalic acid<sup>2</sup> may be con-

(1) U. S. Public Health Service Predoctorate Research Fellow of the National Heart Institute.

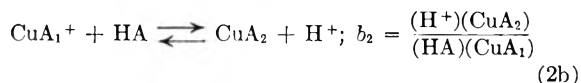
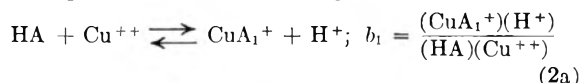
(2) The constants are determined from the data in Martell and Calvin, "Chemistry of the Metal Chelate Compounds," 1952.

sidered as a displacement reaction 1a or as a combination reaction 1b



Both of these constants are well defined because the concentrations of all the substances entering these equations are readily determinable by experiment. The same is not true for binding of copper to a poly-electrolyte such as polyacrylic acid. This is because there is no direct way of measuring the number of adjacent ionized carboxylate sites. This has been recognized by H. Morawetz, *et al.*,<sup>3</sup> for the special case of maleic anhydride copolymers. The general result is that for polyelectrolytes we may only make a rigorous test of equation 1a.

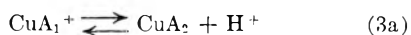
Gregor, *et al.*,<sup>4</sup> employed equation 1a in the expectation that it might lead to a formation constant that would be independent of the net charge carried by the polymer since the reaction involves no net change in charge. They considered the displacement reaction of copper with polyacrylic acid to take place in two steps giving equations<sup>5</sup>



with the over-all competitive complexation constant

$$B_2 = b_1 b_2 = \frac{(\text{CuA}_2)(\text{H}^+)^2}{(\text{Cu}^{++})(\text{HA})^2} \quad (2c)$$

This procedure is in error because the second step in the formation of the Cu-PAA complex is not correctly represented by (2b). If the  $\text{Cu}^{++}$  in  $\text{CuA}_1^+$  reacts further to form  $\text{CuA}_2$  it is most likely that it will react with an adjacent carboxyl group<sup>6</sup> and since the number of adjacent carboxyl groups is two (or less depending on the degree of complexation) reaction (2b) is independent of (HA). Indeed this is the essence of the chelate effect. Thus (2b) should be replaced by



leading to

$$B_2 = \frac{(\text{CuA}_2)(\text{H}^+)^2}{(\text{Cu}^{++})(\text{HA})} \quad (3b)$$

The original values of  $B_2$  and the corrected values for Cu-PAA are given in Table I and compared with  $B_2$  for glutaric acid, the corresponding mono-meric analog.

The internal consistency between the competitive complexation constants in pure water and  $\text{NaNO}_3$  solution is good. The values in KCl are lower and show a steady increase with increasing PAA concentration. The latter values are suspect be-

(3) H. Morawetz, A. M. Kotliar and H. Mark, *THIS JOURNAL*, **58**, 619 (1954).

(4) H. P. Gregor, *et al.*, *ibid.*, **59**, 34 (1955); **59**, 366 (1955); **59**, 559 (1955); **59**, 990 (1955).

(5) See reference 4 for an explanation of the symbolism.

(6) Experimental evidence has been cited for this by F. T. Wall and S. J. Gill, *THIS JOURNAL*, **58**, 1128 (1954).

TABLE I

| Acid     | Concn.,<br>N | Neutral salt          | $B_2(2c)$<br>$\times 10^4$ | $B_2(3b)$<br>$\times 10^7$ |
|----------|--------------|-----------------------|----------------------------|----------------------------|
| PAA      | 0.01         | None                  | 420                        | 420                        |
| PAA      | .01          | 0.2 M $\text{NaNO}_3$ | 460                        | 460                        |
| PAA      | .01          | 2 M $\text{NaNO}_3$   | 1050                       | 1050                       |
| PAA      | .01          | 1 M KCl               | 28                         | 28                         |
| PAA      | .06          | 1 M KCl               | 23                         | 138                        |
| PAA      | .1           | 1 M KCl               | 40                         | 398                        |
| Glutaric | .01          | None                  | 0.174                      | 0.174                      |

cause chloride ion forms a strong complex with cupric ion in aqueous solution. The striking disparity between the values of  $B_2$  for PAA and glutaric acid<sup>7</sup> emphasizes the need for a more comprehensive approach to this problem in which the electrostatic terms would be evaluated directly.

The author wishes to thank Joseph Eigner, Edward Chun and Professor Paul Doty for constructive criticism.

(7) A statistical factor of 2 favors the  $B_2$  for PAA metal binding over glutaric acid metal binding.

## THE ACID DISSOCIATION QUOTIENT OF 3-HYDROXYL-1,3-DIPHENYLTRIAZINE

By R. W. RAMETTE AND T. R. BLACKBURN

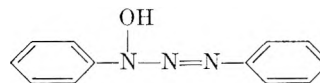
Contribution from Leighton Hall of Chemistry, Carleton College, Northfield, Minn.

Received September 17, 1956

Sogani and Bhattacharya<sup>1</sup> reported that 3-hydroxyl-1,3-diphenyltriazine forms an insoluble chelate with palladium, the latter forming bonds with the oxygen of the hydroxyl group and the nitrogen farthest removed from this group. The present research was concerned with the determination of the quotient governing the ionization of the compound as an acid. The quotient is defined as

$$K = (\text{H}^+)(\text{T}^-)/(\text{HT})$$

where  $\text{T}^-$  represents the anion and HT the undissociated molecular form which has the formula



**Apparatus.**—Absorbances were measured using silica 1-cm. cells in a Beckman DU spectrophotometer. The temperature was controlled at 25° by means of a circulating water-bath and dual thermospacers in the spectrophotometer.

**Reagents.**—The triazine was prepared as described by Sogani and Bhattacharya,<sup>1</sup> and was recrystallized twice from ethanol. Stock solutions were prepared by dissolving weighed amounts in ethanol.

Other reagents were of analytical reagent grade.

### Experimental

A series of solutions containing sodium hydroxide and potassium chloride were prepared in 100-ml. volumetric flasks and were suspended in a water-bath at 25°. The concentrations were such that upon dilution to the mark the pH ranged from 10.85 to 11.60 (assuming  $pK_w = 13.85$ ) with an ionic strength of 0.050. In each case, a 2-ml. portion of the stock triazine solution (freshly prepared, about  $\times 10^{-3}$  M in most cases) was added with a pipet, the solution diluted to the mark immediately and mixed, and the absorbance was measured as soon as possible at 390  $\mu$ . Instability of the solutions made it desirable to take successive readings at known times (every three minutes)

(1) N. C. Sogani and S. C. Bhattacharya, *Anal. Chem.*, **28**, 81 (1956).

and to extrapolate the absorbances back to the values they presumably would have been before any decomposition occurred. It is felt that the uncertainty in this procedure is well under one per cent. Solutions of pH equal to 6 and 14, containing the triazine virtually completely converted to the molecular and anion forms, respectively, were prepared and measured in a similar manner. The absorptivity of the molecular form is about  $3.3 \times 10^3$  liter mole<sup>-1</sup> cm.<sup>-1</sup> and the corresponding value for the anion is about  $2.7 \times 10^4$  at 390 m $\mu$ .

It was found that the addition of small amounts of sodium sulfite to the solutions before adding the triazine resulted in improved stability, probably due to the reduction of oxygen, and that this did not significantly affect the observed values of  $K$ .

The absorption spectra (approximate, because of instability) of the two forms are shown in Fig. 1.

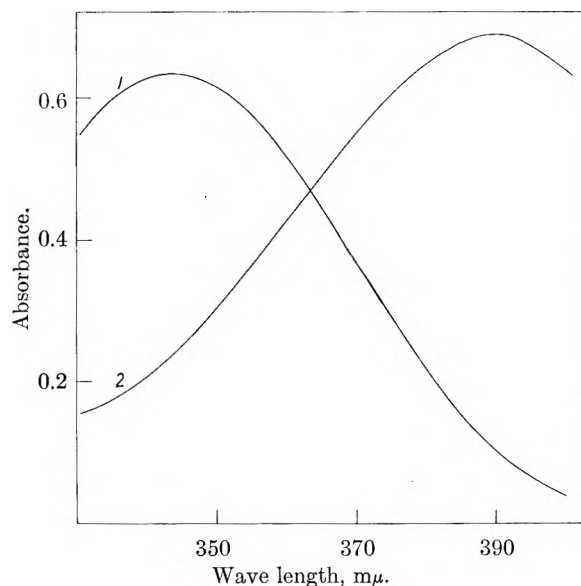


Fig. 1.—Absorption spectra of the two forms of 3-hydroxyl-1,3-diphenyltriazine: concentration about  $2.5 \cdot 10^{-6}$  M. Curve 1, pH 6, all triazine as molecular form; curve 2, pH 14, all triazine present as anion form.

### Results

Table I gives the values of  $K$  found at various pH values. The quotient was calculated by means of the formula

$$K = (H^+)(A - A_a)/(A_b - A)$$

where  $A$  is the observed absorbance of the solution containing both forms,  $A_a$  is the absorbance of the solution containing the triazine completely in the molecular form, and  $A_b$  is the absorbance of the solution containing the triazine completely in the anion form, all solutions having the same total concentration.

TABLE I

DISSOCIATION QUOTIENT OF 3-HYDROXY-1,3-DIPHENYLTRIAZINE

| pH    | $K \times 10^{12}$ | pK           |
|-------|--------------------|--------------|
| 11.30 | 2.63               | 11.58        |
| 11.40 | 2.79, 2.51         | 11.55, 11.60 |
| 11.45 | 2.80, 2.89         | 11.55, 11.54 |
| 11.50 | 2.94, 2.85         | 11.53, 11.55 |
| 11.55 | 2.83               | 11.55        |
| 11.60 | 3.23, 3.05         | 11.49, 11.52 |

These results give an average value of  $K = 2.85$  ( $\pm 0.14$ )  $\times 10^{-12}$ .

**Acknowledgments.**—It is a pleasure to acknowledge that this research was supported through the partial use of grants from the Research Corporation and from E. I. du Pont de Nemours and Co. We are indebted to Mr. Herbert Richardson for the preparation of the triazine.

## THE SOLUBILITY OF SODIUM HYDRIDE IN SODIUM

BY D. D. WILLIAMS, J. A. GRAND AND R. R. MILLER

Chemistry Division, Naval Research Laboratory, Washington, D. C.

Received August 30, 1956

As a continuation of the study of impurities in alkali metals<sup>1</sup> the solubility of sodium hydride in sodium has been determined. This system has implications bearing upon corrosion data interpretation from the standpoint of both direct reaction and apparent oxide content correlation.

This impurity in a sodium system can come from two principal sources, hydrogen-sodium reaction (impure cover gas), and as a product of the reaction between sodium and sodium hydroxide.<sup>2,3</sup> Previous work at NRL<sup>2</sup> established two facts pertinent to this study: that sodium hydride resulted from the Na-NaOH reaction at temperatures above 325°, and that the hydride so produced was stable when in solution in an excess of either primary reactant. Stability in NaOH has been shown by Gilbert,<sup>4</sup> and mutual solubility of sodium-sodium hydride has been reported by Banus, *et al.*<sup>5</sup> The stability in solution results in a lowering of the dissociation pressure of the sodium hydride. Thus, if a sodium system is heated, under other than high vacuum conditions, in order to rid it of any contained hydroxide,<sup>3,6</sup> sodium hydride is introduced as an impurity. A sample drawn from such a system for oxygen analysis, without accounting for the contained hydride would result in erroneous values.

The solubility of sodium hydride in sodium was, of necessity, determined by an indirect method, based upon the lowering of the dissociation pressure<sup>2,4</sup> of this normally unstable material.<sup>2,7,8</sup> Thus, at a given temperature, a mixture of sodium and sodium hydride will exhibit a true dissociation pressure only so long as the condensed portion of the system consists of two phases: saturated sodium and solid sodium hydride. During stepwise temperature increases the first incremental increase in temperature which failed to exhibit a corresponding increase in pressure indicated the temperature of saturation as the lower of the two temperatures.

### Experimental

Three techniques, with different apparatus, were used to establish the curve for the solubility of sodium hydride in sodium. Low temperature (240–300°) runs were made by

- (1) D. D. Williams, J. A. Grand and R. R. Miller, in preparation.
- (2) D. D. Williams, NRL Memorandum Report #33, 1952.
- (3) A. Klemenc and E. Svetlik, *Z. anorg. Chem.*, **269**, 153 (1952).
- (4) H. N. Gilbert, U. S. Patent 2,377,876 (June 1945).
- (5) M. D. Banus, J. J. McSharry and E. A. Sullivan, *J. Am. Chem. Soc.*, **77**, 2007 (1955).
- (6) J. D. Noden and K. Q. Bagley, Culcheth Laboratories, Tech. Note #80, 1954.
- (7) F. G. Keyes, *J. Am. Chem. Soc.*, **34**, 779 (1912).
- (8) A. Herold, *Compt. rend.*, **228**, 686 (1949).

exposing sodium to an excess of sodium hydride and sodium oxide, filtering, and: (1) analyzing the filtrate by amalgamation and titration, and (2) analyzing the filtrate by controlled dissociation in a calibrated volume. Higher temperatures (300–445°) were investigated by both absorption and desorption of hydrogen in an apparatus which provided for simultaneous recording of  $P$ - $V$ - $T$  data.

The low temperature apparatus consisted of two 50-ml. Pyrex flasks joined by an inverted U shaped piece of tubing. One flask was equipped with an inlet port and was used as a still for introducing pure sodium into the second flask. This latter flask was fitted with an inlet port, thermocouple well, vacuum manifold outlet, and a sintered glass filter below which was a thin-walled ampule of about 3-ml. capacity. Sodium hydride (98%) was placed in the saturation chamber and metallic sodium in the distilling pot. The system was purged by evacuation and the sodium was distilled into the saturation chamber. Heat was applied to the Na-NaH mixture and the filter until a desired temperature was reached. The melt was allowed to soak at this temperature for five minutes. (Attack on the glass system, by the sodium, also saturated the melt with sodium oxide.). Nitrogen pressure was then admitted, forcing the saturated metal into the sample bulb, which was then sealed off. This sample was then analyzed in the apparatus described in the NRL modification<sup>9</sup> of the Pepkowitz and Judd method for oxygen in sodium. The total apparent oxide alkalinity thus determined was corrected for that due to oxide saturation,<sup>1</sup> the remainder being alkalinity due to sodium hydride. The presence of traces of sodium hydride was confirmed during analysis by the evolution of gas bubbles when the amalgamation residue was hydrolyzed.

For some runs, this apparatus was modified by replacing the sample ampule with a calibrated volume receiver and a manometer. After saturation and filtration, the analysis for hydride was made by heating the sample under vacuum. The temperature and pressure of evolved hydrogen were noted. The amount of sodium hydride was thus calculable. Sample weight was determined by reaction with alcohol and titration.

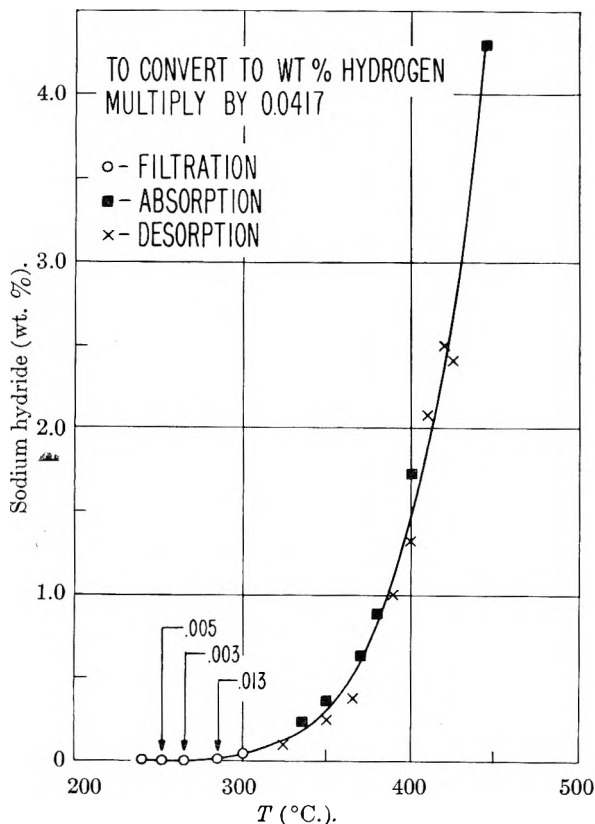


Fig. 1.—The solubility of sodium hydride in metallic sodium.

(9) D. D. Williams and R. R. Miller, *Anal. Chem.*, **23**, 1865 (1951).

Both of the above methods suffer from the presence of sodium oxide in the samples, and they are limited to a low temperature range because of accelerated attack upon the glass systems at higher temperatures. Furthermore, both methods tend to yield low results by reason of the temperature changes involved in the filtering and cooling steps. As the saturated sodium cools, solid sodium hydride separates and dissociates to some indeterminate extent depending upon run temperature and cooling rate. Thus, some hydride is irretrievably lost. The bulk of the hydride solubility data, therefore, was gathered by the indirect method of hydrogen evolution and absorption.

The apparatus for absorption and desorption studies consisted of a metal saturation pot attached by means of a metal ball joint to a Pyrex system which included a 1,250-cc. calibrated volume, a mercury manometer and a vacuum manifold connection. A stopcock between the saturation pot and the calibrated volume allowed for the isolation of the hot from the cold part of the system. The volume of the heated saturation pot was about 1% of the calibrated volume which was at ambient temperature.

For desorption, known weights of sodium metal and sodium hydride were added to the purged and nitrogen-filled saturation chamber. After evacuation and isolation from the vacuum manifold, the temperature of the saturation chamber was raised with the stopcock between the pot and the calibrated volume closed. When the desired temperature was reached, the stopcock was opened slowly and excess solid sodium hydride allowed to dissociate, the hydrogen passing into the calibrated volume. When no further hydrogen evolution was apparent, the pressure and temperature of the system were checked against the known dissociation pressure of sodium hydride.<sup>7,8</sup> If the pressure on the system was less than that specified by these references, then the temperature of the saturation chamber was slowly lowered until the  $P$ - $T$  relation for the system agreed with reference values. If, on the other hand, the first check revealed that the  $P$ - $T$  relation checked the literature values, then the temperature was raised until an incremental increase did not result in a corresponding increase in the pressure. These points of conformity to sodium hydride dissociation data were taken as the saturation temperatures for the various runs. The anticipated range could be predicted, and was shifted by varying the original charge of sodium hydride.

The hot saturation pot was isolated, and the hydrogen in the calibrated volume removed by evacuation. The hydrogen equivalent to the remaining soluble hydride was then recovered and measured by repeated evolution into, and evacuation from, the calibrated volume. Evolution and measurement were always made with appropriate isolation of the hot and cold parts of the system so that the volume measured for removal was always at ambient temperature. This hydrogen removal could be done at saturation temperature because sodium hydride in solution still exhibits a dissociation pressure (a few millimeters at 400°) which is sufficient to effect complete recovery, although the equilibrium pressure becomes lower as the solution becomes more dilute. A second means of dissociating the soluble hydride is to cycle the melt through a temperature range of 300–350° with intervening evacuations. Both methods were used and were equally effective.

The isolation stopcock between the saturation pot and the calibrated volume was closed during the initial heating period so as to minimize the amount of hydride required to satisfy both metal saturation and equilibrium system pressure. Since the apparatus was not designed to operate at pressures greater than one atmosphere, solubility determinations by this method were made only to 425°.

In the absorption studies, the same apparatus was used. It was charged, after purging, with sodium metal and hydrogen gas. The temperature of the saturation pot was raised to the various desired temperatures and the hydrogen pressure drop was recorded until no further absorption was indicated. This method was much slower than the desorption study, but did allow for higher temperatures to be used. In early runs, the reaction pot was constructed of nickel, but diffusion at temperatures above 400° necessitated the substitution of a 304 stainless steel tube.

The data from all runs are shown graphically in Fig. 1. The agreement of the data from the different types of runs lends credence to the indirect approach to the solubility

problem. A brief discussion of the deviations may be in order, however.

It may be seen that the absorption data tend to run somewhat higher than the desorption data. The reason for this is the limited formation of undissolved hydride. The initial  $H_2$  pressure during the absorption runs was between 600 and 650 mm. Thus, at temperatures below 400°, the melt absorbed sufficient  $H_2$  to saturate itself and, in addition, enough to coat the surface with a thin layer of sodium hydride. Since the system was static, this layer prevented further hydride formation,<sup>10</sup> and accounts for the slightly higher solubility figures reported.

The wide deviation of the point at 265° is explained by the fact that, at this temperature, the melt probably was not saturated with sodium oxide, and subsequent correction for anticipated saturation by this material resulted in a low hydride value. The 240° figure was not corrected for oxide, since no attack was in evidence and no alkalinity was found.

This solubility study was limited by the vapor pressure of sodium metal and the dissociation pressure of sodium hydride. Both become significant to these data at 425°. The desorption apparatus would not allow for operation at pressures in excess of one atmosphere, and excessive distillation of sodium vitiated higher temperature results in the absorption runs. Data were collected at 500°, but were not sufficiently reliable to be included in this report. There were indications, however, that the system was approaching a limiting solubility of approximately 5 wt. % NaH (under about 1 atmosphere  $H_2$  pressure). Hence, extrapolation of the data herein reported is not recommended.

The results of this study demonstrate a possible source of error in present sodium analysis for oxygen by the amalgamation method. The error with respect to sodium hydride, as well as the likelihood that it will be present in most sodium systems, is particularly significant. The error will not necessarily be predictable in a sample drawn directly from saturated sodium unless precautions are taken to prevent dissociation of hydride during sample handling and cooling. Excessive local heating during amalgamation in the oxide analysis method can also result in hydride loss.

(10) D. T. Hurd, "Chemistry of Hydrides," John Wiley and Sons, New York, N. Y., 1952, p. 31.

## THE EFFECT OF $D_2O$ ON THE RATE OF THE REACTION BETWEEN OXYGEN AND Pu(III)<sup>1</sup>

BY F. B. BAKER AND T. W. NEWTON

University of California, Los Alamos Scientific Laboratory, Los Alamos, New Mexico

Received August 27, 1956

It has been shown recently that the reaction between Pu(III) and oxygen in aqueous sulfate solutions is in termolecular: first order in the oxygen concentration and second order in the Pu(III) concentration.<sup>2</sup> One possible mechanism would involve an activated complex in which two Pu(III) sulfate complexes were linked by means of an oxygen bridge; this structure would be similar to that postulated for one of the Pu(IV)- $H_2O_2$  complexes.<sup>3</sup> Another possible mechanism would involve the transfer of a hydrogen atom from the hydration shell of each of two Pu(III)- $SO_4^-$  complexes to the oxygen molecule.<sup>4</sup> If a hydrogen atom transfer

(1) This work was done under the auspices of the U. S. Atomic Energy Commission.

(2) T. W. Newton and F. B. Baker, *J. Phys. Chem.*, **60**, 1417 (1956).

(3) R. E. Connick and W. H. McVey, paper 4.12 in "The Transuranium Elements," edited by G. T. Seaborg, J. J. Katz and W. M. Manning, "National Nuclear Energy Series," Division IV, Vol. 14B, McGraw-Hill Book Co., Inc., New York, N. Y., 1949.

(4) This was suggested to us by Professor Norman Davidson, see also R. E. Huffman and N. Davidson, *J. Am. Chem. Soc.*, **78**, 4836 (1956).

mechanism were the correct one, there should be a marked hydrogen isotope effect and a significant decrease in reaction rate in  $D_2O$ .<sup>4</sup> In the hope of deciding between these mechanisms, rates in  $H_2O$  and  $D_2O$  solutions were determined and compared at the same  $O_2$ , Pu(III) and free  $SO_4^-$  concentrations. Only a moderate hydrogen isotope effect was observed.

The solubility of oxygen in  $D_2O$  was determined so that a correction for the concentration difference in the two solvents at the same partial pressure of oxygen could be applied. A known volume of water was saturated with oxygen, transferred to a vacuum line and distilled into a large bulb chilled with Dry Ice. The liberated gas was determined manometrically. For a partial pressure of  $O_2$  of 1 atm. the solubility was found to be  $1.28 \times 10^{-3} M$  in  $H_2O$  and  $1.41 \times 10^{-3} M$  in  $D_2O$ . Three determinations in each solvent were made, the mean deviation was about 2.4%. No measurements have been made in salt solutions, but it is probably safe to assume the same solubility ratio and that  $O_2$  is about 10% more soluble in  $D_2O$  solutions than in  $H_2O$  solutions.

The acid dissociation quotient of  $DSO_4^-$  in  $D_2O$  solutions was needed for the calculation of the free  $SO_4^-$  concentrations in those solutions. It was determined by making optical measurements on the Ce(III)- $SO_4^-$  system. Absorbancies were determined for a series of Ce(III) solutions which were 0.012  $M$  in  $HClO_4$  and with  $Na_2SO_4$  ranging from 0 to 0.05  $M$ . In these solutions, the acid concentration was low enough so that an approximate value for the acid dissociation quotient was sufficient for the determination of free sulfate concentration as a function of absorbancy. Using the same Ce(III) concentration, absorbancies were determined for a series of solutions all 0.05  $M$  in  $Na_2SO_4$ , but with  $HClO_4$  concentrations ranging up to 0.11  $M$ . Free  $SO_4^-$  concentrations were estimated from the absorbancy vs.  $SO_4^-$  function and the acid dissociation quotients were calculated. The results of such determinations in both  $H_2O$  and  $D_2O$  solutions of unit ionic strength are given in Table I. The fact that the values obtained in the

TABLE I

DETERMINATIONS OF THE ACID DISSOCIATION QUOTIENT OF THE BISULFATE ION IN SODIUM PERCHLORATE SOLUTIONS OF UNIT IONIC STRENGTH AT 25°

| Fraction $D_2O$ | $Na_2SO_4$ , $M$ | No. of soln. | $HClO_4$ range, $M$ | Acid dissociation quotient |
|-----------------|------------------|--------------|---------------------|----------------------------|
| 0               | 0.05             | 5            | 0.05 to 0.11        | $0.091 \pm 0.006$          |
| 0.892           | .05              | 4            | .05 to .11          | $.052 \pm .004$            |
| 0.876           | .05              | 5            | .03 to .11          | $.055 \pm .003$            |

$H_2O$  solutions are in good agreement with those obtained potentiometrically<sup>5</sup> indicates that the optical method for determining the acid dissociation quotients is valid. Assuming that the effect of  $D_2O$  is linear in its concentration, the data lead to the estimate that the acid dissociation quotient of  $DSO_4^-$  in pure  $D_2O$  solutions at 25° and unit ionic strength is  $0.051 \pm 0.003$ . The ratio of acid dissociation quotients found here is in substantial agreement with the ratios which have been re-

(5) E. Eichler and S. W. Rabideau, *ibid.*, **77**, 5501 (1955).

ported for other weak acids.<sup>6</sup> It was found to be impossible to make reliable measurements at an ionic strength of 2 due to the formation of a precipitate. However, it is probably safe to assume that the ratio is essentially the same at the two ionic strengths.

Three experiments have been made in which the rates of the reaction between Pu(III) and oxygen (in the presence of Fe(II) to eliminate complications from the reactions of H<sub>2</sub>O<sub>2</sub>) were compared in H<sub>2</sub>O and D<sub>2</sub>O solutions. The rates were determined as previously described.<sup>2</sup> The results of these experiments are shown in Table II.

TABLE II

EFFECT OF D<sub>2</sub>O ON THE RATE OF REACTION BETWEEN Pu(III) AND OXYGEN IN NaClO<sub>4</sub> SOLUTIONS OF IONIC STRENGTH 2 AND 23°

| HClO <sub>4</sub> ,<br>M | Na <sub>2</sub> -<br>SO <sub>4</sub> ,<br>M | Na-<br>ClO <sub>4</sub> ,<br>M | Frac-<br>tion<br>D <sub>2</sub> O | K <sub>a</sub> | SO <sub>4</sub> <sup>2-</sup> ,<br>M | R <sub>H</sub> /R <sub>D</sub> <sup>a</sup> | k <sub>H</sub> /<br>k <sub>D</sub> <sup>b</sup> |
|--------------------------|---|--------------------------------|-----------------------------------|----------------|--------------------------------------|---|---|
| 0.131                    | 0.06  | 1.75                           | 0                                 | 0.10           | 0.03                                 | 1.84 ± 0.05                                 | 1.17  |
| .131                     | .06   | 1.75                           | 0.98                              | .056           | .022 <sub>6</sub>                    |   |   |
| .17                      | .14   | 1.55                           | 0                                 | .10            | .07                                  | 1.53 ± .03                                  | 1.23  |
| .17                      | .14   | 1.55                           | 0.87 <sub>2</sub>                 | .059           | .056 <sub>7</sub>                    |   |   |
| .17                      | .14   | 1.55                           | 0                                 | .10            | .07                                  | 1.15 ± .01                                  | 1.30  |
| .219                     | .189  | 1.45                           | 0.87 <sub>2</sub>                 | .059           | .07                                  |   |   |

<sup>a</sup> Observed rate ratio at the same Pu(III) concentrations.

<sup>b</sup> Rate ratio corrected to the same free SO<sub>4</sub><sup>2-</sup> and oxygen concentrations.

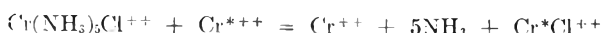
For our purposes, the rates should be compared not at the same stoichiometric concentrations of the reactants but at the same concentrations of the reactive intermediates. Since PuSO<sub>4</sub><sup>+</sup> and Pu(SO<sub>4</sub>)<sub>2</sub><sup>-</sup> are believed to be the reactive intermediates, the possibility that their association quotients are different in the two solvents was considered. Preliminary spectrophotometric determinations of the association quotient of CeSO<sub>4</sub><sup>+</sup> in D<sub>2</sub>O indicate that the association quotient is the same, within 10%, in H<sub>2</sub>O and D<sub>2</sub>O solutions. This lack of effect probably applies to the Pu(III)-SO<sub>4</sub><sup>2-</sup> complexes as well.

In general a hydrogen isotope effect usually depends on the strength of the bonds to hydrogen both in the reactants and the activated complex, and a large range of rate ratios has been observed.<sup>7</sup> In comparing rates in H<sub>2</sub>O and D<sub>2</sub>O solutions the solvent effect cannot be ignored since it may give rise to rate ratios as large as 1.4.<sup>8</sup> Thus a rather large rate ratio is necessary if it is to be considered as evidence for hydrogen atom transfer.<sup>9</sup> The rather small rate ratio of 1.23 found for the oxidation of Pu(III) does not support a mechanism involving transfer of a hydrogen atom, but instead supports an electron transfer mechanism.

(6) C. K. Rule and V. K. LaMer, *ibid.*, **60**, 1974 (1938).

(7) K. B. Wiberg, *Chem. Revs.*, **55**, 713 (1955).

(8) H. Taube, personal communication, has reported that the Cl-atom transfer reaction



is 1.4 times faster in H<sub>2</sub>O than in D<sub>2</sub>O solutions.

(9) For example, J. Hudis and R. W. Dodson, *J. Am. Chem. Soc.*, **78**, 911 (1956), found the rate ratio to be 2 for the Fe(II)-Fe(III) exchange in H<sub>2</sub>O and D<sub>2</sub>O solutions, and considered this to support a H-atom transfer mechanism.

## DECOMPOSITION STUDY OF CONCENTRATED HYDROGEN PEROXIDE

BY A. GREENVILLE WHITTAKER AND CHARLES M. DREW

Contribution from the Chemistry Division, Research Department, U. S. Naval Ordnance Test Station, China Lake, California

Received July 30, 1956

Many investigations have been made on the liquid phase decomposition of H<sub>2</sub>O<sub>2</sub>. Practically all of this early work was done in dilute solution and on catalytic decomposition of H<sub>2</sub>O<sub>2</sub>. The kinetics of decomposition of very concentrated H<sub>2</sub>O<sub>2</sub> has received little attention. Our primary objective was to study the homogeneous thermal decomposition in the concentration range of 100% H<sub>2</sub>O<sub>2</sub> and arrive at a reasonable mechanism for the decomposition. After considerable effort to keep the experiments dust-free and make quartz surfaces catalytically inactive it was found that homogeneous decomposition was still not achieved. Because of this result the work was not continued beyond the first stages of a kinetic study.

### Experimental

Spherical ampoules of fused quartz having a capacity of about one ml. and weighing about 0.4 g. were constructed from selected quartz tubing which previously had been cleaned by the procedure recommended by Schumb.<sup>1</sup> The upper end of the ampoule was drawn out into a thin capillary tube about 5 cm. in length with an inside diameter of 5-10 mils. The end was bent into a hook and left open. When this vessel was half filled it gave a surface to volume ratio of 4.83 cm.<sup>-1</sup>. This ratio was about the same relative to the wetted surface of the vessel as well as the non-wetted surface, and does not include the liquid-gas interface. A small hook was attached to the bottom of the ampoule so that it could be inverted for filling in a special apparatus. After filling about one-half full of sample the ampoule was suspended on a calibrated quartz helix in a dry 25 mm. i.d. glass well. The weight loss of sample was measured by observing the change in helix length. The assembly was thermostated at the desired temperature inside a dry well immersed in an oil-bath (Corning cylindrical jar 12" deep No. 370). The length of the helix was observed through the walls of the bath and well with a Gaertner model M-901 cathetometer. In order to reduce errors due to aberrations in the glass surfaces a flat vertical strip was ground and polished on the outside of the bath jar for a viewing window. Aberrations on the inner surfaces were effectively eliminated by choosing a bath fluid having nearly the same refractive index as Pyrex glass (White paraffin oil, 1.475<sup>20</sup>). The tubing selected for the well had no appreciable optical aberrations.

**Purification of Hydrogen Peroxide Solutions.**—Hydrogen peroxide used in this work was purified by repeated recrystallization of concentrated 97.85% stabilizer-free material obtained from Buffalo Electric Co.<sup>2,3</sup> The material was handled in all quartz glassware under dust-free conditions. The quartz vessels were cleaned and conditioned before use by the previously mentioned procedure of Schumb.<sup>1</sup> The hydrogen peroxide was purified by six crystallizations which were carried out in a closed system constructed in such a way that the crystals always remained in the same flask. After crystallization the material gave an analysis of 99.8% hydrogen peroxide by weight using a method of direct titration against potassium permanganate in dilute sulfuric acid solution. Analyses indicating 100.0% of hydrogen peroxide were obtained by volumetric measurement of total oxygen obtained from complete decomposition of a weighed quantity of material. Since both methods are subject to errors it was felt that the correct value probably lies somewhere between the values given. The material was

(1) W. C. Schumb, *Ind. Eng. Chem.*, **41**, 992 (1949).

(2) O. Maass and W. H. Hatcher, *J. Am. Chem. Soc.*, **42**, 2548 (1920).

(3) D. M. Yost and H. Russell, "Systematic Inorganic Chemistry," Prentice-Hall, Inc., New York, N. Y., 1946, p. 367.

stored at 5° until used. No measurable decomposition was encountered under storage for about one year.

**Sampling Procedure.**—The weighed empty ampules were filled by inverting them in an enclosed flask with the open end of the capillary vent just under the surface of purified hydrogen peroxide. The assembly was partially evacuated through a side arm provided with a dust trap and then released to atmospheric pressure, thus causing the ampule to fill about one-half full of liquid. The ampule was removed, shaken, then emptied in a similar flask in like manner and then filled again. The procedure was repeated three times to ensure complete rinsing. After filling the final time the ampule was shaken down to remove excess liquid from the capillary. A small hand torch was used to warm the capillary vent in order to dry the inside. It was again weighed, then placed on the helix assembly at bath temperature. If bubble streamers appeared at any time during an experiment the ampule was discarded.

**Quartz Helix Balance.**—The quartz helix employed was constructed to the following specifications, giving optimum sensitivity for a one-gram load capacity maximum.<sup>4</sup>

Fiber diameter = 6.1 mils, helix diameter = 8.9 mm. (average), no. of turns = 134, pitch relaxed = 5 turns per mm., extension under 1 gram load = 50 cm., sensitivity about 0.45 mm./mg. The helix sensitivity was carefully determined with known weights at bath temperature before use.

**Rate Measurements.**—The change in weight of the hydrogen peroxide sample with time was followed by periodically observing the change in length of the helix with a cathetometer. Measurements were made to the nearest 0.05 mm. Thus from the previously determined helix sensitivity the total weight loss of the sample could be determined. This loss represents the total loss of oxygen, water and hydrogen peroxide from the ampule. To determine the oxygen loss only, the total weight loss must be corrected for the water and hydrogen peroxide carried out of the ampule by the oxygen. This can be done by an iteration process to any desired degree of accuracy. To start the iteration it was assumed that the total observed weight loss was due to oxygen. From the known partial and total vapor pressure data on the water-hydrogen peroxide system<sup>5,6</sup> and the assumption that the oxygen was saturated at these pressures a first approximation of the water and hydrogen peroxide carried out by the oxygen was calculated. This weight was subtracted from the first assumed weight of oxygen to give the first approximation of the correct weight lost. This corrected weight of oxygen can be used to make further approximations of the correct oxygen loss. Because of the low vapor pressure of concentrated peroxide solutions the first approximation of the weight of oxygen lost was usually accurate enough. Using oxygen loss the amount of decomposition was calculated from the following stoichiometry



The validity of the method was checked by analyzing partially decomposed samples by titration against potassium permanganate. The results agreed within experimental error which was  $\pm 0.1\%$  hydrogen peroxide decomposed.

The long capillary vent eliminated direct evaporation losses by providing a long diffusion path. The effectiveness of this system was verified by observing the weight loss of ampules containing distilled water at maximum bath temperature. The loss was scarcely detectable over a two weeks period and since water has a much higher vapor pressure than concentrated hydrogen peroxide solutions it was assumed that losses by evaporation were negligible.

### Results

Severe demands on cleanliness and handling techniques reduced the number of successful runs severely. The results given in Table I include only those runs which gave no visible evidence of bubble streamers in the liquid during the course of the experiment. When streamers were encountered the decomposition rates were invariably much

greater and not reproducible. In some cases where abnormally high rates were observed without streamers in evidence the ampules were emptied and refilled with considerable improvement noted. All new ampules were therefore given a conditioning treatment prior to use. Once conditioned, an ampule gave reasonably reproducible results and also agreed with results obtained with other similarly treated ampules.

TABLE I  
OBSERVED DECOMPOSITION RATES OF PURE HYDROGEN PEROXIDE AT VARIOUS TEMPERATURES

| Temp., °C. | % Decomposed | Duration, hr. | Decomp. rate, %/hr. $\times 10^2$ | Av. rate, %/hr. $\times 10^2$ |
|------------|--------------|---------------|-----------------------------------|-------------------------------|
| 86.3       | 2.51         | 71            | 3.53                              |                               |
|            | 1.85         | 64            | 2.89                              |                               |
|            | 2.66         | 96            | 2.75                              |                               |
|            | 2.34         | 72            | 3.21                              |                               |
|            | 6.71         | 218           | 3.08                              |                               |
|            | 6.31         | 214           | 2.95                              | 2.70                          |
|            | 4.02         | 213           | 1.89                              |                               |
|            | 4.26         | 213           | 2.00                              |                               |
|            | 8.86         | 240           | 3.69                              |                               |
|            | 3.92         | 239           | 1.64                              |                               |
|            | 5.54         | 239           | 2.32                              |                               |
|            | 7.81         | 238           | 3.28                              |                               |
|            | 4.25         | 233           | 1.82                              |                               |
|            | 70.5         | 3.53          | 330                               | 1.07                          |
| 3.14       |              | 330           | 0.95                              |                               |
| 3.73       |              | 330           | 1.13                              | 1.07                          |
| 3.66       |              | 330           | 1.11                              |                               |
| 59.3       | 3.46         | 720           | 0.48                              |                               |
|            | 3.31         | 720           | 0.46                              |                               |
|            | 4.90         | 720           | 0.68                              | 0.54                          |
|            | 3.39         | 720           | 0.54                              |                               |

It is felt that the chief merits of this method lie in the small amount of surface and sample size required thus eliminating the formidable task of purifying large quantities of hydrogen peroxide and cleaning large surface areas.

All the experimental results showed a linear relationship between the per cent. decomposed and time. The scatter of the points about an average line was  $\pm 0.10\%$  unit for the experiments at 86.3°. At the lower temperatures the scatter was less. These results indicate that the decomposition was showing zero-order behavior. However, even this precision was not good enough to rule out completely the possibility that the decomposition may have been half order. Over the temperature range studied, the reaction gave an average temperature coefficient of 1.83. This is somewhat lower than Schumb's value of 2.12<sup>1</sup> and Roth and Shanley's value of 2.26.<sup>7</sup> It is interesting to note that our value does agree very closely with Roth and Shanley's value of 1.84 which they obtained on concentrated hydrogen peroxide stabilized with phosphoric acid. If the zero-order rate constant  $k$  is expressed as an Arrhenius function of temperature

$$k = PZe^{-E/RT}$$

then the activation energy  $E$  is 14.4 kcal. and the

(4) F. M. Ernsberger and C. M. Drew, *Rev. Sci. Instr.*, **24**, 117 (1953).

(5) P. A. Giguere and O. Maass, *Can. J. Res.*, **18B**, 184 (1940).

(6) O. Maass and P. G. Jiebert, *J. Am. Chem. Soc.*, **46**, 2693 (1924).

(7) E. M. Roth and E. S. Shanley *Ind. Eng. Chem.*, **45**, 2343 (1953).

collision factor  $PZ$  is approximately  $10^4$  moles/l. sec. This result indicates that its apparent normal behavior is the result of both a very low collision factor and a small activation energy.

No induction period ever was observed. This probably was due to the fact that the solutions were of very high purity and free of foreign materials that could act as inhibitors. However, it also tends to rule out mechanisms in which a certain concentration of an intermediate must be built up before the decomposition can proceed.

Many homogeneous mechanisms were considered but none were found that had a low enough activation energy. If it is assumed that the decomposition involves strongly adsorbed hydrogen peroxide on the quartz surface, it is possible to write a mechanism with a sufficiently low activation energy and zero-order kinetics. Unfortunately the results obtained in this study are not complete enough to establish clearly this decomposition mechanism. However, they do support the notion that the decomposition of concentrated liquid hydrogen peroxide takes place primarily if not completely by a heterogeneous mechanism.

## THE STRUCTURE OF THE AMIDE ION

By S. F. MASON<sup>1</sup>

Australian National University, Department of Medical Chemistry,  
University College, London, W.C. 1

Received September 19, 1956

The crystal structures of sodium amide<sup>2</sup> and lithium amide<sup>3</sup> have been reported recently. In these determinations the H...H and N...H distances in the amide ion were assumed<sup>2</sup> to be 1.60 and 1.01 Å., respectively. It has been shown, from the proton magnetic resonance spectrum of potassium amide,<sup>4</sup> that the H...H distance in the amide ion is  $1.63 \pm 0.03$  Å., and in the present work an approximate value of  $10^4$  for the bond angle has been calculated from the infrared spectrum of lithium amide, giving the N...H distance of 1.03 Å. for the ion.

The infrared spectrum was obtained with a weighed sample of purified lithium amide pressed into a disc with potassium bromide, using a Perkin-Elmer Model 12C spectrometer with a lithium fluoride prism. The amount of lithium amide in the disc was subsequently checked by titrating an aqueous solution of the disc potentiometrically against standard acid. The asymmetric stretching frequency was observed at  $3315 \pm 1$  cm.<sup>-1</sup>, with a molecular extinction coefficient of 6.5, and a band half width of 10 cm.<sup>-1</sup>, and the symmetric frequency at  $3231 \pm$  cm.<sup>-1</sup>, with an  $\epsilon_{\max}$  of 17.7, and a band half width of 14 cm.<sup>-1</sup>. These bands are sharp and symmetrical in shape, and no other bands were observed in the N-H stretching vibration region. Thus the amide ion does not hydrogen bond in the crystal, as expected from the large minimum N...N distance (3.81 Å.) in the sodium

salt.<sup>1</sup> The bond angle of the amide ion and the N-H stretching vibration force constant ( $5.99 \times 10^5$  dyne/cm.) were calculated using Linnett's formula.<sup>5</sup>

(5) J. W. Linnett, *ibid.*, **41**, 223 (1945).

## THE VAPOR PRESSURE OF SODIUM FLUORIDE<sup>1</sup>

By KARL A. SENSE, C. A. ALEXANDER, R. E. BOWMAN,  
R. W. STONE AND R. B. FILBERT, JR.

Battelle Memorial Institute, Columbus, Ohio

Received October 26, 1956

This work was undertaken because information on the vapor pressures of sodium fluoride was needed in the 930-1075° temperature range. The apparatus and experimental procedure of the transpiration method used have been adequately described in the previous papers.<sup>2,3</sup> The sodium fluoride used was J. T. Baker highest grade. The results are given in Table I.

TABLE I  
VAPOR PRESSURE OF SODIUM FLUORIDE

| Temp., °C. | Pressure, mm. |        | Dev. % | Flow rate, nitrogen, cm. <sup>3</sup> /min. |
|------------|---------------|--------|--------|---|
|            | Obsd.         | Calcd. |        |   |
| 934.6      | 0.108         | 0.108  | 0.0    | 47.3  |
| 946.9      | .142          | .143   | -0.7   | 50.9  |
| 955.0      | .173          | .172   | +0.6   | 48.2  |
| 964.5      | .211          | .213   | -0.9   | 50.0  |
| 974.0      | .266          | .263   | +1.1   | 49.1  |
| 984.7      | .336          | .332   | +1.2   | 49.2  |
| 992.0      | .385          | .389   | -1.0   | 48.6  |
| 1001       | .452          | .465   | -2.6   | 49.3  |
| 1011       | .563          | .548   | +2.7   | 49.4  |
| 1014       | .580          | .579   | +0.2   | 50.3  |
| 1021       | .653          | .654   | -0.2   | 49.6  |
| 1032       | .797          | .792   | +0.6   | 49.3  |
| 1035       | .832          | .834   | -0.2   | 48.2  |
| 1047       | 1.02          | 1.01   | +1.0   | 45.4  |
| 1064       | 1.30          | 1.32   | -1.5   | 44.0  |
| 1075       | 1.58          | 1.58   | 0.0    | 40.5  |

By use of a least-squares correlation the following  $P$ - $T$  relationships were derived.

From 934-996°

$$\log p \text{ (mm.)} = 11.3315 - \frac{14856}{T, \text{ }^\circ\text{K.}} \quad (1)$$

$$\Delta H_{\text{sublimation}} = 68.0 \text{ kcal./mole} \quad (2)$$

From 996-1075°

$$\log p \text{ (mm.)} = 9.4188 - \frac{12428}{T, \text{ }^\circ\text{K.}} \quad (3)$$

$$\Delta H_{\text{vaporization}} = 56.9 \text{ kcal./mole} \quad (4)$$

The melting point, 996°, was obtained by equating (1) and (3). These results are based on the assumption that, at the temperature range studied, the sodium fluoride molecule exists as a monomer. If dimers or higher polymers are present in the vapor phase, the resulting vapor pressures would, of course, be lower.

(1) Chemistry Department, The University, Exeter, England.

(2) A. Zalkin and D. H. Templeton, *THIS JOURNAL*, **60**, 821 (1956).

(3) R. Jung and K. Opp, *Z. anorg. allgem. Chem.*, **266**, 313 (1951).

(4) R. Freeman and R. E. Richards, *Trans. Faraday Soc.*, **52**, 802 (1956).

(1) Work performed under AEC Contract W-7405-eng-92.

(2) K. A. Sense, M. J. Snyder and J. W. Clegg, *THIS JOURNAL*, **58**, 233 (1954).

(3) K. A. Sense, M. J. Snyder and R. B. Filbert, Jr., *ibid.*, **58**, 995 (1954).

# NATURAL PLANT HYDROCOLLOIDS

103 Pages Devoted to Natural  
Plant Hydrocolloids Of  
Appreciable Commercial Significance

Number 11 in  
Advances in Chemistry Series

edited by the staff of  
Industrial and Engineering Chemistry

|  |     |
|--|-----|
| <b>Introductory Remarks</b> .....  | 1   |
| <i>Leonard Stoloff</i> , Seaplant Chemical Corp., New Bedford, Mass.   |     |
| <b>Calcium Pectinates, Their Preparation and Uses</b> .....  | 3   |
| <i>Clinton W. Woodmansee</i> and <i>George L. Baker</i> , University of Delaware, Newark, Del.   |     |
| <b>Factors Influencing Gelation with Pectin</b> .....  | 10  |
| <i>Harry S. Owens</i> , <i>Harold A. Swenson</i> , and <i>Thomas H. Schultz</i> , Western Regional Research Laboratory, Albany 6, Calif. |     |
| <b>Agar Since 1943</b> .....   | 16  |
| <i>Horace H. Selby</i> , American Agar & Chemical Co., San Diego, Calif.   |     |
| <b>Technology of Gum Arabic</b> .....  | 20  |
| <i>Charles L. Mantell</i> , 457 Washington St., New York 13, N. Y.   |     |
| <b>Chemistry, Properties, and Application of Gum Karaya</b> .....  | 33  |
| <i>Arthur M. Goldstein</i> , Stein, Hall & Co., Inc., New York, N. Y.  |     |
| <b>History, Production, and Uses of Tragacanth</b> .....   | 38  |
| <i>D. C. Beach</i> , S. B. Penick & Co., New York, N. Y.   |     |
| <b>Guar Gum, Locust Bean Gum, and Others</b> .....   | 45  |
| <i>Roy L. Whistler</i> , Purdue University, Lafayette, Ind.  |     |
| <b>Some Properties of Locust Bean Gum</b> .....  | 51  |
| <i>Hans Deuel</i> and <i>Hans Neukom</i> , Swiss Federal Institute of Technology, Zurich, and Meypro, Ltd., Weinfelden, Switzerland      |     |
| <b>Observations on Pectic Substances</b> .....   | 62  |
| <i>Hans Deuel</i> and <i>Jürg Solms</i> , Swiss Federal Institute of Technology, Zurich, Switzerland                                     |     |
| <b>Algin in Review</b> .....   | 68  |
| <i>Arnold B. Steiner</i> and <i>William H. McNeely</i> , Kelco Co., San Diego, Calif.  |     |
| <b>Alginates from Common British Brown Marine Algae</b> .....  | 83  |
| <i>W. A. P. Black</i> and <i>F. N. Woodward</i> , Institute of Seaweed Research, Inveresk, Midlothian, Scotland                          |     |
| <b>Irish Moss Extractives</b> .....  | 92  |
| <i>Leonard Stoloff</i> , Seaplant Chemical Corp., New Bedford, Mass.   |     |
| <b>Effect of Different Ions on Gel Strength of Red Seaweed Extracts</b> .....  | 101 |
| <i>S. M. Marshall</i> and <i>A. P. Orr</i> , Marine Station, Millport, Scotland  |     |

103 pages—paper bound—\$2.50 per copy

order from

**Special Publications Department**  
**American Chemical Society**

1155 Sixteenth Street, N.W.  
Washington 6, D. C.

# ORDER THESE SPECIAL PUBLICATIONS FOR YOUR PERMANENT RECORDS

*Selected For Reprinting Solely On The Basis Of Their Importance To You*

## UNIT OPERATIONS REVIEWS

|                   |        |
|-------------------|--------|
| 1st Annual Review | \$0.50 |
| 2nd Annual Review | 0.50   |
| 4th Annual Review | 0.50   |
| 5th Annual Review | 0.50   |
| 6th Annual Review | 0.50   |
| 7th Annual Review | 0.75   |
| 8th Annual Review | 0.75   |
| 9th Annual Review | 0.75   |

## FUNDAMENTALS REVIEWS

|                   |      |
|-------------------|------|
| 1st Annual Review | 0.75 |
| 2nd Annual Review | 0.75 |

## UNIT PROCESSES REVIEWS

|                   |      |
|-------------------|------|
| 1st Annual Review | 0.50 |
| 5th Annual Review | 0.75 |
| 7th Annual Review | 1.50 |

## MATERIALS OF CONSTRUCTION REVIEWS

|                   |      |
|-------------------|------|
| 3rd Annual Review | 0.50 |
| 4th Annual Review | 0.75 |
| 5th Annual Review | 0.75 |
| 6th Annual Review | 0.75 |
| 7th Annual Review | 0.75 |
| 8th Annual Review | 1.50 |

## ANALYTICAL CHEMISTRY REVIEWS

|                   |      |
|-------------------|------|
| 2nd Annual Review | 1.50 |
| 3rd Annual Review | 1.50 |
| 5th Annual Review | 0.75 |
| 7th Annual Review | 1.50 |

## INDUSTRIAL & ENGINEERING CHEMISTRY REVIEWS

|   |      |
|---|------|
| March 1955 edition includes:                |      |
| 3rd Fundamentals Review                     |      |
| 10th Unit Operations Review                 | 2.00 |
| September 1955 edition includes:            |      |
| 9th Annual Materials of Construction Review |      |
| 8th Unit Processes Review                   | 2.00 |

## RESOURCES SYMPOSIA

|                           |      |
|---------------------------|------|
| Southwest                 | 0.50 |
| Far West                  | 0.50 |
| New England               | 0.75 |
| Mid Atlantic              | 0.75 |
| Rocky Mountain—Part 1     | 0.75 |
| East North Central States | 0.75 |
| West North Central States | 0.75 |
| South Atlantic States     | 0.75 |

## MISCELLANEOUS REPRINTS

|  |      |
|--|------|
| Raman Spectra  | 0.35 |
| Corrosion Testing in Pilot Plants                    | 0.25 |
| Atmospheric Contamination and Purification Symposium | 0.75 |

|   |      |
|---|------|
| Titanium Symposium                          | 0.50 |
| Adsorption Symposium                        | 0.50 |
| Careers in Chemistry & Chemical Engineering | 1.50 |
| Information Please Symposium                | 0.50 |
| Dispersion in Gases                         | 0.50 |
| Statistical Methods in Chemical Production  | 0.50 |
| Liquid Industrial Wastes Symposium          | 0.75 |
| Nucleation Phenomena                        | 0.75 |
| Chemical Facts and Figures—1952             | 1.00 |
| Corrosion Data Charts                       | 0.75 |
| Synthetic Fibers                            | 1.00 |
| Chemical Progress in 1952                   | 0.75 |
| Chemical Facts and Figures 1954             | 1.50 |
| Process Kinetics Symposium                  | 0.75 |
| X-Ray Symposium                             | 0.75 |
| Emulsion Paints                             | 0.75 |
| Industrial Process Water Symposium          | 0.75 |
| Symposium on Pilot Plants                   | 0.75 |
| Symposium on Boiler Water Chemistry         | 0.75 |
| Flow through Porous Media                   | 0.75 |
| Process Instrumentation Symposium           | 0.75 |
| First Air Pollution Review                  | 0.50 |
| Jet Fuels Symposium                         | 0.75 |
| Symposium on Application of Silicones       | 0.75 |
| Pulsatory and Vibrational Phenomena         | 1.25 |
| Plastics as Materials of Construction       | 1.75 |

## ADVANCES IN CHEMISTRY SERIES

|  |      |
|--|------|
| No. 4, Searching the Chemical Literature                           | 2.00 |
| No. 5, Progress in Petroleum Technology                            | 4.00 |
| No. 6, Azeotropic Data   | 4.00 |
| No. 7, Agricultural Applications of Petroleum Products             | 1.50 |
| No. 8, Chemical Nomenclature                                       | 2.50 |
| No. 9, Fire Retardant Paints                                       | 2.50 |
| No. 10, Literature Resources for Chemical Process Industries       | 6.50 |
| No. 11, Natural Plant Hydrocolloids                                | 2.50 |
| No. 12, Use of Sugars and other Carbohydrates in the Food Industry | 3.00 |
| No. 13, Pesticides in Tropical Agriculture                         | 2.50 |
| No. 14, Nomenclature for Terpene Hydrocarbons                      | 3.00 |
| No. 15, Physical Properties of Chemical Compounds                  | 5.85 |

## MISCELLANEOUS

|   |        |
|---|--------|
| Seventy-Five Eventful Years (History of the ACS)                                  | 5.00   |
| Chemistry—Key to Better Living  | 4.00   |
| Combination of Seventy-Five Eventful Years and Chemistry—Key to Better Living     | 7.50   |
| List of Periodicals Abstracted by Chem. Abs.                                      | 3.00   |
| 10 Years Numerical Patent Index (1937-1946)                                       | 6.50   |
| 27 Year Collective Formula Index  | 80.00  |
| 2nd Decennial Index to Chemical Abstracts   | 100.00 |
| 3rd Decennial Index to Chemical Abstracts   | 150.60 |
| 4th Decennial Index to Chemical Abstracts   | 120.60 |
| Directory of Chemical and Chemical Processing Plants in the South Atlantic States | 1.00   |

Supply of the above items is limited, and each will be sold only until present stock is exhausted.

**Order from: Special Publications Department, American Chemical Society  
1155 Sixteenth Street, N.W., Washington 6, D. C.**